RADIOLOGY AND ONCOLOGY

vol.59 no.1
march 2025

RADIOLOGY AND ONCOLOGY

March 2025
Vol. 59 No. 1
Pages 1-152
ISSN 1318-2099
UDC 616-006
CODEN: RONCEM
eISSN: 1581-3207

Publisher
Association of Radiology and Oncology

Aims and Scope
Radiology and Oncology (ISSN 1318-2099) is a multidisciplinary journal devoted to the publishing original and high-quality scientific papers and review articles, pertinent to oncologic imaging, interventional radiology, nuclear medicine, radiotherapy, clinical and experimental oncology, radiobiology, medical physics, and radiation protection. Papers on more general aspects of interest to the radiologists and oncologists are also published (no case reports).

Editorial office

Radiology and Oncology
Zaloška cesta 2
P. O. Box 2217
SI-1000 Ljubljana
Slovenia
Phone: +386 1 5879 369
Phone/Fax: +386 1 5879 434
E-mail: gsersa@onko-i.si

Reader for English
Vida Kološa

Secretary
Mira Klemenčič, Zvezdana Vukmirović, Vijoleta Kaluža, Uroš Kuhar

Design
Monika Fink-Serša, Samo Rovan, Ivana Ljubanović

Layout
Matjaž Lužar

Printed by
Tiskarna Ozimek, Slovenia

Published quarterly in 300 copies

Beneficiary name: DRUŠTVO RADIOLOGIJE IN ONKOLOGIJE
Zaloška cesta 2
1000 Ljubljana
Slovenia

Beneficiary bank account number: SI56 02010-0090006751
IBAN: SI56 0201 0009 0006 751
Our bank name: Nova Ljubljanska banka, d.d.,
Ljubljana, Trg republike 2,
1520 Ljubljana; Slovenia

SWIFT: LJBASI2X

Subscription fee for institutions EUR 100, individuals EUR 50

The publication of this journal is subsidized by the Slovenian Research Agency.

Indexed and abstracted by:

- *Baidu Scholar*
- *Case*
- *Chemical Abstracts Service (CAS) - CAplus*
- *Chemical Abstracts Service (CAS) - SciFinder*
- *CNKI Scholar (China National Knowledge Infrastructure)*
- *CNPIEC - cnpLINKer*
- *Dimensions*
- *DOAJ (Directory of Open Access Journals)*
- *EBSCO (relevant databases)*
- *EBSCO Discovery Service*
- *Embase*
- *Genamics JournalSeek*
- *Google Scholar*
- *Japan Science and Technology Agency (JST)*
- *J-Gate*
- *Journal Citation Reports/Science Edition*
- *JournalGuide*
- *JournalTOCs*
- *KESLI-NDSL (Korean National Discovery for Science Leaders)*
- *Medline*
- *Meta*
- *Microsoft Academic*
- *Naviga (Softweco)*
- *Primo Central (ExLibris)*
- *ProQuest (relevant databases)*
- *Publons*
- *PubMed*
- *PubMed Central*
- *PubsHub*
- *QOAM (Quality Open Access Market)*
- *ReadCube*
- *Reaxys*
- *SCImago (SJR)*
- *SCOPUS*
- *Sherpa/RoMEO*
- *Summon (Serials Solutions/ProQuest)*
- *TDNet*
- *Ulrich's Periodicals Directory/ulrichsweb*
- *WanFang Data*
- *Web of Science - Current Contents/Clinical Medicine*
- *Web of Science - Science Citation Index Expanded*
- *WorldCat (OCLC)*

This journal is printed on acid- free paper

On the web: ISSN 1581-3207
https://content.sciendo.com/raon
http://www.radioloncol.com

contents

clinical oncology

review

Pulsed field ablation in medicine: irreversible electroporation and electropermeabilization theory and applications

Edward J Jacobs[1], Boris Rubinsky[2], Rafael V Davalos[1]

[1] Wallace H Coulter School of Biomedical Engineering, Georgia Institute of Technology & Emory Medical School, Atlanta, Georgia, USA

[2] Department of Bioengineering and Department of Mechanical Engineering, University of California, Berkeley, Berkeley, California, USA

Radiol Oncol 2025; 59(1): 1-22.

Received 21 November 2024
Accepted 7 December 2024

Correspondence: Rafael Davalos, Ph.D., Wallace H. Coulter School of Biomedical Engineering, Georgia Institute of Technology & Emory Medical School, Atlanta, Georgia, USA. E-mail: Rafael.Davalos@bme.gatech.edu

Disclosure: R.D. and B.R. have patents in the field of bioelectrics.

Background. Focal ablation techniques are integral in the surgical intervention of diseased tissue, where it is necessary to minimize damage to the surrounding parenchyma and critical structures. Irreversible electroporation (IRE) and high-frequency IRE (H-FIRE), colloquially called pulsed-field ablation (PFA), utilize high-amplitude, low-energy pulsed electric fields (PEFs) to nonthermally ablate soft tissue. PEFs induce cell death through permeabilization of the cellular membrane, leading to loss of homeostasis. The unique nonthermal nature of PFA allows for selective cell death while minimally affecting surrounding proteinaceous structures, permitting treatment near sensitive anatomy where thermal ablation or surgical resection is contraindicated. Further, PFA is being used to treat tissue when tumor margins are not expected after surgical resection, termed margin accentuation. This review explores both the theoretical foundations of PFA, detailing how PEFs induce cell membrane destabilization and selective tissue ablation, the outcomes following treatment, and its clinical implications across oncology and cardiology.

Conclusions. Clinical experience is still progressing, but reports have demonstrated that PFA reduces complications often seen with thermal ablation techniques. Mounting oncology data also support that PFA produces a robust immune response that may prevent local recurrences and attenuate metastatic disease. Despite promising outcomes, challenges such as optimizing field delivery and addressing variations in tissue response require further investigation. Future directions include refining PFA protocols and expanding its application to other therapeutic areas like benign tissue hyperplasia and chronic bronchitis.

Key words: puled-field ablation; irreversible electroporation; pulsed electric fields; margin accentuation; oncology; atrial fibrillation

Electropermeabilization theory

Electropermeabilization is a biophysical phenomenon in which exogenous electric fields (EFs) increase the permeability of the cellular membrane (Figure 1). The application of an electric potential across tissue generates an EF whose shape and magnitude depend on the local electrical tissue properties. The EF induces ion movement (i.e., current) within the tissue (Figure 2), and the subsequent charge concentration around cells generates an electric potential across the cellular membrane. This transmembrane potential (TMP) permeabilizes the cellular membrane through phospholipid oxidation[1-6], modulation of electrically-induced proteins[7], and the generation of nano-scale pores

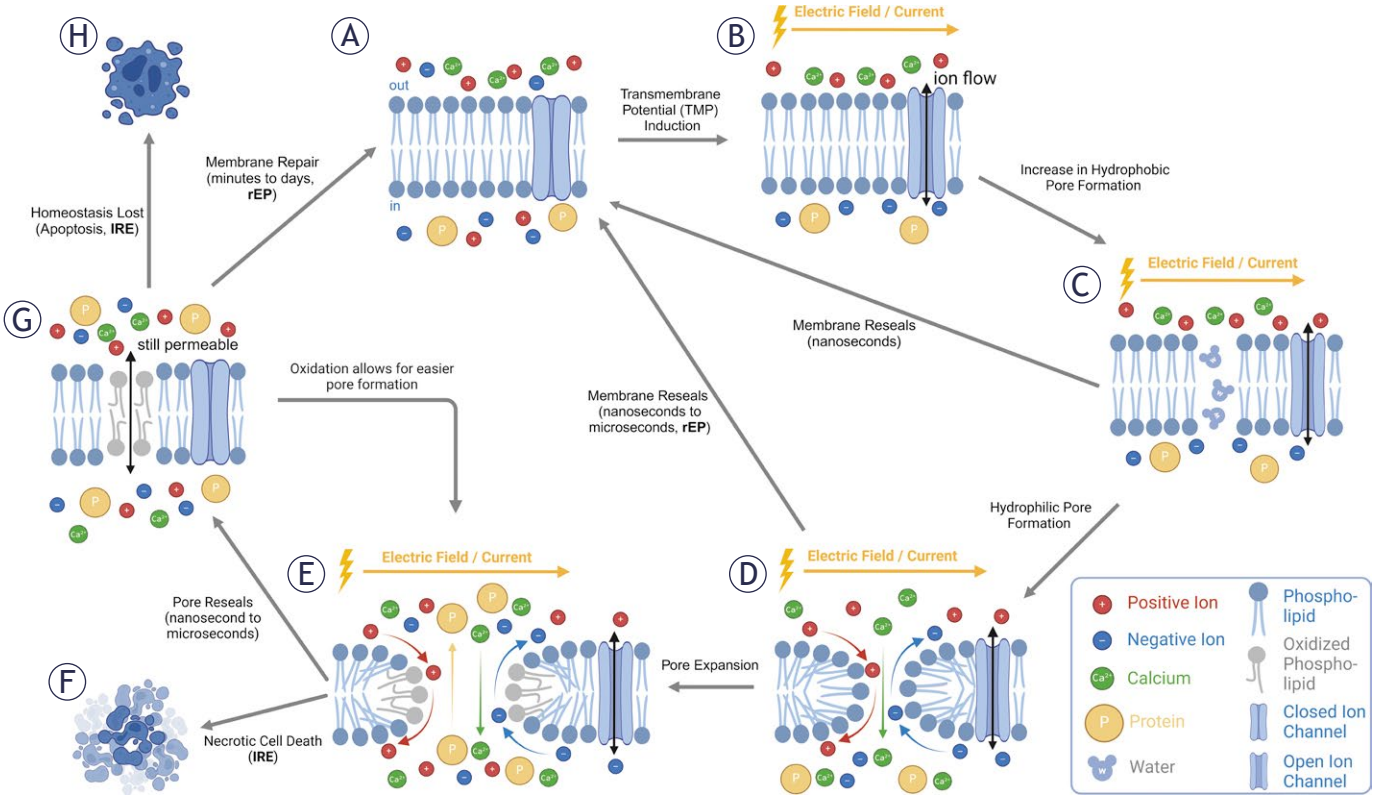

FIGURE 1. Conceptual schematic of the molecular mechanisms of electropermeabilization. **(A)** An intact cell membrane **(B)** in an exogenous electric field experiences an induced transmembrane potential. **(C)** Hydrophobic pores become energetically favorable as water infiltrates the bilayer. With the removal of the applied electric field, the hydrophobic pore reseals within nanoseconds. **(D)** If higher and longer external electric fields are applied, phospholipids invert to form small hydrophilic pores that allow the passage of ions and small molecules. Elastic forces within the membrane allow for these pores to reseal within nanoseconds to microseconds after the removal of the electric field. **(E)** With higher magnitude and longer duration electric fields, pores number may increase, and nucleated pores may expand or combine, allowing the transport of larger molecules and higher quantities across the membrane. Significant lipid oxidation is indicated to occur at high electric fields. **(F)** If excessive, the lipid bilayer may hemorrhage leading to lytic (necrotic) cell death. **(G)** After cessation of the applied electric field, the cell membrane may remain permeable due to the presence of lipid oxidation, which, in return, also allows for easier pore formation upon the introduction of another electric field. **(H)** As significant mass transport occurs over the cell membrane, the cell may lose homeostasis and die through regulated cell death, or **(G)** the cell may repair the permeable and damaged cell membrane to regain homeostasis.

(electroporation).[8] Standard electroporation theory and experiments suggest that pores are the dominant factor in mass transport across the membrane following electropermeabilization[9] and that pore formation occurs when the induced TMP exceeds a critical threshold (~0.258 V).[10] The magnitude of the induced TMP is dependent on the local geometry of the membrane and directly related to cell size and shape.[11,12] Once the exogenous EF is removed, the hydrophobic interactions, Van der Waals forces, and electrostatic interactions within the phospholipid bilayer may cause the pores to reseal within seconds to hours.[13-15] The transitory formation of pores is called reversible electroporation (rEP) and has been used for decades to deliver chemotherapeutics (electrochemotherapy; ECT)[16-18], calcium (calcium electroporation; CaEP)[19-25], genetic material (gene electrotherapy, GET)[26,27], and otherwise impermeable substances[28] into cells. With the application of higher magnitude and protracted pulses, pore nucleation increases within the cellular membrane, and existing pores expand, allowing for increased mass transport, consequently with the increased likelihood of losing homeostasis or causing cellular membrane hemorrhage.[7,29,30]

Concomitant to pore formation, the applied EF generates reactive oxygen species (ROS) that can induce lipid oxidation within the membrane.[1-6] Lipid oxidation increases the spacing between lipids and decreases membrane thickness, leading to increases in membrane permeability and electrical conductivity.[5,6,31] Since oxidative agents are slowly removed from the membrane[32], these effects

also persist after pores reseal.[4,5] Further, subsequent pore formation and increased oxidation may occur more easily at locations of previous oxidation[33], and oxidative lipids may diffuse throughout the membrane between applied pulses.[34] Excessive oxidation can occur using higher magnitude EFs, longer pulses, and more pulses[2-4], leading to complete bilayer disruption and cell death.[31]

Further, PEFs can destabilize and fragment cytoskeletal elements[35], including actin filaments[36-39], microtubules[40,41], and intermediate filaments[41-43], which collectively maintain cell shape, enable intracellular transport, and support membrane stability.[44] The membrane and cytoskeleton are functionally and structurally linked, so disruption can exacerbate membrane deformation and impair cellular mechanical properties, increasing the susceptibility of the membrane to subsequent pore formation and enhancing ion and molecule transport.[39,45] Cytoskeletal disruption may also interfere with cellular signaling pathways reliant on cytoskeletal integrity, affecting processes such as cell adhesion, motility, and division[36,42,45], with implications in blood vessel permeabilization.[46-48] As with membrane oxidation, cytoskeletal damage can persist even after the EF is removed, leading to prolonged changes in cell structure and negatively impacting cell viability and function.[49,50]

Pulsed field ablation techniques in medicine

Irreversible electroporation (IRE) was initially considered the upper limit of rEP and, as such, something to be avoided when post-treatment viability is desired.[11] With their seminal paper, R. Davalos, L. Mir, and B. Rubinsky mathematically described that EFs necessary to induce clinically relevant volumes of IRE did not simultaneously generate significant Joule heating and subsequent thermal damage.[51] Edd *et al.* supported this hypothesis by generating contiguous ablations in rat livers at EFs indicated to not cause thermal damage.[52] Following, Al-Sakere *et al.* reported the first successful use of IRE in oncology, achieving complete regression in 92% (12/13) of treated cutaneous mouse tumors using an optimized waveform (80 monophasic pulses of 100 μs at 0.3 Hz and 2500 V/cm), with a maximum measured temperature of 37.5°C.[53] The results from these studies demonstrated the feasibility of increasing the number of pulses from conventional ECT (8 pulses) without inducing thermal damage and provided the foundation for parameters used in current IRE protocols.

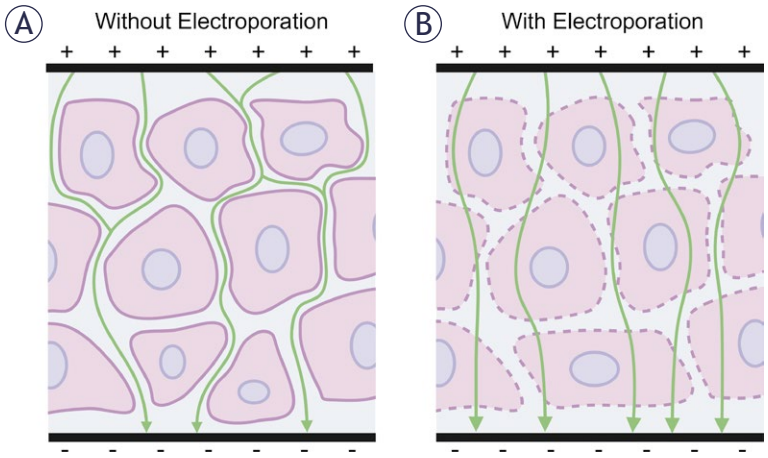

FIGURE 2. Electric field and current through heterogeneous tissue. **(A)** Without electroporation, current (green arrows) passes around the cells (pink) through the extracellular space (blue). **(B)** Electroporation allows for current to pass through the cells, but it is still influenced by tissue heterogeneity.

Shortly after, Bertacchini *et al.* developed the first IRE generator approved for clinical use.[54] Since the introduction of IRE in the clinic in 2010, over 100 clinical trials have been registered worldwide (Figure 3), with hundreds of research articles published demonstrating safe and effective treatment of prostate[55-64], pancreas[65-74], liver[75-84], and kidney[85-97] tumors, but feasibility in many other solid tumors like lung[98-99] and brain[100] has been demonstrated.

IRE as a clinical technique is described as a non-thermal focal ablation modality that employs high-magnitude (1–3 kV) and short (70–100 μs) monophasic pulses (Figure 4A) generated between conductive electrodes placed into or around the targeted tissue. In clinical practice, conventional

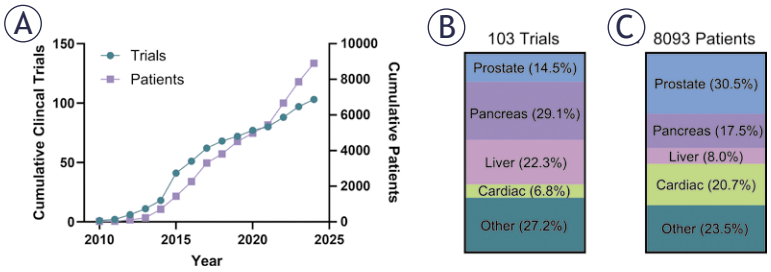

FIGURE 3. **(A)** cumulative registered patient and trial numbers for IRE and PFA on ClinicalTrials.gov. **(B)** Breakdown of trials and **(C)** patient populations by tissue type. Other contains renal, lung, stomach, esophageal, gallbladder, hilus pulmonis, extremity, lymph node, intestinal, rectal, laryngeal, head and neck, and breast cancers; benign prostate hyperplasia; chronic bronchitis; tonsillar hypertrophy.

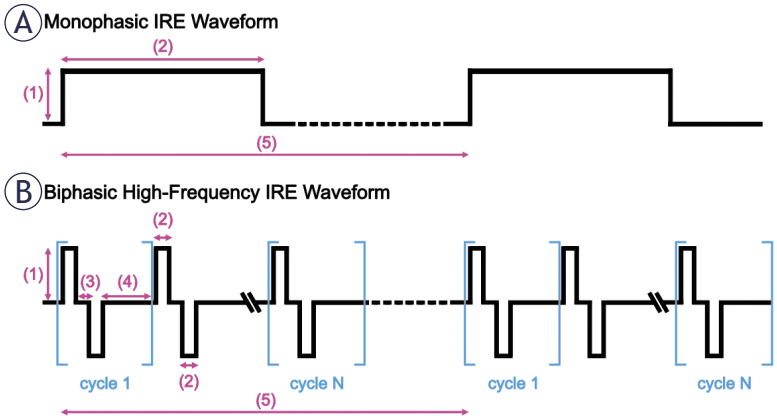

FIGURE 4. (A) Monophasic IRE waveform and **(B)** Biphasic H-FIRE waveform. (1) Magnitude (voltage or current), (2) pulse width, (3) interphase delay, (4) interpulse / intercycle delay, (5) burst repitition interval.

monophasic IRE pulses must be delivered using general anesthesia and prophylactic neuromuscular blockers to reduce muscle contractions.[53,101-103] Induced muscle contractions are undesirable in debilitated patients and can cause an involuntary shift in the electrode locations, leading to incomplete ablation of the target region or puncture of neighboring critical structures (e.g., blood vessels, nerves). Early experience with IRE was also associated with incidence of cardiac dysrhythmia, so pulse delivery is now synchronized to the R-wave on electrocardiogram (ECG) recording with a 0.05 s delay to avoid interference with normal cardiac rhythm.[104] IRE is still contraindicated in patients with cardiac arrhythmia, as pulses cannot be con-

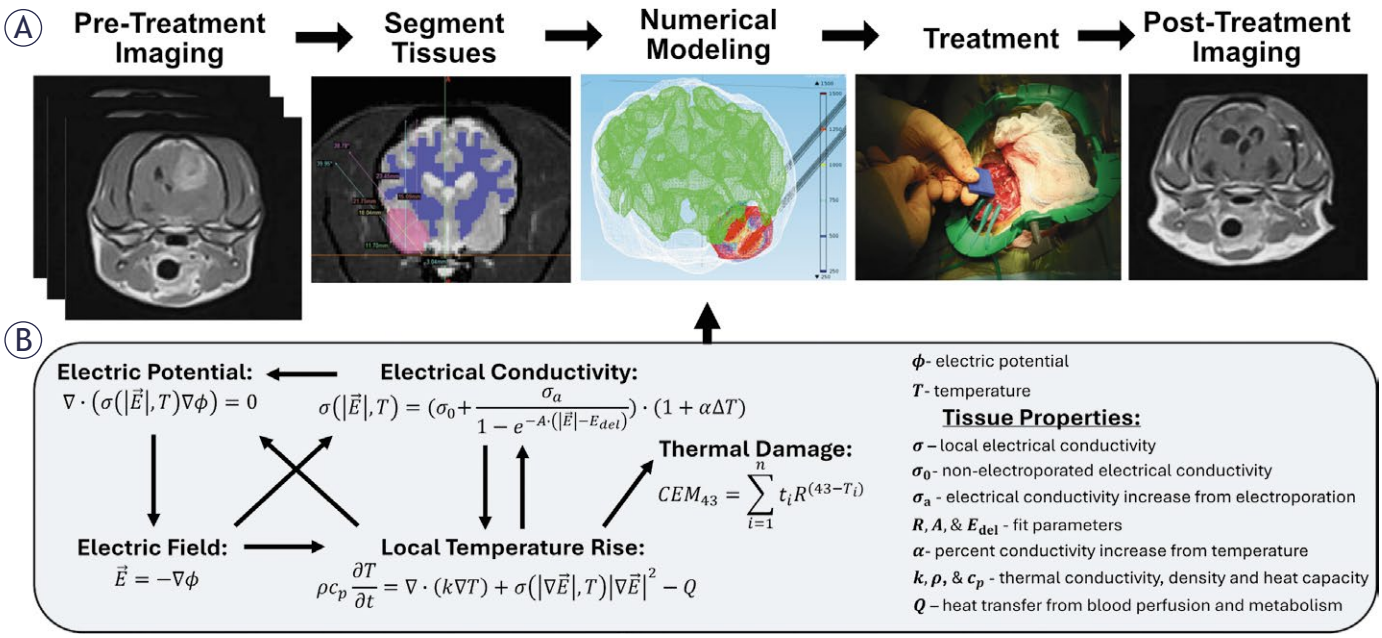

FIGURE 5. Pulsed field ablation treatment planning pipeline. **(A)** Images of the region of interest are taken through CT, MRI, US, or other modalities. Typically, segmentation is performed to define individual tissue regions before computational modeling, as the dynamic electric field, temperature, and conductivity distributions are tissue dependent. Numerical modeling is performed with the intent to maximize targeted tissue coverage with a critical electric field while minimizing deleterious effects on nearby structures. Following, the protocol is implemented for the treatment of the target tissue. While computational modeling can inform treatments, the exact application of PFA can often differ from *a priori* computational modeling. Post-treatment imaging is frequently used to assess acute and long-term ablation success. **(B)** Tissue electroporation modeling is multifaceted and requires knowledge about multiple electroporation-dependent and electroporation-independent tissue properties. The local electric potential depends on the local electrical conductivity and temperature. The electrical conductivity also depends on the local temperature and the electric field, as pore formation due to the local electric field allows for current to flow through cells. Subsequently, temperature generation depends on the electric field magnitude and the local conductivity. Images in panel A were adapted from various sources for instructional purposes.[100,235]

sistently synchronized with the cardiac refractory period.

To overcome these limitations, Arena *et al.* developed High-Frequency IRE (H-FIRE)[105], which utilizes a series of short (0.5–10 μs) biphasic pulses. The H-FIRE waveform is constructed of a positive pulse, interphase delay (d1), negative pulse, and interpulse delay (d2), repeated for several cycles to achieve an on-time comparable to IRE (Figure 4B). H-FIRE significantly reduces muscle contraction during treatment and obviates the use of neuromuscular blockers or cardiac synchronization.[106] Further, the shorter pulses are suggested to provide more predictable ablations when the pulse width is below the cell membrane charging time of 1–2 μs.[107-108] However, as a consequence of the reduced membrane charging, the EF threshold (EFT) required to induce electroporation increases as pulse width decreases, but thermal heating remains relatively the same.[109-110] H-FIRE has been used pre-clinically to treat breast[111], liver[106], brain[112], lung[113], and prostate[114] cancer with mixed results. To date, H-FIRE has not demonstrated the same tumor ablation capability as IRE, but H-FIRE has been evaluated clinically in prostate cancer, offering a potential reduction in experienced complications.[115,116] Notwithstanding, H-FIRE has gained prodigious attention for the treatment of cardiac arrhythmias under the name PFA.[117-129] Between the different groups, H-FIRE (i.e., PFA) is indicated to have been performed in over 100,000 patients as of September 2024, not without appropriate criticism of the lack of transparency for treatment details.

Since PFA primarily induces cell death through permeabilization of the cell membranes, the PEFs minimally affect proteinaceous structures. The nonthermal mechanism is paramount for the control of diseased tissue near critical structures, such as bowels[97], ducts[130], mature blood vessels[131,132], esophagus[133], and nerves[56,134,135], where surgical resection and thermal ablation methods are contraindicated. Further, PFA is not influenced by the "heat sink" effect, where blood flow in adjacent vessels dissipates heat, reducing ablation effectiveness and potentially sparing targeted tissue. This allows PFA to completely treat tissue abutting blood vessels. Narayan *et al.* examined the patency of 158 vessels with a mean distance from the treatment lesions of 2.3 mm and noted abnormal changes in 4.4% (7/158) of vessels.[132] Only 1.4% (2/158) were hemodynamically significant, with many vessels that experienced thrombosis post-treatment already heavily involved before treatment. Tumors abutted 40 vessels and encased 10 vessels, but 96% (48/50) maintained patency despite being directly within the ablation. Further, Li *et al.* found that neurovascular bundles are not destroyed even when directly treated with ablative PEFs.[134] Subsequent studies have observed that there may be some degree of thermal damage to the tissue immediately near the treatment electrodes[136-137], so careful planning and probe placement are still needed.

Pretreatment planning

Computational modeling is necessary for the successful delivery of PFA[138], as the entire target tissue must be covered by a critical EF while minimizing collateral damage to nearby critical structures.[139] Treatment planning includes (Figure 5):

1. Imaging of the treatment area and surrounding structures

Before surgery, the location, size, and geometry of the tissue to be treated are determined with one or more imaging modalities, including contrast-enhanced computed tomography (Ce-CT), positron emission tomography (PET), magnetic resonance imaging (MRI), and 3D-mapping biopsy for prostate cancer (PCa). Except for PCa, Ce-CT is the most used modality due to its availability, high resolution, and ability to rapidly create multi-planar reconstructions of the tumor and surrounding structures.[140] For cancer patients, tumor growth or shifting may cause differences between prior- and intra-procedural images, so Ce-CT also allows for rapid adjustments in the treatment planning and probe position.[140-142]

2. 3D reconstruction of the anatomy of the treatment area

Multi-planar images are imported into a segmentation software (e.g., 3DSlicer) to separate the tumor, parenchyma, and nearby structures. The geometries are then meshed for importing into finite element analysis software (e.g., COMSOL™).

3. Define the electroporation-dependent material properties for the different tissues

A priori information about the target tissue is needed for accurate treatment modeling. Both the EF

and temperature distributions strongly depend on the tissue-specific electrical properties[143,144], which both differ between patients in healthy and malignant tissues and change non-linearly from the electroporation process itself.[145] Results in computational modeling significantly differ when considering electroporation effects[146,147], but validated tissue properties are sparse within the literature.

Conventional methods for tissue characterization use *ex vivo* tissue slices with fixed geometries to translate impedance at different applied EF magnitudes to conductivity.[146,148] Quantifications are often limited to healthy animal tissues due to their availability and can misrepresent the targeted tissue, especially when translating results to tumors. Tissue characterization using patient-derived xenografts is more representative[149], but they can take weeks to grow, are not widely available during treatment planning, and do not replicate *in situ* conditions. Further, even within a specific tumor type, there can be a high degree of tumor tissue heterogeneity between patients and even between tumors at different locations in the body. Translating experimentally found properties to an individual can be unreliable, so improved methods for patient-specific tissue characterizations are greatly needed.[147]

In addition to simulating the EF and thermal distributions, it is necessary to know the EFT of the tissues being treated to quantify the lesion coverage. Values for the lethal EFT are variable within the literature due to the lack of validated and standardized protocols. Thresholds gathered *in vitro* using cuvette systems are typically higher than those gathered using 2D or 3D platforms, but *in-situ* data is the most translatable.[150] Pulse widths from nanoseconds to milliseconds will generate ablations, but pulse width negatively correlates with EFTs.[109,110,151,152]

4. Incorporation of treatment probes within the model and numerical optimization

Intrinsic tissue properties cannot often be changed; thus, treatment parameters (i.e., voltage, probe geometry, and PFA waveform) must be adjusted to find solutions that solve the desired objective. The two main objectives that are usually investigated for PFA are (1) encompassing the target tissue with a lethal EF while (2) minimizing Joule heating and subsequent thermal damage to nearby critical structures.

The number of probes depends on the ability to cover the tumor and margin with a lethal EF. For deep soft tissue neoplasms, typically 2 to 6 monopolar probes are inserted into or around the neoplasm. For lesions smaller than 2 cm, 3 probes are placed at the periphery of the tumor in a triangle; for lesions between 2–3 cm, 4 probes are placed at the periphery in a square; for lesions larger than 3 cm, 4–6 probes are used, with 1–2 of the probes placed within the lesion and the rest at the periphery.[153] The distance between electrode pairs should not exceed 2.2 cm, but values have ranged from 0.7 to 2.9 cm in literature. The electrode exposure can vary from 0.5 to 3 cm, but 1.5 cm is the most common. The applied current scales linearly with electrode exposure, and too large of an exposure can trigger the overcurrent on electroporation generators at 50 A. Therefore, if the target is larger than the possible electrode exposure, the deepest portion of the target should be treated first; then, the electrodes can be "pulled back" for subsequent treatments to ensure overlapping and cohesive ablations.

Applied EFs or "voltage-to-distance ratios" (VDRs) typically range from 1200 V/cm to 2000 V/cm for IRE and 2000 V/cm to 3000 V/cm for H-FIRE. Higher VDRs will generate larger ablations at the consequence of increased Joule heating, neuromuscular excitation, and electrochemical effects.

Probe positioning and treatment

IRE has been successfully performed through intraoperatively[154], laparoscopy[155], and percutaneous[156] insertion of treatment probes. For percutaneous insertion, the probes must be carefully inserted under contrast-enhanced ultrasound (ce-US) or ce-CT guidance to prevent puncturing sensitive structures and maintain parallel insertion of the electrodes. Imaging is used to verify correct probe placement and measure the center-to-center probe separation to calculate the VDR. Probes should be placed parallel to each other with no more than 10-degree deviations to prevent irregular ablations and possible incomplete treatment.

Despite the EF coverage ultimately dictating ablation size, clinicians have found that electrical currents between 20 and 40 A during IRE provide sufficient ablations. With the NanoKnife system, 10 pulses are initially delivered to assess the applied current between each electrode pair. Following, if the current is adequate, the rest of the treatment will be delivered. Otherwise, the clinicians will increase or decrease the VDR to achieve the desired current and then deliver the appropriate number

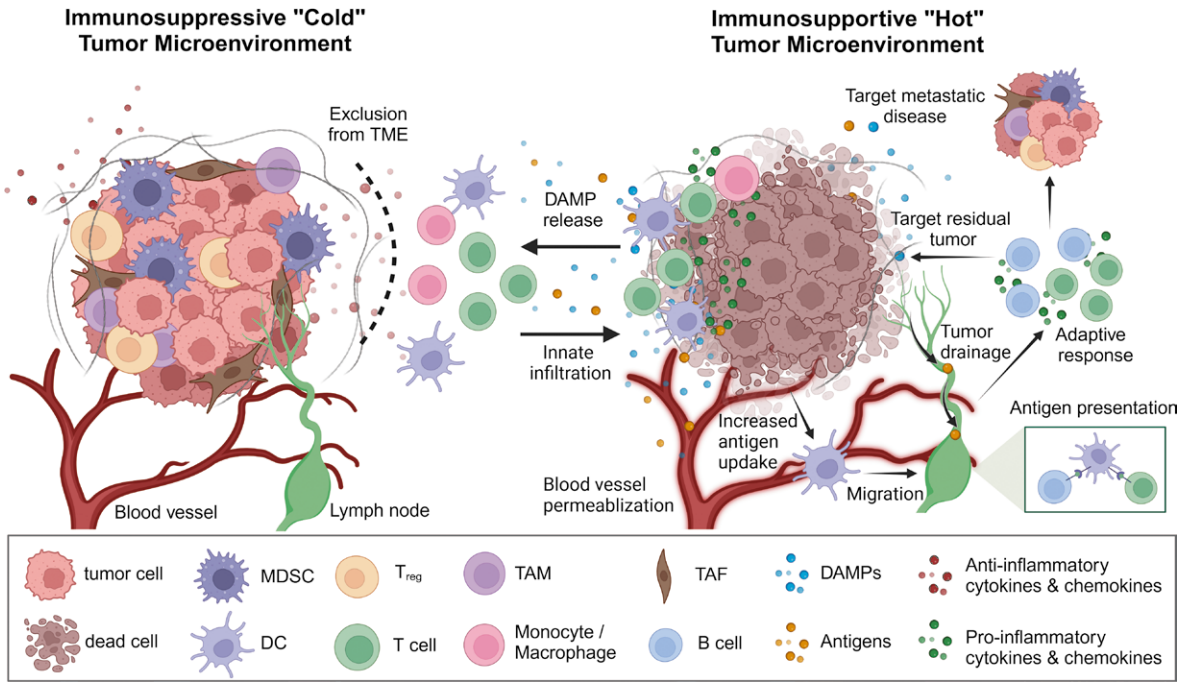

FIGURE 6. Immune response following pulsed field ablation. The tumor microenvironment (TME) evolved through all stages of cancer progression and protects itself through reprogramming immune cells (T regulatory cells [T-reg], myeloid-derived suppressor cells [MDSCs], and tumor-associated macrophages [TAMs]), attracting stromal cells (endothelial cells and fibroblasts) that help deposit a dense extracellular matrix (ECM). This produces an immunosuppressive "cold" tumor that excludes normal immune cells from infiltrating. Pulsed-field ablation indiscriminately kills tumor cells, stromal cells, and immunosuppressive immune cells within the ablation and restructures the ECM. The removal of active immunosuppression, permeabilization of mature blood vessels, and release of Damage Associated Molecular patterns (DAMPs) by IRE entices innate immune cell infiltration. Tumor antigens are released by treated cells, which are either taken up by dendritic cells or drained directly into lymph nodes for antigen presentation. Tumor-specific T- and B-cells mature within the lymph nodes, then antigen-specific T- and B-cells leave the lymph node to potentially remove residual cancer or target distant metastatic disease.

of pulses. An applied potential is only generated between one electrode pair at a time, and the final train of pulses is typically either 70 or 90 pulses between each probe pair.

In addition to cardiac arrhythmia, other absolute contraindications for PFA include the presence of non-removable pacemakers or implantable cardioverter defibrillators, a history of epilepsy or seizures, a history of bleeding disorders, and the presence of anatomical obstacles blocking safe probe insertion.

Post treatment imaging

CT imaging is predominantly used after the procedure to determine treatment success and to evaluate disease recurrence or remission during follow-ups[157], but ablations are also regularly visualized using PET[140], MRI[157], and US.[137] Further, both IRE and H-FIRE produce ablations with sharper delineation than other ablation modalities.[158] Histology of ablations demonstrates demarcation between the ablated and live tissue on the order of 1–2 cells.

Cell death and immune activation

Given the complex and nuanced processes involved, the cell death mechanisms following IRE and H-FIRE are still under investigation. Researchers originally attributed necrosis due to

disruption of the osmotic balance as the killing mechanism of electroporation. However, in the late 1990s, it was demonstrated that electroporation not only caused necrosis but also induced delayed cell death following chromosomal DNA fragmentation, which is an explicit indication of late apoptosis.[159,160]

There is a plethora of competing findings for cell death pathways and mechanisms following PFA, including immunogenic (e.g., necrosis, necroptosis, and pyroptosis) and non-immunogenic (e.g., apoptosis) cell death.[136,159-163] Each pathway has unique implications for treatment side effects, immune activation, and efficacy.[164] Increasing evidence suggests that H-FIRE induces delayed, regulated cell death while IRE induces immediate, lytic cell death.[163,165,166] Further, it is suggested that higher EFs are more likely to induce necrosis through membrane hemorrhaging and thermal damage, while lower EFs may permit membrane recovery but induce regulated cell death following ROS generation, DNA damage, mitochondrial damage, ATP loss, osmotic imbalance, or calcium influx.[29,136,165,166] While apoptosis is frequently highlighted as a key form of cell death in PFA, immediate cell death observed following IRE and H-FIRE often shows characteristics of necrosis. Thus, rather than a single pathway, it is likely a combination of overlapping death mechanisms that lead to the loss of cellular homeostasis.

I. PFA reduces the anti-inflammatory cell populations within the tumor microenvironment

In many solid tumors, multiple cell populations contribute to the immunosuppressive "cold" TME (Figure 6), including differentiated cancer cells, cancer stem cells, tumor-associated fibroblasts (TAFs), and immunosuppressive immune cells (ISICs) (e.g., tumor-associated macrophages [TAMs], myeloid-derived suppressor cells [MDSCs], and regulatory T-cells [T_{reg}]).[167] Further, the epigenetic and cellular composition of tumors can vary between patients, between different tumors within a patient, and even at different locations within the same tumors[168], making it challenging to provide single-target therapeutics. PFA acts indiscriminately on proliferating and non-proliferating cells[169] within the critical EFT. Therefore, recalcitrant (e.g., cancer stem cells[170,171]) and immunosuppressive cells (TAMs, MDSCs, TAFs, and T_{regs}[111,172,173]) are removed in addition to bulk tumor cytoreduction.

II. PFA effectively reverses the stroma-induced immunosuppression

PFA ablation alters the physical properties of the TME through reduction of the extracellular matrix density and rigidity[174,175] and increases tumor-associated blood vessel permeability.[47,48,137,175,176] These both reduce tumor-associated hypoxia that impedes leukocyte function.[175] Increases in microvascular density are indicated after treatment[174,175], but this may be attributed to transient decreases in vascular junction integrity and subsequent increases in the expression of junction proteins to regain microvasculature function. The preservation of mature vasculature patency while increasing permeability allows for infiltration of leukocytes and transport of TAAs to tumor-draining lymph nodes[238]. These results are not replicated in other focal ablation therapies, indicating that IRE may uniquely modulate the TME. Regeneration of the ablation site by parenchymal cells is also indicated at 1–2 weeks post ablations[177], but underlying tissue disease or chemoembolization may prevent the healing process.[95]

III. PFA induces a pro-inflammatory TME and activates the adaptive immune system

In addition to reducing anti-inflammatory cell populations, PFA actively promotes an immune-supportive TME. Damage associated molecular patterns (DAMPs) are released by electroporated cells and recognized by the innate immune system for generating early inflammation.[111,175] Tumor-associated antigens (TAAs) are also released and evaginated by dendritic cells and macrophages for antigen presentation.[178] Unlike with thermal ablation modalities, DAMPs and TAAs released by electroporated cells are presumably not destroyed due to the lack of sufficient thermal heat to denature proteins, potentially allowing for the priming of mature T-cells with receptors directed at the *in-situ* protein motif.[179]

Although PFA treatment success is not predicated by the induction of an anti-tumor immune response, both *in vivo* and clinical data suggest a correlation between immune activation and progression-free survival (PFS) and overall survival (OS). He *et al.* demonstrated the disparity in patient OS when gating by immune activation; when separating patients into high and low T-lymphocyte responses, there was 70–80% and 0% survival at 30 months post-IRE, respectively.[74] Goboers *et al.*

found that T-cell activation correlated with pre-treatment tumor sizes and suggested that antigen release may correlate with the extent of ablation.[173] Larger ablation volumes would presumably induce more TAA and DAMP release while generating a larger variety of cell death mechanisms to create a robust immune response. They also found a decrease in circulating dendritic cell populations indicative of activation-induced migration to lymph nodes and treated tissue, which was supported by the activated T-cells expressing specific receptors against prostate cancer-associated antigens.

IV. PFA can be combined with immunotherapies

To consistently generate persistent peripheral anti-tumor immune activation, current research aims to adjust pulsing waveforms to generate more inflammatory cell death modalities or combine treatment with adjuvant immunotherapies. The combination of IRE and immune checkpoint inhibitors (ICIs), such as anti-CTLA4, anti-PDL1, and anti-PD1, have positive results in both mice and humans.[172,175,178,180] He *et al*. presented promising results when combining IRE with anti-PD1 in Stage III locally advanced pancreatic cancer, achieving an overall survival of 44.3 months versus 23.4 months for IRE alone.[180] Further, they did not observe differences in adverse side effects between the two treatment groups, demonstrating that ICIs may offer a significant increase in IRE efficacy without additional side effects. Primary tumor ablation with IRE in a PCa mouse model, followed by anti-CTLA4 and anti-PD1 immune checkpoint inhibitors, induced a significant increase in both tissue-resident and circulating memory cytotoxic T-cells with T-cell receptors targeting PCa-specific antigen, SPAS-1.[178] Subsequently, this work indicated that a tumor vaccine effect was achieved by the tissue-resident and circulating memory cytotoxic $CD8^+$ T-cells, limiting the reintroduction of new PCa. A recent direct comparison of IRE with cryoablation (CA) and thermal ablation further demonstrated that anti-PD1 synergizes best with IRE, leading to longer tumor-free survival, increased infiltration of CD8+ T-cells, and protection against tumor reintroduction.[181] Due to the modulation of the immunosuppressive TME, the efficacy of dendritic cell vaccination is improved after IRE.[182]

Despite promising results, local and distant tumor recurrence still occurs. A potential reason for the eventual tumor recurrence is that major histocompatibility complex I (MHC I) downregulation occurs 30–100% in many cancer types, with pancreatic cancer having a suppression rate of 40–100%.[183,184] IRE clearly benefits from an induced immune response, but without antigen presentation for T-cell recognition, the local and metastatic micro-tumors are hidden from the heightened immune response and eventually repopulate local and distant sites. Lin *et al.* demonstrated the potential for combining IRE with autologous γδ T-cells, which can recognize and lyse cancers in an MHC-unrestricted manner. Patient γδ T-cells were isolated from the blood, expanded, and then reintroduced after IRE through at least 2 cycles.[185] Patients with multiple infusions survived longer after treatment (17 months) than patients with a single infusion (13.5 months) or IRE alone (11 months). Further, IRE has been combined with natural killer (NK) cells[186-189], which recognize cells that have downregulated MHC I receptors.[190] Despite only evaluating the efficacy at 1-mo post-treatment, a randomized study of 92 LAPC patients found that the IRE-NK group achieved an overall response of 71.7% compared to IRE alone with 56.5%.[188]

Prostate (PCa)

PCa is a leading cause of cancer-related deaths among men[191], and the contemporary treatment for localized PCa is active surveillance, radical prostatectomy, and radiation therapy. Routine prostate examinations are becoming increasingly popular, resulting in earlier detection of manageable small-volume neoplasms. While whole-gland approaches have historically offered the best possible oncological outcome for local disease, low- to intermediate-risk patients may not benefit from radical treatments, as damage to the neurovascular bundle, external sphincter, bladder neck, urethra, and rectum are often associated with gastrourinary dysfunction which could include impotence, incontinence, pain, loss of rectal control, and loss of sensation. IRE offers a valuable treatment option for these patients, as the negative side effects can be circumvented while still achieving sufficient oncological outcomes. Further, IRE can be successfully delivered to any region of the gland (apex, middle, or base) with similar disease control[192], while other focal ablation therapies are known to be preferential for certain areas.[193,194]

The first evaluation of IRE in the prostate was performed by Onik *et al.* in 2007 in six healthy canine prostates.[61] Histology revealed a fine demarcation between the unaffected and necrotic

prostate tissue, spanning only a few cells. When directly including the urethra within the ablation, necrotic glandular tissue abutted urethral structures without necrosis within the sub-mucosa. Vessel patency was also preserved when deliberately treating the neurovascular bundle, though variable endothelial and fibrinoid necrosis was observed. The authors expressed that nerves within the neurovascular bundles did not appear to be affected, with no evidence of ganglion cell death. Following, Onik *et al.* performed the first human clinical trial for IRE, involving 16 patients with low- to moderate-risk prostate cancer in a series of outpatient procedures.[62] All patients were continent immediately after IRE, and all patients who were potent before the procedure were still potent after the procedure. Two patients who had bilateral areas treated required 6 months for a full return of potency. Color Doppler US showed intact flow within the neurovascular bundle immediately after the procedure, and postoperative biopsies taken from the area of previously known cancer in 15 patients showed no evidence of cancer.

A disadvantage of focal ablation therapies is the possible presence of multi-focal disease that is not initially diagnosed through imaging or biopsy. As PCa is frequently multi-focal, IRE application to multiple segments or the entire prostate gland can extend its coverage. A multi-center randomized clinical trial evaluated the control of focal and extended IRE in 106 low- to intermediate- risk patients.[56] A similar total rate of recurrence was observed, but the extended ablation cohort experienced lower recurrence away from the lesion site. Guenter *et al.* also presented encouraging results from a large retrospective assessment of 429 patients with low (n = 25), intermediate (n = 88), and high-risk (n = 312) prostate cancer.[195] Patients were treated focally (n = 123), sub-whole-gland (n = 154), whole gland (n = 134), or for recurrent disease after previous treatment with other modalities (n = 63). During a maximum follow-up time of 72 months, 3 (12%), 18 (20.4%), and 26 (8.3%) recurrent cancers were observed in the low-, intermediate-, and high-risk groups, respectively. Urinary continence was preserved in all patients. Ten patients developed a temporary decrease in erectile function, with 4 patients experiencing a decrease longer than a year. Scheltema *et al.* recently released their longer-term (60 months) oncologic and functional evaluation following IRE as a primary treatment in 229 patients (International Society of Urologic Pathologists [ISUP] grade 1–4).[196] The long-term follow-up confirmed earlier findings that IRE provides acceptable local and distant oncological control with lower loss of continence and potency than radical treatments.

Radiotherapy is a well-established therapy for PCa; however, one in five patients recur with significant disease, forming a difficult-to-treat patient sub-population. Recently, IRE has been evaluated in patients with recurrent PCa, specifically following prostatectomy and radiotherapy.[197-199] Mid-term oncological and safety results demonstrate that IRE can be delivered safely to ISUP 1–5 recurrent patients, with similar in-field oncologic responses to *in situ* treatment.[197]

Dong *et al.* were the first to demonstrate the feasibility of tumor ablation using H-FIRE in humans.[115] They treated 40 PCa patients using a 5 μs pulse width without ECG synchronization and with moderately lower muscle relaxants than conventional treatments. No muscle contractions or abnormalities were observed during H-FIRE delivery, with all patients able to move ~10 hours after treatment. Lesions were clearly visible on MRI at 4 weeks post-treatment. At a median follow-up of 6 months, no major complications were experienced, with sexual function and urinary continence preserved in all patients. A recent multi-center non-randomized prospective clinical study treated 109 patients with low (n = 27) and intermediate (n = 82) risk PCa using an unspecified H-FIRE waveform.[116] One hundred patients underwent a 6-month biopsy, with clinically significant prostate cancer in the treatment zone and out of the treatment zones for 1 and 5 patients, respectively. Urinary continence was maintained in 99.1% of patients, and emergent sexual dysfunction was experienced in 9% of patients.

Pancreas (PC)

Pancreatic cancer is currently the 3rd deadliest malignancy and possesses an insidious prognosis due to its surreptitious progression, with over 80% of patients unfortunately presenting stage III locally advanced pancreatic cancer (LAPC) or metastatic disease at diagnosis. Poor outcomes for LAPC are attributed to diffuse cancer infiltration, the sclerotic and immunosuppressive tumor microenvironment, and significant involvement of sensitive structures. This precludes surgical resection in > 80% of patients. The intervention of unresectable PC consists of chemoradiation, which has not meaningfully increased survival, with a median overall survival of 9.3–11.8 months after

diagnosis.[200,201] IRE provides perhaps one of the largest benefits to patients with LAPC, and numerous clinical evaluations are published yearly, demonstrating its safety and efficacy. Further, multiple studies have evaluated IRE to treat margins after pancreatectomy in borderline resectable pancreatic cancers (BRPCs), termed margin accentuation (MA), when negative margins are not expected.

Martin *et al.* and Narayanan *et al.* published the first clinical series on the treatment of PC using IRE.[156,202] Martin *et al.* treated 27 patients with IRE either *in situ* (n = 19) or for MA following surgical resection (n = 8). They achieved 100% ablation of the primary tumor evaluated at the 90-day follow-up. Nine patients experienced 18 complications, with most being potentially associated with the open surgery approach and 4 being possible device-related complications. In parallel, Narayanan *et al.* treated 11 patients with LAPC and 3 with metastatic disease using a percutaneous approach. Ten of the 11 LAPC patients were still alive at 14 months post-treatment, but the 3 metastatic patients did not benefit from IRE with a median overall survival of 4 months. Contrast-enhanced CT immediately and 24 hours after treatment showed that vascular patency was preserved in all patients. Martin *et al.* subsequently treated 200 Stage III LAPC patients treated with either *in situ* (n = 150) or for MA following surgical resection (n = 50).[203] All patients had initially undergone induction chemotherapy, and 52% were additionally given chemoradiation therapy for a median of 6 months before IRE. At a median follow-up of 29 months, 58 patients developed recurrences (6 local recurrences) with a median progression-free survival of 12.4 months. MA had a higher median overall survival than IRE alone (28.3 *vs.* 23.2 months). Twenty patients (40%) experienced 49 complications in the MA group, and 54 patients (36%) experienced 100 complications in the *in situ* group, with the most common complications being gastrointestinal complaints. Ten severe complications were experienced after treatment. The same group published their results on another prospective multi-institutional assessment with 152 additional patients treated.[67] *In situ* IRE was successfully delivered to all patients with tumors ranging from 1 to 5.4 cm in diameter with a median follow-up of 19 months. There were 9 local recurrences and 27 distant recurrences, resulting in a median progression-free survival of 22.8 months and a median overall survival of 30.7 months. Nineteen patients experienced severe adverse events, with the most common complications being gastrointestinal or hepatic related. In both studies, the liver was the most common site of distant recurrence.

Many clinical studies have evaluated IRE following inductive chemotherapy. A randomized trial demonstrated the additive effect of IRE with or without chemotherapy.[204] Specifically, combinatorial treatment patients had higher OS (20.3 *vs.* 16.2 months). Similarly, the PANFIRE-2 trial found IRE following induction chemotherapy provided a benefit to OS (17 *vs.* 12.4 months).[140] A recent prospective randomized clinical trial compared the safety and efficacy of IRE (n = 34) to MRI-guided stereotactic ablative body radiotherapy (SABR, n = 34) following induction FOLFIRINOX.[205] There were no differences in OS (12.5 *vs.* 16.1 months), PFS (9.5 *vs.* 8.5 months), or number of complications. Distant tumor-free survival was higher following IRE (13.2 *vs.* 8.5 months), but this could be due to a higher percentage of patients receiving adjuvant therapy following IRE. He *et al.* analyzed the SEER and SYUCC databases to compare the efficacy and long-term safety of IRE (n = 206) following induction chemotherapy against chemotherapy alone (n = 3444)[206] and found that IRE following induction chemotherapy had a higher OS (18 *vs.* 8 months) and PFS (7.7 *vs.* 4.1 months). Recently, Suraju *et al.* compared resection (n = 40), MA (n = 13), *in situ* IRE (n = 14), and unresected (n = 35) in BRPC and LPAC patients who received neoadjuvant chemotherapy.[236] Despite having a higher number of patients with LAPC in the MA group, they experienced a non-significantly higher OS and PFS compared to resectable patients; the median OS from diagnoses were 30 months for MA, 28 months for *in situ* IRE, 27 months for resection, and 14 months for the unresected group. Neoadjuvant chemoradiation, IRE, and resection were independently associated with decreased risk of mortality, and IRE with an open approach had fewer severe complications than pancreatectomy.

Liver

Liver cancer is the fifth most fatal malignancy globally, with hepatocellular carcinoma (HCC) comprising over 80% of primary liver tumors.[207] Additionally, the liver is a frequent site of metastasis, especially from colorectal cancer; at least 25% of colorectal cancer patients develop liver metastases (CRLM), accounting for a substantial proportion of secondary liver tumors.[208] Standard treatment approaches for HCC and CRLM, including chemoradiation and surgical resection, are often

limited, and up to 80% of patients are deemed ineligible for resection due to tumor burden, anatomical location, or proximity to critical structures. Following hepatectomy, critical structures like the single remaining portal vein, central bile duct, and one or two major hepatic veins limit further resection, as removal or damage to these could compromise liver function. If further resection of these structures is not feasible, then focal ablation offers an effective treatment, but thermal ablation strategies are limited due to the associated "heat sink" effects and potential damage to critical structures.

Thus, IRE has been an increasingly effective method for treating tumors near these structures.[155,209] Ma *et al.* demonstrated that percutaneous IRE is a safe and effective treatment for HCC abutting the diaphragm.[210] They successfully ablated 36/39 tumors with no major complications and achieved a median 20.4 months to local tumor progression. The COLDFIRE-I ablate and resect clinical trial demonstrated the feasibility and safety of IRE to treat CRLM in 10 patients.[211] The subsequent COLDFIRE-II trial further demonstrated the efficacy and safety of IRE in 51 patients with a total of 76 CRLMs.[237] The 1-year local-progression-free (LPF) rate was 68%, and following repeated procedures in 8 patients, local control was achieved in 37/50 (74%) patients. The median overall survival from treatment was 32 months. Fruhling *et al*. further demonstrate that IRE was a safe ablation modality in 149 patients with HCC (n = 53) and CRLM (n = 71) when other treatment options are unsuitable.[212] At 12 months, they achieved local ablation success of 40.3% in HCC patients and 25.4% in CRLM patients. This translated to a median OS of 35 months and 27 months for HCC and CRLM patients, respectively. Three patients experienced severe complications, with one death due to thromboembolism. In a subsequent analysis of the patient population, they found that smaller decreases in resistance and larger tumor sizes were associated with earlier recurrence in CRLM but not HCC patients.[213]

In an evaluation of IRE as a salvage treatment, Hitpass *et al.* demonstrated that IRE is a safe option when resection and thermal ablation are unsuitable.[84] All tumors were located adjacent to the sole remaining intrahepatic blood vessels and bile ducts, but IRE was successfully delivered with a 5 mm margin in 31/32 lesions across 23 patients, with one incomplete ablation. The local progression-free rate was 64% and 57.4%, and the intrahepatic progression-free rate was 36.4% and 19.5% at 12 and 36 months, respectively. Altogether, five patients were tumor-free at the last follow-up. No vessel injury or thrombosis was observed, and only minor complications occurred, including moderate segmental cholestasis, which spontaneously resolved. Recently, Narayanan *et al.* confirmed that IRE is a safe and viable option for the treatment of unresectable CLRMs close to the portal and hepatic veins, inferior vena cava, bile duct, and gallbladder.[214] They achieved a median OS of 40.4 months with only minor complications. In a recent randomized non-inferiority clinical trial, Zhang *et al.* compared IRE (n = 78) to radiofrequency ablation (RFA) (n = 78) for the treatment of malignant liver tumors.[215] They demonstrated that IRE was not inferior to RFA, with comparable tumor ablation rates (94.9% *vs*. 96%), similar complication rates, and similar 6-mo recurrence rates (13.3% *vs*. 19.7%) between IRE and RFA. In a direct comparison of IRE to RFA and MWA in a propensity score-matched population of early HCC, Wada *et al.* found 2-year local tumor progressions of 0%, 45%, and 25% for IRE, RFA, and MWA, respectively.[216]

A majority of HCC develops in patients with underlying pathologies, and the possibility of damaging diseased hepatic parenchyma (e.g. Child-Pugh B/C) has the associated risk of severe liver failure and mortality.[217] Bhutiani *et al.* compared the tolerability and efficacy of IRE and microwave ablation for treating HCC patients with moderate Child-Pugh B liver dysfunction.[218] They found that both modalities had comparable success rates, but IRE was better tolerated with a significantly lower length of stay and 90-day readmission rate.

Kidney

Small renal cell carcinoma (RCC) has traditionally been treated with surgical resection, with radical nephrectomy being the most common treatment. IRE has yet to be fully established for the treatment of renal tumors, but it may be considered when surgical resection or thermal ablation is not an option. Thomson *et al.* treated 7 patients with RCC using IRE.[95] Transient hematuria was observed in two patients with treatments near the center of the kidney, which resolved in under 24 hours. Follow-up CT at 3 months confirmed successful ablations in 71.4% (5/7) of patients, with the other 2 receiving a second IRE procedure. The first large cohort of patients with renal tumors treated with IRE was reported by Trimmer *et al.,* in which 20 patients with T1a renal carcinoma (n = 13), indeterminate

masses (n = 5), or benign masses (n = 2) underwent CT-guided IRE.[86] All ablations were initially technically successful, as verified with ce-CT, but two patients required salvage therapy at 2 weeks due to incomplete ablation. All 15 patients imaged at 6 months had no evidence of recurrence, and only one patient was observed to experience recurrence at 1 year after IRE.

Despite initial data supporting the feasibility and safety of IRE, a few clinical studies have found suboptimal short- and mid-term disease control. Canvasser *et al.* found that the initial treatment was successful in 93% (39/42) of tumors, but the 2-year local-recurrence-free rate was 83%[89], which is unfavorably compared to contemporary local-recurrence-free rates of >97% for partial nephrectomy of tumors < 3.0 cm. Further, the first prospective Phase II clinical trial (IRENE) found "complexities in the overall procedure".[92] All tumors were resected after treatment to assess the lesion. Four patients had no residual tumor, while 3 had microscopic residual tumor due to incomplete ablation. Dai *et al.* found similar results in a retrospective study of 47 patients with 48 tumors, with 45.8% (22/44) being biopsy-proven RCC.[219] At a median follow-up of 50.4 months, their 5-year local recurrence-free rate was 81.4% in biopsy-confirmed RCC patients and 81.0% in all patients.

None of the studies observed major complications, supporting the safe initial use of IRE for RCC. While the safety profile after IRE is compelling, if it is concluded that IRE does not present a significant advantage over conventional therapies, patient selection for IRE could include those with central renal tumors near blood vessels and collecting systems in which the nonthermal mode of ablation can be exploited. Min Wah *et al.* evaluated the safety and efficacy of CT-guided IRE in 26 patients with 30 biopsy-proven RCCs near vital structures of the kidney.[96] Nearby structures included the colon (n = 11), ureter (n = 11), and renovascular pedicles (n = 7). They specified that the initial technical success of 73.3% was due to an early operator's learning curve, and 7/8 of the residual tumors were treated with CA to achieve a technical success rate of 97%. They state that one patient was not retreated due to an unexpected stroke at 4 months post-IRE. The 2- and 3-year recurrence-free survival was 91% for both time points. Six patients experienced minor complications, and 1 patient experienced a major complication (Clavien-Dindo III), as the patient developed post-proximal ureteral stricture that required long-term retrograde ureteric stenting.

Lung

Lung cancer is the deadliest and most prevalent cancer globally, with few curative treatment options. Central tumors near the central bronchial structures and large blood vessels are especially challenging to treat with surgical resection and thermal ablation modalities. IRE can potentially spare critical structures, but current oncological outcomes are lacking.

Thomson *et al.* treated 1 patient with 1 non-small-cell carcinoma and 3 patients with 5 colorectal lung metastases.[95] None of these patients treated with IRE had a satisfactory tumor response, and they all presented with progressive disease when assessed by the 3-mo time point. A biopsy from one of the patients showed coagulative necrosis in a portion of the tumor with viable cancerous tissue at the margin of the treated lesion. All four patients experienced transient ventricular arrhythmia, one patient presented transient supraventricular tachycardia, and one patient required cardioversion as a response to atrial fibrillation. Pneumothorax was observed in two out of the four patients which resolved spontaneously. Usman *et al.* reported on the use of IRE to treat two patients with lung neoplasms that had been previously deemed unresectable.[98] One of the patients presented with an increase of the right suprahilar mass with ce-CT, suggesting tumor growth reported 2 months after the procedure. Moderate parenchymal hemorrhage was observed during the procedure, and at the 9-month follow-up, it was suggested that the tumor had invaded the trachea. The cancer continued to progress, and the patient succumbed to the disease within a year post-IRE. The other patient was reported to still be alive 2.5 years after the procedure, with no major complications described. The authors explain that challenges still remain with using IRE to treat lung tumor masses due to the heterogeneity, geometry, and low density of lung tissue. It is clear that further research is needed to optimize IRE treatment of lung cancer through collaboration between engineers and clinicians. It can be argued that these studies were limited because the probes themselves were not designed for lung treatments, and thus, surgical probes need to be tailored for this particular application.

Kodama *et al.* determined that electroporation applied through an endobronchial catheter is a feasible technique for the treatment of parabronchial tumors in a pig lung tumor model.[220] The ablations measured on gross pathology were signifi-

cantly smaller than the treatment-related changes measured on CT, contrasting observations in other organ systems. Using FEM, they predicted EFs sufficient to induce irreversible electroporation (500–2000 V/cm) within a 1 cm circumference around the probe, which was reflected by extensive ablations seen in gross histology. However, large blood vessels and airways significantly affected the EF distribution, reducing the local EF in portions of the tumor below the lethal EFT. Lastly, they found that electroporation does not affect the patency of the treated bronchi.

Cardiac

Catheter-based PFA is emerging as a promising alternative to thermal techniques (RFA & CA) in treating cardiac arrhythmias due to the better safety profile and similar efficacy.[221,222] The rapid success of PFA in the clinic has led many research groups and companies to develop their own probes and electroporation systems (Figure 8), often keeping technical details and treatment parameters secret. Direct electric currents were first used to treat cardiac arrhythmias in the 1980s; however, the continuous application of the EF caused electrical arcing, barotrauma, and proarrhythmic effects. Lavee *et al.* were the first to utilize IRE for atrial ablation in 5 pigs, which mitigated the previous complications experienced with direct current applications[124] and achieved sharp transmural with no evidence of thermal damage. Subsequently, preclinical and clinical studies have demonstrated that PFA selectively ablates cardiac tissue while minimally affecting peri-atrial tissue, such as the esophagus and phrenic nerve[223], and lowers the risk of pulmonary vein stenosis compared to thermal ablation. Recently, the results from multiple large clinical trials have been released.

The first and most studied PFA catheter is the multi-electrode pentaspline catheter.[122] The Impulse, PEFCAT, PEFCAT2, and PersAFONE trials demonstrated the initial feasibility and safety of this catheter for treating paroxysmal and persistent AF in relatively small cohorts.[224] Recently, the MANIFEST-PF[117] and MANIFEST-17k[225] clinical trials provide compelling safety and efficacy results in larger patient cohorts and across more centers. The MANIFEST-PF trial included 24 centers and 1,758 patients to determine the acute effectiveness and safety of PFA and found that PFA achieved complete acute pulmonary vein isolation in 99.9% of patients on immediate electroanatomical mapping. The 1-year recurrence rates were 31% for the total cohort, 27% for paroxysmal AF, and 42% for persistent AF. The MANIFEST-17k trial evaluated the safety of PFA across at 106 centers across 20 countries in 17,642 patients with paroxysmal (57.8%) and persistent (35.2%) AF. At a median of 15 months follow-up, no esophageal damage, pulmonary vein stenosis, or persistent phrenic nerve palsy were reported. Major complications were reported in 0.98% of patients, with the most common being pericardial tamponade (0.36%), vascular events (0.30%), stroke (0.12%), hemolysis-related acute renal failure (0.03%), and death (0.03%). Two of the deaths (0.01%) were procedure-related from irreversible neurological damage; post-procedural brain MRI was performed in 96 asymptomatic patients to determine the rate of silent cerebral lesions (SCLs), of which 9.4% of patients showed abnormalities. Further, the recent ADVENT trial demonstrated the non-inferiority of PFA using the pentaspline catheter in a randomized, single-blind prospective comparison to conventional thermal ablation (RFA or CA) in 707 paroxysmal AF patients[221,222] evaluating the safety and 1-year recurrence rates of pulsed-field ablation against thermal ablation (RFA or CA). Urbanek *et al.* found similar results in 400 patients and achieved similar 1-year success rates between CA and pentaspline PFA in both paroxysmal AF (83.1% CA *vs.* 80.3% PFA) and persistent AF (71% CA *vs.* 66.8% PFA).[126]

The PULSED AF pivotal trial evaluated the circular-lasso-type 9-electrode catheter in 150 paroxysmal and 150 symptomatic persistent AF patients.[125] They achieved 100% acute pulmonary vein isolation rates for both groups, but at the 90-day follow-up, the recurrence rate was already 30.5% and 37.7% for the paroxysmal and persistent AF groups, respectively. The 1-year recurrence rates did not increase much from the 90-day rates, with 33.8% for the paroxysmal AF and 44.9% for the persistent AF patients. Two severe adverse effects occurred due to treatment (0.7%): one cerebrovascular accident occurred the same day as treatment and one pericardial effusion that required draining.

The SPHERE PER-AF trial is a randomized, 2-arm prospective study evaluating a large-tip catheter dual PFA and RFA ablation system against a control RFA system.[226] They found that PFA had significantly lower energy application times, transpired ablation times, and skin-to-skin procedural times. At a 1-year follow-up, 73.8% and 65.8% of patients were arrhythmia-free for the large-tip

catheter and control system, respectively, with no major complications observed in either group.

The insPIRE and admIRE trials investigated the safety and efficacy of using a variable-loop circular catheter (VLCC).[227,228] The inspIRE trial investigated the safety and efficacy of the VLCC in 226 patients with paroxysmal AF. The 12-month freedom from symptomatic arrhythmia was 79%. Pre- and post-treatment MRI imaging detected SCLs in 4 of the first 6 patients. After adjusting treatment to include a 10-second pause between PFA applications and strictly adhering to the anticoagulation regimen, SCLs were found in 4 of the remaining 33 patients. All the SCLs were asymptomatic and resolved spontaneously. The VLCC can be used for guidance, stimulation/recording of cardiac signals, and applying PFA, so the admIRE trial investigated the use of the VLCC for real-time non-fluoroscopic procedural guidance and lesion indexing in 277 patients with paroxysmal AF. They achieved 97.5% success on first-pass per vein isolation, with 100% of veins ultimately isolated. At 12 months, they found similar efficacy to patients treated without fluoroscopy (75% *vs*. 72.7%), demonstrating that treatments can be delivered without fluoroscopy, which can potentially speed up procedures, minimizing procedure-related complications and exposure to X-rays.

Collectively, these results indicate that H-FIRE is a safe and effective method for pulmonary isolation, but high acute pulmonary isolation rates have not necessarily translated to long-term freedom from disease. Nevertheless, PFA has similar, if not slightly better, efficacy than thermal ablation, but currently, methods are still needed to generate deeper and wider transmural lesions to prevent recurrence.

Multiple preclinical and early clinical evaluations have also demonstrated the feasibility of PFA for the treatment of ventricular arrhythmias (VAs).[229-231] VAs pose a unique challenge due to the thickness of the tissue and frequent scar tissue, making it challenging to develop deep lesions. PFA is indicated to better penetrate through scar tissue[231-233], allowing for treatment of tissue that other focal ablation therapies cannot reach and for redo ablations. Peich *et al.* evaluated focal PFA in 21 patients with ventricular premature complexes and 23 partients with scar-related ventricular tachycardia.[234] Using the highest energy setting (25A), they achieve 81% and 52% success for the premature complex and tachycardia patients, respectively, at a mean follow-up of 116 days.

Concluding remarks

It has almost been 300 years since the earliest recording of electrically mediated tissue damage by Jean-Antoine Nollet in 1754. He observed the formation of red spots, presumably due to IRE, following the application of high voltages to human and animal skin. Only 20 years ago was IRE again described as a viable option for controlled tissue destruction. In such a short period, it has significantly impacted the treatment of soft tumors and cardiac tissue. However, there are still multiple areas of improvement:

(1) Factors influencing electroporation at the cellular and tissue level are still not fully understood, and there is still a large gap in knowledge on the precise mechanisms of cell death following different PFA procedures. PFA is unique compared to every other focal therapy, and understanding genetic and proteomic changes following treatment is paramount for developing synergistic therapies.

(2) Accordingly, the dynamics of tumor microenvironmental changes following PFA have only recently started being investigated.

(3) Electroporation-dependent tissue properties for many tissues and tumors are not available, and there are currently no guidelines on appropriate methods for gathering and validating data. This limits confidence in computational models for predicting ablation outcomes before treatment.

(4) Inserting and maintaining multiple probes is the most technically challenging and time-consuming aspect of IRE treatments. Improved methods for delivering PEFs will presumably help increase the adoption of PFA and decrease operating room times.

(5) While ablations can be measured soon after treatment, there are no clinically ready methods for real-time ablation progression or temperature monitoring. The lack of real-time feedback can lead to unnecessary thermal damage and avoidable complications.

(6) Due to the multifaceted nature of PFA, optimized waveforms for oncology and cardiology have yet to be developed.

Therefore, it is important for industry, clinicians, and researchers to work together to allow for independent analysis and validation of data. If clinicians are aware of the capabilities and limitations of PFA procedures, tissues that were once considered untreatable and unresectable may now find a legitimate contender with IRE.

References

1. Gabriel B, Teissie J. Generation of reactive-oxygen species induced by electropermeabilization of Chinese hamster ovary cells and their consequence on cell viability. *Eur J Biochem* 1994; **223:** 25-33. doi: 10.1111/j.1432-1033.1994.tb18962.x

2. Maccarrone M, Rosato N, Agro AF. Electroporation enhances cell membrane peroxidation and luminescence. *Biochem Biophys Res Commun* 1995; **206:** 238-45. doi: 10.1006/bbrc.1995.1033

3. Maccarrone M, Bladergroen MR, Rosato N, Agro AF. Role of lipid peroxidation in electroporation-induced cell permeability. *Biochem Biophys Res Commun* 1995; **209:** 417-25. doi: 10.1006/bbrc.1995.1519

4. Bonnafous P, Vernhes MC, Teissié J, Gabriel B. The generation of reactive-oxygen species associated with long-lasting pulse-induced electropermeabilisation of mammalian cells is based on a non-destructive alteration of the plasma membrane. *Biochim Biophys Acta Biomembranes* 1999; **1461:** 123-34. doi: 10.1016/S0005-2736(99)00154-6

5. Rems L, Viano M, Kasimova MA, Miklavčič D, Tarek M. The contribution of lipid peroxidation to membrane permeability in electropermeabilization: a molecular dynamics study. *Bioelectrochemistry* 2019; **125:** 46-57. doi: 10.1016/j.bioelechem.2018.07.018

6. Balantič K, Weiss VU, Pittenauer E, Miklavčič D, Kramar P. The role of lipid oxidation on electrical properties of planar lipid bilayers and its importance for understanding electroporation. *Bioelectrochemistry* 2023; **153:** 108498. doi: 10.1016/j.bioelechem.2023.108498

7. Rems L, Kasimova MA, Testa I, Delemotte L. Pulsed electric fields can create pores in the voltage sensors of voltage-gated ion channels. *Biophys J* 2020; **119:** 190-205. doi: 10.1016/j.bpj.2020.05.030

8. Geboers B, Scheffer HJ, Graybill PM, Ruarus AH, Nieuwenhuizen S, Puijk RS, et al. High-voltage electrical pulses in oncology: Irreversible electroporation, electrochemotherapy, gene electrotransfer, electrofusion, and electroimmunotherapy. *Radiology* 2020; **295:** 254-72. doi: 10.1148/RADIOL.2020192190

9. Neumann E, Rosenheck K. Permeability changes induced by electric impulses in vesicular membranes. *J Membr Biol* 1972; **10:** 279-90. doi: 10.1007/BF01867861

10. DeBruin KA, Krassowska W. Modeling electroporation in a single cell. I. Effects of field strength and rest potential. *Biophys J* 1999; **77:** 1213-24. doi: 10.1016/S0006-3495(99)76973-0

11. Lee RC, Gaylor DC, Bhatt D, Israel DA. Role of cell membrane rupture in the pathogenesis of electrical trauma. *J Surg Res* 1988; **44:** 709-19. doi: 10.1016/0022-4804(88)90105-9

12. Jacobs IV EJ, Graybill PM, Jana A, Agashe A, Nain AS, Davalos R V. Engineering high post-electroporation viabilities and transfection efficiencies for elongated cells on suspended nanofiber networks. *Bioelectrochemistry* 2023; **152:** 108415. doi: 10.1016/j.bioelechem.2023.108415

13. Böckmann RA, De Groot BL, Kakorin S, Neumann E, Grubmü H. Kinetics, statistics, and energetics of lipid membrane electroporation studied by molecular dynamics simulations. *Biophys J* 2008; **95:** 1837-50. doi: 10.1529/biophysj.108.129437

14. Neumann E, Kakorin S. Membrane electroporation: chemical thermodynamics and flux kinetics revisited and refined. *Eur Biophys J* 2018; **47:** 373-87. doi: 10.1007/S00249-018-1305-3

15. Saulis G. Pore disappearance in a cell after electroporation: theoretical simulation and comparison with experiments. *Biophy J* 1997; **73:** 1299-309. doi: 10.1016/S0006-3495(97)78163-3

16. Ottlakan A, Lazar G, Olah J, Nagy A, Vass G, Vaset M, et al. Current updates in bleomycin-based electrochemotherapy for deep-seated soft-tissue tumors. *Electrochem* 2023; **4:** 282-90. doi: 10.3390/electrochem4020019

17. Mir LM, Orlowski S, Belehradek J, Paoletti C. Electrochemotherapy potentiation of antitumour effect of bleomycin by local electric pulses. *Eur J Cancer Clin Oncol* 1991; **27:** 68-72. doi: 10.1016/0277-5379(91)90064-K

18. Spiliotis AE, Holländer S, Rudzitis-Auth J, Wagenpfeil G, Eisele R, Nika S, et al. Evaluation of electrochemotherapy with bleomycin in the treatment of colorectal hepatic metastases in a rat model. *Cancers* 2023; **15:** 1598. doi: 10.3390/cancers15051598

19. Pakhomova ON, Gregory B, Semenov I, Pakhomov AG. Calcium-mediated pore expansion and cell death following nanoelectroporation. *Biochim Biophys Acta Biomembr* 2014; **1838:** 2547-54. doi: 10.1016/j.bbamem.2014.06.015

20. Szewczyk A, Gehl J, Daczewska M, Saczko J, Krog Frandsen S, Kulbacka J. Calcium electroporation for treatment of sarcoma in preclinical studies. *Oncotarget* 2018; **9:** 11604-18. doi: 10.18632/oncotarget.24352

21. Falk H, Matthiessen LW, Wooler G, Gehl J. Calcium electroporation for treatment of cutaneous metastases; a randomized double-blinded phase II study, comparing the effect of calcium electroporation with electrochemotherapy. *Acta Oncol* 2018; **57:** 311-9. doi: 10.1080/0284186X.2017.1355109

22. Frandsen SK, Gissel H, Hojman P, Tramm T, Eriksen J, Gehl J. Direct therapeutic applications of calcium electroporation to effectively induce tumor necrosis. *Cancer Res* 2012; **72:** 1336-41. doi: 10.1158/0008-5472.CAN-11-3782

23. Plaschke CC, Gehl J, Johannesen HH, Fisher BM, Kjaer A, Lomholt AF, et al. Calcium electroporation for recurrent head and neck cancer: a clinical phase I study. *Laryngoscope Investig Otolaryngol* 2019; **4:** 49-56. doi:10.1002/lio2.233

24. Kraemer MM, Tsimpaki T, Berchner-Pfannschmidt U, Bechrakis NE, Seitz B, Fiorentzis M. Calcium electroporation reduces viability and proliferation capacity of four uveal melanoma cell lines in 2D and 3D cultures. *Cancers* 2022; **14:** 2889. doi:10.3390/cancers14122889

25. Frandsen SK, Gibot L, Madi M, Gehl J, Rols MP. Calcium electroporation: Evidence for differential effects in normal and malignant cell lines, evaluated in a 3D spheroid model. *PLoS One* 2015; **10:** e0144028. doi: 10.1371/journal.pone.0144028

26. Neumann E, Schaefer-Ridder M, Wang Y, Hofschneider PH. Gene transfer into mouse lyoma cells by electroporation in high electric fields. *EMBO J* 1982; **1:** 841-5. doi: 10.1002/j.1460-2075.1982.tb01257.x

27. Rosazza C, Haberl Meglic S, Zumbusch A, Rols MP, Miklavcic D. Gene electrotransfer: a mechanistic perspective. *Curr Gene Ther* 2016; **16:** 98-129. doi: 10.2174/1566523216666160331130040

28. Alex A, Piano V, Polley S, Stuiver M, Voss S, Ciossani G, et al. Electroporated recombinant proteins as tools for in vivo functional complementation, imaging and chemical biology. *Elife* 2019; **8:** e48287. doi: 10.7554/eLife.48287.001

29. Batista Napotnik T, Polajžer T, Miklavčič D. Cell death due to electroporation – a review. *Bioelectrochemistry* 2021; **141:** 107871. doi: 10.1016/J.BIOELECHEM.2021.107871

30. Saulis G, Saule R. Size of the pores created by an electric pulse: microsecond vs millisecond pulses. *Biochim Biophys Acta* 2012; **1818:** 3032-9. doi: 10.1016/j.bbamem.2012.06.018

31. Runas KA, Malmstadt N. Low levels of lipid oxidation radically increase the passive permeability of lipid bilayers. *Soft Matter* 2015; **11:** 499-505. doi: 10.1039/c4sm01478b

32. Ayala A, Muñoz MF, Argüelles S. Lipid peroxidation: production, metabolism, and signaling mechanisms of malondialdehyde and 4-hydroxy-2-nonenal. *Oxid Med Cell Longev* 2014; **2014:** 360438. doi: 10.1155/2014/360438

33. Vernier PT, Levine ZA, Wu YH, Joubert V, Ziegler MJ, Mir LM, et al. Electroporating fields target oxidatively damaged areas in the cell membrane. *PLoS One* 2009; **4:** e7966. doi: 10.1371/journal.pone.0007966

34. Leguèbe M, Silve A, Mir LM, Poignard C. Conducting and permeable states of cell membrane submitted to high voltage pulses: mathematical and numerical studies validated by the experiments. *J Theor Biol* 2014; **360:** 83-94. doi: 10.1016/j.jtbi.2014.06.027

35. Graybill PM, Davalos R V. Cytoskeletal disruption after electroporation and its significance to pulsed electric field therapies. *Cancers* 2020; **12:** 1132. doi: 10.3390/cancers12051132

36. Steuer A, Schmidt A, Labohá P, Babica P, Kolb JF. Transient suppression of gap junctional intercellular communication after exposure to 100-nanosecond pulsed electric fields. *Bioelectrochemistry* 2016; **112:** 33-46. doi: 10.1016/j.bioelechem.2016.07.003

37. Steuer A, Wende K, Babica P, Kolb JF. Elasticity and tumorigenic characteristics of cells in a monolayer after nanosecond pulsed electric field exposure. *Eur Biophys J* 2017; **46:** 567-80. doi: 10.1007/s00249-017-1205-y

38. Thompson GL, Roth C, Tolstykh G, Kuipers M, Ibey BL. Disruption of the actin cortex contributes to susceptibility of mammalian cells to nanosecond pulsed electric fields. *Bioelectromagnetics* 2014; **35:** 262-72. doi: 10.1002/bem.21845

39. Graybill PM, Jana A, Kapania RK, Nain AS, Davalos R V. Single cell forces after electroporation. *ACS Nano* 2021; **15:** 2554-68. doi: 10.1021/acsnano.0c07020

40. Thompson GL, Roth CC, Dalzell DR, Kuipers MA, Ibey BL. Calcium influx affects intracellular transport and membrane repair following nanosecond pulsed electric field exposure. *J Biomed Opt* 2014; **19:** 055005. doi: 10.1117/1.jbo.19.5.055005

41. Kanthou C, Kranjc S, Sersa G, Tozer G, Zupanic A, Cemazar M. The endothelial cytoskeleton as a target of electroporation-based therapies. *Mol Cancer Ther* 2006; **5:** 3145-52. doi: 10.1158/1535-7163.MCT-06-0410

42. Harkin DG, Hay ED. Effects of electroporation on the tubulin cytoskeleton and directed migration of corneal fibroblasts cultured within collagen matrices. *Cell Motil Cytoskeleton* 1996; **35:** 345-57. doi: 10.1002/(SICI)1097-0169(1996)35:4<345::AID-CM6>3.0.CO;2-5

43. Thompson GL, Roth CC, Kuipers MA, Tolstykh GP, Beier HT, Ibey BL. Permeabilization of the nuclear envelope following nanosecond pulsed electric field exposure. *Biochem Biophys Res Commun* 2016; **470:** 35-40. doi: 10.1016/j.bbrc.2015.12.092

44. Fletcher DA, Mullins RD. Cell mechanics and the cytoskeleton. *Nature* 2010; **463:** 485-92. doi: 10.1038/nature08908

45. Rols MP, Teissié J. Experimental evidence for the involvement of the cytoskeleton in mammalian cell electropermeabilization. *Biochim Biophys Acta* 1992; **1111:** 45-50. doi: 10.1016/0005-2736(92)90272-N

46. Partridge BR, Kani Y, Lorenzo MF, Campelo SN, Allen IC, Hinckley J, et al. High-frequency irreversible electroporation (H-FIRE) induced blood–brain barrier disruption is mediated by cytoskeletal remodeling and changes in tight junction protein regulation. *Biomedicines* 2022; **10:** 1384. doi: 10.3390/biomedicines10061384

47. Arena CB, Garcia PA, Sano MB, et al. Focal blood-brain-barrier disruption with high-frequency pulsed electric fields. *Technology* 2014; **2:** 206-13. doi: 10.1142/s2339547814500186

48. Garcia PA, Rossmeisl JH, Robertson JL, Olson JD, Johnson AJ, Ellis TL, et al. 7.0-T magnetic resonance imaging characterization of acute blood-brain-barrier disruption achieved with intracranial irreversible electroporation. *PLoS One* 2012; 7: e50482. doi: 10.1371/journal.pone.0050482

49. Stacey M, Fox P, Buescher S, Kolb J. Nanosecond pulsed electric field induced cytoskeleton, nuclear membrane and telomere damage adversely impact cell survival. *Bioelectrochemistry* 2011; **82:** 131-4. doi: 10.1016/j.bioelechem.2011.06.002

50. Xiao D, Tang L, Zeng C, Wang J, Luo X, Yao C, et al. Effect of actin cytoskeleton disruption on electric pulse-induced apoptosis and electroporation in tumour cells. *Cell Biol Int* 2011; **35:** 99-104. doi: 10.1042/cbi20100464

51. Davalos R V, Mir LM, Rubinsky B. Tissue ablation with irreversible electroporation. *Ann Biomed Eng* 2005; **33:** 223-31. doi: 10.1007/s10439-005-8981-8

52. Edd JF, Horowitz L, Davalos R V., Mir LM, Rubinsky B. In vivo results of a new focal tissue ablation technique: Irreversible electroporation. *IEEE Trans Biomed Eng* 2006; **53:** 1409-15. doi: 10.1109/TBME.2006.873745

53. Al-Sakere B, André F, Bernat C, Connault E, Opolon P, Davalos RV, et al. Tumor ablation with irreversible electroporation. *PLoS One* 2007; **2:** e1135. doi: 10.1371/JOURNAL.PONE.0001135

54. Bertacchini C, Margotti PM, Bergamini E, Lodi A, Ronchetti M, Cadossi R. Design of an irreversible electroporation system for clinical use. *Technol Cancer Res Treat* 2007; **6:** 313-20. doi: 10.1177/15330346070060040

55. Gielchinsky I, Lev-Cohain N. Focal irreversible electroporation for localized prostate cancer – oncological and safety outcomes using mpMRI and transperineal biopsy follow-up. *Res Rep Urol* 2023; **15:** 27-35. doi: 10.2147/RRU.S393243

56. Zhang K, Teoh J, Laguna P, Dominguez-Escrig J, Barret E, Ramon-Borja JC, et al. Effect of focal vs extended irreversible electroporation for the ablation of localized low- or intermediate-risk prostate cancer on early oncological control: a randomized clinical trial. *JAMA Surg* 2023; **158:** 343-9. doi: 10.1001/jamasurg.2022.7516

57. Prabhakar P, Avudaiappan AP, Sandman M, Eldefrawy A, Caso J, Narayanan G, et al. Irreversible electroporation as a focal therapy for localized prostate cancer: a systematic review. *Indian J Urol* 2024; **40:** 6-16. doi: 10.4103/iju.iju_370_23

58. van den Bos W, Jurhill RR, de Bruin DM, Savci-Heijink CD, Postema AW, Wagstaff PG, et al. Histopathological outcomes after irreversible electroporation for prostate cancer: results of an ablate and resect study. *J Urol* 2016; **196:** 552-9. doi: 10.1016/j.juro.2016.02.2977

59. Valerio M, Dickinson L, Ali A, Ramachadran N, Donaldson I, Mccartan N, et al. Nanoknife electroporation ablation trial: a prospective development study investigating focal irreversible electroporation for localized prostate cancer. *J Urol* 2017; **197:** 647-54. doi: 10.1016/j.juro.2016.09.091

60. van den Bos W, Scheltema MJ, Siriwardana AR, Kalsbeek AMF, Thompson JE, Ting F, et al. Focal irreversible electroporation as primary treatment for localized prostate cancer. *BJU Int* 2018; **121:** 716-24. doi: 10.1111/bju.13983

61. Onik G, Mikus P, Rubinsky B. Irreversible electroporation: Implications for prostate ablation. *Technol Cancer Res Treat* 2007; **6:** 295-300. doi: 10.1177/153303460700600405

62. Onik G, Rubinsky B. Irreversible electroporation: first patient experience focal therapy of prostate cancer. In: *Irreversible electroporation*. [internet]. 1970: 235-47. [cited 2024 Oct 15]. doi: 10.1007/978-3-642-05420-4_10. Available at: https://www.researchgate.net/publication/225882920

63. Valerio M, Stricker PD, Ahmed HU, Dickinson L, Ponsky L, Shnier R, et al. Initial assessment of safety and clinical feasibility of irreversible electroporation in the focal treatment of prostate cancer. *Prostate Cancer Prostatic Dis* 2014; **17:** 343-7. doi: 10.1038/pcan.2014.33

64. Van den Bos W, De Bruin D, Veelo D, Postema AW1, Muller BG1, Varkarakis IM, et al. Quality of life and safety outcomes following irreversible electroporation treatment for prostate cancer: results from a phase I-II study. *J Cancer Sci Ther* 2015; **7:** 312-21. doi: 10.4172/1948

65. Tian G, Guan J, Chu Y, Zhao Q, Jiang T. Immunomodulatory effect of irreversible electroporation alone and its cooperating with immunotherapy in pancreatic cancer. *Front Oncol* 2021; **11:** 712042. doi: 10.3389/fonc.2021.712042

66. Kwon D, McFarland K, Velanovich V, Martin RCG. Borderline and locally advanced pancreatic adenocarcinoma margin accentuation with intraoperative irreversible electroporation. *Surgery* 2014; **156:** 910-20. doi: 10.1016/j.surg.2014.06.058

67. Holland MM, Bhutiani N, Kruse EJ, Weiss MJ, Christein JD, White RR, et al. A prospective, multi-institution assessment of irreversible electroporation for treatment of locally advanced pancreatic adenocarcinoma: initial outcomes from the AHPBA pancreatic registry. *HPB (Oxford)* 2019; **21:** 1024-31. doi: 10.1016/j.hpb.2018.12.004

68. Belfiore MP, Ronza FM, Romano F, Ianniello GP, De Lucia G, Gallo C, et al. Percutaneous CT-guided irreversible electroporation followed by chemotherapy as a novel neoadjuvant protocol in locally advanced pancreatic cancer: our preliminary experience. *Int J Surg* 2015; **21(Suppl 1):** S34-9. doi: 10.1016/j.ijsu.2015.06.049

69. Spiliopoulos S, Reppas L, Filippiadis D, Delvecchio A, Conticchio M, Memeo R, et al. Irreversible electroporation for the management of pancreatic cancer: current data and future directions. *World J Gastroenterol* 2023; **29:** 223-31. doi: 10.3748/wjg.v29.i2.223

70. Stephens K, Philips PP, Egger ME, Scoggins CR, McMasters KM, Martin RCG. Multi-institutional review of adverse events associated with irreversible electroporation in the treatment of locally advanced pancreatic cancer. *Surgery* 2024; **175:** 704-11. doi: 10.1016/j.surg.2023.08.042

71. Shuiqing H, Sheng L. Is irreversible electroporation (IRE) an effective and safe ablation method for local advanced pancreatic cancer: a meta-analysis. *Health Sciences Review* 2022; **3:** 100029. doi: 10.1016/j.hsr.2022.100029

72. Woeste MR, Wilson KD, Kruse EJ, Weiss MJ, Christein JD, White RR, et al. Optimizing patient selection for irreversible electroporation of locally advanced pancreatic cancer: analyses of survival. *Front Oncol* 2022; **11:** 817220. doi: 10.3389/fonc.2021.817220

73. Pishvaian MJ, Blais EM, Brody JR, Lyons E, DeArbeloa P, Hendifar A, et al. Overall survival in patients with pancreatic cancer receiving matched therapies following molecular profiling: a retrospective analysis of the Know Your Tumor registry trial. *Lancet Oncol* 2020; **21:** 508-18. doi: 10.1016/S1470-2045(20)30074-7

74. He C, Wang J, Sun S, Zhang Y, Li S. Immunomodulatory effect after irreversible electroporation in patients with locally advanced pancreatic cancer. *J Oncol* 2019; **2019:** 9346017. doi: 10.1155/2019/9346017

75. Dai Z, Wang Z, Lei K, Liao J, Peng Z, Lin M, et al. Irreversible electroporation induces CD8+ T cell immune response against post-ablation hepatocellular carcinoma growth. *Cancer Lett*. 2021; **503:** 1-10. doi: 10.1016/j.canlet.2021.01.001

76. Sugimoto K, Kakimi K, Takeuchi H, Fujieda N, Saito K, Sato E, et al. Irreversible electroporation versus radiofrequency ablation: comparison of systemic immune responses in patients with hepatocellular carcinoma. *J Vasc Interv Radiol* 2019; **30:** 845-53.e6. doi: 10.1016/j.jvir.2019.03.002

77. Lu LC, Shao YY, Chan SY, Hsu CH, Cheng AL. Clinical characteristics of advanced hepatocellular carcinoma patients with prolonged survival in the era of anti-angiogenic targeted-therapy. *Anticancer Res* 2014; **34:** 1047-52. doi: 10.1016/j.jvir.2019.03.002

78. Dai Z, Wang Z, Lei K, Liao J, Peng Z, Lin M, et al. Irreversible electroporation induces CD8+ T cell immune response against post-ablation hepatocellular carcinoma growth. *Cancer Lett* 2021; **503:** 1-10. doi: 10.1016/j.canlet.2021.01.001

79. Narayanan G, Koethe Y, Gentile N. Irreversible electroporation of the hepatobiliary system: current utilization and future avenues. *Medicina (Kaunas)* 2024; **60:** 251. doi: 10.3390/medicina60020251

80. Yang Y, Qin Z, Du D, Wu Y, Qiu S, Mu F, et al. Safety and short-term efficacy of irreversible electroporation and allogenic natural killer cell immunotherapy combination in the treatment of patients with unresectable primary liver cancer. *Cardiovasc Intervent Radiol* 2019; **42:** 48-59. doi: 10.1007/s00270-018-2069-y

81. Guo X, Du F, Liu Q, Guo Y, Wang Q, Huang W, et al. Immunological effect of irreversible electroporation on hepatocellular carcinoma. *BMC Cancer* 2021; **21:** 443. doi: 10.1186/s12885-021-08176-x

82. Eller A, Schmid A, Schmidt J, May M, Brand M, Saake M, et al. Local control of perivascular malignant liver lesions using percutaneous irreversible electroporation: initial experiences. *Cardiovasc Intervent Radiol* 2015; **38:** 152-9. doi: 10.1007/s00270-014-0898-x

83. Beyer LP, Pregler B, Michalik K, Niessen C, Dollinger M, Müller M, et al. Evaluation of a robotic system for irreversible electroporation (IRE) of malignant liver tumors: initial results. *Int J Comput Assist Radiol Surg* 2017; **12:** 803-9. doi: 10.1007/s11548-016-1485-1

84. Hitpass L, Distelmaier M, Neumann UP, Schöning W, Isfort P, Keil S, Kuhl CK, et al. Recurrent colorectal liver metastases in the liver remnant after major liver surgery - IRE as a salvage local treatment when resection and thermal ablation are unsuitable. *Cardiovasc Intervent Radiol* 2022; **45:** 182-9. doi: 10.1007/s00270-021-02981-4

85. Buijs M, Zondervan PJ, de Bruin DM, van Lienden KP, Bex A, van Delden OM. Feasibility and safety of irreversible electroporation (IRE) in patients with small renal masses: results of a prospective study. *Urolo Oncol* 2019; **37:** 183.e1-183.e8. doi: 10.1016/j.urolonc.2018.11.008

86. Trimmer CK, Khosla A, Morgan M, Stephenson SL, Ozayar A, Cadeddu JA. Minimally invasive percutaneous treatment of small renal tumors with irreversible electroporation: a single-center experience. *J Vasc Interv Radiol* 2015; **26:** 1465-71. doi: 10.1016/j.jvir.2015.06.028

87. Narayanan G, Doshi MH. Irreversible electroporation (IRE) in renal tumors. *Curr Urol Rep* 2016; **17:** 1-7. doi: 10.1007/s11934-015-0571-1

88. Hilton A, Kourounis G, Georgiades F. Irreversible electroporation in renal tumours: a systematic review of safety and early oncological outcomes. *Urologia* 2022; **89:** 329-37. doi: 10.1177/03915603221077590

89. Canvasser NE, Sorokin I, Lay AH, Morgan MSC, Ozayar A, Trimme C, et al. Irreversible electroporation of small renal masses: suboptimal oncologic efficacy in an early series. *World J Urol* 2017; **35:** 1549-55. doi: 10.1007/s00345-017-2025-5

90. Pech M, Janitzky A, Wendler JJ, Morgan MSC, Ozayar A, Trimmer C, et al. Irreversible electroporation of renal cell carcinoma: a first-in-man phase i clinical study. *Cardiovasc Intervent Radiol* 2011; **34:** 132-8. doi: 10.1007/s00270-010-9964-1

91. Deodhar A, Monette S, Single GW, Hamilton WC Jr, Thornton R, Maybody M, et al. Renal tissue ablation with irreversible electroporation: preliminary results in a porcine model. *Urology* 2011; **77:** 754-60. doi: 10.1016/j.urology.2010.08.036

92. Wendler JJ, Pech M, Fischbach F, Jürgens J, Friebe B, Baumunk D, et al. Initial assessment of the efficacy of irreversible electroporation in the focal treatment of localized renal cell carcinoma with delayed-interval kidney tumor resection (Irreversible Electroporation of Kidney Tumors Before Partial Nephrectomy [IRENE] trial - an ablate-and-resect pilot study). *Urology* 2018; **114:** 224-32. doi: 10.1016/j.urology.2017.12.016

93. Neal RE, Garcia PA, Kavnoudias H, Rosenfeldt F, Mclean CA, Earl V, Bergman J, et al. In vivo irreversible electroporation kidney ablation: experimentally correlated numerical models. *IEEE Trans Biomed Eng* 2015; **62:** 561-9. doi: 10.1109/TBME.2014.2360374

94. Deodhar A, Monette S, Single GW, Hamilton WC Jr, Thornton R, Maybody M, et al. Renal tissue ablation with irreversible electroporation: preliminary results in a porcine model. *Urology* 2011; **77:** 754-60. doi: 10.1016/j.urology.2010.08.036

95. Thomson KR, Cheung W, Ellis SJ, Federman D, Kavnoudias H, Loader-Oliver D, et al. Investigation of the safety of irreversible electroporation in humans. *J Vasc Interv Radiol* 2011; **22:** 611-21. doi: 10.1016/j.jvir.2010.12.014

96. Min Wah T, Lenton J, Smith J, Bassett P, Jagdev S, Ralph C, et al. Irreversible electroporation (IRE) in renal cell carcinoma (RCC): a mid-term clinical experience. *Eur Radiol* 2021; **31:** 7491-9. doi: 10.1007/s00330-021-07846-5

97. Sorokin I, Canvasser N, Johnson B, Lucas E, Cadeddu JA. Irreversible electroporation for renal ablation does not cause significant injury to adjacent ureter or bowel in a porcine model. *J Endourol* 2021; **35:** 873-7. doi: 10.1089/END.2020.0856

98. Usman M, Moore W, Talati R, Watkins K, Bilfinger T V. Irreversible electroporation of lung neoplasm: a case series. *Med Sci Monit* 2012; **18:** CS43-7. doi: 10.12659/MSM.882888

99. Ricke J, Jürgens JHW, Deschamps F, Tselikas L, Uhde K, Kosiek O, et al. Irreversible electroporation (IRE) fails to demonstrate efficacy in a prospective multicenter phase II trial on lung malignancies: The ALICE Trial. *Cardiovasc Intervent Radiol* 2015; **38:** 401-8. doi: 10.1007/s00270-014-1049-0

100. Garcia PA, Kos B, Rossmeisl JH, Pavliha D, Miklavčič D, Davalos R V. Predictive therapeutic planning for irreversible electroporation treatment of spontaneous malignant glioma. *Med Phys* 2017; **44:** 4968-80. doi: 10.1002/mp.12401

101. Narayanan G. Irreversible electroporation. *Semin Intervent Radiol* 2015; **32:** 349-55. doi: 10.1055/s-0035-1564706

102. Cannon R, Ellis S, Hayes D, Narayanan G, Martin RCG. Safety and early efficacy of irreversible electroporation for hepatic tumors in proximity to vital structures. *J Surg Oncol* 2013; **107:** 544-9. doi: 10.1002/jso.23280

103. Aycock KN, Davalos RV. Irreversible electroporation: background, theory, and review of recent developments in clinical oncology. *Bioelectricity* 2019; **1:** 214-34. doi: 10.1089/BIOE.2019.0029

104. Mali B, Jarm T, Jager F, Miklavčič D. An algorithm for synchronization of in vivo electroporation with ECG. *J Med Eng Technol* 2005; **29:** 288-96. doi: 10.1080/03091900512331332591

105. Arena CB, Sano MB, Rossmeisl JH, Caldwell JL, Garcia PA, Rylander MN, et al. High-frequency irreversible electroporation (H-FIRE) for non-thermal ablation without muscle contraction. *Biomed Eng Online* 2011; **10:** 102. doi: 10.1186/1475-925X-10-102

106. Partridge BR, O'Brien TJ, Lorenzo MF, Coutermarsh-Ott SL, Barry SL, Stadler K, et al. High-frequency irreversible electroporation for treatment of primary liver cancer: a proof-of-principle study in canine hepatocellular carcinoma. *J Vasc Interv Radiol* 2020; **31:** 482-91.e4. doi: 10.1016/j.jvir.2019.10.015

107. Bhonsle S, Arena C, Sweeney D, Davalos R. Mitigation of impedance changes due to electroporation therapy using bursts of high-frequency bipolar pulses. *Biomed Eng Online* 2015; **14(Suppl 3):** S3. doi: 10.1186/1475-925X-14-S3-S3

108. Siddiqui IA, Latouche EL, DeWitt MR, Swet JH, Kirks RC, Baker EH, et al. Induction of rapid, reproducible hepatic ablations using next-generation, high frequency irreversible electroporation (H-FIRE) in vivo. *HPB (Oxford)* 2016; **18:** 726-34. doi: 10.1016/j.hpb.2016.06.015

109. Jacobs IV EJ, Campelo SN, Charlton A, Altreuter S, Davalos R V. Characterizing reversible, irreversible, and calcium electroporation to generate a burst-dependent dynamic conductivity curve. *Bioelectrochemistry* 2024; **155:** 108580. doi: 10.1016/j.bioelechem.2023.108580

110. Aycock KN, Vadlamani RA, Jacobs EJ, Imran KM, Verbridge SS, Allen IC, et al. Experimental and numerical investigation of parameters affecting high-frequency irreversible electroporation for prostate cancer ablation. *J Biomech Eng* 2022; **144:** 061003. doi: 10.1115/1.4053595

111. Ringel-Scaia VM, Beitel-White N, Lorenzo MF, Brock RM, Huie KE, Coutermarsh-Ott S, Eden K, et al. High-frequency irreversible electroporation is an effective tumor ablation strategy that induces immunologic cell death and promotes systemic anti-tumor immunity. *EBioMedicine* 2019; **44:** 112-5. doi: 10.1016/j.ebiom.2019.05.036

112. Campelo SN, Lorenzo MF, Partridge B, Alinezhadbalalami N, Kani Y, Garcia J, et al. High-frequency irreversible electroporation improves survival and immune cell infiltration in rodents with malignant gliomas. *Front Oncol* 2023; **13:** 1171278. doi: 10.3389/fonc.2023.1171278

113. Hay AN, Aycock KN, Lorenzo M, David K, Coutermarsh-Ott S, Salameh Z, et al. Investigation of high frequency irreversible electroporation for canine spontaneous primary lung tumor ablation. *Biomedicines* 2024; **12:** 2038. doi: 10.3390/biomedicines12092038

114. Xing R, Ji S, Li X, Gong T, Jiang Q. High-frequency irreversible electroporation ablation for the prostate in Beagle dogs. *Transl Androl Urol* 2024; **13:** 2016-26. doi: 10.21037/tau-24-108

115. Dong S, Wang H, Zhao Y, Sun Y, Yao C. First human trial of high-frequency irreversible electroporation therapy for prostate cancer. *Technol Cancer Res Treat* 2018; **17:** 1-9. doi: 10.1177/1533033818789692

116. Wang H, Xue W, Yan W, Yin L, Dong B, He B, et al. Extended focal ablation of localized prostate cancer with high-frequency irreversible electroporation: a nonrandomized controlled trial. *JAMA Surg* 2022; **157:** 693-700. doi: 10.1001/jamasurg.2022.2230

117. Ekanem E, Reddy VY, Schmidt B, Reichlin T, Neven K, Metzner A, et al. Multi-national survey on the methods, efficacy, and safety on the post-approval clinical use of pulsed field ablation (MANIFEST-PF). *Europace* 2022; **24:** 1256-66. doi: 10.1093/europace/euac050

118. Reddy VY, Neuzil P, Koruth JS, Petru J, Funosako M, Cochet H, et al. Pulsed field ablation for pulmonary vein isolation in atrial fibrillation. *J Am Coll Cardiol* 2019; **74:** 315-26. doi: 10.1016/j.jacc.2019.04.021

119. Reddy VY, Anic A, Koruth J, Petru J, Funasako M, Minami K, et al. Pulsed field ablation in patients with persistent atrial fibrillation. *J Am Coll Cardiol* 2020; **76:** 1068-80. doi: 10.1016/j.jacc.2020.07.007

120. Loh P, Van Es R, Groen MHA, Neven K, Kassenberg W, Wittkampf FHM, et al. Pulmonary vein isolation with single pulse irreversible electroporation: a first in human study in 10 patients with atrial fibrillation. *Circ Arrhythm Electrophysiol* 2020; **13:** E008192. doi: 10.1161/CIRCEP.119.008192

121. Reddy VY, Anter E, Rackauskas G, Peichl P, Koruth JS, Petru J, et al. Lattice-tip focal ablation catheter that toggles between radiofrequency and pulsed field energy to treat atrial fibrillation: a first-in-human trial. *Circ Arrhythm Electrophysiol* 2020; **13:** E008718. doi: 10.1161/CIRCEP.120.008718

122. Reddy VY, Koruth J, Jais P, Petru J, Timko F, Skalsky I, et al. Ablation of atrial fibrillation with pulsed electric fields: an ultra-rapid, tissue-selective modality for cardiac ablation. *JACC Clin Electrophysiol* 2018; **4:** 987-95. doi: 10.1016/j.jacep.2018.04.005

123. Kueffer T, Madaffari A, Muehl A, Maurhofer J, Stefenova A, Seiler J, et al. Pulsed-field- vs. cryo- vs. radiofrequency ablation: one-year recurrence rates after pulmonary vein isolation in patients with paroxysmal atrial fibrillation. *EP Europace* 2023; **25(Suppl 1):** euad122.157. doi: 10.1093/europace/euad122.157

124. Lavee J, Onik G, Mikus P, Rubinsky B. A novel nonthermal energy source for surgical epicardial atrial ablation: Irreversible electroporation. *Heart Surgery Forum* 2007; **10:** 96-101. doi: 10.1532/HSF98.20061202

125. Verma A, Haines DE, Boersma LV, Sood N, Natale A, Marchlinski FE, et al. Pulsed field ablation for the treatment of atrial fibrillation: PULSED AF pivotal trial. *Circulation* 2023; **147:** 1422-32. doi: 10.1161/CIRCULATIONAHA.123.063988

126. Urbanek L, Bordignon S, Schaack D, Chen S, Tohoku S, Efe TH, et al. Pulsed field versus cryoballoon pulmonary vein isolation for atrial fibrillation: efficacy, safety, and long-term follow-up in a 400-patient cohort. *Circ Arrhythm Electrophysiol* 2023; **16:** 389-98. doi: 10.1161/CIRCEP.123.011920

127. Tabaja C, Younis A, Hussein AA, Taigen TL, Nakagawa H, Saliba WI, et al. Catheter-based electroporation: a novel technique for catheter ablation of cardiac arrhythmias. *JACC Clin Electrophysiol* 2023; **9:** 2008-23. doi: 10.1016/j.jacep.2023.03.014

128. Bradley CJ, Haines DE. Pulsed field ablation for pulmonary vein isolation in the treatment of atrial fibrillation. *J Cardiovasc Electrophysiol* 2020; **31:** 2136-47. doi: 10.1111/jce.14414

129. Sugrue A, Maor E, Ivorra A, Vaidya V, Witt C, Kapa S, et al. Irreversible electroporation for the treatment of cardiac arrhythmias. *Expert Rev Cardiovasc Ther* 2018; **16:** 349-60. doi: 10.1080/14779072.2018.1459185

130. Ueshima E, Schattner M, Mendelsohn R, Gerdes H, Monette S, Takaki H, et al. Transmural ablation of the normal porcine common bile duct with catheter-directed irreversible electroporation is feasible and does not impact duct patency. *Gastrointest Endosc* 2018; **87:** 300.e1-6. doi: 10.1016/j.gie.2017.05.004

131. Maor E, Ivorra A, Leor J, Rubinsky B. The effect of irreversible electroporation on blood vessels. *Technol Cancer Res Treat* 2007; **6:** 307-12. doi: 10.1177/153303460700600407

132. Narayanan G, Bhatia S, Echenique A, Suthar R, Barbery K, Yrizarry J. Vessel patency post irreversible electroporation. *Cardiovasc Intervent Radiol* 2014; **37:** 1523-9. doi: 10.1007/s00270-014-0988-9

133. Koruth JS, Kuroki K, Kawamura I, Brose R, Viswanathan R, Buck ED, et al. Pulsed field ablation versus radiofrequency ablation: esophageal injury in a novel porcine model. *Circ Arrhythm Electrophysiol* 2020; **13:** E008303. doi: 10.1161/CIRCEP.119.008303

134. Li W, Fan Q, Ji Z, Qiu X, Li Z. The effects of irreversible electroporation (IRE) on nerves. *PLoS One* 2011; **6:** e18831. doi: 10.1371/journal.pone.0018831

135. Moshkovits Y, Grynberg D, Heller E, Maizels L, Maor E. Differential effect of high-frequency electroporation on myocardium vs. non-myocardial tissues. *Europace* 2023; **25:** 748-55. doi: 10.1093/europace/euac191

136. Faroja M, Ahmed M, Appelbaum L, Ben-David E, Moussa M, Sosna J, et al. Irreversible electroporation ablation: is all the damage nonthermal? *Radiology* 2013; **266:** 462-70. doi: 10.1148/radiol.12120609/-/DC1

137. Appelbaum L, Ben-David E, Sosna J, Nissenbaum Y, Goldberg SN. US findings after irreversible electroporation ablation: radiologic-pathologic correlation. *Radiology* 2012; **262:** 117-25. doi: 10.1148/radiol.11110475

138. Kos B, Voigt P, Miklavcic D, Moche M. Careful treatment planning enables safe ablation of liver tumors adjacent to major blood vessels by percutaneous irreversible electroporation (IRE). *Radiol Oncol* 2015; **49:** 234-41. doi: 10.1515/raon-2015-0031

139. Kranjc M, Kranjc S, Bajd F, Serša G, Serša I, Miklavčič D. Predicting irreversible electroporation-induced tissue damage by means of magnetic resonance electrical impedance tomography. *Sci Rep* 2017; **7:** 10323. doi: 10.1038/s41598-017-10846-5

140. Ruarus AH, Vroomen LGPH, Geboers B, van Veldhuisen E, Puijk RS, Nieuwenhuizen S, et al. Percutaneous irreversible electroporation in locally advanced and recurrent pancreatic cancer (PANFIRE-2): a multicenter, prospective, single-arm, phase II study. *Radiology* 2020; **294:** 212-20. doi: 10.1148/radiol.2019191109

141. Geboers B, Timmer FEF, Ruarus AH, Pouw JEE, Schouten EAC, Bakker J, et al. Irreversible electroporation and nivolumab combined with intratumoral administration of a toll-like receptor ligand, as a means of in vivo vaccination for metastatic pancreatic ductal adenocarcinoma (Panfire-iii). A phase-I study protocol. *Cancers* 2021; **13:** 3902. doi: 10.3390/cancers13153902

142. Geboers B, van der Lei S, Kloppenborg LTE, Boon RM, Timmer FE, Puijk RS, et al. Transcatheter CT arteriography-guided irreversible electroporation of locally advanced pancreatic adenocarcinoma: a pictorial essay. *J Med Imaging Radiat Oncol* 2023; **67:** 428-34. doi: 10.1111/1754-9485.13535

143. Miklavcic D, Semrov DS, Mekid H, Mir LM. A validated model of in vivo electric field distribution in tissues for electrochemotherapy and for DNA electrotransfer for gene therapy. *Biochim Biophys Acta* 2000; **1523:** 73-83. doi: 10.1016/S0304-4165(00)00101-X

144. Ivorra A, Rubinsky B. In vivo electrical impedance measurements during and after electroporation of rat liver. *Bioelectrochemistry* 2007; **70:** 287-95. doi: 10.1016/j.bioelechem.2006.10.005

145. Pavšelj N, Bregar Z, Cukjati D, Batiuskaite D, Mir LM, Miklavčič D. The course of tissue permeabilization studied on a mathematical model of a subcutaneous tumor in small animals. *IEEE Trans Biomed Eng* 2005; **52:** 1373-81. doi: 10.1109/TBME.2005.851524

146. Beitel-White N, Lorenzo MF, Zhao Y, Brock RM, Coutermarsh-Ott S, Allen IC, et al. Multi-tissue analysis on the impact of electroporation on electrical and thermal properties. *IEEE Trans Biomed Eng* 2021; **68:** 771-82. doi: 10.1109/TBME.2020.3013572

147. Jacobs EJ, Aycock KN, Santos PP, Tuohy JL, Davalos R V. Rapid estimation of electroporation-dependent tissue properties in canine lung tumors using a deep neural network. *Biosens Bioelectron* 2024; **244:** 115777. doi: 10.1016/j.bios.2023.115777

148. Beitel-White N, Bhonsle S, Martin RCG, Davalos RV. Electrical characterization of human biological tissue for irreversible electroporation treatments. *Annu Int Conf IEEE Eng Med Biol Soc* 2018; **2018:** 4170-3. doi: 10.1109/EMBC.2018.8513341

149. Brock RM, Beitel-White N, Coutermarsh-Ott S, Grider DJ, Lorenzo MF, Ringel-Scaia VM, et al. Patient derived xenografts expand human primary pancreatic tumor tissue availability for ex vivo irreversible electroporation testing. *Front Oncol* 2020; **10:** 843. doi: 10.3389/fonc.2020.00843

150. Kos B, Mattison L, Ramirez D, Cindrič H, Sigg DC, Iaizzo PA, et al. Determination of lethal electric field threshold for pulsed field ablation in ex vivo perfused porcine and human hearts. *Front Cardiovasc Med* 2023; **10:** 1160231. doi:10.3389/fcvm.2023.1160231

151. Rao X, Chen S, Alfadhl Y, Chen X, Sun L, Yu L, Zhou J, et al. Pulse width and intensity effects of pulsed electric fields on cancerous and normal skin cells. *Sci Rep* 2022; **12:** 18039. doi: 10.1038/s41598-022-22874-x

152. Fesmire CC, Williamson RH, Petrella RA, Kaufman JD, Topasna N, Sano MB. Integrated time nanosecond pulse irreversible electroporation (INSPIRE): assessment of dose, temperature, and voltage on experimental and clinical treatment outcomes. *IEEE Trans Biomed Eng* 2024; **71:** 1511-20. doi:10.1109/TBME.2023.3340718

153. Yun JH, Fang A, Khorshidi F, Habibollahi P, Kutsenko O, Etezadi V, et al. New developments in image-guided percutaneous irreversible electroporation of solid tumors. *Curr Oncol Rep* 2023; **25:** 1213-26. doi: 10.1007/s11912-023-01452-y

154. Martin II R, Mcfarland K, Ellis S, Velanovich V. Irreversible electroporation in locally advanced pancreatic cancer: potential improved overall survival. *Ann Surg Oncol* 2013; **20(Suppl 3):** S443-9. doi: 10.1245/s10434-012-2736-1

155. Cannon R, Ellis S, Hayes D, Narayanan G, Martin RCG. Safety and early efficacy of irreversible electroporation for hepatic tumors in proximity to vital structures. *J Surg Oncol* 2013; **107:** 544-9. doi: 10.1002/jso.23280

156. Narayanan G, Hosein PJ, Arora G, Barbery KJ, Froud T, Livingstone AS, et al. Percutaneous irreversible electroporation for downstaging and control of unresectable pancreatic adenocarcinoma. *J Vasc Interv Radiol* 2012; **23:** 1613-21. doi: 10.1016/j.jvir.2012.09.012

157. Akinwande O, Ahmad SS, Van Meter T, Schulz B, Martin RCG. CT Findings of patients treated with irreversible electroporation for locally advanced pancreatic cancer. *J Oncol* 2015; **2015:** 680319. doi: 10.1155/2015/680319

158. Lee EW, Thai S, Kee ST. Irreversible electroporation: a novel image-guided cancer therapy. *Gut Liver* 2010; **4(Suppl 1):** S99-104. doi: 10.5009/gnl.2010.4.S1.S99

159. Hofmann F, Ohnimus H, Scheller C, Strupp W, Zimmermann U, Jassoy C. Electric field pulses can induce apoptosis. *J Membr Biol* 1999; **169:** 103-9. doi: 10.1007/s002329900522

160. Piñero J, López-Baena M, Ortiz T, Cortés F. Apoptotic and necrotic cell death are both induced by electroporation in HL60 human promyeloid leukaemia cells. *Apoptosis* 1997; **2:** 330-6. doi: 10.1023/A:1026497306006

161. Lee EW, Chen C, Prieto VE, Dry SM, Loh CT, Kee ST. Advanced hepatic ablation technique for creating complete cell death: Irreversible electroporation. *Radiology* 2010; **255:** 426-33. doi: 10.1148/radiol.10090337

162. Lee EW, Loh CT, Kee ST. Imaging guided percutaneous irreversible electroporation: ultrasound and immunohistological correlation. *Technol Cancer Res Treat* 2007; **6:** 287-93. doi: 10.1177/153303460700600404

163. Mercadal B, Beitel-White N, Aycock KN, Castellví Q, Davalos RV, Ivorra A. Dynamics of cell death after conventional IRE and H-FIRE treatments. *Ann Biomed Eng* 2020; **48:** 1451-62. doi: 10.1007/s10439-020-02462-8

164. Brock RM, Beitel-White N, Davalos RV, Allen IC. Starting a fire without flame: the induction of cell death and inflammation in electroporation-based tumor ablation strategies. *Front Oncol* 2020; **10:** 1235. doi: 10.3389/fonc.2020.01235

165. Polajžer T, Miklavčič D. Immunogenic cell death in electroporation-based therapies depends on pulse waveform characteristics. *Vaccines* 2023; **11:** 1036. doi: 10.3390/vaccines11061036

166. Peng W, Polajžer T, Yao C, Miklavčič D. Dynamics of cell death due to electroporation using different pulse parameters as revealed by different viability assays. *Ann Biomed Eng* 2024; **52:** 22-35. doi: 10.1007/s10439-023-03309-8

167. de Visser KE, Joyce JA. The evolving tumor microenvironment: from cancer initiation to metastatic outgrowth. *Cancer Cell* 2023; **41:** 374-403. doi: 10.1016/j.ccell.2023.02.016

168. Liu M, Bertolazzi G, Sridhar S, Mulder K, Syn N, Hoppe MM, et al. Spatially-resolved transcriptomics reveal macrophage heterogeneity and prognostic significance in diffuse large B-cell lymphoma. *Nat Commun* 2024; **15:** 2113. doi: 10.1038/s41467-024-46220-z

169. Ivey JW, Latouche EL, Sano MB, Rossmeisl JH, Davalos R V, Verbridge SS. Targeted cellular ablation based on the morphology of malignant cells. *Sci Rep* 2015; **5:** 17157. doi: 10.1038/srep17157

170. Ivey JW, Wasson EM, Alinezhadbalalami N, Kanitkar A, Debinski W, Sheng Z, et al. Characterization of ablation thresholds for 3D-cultured patient-derived glioma stem cells in response to high-frequency irreversible electroporation. *Research* 2019; **2019:** 8081351. doi: 10.34133/2019/8081315

171. Rolong A, Schmelz EM, Davalos RV. High-frequency irreversible electroporation targets resilient tumor-initiating cells in ovarian cancer. *Integr Biol* 2017; **9:** 979-87. doi: 10.1039/c7ib00116a

172. Ma Y, Xing Y, Li H, Yuan T, Liang B, Li R, et al. Irreversible electroporation combined with chemotherapy and PD-1/PD-L1 blockade enhanced antitumor immunity for locally advanced pancreatic cancer. *Front Immunol* 2023; **14:** 1193040. doi: 10.3389/fimmu.2023.1193040

173. Geboers B, Scheltema MJ, Jung J, Bakker J, Timmer FEF, Cerutti X, et al. Irreversible electroporation of localised prostate cancer downregulates immune suppression and induces systemic anti-tumour T-cell activation – IRE-IMMUNO study. *BJU Int* 2024. doi:10.1111/bju.16496

174. He C, Huang X, Zhang Y, Lin X, Li S. T-cell activation and immune memory enhancement induced by irreversible electroporation in pancreatic cancer. *Clin Transl Med* 2020; **10:** E39. doi: 10.1002/ctm2.39

175. Zhao J, Wen X, Tian L, Xu C, Wen X, Melancon MP, et al. Irreversible electroporation reverses resistance to immune checkpoint blockade in pancreatic cancer. *Nat Commun* 2019; **10:** 899. doi: 10.1038/s41467-019-08782-1

176. Markelc B, Čemažar M, Serša G. Effects of reversible and irreversible electroporation on endothelial cells and tissue blood flow. In: *Handbook of electroporation*. Springer International Publishing; 2017: 607-20. doi: 10.1007/978-3-319-32886-7_70

177. Monleón E, Lucía Ó, Güemes A, López-Alonso B, Arribas D, Sarnago H, et al. Liver tissue remodeling following ablation with irreversible electroporation in a porcine model. *Front Vet Sci* 2022; **9:** 1014648. doi: 10.3389/fvets.2022.1014648

178. Burbach BJ, O'Flanagan SD, Shao Q, Young KM, Slaughter JR, Rollins MR, et al. Irreversible electroporation augments checkpoint immunotherapy in prostate cancer and promotes tumor antigen-specific tissue-resident memory CD8+ T cells. *Nat Commun* 2021; **12:** 3862. doi: 10.1038/s41467-021-24132-6

179. Shao Q, O'Flanagan S, Lam T, Roy P, Pelaez F, Burbach BJ, et al. Engineering T cell response to cancer antigens by choice of focal therapeutic conditions. *Int J Hyperthermia* 2019; **36:** 130-8. doi: 10.1080/02656736.2018.1539253

180. He C, Sun S, Zhang Y, Li S. Irreversible electroporation plus anti-pd-1 antibody versus irreversible electroporation alone for patients with locally advanced pancreatic cancer. *J Inflamm Res* 2021; **14:** 4795-807. doi: 10.2147/JIR.S331023

181. Jiang M, Shao Q, Slaughter J, Bischof J. Irreversible electroporation has more synergistic effect with anti-PD-1 immunotherapy than thermal ablation or cryoablation, in a colorectal cancer model. *Adv Ther* 2024; **7:** 2400068. doi:10.1002/adtp.202400068

182. Yang J, Eresen A, Shangguan J, Ma Q, Yaghmai V, Zhang Z. Irreversible electroporation ablation overcomes tumor-associated immunosuppression to improve the efficacy of DC vaccination in a mice model of pancreatic cancer. *Oncoimmunology* 2021; **10:** 1875638. doi: 10.1080/2162402X.2021.1875638

183. Dhatchinamoorthy K, Colbert JD, Rock KL. Cancer immune evasion through loss of MHC class I antigen presentation. *Front Immunol* 2021; **12:** 636568. doi: 10.3389/fimmu.2021.636568

184. Cornel AM, Mimpen IL, Nierkens S. MHC class I downregulation in cancer: underlying mechanisms and potential targets for cancer immunotherapy. *Cancers* 2020; **12:** 1-33. doi: 10.3390/cancers12071760

185. Lin M, Zhang X, Liang S, Luo H, Alnaggar M, Liu A, et al. Irreversible electroporation plus allogenic Vγ9Vδ2 T cells enhances antitumor effect for locally advanced pancreatic cancer patients. *Signal Transduct Target Ther* 2020; **5:** 215. doi: 10.1038/s41392-020-00260-1

186. Alnaggar M, Lin M, Mesmar A, Liang S, Qaid A, Xu K, et al. Allogenic natural killer cell immunotherapy combined with irreversible electroporation for stage IV hepatocellular carcinoma: Survival outcome. *Cell Physiol Biochem* 2018; **48:** 1882-93. doi: 10.1159/000492509

187. Eresen A, Yang J, Scotti A, Cai K, Yaghmai V, Zhang Z. Combination of natural killer cell-based immunotherapy and irreversible electroporation for the treatment of hepatocellular carcinoma. *Ann Transl Med* 2021; **9:** 1089. doi: 10.21037/atm-21-539

188. Pan Q, Hu C, Fan Y, Wang Y, Li R, Hu X. Efficacy of irreversible electroporation ablation combined with natural killer cells in treating locally advanced pancreatic cancer. *J BUON*. 2020; **25:** 1643-49. PMID: 32862617.

189. Lin M, Liang S, Wang X, Liang Y, Zhang M, Chen J, et al. Short-term clinical efficacy of percutaneous irreversible electroporation combined with allogeneic natural killer cell for treating metastatic pancreatic cancer. *Immunol Lett* 2017; **186:** 20-27. doi: 10.1016/j.imlet.2017.03.018

190. Paul S, Lal G. The molecular mechanism of natural killer cells function and its importance in cancer immunotherapy. *Front Immunol* 2017; **8:** 1124. doi: 10.3389/fimmu.2017.01124

191. Siegel RL, Giaquinto AN, Jemal A. Cancer statistics, 2024. *CA Cancer J Clin* 2024; **74:** 203. doi: 10.3322/caac.21820

192. Blazevski A, Scheltema MJ, Yuen B, Masand N, Nguyen TV, Delprado W, Shnier R, et al. Oncological and quality-of-life outcomes following focal irreversible electroporation as primary treatment for localised prostate cancer: a biopsy-monitored prospective cohort. *Eur Urol Oncol* 2020; **3:** 283-90. doi: 10.1016/j.euo.2019.04.008

193. Sivaraman A, Barret E. Focal Therapy for prostate cancer: an "à la carte" approach. *Eur Urol* 2016; **69:** 973-5. doi: 10.1016/j.eururo.2015.12.015

194. Ganzer R, Arthanareeswaran VKA, Ahmed HU, Cestari A, Rischmann P, Salomon G, et al. Which technology to select for primary focal treatment of prostate cancer? European Section of Urotechnology (ESUT) position statement. *Prostate Cancer Prostatic Dis* 2018; **21:** 175-86. doi: 10.1038/s41391-018-0042-0

195. Guenther E, Klein N, Zapf S, Weil S, Schlosser C, Rubinsky B, et al. Prostate cancer treatment with irreversible electroporation (IRE): safety, efficacy and clinical experience in 471 treatments. *PLoS One* 2019; **14:** e0215093. doi: 10.1371/journal.pone.0215093

196. Scheltema MJ, Geboers B, Blazevski A, Doan P, Katelaris A, Agrawal S, et al. Median 5-year outcomes of primary focal irreversible electroporation for localised prostate cancer. *BJU Int* 2023; **131(Suppl 4):** 6-13. doi: 10.1111/bju.15946

197. Geboers B, Scheltema MJ, Blazevski A, Katelaris A, Doan P, Ali I, et al. Median 4-year outcomes of salvage irreversible electroporation for localized radio-recurrent prostate cancer. *BJU Int* 2023; **131(Suppl 4):** 14-22. doi: 10.1111/bju.15948

198. Scheltema MJ, van den Bos W, Siriwardana AR, Doan P, Katelaris A, Agrawal S, et al. Feasibility and safety of focal irreversible electroporation as salvage treatment for localized radio-recurrent prostate cancer. *BJU Int* 2017; **120:** 51-8. doi: 10.1111/bju.13991

199. Yaxley WJ, Gianduzzo T, Kua B, Oxford R, Yaxley JW. Focal therapy for prostate cancer with irreversible electroporation: oncological and functional results of a single institution study. *Investig Clin Urol* 2022; **63:** 285-93. doi: 10.4111/icu.20210472

200. Park W, Chawla A, O'Reilly EM. Pancreatic cancer: a review. *JAMA* 2021; **326:** 851-62. doi: 10.1001/jama.2021.13027

201. Wang ZQ, Zhang F, Deng T, Zhang L, Feng F, Wang FH, et al. The efficacy and safety of modified FOLFIRINOX as first-line chemotherapy for Chinese patients with metastatic pancreatic cancer. *Cancer Commun* 2019; **39:** 26. doi: 10.1186/s40880-019-0367-7

202. Martin RCG, McFarland K, Ellis S, Velanovich V. Irreversible electroporation therapy in the management of locally advanced pancreatic adenocarcinoma. *J Am Coll Surg* 2012; **215:** 361-9. doi: 10.1016/j.jamcollsurg.2012.05.021

203. Martin RCG, Kwon D, Chalikonda S, Sellers M, Kotz E, Scoggins C, et al. Treatment of 200 locally advanced (Stage III) pancreatic adenocarcinoma patients with irreversible electroporation safety and efficacy. *Anna Surg* 2015; **262:** 486-94. doi: 10.1097/SLA.0000000000001441

204. Liu S, Qin Z, Xu J, Zeng J, Chen J, Niu L, et al. Irreversible electroporation combined with chemotherapy for unresectable pancreatic carcinoma: a prospective cohort study. *Onco Targets Ther* 2019; **12:** 1341-50. doi: 10.2147/OTT.S186721

205. Timmer FEF, Geboers B, Ruarus AH, Vroomen LGPH, Schouten EAC, van der Lei S, et al. MRI-guided stereotactic ablative body radiotherapy versus CT-guided percutaneous irreversible electroporation for locally advanced pancreatic cancer (CROSSFIRE): a single-centre, open-label, randomised phase 2 trial. *Lancet Gastroenterol Hepatol* 2024; **9:** 448-59. doi: 10.1016/S2468-1253(24)00017-7

206. He C, Huang X, Zhang Y, Cai Z, Lin X, Li S. Comparison of survival between irreversible electroporation followed by chemotherapy and chemotherapy alone for locally advanced pancreatic cancer. *Front Oncol* 2020; **10:** 6. doi: 10.3389/fonc.2020.00006

207. Oh JH, Jun DW. The latest global burden of liver cancer: a past and present threat. *Clin Mol Hepatol* 2023; **29:** 355-7. doi: 10.3350/cmh.2023.0070

208. Martin J, Petrillo A, Smyth EC, Shaida N, Khwaja S, Cheow HK, et al. Colorectal liver metastases: current management and future perspectives. *World J Clin Oncol* 2020; **11:** 761-808. doi: 10.5306/wjco.v11.i10.761

209. Niessen C, Thumann S, Beyer L, Pregler B, Kramer J, Lang S, et al. Percutaneous irreversible electroporation: long-term survival analysis of 71 patients with inoperable malignant hepatic tumors. *Sci Rep* 2017; **7:** 43687. doi: 10.1038/srep43687

210. Ma Y, Chen Z, Liang B, Li R, Li J, Li Z, et al. Irreversible electroporation for hepatocellular carcinoma abutting the diaphragm: a prospective single-center study. *J Clin Transl Hepatol* 2022; **10:** 190-6. doi: 10.14218/JCTH.2021.00019

211. Scheffer HJ, Nielsen K, van Tilborg AAJM, Vieveen JM, Bouwman RA, Kazemier G, et al. Ablation of colorectal liver metastases by irreversible electroporation: results of the COLDFIRE-I ablate-and-resect study. *Eur Radiol* 2014; **24:** 2467-75. doi: 10.1007/s00330-014-3259-x

212. Frühling P, Stillström D, Holmquist F, Nilsson A, Freedman J. Irreversible electroporation of hepatocellular carcinoma and colorectal cancer liver metastases: a nationwide multicenter study with short- and long-term follow-up. *EJSO* 2023; **49:** 107046. doi: 10.1016/j.ejso.2023.107046

213. Frühling P, Stillström D, Holmquist F, Nilsson A, Freedman J. Change in tissue resistance after irreversible electroporation in liver tumors as an indicator of treatment success - a multi-center analysis with long term follow-up. *EJSO* 2024; **50:** 108508. doi: 10.1016/j.ejso.2024.108508

214. Narayanan G, Gentile NT, Eyshi J, Schiro BJ, Gandhi RT, Peña CS, et al. Irreversible electroporation in treating colorectal liver metastases in proximity to critical structures. *J Vasc Interv Radiol* 2024; **35:** 1806-13. doi: 10.1016/j.jvir.2024.08.021

215. Zhang X, Zhang X, Ding X, Wang Z, Fan Y, Chen G, et al. Novel irreversible electroporation ablation (Nano-knife) versus radiofrequency ablation for the treatment of solid liver tumors: a comparative, randomized, multicenter clinical study. *Front Oncol* 2022; **12:** 945123. doi: 10.3389/fonc.2022.945123

216. Wada T, Sugimoto K, Sakamaki K, Takahashi H, Kakegawa T, Tomita Y, et al. Comparisons of radiofrequency ablation, microwave ablation, and irreversible electroporation by using propensity score analysis for early stage hepatocellular carcinoma. *Cancers* 2023; **15:** 732. doi: 10.3390/cancers15030732

217. Schlageter M, Terracciano LM, D'Angelo S, Sorrentino P. Histopathology of hepatocellular carcinoma. *World J Gastroenterol* 2014; **20:** 15955-64. doi: 10.3748/wjg.v20.i43.15955

218. Bhutiani N, Philips P, Scoggins CR, McMasters KM, Potts MH, Martin RCG. Evaluation of tolerability and efficacy of irreversible electroporation (IRE) in treatment of Child-Pugh B (7/8) hepatocellular carcinoma (HCC). *HPB* 2016; **18:** 593-9. doi: 10.1016/j.hpb.2016.03.609

219. Dai JC, Morgan TN, Steinberg RL, Johnson BA, Garbens A, Cadeddu JA. Irreversible lectroporation for the treatment of small renal masses: 5-year outcomes. *J Endourol* 2021; **35:** 1586-92. doi: 10.1089/end.2021.0115

220. Kodama H, Vroomen LG, Ueshima E, Reilly J, Brandt W, Paluch LR, et al. Catheter-based endobronchial electroporation is feasible for the focal treatment of peribronchial tumors. *J Thorac Cardiovasc Surg* 2018; **155:** 2150-9.e3. doi: 10.1016/j.jtcvs.2017.11.097

221. Reddy VY, Gerstenfeld EP, Natale A, Whang W, Cuoco FA, Patel C, et al. Pulsed field or conventional thermal ablation for paroxysmal atrial fibrillation. *N Engl J Med* 2023; **389:** 1660-71. doi: 10.1056/nejmoa2307291

222. Reddy VY, Mansour M, Calkins H, d'Avila A, Chinitz L, Woods C, et al. Pulsed field vs conventional thermal ablation for paroxysmal atrial fibrillation: recurrent atrial arrhythmia burden. *J Am Coll Cardiol* 2024; **84:** 61-74. doi: 10.1016/j.jacc.2024.05.001

223. Neven K, Van Es R, Van Driel V, van Wessel H, Fidder H, Vink A, et al. Acute and long-term effects of full-power electroporation ablation directly on the porcine esophagus. *Circ Arrhythm Electrophysiol* 2017; **10:** d e004672. doi: 10.1161/CIRCEP.116.004672

224. Reddy VY, Dukkipati SR, Neuzil P, Anic A, Petru J, Funasako M, et al. Pulsed field ablation of paroxysmal atrial fibrillation: 1-year outcomes of IMPULSE, PEFCAT, and PEFCAT II. *JACC Clin Electrophysiol* 2021; **7:** 614-27. doi: 10.1016/j.jacep.2021.02.014

225. Ekanem E, Neuzil P, Reichlin T, Kautzner J, van der Voort P, Jais P, et al. Safety of pulsed field ablation in more than 17,000 patients with atrial fibrillation in the MANIFEST-17K study. *Nat Med* 2024; **30:** 2020-9. doi: 10.1038/s41591-024-03114-3

226. Anter E, Mansour M, Nair DG, Sharma D, Taigen TL, Neuzil P, et al. Dual-energy lattice-tip ablation system for persistent atrial fibrillation: a randomized trial. *Nat Med* 2024; **30:** 2303-10. doi: 10.1038/s41591-024-03022-6

227. Duytschaever M, De Potter T, Grimaldi M, Anic A, Vijgen J, Neuzil P, et al. Paroxysmal atrial fibrillation ablation using a novel variable-loop biphasic pulsed field ablation catheter integrated with a 3-dimensional mapping system: 1-year outcomes of the multicenter inspIRE study. *Circ Arrhythm Electrophysiol* 2023; **16:** E011780. doi: 10.1161/CIRCEP.122.011780

228. Reddy VY, Calkins H, Mansour M, Wazni O, Di Biase L, Bahu M, et al. Pulsed field ablation to treat paroxysmal atrial fibrillation: safety and effectiveness in the ADMIRE pivotal trial. *Circulation* 2024; **150:** 1174-86. doi: 10.1161/CIRCULATIONAHA.124.070333

229. van Zyl M, Ladas TP, Tri JA, Yasin OZ, Ladejobi AO, Tan NY, et al. Bipolar electroporation across the interventricular septum: electrophysiological, imaging, and histopathological characteristics. *JACC Clin Electrophysiol* 2022; **8:** 1106-18. doi: 10.1016/j.jacep.2022.06.002

230. Koruth JS, Kuroki K, Iwasawa J, Viswanathan R, Brose R, Buck ED, et al. Endocardial ventricular pulsed field ablation: a proof-of-concept preclinical evaluation. *Europace* 2020; **22:** 434-9. doi: 10.1093/europace/euz341

231. Younis A, Buck E, Santangeli P, Tabaja C, Garrott K, Lehn L, et al. Efficacy of pulsed field vs radiofrequency for the reablation of chronic radiofrequency ablation substrate. *JACC Clin Electrophysiol* 2024; **10:** 222-34. doi: 10.1016/j.jacep.2023.09.015

232. Im S Il, Higuchi S, Lee A, Morrow B, Schenider K, Speltz M, et al. Pulsed field ablation of left ventricular myocardium in a swine infarct model. *JACC Clin Electrophysiol* 2022; **8:** 722-31. doi: 10.1016/j.jacep.2022.03.007

233. Sandhu U, Alkukhun L, Kheiri B, Hodovan J, Chiang K, Splanger T, et al. In vivo pulsed-field ablation in healthy vs. chronically infarcted ventricular myocardium: biophysical and histologic characterization. *Europace* 2023; **25:** 1503-9. doi: 10.1093/europace/euac252

234. Peichl P, Bulava A, Wichterle D, Schlosser F, Stojadinović P, Borišincová E, et al. Efficacy and safety of focal pulsed-field ablation for ventricular arrhythmias: two-centre experience. *Europace* 2024; **26:** euae192. doi: 10.1093/europace/euae192

235. Garcia PA, Pancotto T, Rossmeisl JH, Henao-Guerrero N, Gustafson NR, Daniel GB, et al. Non-thermal irreversible electroporation (N-TIRE) and adjuvant fractionated radiotherapeutic multimodal therapy for intracranial malignant glioma in a canine patient. *Technol Cancer Res Treat* 2011; **10:** 73-83. doi: 10.7785/tcrt.2012.500181

236. Suraju MO, Su Y, Chang J, Katwala A, Nayyar A, et al. Impact of irreversible electroporation on survival among patients with borderline resectable/locally advanced pancreatic cancer: A single center experience. Surgical Oncology Insight 2024; 1: 100075. doi: 10.1016/j.soi.2024.100075.

237. Meijerink MR, Ruarus AH, Vroomen LG, Puijk RS, Geboers B, et al. Irreversible electroporation to treat unresectable colorectal liver metastases (COLDFIRE-2): A phase II, two-center, single-arm clinical trial. Radiology 2021; 299: 470 - 480. doi: 10.1148/RADIOL.2021203089.

238. Esparza S, Jacobs E, Hammel J, Michelhaugh SK, Alinezhadbalamani, Nagai-Singer M, et al. Transient Lymphatic Remodeling Follows Sub-Ablative High-Frequency Irreversible Electroporation Therapy in a 4T1 Murine Model. Annals of Biomedical Engineering 2025; 3674. doi.org/10.1007/s10439-024-03674-y.

review

Recurrent respiratory papillomatosis: role of bevacizumab and HPV vaccination. A literature review with case presentations

Silvio Sporeni[1], Francesca Rifaldi[1], Irene Lanzetta[1], Ilaria Imarisio[2], Benedetta Montagna[2], Francesco Serra[1,2], Francesco Agustoni[1,2], Paolo Pedrazzoli[1,2], Marco Benazzo[3,4], Giulia Bertino[3]

[1] Department of Internal Medicine and Medical Therapy, University of Pavia, Pavia, Italy
[2] Department of Oncology, Hospital IRCCS Policlinico San Matteo Foundation, Pavia, Italy
[3] Department of Otolaryngology, Hospital IRCCS Policlinico San Matteo Foundation, Pavia, Italy
[4] Department of Clinical, Surgical, Diagnostic and Pediatric Sciences, University of Pavia, Pavia, Italy

Radiol Oncol 2025; 59(1): 23-30.

Received 3 November 2024
Accepted 26 November 2024

Correspondence to: Silvio Sporeni, M.D., Department of Internal Medicine and Medical Therapy, University of Pavia and Department of Oncology, IRCCS Policlinico San Matteo Foundation, Pavia, Italy. E-mail: silvio.sporeni01@universitadipavia.it and Francesco Agustoni, M.D., Department of Internal Medicine and Medical Therapy, University of Pavia and Department of Oncology, IRCCS Policlinico San Matteo Foundation, Pavia, Italy. E-mail: f.agustoni@smatteo.pv.it

Disclosure: No potential conflicts of interest were disclosed.

Background. Recurrent respiratory papillomatosis (RRP) is a condition caused by human papilloma virus (HPV) infection. Curative treatments aren't identifiable, and conservative surgery is often the best option to preserve respiratory functions. To date monoclonal antibodies are considered to be a treatment choice with both good efficacy and safety profile.

Materials and methods. A web-based search of MEDLINE/PubMed library from 2000 to 2024 of English-language papers was performed to identify articles by using "respiratory or laryngeal papillomatosis" and "HPV respiratory infection, papillomatosis treatment, papillomatosis vaccine immunization, papillomatosis systemic treatment". Furthermore, a manual screening of references from original articles was done to identify additional studies. We selected 34 articles.

Results. Since 2009, the systemic administration of Bevacizumab has been used to treat RRP not responding to surgical treatment. The efficacy of an anti-VEGF monoclonal antibody in RRP lesions can be related to their vascular nature. The major concern is the rebound papilloma growth within the cessation of treatment. An interesting solution could be the concomitant use of immunotherapy to both reduce the burden of residual disease and activate the immune system against the HPV-infected cells.

Conclusions. Bevacizumab has a safe profile with a short-term local eradication of HPV. Further prospective research with long-term follow-up is needed to better define its safety and results against the disease recurrence. Considering the role of the anti-HPV vaccine, both, in the prophylaxis of the infection and in the adjuvant setting, the actual data underline the need for evaluation of its therapeutic efficacy for the management of RRP.

Key words: oral cavity papillomatosis; respiratory recurrent papillomatosis; multimodal treatment; systemic therapy; vaccine immunization

Introduction

Recurrent respiratory papillomatosis (RRP) describes a morbid benign condition caused by the infection of the upper aerodigestive tract operated by human papillomavirus (HPV), a non-encapsulated, double chain icosahedral structured virus composed of 72 capsomeres.

There is currently no curative treatment for RRP. The primary approach consists in surgical excision to debulk the papilloma and ensure an adequate vocal outcome, as much as possible.

HPV

The term "Papillomatosis" collects a heterogeneous group of non-oncological lesions that affect the mucosal tissue of the oral cavity and upper respiratory tract.

The etiopathogenesis of this morbid condition isn't totally understood yet, although some potential risk factors were identified: mostly the same that could potentially lead to the develop of Squamocellular Carcinoma (SCC) and can be classified in non-viral and viral risk factors. Excessive smoking, chronic alcoholism, poor oral hygiene, edentations and mucosal trauma inducted by incorrect prosthetic works are fundamental in producing a persistent inflammation and irritation.[1] Nowadays, especially with the improvement of diagnostic molecular biology techniques, human papillomavirus (HPV) is identified as essential cause of papillomatous lesions.[2]

HPV is a non-enveloped double-stranded circular genome DNA virus classified into Papillomaviridae family, whose 200 different genotypes are known. Up to 90% of the infections are related to genotypes 6 and 11, which are characterized by a weak potential of malignant transformation. The remaining 10% of infections are caused by genotypes 16, 18, 31 and 33, which are associated to a high carcinogenic power and can induce the development of malignancies such as squamous cell carcinoma of the oropharynx, cervix, vagina, uterus, anus and penis.[3,4] The viral infection is globally widespread, nevertheless with a geographical linked incidence variability. It's higher in East African countries, due to the underdeveloped economic system and the inefficacy of the medical system in promoting the vaccination program, while the rate in West Asia is the lowest. The transmission can be sexual or non-sexual and, in 1% of general population, HPV 6 and 11 can be "commensal" of the oral cavity, especially in the larynx.[5] The virus infiltrates the mucosal basal membrane and the profound cell layer, through epithelial discontinuation, where is able to multiply; all the process is mainly driven by genes E6 and E7, key regulators of cell cycle progression.[6]

In order to sustain its proliferation, HPV maintains itself inside the host cell, fusing its genes with the host cell genome: this phenomenon is probably responsible for a persistent viral infection defined as Recurrent Respiratory Papillomatosis (RRP).[7]

Recurrent Respiratory Papillomatosis (RRP)

Is a rare pathological condition that usually primary affects the upper aerodigestive tract.[8] Three peaks of onset are recognized at ages 7, 35, and 64.[9] The juvenile form (JoRRP) is more aggressive, and it's estimated to affect 4.3 per 100000 children, otherwise the adult form (AoRRP) involves 1.8 per 100000.[5,10] It's known a geographical as previously said, even if, interestingly, the incidence of RRP is similar in both developed and developing countries.[11]

Diagnosis

Starting from the larynx, the infection can spread to extra laryngeal structures such as trachea, oropharynx, nasopharynx, nose, oral cavity, and rarely the lung. The involvement of these anatomical structure explains the most frequent symptoms onset: hoarseness, typical of young age, and dysphonia, common in the adults' forms. Dyspnoea, chronic cough, recurrent respiratory infections, pneumonia, acute respiratory distress, dysphagia are usually result of an upper airway involvement.[12]

Clinical pattern is the first thing to consider, then a tissue biopsy must be performed, leaded with flexible fiberoptic laryngoscopy or direct laryngoscopy. While bronchoscopy is considered the most accurate technique for diagnosis of lesions in the central airways.[13]

Histologically, RRP is composed by papillomatous structures made of abnormal squamous epithelium, where keratinization and basal cell hyperplasia are in excess, with exophytic projections overlying supporting fibrovascular cores. Epithelial atypia is usually absent, although these benign lesions can undergo malignant transformation. Pathological changes include atypia, focal necrosis, foci of keratinization and sheets of polygonal tumoral cells.[5]

Radiological diagnostic strategies include x-rays, particularly indicated for RPP with lung involvements; CT scan, that allow to find the presence of focal or diffused airway narrowing on the mucosal surface; MRI, that can detect the presence of lesions in the larynx, tracheobronchial and pulmonary regions. Radiological assessments are nec-

essary to determine the correct staging and, consequently, the correct treatment option.[13,14]

Treatment

Currently, there is no curative treatment for RRP. However, the primary approach is surgical excision. The aim of the surgical strategy is to debulk the papillomatous lesions at the same time preserving the integrity of the underlying anatomical structures and maintain the airway patency. The excision modalities are multiple and surgeon-dependent; the focus is to prevent damage of surrounding tissue. Recurrences are common, and repeated surgery is often necessary to preserve good respiratory and phonatory quality. For these reasons, double-stage procedures or subtotal resections are preferred, reducing the risks of webbing and scarring.[15]

Different surgical techniques have evolved in the management of RRP, moving from cold instruments and microdebriders to different types of lasers, mainly: ablative/cutting lasers or photoangiolytic lasers.[15]

On the other hand, this strategy can increase the risk of local damage and complications such as laryngeal stenosis, reduction of the respiratory space, formation of tracheoesophageal fistulas and increase expression of HPV dormant in nearby cells.[16]

Adjuvant treatment

In about 1 out of 5 patients, the disease cannot be controlled by surgery alone and adjuvant treatments are needed. The adjuvant therapy should be considered if palliative surgery is needed more than 4 times a year, in case of rapid recurrence of papillomatous lesions with the risk of airway obstruction and in case of disease spread to the distal respiratory tree. The main purpose of adjuvant treatments is to remodulate the action of the immune system against the effective agent to inhibit the replication of the virus.

Several adjuvant therapies have been administered, with a little consensus on which treatments are most effective and the timing of their administration. Antiviral agents such as interferon-alpha and cidofovir were commonly considered the first line treatment. The mechanism of action is predominantly inhibition of viral nucleic acid synthesis. But the results were heterogeneous and, in some cases, burdened by considerable side effects including neurological disorders, leukopenia and thrombocytopenia.[15,17]

To date, in locally advanced disease or metastatic forms, other therapeutic options taken into account are antiangiogenic monoclonal antibodies, approved as single agent or in combination with chemotherapy, and targeted therapies. Bevacizumab, a recombinant human monoclonal antibody that acts selectively, binding the circulating vascular endothelial growth factor VEGF-A[18], is one of the agents that have been investigated in these settings.

Interferon

In the 1980s interferon-alpha was one of the first adjuvant treatments adopted for the treatment of RRP and it was used either intralesional or intramuscular. It is a cytokine that binds to specific cell receptors and modifies the immune response with an anti-proliferative and anti-viral effect.[19] Its use was progressively abandoned due to the severe side effects, mainly hepatotoxicity.

Antiviral agents (acyclovir, ribavirin, cidofovir)

The efficacy of Acyclovir and Ribavirin was tested in the 1990s by Bergler *et al.* and in a few case series and seemed to be linked to the presence of viral co-infections (Herpes Syimplex, Cytomegalovirus, or Epstein-Barr virus).[20] These clinical studies were insufficient to conclude a beneficial effect of these drugs.

Cidofovir on the other hand is a cytosine nucleotide analogue and its introduction resulted in a great improvement in the control of the disease. Once converted in its active form, it is incorporated into DNA and exerts its toxicity in the Papilloma and Herpesviridae families. It can be administered intravenously or intralesional. Unfortunately, systemic treatment has been associated with neutropenia and nephrotoxicity.[21] The intralesional off-label use has been adopted for the treatment of genital HPV or RRP, but there are no clear protocols for dose, concentration, and frequency.[22]

Even if many studies have reported significant response rates with almost no side effects in January 2011, a communication provided by the manufacturer of cidofovir addressed very serious side effects concerning its off-label use: reporting nephrotoxicity, neutropenia, oncogenicity and even some fatalities. In 2012 followed a study involving 16 different hospitals in 11 different countries worldwide which submitted 635 RRP patients, of whom 275 were treated with intralesional

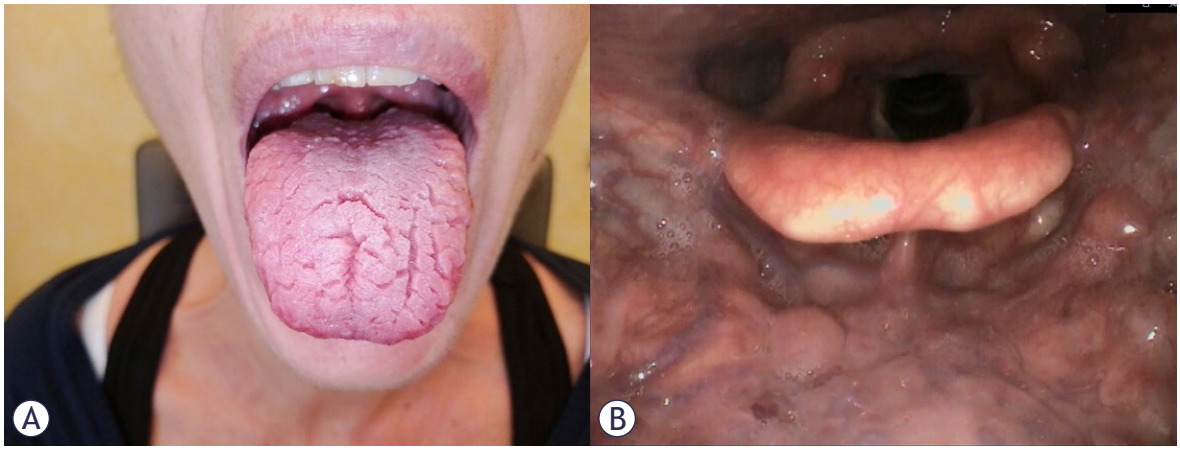

FIGURE 1. Inspection of the oral cavity and fiberoptic images of patient 1, a 44 yar-old woman, after systemic treatment. **(A)** Picture of tongue fissurization and oral cavity of the patient. **(B)** Oropharyngeal overview of the patient, with no sign of papillomatosis

cidofovir, with no clinical evidence for long-term nephrotoxicity, neutropenia, or malignancies.[19] Nevertheless, drug import is now allowed only for authorised clinical trials.

Bevacizumab

Bevacizumab is a recombinant monoclonal humanised antibody that blocks angiogenesis by inhibiting human vascular endothelial growth factor A (VEGF-A) and by preventing the activation of its receptor (VEGF-R).[18] A retrospective study conducted by Rahbar *et al*. demonstrated the role of VEGF-A in the pathogenesis of RRP.[23] The squamous epithelium of papilloma presented a strong expression of VEGF-A mRNA, and VEGFR-1 and VEGFR-2 were strongly expressed in papilloma's blood vessels endothelial cells. From these observations Bevacizumab was considered as a treatment. The predominant effect of Bevacizumab in RRP is modulation of vasculature and not the induction of apoptosis, stronger effects are seen coupling the use of this drug with photoangiolytic lasers.[23]

Bevacizumab can be administered both intravenously and intralesionaly, where the intravenous use is indicated for patients with non-accessible lesions, at the dose of 5-15 mg/kg every 2-3 weeks in adults and 5-10 mg/kg every 2-4 weeks in children.[24,25] Intralesional use instead has an approved dose of 7.5-12.5 mg at 25 mg/ml.[26]

Studies have not yet shown statistically significant differences between the use of intralesional Cidofovir and Bevacizumab, however Bevacizumab shows a higher rate of partial remissions and fewer adverse events.[27]

Other adjuvant treatments

Other compounds have been proposed, such as celecoxib, indole-3-carbinol, anti-reflux drugs, PD-1 inhibitors, and gefitinib. Unfortunately, no clinical trials are yet available to assess the actual efficacy of these adjuvant treatments.[15]

Vaccination

Recent research has shown that the HPV vaccine plays a significant role in not only preventing the transmission of RRP but also in aiding the eradication of the disease in an adjuvant context. Currently, two safe and highly immunogenic vaccines are available that effectively stimulate both humoral and cellular immunity: Gardasil, a quadrivalent vaccine containing recombinant HPV proteins targeting genotypes 6, 11, 16, and 18, which aims to prevent cervical and anal cancers[28], and Gardasil 9, which offers protection against additional HPV genotypes 31, 33, 45, 52, and 58, and is recommended for individuals aged 9 to 45.

Now there are interesting clinical trials ongoing like the INO-3107 (NCT04398433), a DNA immunotherapy designed to elicit targeted T-cell responses against human papillomavirus (HPV) types 6 and 11, in adult patients with recurrent respiratory papillomatosis. Which shows promising results with a tolerable and beneficial effect.[29]

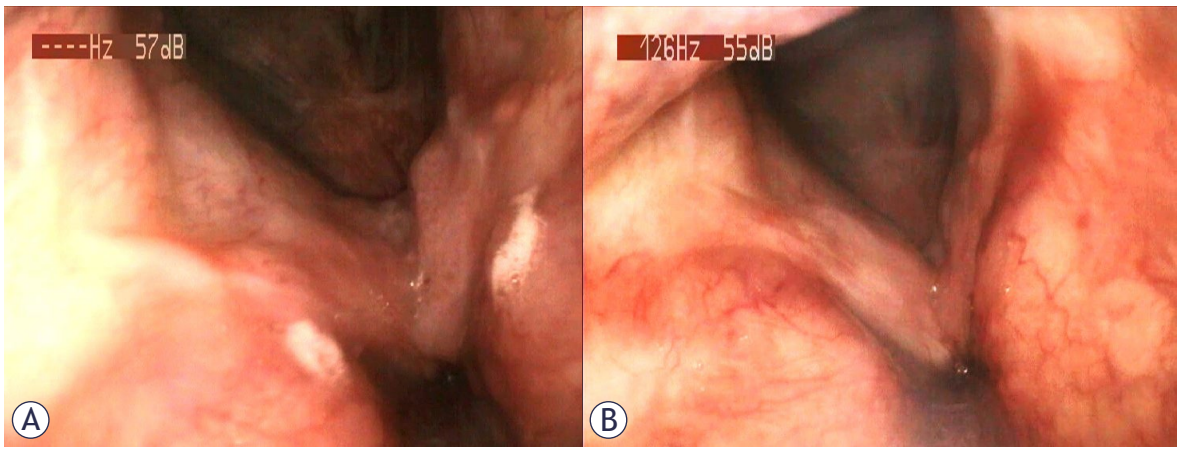

FIGURE 2. Inspection of the oral cavity and fiberoptic images of patient 2, a 58 years-old male, after systemic treatment. **(A)** Oropharyngeal overview at slightly different angles of the patient **(B)**, with no sign of papillomatosis.

Presentation of successful treatment cases

We present two cases of RRP successfully treated with surgery, adjuvant systemic Bevacizumab and HPV vaccination.

Patient 1

A 44-year-old woman, with a previous history of uterus conizations for LSIL (Low grade Squamous Intraepithelial Lesion) / CIN1 (Cervical Intraepithelial Neoplasia) lesions, underwent an ENT evaluation after the onset of widespread papillomatous lesions located on the tip, base and margins of the tongue and on the median raphe of the upper lip.

An excisional biopsy and scraping of the oral cavity were performed. The histological examination of the squamous papillomatous lesions reported the positivity for Human Papillomavirus of genotype 6.

Surgery was evaluated as the best first line treatment option, therefore a bilateral laser vaporization of most of the visible papillomatous lesions on the tip, margins, ventral face, dorsal face and base of the tongue was performed.

Since this surgical treatment resulted in an incomplete removal of the widespread papillomatosis, the case was discussed by our tumor board, and we decided to proceed with systemic adjuvant therapy with Bevacizumab at the dose of 10 mg/kg every three weeks, repeated for six cycles.

At our first oncological evaluation, before the beginning of treatment, the patient was in good clinical conditions, with an ECOG PS equal to 0 and no pathological signs at the physical examination. The inspection of the oral cavity showed papillomatous lesions of the tongue without any symptoms referred.

For each infusion, 470 mg of Bevacizumab were administered. Due to the patient's previous history of serious allergic reactions both after the administration of the anti-SARS-COV2 vaccine and amoxicillin, an appropriate premedication of hydrocortisone 250 mg and chlorphenamine 10 mg was administered at every cycle. Following the first Bevacizumab infusion the patient reported pain in the right cubital fossa and low-grade edema of the ipsilateral hand with symmetrical isosphygmic peripheral pulses. Deep vein thrombosis was suspected; but the venous doppler ultrasound scan of the arms resulted negative. The edema then resolved spontaneously. Furthermore, after the third infusion, an isolated case of proteinuria G1 was detected at urine analysis. The treatment was overall well tolerated with no clinically significant side effects reported.

After the treatment completion, at the first oncological re-evaluation the patient complained of sore throat and foreign body sensation. At the oral cavity examination, diffuse papillomatous lesions in the left edge, lingual base and right labial fornix were observed, although decreased in number and locations; hypertrophy of the right tonsil was also noticed. New biopsies and scraping of the oral cav-

ity were performed. On the right anterior lingual margin and on the left posterior lingual margin, squamous papillomas with diffuse superficial erosion were diagnosed. The Innogenetics tests performed on the scrapings of the oropharynx resulted as negative, both for the identification of HPV DNA and HPV genotypes.

The patient performed a facial MRI, which reported the absence of signal alterations affecting the lingual body or suspicious DWI signal abnormalities; only some immunoreactive lymph nodes at the IIa level of the right neck were highlighted (the largest one of 11 x 7 mm of diameter).

Three months after the completion of treatment with Bevacizumab, the patient underwent the anti-HPV vaccination for therapeutic purposes and two doses of Gardasil 9 were administered without remarkable side effects.

The patient will undergo an annual ENT follow-up.

Patient 2

A 58-year-old male, with no significant pathological anamnesis (GERD, disc herniation), underwent ENT evaluation due to breathing difficulty and hoarseness; turbinates' hypertrophy and vegetative exophytic neoformation on the left epiglottis were diagnosed, so the specialist recommended the turbinates' reduction with radiofrequency and the neoformation's removal. The patient underwent both procedures, and the histological examination came back positive for HPV-related squamous cells laryngeal papillomatosis, p16-, low risk strains (genotyping not executable). Three months later, a new episode of dysphonia occurred; again, ENT evaluation was requested, and the reappearance of papillomatous lesions was diagnosed. The patient then underwent a second exeresis (CO2 laser mediated) of a right arrhythmenoideal neoformation and a left anterior commissural lesion. To histological examination: HPV-related squamous cells papillomatosis; HPV-DNA positive for low-risk strains. Two months later, at ENT follow-up re-evaluation, the patient was diagnosed with a recurrence of the disease (appearance of: four laryngeal papillomatosis lesions, one infrahyoid lesion, one right false vocal cord lesion, one left true vocal cord lesion conditioning phonatory difficulty). He then underwent HPV-vaccination (3 inoculations) and surgical exeresis of the above-mentioned lesions, again with histological positivity for HPV.

Because of the evidence of a new recurrence of disease on the left vocal cord one month later, the patient was candidate to systemic treatment with intravenous Bevacizumab, at the dose of 10 mg/kg q21 for 6 cycles, after which an instrumental restaging with CT scan will be carried out. The treatment was overall well tolerated; drug-induced hypertension (maximum values of 140/90 mmHg) responsive to low dose antihypertensive, and occasional itching well responsive to low doses of antihistamines were observed.

Due to the appearance of leukoplakia e aphthous stomatitis of the oral cavity, the patient underwent local ozone therapy treatment sessions with clinical benefit.

The CT scan performed at the end of the treatment administration reported the complete resolution of the two lesions on the left vocal cord previously described and the total absence of new ones.

The patient will undergo an annual ENT follow-up.

Discussion

In 2009 Nagel *et al.* described a case of pulmonary and tracheal RRP requiring laser-debridement 4 times a year over a 10-year period.[30] The patient had a significant regression of the disease following the first systemic administration of Bevacizumab. In 2017, after many years of clinical experimentation with a nationwide survey, Best *et al.* concluded that systemic Bevacizumab at a dose of 5–10 mg/kg every 2–4 weeks showed significant positive outcome in patients with advanced, treatment-resistant papillomatosis.[31] The reason behind these results is that RRP lesions possess a vascular nature, therefore drugs designed to disrupt blood vessels' density or formation are effective in hindering papillomatous lesions' progression. Bevacizumab, being an anti-VEGF monoclonal antibody, administered both locally (intralesional injection) or systemically (intravenous injection) has shown excellent results.[32]

The major concern about the use of an antiangiogenic therapy is the rebound papilloma's growth within the cessation of the treatment, since VEGF-blockade alone does not intrinsically activate immunity against HPV. Moreover, Bevacizumab has a known side effect profile (renal insufficiency), and prospective studies are needed to determine optimal long-term dosing schedules aimed at keeping enough drug in the system to suppress papilloma's growth while reducing the risk of adverse events. An interesting solution could be the concomitant use of immunotherapy, to both reduce

the burden of the residual disease and activate the immune system against the HPV infected cells. These aspects certainly deserve further studies. Promising data concern the possible use of HPV vaccine in the adjuvant treatment of RRP, despite the primary purpose of vaccination is to prevent future HPV infection. In their study, Young *et al*. showed a clinical benefit of HPV vaccination in RRP patients: eight patients experienced complete remission, and five patients experienced partial remission.[28] Also, Yiu *et al*. demonstrated an increase in the time interval between repeated surgeries in vaccinated patients.[33] The mechanism that underlies the vaccine's potential therapeutic efficacy against HPV is still unknown.

Therefore, two strategies against RRP should be considered: firstly, the vaccine reduces the risk of infection and consequently the incidence of HPV-related pathologies; secondly, patients who tested anti-HPV positive at baseline could develop a booster response to vaccination that prevents the infection from recurring.[34] For these reasons HPV vaccination is the most promising development in the treatment of RRP.[15]

Despite the encouraging literature on adjuvant HPV vaccination for secondary prevention in RRP, this strategy has not yet been accepted widely in treating the RRP population: the inconsistent findings data from published reports underline the need for evaluation of therapeutic efficacy of currently available HPV vaccines for the management of RRP.

Conclusions

RRP is a chronic disease currently difficult to treat due to the unpredictability of its recurrences and aggressive nature. The cases we reported are an example of the efficacy of systemic Bevacizumab at the dose of 10 mg/kg as a first line adjuvant therapy. As previously published clinical cases and series suggest, this treatment has shown a safe profile with overall good results, with the short-term local eradication of HPV. Further randomized prospective research with long-term follow-up is needed to better define the safety of this agent and the results against the disease's recurrence.

We also discussed the effectiveness of anti-HPV vaccination, not only as a prophylaxis of the infection but also as adjuvant treatment in preventing or delaying the recurrence of the disease, a role that needs to be demonstrated with further studies.

References

1. Andrei EC, Baniță IM, Munteanu MC, Busuioc CJ, Mateescu GO, Mălin RD, et al. Oral papillomatosis: its relation with human papilloma virus infection and local immunity - an update. *Medicina (Kaunas)* 2022; **58:** 1103. doi: 10.3390/medicina58081103
2. Betz SJ. HPV-related papillary lesions of the oral mucosa: a review. *Head Neck Pathol* 2019; **13:** 80-90. doi: 10.1007/s12105-019-01003-7
3. Gillison ML, Alemany L, Snijders PJF, Chaturvedi A, Steinberg BM, Schwartz S, et al. Human papillomavirus and diseases of the upper airway: head and neck cancer and respiratory papillomatosis. *Vaccine* 2012; **30 (Suppl 5):** F34-54. doi: 10.1016/j.vaccine.2012.05.070
4. Syrjänen S. Human papillomavirus infections and oral tumors. *Med Microbiol Immunol* 2003; **192:** 123-8. doi: 10.1007/s00430-002-0173-7
5. Welschmeyer A, Berke G S. An updated review of the epidemiological factors associated with recurrent respiratory papillomatosis. *Laryngoscope Investig Otolaryngol* 2021; **6:** 226-33. doi: 10.1002/lio2.521
6. Wang HFan, Wang SS, Tang YJ, Chen Y, Zheng M, Tang YL, et al. The double-edged sword-how human papillomaviruses interact with immunity in head and neck cancer. *Front Immunol* 2019; **10:** 653. doi: 10.3389/fimmu.2019.00653
7. Shanmugasundaram S, You J. Targeting persistent human papillomavirus infection. *Viruses* 2017; **9:** 229. doi: 10.3390/v9080229
8. Langer C, Wittekindt C, Wolf G. [Recurrent respiratory papillomatosis: current information on diagnosis and therapy]. [German]. *Onkol up2date* 2020; **2:** 107-18. doi: 10.1055/a-1132-0051
9. San Giorgi MRM, van den Heuvel ER, Tjon Pian Gi REA, Brunings JW, Chirila M, Friedrich G, et al. Age of onset of recurrent respiratory papillomatosis: a distribution analysis. *Clin Otolaryngol* 2016; **41:** 448-53. doi: 10.1111/coa.12565
10. Evers G, Schliemann C, Beule A, Schmidt LH, Schulze AB, Kessler C, et al. Long-term follow-up on systemic bevacizumab treatment in recurrent respiratory papillomatosis. *Laryngoscope* 2021; **131:** E1926-E33. doi: 10.1002/lary.29351
11. Seedat RY. Juvenile-onset recurrent respiratory papillomatosis diagnosis and management – a developing country review. *Pediatr Heal Med Ther* 2020; **11:** 39-46. doi: 10.2147/PHMT.S200186
12. Ouda AM, Elsabagh AA, Elmakaty IM, Gupta I, Vranic S, Hamda Al-Thawadi H, et al. HPV and recurrent respiratory papillomatosis: a brief review. *Life* 2021; **11:** 1-17. doi: 10.3390/life11111279
13. Fortes HR, von Ranke FM, Escuissato DL, Araujo Neto CA, Zanetti G, Hochhegger B, et al. Recurrent respiratory papillomatosis: a state-of-the-art review. *Respir Med* 2017; **126:** 116.21. doi: 10.1016/j.rmed.2017.03.030
14. Mauz P S, Zago M, Kurth R, Pawlita M, Holderried M, Thiericke J, et al. A case of recurrent respiratory papillomatosis with malignant transformation, HPV11 DNAemia, high L1 antibody titre and a fatal papillary endocardial lesion. *Virol J* 2014; **11:** 1-6. doi: 10.1186/1743-422X-11-114
15. Bertino G, Pedretti F, Mauramati S, Filauro M, Vallin A, Mora F, et al. Recurrent laryngeal papillomatosis: multimodal therapeutic strategies. Literature review and multicentre retrospective study. *Acta Otorhinolaryngol Ital* 2023; **43:** S111-S122. doi: 10.14639/0392-100X-suppl.1-43-2023-14
16. Torres-Canchala L, Cleves-Luna D, Arias-Valderrama O, Candelo E, Guerra MA, Pachajoa H, et al. Systemic bevacizumab for recurrent respiratory papillomatosis: a scoping review from 2009 to 2022. *Child* 2022; **10:** 54. doi: 10.3390/children10010054
17. Derkay CS, Wikner EE, Pransky S, Best SR, Zur K, Sidell DR, et al. Systemic use of bevacizumab for recurrent respiratory papillomatosis: who, what, where, when, and why? *Laryngoscope* 2023; **133:** 2-3. doi: 10.1002/lary.30180
18. Pogoda L, Ziylan F, Smeeing DPJ, Dikkers FG, Rinkel RNPM. Bevacizumab as treatment option for recurrent respiratory papillomatosis: a systematic review. *Eur Arch Otorhinolaryngol* 2022; **279:** 4229-40. doi: 10.1007/s00405-022-07388-6
19. Gerein V, Rastorguev E, Gerein J, Jecker P, Pfister H. Use of interferon-alpha in recurrent respiratory papillomatosis: 20-year follow-up. *Ann Otol Rhinol Laryngol* 2005; **114:** 463-71. doi: 10.1177/000348940511400608

20. Bergler WF, Götte K. Current advances in the basic research and clinical management of juvenile-onset recurrent respiratory papillomatosis. *Eur Arch Otorhinolaryngol* 2000; **257:** 263-9. doi: 10.1007/s004050050236

21. Patel A, Orban N. Infantile recurrent respiratory papillomatosis: review of adjuvant therapies. *J Laryngol Otol* 2021; **135:** 958-63. doi: 10.1017/S0022215121002322

22. Tjon Pian GiREA, Dietz A, Djukic V, Eckel HE, Friedrich G, Golusinski W, et al. Treatment of recurrent respiratory papillomatosis and adverse reactions following off-label use of cidofovir (Vistide®). *Eur Arch Otorhinolaryngol* 2012; **269:** 361-2. doi: 10.1007/s00405-011-1804-7

23. Rahbar R, Vargas SO, Folkman J, McGill TJ, Healy GB, Tan X, et al. Role of vascular endothelial growth factor-A in recurrent respiratory papillomatosis. *Ann Otol Rhinol Laryngol* 2005; **114:** 289-95. doi: 10.1177/000348940511400407

24. Mohr M, Schliemann C, Biermann C, Schmidt LH, Kessler T, Schmidt J, et al. Rapid response to systemic bevacizumab therapy in recurrent respiratory papillomatosis. *Oncol Lett* 2014; **8:** 1912-8 doi: 10.3892/ol.2014.2486

25. Ryan MA, Leu GR, Upchurch PA, Tunkel DE, Walsh JM, Boss EF, et al. Systemic bevacizumab (Avastin) for juvenile-onset recurrent respiratory papillomatosis: a systematic review. *Laryngoscope* 2021; **131:** 1138-46. doi: 10.1002/lary.29084

26. Zeitels SM, Barbu AM, Landau-Zemer T, Lopez-Guerra G, Burns JA, Friedman AD, et al. Local injection of bevacizumab (Avastin) and angiolytic KTP laser treatment of recurrent respiratory papillomatosis of the vocal folds: a prospective study. *Ann Otol Rhinol Laryngol* 2011; **120:** 627-34. doi: 10.1177/000348941112001001.

27. Zagzoog FH, Mogharbel AM, Alqutub A, Bukhari M, Almohizea MI. Intralesional cidofovir vs. bevacizumab for recurrent respiratory papillomatosis: a systematic review and indirect meta-analysis. *Eur Arch Otorhinolaryngol* 2024; **281:** 601-27. doi: 10.1007/s00405-023-08279-0

28. Young DL, Moore MM, Halstead LA. The use of the quadrivalent human papillomavirus vaccine (gardasil) as adjuvant therapy in the treatment of recurrent respiratory papilloma. *J. Voice* 2015; **29:** 223-9. doi: 10.1016/j.jvoice.2014.08.003

29. Mau T, Amin MR, Belafsky PC, Best SR, Friedman AD, Klein AM, et al. Interim results of a phase 1/2 open-label study of INO-3107 for HPV-6 and/or HPV-11-associated recurrent respiratory papillomatosis. *Laryngoscope* 2023; **133:** 3087-93. doi: 10.1002/lary.30749

30. Nagel S, Busch C, Blankenburg T, Schütte W. [Treatment of respiratory papillomatosis – a case report on systemic treatment with bevacizumab]. [German]. *Pneumologie* 2009; **63:** 387-9. doi: 10.1055/s-0029-1214714

31. Best S R, Mohr M, Zur K. B. Systemic bevacizumab for recurrent respiratory papillomatosis: a national survey. *Laryngoscope* 2017; **127:** 2225-9. doi: 10.1002/lary.26662

32. Allen CT. Biologics for the treatment of recurrent respiratory papillomatosis. *Otolaryngol Clin North Am* 2012; **54:** 769-77. doi: 10.1016/j.otc.2021.05.002

33. Yiu Y, Fayson S, Smith H, Matrka L. Implementation of routine HPV vaccination in the management of recurrent respiratory papillomatosis. *Ann Otol Rhinol Laryngol* 2019; **128:** 309-15. doi: 10.1177/0003489418821695

34. Chirilă M, Bolboacă SD. Clinical efficiency of quadrivalent HPV (types 6/11/16/18) vaccine in patients with recurrent respiratory papillomatosis. *Eur Arch Otorhinolaryngol* 2014; **271:** 1135-42. doi: 10.1007/s00405-013-2755-y

review

The financial toxicity of breast cancer: a systematic mapping of the literature and identification of research challenges

Ivica Ratosa[1,2], Mojca Bavdaz[3], Petra Dosenovic Bonca[3], Helena Barbara Zobec Logar[1,2], Andraz Perhavec[2,4], Marjeta Skubic[2], Katja Vörös[2], Ana Mihor[5], Vesna Zadnik[2,5,6], Tjasa Redek[3]

[1] Division of Radiotherapy, Institute of Oncology Ljubljana, Ljubljana, Slovenia
[2] Faculty of Medicine, University of Ljubljana, Ljubljana, Slovenia
[3] School of Economics and Business, University of Ljubljana, Slovenia
[4] Sector for Oncology Epidemiology and Cancer Registry, Institute of Oncology Ljubljana, Ljubljana, Slovenia
[5] Sector for Oncology Epidemiology and Cancer Registry, Institute of Oncology Ljubljana, Ljubljana, Slovenia
[6] Faculty of Health Sciences, University of Primorska, Izola, Slovenia

Radiol Oncol 2025; 59(1): 31-42.

Received 3 April 2024
Accepted 16 August 2024

Correspondence to: Assist. Prof. Ivica Ratoša, M.D., Ph.D., Division of Radiotherapy, Institute of Oncology Ljubljana, Ljubljana, Slovenia.
E-mail: iratosa@onko-i.si

Disclosure: No potential conflicts of interest were disclosed.

Background. Breast cancer is one of the most common cancers, increasingly prevalent also among working-age populations. Regardless of age, breast cancer has significant direct and indirect costs on the individuals, families and society. The aim of the research was to provide a comprehensive bibliometric analysis of the financial toxicity of breast cancer, to identify research voids and future research challenges.

Materials and methods. The systematic mapping of literature relied on a multi-method approach, combining bibliometric methods with a standard review/discussion of most important contributions. The analysis employed Bibliometrics in R and VosViewer.

Results. The results highlighted the key authors, journals and research topics in the investigation of the financial toxicity of cancer and stressed the concentration of work around several authors and journals.

Conclusions. The results also revealed a lack of a comprehensive approach in the study of financial toxicity, as the literature often focuses on one or few selected aspects of financial toxicity. In addition, geographic coverage is uneven and differences in the healthcare systems represent a challenge to straightforward comparisons.

Key words: breast cancer; financial toxicity; bibliometric analysis

Introduction

Cancer care is not only a medical challenge, but also a complex socio-economic issue. The term financial toxicity has gained prominence in recent years to describe the adverse financial effects experienced by cancer patients as they navigate diagnosis, treatment, and survivorship.[1] Financial toxicity in cancer care is prevalent and causes significant financial loss, psychological distress, and maladaptive coping strategies, requiring multilevel, coordinated efforts among stakeholders.[2] Patients with breast cancer frequently experience financial toxicity as a result of extended and multimodal treatment; in low- and middle-income countries, this was reported to affect 78.8% of patients, while in high-income countries, it affected 35.3% of patients.[3] Systematic reviews of the literature

have shown that patients with cancer from various income-group countries experience a significant financial burden during their treatment[4], and despite publicly funded universal public healthcare, financial toxicity remains a concern for patients with cancer and their families.[5] However, patients with cancer in countries with more market-driven health care face more financial toxicity since they have to co-pay for medical services and medicines, even if they have insurance. This is one of the reasons why the prevalence of financial toxicity is higher in the US compared to nations with universal health care (22–27%).[5,6] Although financial toxicity levels vary by country, the data indicate that financial protection is inadequate in many countries and highlight the need for targeted interventions to alleviate financial strain among affected individuals.[5] Generally, women fare worse financially than men after cancer treatment.[7]

Various factors contribute to the development and exacerbation of financial toxicity among patients with breast cancer. Socioeconomic factors, such as income level, employment status, and education, play a significant role in determining an individual's vulnerability to financial strain. Additionally, clinical factors, such as disease stage, further compound the financial burden experienced by patients. Geospatial differences also exist, with certain counties exhibiting higher risk profiles for financial toxicity due to disparities in healthcare infrastructure and access to supportive resources.[7-9]

In a single-institution cross-sectional survey of adult female patients with breast cancer who underwent lumpectomy or mastectomy, lower financial distress was associated with factors such as having supplemental insurance, higher household income, and a higher credit score, while work reduction, increased out-of-pocket spending, advanced tumour stage, and being employed at diagnosis were associated with increased distress.[10] For survivors of breast and gynaecologic cancer, greater financial toxicity is associated with greater distress and a lower quality of life.[11]

As the incidence and prevalence of breast cancer continues to rise worldwide[12], understanding its impact on financial toxicity in Europe is essential for guiding policy interventions and improving patient outcomes. In light of these challenges, there is a growing recognition of the need to address financial toxicity as an integral component of comprehensive cancer care. In recent years, the utilization of visualization analysis has surged as a prominent approach for scrutinizing vast bibliometric datasets and results of scientific contributions. This methodology employs specialized software to conduct correlations within data, translating findings into visual representations that facilitate a more intuitive comprehension of pertinent information. By doing so, it facilitates the detection of underlying patterns concealed within extensive datasets, streamlining the assimilation of valuable insights.[13] While existing literature has comprehensively summarized various aspects of financial toxicity[3,5,13], there remains a notable need for bibliometric and visual studies examining the current landscape of financial toxicity in patients with breast cancer. Therefore, the aim of present study was to gain insights into the current literature and trends on financial toxicity in patients with breast cancer using bibliometrics and visualization analysis to identify key journals, countries, researchers, institutions, and collaborations among them to identify research voids and future research challenges and discuss most important contributions.

Materials and methods

Research goals

This paper relies on a multi-method approach to identify research challenges in the field of the financial toxicity of breast cancer, primarily relying on bibliometric analysis with text mining to provide a solid base for a classic problem-based literature review. The research goal of the bibliometric analysis of the research done within the field of financial toxicity of breast cancer focuses on identifying key challenges and research gaps in understanding the causal relationships between breast cancer, its treatment and direct and indirect financial burden. To do so, the following research questions were addressed:

1. What was the evolution of research in this topic and its dynamics throughout time?
2. Which were the important journals and influential authors who have contributed to the understanding of financial toxicity in cancer, as well as what was the influence of collaboration between authors and countries?
3. Which were the main topics that were investigated in relation to the financial toxicity of cancer? and
4. Which are the current gaps in the literature?
5. While the first two research questions are predominantly explored using bibliometric analysis, the last two are explored using a multi-method approach: the bibliometric analysis is used

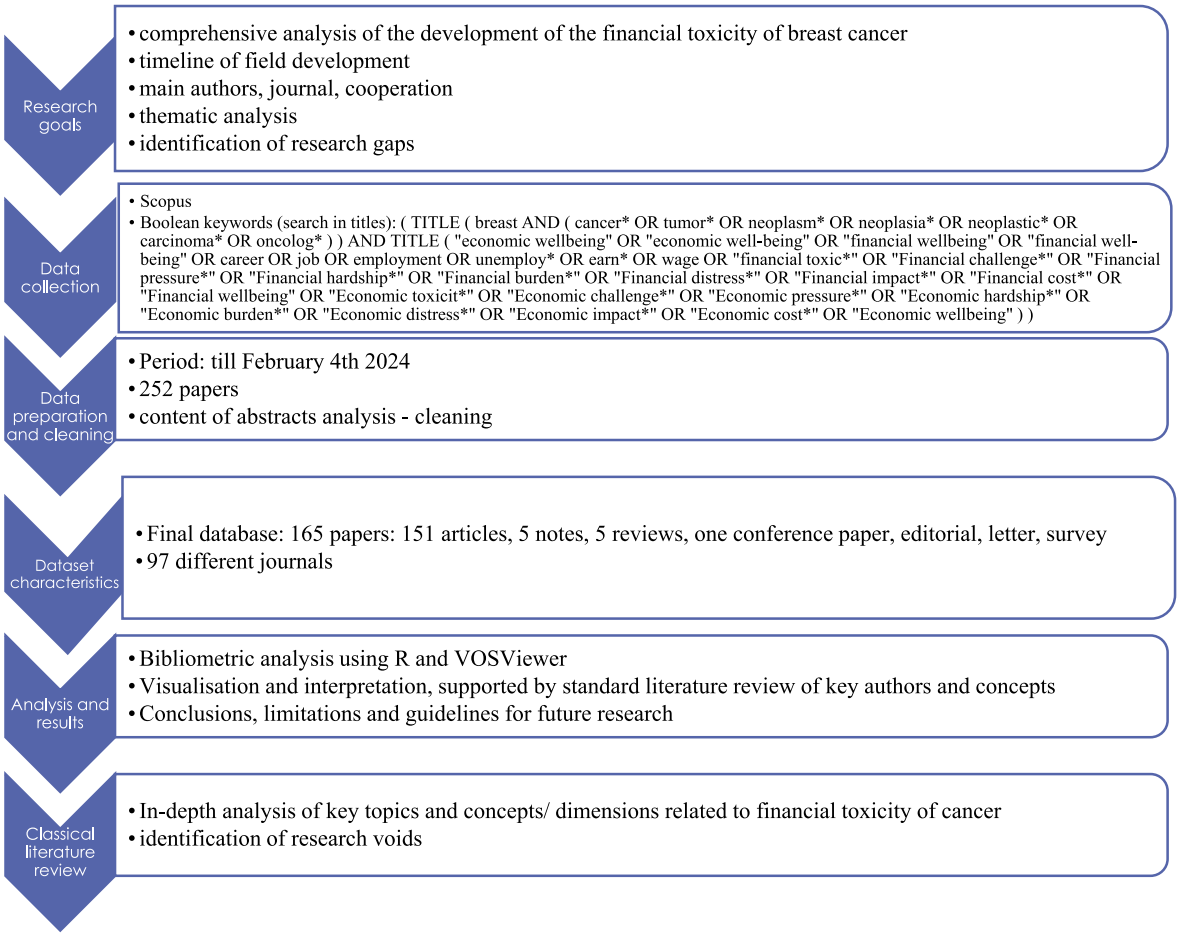

FIGURE 1. Step-by-step research approach summary (based on ref.[16]).

to provide the general guidelines for further research using content analysis and extended by a standard review of key contributions.

Methodology

Scopus was used as a base for the bibliometric analysis due to its wide coverage in the field of medicine (including Medline) as well as wider coverage of publication types than Web of Science.*

Initially, 252 papers were obtained from the Scopus database on February 4th 2024, using the search focusing on a wider span of relevant keywords in paper titles (see Figure 1). The final database was prepared based on content analysis of the paper titles and abstracts to limit the analysis only to those relevant for the study. The final set of studied papers comprised 165 papers (151 articles, 5 notes, 5 reviews, one conference paper, one editorial, one letter, one survey), published in 97 different sources between 1995 and 2024. The papers were prepared by in total 926 authors, with an average of 6.76 authors per paper and only 9 papers being single authored. The content was summarized in 293 different keywords and 1065 key-words plus. The research, presented in the investigated papers, relied on a broad set of knowledge, the total number of cited references was 5323. The investigated body of literature already made a significant impact in the field, since the studied papers were on average cited close to 23 times. Figure 1 summarizes the research approach summary.

Methodologically, the paper combines two approaches: (1) bibliometric analysis, serving as a base for a [2] more detailed review of the key lit-

* For example, in December 2023 Scopus included more than 29200 active serial publications, more than 330 thousand books and 23.4 million open access items from more than 7000 publishers. In total, the data comprised the work of almost 20 million authors, and almost 100 thousand affiliations.[14] Scopus also includes data from MEDLINE and EMBASE.[15] The wider and highly topic-relevant coverage were the main reasons why Scopus was chosen over Web of Science.[16]

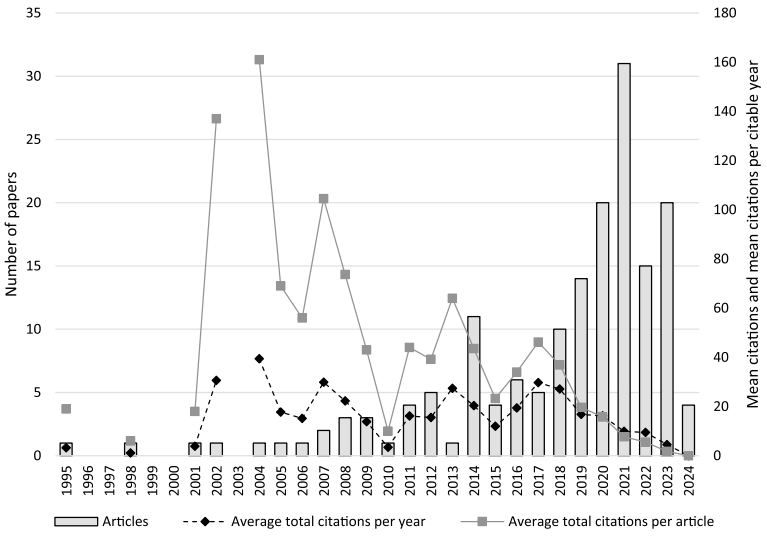

FIGURE 2. Published number of papers by year (left axis) and mean citations per paper and mean citations per citable year (right axis).

erature, identified by the bibliometric analysis. The bibliometric analysis relies on the established bibliometric approaches.[17-20] The analysis provides first the dynamics of the field development, including key authors, outlets, citation and collaboration. Co-citation and collaboration analyses were used to further explore the relationships between papers, clusters of papers with common topics or origin and also to identify the teams of authors, collaborations that contributed most to the development of the field. The more general thematic analysis was conducted in Bibliometrix package in R online environment (R-Studio 0.98.1091 software).[21] It was used to extract key topics using keywords and also identify the topics using keyword co-occurrences. Namely, key-words are according to the literature the first and most general summary of the main topics in the text.[22-25] To further investigate the evolution of themes in the field, a conceptual structure was created using the Multiple Correspondence Analysis (MCA), an exploratory multivariate technique that identifies themes based on distances.[18] Content analysis relying on keywords was conducted also in R.[26] The research also utilized VOSviewer (version 1.6.20) for visualization.[27]

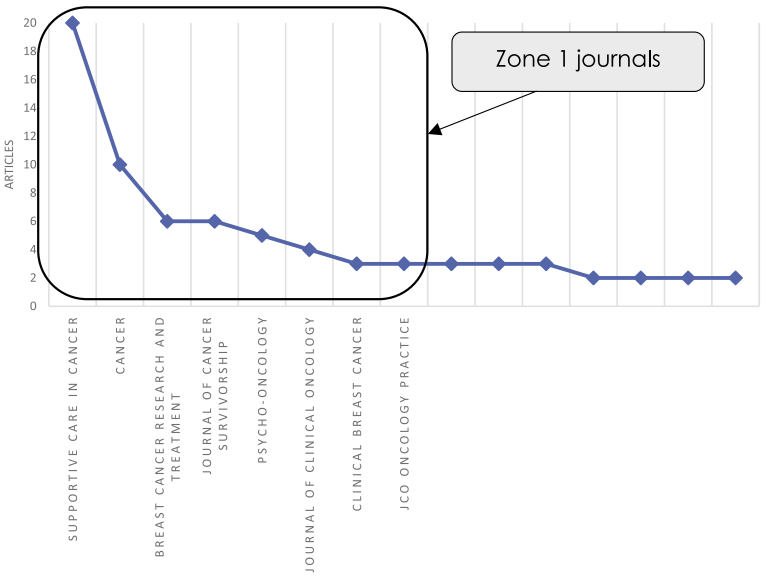

FIGURE 3. Bradford law with Zone 1 journals.

Results

The interest in the topic of financial toxicity of cancer in the literature (focusing on Scopus) has been growing since the 1990s, with the number of papers increasing fast in particular after 2010. In 2021, 31 papers, dealing with the topic of financial toxicity of breast cancer were published. The published papers were on average cited more than 20 times over the observed period. In some years, though, the number of citations in the investigated body of the literature on average exceeded 160 in 2004, 137 in 2002 and 100 citations in 2007, when also some of the more cited papers were published.[28,29] But, even if the total number of citable years is considered, the investigated body of literature on average still received several citations, apart from the papers published in 2024 (Figure 2).

The outlets, that published most papers on the topic, are the following: *Supportive Care in Cancer*, with 20 papers studying financial toxicity of cancer, followed by *Cancer* (10 papers), *Breast Cancer Research and Treatment* (6), *Journal of Cancer Survivorship* (6), *Psycho-oncology* (5). Bradford law states that there are only a few very productive publications, and a much larger number of those of low(er) relevance. The so-called Zone 1 or core journals are those most often cited in the literature for a specific field and thus most important. Mathematically, the rank is inverse with a proportion of the articles in the journal using a logarithmic scale.[30]

The Bradford law analysis of the investigated body of literature suggests that the most important sources are indeed *Supportive Care in Cancer, Cancer, Breast Cancer Research and Treatment, Journal of Cancer Survivorship, Psycho-oncology*, but also *Journal of Clinical Oncology, Clinical Breast Cancer*

and *JCO Oncology Practice*, which all are in Zone 1 (or most important journals) (Figure 3).

Hawley[31-33], Offodile[10,34,35], Wheeler[36-38], Bradley[29,39,40] and Jagsi[31,32,41] are some of the most important authors, authoring or co-authoring at least 6 published articles or 3.6% or more of the investigated body of literature (Table 1, for each author the citations in the brackets in the text refer to the 3 most cited papers).

Lotka Law[42], which investigates the concentration (or distribution of papers by authorship) also highlights that 3 authors (Hawley, Offodile, Wheeler), who in total represent 0.3% of all authors, have contributed a significant proportion of the studied papers, while on the other hand 87% of authors have only contributed one paper. H index[43], measuring authors' local impact, shows that Hawley, Jagsi, Wheeler and Offodile have the highest H-index of 6, indicating that each has at least 6 papers, each cited at least 6 times.

Authors are international, coming from a number of different countries, most often collaborating with the US (25 papers), UK (13), Switzerland (7), Australia (6). While authors are from a number of different institutions, the most common affiliations are: University of Michigan, University of Texas (MD Anderson Cancer Center), University of California, University of North Carolina, Shiraz University of Medical Sciences, Johns Hopkins University, University of Maryland and Harvard Medical School, each with at least 13 mentions with Michigan in total with 38. USA dominates also among the cited references, with in total 2565 cited papers, followed by Australia with 233, Canada with 180 papers and UK with 145 cited papers in the list of references. Further investigation of the collaboration between groups of authors shows that there are five strong groups of authors, who collaborate frequently. Among those are: (1) Wheeler, Spencer, Blinder, Reeder-Hayes, Swanberg and Vanderpool, (2) Hawley, Bradley, Jagsi, Katz, Hamilton, Abrahamse, Griggs, Janz, Kurian, Wallner, Blinder, and (3) Offodile, Asaad,

TABLE 1. A list of authors with at least 4 published papers in the investigated set of literature

Authors	Articles	Articles Fractionalized*	No of documents (in % of all)
HAWLEY ST[31-33]	7	0.919	4.2
OFFODILE AC[10,34,35]	7	0.774	4.2
WHEELER SB[36-38]	7	0.868	4.2
BRADLEY CJ[29,39,40]	6	1.569	3.6
JAGSI R[31,32,41]	6	0.701	3.6
ASAAD M[10,34,35]	5	0.549	3
BOUKOVALAS S[10,34,35]	5	0.549	3
KATZ SJ[31-33]	5	0.576	3
AZUERO A[46]	4	0.522	2.4
CHAN A[64–67]	4	0.342	2.4
COOPER B[64–67]	4	0.342	2.4
GORDON L[45]	4	0.501	2.4
HAMILTON AS[31,32]	4	0.476	2.4
KOCZWARA B[64–67]	4	0.342	2.4
MIASKOWSKI C[64–67]	4	0.342	2.4

* Fractionalized authorship to papers assesses individual productivity taking into account co-authorships, assuming equal distribution of contributions across all authors

TABLE 2. A list of 10 most cited papers in the investigated set of literature (only the first author is listed in case of multiple authors)*

Paper	DOI/PMID	Total citations	TC per year	Normalized TC
Jagsi *et al.*, 2014, J Clin Oncol[31]	10.1200/JCO.2013.53.0956	206	18.73	4.73
Arozullah *et al.*, 2004, J Support Oncol[28]	PMID: 15328826	161	7.67	1.00
Bradley *et al.*, 2002, J Health Econ[29]	10.1016/S0167-6296(02)00059-0	137	5.96	1.00
Bradley *et al.*, 2007, Cancer Invest[39]	10.1080/07357900601130664	117	6.50	1.12
Lauzier *et al.*, 2008, J Natl Cancer Inst[44]	10.1093/jnci/djn028	111	6.53	1.51
Jagsi *et al.*, 2018, Cancer[32]	10.1002/cncr.31532	104	14.86	2.82
Meneses *et al.*, 2012, Gynecol Oncol[46]	10.1016/j.ygyno.2011.11.038	94	7.23	2.40
Gordon L *et al*, 2007, Psycho-Oncology[45]	10.1002/pon.1182	92	5.11	0.88
Greenup *et al*, 2019, J Oncol Pract[37]	10.1200/JOP.18.00796	81	13.50	4.12
Wheeler *et al.*, 2018, J Clin Oncol[36]	10.1200/JCO.2017.77.6310	81	11.57	2.20

* TC per year = total citations per year; Normalized TC = Normalized total citations

Boukovalas, Greenup, Lin, Bailey, and Butler, to list just the first three groups of authors.

The investigation of the financial toxicity of breast cancer was highly influenced by a smaller set of highly cited papers (Table 2).

Below, a summary of the most cited is provided. Jagsi and co-authors[31] published in 2014 the most cited paper with in total 206 citations. They used a longitudinal approach to study the long-term financial burden of breast cancer that showed that a quarter of women suffered financial decline due to breast cancer, and that the minorities were more vulnerable to the effects. Arozullah *et al*.[28] showed that the financial burden of cancer in the US accounted for at least 26% of monthly income to as much as 98%, depending on income group, and that the insurance policies covered on average only around 3% of out-of-pocket expenditures of the studied women, providing valuable policy input that affordable compensation plans should be available in particular to those in low income brackets. Bradley *et al*.[29] in 2007 investigated the relationship between breast cancer survival, work and earnings in the US and found that while breast cancer does have a negative impact on employment, the responses of women are heterogenous and that the survivors who do work in fact worked and earned more than those in the control group. In 2002, Bradley *et al*.[39] showed in a US-based longitudinal study that the greatest impact on labour supply was present in the first six months after diagnosis, while between 12 and 18 months after diagnosis many already returned to work. Among the papers with more than 100 citations is also the work of Lauzier *et al*.[44] who showed that in Canada on average around a quarter of projected annual wage was lost due to breast cancer, more among those with lower education, those with lower social support, receiving chemotherapy, self-employed and short work-experience, to list just those with highest significance. A longitudinal study in Australia showed that economic costs continue to affect women even 1.5 years after surgery, where income loss and the costs of health service were the most important sources of economic burden, which is higher for women with positive lymph nodes.[45] Related to the longer-term analysis of financial toxicity of cancer, a follow-up study of 132 survivors showed that the impacts in the longer term are significant in the financial sense (e.g. increased insurance premiums) and otherwise (lower motivation, productivity, quality of work, impact on absence from work), stressing the extended impact of cancer burden on post-treatment period in the US.[46] Wheeler *et al*.[36] discuss the racial differences in breast cancer financial toxicity in the US and find that the impact of race was significant for job loss, transportation barriers, income loss, and overall financial impact. Jagsi *et al*.[32] investigated the role of clinicians' engagement in the patient care also from the perspective of financial toxicity of cancer, not just health aspects of the disease in the US. Between 15–30% of patients, depending on ethnicity, expressed desire to discuss also financial burden of cancer, however, depending on the topic, between 50 and 70% of those longing to talk also about the financial aspect, did not report or receive such support. Financial toxicity impacts also the decision for the type of breast cancer surgery. For example, more than a quarter of studied women in the US reported that costs were considered when deciding about preservation and appearance.[37] Bilateral mastectomy was associated with higher debt, very high financial burden and changed employment.[37]These findings, which refer to the most cited papers, mainly refer to the US, which has a specific health insurance system.

Although the investigated literature focuses on the financial toxicity of breast cancer, the literature deals with a wide array of subtopics. The simplest content analysis is done using keywords, as they are used to efficiently summarize the text.[47] Most common author-used keywords by frequency are the following: breast cancer and financial toxicity, return to work, quality of life, survivorship, cost of illness, costs, metastatic breast cancer, oncology, cancer survivors/survivorship, chemotherapy, financial burden, lymphedema, fatigue, healthcare costs, treatment, financial stress, occupation, rehabilitation, social support, unemployment, work.

Thematic map, investigating the relationships between the words, prepared in Bibliometrix, allows the division of the topic also into basic themes, motor themes, niche themes and emerging/declining themes, which are investigated using keywords for each theme (100 words were included, minimum cluster frequency 5, Walktrap clustering algorithm). Table 3 summarizes the main topics and provides selected references for each of the identified topics.

The **motor themes** are three (T1–T3, Table 3). The first motor topic is related to the individual and the consequences of the **disease** for the individual, in particular **in relation to employment and financial toxicity**. This topic deals with cancer survivorship, employment and the return to work, occupational differences, related disability

TABLE 3. Thematic map of (financial) toxicity of breast cancer with most common author keywords for each of the themes and selected references

	Key term(s)	Other key terms*	Selected papers (No. of reference)
Motor themes	T1: Breast cancer (neoplasms), employment, financial toxicity	Quality of life, return to work, (cancer) survivor(ship), treatment, financial burden / stress, fatigue, chemotherapy, mental health, caregivers, social support, disability, occupation, burnout complaints	29, 33, 39
	T2: Metastatic breast cancer	Prevalence, healthcare use, healthcare utilization, healthcare costs, advanced breast cancer, adverse effects, administrative claims, breast cancer costs	48, 49
	T3: COVID-19	Depression, job loss, access to healthcare, breast cancer survivors, cognition, anxiety, autonomy	50, 51
Basic themes	T1 Economic burden	Cost(s), oncology, lymphedema, rehabilitation, breast neoplasm, cost-effectiveness, recurrence, screening, cost of illness, cancer, resource utilization, healthcare use	52-54
Emerging or declining themes	T1: Coping strategies	Breast cancer, healthcare, costs, regional, ethnic differences	55, 56
Niche themes	T1: Reasonable accommodations	Sick leave, assessment and planning	57, 58

* Other key terms (T) selected based on centrality and repetition (overlap with other similar key terms within same topic).

and the consequences of treatment (chemotherapy, fatigue, burnout) as well as mental health aspects of the disease. In terms of financial toxicity, a number of aspects are investigated, besides employment also unemployment, social support, rehabilitation, return to work, occupations, needs assessment (which can also be related to return to work), socio-economic status, sick-leave, career change, fatigue, job loss, quality of life, and other.[29,33,39] The second motor topic is related to metastatic breast cancer, its prevalence, the impact on healthcare use, utilization and costs. This topic is more closely related to the wider healthcare aspect of cancer-related cost.[48,49] The third motor topic was dealing with COVID-19 and breast cancer.[50,51] The COVID-19 is on the margin between a niche and a motor theme, indicating a fast development of a narrow theme, which focuses on the impact of cancer during COVID-19, to job-loss and mental health. The access to healthcare was also highlighted. The topic of financial toxicity of cancer (T1, Table 3) is also close to the border between basic and motor themes, while the broader economic burden is a major motor theme. General economic burden, cost of illness and cancer is a **basic theme**. The key words stress the cost-effectiveness, resource utilization, healthcare use and healthcare costs, screening. The topic also highlights differences between diagnoses (e.g. metastatic, hormone positive, premenopausal). A close link between the motor theme (T1) and basic theme is for example productivity loss, which highlights the aggregate effects of the impact of the disease on the individuals' labour market outcome.[52-54] **Niche themes** revolve around reasonable accommodations and sick-leave, highlighting also the importance of assessment and planning.[55,56] **Emerging or declining themes** revolve around coping strategies, healthcare costs as well as regional and ethnic differences.[57,58]

An investigation into the evolution of the themes between 1995 and 2024 shows that before 2010, the number and diversity of the topics in the literature was significantly narrower, focusing primarily on (1) employment (hours worked, labour market effects, disability, earnings), (2) process of treatment and return to work (oncology, breast neoplasms, chemotherapy, rehabilitation, occupation, return to work), (3) process of the return to work (assessment and planning, reasonable accommodations, job retention), (4) healthcare system and costs (prevalence, direct and indirect costs, cost of illness, administrative claims) and (5) selected demographic aspects. After 2010, the number of topics significantly increased, predominantly due to further disaggregation of selected aspects. In addition to the aforementioned key aspects, which were driving the literature before 2010, several additional aspects emerge: (1) financial toxicity in relation to coping strategies, social supports, community programs, (2) metastatic cancer is studied in relation to cancer distress, costs, role of screening, (3) healthcare costs and use are studied in relation to cost drivers and adverse events, while also (4) covid-19 emerges as a topic, both in relation to financial toxicity as well as anxiety, and cognition.

TABLE 4. A systematization of (financial) toxicity of breast cancer at the level of the individual (left column) and research gap (right column)

Type of financial burden/burden	Coverage in the literature and research gap
1. Medical costs	
Treatment expenses	Weaker coverage, survey based, depends on social security system, more relevant for private-insurance based system (e.g. US)
Hospitalization costs	
2. Non-medical costs	
Travel expenses	Weaker coverage, survey based, depends on social security system, more relevant for private-insurance based system (e.g. US)
Accommodation costs	
Other	
3. Out-of-pocket costs	
Deductibles and co-payments	Weak coverage, survey based
Prescription drug costs*	
4. Loss of income	
Changed work hours	Well-documented employment impacts, income impacts, less focus on occupational change
Job loss	
Change in occupation	
Loss/change in income	
5. Insurance-related costs	Weak coverage, depends on social security system, but has broader relevance for other non-medical insurances (life, travel, etc.)
6. Impact on finances and assets:	
Debt accumulation	Weak coverage
Asset depletion	
7. Psychosocial impact:	
Stress and anxiety	Well-documented, focus on stress, anxiety, less focus on quality of life as a whole
Quality of life	
8. Long-term financial consequences	
Survivorship costs	Increasing interest on recurrence, screening
Cancer recurrence	
9. Geographical coverage	
US	Vast body of evidence for the US, poorer coverage for EU/European context
Europe	

* Can differ between countries depending on health-care system

Discussion

Discussion of bibliometric analysis: a review of most important findings

According to the results of the bibliometric analysis, the literature on the financial toxicity of breast cancer is marked with a significant concentration in terms of relevant research journals (*Supportive Care in Cancer, Cancer, Breast Cancer Research and Treatment, Journal of Cancer Survivorship*), authors (Hawley[31-33], Offodile[10,34,35], Wheeler[36-38], Bradley[29,39,40] and Jagsi[31,32,41]) as well as concentration of topics, with the two most important and widest being the (1) individual-level investigation of financial toxicity of cancer in relation to earnings, employment and other related topics and (2) a more aggregated health-care and social system perspective related to cancer treatment and its costs.

However, the financial toxicity of cancer is a much wider concept, encompassing (i) direct or active financial spending, (ii) passive financial resources' spending, (iii) psychosocial impacts, (iv) the need for external support, (v) coping with care and (vi) changes in lifestyle.[47] The direct payments

include medical (potential treatment expenses, hospitalization expenses, depending on social security system), non-medical costs (travel, accommodation, other travel related costs), out-of-pocket costs (medications, deductibles and co-payments, depending on social system).[59,60] Second, the individual suffers loss of income due to reduced working hours or even job-loss[61], domestic finances and assets can be affected due to the use of savings[62], and individuals can suffer insurance-related costs (increased premiums).[63] In the short and in the long-term, the disease can bear significant costs due to stress and anxiety, while the quality of life can also suffer. In the long term, primarily the so-called survivorship costs, related to on-going care or long-term effects of cancer and potential recurrence are important.

The investigated body of literature, which examines financial toxicity of breast cancer, focuses most on the employment, job, and income related consequences (Table 4).

These are also the consequences that can more easily and reliably be measured, either via surveys or registry-data, both cross-sectional and longitudinal, focusing also on the differences conditional on the demographic characteristics of patients. The literature also demonstrates a lot of focus on phycological impacts on the individual, which can have longer-term effects on both health as well as financial stress. The aggregated perspective on the health-care system is also at the forefront of research. On the other hand, the reviewed body of literature on financial toxicity of breast cancer displayed little interest in the non-medical costs, insurance related costs, impact on debt accumulation and depletion of savings. However, cross-country differences are notable, depending not only on the health-care system, but also on the income (development) level of the countries.[4,68] In particular, when comparing developed economies, the evidence is widely focused on the experiences of the US patients, there is significantly less evidence for European context.[69-72] The studies show a significant level of financial burden of cancer in both US and EU, however, in the US the private insurance, varying insurance coverage and reimbursement policies referring to cancer care, including diagnostics, treatments (chemotherapy and radiation), medications and also supportive care medications cause substantial out-of-pocket expenses for patients.[60] In Europe, where health-care systems are predominantly publicly funded and universal, breast cancer patients generally face lower out-of-pocket costs for medical services. However, disparities in access to innovative treatments and supportive care services may still exist across different European countries, contributing to variations in financial toxicity among patients[4,73,74], which highlights also the need for using an adjusted methodology.[75]

Limitations and future research orientation

This analysis contributes to the literature in several aspects. First, it studies the body of literature on the financial toxicity of breast cancer in Scopus. A comparable analysis using Web of Science[76] is narrower due to the coverage as well as due to its focus on solely bibliometric issues. This paper relies on a multi-method approach to provide a more comprehensive overview – first, it highlights in a systematic manner the most notable authors and papers as well as stresses the concentration of authors, journals and topics in the literature. Second, the paper shows that the majority of the literature focuses on selected aspects of financial toxicity of cancer. Thereby, it identified a research gap that can propel future development of the study area.

The analysis can in the future also be extended and improved to overcome some of the limitations of the existing analysis. First of all, a more detailed analysis into each of the key topics would allow identification of main linkages between the variables of interest within a specific topic. An in-depth investigation of each of these variables would allow identification of possible causal mechanisms in the existing literature that explain the channels through which cancer is related to financial toxicity in both short and long term. It is also important to highlight the methodological downsides of bibliometric analysis[77], which is in fact quantitative, although it often seeks to provide qualitative conclusions. Furthermore, the body of literature is focusing on different health-care systems, revealing also the differences in the financial toxicity. Future research should adequately address these differences in empirical assessment[75], in particular when comparing different countries. This could also imply that data gathered based on established international methodology (questionnaires such as Comprehensive Score for financial Toxicity - Functional Assessment of Chronic Illness Therapy (COST-FACIT)[78] should be used with care and questionnaires should be extended to capture national specifics.

Conclusions

The financial toxicity of breast cancer represents a burden that encompasses a wide range of effects, from the direct to the indirect financial costs as well as wider socio-economic impacts on patients. This paper provides a systematic mapping of the literature, relying on the bibliometric analysis that shows that despite the relatively wide coverage, there are still significant research gaps in the literature. The literature often concentrates on specific aspects of financial toxicity, is often focusing on one country and thereby also one specific healthcare system, or is not addressing the broader, more holistic aspects of the problem. In particular, the literature is focusing on the aspects that are easier to measure or capture, while a more holistic approach would require both a broader as well more often also a longitudinal approach. Such an approach would also allow better informed policy-making to alleviate the short- and long-term effects of the financial toxicity of breast and other cancers.

Acknowledgments

This work was financed by Slovenian Research and Innovation Agency grants No. J7-4540, P5-0128, P5-0117, P5-0441 and P3-0429.

References

6. Zafar SY. Financial toxicity of cancer care: it's time to intervene. *J Natl Cancer Inst* 2016; **108:** djv370. doi: 10.1093/jnci/djv370

7. Lentz R, Benson AB, Kircher S. Financial toxicity in cancer care: prevalence, causes, consequences, and reduction strategies. *J Surg Oncol* 2019; **120:** 85-92. doi: 10.1002/jso.25374

8. Ehsan AN, Wu CA, Minasian A, Singh T, Bass M, Pace L, et al. Financial toxicity among patients with breast cancer worldwide: a systematic review and meta-analysis. [Internet]. *JAMA Netw Open* 2023; **6:** e2255388. doi: 10.1001/jamanetworkopen.2022.55388. [cited 2024 Mar 15]. Available at: https://www.scopus.com/inward/record.uri?eid=2-s2.0-85147783077&doi=10.1001%2fjamanetworkopen.2022.55388&partnerID=40&md5=c2a7253b842dc09af15f9af533d51bb2

9. Azzani M, Atroosh WM, Anbazhagan D, Kumarasamy V, Abdalla MMI. Describing financial toxicity among cancer patients in different income countries: a systematic review and meta-analysis. *Front Public Health* 2024; **11:** 1266533. doi: 10.3389/fpubh.2023.1266533

10. Longo CJ, Fitch MI, Banfield L, Hanly P, Yabroff KR, Sharp L. Financial toxicity associated with a cancer diagnosis in publicly funded healthcare countries: a systematic review. *Support Care Cancer* 2020; **28:** 4645-65. doi: 10.1007/s00520-020-05620-9

11. Pauge S, Surmann B, Mehlis K, Zueger A, Richter L, Menold N, et al. Patient-reported financial distress in cancer: a systematic review of risk factors in universal healthcare systems. *Cancers* 2021; **13:** 5015. doi: 10.3390/cancers13195015

12. Smith GL, Lopez-Olivo MA, Advani PG, Ning MS, Geng Y, Giordano SH, et al. Financial burdens of cancer treatment: a systematic review of risk factors and outcomes. *J Natl Compr Canc Netw* 2019; **17:** 1184-92. doi: 10.6004/jnccn.2019.7305

13. Çelik Y, Çelik SŞ, Sarıköse S, Arslan HN. Evaluation of financial toxicity and associated factors in female patients with breast cancer: a systematic review and meta-analysis. *Support Care Cancer* 2023; **31:** 691. doi: 10.1007/s00520-023-08172-w

14. Verhoeven D, Allemani C, Kaufman C, Mansel R, Siesling S, Anderson B. Breast cancer: global quality care optimizing care delivery with existing financial and personnel resources. *ESMO Open* [internet] 2019; **4(Suppl 2):** e000861. [cited 2024 Mar 21]; Available at: https://www.esmoopen.com/article/S2059-7029(20)32629-6/fulltext

15. Offodile AC, Asaad M, Boukovalas S, Bailey C, Lin YL, Teshome M, et al. Financial toxicity following surgical treatment for breast cancer: a cross-sectional pilot study. *Ann Surg Oncol* 2021; **28:** 2451-62. doi: 10.1245/s10434-020-09216-9

16. Benedict C, Fisher S, Schapira L, Chao S, Sackeyfio S, Sullivan T, et al. Greater financial toxicity relates to greater distress and worse quality of life among breast and gynecologic cancer survivors. *Psychooncology* 2022; **31:** 9-20. doi: 10.1002/pon.5763

17. International Agency for Research on Cancer. Cancer today [internet]. 2024 [cited 2024 Mar 21]. Available at: https://gco.iarc.who.int/today/

18. Cheng H, Lin L, Liu T, Wang S, Zhang Y, Tian L. Financial toxicity of breast cancer over the last 30 years: a bibliometrics study and visualization analysis via CiteSpace. *Medicine* 2023; **102:** e33239. doi: 10.1097/MD.0000000000033239

19. Elsevier. Scopus. Scopus content [internet]. 2024 [cited 2024 Feb 15]. Available at: https://www.elsevier.com/products/scopus/content

20. Tuttle B; LibGuides. Database Search Tips. Scopus [internet]. 2023 [cited 2024 Feb 15]. Available at: https://guides.mclibrary.duke.edu/searchtips/scopus

21. Matthews T. LibGuides: resources for librarians and administrators. Web of Science Coverage Details [internet]. 2024 [cited 2024 Feb 15]. Available at: https://clarivate.libguides.com/librarianresources/coverage

22. Roblek V, Dimovski V, Mesko M, Peterlin J. Evolution of organisational agility: a bibliometric study. *Kybernetes* 2022; **51:** 119-37. doi: 10.1108/K-11-2021-1137

23. Aria M, Cuccurullo C. Bibliometrix: an R-tool for comprehensive science mapping analysis. *J Informetr* 2017; **11:** 959-75. doi: 10.1016/j.joi.2017.08.007

24. Zupic I, Čater T. Bibliometric methods in management and organization. *Organizational Research Methods* [internet]. 2014 [cited 2020 May 19]. **18:** 429-72. doi: 10.1177/1094428114562629. Available at: https://journals.sagepub.com/doi/10.1177/1094428114562629

25. Perianes-Rodriguez A, Waltman L, van Eck NJ. Constructing bibliometric networks: a comparison between full and fractional counting. *J Inform* 2016; **10:** 1178-95. doi: 10.1016/j.joi.2016.10.006

26. Bibliometrix. Home [internet]. 2024 [cited 2024 Jan 26]. Available at: https://www.bibliometrix.org/home/index.php

27. Feinerer I, Hornik K, Meyer D. Text Mining Infrastructure in *R* [internet]. *J Stat Softw* 2008 [cited 2017 Feb 2]; **25:** 1-54. Available at: http://www.jstatsoft.org/v25/i05/

28. Feldman R, Dagan I, Hirsh H. Mining text using keyword distributions. *J Intell Inf Syst* 1998; **10:** 281-300. doi: 10.1023/A:1008623632443

29. Godnov U, Redek T. Application of text mining in tourism: case of Croatia. *Ann Tour Res* 2016; 58: 162-6. doi: 10.1016/j.annals.2016.02.005

30. Liu B. *Sentiment analysis and opinion mining*. San Rafael, Calif.: Morgan & Claypool Publishers; 2012. p. 180.

31. Benoit K, Watanabe K, Wang H, Nulty P, Obeng A, Müller S, et al. quanteda: an R package for the quantitative analysis of textual data. *J Open Source Soft* 2018; **3:** 774. doi: 10.21105/joss.00774 P

32. Centre for Science and Technology Studies. VOSviewer. Visualizing scientific landscapes [Internet]. *VOSviewer* 2021 [cited 2021 Mar 7]. Available at: https://www.vosviewer.com//

33. Arozullah AM, Calhoun EA, Wolf M, Finley DK, Fitzner KA, Heckinger EA, et al. The financial burden of cancer: estimates from a study of insured women with breast cancer. *J Support Oncol* 2004; **2:** 271-8. PMID: 15328826

34. Bradley CJ, Neumark D, Luo Z, Schenk M. Employment and cancer: findings from a longitudinal study of breast and prostate cancer survivors. *Cancer Invest* 2007; **25:** 47-54. 10.1080/07357900601130664

35. Nash-Stewart CE, Kruesi LM, Del Mar CB. Does Bradford's law of scattering predict the size of the literature in Cochrane reviews? *J Med Libr Assoc* 2012; **100:** 135-8. doi: 10.3163/1536-5050.100.2.013

36. Jagsi R, Pottow JAE, Griffith KA, Bradley C, Hamilton AS, Graff J, et al. Long-term financial burden of breast cancer: experiences of a diverse cohort of survivors identified through population-based registries. *J Clin Oncol* 2014; **32:** 1269-76. doi: 10.1200/JCO.2013.53.0956

37. Jagsi R, Ward KC, Abrahamse PH, Wallner LP, Kurian AW, Hamilton AS, et al. Unmet need for clinician engagement regarding financial toxicity after diagnosis of breast cancer. *Cancer* 2018; **124:** 3668-76. doi: 10.1002/cncr.31532

38. Jagsi R, Hawley ST, Abrahamse P, Li Y, Janz NK, Griggs JJ, et al. Impact of adjuvant chemotherapy on long-term employment of survivors of early-stage breast cancer. *Cancer* 2014; **120:** 1854-62. doi: 10.1002/cncr.28607

39. Sidey-Gibbons C, Pfob A, Asaad M, Boukovalas S, Lin YL, Selber JC, et al. Development of machine learning algorithms for the prediction of financial toxicity in localized breast cancer following surgical treatment. *JCO Clin Cancer Inform* 2021; **5:** 338-47. doi: 10.1200/CCI.20.00088

40. Coroneos CJ, Lin YL, Sidey-Gibbons C, Asaad M, Chin B, Boukovalas S, et al. Correlation between financial toxicity, quality of life, and patient satisfaction in an insured population of breast cancer surgical patients: a single-institution retrospective study. *J Am Coll Surg* 2021; **232:** 253-63. 10.1016/j.jamcollsurg.2020.10.023

41. Wheeler SB, Spencer JC, Pinheiro LC, Carey LA, Olshan AF, Reeder-Hayes KE. Financial impact of breast cancer in black versus white women. *J Clin Oncol* 2018; **36:** 1695-701. doi: 10.1200/JCO.2017.77.6310

42. Greenup RA, Rushing C, Fish L, Campbell BM, Tolnitch L, Hyslop T, et al. Financial costs and burden related to decisions for breast cancer surgery. *J Oncol Pract* 2019; **15:** e666-76. doi: 10.1200/JOP.18.00796

43. Spencer JC, Rotter JS, Eberth JM, Zahnd WE, Vanderpool RC, Ko LK, et al. Employment changes following breast cancer diagnosis: the effects of race and place. *J Natl Cancer Inst* 2020; **112:** 647-50. doi: 10.1093/jnci/djz197

44. Bradley CJ, Bednarek HL, Neumark D. Breast cancer survival, work, and earnings. *J Health Econ* 2002; **21:** 757-79. doi: 10.1016/S0167-6296(02)00059-0

45. Veenstra CM, Wallner LP, Jagsi R, Abrahamse P, Griggs JJ, Bradley CJ, et al. Long-term economic and employment outcomes among partners of women with early-stage breast cancer. *J Oncol Pract* 2017; **13:** e916-26. doi: 10.1200/JOP.2017.023606

46. Jagsi R, Hawley ST, Abrahamse P, Yun Li, Nancy K Janz, Jennifer J Griggs, et al. Impact of adjuvant chemotherapy on long-term employment of survivors of early-stage breast cancer. *Cancer* 2014; **120:** 1854-62. doi: 10.1002/cncr.28607

47. Bensman SJ, Smolinsky LJ. Lotka's inverse square law of scientific productivity: its methods and statistics [Internet]. *arXiv 1601.04950*; 2016 [cited 2024 Feb 18]. Available at: http://arxiv.org/abs/1601.04950

48. Costas R, Bordons M. The h-index: advantages, limitations and its relation with other bibliometric indicators at the micro level. *J Inform* 2007; **1:** 193-203. doi: 10.1016/j.joi.2007.02.001

49. Lauzier S, Maunsell E, Drolet M, Coyle D, Hébert-Croteau N, Brisson J, et al. Wage losses in the year after breast cancer: extent and determinants among Canadian women. *J Natl Cancer Instit* 2008; **100:** 321-32. doi: 10.1093/jnci/djn028.

50. Gordon L, Scuffham P, Hayes S, Newman B. Exploring the economic impact of breast cancers during the 18 months following diagnosis. *Psychooncology* 2007; 1**6:** 1130-9. doi: 10.1002/pon.1182

51. Meneses K, Azuero A, Hassey L, McNees P, Pisu M. Does economic burden influence quality of life in breast cancer survivors? *Gynecol Oncol* 2012; **124:** 437-43. doi: 10.1016/j.ygyno.2011.11.038

52. Zha H. Generic summarization and keyphrase extraction using mutual reinforcement principle and sentence clustering [internet]. 2002. [cited 2024 Mar 16]. Available at: https://citeseerx.ist.psu.edu/document?repid=rep1&type=pdf&doi=42e0376c29ad9510464b7a643a49cfc3b60c2cad

53. Montero AJ, Eapen S, Gorin B, Adler P. The economic burden of metastatic breast cancer: a U.S. managed care perspective. *Breast Cancer Res Treat* 2012; **134:** 815-22. doi: 10.1007/s10549-012-2097-2

54. Max W, Sung HY, Stark B. The economic burden of breast cancer in California. *Breast Cancer Res Treat* 2009; **116:** 201-7. doi: 10.1007/s10549-008-0149-4

55. Wadasadawala T, Sen S, Watekar R, Rane P, Sarin R, Gupta S, et al. Economic distress of breast cancer patients seeking treatment at a tertiary cancer center in Mumbai during COVID-19 pandemic: a cohort study. *Asian Pac J Cancer Prev* 2021; **22:** 793-800. doi: 10.31557/APJCP.2021.22.3.793

56. Chapman B, Swainston J, Grunfeld EA, Derakshan N. COVID-19 outbreak effects on job security and emotional functioning amongst women living with breast cancer. *Front Psychol* 2020; **11:** 582014. doi: 10.3389/fpsyg.2020.582014

57. Boyages J, Xu Y, Kalfa S, Koelmeyer L, Parkinson B, Mackie H, et al. Financial cost of lymphedema borne by women with breast cancer. *Psychooncology* 2017; **26:** 849-55. doi: 10.1002/pon.4239

58. Foster TS, Miller JD, Boye ME, Blieden MB, Gidwani R, Russell MW. The economic burden of metastatic breast cancer: a systematic review of literature from developed countries. *Cancer Treat Rev* 2011; **37:** 405-15. doi: 10.1016/j.ctrv.2010.12.008

59. Lamerato L, Havstad S, Gandhi S, Jones D, Nathanson D. Economic burden associated with breast cancer recurrence: findings from a retrospective analysis of health system data. *Cancer* 2006; **106:** 1875-82. doi: 10.1002/cncr.21824

60. Jing J, Feng R, Zhang X, Li M, Gao J. Financial toxicity and its associated patient and cancer factors among women with breast cancer: a single-center analysis of low-middle income region in China. *Breast Cancer Res Treat* 2020; **181:** 435-43. doi: 10.1007/s10549-020-05632-3

61. Ruan J, Liu C, Yang Z, Kuang Y, Yuan X, Qiu J, et al. Suffering and adjustment: a grounded theory of the process of coping with financial toxicity among young women with breast cancer. *Support Care Cancer* 2024; **32:** 96. doi: 10.1007/s00520-024-08305-9

62. Rumrill PD, Nutter DL, Hennessey M, Ware ME. Job retention and breast cancer: employee perspectives and implications for rehabilitation planning. *Work* 1998; **10:** 251-9. doi: 10.3233/WOR-1998-10306

63. Monteiro I, Morais S, Costa AR, Lopes-Conceição L, Araújo N, Fontes F, Dias T, Pereira S, Lunet N. Changes in employment status up to 5 years after breast cancer diagnosis: a prospective cohort study. *Breast* 2019; **48:** 38-44. doi: 10.1016/j.breast.2019.07.007

64. Witte J, Mehlis K, Surmann B, Lingnau R, Damm O, Greiner W, et al. Methods for measuring financial toxicity after cancer diagnosis and treatment: a systematic review and its implications. *Ann Oncol* 2019; **30:** 1061-70. doi: 10.1093/annonc/mdz140

65. Zafar SY, Peppercorn JM, Schrag D, Taylor DH, Goetzinger AM, Zhong X, et al. The financial toxicity of cancer treatment: a pilot study assessing out-of-pocket expenses and the insured cancer patient's experience. *Oncologist* 2013; **18:** 381-90. doi: 10.1634/theoncologist

66. Vaalavuo M. The unequal impact of ill health: earnings, employment, and mental health among breast cancer survivors in Finland [Internet]. *Labour Econ* 2021 [cited 2024 Mar 17]; **69:** 101967. doi: 10.1016/j.labeco.2021.101967. Available at: https://www.scopus.com/inward/record.uri?eid=2-s2.0-85100212299&doi=10.1016%2fj.labeco.2021.101967&partnerID=40&md5=0676064fbcadefe09abdd1671fda55d0

67. Gilligan AM, Alberts DS, Roe DJ, Skrepnek GH. Death or debt? National estimates of financial toxicity in persons with newly-diagnosed cancer. *Am J Med* 2018; **131:** 1187-99.e5. doi: 10.1016/j.amjmed.2018.05.020

68. Ng AP, Sanaiha Y, Verma A, Lee C, Akhavan A, Cohen JG, et al. Insurance-based disparities and risk of financial toxicity among patients undergoing gynecologic cancer operations. *Gynecol Oncol* 2022; **166:** 200-6. doi: 10.1016/j.ygyno.2022.05.017

69. Chan R, Cooper B, Paul S, Conley Y, Kober K, Koczwara B, et al. Distinct financial distress profiles in patients with breast cancer prior to and for 12 months following surgery. *BMJ Support Palliat Care* 2022; **12:** 347-354. doi: 10.1136/bmjspcare-2020-002461

70. Chan RJ, Cooper B, Gordon L, Hart N, Tan CJ, Koczwara B, et al. Distinct employment interference profiles in patients with breast cancer prior to and for 12 months following surgery. *BMC Cancer* 2021; **21:** 883. doi: 10.1186/s12885-021-08583-0

71. Chan RJ, Cooper B, Koczwara B, Chan A, Tan CJ, Paul SM, et al. A longitudinal analysis of phenotypic and symptom characteristics associated with inter-individual variability in employment interference in patients with breast cancer. *Support Care Cancer* 2020; **28:** 4677-86. doi: 10.1007/s00520-020-05312-4

72. Chan RJ, Cooper B, Koczwara B, Chan A, Tan CJ, Gordon L, et al. Characteristics associated with inter-individual variability in financial distress in patients with breast cancer prior to and for 12 months following surgery. *Support Care Cancer* 2022; **30:** 1293-302. doi: 10.1007/s00520-021-06524-y

73. Mollica MA, Zaleta AK, Gallicchio L, Brick R, Jacobsen PB, Tonorezos E, et al. Financial toxicity among people with metastatic cancer: findings from the Cancer Experience Registry. *Support Care Cancer* 2024; **32:** 137. doi: 10.1007/s00520-024-08328-2

74. Ribi K, Pagan E, Sala I, Ruggeri M, Bianco N, Bucci EO, et al. Employment trajectories of young women with breast cancer: an ongoing prospective cohort study in Italy and Switzerland. *J Cancer Surviv* 2023; **17:** 1847-58. doi: 10.1007/s11764-022-01222-y

75. Dumas A, Luis IV, Bovagnet T, El Mouhebb M, Di Meglio A, Pinto S, et al. Impact of breast cancer treatment on employment: results of a multicenter prospective cohort study (CANTO). *J Clin Oncol* 2020; **38:** 734-43. doi: 10.1200/JCO.19.01726

76. Foster TS, Miller JD, Boye ME, Blieden MB, Gidwani R, Russell MW. The economic burden of metastatic breast cancer: a systematic review of literature from developed countries. *Cancer Treat Rev* 2011; **37:** 405-15. doi: 10.1016/j.ctrv.2010.12.008

77. Kuper H, Yang L, Theorell T, Weiderpass E. Job strain and risk of breast cancer. *Epidemiology* 2007; **18:** 764-8. doi: 10.1097/EDE.0b013e318142c534

78. Desai A, Gyawali B. Financial toxicity of cancer treatment: moving the discussion from acknowledgement of the problem to identifying solutions. *eClinicalMedicine* [Internet]. 2020 [cited 2024 Mar 21]; **20:** 100269. doi: 10.1016/j.eclinm.2020.100269. Available at: https://www.thelancet.com/journals/eclinm/article/PIIS2589-5370(20)30013-4/fulltext

79. Winkler EC, Mehlis K, Surmann B, Witte J, Lingnau R, Apostolidis L, et al. Financial toxicity in German cancer patients: how does a chronic disease impact the economic situation? 43rd ESMO Congress (ESMO). *Ann Oncol* 2018; **29(Suppl 8):** 568. doi: 10.1093/annonc/mdy424.079

80. Witte J, Mehlis K, Surmann B, Lingnau R, Damm O, Greiner W, et al. Methods for measuring financial toxicity after cancer diagnosis and treatment: a systematic review and its implications. *Ann Oncol* 2019; **30:** 1061-70. doi: 10.1093/annonc/mdz140

81. Cheng H, Lin L, Liu T, Wang S, Zhang Y, Tian L. Financial toxicity of breast cancer over the last 30 years: a bibliometrics study and visualization analysis via CiteSpace. *Medicine* 2023; **102:** e33239. doi: 10.1097/MD.0000000000033239

82. Donthu N, Kumar S, Mukherjee D, Pandey N, Lim WM. How to conduct a bibliometric analysis: an overview and guidelines. *J Bus Res* 2021; **133:** 285-96. doi: 10.1016/j.jbusres.2021.04.070

83. FACIT.org. FACIT-COST. COST: a FACIT measure of financial toxicity [Internet]. FACIT Group. 2024 [cited 2024 Mar 21]. Available at: https://www.facit.org/measures/facit-cost

research article

Early-time-point ^{18}F-FDG-PET/CT and other prognostic biomarkers of survival in metastatic melanoma patients receiving immunotherapy

Nezka Hribernik[1,2], Katja Strasek[3], Andrej Studen[3,6], Katarina Zevnik[7], Katja Skalic[7], Robert Jeraj[3,4,5,6], Martina Rebersek[1,2]

[1] Department of Medical Oncology, Institute of Oncology Ljubljana, Ljubljana, Slovenia
[2] Faculty of Medicine, University of Ljubljana, Ljubljana, Slovenia
[3] Faculty of Mathematics and Physics, University of Ljubljana, Ljubljana, Slovenia
[4] University of Wisconsin Carbone Cancer Centre, Madison, WI, USA
[5] Department of Medical Physics, University of Wisconsin-Madison, Madison, WI, USA
[6] Experimental Particle Physics Department, Jozef Stefan Institute, Ljubljana, Slovenia
[7] Department of Nuclear Medicine, Institute of Oncology Ljubljana, Ljubljana, Slovenia

Radiol Oncol 2025; 59(1): 43-53.

Received 12 December 2024
Accepted 4 January 2025

Correspondence to: Assoc. Prof. Martina Reberšek, M.D., Ph.D., Department of Medical Oncology, Institute of Oncology Ljubljana, Zaloška 2, SI-1000 Ljubljana, Slovenia. E-mail: mrebersek@onko-i.si

Disclosure: Robert Jeraj is a cofounder and CSO of AIQ Solutions, Madison, WI, USA. Funding. No potential conflicts of interest are disclosed by the other co-authors.

Background. A considerable proportion of metastatic melanoma (mM) patients do not respond to immune checkpoint inhibitors (ICIs). There is a great need to develop noninvasive biomarkers to detect patients, who do not respond to ICIs early during the course of treatment. The aim of this study was to evaluate the role of early [^{18}F]2fluoro-2-deoxy-D-glucose PET/CT (^{18}F-FDG PET/CT) at week four (W4) and other possible prognostic biomarkers of survival in mM patients receiving ICIs.

Patients and methods. In this prospective noninterventional clinical study, mM patients receiving ICIs regularly underwent ^{18}F-FDG PET/CT: at baseline, at W4 after ICI initiation, at week sixteen and every 16 weeks thereafter. The tumor response to ICIs at W4 was assessed via modified European Organisation for Research and Treatment of Cancer (EORTC) criteria. Patients with progressive metabolic disease (PMD) were classified into the no clinical benefit group (no-CB), and those with other response types were classified into the clinical benefit group (CB). The primary end point was survival analysis on the basis of the W4 ^{18}F-FDG PET/CT response. The secondary endpoints were survival analysis on the basis of LDH, the number of metastatic localizations, and immune-related adverse events (irAEs). Kaplan-Meier analysis and univariate Cox regression analysis were used to assess the impact on survival.

Results. Overall, 71 patients were included. The median follow-up was 37.1 months (95% CI = 30.1–38.0). Three (4%) patients had only baseline scans due to rapid disease progression and death prior to W4 ^{18}F-FDG-PET/CT. Fifty-one (72%) patients were classified into the CB group, and 17 (24%) were classified into the no-CB group. There was a statistically significant difference in median overall survival (OS) between the CB group (median OS not reached [NR]; 95% CI = 17.8 months – NR) and the no-CB group (median OS 6.2 months; 95% CI = 4.6 months – NR; p = 0.003). Univariate Cox analysis showed HR of 0.4 (95% CI = 0.18 – 0.72; p = 0.004). median OS was also significantly longer in the group with normal serum LDH levels and the group with irAEs and cutaneous irAEs.

Conclusions. Evaluation of mM patients with early ^{18}F-FDG-PET/CT at W4, who were treated with ICIs, could serve as prognostic imaging biomarkers. Other recognized prognostic biomarkers were the serum LDH level and occurrence of cutaneous irAEs.

Key words: early time-point ^{18}F-FDG-PET/CT; prognostic biomarkers; immune-related adverse effects metastatic melanoma; immune-checkpoint inhibitor

Introduction

Immunotherapy with immune checkpoint inhibitors (ICIs) has greatly impacted the treatment landscape of metastatic melanoma (mM) patients. Final, 10-year results from pivotal randomized clinical trial have shown ongoing benefits, with 10-year overall survival (OS) rates of 34%, 37%, and 43% in mM patients receiving pembrolizumab, nivolumab, and ipilimumab/nivolumab, respectively.[1,2] However, a considerable proportion of mM patients do not respond to ICIs.

Normal serum levels of lactate dehydrogenase (LDH) and a small number of organs with metastatic involvement are two very strong and well-recognized prognostic biomarkers of better survival in mM patients.[3-5] In addition, immune-related adverse events (irAEs) have been proven in some studies to be biomarkers of improved response rates and longer survival in patients treated with ICIs.[6,7] Specifically, endocrine and cutaneous irAEs were associated with favourable survival outcomes compared with patients without this type of irAE in a large retrospective multicohort study.[6] There is a great need to develop other non-invasive imaging biomarkers (IBM) to detect mM patients who do not respond to ICIs early in the course of treatment.

Positron emission tomography/computed tomography with [^{18}F]2fluoro-2-deoxy-D-glucose PET/CT (^{18}F-FDG PET/CT) is a noninvasive method that combines anatomical and functional data. It is generally used as a diagnostic tool for the staging of melanoma patients and is now gaining valuable value in immunotherapy treatment response evaluation and prognosticating outcomes.[7,8] In addition to staging and response monitoring, ^{18}F-FDG PET/CT has also shown some potential for detecting immune-related side effects (irAEs), such as the use of organ ^{18}F-FDG uptake, quantified by percentiles of standardized uptake values (SUV) distribution as a quantitative IBM of irAEs.[9-11]

The optimal timing of the first on-treatment ^{18}F-FDG PET/CT evaluation of mM patients on ICIs is a matter of ongoing investigations. Joint EANM/SNMMI/ANZSNM practice guidelines/procedure standards recommended an interim ^{18}F-FDG PET/CT scan during immunomodulatory treatment in patients with solid tumors at 8–12 weeks after the start of treatment (i.e., after 3–4 cycles of immunotherapy).[7] However, there are studies analysing ^{18}F-FDG PET/CT scans performed earlier after ICI initiation. In a prospective study with 20 mM patients treated with ipilimumab, ^{18}F-FDG PET/CT was performed between 21-28 days after treatment start. They concluded that the combination of changes in lesion dimensions along with changes in ^{18}F-FDG uptake may be associated with immune activation and a favourable outcome.[12]

We previously reported the results of our prospective study regarding the role of quantitative IBM in early ^{18}F-FDG PET/CT, which was performed four weeks after ICI initiation, for the detection of immune-related adverse events in melanoma patients.[10] Here, we evaluated the role of early ^{18}F-FDG-PET/CT at week four and other possible prognostic biomarkers of survival in mM patients receiving ICIs.

Patients and methods

Patients

We enrolled patients 18 years of age or older who had histologically confirmed, unresectable, advanced melanoma and were planned to be treated per standard of care with ICIs with anti-cytotoxic T-lymphocyte-associated antigen 4 (anti-CTLA-4) and/or anti-programmed death-1 (anti-PD-1) treatment in the first or second line of systemic treatment at the Institute of Oncology Ljubljana, Slovenia. The key exclusion criteria included symptomatic brain metastases and malignant diseases other than melanoma.

Trial design

In this noninterventional, prospective study, patients underwent baseline ^{18}F-FDG PET/CT within four weeks before treatment initiation and were monitored regularly with serial ^{18}F-FDG PET/CT: at week four (W4) (+/- 5 days), week 16 (W16) (+/- 7 days), and week 32 (W32) (+/- 7 days) after treatment initiation and every 16 weeks thereafter. The first follow-up ^{18}F-FDG PET/CT at W4 was performed for investigational purposes and was not necessarily used to guide treatment decisions. The clinical data and images included in this analysis were obtained from disease diagnosis up to 1st September 2024.

All ^{18}F-FDG PET/CT data were acquired before and during ICI treatment, and all clinical data were collected for review. The irAE grade was assigned prospectively and scored with the use of the National Cancer Institute Common Terminology Criteria for Adverse Events (CTCAE, v.5.0).[13] The irAE were classified as serous irAE in case of higher grade of irAE of 3 and above. Imaging and clini-

cal data were anonymized and stored in a secure LabKey database server.[14]

The clinical protocol was approved by the Ethics Committee ERIDEK-0034/2020 and the Clinical Trials Protocol Review Committee ERID-KSOPKR-0032/2020 at the Institute of Oncology Ljubljana and by the Commission of the Republic of Slovenia for Medical Ethics (approval number: 0120-256/2020-14, September 15th 2020). It was conducted following the ethical standards defined by the Declaration of Helsinki and the International Conference on Harmonization Guidelines for Good Clinical Practice. The study was registered with ClinicalTrials.gov under the registration number NCT06207747.

The study was conducted with the acknowledgment and consent of the subjects. All patients provided signed informed consent for treatment and consent allowing the use of their data for scientific purposes.

^{18}F-FDG PET/CT acquisition and analysis

All ^{18}F-FDG PET/CT scans were obtained on Biograph mCT PET/CT (Siemens, Knoxville, TN). Imaging protocol required patients to fast for 6 hours prior to injection of the radiotracer and have a blood glucose level below 10 mmol/L at the time of the scan. Patients were required to hold all diabetic medication, including metformin, for 6 hours prior to radiotracer injection. All scans were acquired per standard of care. CT that meets response evaluation criteria in solid tumours (RECIST) analysis needs was acquired according to adjusted protocol including sinogram affirmed iterative reconstruction (SAFIR) to minimize dose. Following reconstruction, PET images were normalized by patient weight and injected dose to compute SUV. More details about image acquisition can be found in our previous paper, where the same cohort of patients was used for analysis.[11]

The tumor response to ICIs on ^{18}F-FDG PET/CT was evaluated by a nuclear medicine specialist combining the European Organisation for Research and Treatment of Cancer (EORTC) criteria and visual response assessment.[15] The SUV_{max} and size of the lesions were measured in all most representative tumor lesions, which are the largest lesions of a certain area or organ with the highest FDG uptake at baseline, W4 and all consecutive ^{18}F-FDG PET/CT scans. Patients were classified into four major categories on the basis of the tumor response to ICIs: complete metabolic response (CMR), partial metabolic response (PMR), stable

TABLE 1. Patient demographics, cancer staging, treatment details, and outcomes

Characteristics	No = 71 (%)
Age; mean (+/-SD) (yr)	62 ± 12
Gender	
Male	43 (61)
Female	28 (39)
ECOG performance status	
0	30 (42)
1	41 (58)
AJCC	
III.D	1 (1)
M1a	16 (23)
M1b	10 (14)
M1c	32 (45)
M1d	12 (17)
Anatomic site of primary	
Cutaneous	58 (82)
Ocular	4 (6)
Mucosal	3 (4)
Unknown primary	6 (8)
Line of systemic treatment for metastatic disease	
1st line	63 (89)
2nd line	8 (11)
Baseline LDH	
Elevated	23 (32)
Normal	49 (68)
Number of organs with metastatic involvement	
1	25 (35)
2	21 (30)
3	11 (15)
> 3	14 20)
Actionable mutation	
BRAF wild type	21 (30)
BRAF V600E	28 (39)
BRAF V600K	10 (14)
BRAF V600 - others	1 (1)
NRAS	11 (16)
Type of systemic treatment	
PD-1 inhibitors	47 (66)
Combination of PD-1 and CTLA-4 inhibitors	24 (34)
Tumor response on week 4 ^{18}F-FDG PET/CT	
Complete metabolic response	3 (4)
Partial metabolic response	12 (17)
Stable metabolic disease	10 (14)
Heterogenous response	6 (8)
Possible pseudoprogression	20 (28)
Progressive metabolic disease	17 (24)

AJCC = American Joint Classification of Cancer; BRAF = V-Raf murine sarcoma viral oncogene homolog B; CTLA-4 = Cytotoxic T lymphocyte-associated antigen 4; ECOG = Eastern Cooperative Oncology Group; ICI = Immune checkpoint inhibitors; No = number of patients; NRAS = neuroblastoma RAS viral homolog; PD-1 = programmed death-1; SD = standard deviation

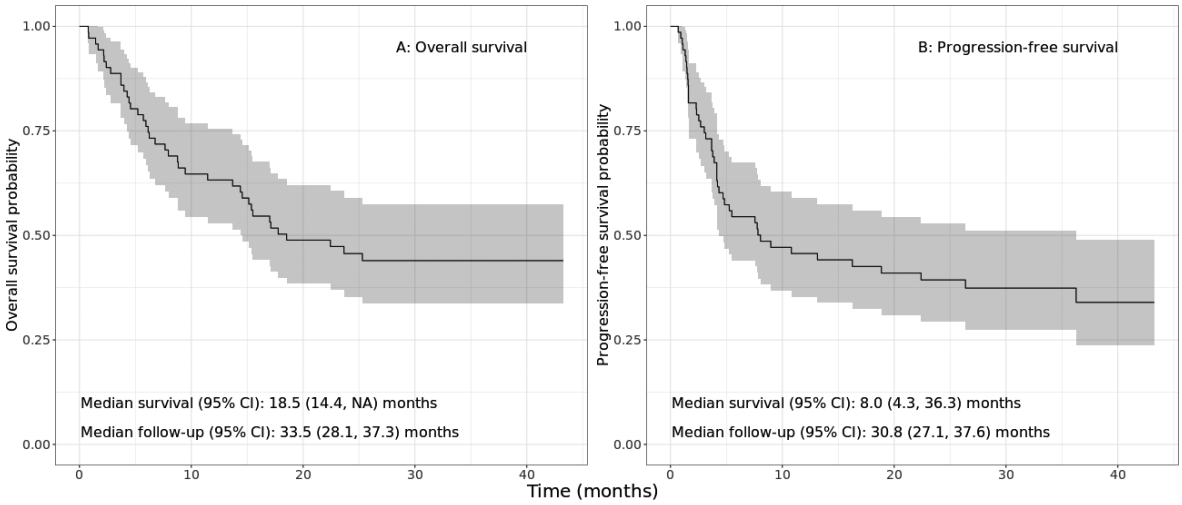

FIGURE 1. Kaplan-Meier curves show overall survival (OS) probability **(A)** and progression-free survival (PFS) probability **(B)** over time in patients with metastatic melanoma treated with immune checkpoint inhibitors. The grey shading reflects the 95% confidence interval.

metabolic disease (SMD) and progressive metabolic disease (PMD).[15] According to the information gathered after the whole -body ^{18}F-FDG PET/CT visual assessment, two new categories, of heterogenous response (HGR) and possible pseudoprogressive disease (PPD), were added for tumor response evaluation. HGR was assigned when multiple lesions were variably meeting the criteria of PMD, SMD, PMR and CMR and could not be classified into only one response evaluation category. PPD was assigned in the case of moderate metabolic progression of the baseline tumor lesions with few locally distributed new lesions. Obvious progression with multiple new tumor lesion sites was classified as true progression (PMD). The patients were further stratified into two groups: patients with PMD were classified into the no clinical benefit (no-CB) group and patients with other response categories into the clinical benefit (CB) group. A summary of the response criteria is presented in Supplementary Table 1.

Outcomes and statistical analysis

The primary end point of this study was the analysis of median OS based on the W4 ^{18}F-FDG PET/CT response. The secondary endpoint was the median OS, which was analysed on the basis of the level of LDH, the number of organs with metastatic involvement at the beginning of ICI treatment, occurrence of irAE, higher irAE, cutaneous irAEs, endocrine irAEs and immune-related thyroiditis (irThyroiditis).

Patient characteristics were summarized via descriptive statistics. Survival analysis was performed via the Kaplan–Meier method, and 95% confidence intervals (CIs) were calculated. The associations of each of the eight metrics with OS were assessed with a univariate Cox proportional hazard model. With the use of the Bonferroni correction for testing multiple hypothesis, probability values $p < 0.006$ were considered statistically significant.

Results

From September 2020 through September 2022, a total of 71 patients were enrolled. The characteristics of the patients are summarized in Table 1. At the cut-off date of the observational period for this analysis on 1st September 2024, the median follow-up was 37.1 months (95% CI = 30.1-38.0). The median duration of ICI therapy was 10.2 months (range: 1-39.4 months). Three (4%) patients had only baseline scans due to rapid disease progression and death prior to W4 ^{18}F-FDG-PET/CT. The timing of ^{18}F-FDG PET/CT relative to ICI treatment initiation and the number of ^{18}F-FDG-PET/CT images are shown in the Supplementary Table 2.

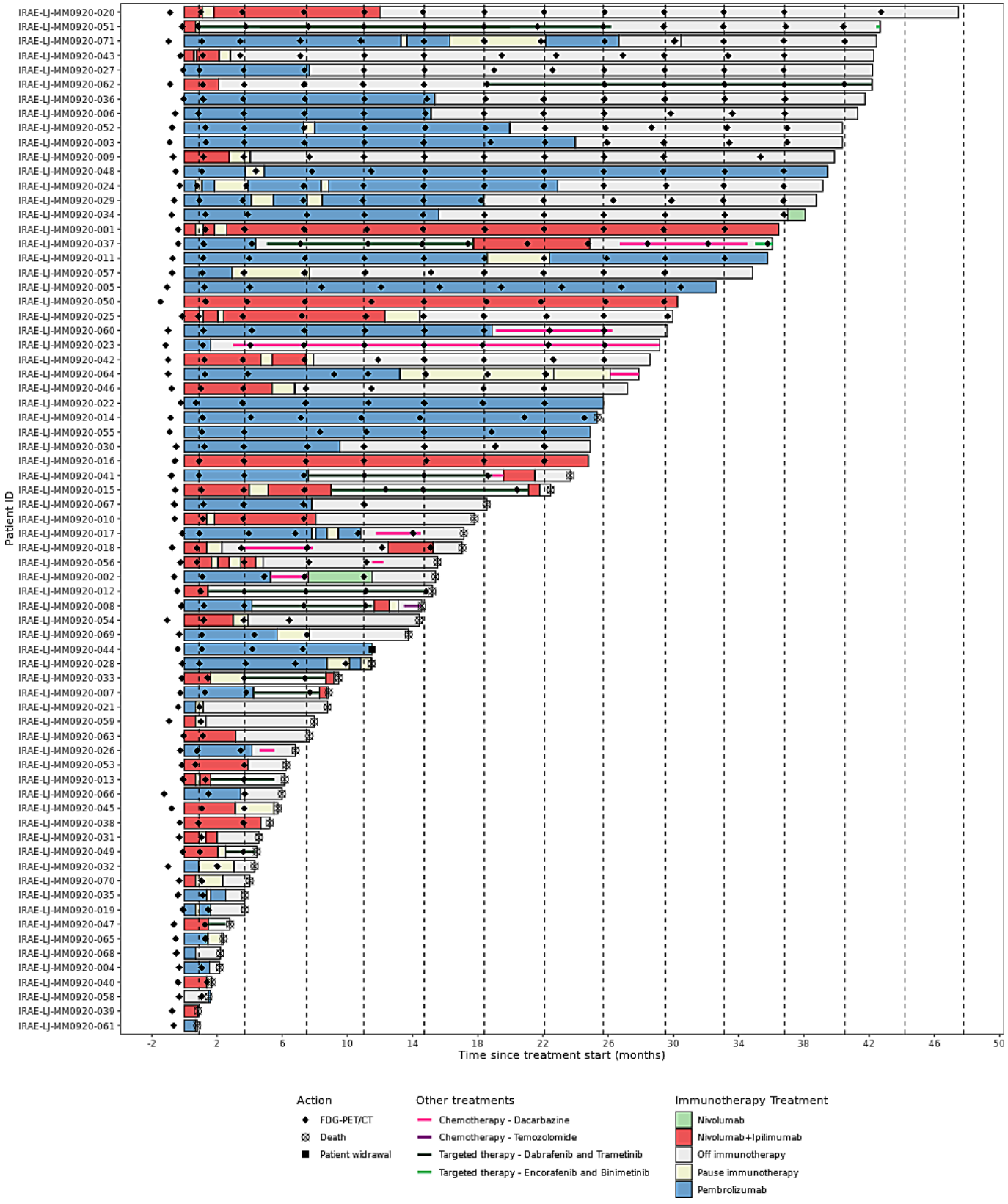

FIGURE 2. Swimmer plot shows individual patient's treatment progression in each horizontal line. Colourful bars and lines indicate type and duration of treatment, while dots indicate specific action - ^{18}F-FDG-PET/CT imaging or reason for end-of-study (if applicable). Vertical dashed lines indicate a time when ^{18}F-FDG-PET/CT scan should be performed for patients in this study.

TABLE 2. Clinical diagnosis of immune-related adverse events

Immune-related adverse event	Any grade No (%)	Grade 3-5 No (%)	Time to onset of irAE (mean ± SD) [weeks]
No. of pts with at least one irAE	56 (79)	13 (18)	-
Number of all irAE events	144	14	144 ± 161
Gastrointestinal			
Diarrhea	14 (20)	2 (3)	31.7 ± 30.6
Colitis	7 (10)	2 (3)	39 ± 32
Xerostomia	2 (3)	0	30.1 ± 4.4
Gastritis	2 (3)	0	64.4 ± 7.7
Stomatitis	1 (1)	0	3 ± 0
Respiratory			
Pneumonitis	5 (7)	0 (0)	40.9 ± 45.7
Sarcoid reaction	2 (3)	0 (0)	6.3 ± 0.3
Hepatic			
Increased AST/ALT	16 (23)	4 (6)	7.7 ± 8.3
Endocrine			
Hypothyroidism	10 (14)	0	12.3 ± 6
Hyperthyroidism	7 (10)	0	7.3 ± 7.1
Adrenal insufficiency	2 (3)	2 (3)	34.4 ± 20.1
Diabetes mellitus	1 (1)	1 (1)	72.7 ± 0
Pancreatitis	1 (1)	1 (1)	32.4 ± 0
Cutaneous			
Pruritus	23 (32)	0	10.7 ± 10
Skin rash	16 (23)	0	14 ± 16.3
Vitiligo	9 (13)	0	37.4 ± 31.6
Poliosis of hair	1 (1)	0	34.7 ± 0
Musculoskeletal			
Arthritis	10 (14)	0	28.7 ± 27.3
Myalgia	2 (3)	0	16.7 ± 12.3
Arthralgia	1 (1)	0	14 ± 0
Synovitis	1 (1)	0	65.4 ± 0
Neurological			
Encephalitis	2 (3)	1 (1)	36.4 ± 32.9
Psychosis	1 (1)	0	25.4 ± 0
Other			
Fatigue	6 (8)	0	6.5 ± 4.9
Hypophosphatemia	1 (1)	0	17 ± 0

AST/ALT = aspartate transaminase / alanín aminotransferaza; irAE = immune-related adverse events

Survival outcomes

The Kaplan–Meier estimated OS and progression-free survival (PFS) for the whole patient group were 18.5 months (95% CI = 14.4 months – not reached [NR]) and 8.1 months (95% CI = 4.3–26.3 months), respectively (Figure 1). Among the whole group, 39 (55%) patients died, and 44 (62%) patients progressed to immunotherapy before the cut-off date. On Figure 2, the swimmer plot displays data for individual patients, where each horizontal line or bar shows type and duration of treatment, and each point represents either ^{18}F-FDG-PET/CT or end-of-study reason (if applicable).

W4 ^{18}F-FDG PET/CT and survival outcomes

Among the 68 (96%) patients who underwent W4 ^{18}F-FDG PET/CT, 51 (72%) patients were classified into the CB group, and 17 (24%) were classified into the no-CB group. The median OS was not reached (NR) (95% CI = 17.8 months - NR) in the CB group and was 6.2 months (95% CI = 4.6 months - NR) in the no-CB group (Figure 3). In univariate Cox analysis classification was statistically significantly correlated to OS with hazard ratio (HR) of 0.4 (95% CI = 0.18–0.72; p = 0.004).

Among the 17 patients with PMD, who were classified into the no-CB group, 7 (42%) died before the W16 ^{18}F-FDG PET/CT scan. Three (18%) patients had PMD on W16 ^{18}F-FDG PET/CT, 6 (35%) had PMR, and one (6%) patient had CMR. Two (12%) patients with PMD on W4 ^{18}F-FDG PET/CT changed systemic therapy from ICI therapy to targeted therapy because of clinical and radiological signs of rapid progression affecting vital organs.

Three patients were classified as CMR on W4 ^{18}F-FDG PET/CT. One patient achieved a durable response with CMR, one patient experienced fatal grade 5 immune-related encephalitis during treatment and one experienced local progression in soft tissues 25 months after CMR imaging on W4 ^{18}F-FDG PET/CT. The site of progression was amenable for local treatment with radiotherapy, and a complete metabolic response was achieved.

In Figure 4, the alluvial plot shows the responses on ^{18}F-FDG PET/CT scans for each patient at week 4, 16, 48 and 96.

Other biomarkers and survival outcomes

LDH and the number of organs with metastatic involvement

Twenty-three (32%) patients had elevated serum LDH at ICI initiation. The median OS of patients with normal LDH levels was NR (95% CI = 17.8 months - NR), and that of patients with elevated

LDH levels was 6.5 months (95% CI = 4.0 months - NR). The difference in OS was statistically significant between these two groups (p = 0.004) (Figure 5A); Univariate Cox analysis showed a HR = 0.4 (95% CI = 0.21–0.76; p = 0.005).

The difference in OS based on the number of organs with metastatic involvement was not statistically significant (p = 0.094) (Figure 5B).

Immune-related adverse events (irAEs)

Among the 71 included patients, 56 (79%) developed irAEs, including 13 (18%) with grade 3 or higher irAEs. All irAE, their number and time to onset, are presented in Table 2. One (2%) patient died of immune-related encephalitis. Due to irAEs, 7 (10%) patients were hospitalized. Three (4%) patients were diagnosed with autoimmune disease prior to ICI initiation: one had vitiligo, one had scalp psoriasis, and one was diagnosed with rheumatoid arthritis at the time of ICI initiation. None of them experienced an exacerbation of their autoimmune disease or needed special treatment for that reason.

The median OS was 25.3 months (95% CI = 17 months - NR) in patients with irAEs and 4.6 months (95% CI = 3.7 months - NR) in patients without irAEs (p = 0.004) (Figure 6A). Univariate Cox analysis showed a HR 0.9 (95% CI = 0.18–0.75; p = 0.006). The median OS was not reached (95% CI = 23.7 months - NR) in patients who experienced cutaneous irAEs and was 8.2 months (95% CI = 4.6–17.8) in patients without cutaneous irAEs (p < 0.0001) (Figure 6C); Cox analysis showed a HR 0.36 (95% CI = 0.19–0.66; p = 0.001). Using Kaplan-Meier analysis, a significant statistical difference in OS was not observed between patients with and without higher-grade irAEs (p = 0.783) (Figure 6B), endocrine irAEs (p = 0.7) (Figure 6D) or immune-related thyroiditis (p = 0.711) (Supplementary Figure 1).

Discussion

The evaluation of mM pts with early ^{18}F-FDG-PET/CT at W4, when treated with ICIs, can serve as a survival imaging biomarker (IBM). Based on our results, patients with no-CB at W4 had a shorter survival compared with the CB group (p = 0.001). This was also observed in the study by Cho *et al.*, where early ^{18}F-FDG-PET/CT scans of 20 patients 21–28 days after treatment started showed a predictive role for response. Unlike in our group, patients in their study were mostly treated with the CTLA-4 inhibitor ipilimumab and tumor response was assessed according to RECIST, immune-related response criteria, PERCIST and EORTC criteria.[12] In another study by Anderson *et al.*, ^{18}F-FDG-PET/CT was performed after a single dose of pembrolizumab, at a median of 7 days (range: 3–21 days) after the start of treatment. They concluded that early scan could identify metabolic changes in metastases that are potentially predictive of response to ICIs.[16] Additionally, in recent studies on neoad-

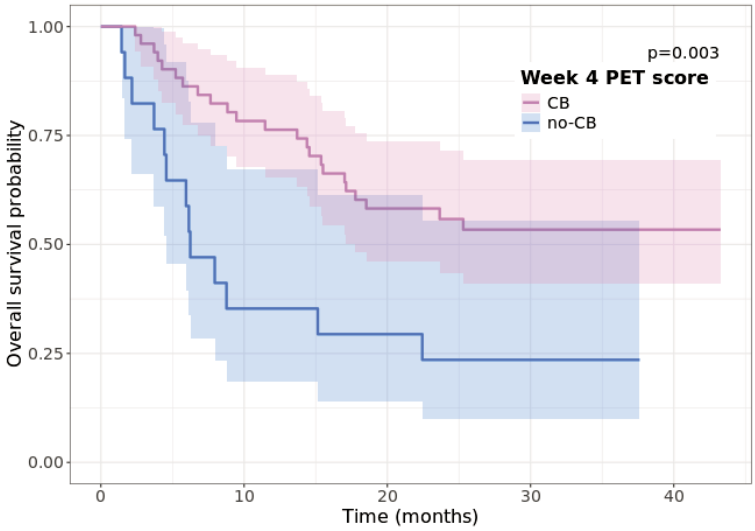

FIGURE 3. Kaplan-Meier curves showing probability of median overall survival (OS) between clinical benefit (CB) and no-CB group as classified by findings on week four (W4) ^{18}F-FDG PET/CT. The curves are statistically significantly different (p = 0.03).

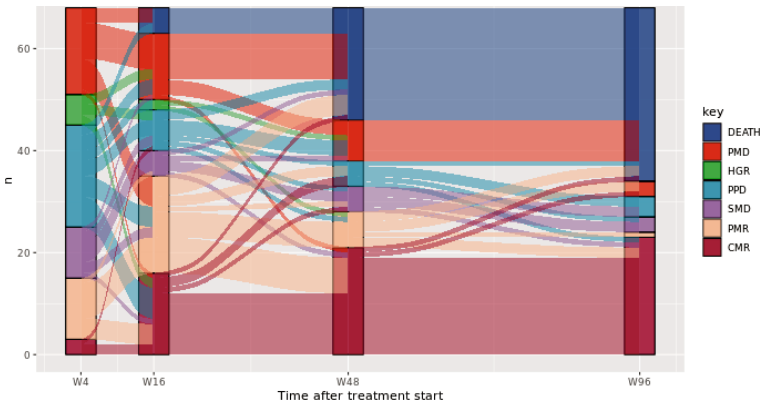

FIGURE 4. Alluvial plot illustrates the flow of patients between different response categories on ^{18}F-FDG PET/CT scan across four evaluation time points: at week 4 (W4), week 16 (W16), week 48 (W48) and week 96 (W96).

CMR = complete metabolic response; HGR = heterogeneous response; PMD = progressive metabolic disease; PPD = pseudoprogressive disease; SMD = stable metabolic disease; PMR = partial metabolic response; n = number of patients

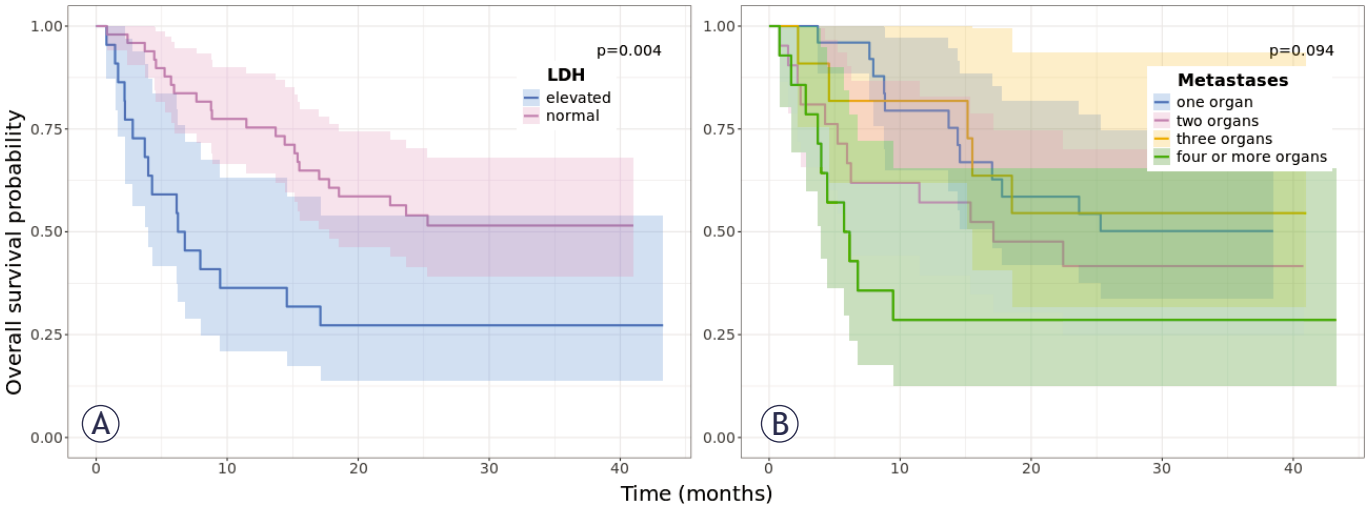

FIGURE 5. Kaplan-Meier curves show the median overall survival (OS) probability of patients with metastatic melanoma treated with immune checkpoint inhibitors according to **(A)** LDH level and **(B)** the number of organs with metastatic involvement. The shading reflects the 95% confidence interval.

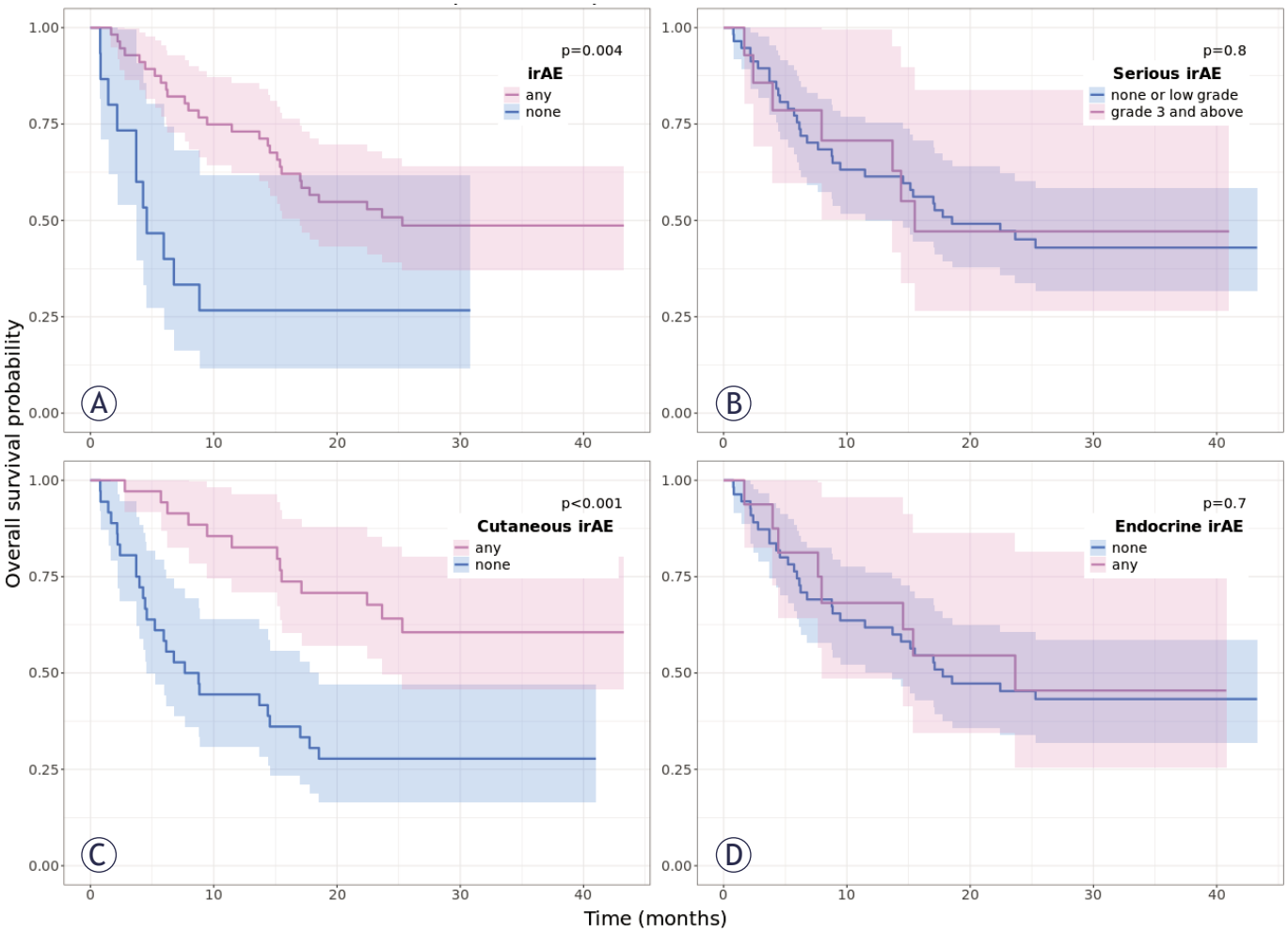

FIGURE 6. Kaplan-Meyer curves of the median overall survival **(OS)** over time in patients with metastatic melanoma treated with immune checkpoint inhibitors according to **(A)** occurrence of immune-related adverse events, **(B)** occurrence of serious immune-related adverse events, **(C)** cutaneous immune-related side effects, **(D)** immune-related endocrine immune-related side effects. The blue and pink shading reflects the 95% confidence intervals for respecting groups.

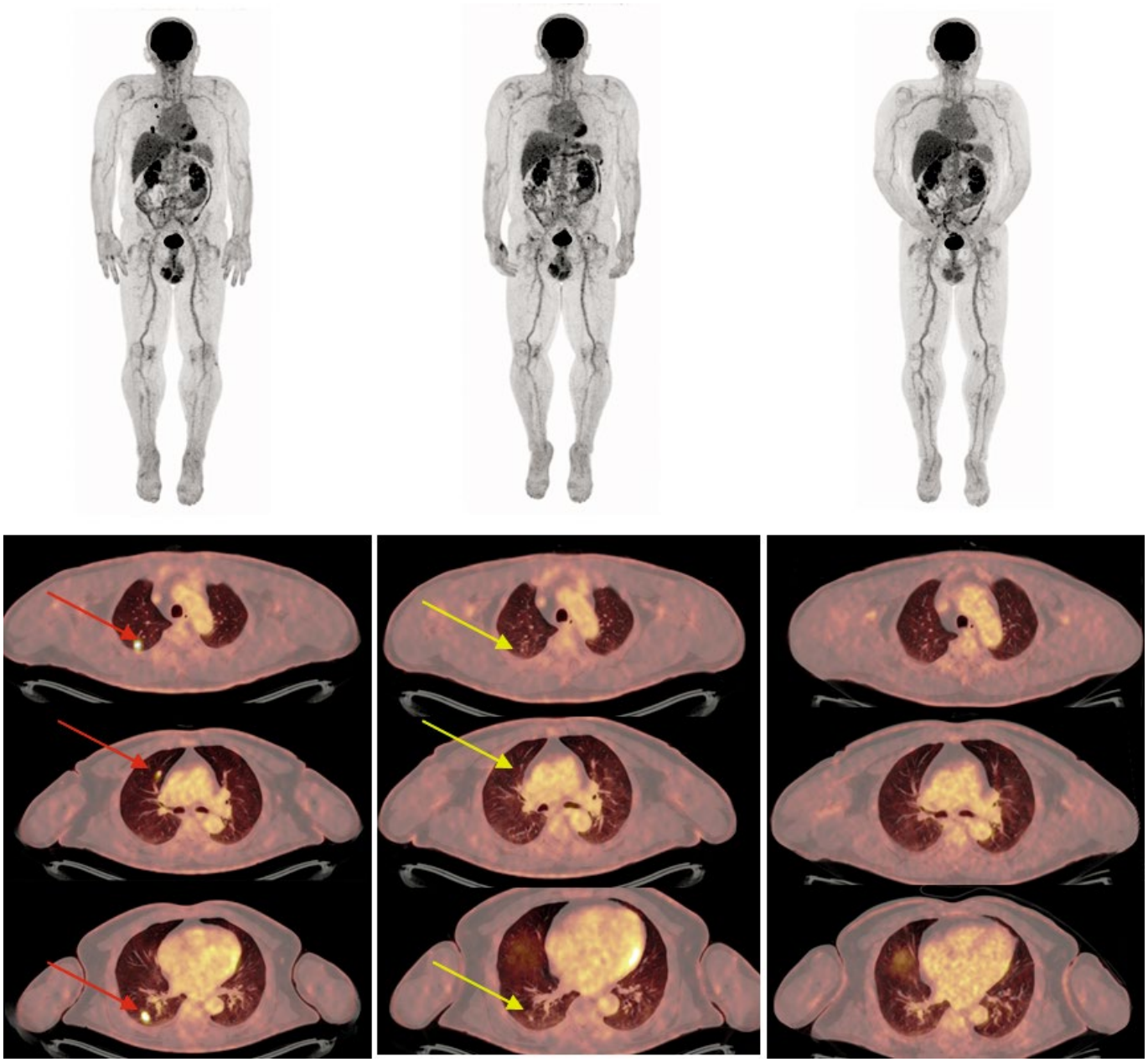

FIGURE 7. A 67-year-old male patient, diagnosed with metastatic NRAS-mutated cutaneous melanoma with lung metastases in January 2021, was treated with pembrolizumab in the first-line setting. Serial 18F-FDG PET/CT scans were obtained per the study protocol. The images above show the maximal intensity projection (MIP) on the baseline PET/CT (left), on the week 4 evaluation PET/CT (middle) and at the endpoint of the study (right). The images below show transverse sections of the lungs in different planes, revealing three FDG-avid metastatic nodules in the right lung (lower left images, red arrows), only small nodules with no FDG uptake on week 4 PET/CT (lower middle images, yellow arrows), a complete metabolic response, and no residual nodules found at the end point of the PET/CT images with persistent complete remission (lower right images).

juvant immunotherapy in melanoma patients, responses were reported as early as two weeks after ICI initiation, and pathological responses were reported at 4-6 weeks after treatment start.[17,18] The use of this strategy with early evaluation is not yet fully understood, but it may lead to new imaging evaluation strategies for patients undergoing immunotherapy.

Seven (10%) patients in our study who were classified as PMD on W4 ^{18}F-FDG-PET/CT showed a later response, as seen on subsequent ^{18}F-FDG PET/CT scans (Figure 4). For this subgroup of patients,

early cessation of ICI therapy has a detrimental effect. More analysis is needed to identify optimal early timepoint scans and to find more specific biomarkers, perhaps using artificial intelligence with automated deep learning-based lesion segmentation, to distinguish patients and lesions that are in progress from those patients who are just late responders to ICIs.[19,20]

^{18}F-FDG-PET/CT seems to play an important role not only at the early beginning of treatment with ICIs at W4 but also later during treatment. In a retrospective analysis of 104 patients with baseline and 1-year CT and PET/CT scans, Dimitriou *et al*. reported that almost all patients with CMR at one year had an ongoing response to ICIs thereafter.[8] In our cohort of patients, most of the patients with CMR at week 42 remained in remission, as shown in the alluvial plot in Figure 4. The case presentation in Figure 5 shows a patient with early and long-lasting CMR.

In our cohort, occurrence of cutaneous irAEs was clearly associated with longer survival. Cutaneous irAEs, especially vitiligo, are more common in patients with melanoma than in other cancers. The higher frequency can be explained by shared immunogenic antigens between healthy tissue and tumors.[21,22] Cutaneous irAEs are usually lower grade and vigorous immunosuppressive management is not necessary; therefore, there is no unfavorable effect of irAE management on ICI efficacy or survival.[22] Contrary to the results from a large retrospective multicohort study[6], our study proved no survival benefit for patients with irThyroiditis or endocrine irAEs, possibly due to the low number of patients with this type of adverse event. Further studies will clarify the prognostic role of this type of irAE.

Our study is limited by not performing analysis of circulating tumor DNA in plasma, not available at Institute of Oncology Ljubljana when the study started, and not using other volumetric PET parameters, like metabolic tumor volume or total lesion glycolysis.[16,23,24] Another limitation of this study is that we did not perform lesion-level response analysis, which would provide even better insights into lesion-level and patient-level response patterns. Regarding response criteria to ICIs, a wide range of criteria have been proposed and compared in recent years: PERCIST, PECRIT, PERCIMT iPERCIST and imPERCIST5.[7,24-26] As further evaluation of these newly proposed criteria is still warranted, our decision was to use standard EORTC criteria, adapted based on recommendations from the EANM/SNMMI/ANZSNM.

Whole-body PET imaging has great potential for future work, especially the use of artificial intelligence.[27] In line with this, our future work will include segmentation of all disease with lesion-by-lesion analysis on W4 and later ^{18}F-FDG-PET/CT images in our cohort of patients. With more in-depth analysis, we hope to identify specific lesions that do not respond to treatment early in the start of the treatment and offer our patients more personalized treatment. Larger, possibly multicenter studies using same steps in analysis are needed to develop new biomarkers, including imaging biomarkers, to guide patient and treatment selection.[28]

Conclusions

The evaluation of mM patients with early ^{18}F-FDG-PET/CT at W4 who were treated with ICIs revealed a strong prognostic IBM. To obtain more information from early ^{18}F-FDG-PET/CT, artificial intelligence will likely play an important role.

Acknowledgments

The research was financially supported by The Slovenian Research Agency (ARIS), grant numbers P3-0321 and P1-0389.

The manuscript was edited by AJE Digital/Curie.

References

1. Wolchok JD, Chiarion-Sileni V, Rutkowski P, Cowey CL, Schadendorf D, Wagstaff J, et al; CheckMate 067 Investigators. Final, 10-Year outcomes with nivolumab plus ipilimumab in advanced melanoma. *N Engl J Med* 2024; **392:** 11-22. doi: 10.1056/NEJMoa2407417

2. Long GV, Carlino MS, McNeil C, Ribas A, Gaudy-Marqueste C, Schachter J, et al. Pembrolizumab versus ipilimumab for advanced melanoma: 10-year follow-up of the phase III KEYNOTE-006 study. *Ann Oncol* 2024; **35:** 1191-9. doi: 10.1016/j.annonc.2024.08.2330

3. Pires da Silva I, Ahmed T, McQuade JL, Nebhan CA, Park JJ, Versluis JM, et al. Clinical models to define response and survival with anti-PD-1 antibodies alone or combined with ipilimumab in metastatic melanoma. *J Clin Oncol* 2022; **40:** 1068-80. doi: 10.1200/JCO.21.01701

4. Schadendorf D, Livingstone E, Zimmer L. Treatment in metastatic melanoma-time to rethink. *Ann Oncol* 2019; **30:** 501-3. doi: 10.1093/annonc/mdz050

5. Hribernik N, Boc M, Ocvirk J, Knez-Arbeiter J, Mesti T, Ignjatovic M, et al. Retrospective analysis of treatment-naive Slovenian patients with metastatic melanoma treated with pembrolizumab - real-world experience. *Radiol Oncol* 2020; **54:** 119-27. doi: 10.2478/raon-2020-0003.

6. Wan G, Chen W, Khattab S, Roster K, Nguyen N, Yan B, et al. Multiorgan immune-related adverse events from immune checkpoint inhibitors and their downstream implications: a retrospective multicohort study. *Lancet Oncol* 2024; **25:** 1053-69. doi: 10.1016/S1470-2045(24)00278-X

7. Lopci E, Hicks RJ, Dimitrakopoulou-Strauss A, Dercle L, Iravani A, Seban RD, et al. Joint EANM/SNMMI/ANZSNM practice guidelines/procedure standards on recommended use of [18F] FDG PET/CT imaging during immunomodulatory treatments in patients with solid tumors version 1.0. *Eur J Nucl Med Mol Imaging* 2022; **49:** 2323-41. doi: 10.1007/s00259-022-05780-2

8. Dimitriou F, Lo SN, Tan AC, Emmett L, Kapoor R, Carlino MS, et al. FDG-PET to predict long-term outcome from anti-PD-1 therapy in metastatic melanoma. *Ann Oncol* 2022; **33:** 99-106. doi: 10.1016/j.annonc.2021.10.003

9. Santo G, Cucè M, Restuccia A, Del Giudice T, Tassone P, Cicone F, et al. Immune-related [18F]FDG PET findings in patients undergoing checkpoint inhibitors treatment: correlation with clinical adverse events and prognostic implications. *Cancer Imaging* 2024; **24:** 125. doi: 10.1186/s40644-024-00774-9

10. Hribernik N, Strasek K, Huff DT, Studen A, Zevnik K, Skalic K, et al. Role of quantitative imaging biomarkers in an early FDG-PET/CT for detection of immune-related adverse events in melanoma patients: a prospective study. *Radiol Oncol* 2024; **58:** 335-47. doi: 10.2478/raon-2024-0045

11. Hribernik N, Huff DT, Studen A, Zevnik K, Klaneček Ž, Emamekhoo H, et al. Quantitative imaging biomarkers of immune-related adverse events in immune-checkpoint blockade-treated metastatic melanoma patients: a pilot study. *Eur J Nucl Med Mol Imaging* 2022; **49:** 1857-69. doi: 10.1007/s00259-021-05650-3

12. Cho SY, Lipson EJ, Im HJ, Rowe SP, Gonzalez EM, Blackford A, et al. Prediction of response to immune checkpoint inhibitor therapy using early-time-point 18F-FDG PET/CT imaging in patients with advanced melanoma. *J Nucl Med* 2017; **58:** 1421-8. doi: 10.2967/jnumed.116.188839

13. National Cancer Institute (NCI). NCI Common Terminology Criteria for Adverse Events (CTCAE). Version 5.0.2021. [cited 2023 Oct 23]. Available at: https://ctep.cancer.gov/protocoldevelopment/electronic_applications/docs/ctcae_v5_quick_reference_8.5x11.pdf

14. Nelson EK, Piehler B, Eckels J, Rauch A, Bellew M, Hussey P, et al. LabKey Server: an open source platform for scientific data integration, analysis and collaboration. *BMC Bioinformatics* 2011; **12:** 71. doi: 10.1186/1471-2105-12-71

15. Young H, Baum R, Cremerius U, Herholz K, Hoekstra O, Lammertsma AA, et al. Measurement of clinical and subclinical tumor response using [18F]-fluorodeoxyglucose and positron emission tomography: review and 1999 EORTC recommendations. European Organization for Research and Treatment of Cancer (EORTC) PET Study Group. *Eur J Cancer* 1999; **35:** 1773-82. doi: 10.1016/s0959-8049(99)00229-4

16. Anderson TM, Chang BH, Huang AC, Xu X, Yoon D, Shang CG, et al. FDG PET/CT imaging 1 week after a single dose of pembrolizumab predicts treatment response in patients with advanced melanoma. *Clin Cancer Res* 2024; **30:** 1758-67. doi: 10.1158/1078-0432.CCR-23-2390

17. Reijers ILM, Menzies AM, van Akkooi ACJ, Versluis JM, van den Heuvel NMJ, Saw RPM, et al. Personalized response-directed surgery and adjuvant therapy after neoadjuvant ipilimumab and nivolumab in high-risk stage III melanoma: the PRADO trial. *Nat Med* 2022; **28:** 1178-88. doi: 10.1038/s41591-022-01851-x

18. Blank CU, Lucas MW, Scolyer RA, van de Wiel BA, Menzies AM, Lopez-Yurda M, et al. Neoadjuvant nivolumab and ipilimumab in resectable stage III melanoma. *N Engl J Med* 2024; **391:** 1696-708. doi: 10.1056/NEJMoa2402604

19. Taghanaki SA, Zheng Y, Kevin Zhou S, Georgescu B, Sharma P, Xu D, et al. Combo loss: handling input and output imbalance in multiorgan segmentation. *Comput Med Imaging Graph* 2019; **75:** 24-33. doi: 10.1016/j.compmedimag.2019.04.005

20. Huff DT, Ferjancic P, Namías M, Emamekhoo H, Perlman SB, Jeraj R. Image intensity histograms as imaging biomarkers: application to immune-related colitis. *Biomed Phys Eng Express* 2021; **7:** 065019. doi: 10.1088/2057-1976/ac27c3

21. Suijkerbuijk KPM, van Eijs MJM, van Wijk F, Eggermont AMM. Clinical and translational attributes of immune-related adverse events. *Nat Cancer* 2024; **5:** 557-71. doi: 10.1038/s43018-024-00730-3

22. Verheijden RJ, van Eijs MJM, May AM, van Wijk F, Suijkerbuijk KPM. Immunosuppression for immune-related adverse events during checkpoint inhibition: an intricate balance. *NPJ Precis Oncol* 2023; **7:** 41. doi: 10.1038/s41698-023-00380-1

23. Wong A, Callahan J, Keyaerts M, Neyns B, Mangana J, Aberle S, et al. ^{18}F-FDG PET/CT based spleen to liver ratio associates with clinical outcome to ipilimumab in patients with metastatic melanoma. *Cancer Imaging* 2020; **20:** 36. doi: 10.1186/s40644-020-00313-2

24. Ayati N, Sadeghi R, Kiamanesh Z, Lee ST, Zakavi SR, Scott AM. The value of 18F-FDG PET/CT for predicting or monitoring immunotherapy response in patients with metastatic melanoma: a systematic review and meta-analysis. *Eur J Nucl Med Mol Imaging* 2021; **48:** 428-48. doi: 10.1007/s00259-020-04967-9

25. Kitajima K, Watabe T, Nakajo M, Ishibashi M, Daisaki H, Soeda F, et al. Tumor response evaluation in patients with malignant melanoma undergoing immune checkpoint inhibitor therapy and prognosis prediction using 18F-FDG PET/CT: multicenter study for comparison of EORTC, PERCIST, and imPERCIST. *Jpn J Radiol* 2022; **40:** 75-85. doi: 10.1007/s11604-021-01174-w

26. Iravani A, Hicks RJ. Imaging the cancer immune environment and its response to pharmacologic intervention, Part 1: The role of ^{18}F-FDG PET/CT. *J Nucl Med* 2020; **61:** 943-50. doi: 10.2967/jnumed.119.234278

27. Shreve JT, Khanani SA, Haddad TC. Artificial intelligence in oncology: current capabilities, future opportunities, and ethical considerations. *Am Soc Clin Oncol Educ Book* 2022; **42:** 1-10. doi: 10.1200/EDBK_350652

28. de Groot DJA, Lub-de Hooge MN, van Meerten T, Brouwers AH, de Vries EGE. Facts and hopes for PET imaging-derived immunotherapy biomarkers. *Clin Cancer Res* 2024; **30:** 5252-9. doi: 10.1158/1078-0432.CCR-24-1427

research article

Prevalence of diffuse idiopathic skeletal hyperostosis and association with coronary artery calcifications in Slovenia

Vesna Lesjak[1], Timea Hebar[1], Maja Pirnat[1,2]

[1] Radiology Department, University Medical Centre Maribor, Maribor, Slovenia
[2] Medical Faculty, University of Maribor, Maribor, Slovenia

Radiol Oncol 2025; 59(1): 54-62.

Received 4 August 2024
Accepted 19 November 2024

Correspondence to: Vesna Lesjak, M.D., Radiology Department, University Medical Centre Maribor, Ljubljanska 5, SI-2000 Maribor, Slovenia. E-mail: vesna.lesjak@ukc-mb.si

Disclosure: No potential conflicts of interest were disclosed.

Background. The aim of this study was to analyze the epidemiological aspects of diffuse idiopathic skeletal hyperostosis (DISH) patients in Slovenia, to evaluate the relationship between coronary CT angiography (CCTA)-derived epicardial adipose tissue (EAT) density and coronary artery calcifications (CAC) in patients with and without DISH, and study influencing factors of these parameters.

Patients and methods. The research comprised patients referred for CCTA due to a clinical suspicion of coronary artery disease. DISH, CAC score and EAT attenuation were quantified using non-contrast imaging. Diagnosis of DISH was based on Resnick criteria. The CCTA was assessed for the presence of obstructive coronary artery disease (CAD). The association between DISH and the extent of CAC was explored, using correlation analysis and multivariate regression.

Results. The study cohort included 219 participants. The prevalence of DISH was 7.8%. In univariate logistic regression, body mass index (BMI) (odds ratio [OR] 1.133, p = 0,005), age (OR 1.055, p = 0,032) and diabetes (OR 3.840, p = 0,015) were significantly associated with the condition. However, this association did not persist on multinomial multivariate analysis, but gender, age, hypertension and EAT attenuation were found to be significantly associated with the increasing CAC strata.

Conclusions. The prevalence of DISH found is comparable with prior literature. There was no independent relationship between the prevalence of DISH and CAC. Our data point to a more nuanced and perhaps non-causal link between coronary artery disease and DISH.

Key words: diffuse idiopathic skeletal hyperostosis; coronary artery calcification; epicardial adipose tissue; metabolic syndrome; body mass index; coronary artery disease

Introduction

Diffuse idiopathic skeletal hyperostosis (DISH) is a systemic condition, originally described in 1950 by Forestier and Querol.[1] In 1976 most commonly used criteria to diagnose DISH were introduced by Resnick and Niwayama.[2] New bone formation, partially in entheses, is the condition's defining feature.[3] It is known that DISH affects more men than women, and its incidence rises with age.[4] Prevalence in Asian countries varies between 3.8% and 27.0%, in the USA between 7.7% and 13.2%, and in Italy 12.8%.[5,6] The etiology of DISH is not utterly understood. The disorder is linked to metabolic syndrome and its components, including diabetes, obesity, and hypertension[7,8], associations were reported with large waist circumference, cardiomegaly, hyperinsulinaemia, dyslipidaemia and hyperuricaemia.[3] DISH is associated with increased calcifications in coronary arteries[3], and

also in thoracic[9] and abdominal aorta.[10] The risk of myocardial infarction is considerably higher in DISH patients.[11]

Between the myocardium and the visceral pericardium is a visceral fat deposit called epicardial adipose tissue (EAT).[12] It surrounds the heart and coronary arteries, being vascularized by branches of the coronary arteries.[12,13] EAT is metabolically active, has a thermogenic role, secretes cytokines with pro- and anti-atherosclerotic qualities, and is hypothesized to defend against mechanical injuries to the heart and coronary vessels.[14] It is thought to have a role in the onset of atherosclerosis, although it is unclear whether systemic processes or paracrine effects of EAT directly contribute to the development of atherosclerosis.[15] The research has shown abundant evidence of the correlation between EAT volume and cardiovascular risk factors, coronary artery calcification and major adverse cardiac events.[16] There has been recently increased interest in EAT attenuation as a marker of risk.[17] In some studies a lower EAT attenuation on non-contrast enhanced cardiac CT scans has been linked to the risk of future events[18], whereas in other studies a higher EAT attenuation has been linked to an increased risk.[19]

Up until recently, vascular calcification was thought to be an inevitable result of aging, and the development of coronary artery calcification (CAC) was thought to be a passive process. The development of CAC is now recognized as an active pathogenic process.

The common feature of atherosclerosis - ectopic bone production is known as the cause of coronary artery calcification, and new bone formation being the defining feature of DISH led us to hypothesize that arterial calcification and the occurrence of DISH are strongly correlated.

To our knowledge, the prevalence of DISH in the Slovenian population has not been evaluated. Based on this framework, the objective of our study is to analyze the epidemiological aspects of DISH patients in Slovenia, to evaluate the relationship between coronary CT angiography (CCTA)-derived EAT density and CAC in patients with and without DISH, and study influencing factors of these parameters.

Patients and methods

This cross-sectional study was conducted at the Department of Radiology, University Medical Centre Maribor. This study was conducted with approval of local ethics committee (UKC-MB-KME-24/21) and performed accordingly to the Declaration of Helsinki. All participants gave written informed consent.

Study protocol

Between January 2022 and January 2024, adult patients referred for CCTA were included in the study. Participants responded to questionnaires assessing socio-demographic information, lifestyle and health-related factors, which contains self-reported information on age, gender, weight status, chronic diseases, smoking and physical activity. Exclusion criteria were age < 18 years, known malignancy and prior coronary artery bypass surgery. A total of 219 cases were included in the study.

Body mass index (BMI)

We calculated the BMI by using self-reported height and weight following the formula: weight (kg) divided by height (m) squared. According to WHO standards, BMI was categorized into underweight (BMI < 18.5), normal (18,5–24.99), overweight (BMI ≥ 25) and obese (BMI ≥ 30).[20]

CT acquisition protocol

All examinations were performed on Somatom Drive CT scanner (Siemens Medical Solutions, Erlengen, Germany). Noncontrast, non-gated CT scan was performed to measure the Agatson coronary artery calcification score (CACS), as described previously.[21] The sum of the individual lesion scores from the four vessels; left main (LM), left anterior descending (LAD), circumflex (LCX), and right coronary artery (RCA) produced the total coronary calcium score. The Agatson Units were classified into four categories: 0, > 0 and < 100, 100–400, and > 400. These categories represent no, mild/minimal, moderate, and substantial plaque burden. In the same way the calcium score (Agatson) was measured for proximal thoracic aorta (from aortic root to the first branch of the aortic arch), aortic root and ascending aorta.

The EAT attenuation was measured on the same axial images used for CACS. Epicardial adipose tissue Hounsfield units (HU) were measured using regions of interest (ROI) near the proximal part of RCA, between the right atrium and right ventricular outflow tract, as previously described.[15]

Hepatic and splenic HU attenuation values were quantified by placing two ROI in the liver

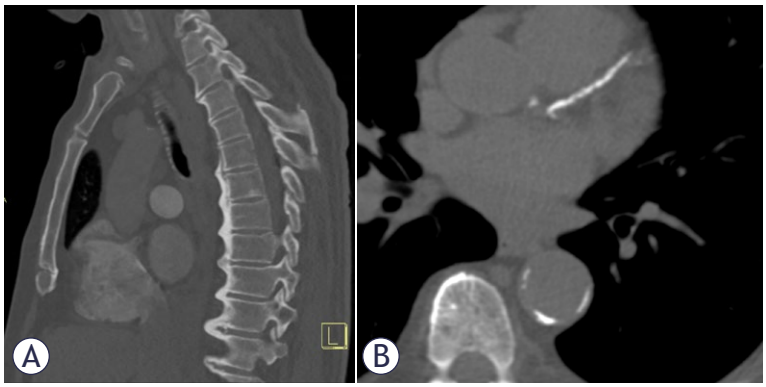

FIGURE 1. A 68-year old male with diffuse idiopathic skeletal hyperostosis (DISH) coronary artery calcification score (CACS) > 400. **(A)** Typical appearance of DISH in thoracic spine, sagittal plane. **(B)** Calcifications in LAD = left anterior descending artery

and one in spleen, in the same axial slice. Liver to spleen ratio was calculated by dividing the mean liver attenuation by the splenic HU. Nonalcoholic fatty liver disease (NAFLD) was defined as liver to spleen ratio < 1 and/or mean liver attenuation < 40 HU.[22]

A retrospective ECG-gated CCTA examination was done in all participants, to assess coronary artery disease (CAD). CCTA datasets were transferred to a workstation (Syngo.via VB10. Siemens Healthcare, Forchheim, Germany), and coronary arteries were evaluated for the presence of obstructive CAD (defined as at least one lesion causing the stenosis of lumen ≥ 50%). CCTA images were reconstructed with a slice thickness of 0.6 mm. The CT studies were evaluated by radiologists having more than five years of experience in cardiac imaging.

Diffuse idiopathic skeletal hyperostosis (DISH)

Resnick classification criteria were used to define DISH: the presence of flowing bridging ossification of at least four contiguous vertebrae, (relative) preservation of the intervertebral disc height and the absence of apophyseal joint bony ankylosis, as described. The prevalence of DISH was diagnosed by a single musculoskeletal radiologist evaluating CT images.

Metabolic syndrome

The metabolic syndrome (MetS) was defined according to the International Diabetes Federation (IDF) definition[23]: BMI greater than 30 kg/m^2 (in this case the central obesity can be assumed and waist circumference measure is not necessary) plus any two of the four factors: 1 raised triglycerides (≥ 1.7 mmol/l) or specific treatment for this abnormality, 2 reduced HDL cholesterol (< 1.03 mmol/l in males or < 1.29 mmol/l in females) or specific treatment, 3 raised blood pressure (systolic BP ≥ 130 or diastolic ≥ 85 mmHg) or treatment for diagnosed hypertension, and 4 raised fasting plasma glucose (≥ 5.6 mmol/l) or previously diagnosed diabetes type 2.

Covariates

Additional data were collected: age in years, sex (male, female), smoking behavior (current smoker yes/no) and physical activity (days per week). The presence of hypertension, diabetes mellitus type 2 and hypercholesterolemia was established by the question 'Have you had these condition?' and/or the self-reported usage of antihypertensive drugs, glucose lowering and lipid lowering drugs. Other chronic health conditions included angina pectoris, and previous myocardial infarction.

Statistical analysis

All continuous variables were tested for normal distribution (Shapiro-Wilk test). Normally distributed variables are given as means and standard deviations (SD), non-normally distributed variables are given as median (interquartile range [Q1–Q3]) and categorical variables are presented as numbers and percentages (%). Comparisons of demographic characteristics and potential covariates between the DISH and no DISH groups were conducted using Mann-Whitney U test and independent sample t-test for continuous variables, and Chi-square test for categorical variables. Group-wise comparisons were performed with the Kruskal-Wallis test. Independent sample t-test, Pearson or Spearman rank correlations were calculated to determine the relationships between EAT attenuation and risk factors. We also evaluated the relationship between EAT attenuation and CT parameters using multivariable linear regression analyses. To determine the association between the presence of DISH, EAT and CAC, univariate and multivariate logistic regression analyses were performed. The models included DISH status (present or absent) as dependent factor and age, gender, BMI, eight, smoking status, diabetes, hypertension and hypercholesterolemia as independent variables. A multivari-

TABLE 1. Characteristics of the cohort

	DISH	no DISH	p-value
Age (years), mean (SD)	67.3 ± 10.1	60.5 ± 12.2	**0.029**
Gender (f/m), N	5/12	99/103	0.120
Weight (kg), mean (SD)	96.6 ± 20.3	84.5 ± 17.5	**0.008**
Height (cm), mean (SD)	170.9 ± 6.5	171.0 ± 9.7	0.980
BMI (kg/m^2), mean (SD)	32.8 ± 7.2	28.9 ± 5.3	**0.011**
Family history of cardiovascular disease, N (%)	11 (64.7%)	119 (59.2%)	0.657
Diabetes, N (%)	6 (35.3%)	25 (12.4%)	**0.010**
Hypercholesterolemia, N (%)	6 (35.3%)	51 (25.4%)	0.371
Hypertension, N (%)	12 (70.6%)	110 (54.7%)	0.206
Current smoker, N (%)	2 (11.8%)	38 (18.9%)	0.465
Angina pectoris, N (%)	4 (23.5%)	92 (44%)	0.076
Metabolic syndrome, N (%)	7 (43.8%)	25 (13.0%)	**0.001**
EAT attenuation (HU), mean (SD)	-98.5 ± 11.8	-101.7 ± 13.0	0.347
NAFLD	5 (29.4%)	52 (26.0%)	0.759
CACS (au) = 0	2 (11.8%)	68 (33.8%)	0.063
CACS (au), median (IQR)	101.0 (4.7-569.0)	27.3 (0-391.8)	0.241
Calcifications in proximal thoracic aorta, median (IQR)	196.4 (12.3-759.5)	14.3 (0-244.6)	**0.023**
Calcifications in aortic root, median (IQR)	146.8 (8.3-758.0)	1.8 (0-175.0)	**0.013**
Calcifications in ascending aorta, median (IQR)	2.1 (0-35.2)	0.0 (0-3.9)	0.109
Myocardial infarction, N (%)	1 (6.0%)	12 (6.0%)	0.988

BMI = body mass index; CACS (au) = Agatson coronary artery calcification score; DISH = diffuse idiopathic skeletal hyperostosis (DISH); EAT = epicardial adipose tissue; f/m = female/male; IQR = interquartile range; N = number, NAFLD = nonalcoholic fatty liver disease; SD = standard deviation

ate multinomial logistic regression was performed with CAC categories (> 0 and < 100, 100−400, > 400) as independent factor and CACS = 0 as reference category and DISH status as dependent factor. Multivariate analyses were done in a stepwise backward elimination based on a p-value < 0,10. We analyzed the prevalence of DISH and CACS in the relation to the amount of risk factors (diabetes, BMI > 30, hypertension, hypercholesterolemia) present. Comparisons between the DISH and no DISH groups were conducted using Chi-square test. All statistical analyses were performed using the SPSS 29.0 software package (IBM, Armonk, NY, USA). All tests were 2-sided and a 'P' value of less than 0.05 was considered statistically significant.

Results

A total of 219 participants were included in the study. The overall prevalence of DISH was 7.8%. The prevalence of DISH was about twice as high in males than in females (10.4% *vs*. 4.8%). The characteristics of the demographics and cardiovascular risk factors of participants with and without DISH are shown in Table 1. Compared to patients without DISH, those with DISH were significantly older (67.3 *vs*. 60.5 years). 42.6% of subjects were obese (45.5% men and 39.4% women). Among subjects with DISH, 68.8% were obese, compared to 40.4% of patients without DISH. NAFLD was present in 26.3% of participants; in 29.4 % of patients with DISH and in 26.0% of patients without DISH. Metabolic syndrome was present in 15.4% of participants, in subjects with DISH in 43.8%, compared to 13.0% of subjects without DISH.

Additionally, in subjects with DISH a significantly higher BMI was noted (32.8 *vs*. 28.9) and more diabetes (35.3% *vs*. 12.4%). Figure 1 shows an example of a male patient with DISH and abundant calcifications in left anterior descending coronary artery.

Subjects without DISH were about three times more likely to not have coronary artery calcifica-

TABLE 2. Prevalence of diffuse idiopathic skeletal hyperostosis (DISH) among Agatson coronary artery calcification score (CACS) categories

	CACS = 0 (N = 70)	CACS > 0 and < 100 (N = 62)	CACS = 100–400 (N = 33)	CACS > 400 (N = 53)
DISH	2.8%	10.3%	6.6%	13.3%
No DISH	97.2%	89.7%	93.4%	86.7%

TABLE 3. Association of epicardial adipose tissue (EAT) attenuation with conventional coronary artery disease (CAD) risk factors and CT parameters

Variable	EAT attenuation (HU)	p-value
Gender	M - 98.3 ± 11.3 F - 105.4 ± 13.6	**< 0.001**
NAFLD	Y - 98.3 ± 12.8 N - 102.7 ± 12.8	**0.022**
Family history of cardiovascular disease	Y - 100.1 ± 12.8 N - 104.5 ± 14.1	0.261
Diabetes	Y - 104.2 ± 14.3 N - 101.3 ± 13.3	0.883
Hypercholesterolemia	Y - 99.4 ± 13.5 N - 102.6 ± 13.3	0.402
Hypertension	Y - 99.2 ± 12.4 N - 105.2 ± 14.1	0.129
Smoking	Y - 97.8 ± 13.3 N - 102.9 ± 13.3	0.361
Regular physical activity	Y - 101.6 ± 12.8 N - 101.9 ± 14.4	0.653
	Correlation coefficient	
CACS (Agatson)	0.306	**< 0.001**
CACS per vessel		
LM	0.159	**0.018**
LAD	0.247	**< 0.001**
LCX	0.269	**< 0.001**
RCA	0.289	**< 0.001**
Calcifications in proximal thoracic aorta	0.110	0.103
Calcifications in aortic root	0.082	0.226
Calcifications in ascending aorta	0.172	**0.011**
Age	0.006	0.834
BMI	0.243	**< 0.001**

BMI = body mass index; CACS = coronary artery calcification score; f = female; HU = Hounsfield units; LAD = left anterior descending artery; LCX = left circumflex artery; m = male; LM = left main coronary artery; NAFLD = nonalcoholic fatty liver disease; RCA = right coronary artery

tions compared to subjects with DISH (33.8% *vs.* 11.0%). In subjects with a CACS > 400, DISH was present in 13.3%, while in subjects with CACS = 0 DISH was present in 2.8% (Table 2).

Associations between EAT attenuation, cardiovascular risk factors and CT parameters are depicted in Table 3. There is a significant correlation between EAT attenuation and BMI (rho = 0.243, p < 0.001), CACS (rho = 0.256, p < 0.001) and calcifications in ascending aorta (rho = 0.052, p = 0.011), as well as significant association between EAT attenuation and gender (p < 0.001) and NAFLD (p = 0.022).

Figure 2A shows EAT attenuation for patients with different Agatson score CACS category. Mean EAT attenuation was lower in patients with CACS = 0 than in patients with CACS > 400 (-103.7 ± 13.8 HU *vs.* -95.9 ± 11.3 HU [p < 0.001]), also in patients with CACS > 0 and < 100 the mean EAT attenuation was lower than in patients with CACS > 400 (-104.5 ± 12.2 HU *vs.* -95.9 ± 11.3 HU (p < 0.001)).

Group-wise comparisons between BMI categories showed significant differences in EAT attenuation (p = 0.007), as shown in Figure 2B. In patients with BMI < 18.5 EAT attenuation was -96.0 ± 9.9 HU (there were only two patients in this group). In patients with BMI 18.5–24.9 -107.1 ± 13.9 HU, with BMI between 25 and 29.9 -102.1 ± 13.2 HU and in patients with BMI > 30 -98.4 ± 11.6 HU.

On univariate analysis, it was observed that age (p = 0.032), BMI (p = 0.005) and diabetes (p = 0.015) were found to be significantly associated with the presence of DISH (Table 4). In multiple logistic regression model age and BMI were found to be significantly associated with the presence of DISH, odds ratio (OR) 1.060, p = 0.029 and OR 1.132, p = 0.009.

In the multinomial multivariate logistic regression analysis with the different CACS categories as outcome and those without coronary artery calcifications (CACS = 0) as a reference category, gender, age, hypertension and epicardial fat attenuation were found to be significantly associated with the increasing CAC strata (Table 5). Male gender has a 16.786 time greater odds of having CACS > 400 than female gender, compared to subjects with CACS = 0 (p < 0.001). Subjects with hypertension have a 5.423 times greater odds of having CACS > 400 than subjects without hypertension, compared to subjects with CACS = 0 (p < 0.001). There is a 1.227-fold increase in the likelihood of having CACS > 400 with every additional year of age, compared to subjects with CACS = 0 (p < 0.001). Every additional unit of EAT attenuation (HU) increases the odds of hav-

ing CACS > 400 by 1.052 times when compared to subjects with CACS = 0 (p = 0.022). DISH, smoking status, diabetes, hypercholesterolemia and metabolic syndrome were excluded from the model, since they did not meet the criteria (p < 0.1).

Discussion

Despite the fact that DISH is a common condition, epidemiology of the disease in Slovenia is unknown. The overall prevalence of DISH in our cohort was 7.8% (10.4% in men and 4.8% in women). Our results are consistent with the literature, varying from 3.8% in China[24] to 30.8% in Pakistan[25], 7.8% in Iceland[26] and 12.8% in Italy.[5] The differences can to some extent be explained by the differences in study population, diagnostic criteria and variety of imaging methods used – chest x-ray or CT scan, whole- spine scans or partial (chest) scans.[26] Prevalence of DISH increases with age and male to female prevalence ratio is 2:1.[27] In the current study, subjects with DISH were significantly older than patients without DISH, however, the logistic analysis confirmed ageing to influence the prevalence of DISH significantly.

Previous studies reported higher BMI in patients with DISH than in those without DISH.[26-28] Also, various metabolic variables are associated with DISH, in particular obesity and type 2 diabetes mellitus.[29,30] Several paleopathological studies showed that the prevalence of DISH varied significantly between groups of different social standing, with speculation that the upper socioeconomic status groups were excessively nourished, with likely increased incidence of obesity, in comparison with the individuals with lower social status.[29] In the present study, diabetes and BMI significantly affected the prevalence of DISH in logistic regression analysis. Insulin, a peptide that promotes bone development, is raised in diabetes. It is speculated, that in patients with diabetes, insulin can promote the new bone growth and thereby excess bone formation.[31] Chondrocytes and periosteal mesenchymal cells inside the enthesis can proliferate under the impact of several factors (i.e. insulin, transforming growth factor-β1,…) to form osteoblasts, fibroblasts and myoblasts. Furthermore, different metabolic agents (i.e. insulin, insulin-like growth factor 1,…) have the potential to induce bone formation by stimulating the proliferation of chondrocytes, fibroblasts and osteoblasts.[29] Increased rates of obesity in DISH patients may indicate that certain adipokines have

TABLE 4. Univariate logistic regression analysis with diffuse idiopathic skeletal hyperostosis (DISH) status as the dependent factor

Variable	units	OR	p-value
Age	+ 1 year	1.055	**0.032**
Gender	Male vs. female	2.307	0.129
BMI	+ 1 kg/m^2	1.133	**0.005**
Diabetes	Present vs. absent	3.840	**0.015**
Hypertension	Present vs. absent	1.985	0.213
Hypercholesterolemia	Present vs. absent	0.623	0.375
Smoking	Present vs. absent	1.748	0.470

BMI = body mass index; OR = odds ratio

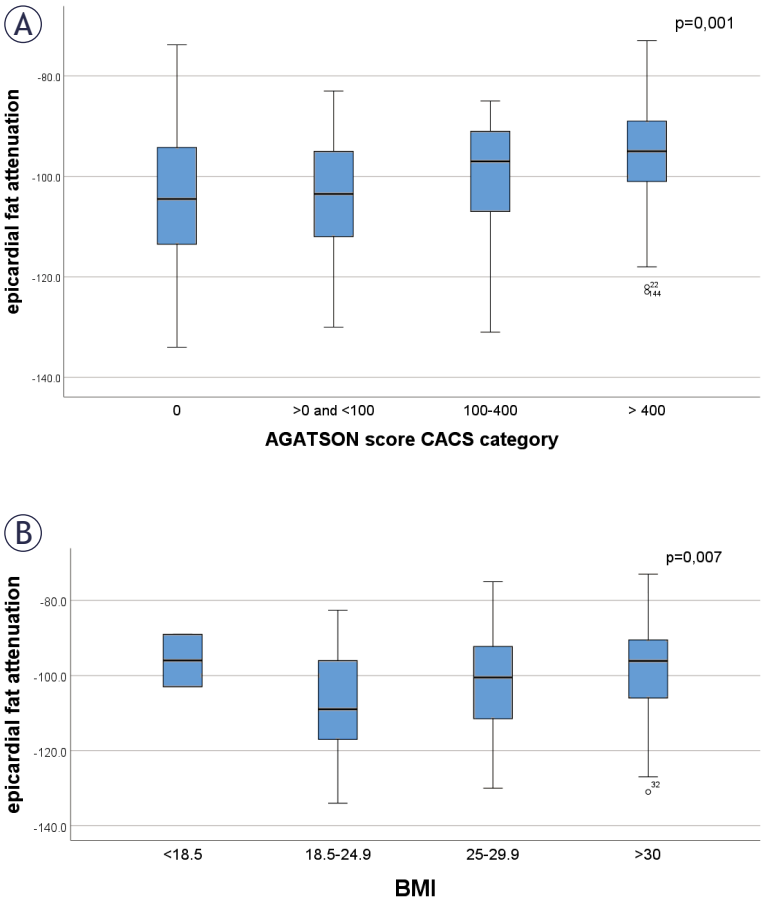

FIGURE 2. Epicardial fat attenuation in subjects with **(A)** different coronary artery calcium score and **(B)** different body mass index (BMI) categories. Data are presented as box plots, where boxes represent the interquartile range (IQR), the lines within the box represent the median, and the lines outside the boxes represent the upper quartile plus 1.5 times IQR or the lower quartile minus 1.5 times the IQR.

CACS = coronary artery calcification score

TABLE 5. Multinomial multivariate logistic regression analysis on the association of diffuse idiopathic skeletal hyperostosis (DISH) and coronary artery calcification score (CACS) category

CACS category	gender		age		hypertension		EAT attenuation	
	OR	p-value	OR	p-value	OR	p-value	OR	p-value
>0 and <100	3.515	0.008	1.087	<0.001	3.956	0.001	0.980	0.225
100-400	7.583	<0.001	1.156	<0.001	5.023	0.003	1.005	0.804
> 400	16.786	<0.001	1.227	<0.001	5.423	0.001	1.052	0.022

OR = odds ratio

Coronary artery calcifications (CAC) category is the outcome compared to the subjects without CAC (CACS = 0) as reference category

a role in the disorder's development. Several of these fat-derived hormones (i.e. leptin) have an association with bone metabolism growth.[3] Obesity-related chronic inflammation with proinflammatory cytokines such as IL-6, TNF-α etc. could contribute to the formation of calcifications, as discs and ligaments of the spine may have receptors for them. Leptin causes chondrocytes to release more chondrocyte degradation mediators and promotes the proliferation of intervertebral disc cells. Leptin stimulates the inflammatory response by raising IL-6, which causes ligamentum flavum hypertrophy and fibrosis.[32] In this study, subjects with DISH had a higher prevalence of metabolic syndrome and NAFLD than those without DISH. The prevalence of NAFLD and metabolic syndrome rises with obesity; and NAFLD is considered as both, a cause and a result of metabolic syndrome. It is widely documented that NAFLD increases the risk of development of atherosclerosis and cardiac events. Studies showed that NAFLD diagnosed on non-contrast CT to be a strong predictor of MACE (major adverse cardiovascular events) at 14-year follow-up.[22] We found no correlation between NAFLD and DISH, however there is a significant association between EAT attenuation and NAFLD.

Our study's findings support earlier research suggesting that DISH is linked to a greater extent of calcifications in blood vessels.[3,9,33] Indeed, we observed an increase of DISH prevalence across CACS categories. CACS was higher in subjects with DISH compared to the non-DISH group, but the association did not perseverate on multivariate analysis, similar as in previous studies.[34] It is hypothesized that subjects with DISH may be prone to form calcifications in arteries and in aortic valve, amongst other locations, however, our data point to a more nuanced, maybe non-causal link between CAD and DISH.

The relationship between EAT volume and attenuation, coronary artery plaque load, and coronary artery disease is widely recognized in the literature. In our study EAT attenuation was significantly higher in subjects with CACS > 400 compared to subjects with CACS = 0. Higher EAT attenuation might reflect inflammation in epicardial fat, which was described in patients with acute coronary syndrome.[35] EAT also increases with vascularization and higher amount of mitochondria and decreases with fatty acids overload.[19] Statins also decrease EAT attenuation over time, via reducing metabolic activity within the EAT by reducing vascularity, cellularity and inflammation[15], therefore, an influence of therapy with statins might have influenced the observed EAT attenuation. Among patients with coronary artery disease having open heart surgery, an increase in pro-inflammatory mediators and cytokines in the EAT was reported, as EAT regulates local inflammation in the immediate vicinity of the coronaries.[36] In our study, chronic, low-grade inflammation might be a significant pathophysiologic connection between DISH, NAFLD, EAT, and CAC. However, to further understand the underlying processes, more research should be conducted correlating EAT attenuation to local and systemic metabolic and inflammatory mechanisms.

The limitations of the current study include its small sample size, the possibility of selection bias due to the inclusion of many individuals with medical disorders, and a cross-sectional design of the study, as a result of which, the possible impact of DISH on mortality cannot be assessed.

To understand the mechanism connecting DISH and coronary artery calcification a multidisciplinary approach that investigates inflammatory, metabolic, genetic, molecular, and environmental factors is required. Future research needs to focus on elucidating common signaling pathways and

risk factors that underlie both conditions, employing a combination of molecular, imaging, genetic, and clinical methodologies, with prospective studies and clinical trials, to enhance our comprehension of the fundamental mechanisms.

Conclusions

There was no independent relationship identified between the prevalence of DISH and CACS. The specific processes that lead to new bone development in DISH patients, particularly in entheses, still remain unclear.

Acknowledgements

The authors would like to thank Laura Kocet for her assistance with statistical processing. The project described was funded by University Medical Centre Maribor, internal research grant number IRP-2021/01-11.

References

1. Forestier J, Rotes-Querol J. Senile ankylosing hyperostosis of the spine. *Ann Rheum Dis* 1950; **9:** 321-30. doi: 10.1136/ard.9.4.321
2. Resnick D, Niwayama G. Radiographic and pathologic features of spinal involvement in diffuse idiopathic skeletal hyperostosis (DISH) *Radiology* 1976; **119:** 559-68. doi: 10.1148/119.3.559
3. Oudkerk SF, Mohamed Hoesein FAA, W PTM, Öner FC, Verlaan JJ, de Jong PA, et al. Subjects with diffuse idiopathic skeletal hyperostosis have an increased burden of coronary artery disease: an evaluation in the COPDGene cohort. *Atherosclerosis* 2019; **287:** 24-9. doi: 10.1016/j.atherosclerosis.2019.05.030
4. Weinfeld RM, Olson PN, Maki DD, Griffiths HJ. The prevalence of diffuse idiopathic skeletal hyperostosis (DISH) in two large American Midwest metropolitan hospital populations. *Skelet Radiol* 1997; **26:** 222-5. doi: 10.1007/s002560050225
5. Ciaffi J, Borlandelli E, Visani G, Facchini G, Miceli M, Ruscitti P, et al. F. Prevalence and characteristics of diffuse idiopathic skeletal hyperostosis (DISH) in Italy. *Radiol Med* 2022; **127:** 1159-69. doi: 10.1007/s11547-022-01545-x
6. Yoshihara H, Nadarajah V, Horowitz E. Prevalence and characteristics of thoracic diffuse idiopathic skeletal hyperostosis in 3299 black patients. *Sci Rep* 2021; **11:** 22181. doi: 10.1038/s41598-021-01092-x
7. Mader R, Novofestovski I, Adawi M, Lavi I. Metabolic syndrome and cardiovascular risk in patients with diffuse idiopathic skeletal hyperostosis. *Semin Arthritis Rheum* 2009; **38:** 361-5. doi: 10.1016/j.semarthrit.2008.01.010
8. Mattera M, Reginelli A, Bartollino S, Russo C, Barile A, Albano D, et al. Imaging of metabolic bone disease. *Acta Biomed* 2018; **89(1-S):** 197-207. doi: 10.23750/abm.v89i1-S.7023
9. Harlianto NI, Westerink J, Hol ME, Wittenberg R, Foppen W, van der Veen PH, et al. Patients with diffuse idiopathic skeletal hyperostosis have an increased burden of thoracic aortic calcifications. *Rheumatol Adv Pract* 2022; **6:** rkac060. doi: 10.1093/rap/rkac060
10. Pariente-Rodrigo E, Sgaramella GA, Olmos-Martínez JM, Pini-Valdivieso SF, Landeras-Alvaro R, Hernández-Hernández JL. Relationship between diffuse idiopathic skeletal hyperostosis, abdominal aortic calcification and associated metabolic disorders: data from the Camargo cohort. *Med Clin* 2017; **149:** 196-202. doi: 10.1016/j.medcli.2017.01.030
11. Glick K, Novofastovski I, Schwartz N, Mader R. Cardiovascular disease in diffuse idiopathic skeletal hyperostosis (DISH): from theory to reality-a 10-year follow-up study. *Arthritis Res Ther* 2020; **22:** 190. doi: 10.1186/s13075-020-02278-w
12. Wu Y, Zhang A, Hamilton DJ, Deng T. Epicardial fat in the maintenance of cardiovascular health. *Methodist Debakey Cardiovasc J* 2017; **13:** 20-4. doi: 10.14797/mdcj-13-1-20
13. Bertaso AG, Bertol D, Duncan BB, Foppa M. Epicardial fat: definition, measurements and systematic review of main outcomes. *Arq Bras Cardiol* 2013; **101:** e18-28. doi: 10.5935/abc.20130138
14. Iacobellis G. Aging effects on epicardial adipose tissue. *Front Aging* 2021; **2:** 666260. doi: 10.3389/fragi.2021.666260
15. Raggi P, Gadiyaram V, Zhang C, Chen Z, Lopaschuk G, Stillman AE. Statins reduce epicardial adipose tissue attenuation independent of lipid lowering: a potential pleiotropic effect. *J Am Heart Assoc* 2019; **8:** e013104. doi: 10.1161/JAHA.119.013104
16. Rosito GA, Massaro JM, Hoffmann U, Ruberg FL, Mahabadi AA, Vasan RS, et al. Pericardial fat, visceral abdominal fat, cardiovascular disease risk factors, and vascular calcification in a community-based sample the Framingham heart study. *Circulation* 2008; **117:** 605-13. doi: 10.1161/CIRCULATIONAHA.107.743062
17. Archer JM, Raggi P, Amin SB, Zhang C, Gadiyaram V, Stillman AE. Season and clinical factors influence epicardial adipose tissue attenuation measurement on computed tomography and may hamper its utilization as a risk marker. *Atherosclerosis* 2021; **321:** 8-13. doi: 10.1016/j.atherosclerosis.2021.01.025
18. Goeller M, Achenbach S, Marwan M, Doris MK, Cadet S, Commandeur F, et al. Epicardial adipose tissue density and volume are related to subclinical atherosclerosis, inflammation and major adverse cardiac events in asymptomatic subjects, *J Cardiovasc Comput Tomogr* 2018; **12:** 67-73. doi: 10.1016/j.jcct.2017.11.007
19. Mahabadi AA, Balcer B, Dykun I, Forsting M, Schlosser T, Heusch G, et al. Cardiac computed tomography-derived epicardial fat volume and attenuation independently distinguish patients with and without myocardial infarction. *PLoS One* 2017; **12:** e0183514. doi: 10.1371/journal.pone.0183514
20. World Health Organization. Obesity and overweight. [internet]. [cited 2024 Mar 13]. Available at: https://www.who.int/news-room/fact-sheets/detail/obesity-and-overweight
21. Agatston AS, Janowitz WR, Hildner FJ, Zusmer NR, Viamonte M Jr, Detrano R. Quantification of coronary artery calcium using ultrafast computed tomography. *J Am Coll Cardiol* 1990; **15:** 827-32. doi: 10.1016/0735-1097(90)90282-t
22. Lin A, Wong ND, Razipour A, McElhinney PA, Commandeur F, Cadet SJ, et al. Metabolic syndrome, fatty liver, and artificial intelligence-based epicardial adipose tissue measures predict long-term risk of cardiac events: a prospective study. *Cardiovasc Diabetol* 2021; **20:** 27. doi: 10.1186/s12933-021-01220-x
23. Alberti KG, Zimmet P, Shaw J. Metabolic syndrome – a new world-wide definition. A Consensus Statement from the International Diabetes Federation. *Diabet Med* 2006; **23:** 469-80. doi: 10.1111/j.1464-5491.2006.01858.x
24. Liang H, Liu G, Lu S, Chen S, Jiang D, Shi H, et al. Epidemiology of ossification of the spinal ligaments and associated factors in the Chinese population: a cross-sectional study of 2000 consecutive individuals. *BMC Musculoskelet Disord* 2019; **20:** 253. doi: 10.1186/s12891-019-2569-1
25. Adel H, Khan SA, Adil SO, Huda F, Khanzada U, Manohar M, et al. CT-based evaluation of diffuse idiopathic skeletal hyperostosis in adult population; prevalence, associations and interobserver agreement. *J Clin Densitom* 2020; **23:** 44-52. doi: 10.1016/j.jocd.2018.12.001
26. Auðunsson AB, Elíasson GJ, Steingrímsson E, Aspelund T, Sigurdsson S, Launer L, et al. Diffuse idiopathic skeletal hyperostosis in elderly Icelanders and its association with the metabolic syndrome: the AGES-Reykjavik Study. *Scand J Rheumatol* 2021; **50:** 314-8. doi: 10.1080/03009742.2020.1846779

27. Harlianto NI, Oosterhof N, Foppen W, Hol ME, Wittenberg R, van der Veen PH, van Ginneken B, et al. Diffuse idiopathic skeletal hyperostosis is associated with incident stroke in patients with increased cardiovascular risk. *Rheumatology* 2022; **61:** 2867-74. doi: 10.1093/rheumatology/keab835

28. Ishimura D, Morino T, Murakami Y, Yamaoka S, Kinoshita T, Takao M. Examining the association between the extent of anterior longitudinal ligament ossification progression and comorbidities in diffuse idiopathic skeletal hyperostosis. *Cureus* 2023; **15:** e51357. doi: 10.7759/cureus.51357

29. Pillai S, Littlejohn G. Metabolic factors in diffuse idiopathic skeletal hyperostosis-a review of clinical data. *Open Rheumatol J* 2014; **8:** 116-28. doi: 10.2174/1874312901408010116

30. Okada E, Ishihara S, Azuma K, Michikawa T, Suzuki S, Tsuji O, et al. Metabolic syndrome is a predisposing factor for diffuse idiopathic skeletal hyperostosis. *Neurospine* 2021; **18:** 109-16. doi: 10.14245/ns.2040350.175

31. Sencan D, Elden H, Nacitarhan V, Sencan M, Kaptanoglu E. The prevalence of diffuse idiopathic skeletal hyperostosis in patients with diabetes mellitus. *Rheumatol Int* 2005; **25:** 518-21. doi: 10.1007/s00296-004-0474-9

32. Chaput CD, Siddiqui M, Rahm MD. Obesity and calcification of the ligaments of the spine: a comprehensive CT analysis of the entire spine in a random trauma population. *Spine J* 2019; **19:** 1346-53. doi: 10.1016/j.spinee.2019.03.003

33. Orden AO, David JM, Díaz RP, Nardi NN, Ejarque AC, Yöchler AB. Association of diffuse idiopathic skeletal hyperostosis and aortic valve sclerosis. *Medicina (B Aires)* 2014; **74:** 205-9. PMID: 24918668

34. Lantsman CD, Brodov Y, Matetzky S, Beigel R, Lidar M, Eshed I, et al. No correlation between diffuse idiopathic skeletal hyperostosis and coronary artery disease on computed tomography using two different scoring systems. *Acta Radiol* 2023; **64:** 508-14. doi: 10.1177/02841851221090890

35. Konishi M, Sugiyama S, Sato Y, Oshima S, Sugamura K, Nozaki T, et al. Pericardial fat inflammation correlates with coronary artery disease. *Atherosclerosis* 2010; **213:** 649-55. doi: 10.1016/j.atherosclerosis.2010.10.007

36. Baker AR, Silva NF, Quinn DW, Harte AL, Pagano D, Bonser RS, et al. Human epicardial adipose tissue expresses a pathogenic profile of adipocytokines in patients with cardiovascular disease. *Cardiovasc Diabetol* 2006; **5:** 1. doi: 10.1186/1475-2840-5-1.

research article

Accuracy of transthoracic echocardiography in diagnosis of cardiac myxoma: single center experience

Polona Kacar[1], Nejc Pavsic[1], Mojca Bervar[1], Zvezdana Dolenc Strazar[2], Katja Prokselj[1,2]

[1] Department of Cardiology, University Medical Center Ljubljana, Ljubljana, Slovenia
[2] Faculty of Medicine, University of Ljubljana, Ljubljana, Slovenia

Radiol Oncol 2025; 59(1): 63-68.

Received 10 February 2024
Accepted 8 December 2024

Correspondence to: Assoc. Prof. Katja Prokšelj, M.D., Ph.D., Department of Cardiology, University Medical Center Ljubljana, Zaloška cesta 7, SI-1525 Ljubljana, Slovenia. E-mail: katja.prokselj@gmail.com

Disclosure: No potential conflicts of interest were disclosed.

Background. The differential diagnosis of cardiac myxomas (CM), the most common benign primary cardiac tumors, is broad and a thorough diagnostic workup is required to establish accurate diagnosis prior to surgical resection. Transthoracic echocardiography (TTE) is usually the first imaging modality used for diagnosis of suspected CM. In a single tertiary centre study, we sought to determine the accuracy, sensitivity, and specificity of TTE in the diagnosis of CM and to determine echocardiographic characteristics indicative of CM.

Patients and methods. We retrospectively analyzed clinical, echocardiographic, and pathohistological findings of 73 patients consecutively admitted for suspected CM.

Results. After diagnostic workup, 53 (73%) patients were treated surgically at our institution. Based on preoperative TTE, patients were divided into a CM group (n=45, 85%) and non-myxoma (NM) group. Of the 53 pathohistological specimens obtained during surgery, 39 (73%) were CM. The sensitivity and specificity of preoperative echocardiography were 97% and 50%, respectively. The overall accuracy was 85%. All NM tumors were found in an atypical location and 72% of CM were found in a typical position in the left atrium ($p < 0.001$). Tumors in NM group were significantly smaller than CM (24.3 ± 13.2 mm *vs.* 37.9 ± 18.3 mm, $p = 0.017$).

Conclusions. Our study confirms very good accuracy of TTE in the diagnosis of CM. The most important echocardiographic characteristics to differentiate between CM and tumors of different etiology are tumor location and size. Smaller tumors presenting at an atypical location are less likely to be diagnosed as CM, and these require additional imaging modalities for accurate diagnosis.

Key words: cardiac mass; cardiac myxoma; cardiovascular imaging; echocardiography

Introduction

Although rare, cardiac myxoma (CM) represents the most common benign primary cardiac tumor.[1] Many patients are asymptomatic and CM is often an incidental finding.[2] Potentially life-threatening complications such as tumor obstruction or embolization can occur, making accurate diagnosis crucial.[3,4] However, diagnosis is challenging due to the broad differential diagnosis of CM, which includes other cardiac tumors and cardiac masses such as thrombi, vegetations, calcific lesions, and other rare conditions.

Transthoracic echocardiography (TTE) nowadays represents the most commonly used initial imaging modality in the diagnostic workup of CM. It provides information on tumor size, location, attachment point, morphology, mobility, and its relation to surrounding structures. The majority of CM are located in the left atrium, attached to

the atrial septum in the region of the fossa ovalis. These are considered as typical CM, but atypical localizations outside the left atrium have been described in around 30%.[5] Size and appearance (solid and round or polypoid) may also vary considerably in CM.[6]

TTE has an excellent detection rate for CM and a sensitivity of 90–96% in diagnosing CM has been reported.[4] However, the heterogeneous morphological presentation leads to overlap with other cardiac masses and may affect the specificity and accuracy of TTE in CM diagnosis. Furthermore, TTE lacks tissue characterization.[7] Multimodality cardiac imaging ensures a more detailed analysis. Ultimately, the final diagnosis is made by histopathological examination of the excised tumor.[8]

The aim of our single-center study was to evaluate the utility and accuracy of TTE in the diagnosis of CM and to determine echocardiographic characteristics indicative of pathohistologically confirmed CM.

Patients and methods

The study was conducted in accordance with the Declaration of Helsinki (as revised in 2013). The study was approved by national ethics committee of Slovenia (NO.: 0120-512/2020-3) and informed consent was obtained from individual participants.

We retrospectively analyzed clinical, echocardiographic, and pathohistological findings of all consecutive adult patients (≥ 18 years of age) referred to our Department of Cardiology in the largest tertiary hospital in Slovenia for suspected CM between 2005 and 2020. Our tertiary centre receives approximately 75% of all referrals for suspected CM in the country.

All patients had TTE performed as part of the standard diagnostic workup. Echocardiographic characteristics of the cardiac mass were obtained, including mass location, surface (smooth or lobulated *vs.* villous) and appearance (homogenous *vs.* heterogenous). The mobility of the mass and the presence or absence of obstruction were also noted. Based on TTE findings, patients were diagnosed with either CM, other non-myxomal (NM) cardiac tumor, or cardiac masses of other etiology (thrombus, infective endocarditis, etc.). Diagnosis of CM was made individually by the cardiologist performing TTE based on typical morphological characteristics of the cardiac mass. In some cases, additional imaging methods were used, either due to poor TTE acoustic windows or atypical tumor presentation. TTE contrast imaging was not performed in any of the cases.

Patients with CM or NM cardiac tumors were referred for surgery and pathohistological samples of the tumors were collected and analyzed to determine the final diagnosis. The accuracy, sensitivity, and specificity of TTE were determined by comparing echocardiographic and pathohistological diagnosis. Furthermore, echocardiographic characteristics of pathohistologically proven CM were compared to NM cardiac tumors.

Statistical analysis

Continuous variables are presented as mean ± standard deviation and categorical variables as numbers and percentage. The independent Student's t-test was used to compare continuous variables. Categorical variables were analyzed using the χ^2test. The sensitivity, specificity, negative predictive value, and positive predictive value of echocardiographic diagnosis of CM were calculated using the results of pathohistological examination as the gold standard. Accuracy was determined as the sum of true negative and positive tests divided by all tests. All statistical analyzes were performed using SPSS version 26.0 software. Values of $p < 0.05$ were considered statistically significant.

Results

Baseline characteristics

During the 15-year period, 73 patients were referred for evaluation of suspected CM. All patients underwent TTE and 63 (86%) were diagnosed with CM or NM cardiac tumor. Of the remaining 10 (14%) patients, five were diagnosed with thrombus and were treated accordingly with anticoagulation therapy. In three cases pseudotumor was diagnosed; one had a prominent Eustachian valve, one had a prominent Chiari network, and one had lipomatous hypertrophy of the interatrial septum. In two patients no obvious cardiac mass was found on repeat TTE.

Out of 63 patients diagnosed with either CM or NM, 35 (56%) underwent one or more additional imaging techniques to confirm the diagnosis, either due to suboptimal image quality on TTE or atypical tumor presentation. CMR was used most frequently (n = 23, 66%), followed by TEE (n = 20, 57%) and CT (n = 3, 9%). In two patients PET-CT

was performed to detect possible distant metastases. No working diagnosis changed after additional imaging techniques.

After complete diagnostic workup, 53 (84%) of the 63 patients diagnosed with either CM or NM underwent surgery at our institution and were included for further analysis in our study. Of the 10 remaining patients, one underwent surgery at another institution, 4 had very small intracardiac masses, prompting periodic TTE follow-up, 4 were unfit for surgery, and 1 declined surgical intervention.

The mean age of the operated patients was 64 ± 14 years (26–85 years), 35 patients (66%) were female. The most common complaint was dyspnea (18 patients, 34%), followed by embolic events in 8 patients (15%), chest pain in 5 patients (9%), constitutional signs in 3 patients (6%) and palpitations in 2 patients (4%). Seventeen patients (32%) were asymptomatic. The mass was an incidental finding in 23 patients (43%), most commonly on TTE (61%) and chest CT (39%) performed for other indication.

Echocardiographic characteristics

Based on preoperative echocardiographic findings, the 53 operated patients were divided into two groups: a CM group (45 patients, 85%) and a NM group (8 patients, 15%). Preoperative echocardiographic characteristics are depicted in Table 1. All tumors were solitary. The mean tumor size in the CM group was 35.3 ± 18.6 mm (range: 10–81 mm). The majority of CM were located in the atria; 80% in the left atrium and 18% in the right atrium. One tumor was found in the left ventricle. Tumors found in the left atrium were most frequently attached to the atrial septum in the region of the fossa ovalis (n = 27, 75%) (Figure 1). Other attachment sites in the left atrium included the mitral valve (n = 4, two were attached to the posterior leaflet, one to the anterior leaflet, and one to the posterior annulus of the mitral valve), other areas of the atrial septum (n = 3, posterior part of the atrial septum), the free atrial wall (n = 1) and left atrial appendage (n = 1). The tumors were mostly mobile (n = 32, 71%). Mitral valve obstruction was observed in 10 (22%) patients and tricuspid valve obstruction in 1 (2%) patient.

The mean tumor size in the NM group was 30.3 ± 16.9 mm (range: 8–50 mm) (Table 1). All NM tumors were found in an atypical location, most frequently in the right atrium (n = 4, 50%). Two were attached to the left atrial free wall or posterior mitral valve leaflet and one to the aortic valve.

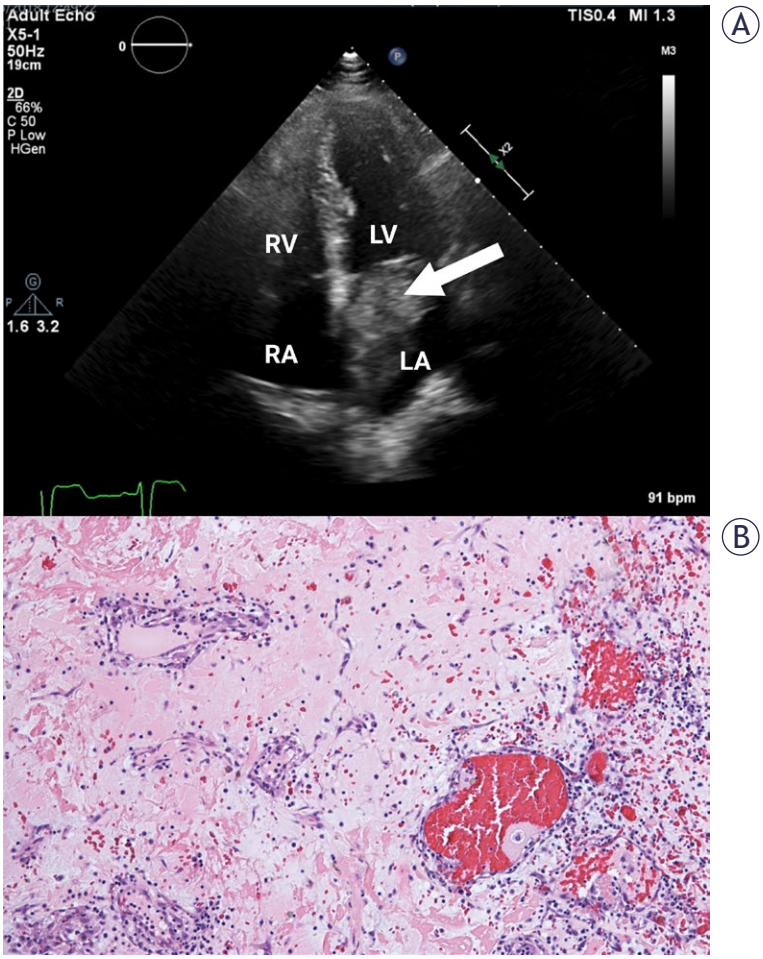

FIGURE 1. (A) Transthoracic echocardiography, apical 4-chamber view. Cardiac mass in left atrium is attached to the interatrial septum in the region of the fossa ovalis (arrow). Histopathological characterization confirmed cardiac myxoma. **(B)** Abundant myxoid stroma with clusters of myxoma cells forming cords and ring structures (HE 100x).

LA = left atrium; LV = left ventricle; RA = right atrium; RV = right ventricle

TTE sensitivity, specificity, and accuracy analysis

Pathohistological samples were obtained from the resected tumors in all 53 surgical procedures performed at our institution. Pathohistological evaluation confirmed CM in 39 of 53 operated patients (73%) (Figure 1).

The calculated sensitivity and specificity of preoperative echocardiography in 53 patients who underwent surgery at our institution were 97% and 50%, respectively. The overall accuracy of TTE in diagnosing CM in those patients was 85% (Figure 2). In 7 patients (13%) diagnosed as CM on

TABLE 1. Preoperative echocardiographic characteristics of the cardiac myxoma (CM) and non-myxoma (NM) group

Echocardiographic characteristics	CM (n=45)	NM (n =8)
Mean size (mm)	35.3 ± 18.6 (range: 10–81)	30.3 ± 16.9 (range: 8–50)
Location		
Left atrium	36 (80)	2 (25)
Fossa ovalis	27 (75)	
Mitral valve	4 (11)	1 (50)
Posterior interatrial septum	3 (8)	
Free left atrial wall	1 (3)	1 (50)
Left atrial appendage	1 (3)	
Right atrium	8 (18)	4 (50)
Left ventricle	1 (2)	1 (12)
Aortic valve		1 (12)
Mobility		
Mobile	32 (71)	7 (88)
Non-mobile	5 (11)	
No data available	8 (18)	1 (12)
Surface		
Smooth or lobulated	28 (62)	1 (12)
Villous	8 (18)	3 (38)
No data available	9 (20)	4 (50)
Obstruction (present)	11 (24)	2 (25)
Mitral valve	10 (21)	1 (50)
Tricuspid valve	1 (9)	1 (50)

Values are presented as mean ± standard deviation or number (percentage).

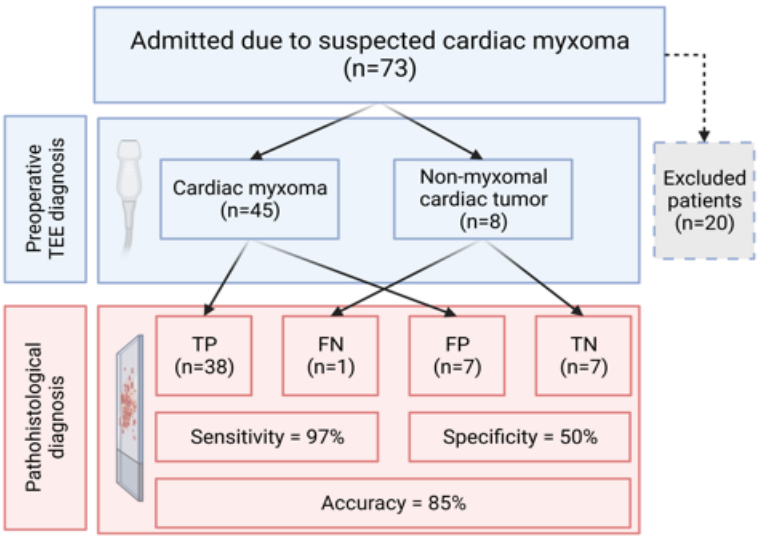

FIGURE 2. Flow diagram showing the diagnostic accuracy of preoperative TTE in patients with suspected CM. The predictive value and accuracy of preoperative TTE was calculated using the results of pathohistological examination as the gold standard.

FN = false negative; FP = false positive; TP = true positive; TN = true negative; TTE = transthoracic echocardiography

preoperative TTE, pathohistology revealed different NM cardiac tumors: papillary fibroelastoma in 5 cases, one case of angioleiomyoma and one malignant melanoma metastasis. Only one patient preoperatively classified as NM cardiac tumor had CM.

Pathohistologically confirmed NM cardiac tumors were significantly smaller than CM (24.3 ± 13.2 mm *vs.* 37.9 ± 18.3 mm, p = 0.017) (Table 2). There was also a statistically significant difference in tumor location between the two groups. All NM tumors were located at an atypical position (seven in the right atrium, five in the left atrium but at an atypical site and two in the left ventricle) and 72% of CM were found at the typical location within the left atrium (p < 0.001). The calculated sensitivity and specificity of tumor location in diagnosis of myxoma was 100% and 56%, respectively. There was no significant difference in other demographic (age, sex) or echocardiographic characteristics (mobility, surface, appearance) between groups.

Discussion

Our single-center study confirms very good overall accuracy of TTE in CM diagnosis. This is clinically important as accurate assessment of cardiac masses is essential for appropriate clinical management and treatment of these patients.

Diagnosis of CM can be challenging since patients are frequently asymptomatic or have only non-specific signs and symptoms. Dyspnea, a frequent and non-specific symptom of cardiac disease, was the most common complaint in our CM group, which is consistent with previous reports.[9–11] Clinical presentation itself rarely suggests the diagnosis of CM; therefore, cardiac imaging is essential in the evaluation of patients with suspected CM. Echocardiography is the most widely used imaging modality that provides important information about the location, size, and appearance of the cardiac mass, as well as possible complications (e.g. obstruction). Previous studies have shown that CM are typically solitary, located in the left atrium, smooth in surface and mobile.[12,13] However, the morphological presentations of CM are often atypical and heterogeneous, leading to overlap with other NM cardiac tumors and cardiac masses.

The results of our study show very good overall accuracy (85%) of TTE in CM diagnosis with excellent sensitivity (97%). However, the specificity of TTE is modest (50%) and caution is warranted

as misdiagnosis of CM is possible. In our study, 5 of the misdiagnosed cases of CM were actually papillary fibroelastoma, which is also a common primary benign cardiac tumor. One of the suspected CM was actually a metastasis of malignant melanoma, underlying the importance of surgical excision and pathohistological examination of all suspected CM.

According to our results tumor localization and tumor size are the best echocardiographic characteristics to distinguish between CM and NM cardiac tumors. CM are typically located in the left atrium attached to the interatrial septum at the region of fossa ovalis, which was also shown in our study.[14] In our patients, 72% of CM were located typically. However, all tumors preoperatively misdiagnosed as CM were located in atypical locations, such as the right atrium and left ventricle. Tumors in the NM group were also significantly smaller compared to tumors in the CM group. However, there was no significant difference in age, sex, and other echocardiographic characteristics (mobility and surface) between the groups.

The differential diagnosis of CM is broad and definite diagnosis is crucial, as treatment varies depending on the diagnosis. Multimodality cardiac imaging improves the diagnostic accuracy of different cardiac masses. In the majority of our patients, at least one additional imaging modality was used as a part of the diagnostic workup. TEE improves image quality and provides more morphological information than TTE.[15] Computed tomography and cardiac magnetic resonance provide additional information on topographic relationships and tissue characteristics, and may detect other pathological conditions within the thorax.[16,17] Assessment of cardiac tumors by CMR is more accurate than echocardiography and can reliably distinguish between benign and malignant cardiac tumors.[18-20]

There are some limitations to this study. First, this is a retrospective study with a relatively small study population, precluding further analyses (e.g. Receiver Operating Characteristic). However, the population size is comparable to other studies on CM. Due to the low incidence of cardiac tumors, only multicenter studies can provide a larger scale patient population. Second, preoperative echocardiography was performed by different echocardiographers, potentially exposing the results to inter-investigator variability in determining the diagnosis. Due to the study inherently including participants already given a working diagnosis of CM, any cardiologist performing TTE was likely influenced by the information provided upon referral. A larger, multicenter, prospective study could serve to identify echocardiographic and clinical characteristics specific to CM, as well as other cardiac tumors, further increasing the utility of preoperative diagnostic modalities.

TABLE 2. Comparison of demographic and echocardiographic characteristics between pathohistologically confirmed cardiac myxoma (CM) and non-myxoma (NM) groups

Characteristic	CM (n= 39)	NM (n = 14)	p value
Age (years)	63.1 ± 13.6	66.6 ± 15.1	0.434
Sex (female)	25 (64)	10 (71)	0.620
Location			
Typical	28 (72)	0	P < 0.001
Atypical	11 (28)	14 (100)	P < 0.001
Size (mm)	37.9 ± 18.3	24.3 ± 13.2	0.017

Values are presented as mean ± standard deviation or number (percentage).

Conclusions

TTE is very accurate in diagnosing CM. Tumor localization and size are the most important echocardiographic characteristics that can differentiate between CM and NM. The diagnosis of CM is less likely in atypical tumor location and smaller tumor size. In such cases, caution is advised and other non-invasive imaging modalities, such as CMR or CT, should be performed to confirm the diagnosis.

Acknowledgments

Funding: The study was financially supported by the Slovenian Research Agency -research core funding No. P3-0429, Slovenian research programme for comprehensive cancer control SLORApro.

References

1. Roberts WC. Primary and secondary neoplasms of the heart. *Am J Cardiol* 1997; **80:** 671-82. doi: 10.1016/S0002-9149(97)00587-0
2. Karabinis A, Samanidis G, Khoury M, Stavridis G, Perreas K. Clinical presentation and treatment of cardiac myxoma in 153 patients. *Medicine* 2018; **97:** e12397-97. doi: 10.1097/MD.0000000000012397
3. Lee S, Kim JH, Na CY, Oh SS. Eleven years' experience with korean cardiac myxoma patients: focus on embolic complications. *Cerebrovasc Dis* 2012; **33:** 471-9. doi: 10.1159/000335830

4. Samanidis G, Khoury M, Balanika M, Perrea DN. Current challenges in the diagnosis and treatment of cardiac myxoma. *Kardiol Pol* 2020; **78:** 269-77. doi: 10.33963/KP.15254

5. Poterucha TJ, Kochav J, O'Connor DS, Rosner GF. Cardiac tumors: clinical presentation, diagnosis, and management. *Curr Treat Options Oncol* 2019; **20:** 1-15. doi: 10.1007/s11864-019-0662-1

6. Tyebally S, Chen D, Bhattacharyya S, Mughrabi A, Hussain Z, Manisty C, et al. Cardiac tumors JACC CardioOncology State-of-the-Art Review. *Jacc Cardiooncology* 2020; **2:** 1-19. doi: 10.1016/j.jaccao.2020.05.009

7. Colin GC, Gerber BL, Amzulescu M, Bogaert J. Cardiac myxoma: a contemporary multimodality imaging review. *Int J Cardiovasc Imaging* 2018; **34:** 1789-808. doi: 10.1007/s10554-018-1396-z

8. Basso C, Rizzo S, Valente M, Thiene G. Cardiac masses and tumours. *Heart* 2016; **102:** 1230-45. doi: 10.1136/heartjnl-2014-306364

9. Pinede L, Duhaut P, Loire R. Clinical presentation of left atrial cardiac myxoma: a series of 112 consecutive cases. *Medicine* 2001; **80:** 159-72. doi: 10.1097/00005792-200105000-00002

10. Cianciulli TF, Cozzarin A, Soumoulou JB, Saccheri MC, Méndez RJ, Beck MA, et al. Twenty years of clinical experience with cardiac myxomas: diagnosis, treatment, and follow up. *J Cardiovasc Imaging* 2019; **27:** 37-47. doi: 10.4250/jcvi.2019.27.e7

11. Yu SH, Lim SH, Hong YS, Yoo KJ, Chang BC, Kang MS. Clinical experiences of cardiac myxoma. *Yonsei Med J* 2006; **47:** 367-71. doi: 10.3349/ymj.2006.47.3.367

12. Bjessmo S, Ivert T. Cardiac myxoma: 40 years' experience in 63 patients. *Ann Thorac Surg* 1997; **63:** 697-700. doi: 10.1016/S0003-4975(97)00003-9

13. Grebenc ML, Rosado-De-Christenson ML, Green CE, Burke AP, Galvin JR. Cardiac myxoma: imaging features in 83 patients. *Radiographics* 2002; **22:** 673-89. doi: 10.1148/radiographics.22.3.g02ma02673

14. Zipes D, Libby P, Bonow R, Mann D, Tomaselli G. *Braunwald's heart disease: a textbook of cardiovascular medicine*. 11th Edition. Philadelphia: Elsevi 2018. p. 555-62.

15. Engberding R, Daniel WG, Erbel R, Kasper W, Lestuzzi C, Curtius JM, et al. Diagnosis of heart tumours by transoesophageal echocardiography: a multicentre study in 154 patients. *Eur Heart J* 1993; **14:** 1223-8. doi: 10.1093/eurheartj/14.9.1223

16. Wintersperger BJ, Becker CR, Gulbins H, Knez A, Bruening R, Heuck A, et al. Tumors of the cardiac valves: imaging findings in magnetic resonance imaging, electron beam computed tomography, and echocardiography. *Eur Radiol* 2000; **10:** 443-9. doi: 10.1007/s003300050073

17. Mendes GS, Abecasis J, Ferreira A, Ribeiras R, Abecasis M, Gouveia R, et al. Cardiac tumors: three decades of experience from a tertiary center: are we changing diagnostic work-up with new imaging tools? *Cardiovasc Pathol* 2020; **49:** 107242. doi: 10.1016/j.carpath.2020.107242

18. Hoey ETD, Mankad K, Puppala S, Gopalan D, Sivananthan MU. MRI and CT appearances of cardiac tumours in adults. *Clin Radiol* 2009; **64:** 1214-30. doi: 10.1016/j.crad.2009.09.002

19. Pazos-López P, Pozo E, Siqueira ME, García-Lunar I, Cham M, Jacobi A, et al. Value of CMR for the differential diagnosis of cardiac masses. *JACC Cardiovasc Imaging* 2014; **7:** 896-905. doi: 10.1016/j.jcmg.2014.05.009

20. Giusca S, Mereles D, Ochs A, Buss S, André F, Seitz S, et al. Incremental value of cardiac magnetic resonance for the evaluation of cardiac tumors in adults: experience of a high volume tertiary cardiology centre. *Int J Cardiovasc Imaging* 2017; **33:** 879-88. doi: 10.1007/s10554-017-1065-7

research article

Comparison of 2D and 3D radiomics features with conventional features based on contrast-enhanced CT images for preoperative prediction the risk of thymic epithelial tumors

Yu-Hang Yuan[1], Hui Zhang[1], Wei-Ling Xu[1], Dong Dong[1], Pei-Hong Gao[1], Cai-Juan Zhang[1], Yan Guo[2], Ling-Ling Tong[3], Fang-Chao Gong[4]

[1] Department of Radiology, The First Hospital of Jilin University, Jilin, China
[2] GE Healthcare, China
[3] Department of Pathology, The First Hospital of Jilin University, Jilin, China
[4] Department of Thoracic Surgery, The First Hospital of Jilin University, Jilin, China

Radiol Oncol 2025; 59(1): 69-78.

Received 31 July 2024
Accepted 27 January 2025

Correspondence to: Fang-Chao Gong, Department of Thoracic Surgery, The First Hospital of Jilin University, No. 71 Xinmin Street, Chaoyang District, Changchun 130021, Jilin, China. E-mail: fangchao_gong@163.com

Yu-Hang Yuan and Hui Zhang contributed equally to this work.

Disclosure: No potential conflicts of interest were disclosed.

Background. This study aimed to develop and validate 2-Dimensional (2D) and 3-Dimensional (3D) radiomics signatures based on contrast-enhanced computed tomography (CECT) images for preoperative prediction of the thymic epithelial tumors (TETs) risk and compare the predictive performance with conventional CT features.

Patients and methods. 149 TET patients were retrospectively enrolled from January 2016 to December 2018, and divided into high-risk group (B2/B3/TCs, n = 103) and low-risk group (A/AB/B1, n = 46). All patients were randomly assigned into the training (n = 104) and testing (n = 45) set. 14 conventional CT features were collected, and 396 radiomic features were extracted from 2D and 3D CECT images, respectively. Three models including conventional, 2D radiomics and 3D radiomics model were established using multivariate logistic regression analysis. The discriminative performances of the models were demonstrated by receiver operating characteristic (ROC) curves.

Results. In the conventional model, area under the curves (AUCs) in the training and validation sets were 0.863 and 0.853, sensitivity was 78% and 55%, and specificity was 88% and 100%, respectively. The 2D model yielded AUCs of 0.854 and 0.834, sensitivity of 86% and 77%, and specificity of 72% and 86% in the training and validation sets. The 3D model revealed AUC of 0.902 and 0.906, sensitivity of 75% and 68%, and specificity of 94% and 100% in the training and validation sets.

Conclusions. Radiomics signatures based on 3D images could distinguish high-risk from low-risk TETs and provide complementary diagnostic information.

Key words: thymic epithelial tumors; radiomics; computed tomography; World Health Organization; classification

Introduction

Thymic epithelial tumors (TETs) are the most prevalent neoplasms in the anterior mediastinum. They generally exhibit low malignancy in both histological and clinical presentations.[1] The WHO classification of TETs, based on lymphocyte-to-epithelial cell ratio and epithelial cell morphology, is widely adopted. According to the 2015 criteria, TETs are categorized into thymomas (with six subtypes)

and thymic carcinomas (TCs).[2,3] This classification serves as an independent prognostic factor and is simplified into low-risk (Type A, AB, B1) and high-risk (Type B2, B3, TCs) categories, influencing patient outcomes.[4] The WHO classification reflects the tumor's clinical and functional features, aiding preoperative diagnosis and treatment planning.[5] Accurate, noninvasive identification and subgroup classification of TETs prior to treatment hold significant clinical value.

CT imaging is the primary diagnostic tool for TETs, revealing a wide range of biological and morphological features.[6,7] Studies have reported specific CT characteristics of TETs.[8,9] While chest contrast-enhanced computed tomography (CECT) provides general morphological parameters, distinguishing between histological subgroups remains challenging due to significant overlap. Radiomics, leveraging radiomic signatures, extracts diverse, high-throughput imaging features, transforming medical images into mineable data.[10,11] Radiomic features can predict disease, cancer, metastasis, and prognosis.[12] Previous studies have used 2D radiomics to determine thymoma risk levels.[13,14] Wang *et al*. differentiated low-risk from high-risk thymomas and early from advanced tumors using contrast-enhanced CECT and non-enhanced CT[15], but their study had a small sample size and the sample size was imbalanced.

Despite several CT-based radiomics analyses being used to classify TET risk, most studies rely on 2D imaging features. Further research is needed to explore 3D radiomic signatures, which may provide more comprehensive and accurate information for TET diagnosis and risk assessment. The available models still require refinement and validation.

This study aimed to develop conventional and 2D/3D radiomics signatures using the conventional and texture features extracted from CECT images for preoperative prediction of the WHO's TET risk classification.

Patients and methods

Patients

This retrospective study was approved by the Ethics Committee of the First Hospital of Jilin University, and the requirement for informed consent was waived due to the retrospective nature of the study (Studi Approval Number: 2020-541). From January 2016 to December 2018, data from 175 patients who undergoing CECT examination within one week to two months before surgery who were pathologically diagnosed as TET were collected in our hospital consecutively. The inclusion criteria were: 1) underwent CECT within one week to two months before surgery without chemotherapy; 2) high CT image quality without artifacts; and 3) available clinical and surgical data. The exclusion criteria were shown in Figure 1. Finally, 149 patients with pathologically confirmed TET were enrolled in this study. The baseline characteristics of all patients including age, sex and symptoms (thoracalgia and myasthenia gravis) were collected. The patients were divided into the high-risk group (B2/B3/TCs, n = 103) and the low-risk group (A/AB/B1, n = 46) according to the WHO classification criteria of TET. All patients were randomly assigned into the training group (n = 104) and test (n = 45) group at a ratio of 7:3. Figure 1 illustrates the flow chart of the case selection process.

CT scanning

All patients underwent routine two-phase chest CECT scans using either a 64-MDCT scanner (Definition, Siemens Healthcare, Erlangen, Germany) or a 128-MDCT scanner (iCT, Philips Healthcare, Amsterdam, Netherlands). The scanning parameters were as follows: (1) Philips iCT: tube voltage 120 kV, automatic mAs, layer thickness 5 mm, pitch 0.980; (2) GE Lightspeed VCT: tube voltage 120 kV, automatic mAs, slice thickness 5 mm, pitch 0.992. All patients were examined in a supine position, arms up, deep inspiration and scanning. The contrast agent was injected into the patient using a high-pressure syringe (Visipaque 320, Amersham Health, Cork, Ireland). A total of 60-80 mL of contrast agent was administered through the antecubital vein at a rate of 3 ml/s, which was followed by 30 ml of saline injection at the same rate.

Conventional CT features measurement

The CT images were reviewed on the picture archiving and communication system (PACS). The conventional CT features of all patients were analyzed and recorded, including tumor's long diameter, short diameter, vertical diameter, area, perimeter and CT values. The tumor heterogeneity evaluated by the radiologist is also recorded, consisting of location (right, middle or left), morphology (lobular, /shallowly-lobulated or non-lobular), demarcation (clear, unclear or infiltrating), internal calcification and necrosis. The workflow of conventional CT feature analysis was shown in Figure 2.

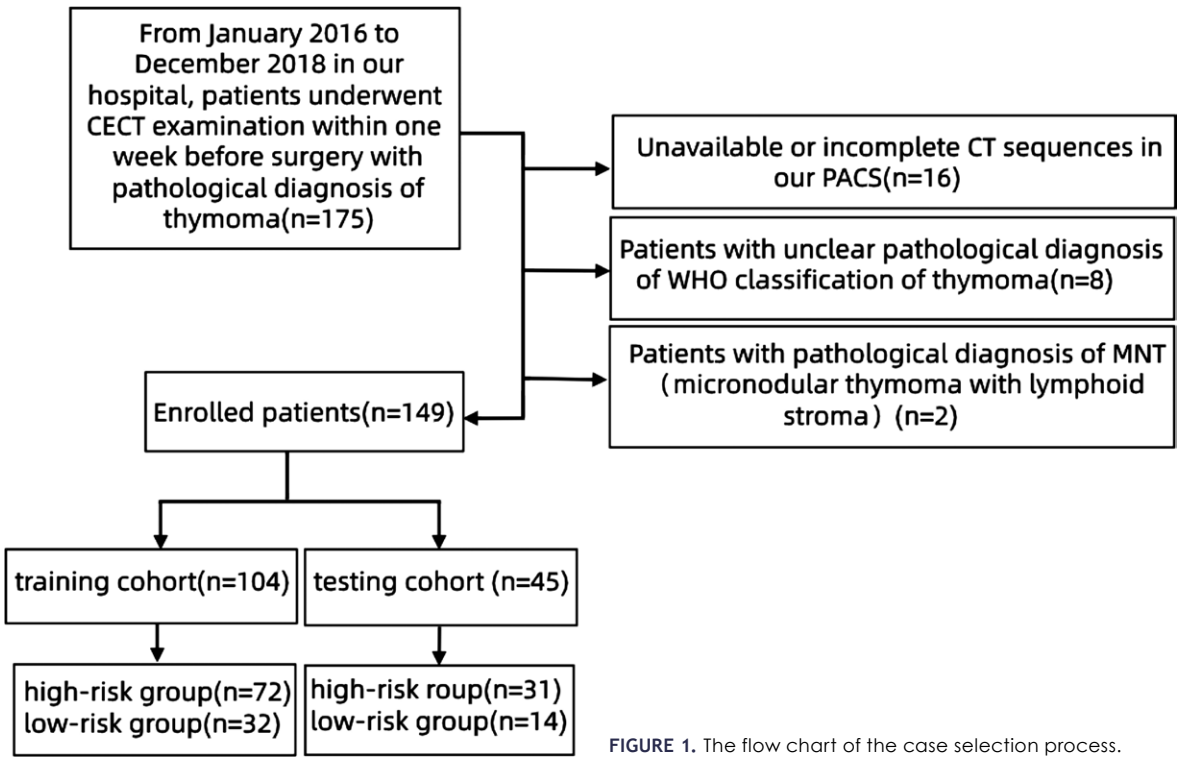

FIGURE 1. The flow chart of the case selection process.

2D and 3D Tumor segmentation

The original CT images with a thickness of 5 mm were uploaded to the A.K. software (Artificial Intelligence Kit, A.K., GE Healthcare, China) for 2D and 3D manual segmentation. First, using a linear interpolation algorithm, the raw data were resampled to a common voxel spacing of 1 mm^3 to construct new data points within the range of a discrete set of known data points, and the voxel would be isotropic. The data with a window width of 350 HU and a window level of 50 HU were used. The 2D and 3D regions of interest (ROIs) were delineated by two independent experienced radiologists (reader 1, XWL with 15 years of experience in chest imaging and reader 2, ZH with 10 years of experience in chest imaging) who were blinded to the pathology results. The 2D ROIs were delineated at the level of the single largest cross-sectional area around the tumor outline. The 3D ROIs were achieved from different continuous levels. To segment the ROI in axial CT images, a manual method was used on the AK software. The lesion was manually separated from the large blood vessels, lung, air, fat tissue and chest wall. The workflow of radiomics analysis was shown in Figure 2.

2D and 3D radiomic features extraction

According to the CECT images of each patient, a total of 396 radiomic features were extracted automatically from the 3D and 2D ROI respectively using A.K. software. The radiomic features were composed of the following classes: first-order histogram features (N = 42), second-order texture features (N = 345, including the Haralick texture (N = 10), gray level co-occurrence matrix (N = 144), gray level run length matrix (N = 180) and gray level size zone matrix (N = 11), and morphological features (N = 9). Details of the radiomics features were described in Supplementary Figure. S1.

Features selection

To reduce the dimensionality of the conventional and 2D/3D radiomic features, the least absolute shrinkage and selection operator (LASSO) method was applied to identify the most valuable features from the training dataset. For better performance of the model, the best penalty parameters λ was obtained based on the loss function with the least squares during 10-fold-cross-validation procedure.

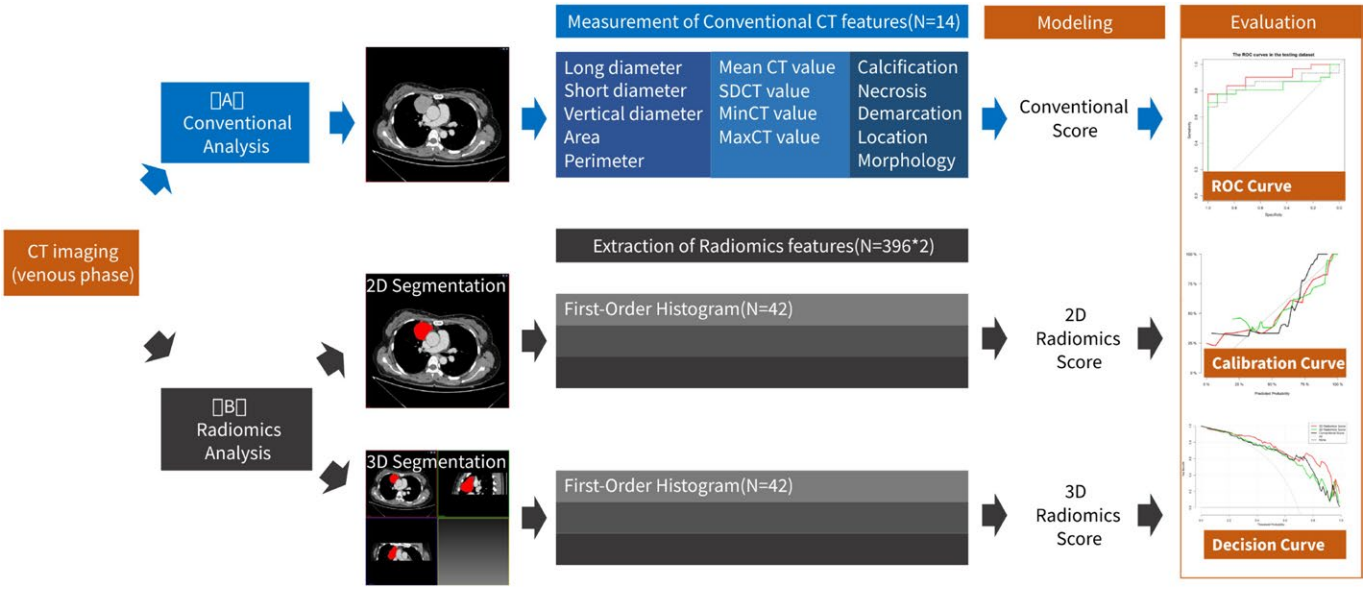

FIGURE 2. The flow chart of the CT imaging analysis. **(A)** shows the workflow of conventional analysis and 14 conventional features were recorded. **(B)** shows the workflow of radiomics analysis. 2D and 3D segmentation were performed on the CT images and 396 radiomics features were extracted respectively. The most predictive feature variables were selected, and the multivariate logistic regression analysis was applied to build the prediction models. The predicting abilities of the conventional and radiomics models were demonstrated by receiver operating characteristic (ROC) curves. The goodness of fit was assessed using calibration curve of the Hosmer-Lemeshow test. Additionally, decision curve analysis (DCA) was conducted to determine the clinical usefulness of the models.

Model building and evaluation

Three models, including the conventional model, 2D radiomics model and 3D radiomics model, were established using multi-variate logistic regression based on the selected features. Then the conventional score, 2D radiomics score and 3D radiomics score were calculated for each patient via a linear combination of selected features weighted by coefficients.

The discriminative performance of the three models were evaluated by ROC curves. The area under the curves (AUC), sensitivity, specificity and the optimal cutoff value were obtained from ROC analysis. Delong test was used to identify the difference of AUC between different models, and $P < 0.05$ indicated a significant difference. The degree of calibration was assessed in the calibration curve of the Hosmer-Lemeshow test, and $P > 0.05$ indicated a good fit. Furthermore, decision curve analysis (DCA) was conducted to determine the clinical applicability of the models by quantifying the net benefit under different threshold probabilities.

Statistical analysis

Continuous data with a normal distribution (according to the Kolmogorov-Smirnov test) were expressed as mean ± standard deviation (SD) and analyzed using Student's t-test. Continuous variables with a non-normal distribution were expressed as medians (interquartile range) and analyzed using the Mann-Whitney test. Categorical variables were represented as frequencies and percentages and analyzed using the chi-square test. The statistical analysis was conducted using R software (v. 3.6.1, http://www.R-project.org). A two-tailed p value of less than 0.05 was considered significant.

Results

Baseline characteristics of the patients

There were 104 patients in the training set, among which 72 (69.2%) cases were in the high-risk group. The testing set involved 45 patients, and 31 (68.9%) cases were in the high-risk group. Age, sex, and

TABLE 1. Baseline characteristics of the patients in training and testing dataset

	Training set			Testing set		
	Low-risk (n=32)	High-risk (n= 72)	P	Low-risk (n=14)	High-risk (n=31)	P
Age, (Mean ± SD) years	53.6±11.2	52.5±11.4	0.656	54.0±10.7	56.4±8.9	0.446
Sex (male, No. (%))	14 (43.8)	37 (51.4)	0.472	7 (50.0)	18 (58.1)	0.614
Myasthenia gravis, No. (%)	7 (21.9)	24 (33.3)	0.238	0 (0.0)	8 (25.8)	0.094
Thoracalgia, No. (%)	3 (9.4)	18 (25.0)	0.067	1 (7.1)	11 (35.5)	0.104

frequency of myasthenia gravis and thoracalgia were similar between the high-risk and low-risk groups in both the training and testing sets (all P > 0.05). The characteristics of the patients are presented in Table 1.

Three models building

Conventional model

In the training set, compared with the low-risk group, the high-risk group had a lower mean HU value (62.0 *vs*. 79.5 HU, P < 0.001), a lower maximum HU value (118.0 *vs*. 148.5 HU, P < 0.001), a smaller short diameter 23.2 *vs*. 34.7 mm, P = 0.009), a smaller area (628.5 *vs*. 1321.5 mm^2, P = 0.008), and a smaller perimeter (112.5 *vs*. 143.0 mm, P = 0.021). In addition, the lesions in the high-risk group were often non-lobular (P = 0.010), and there was no clear demarcation (P = 0.023). The patient's CT conventional parameters are listed in Table 2.

In the testing set, the maximum HU value of the high-risk group was lower than that of the low-risk group (median HU 129.0 *vs*. 162.0, P = 0.002). The lesions in the high-risk group tended to be non-lobular (P < 0.001), with no clear demarcation (P = 0.010).

After LASSO regression analysis, seven conventional CT features with non-zero coefficients were remained. The calculation formula of the conventional score was as follows:

Conventional Score = 5.71-0.012*Circle.mm-0.051*Mean CT value + 0.023*Minimum CT value-0.009*Maximum CT value-0.903*Necrosis + 1.859*adjacent-0.595*Location.

2D Radiomics model

After LASSO regression analysis, five CT features including Min Intensity, Percentila75, Correlation_angle0_offset7, LongRunEmphasis_angle90_offset1, and Small Area Emphasis were retained. The formula for the calculation of the 2D radiomics score was as follows:

2D Radiomics Score = 1.343-0.528 *Min intensity-0.805* Percentile75-0.557* Correlation_angle0_offset7 + 1.343* LongRunEmphasis_angle90_offset 1-0.900* SmallAreaEmphasis

3D radiomics model

The 3D radiomics model was established using eight selected CT features, and the calculation formula of the 3D radiomics score was as follows:

3D Radiomics Score = 1.330-1.731 *Percentile75-0.915* ClusterProminence_angle135_offset4-1.266 *GLCMEnergy_angle0_offset7 + 0.635* AngularSecondMoment-0.559 *LongRunEmphasis_AllDirection_offset1 + 0.678* LowGreyLevelRunEmphasis_AllDirection_offset7_SD-0.573 *Compactness1-0.714* IntensityVariability.

The performance of the three models

Discriminative degree

In the training set, this conventional model had an AUC of 0.863 (95% confidence interval (CI): 0.786-0.940), a sensitivity of 78%, and a specificity of 88%. In the testing set, the AUC was 0.853 (95% CI: 0.740-0.965), the sensitivity was 55%, and the specificity was 100%. The 2D radiomics model yielded an AUCs of 0.854 (95% CI: 0.7-0.931) and 0.834 (95%CI: 0.714-0.954), a sensitivity of 86% and 77%, and a specificity of 72% and 86% in the training and testing set, respectively. For the 3D radiomics model, the AUC of the training and testing set was 0.902 (95%CI: 0.842-0.963) and 0.906 (95%CI: 0.820-0.991), respectively, the sensitivity was 75% and 68%, respectively, and the specificity was 94% and 100%, respectively. The ROC curves and the detailed results were shown in Figure 3 and Table 3.

As shown in Figure 3, the AUC of 3D model was usually higher compared with the conventional parameter model and 2D model. However,

TABLE 2. Distribution of conventional CT features in training and testing dataset

	Training set			Testing set		
	Low-risk (n=32)	High-risk (n= 72)	P	Low-risk (n=14)	High-risk (n=31)	P
Mean CT value (HU)	79.5 (68.4, 91.6)	62.0 (51.0, 78.8)	**<0.001**	88.5 (76.0, 95.1)	67.0 (59.2, 74.0)	**<0.001**
Standard deviation	18.0 (16.0, 22.6)	16.5 (14.0, 19.0)	0.050	18.0 (15.9, 26.2)	17.0 (14.2, 21.6)	0.548
Minimum CT value (HU)	-6.10±30.2	-8.5±25.0	0.678	-0.7±31.6	-7.3±17.9	0.477
Maximum CT value (HU)	148.5 (131.0, 172.1)	118.0 (105.5, 138.6)	**<0.001**	162.0 (148.9, 166.1)	129.0 (105.4, 146.8)	**0.002**
Long diameter (mm)	50.6±17.0	44.1±19.4	0.106	47.8 (40.9, 57.8)	38.0 (27.7, 61.3)	0.198
Short diameter (mm)	34.7 (23.9, 41.7)	23.2 (17.7, 34.6)	**0.009**	36.5 (26.0, 45.4)	25.6 (19.0, 39.3)	0.073
Vertical diameter (mm)	48.6 (44.1, 60.2)	40.4 (29.1, 55.2)	0.204	50.5 (44.4, 63.6)	38.9 (33.1, 55.1)	0.059
Area (mm^2)	1321.5 (692.0, 1889.8)	628.5 (397.4, 1409.7)	**0.008**	1024.0 (747.7, 1623.3)	651.0 (346.0, 1362.8)	0.315
Perimeter (mm)	143.0 (110.8, 167.7)	112.5 (78.6, 153.8)	**0.021**	143.5 (118.6, 255.4)	100.0 (84.1, 194.8)	0.098
Location			0.373			0.790
Right mediastinum	10 (31.3%)	33 (45.8%)		7 (50.0%)	11 (35.5%)	
Middle	8 (25.0%)	15 (20.8%)		1 (7.1%)	3 (9.7%)	
Left mediastinum	14 (43.8%)	24 (33.3%)		6 (42.9%)	17 (54.8%)	
Morphology			**0.010**			**<0.001**
Lobular	5 (15.6%)	10 (13.9%)		7 (50.0%)	2 (6.5%)	
Shallowly-lobulated	15 (46.9%)	14 (19.4%)		7 (50.0%)	15 (48.4%)	
Non-lobular	12 (37.5%)	48 (66.7%)		0 (0.0%)	14 (45.2%)	
Demarcation			**0.023**			**0.010**
Clear	15 (46.9%)	17 (23.6%)		10 (71.4%)	8 (25.8%)	
Unclear	16 (50.0%)	43 (59.7%)		4 (28.6%)	17 (54.8%)	
Infiltration	1 (3.1%)	12 (16.7%)		0 (0%)	6 (19.4%)	
Internal calcification	8 (25.0%)	13 (18.1%)	0.416	4 (28.6%)	9 (29.0%)	0.746
Necrosis	12 (37.5%)	20 (27.8%)	0.321	9 (64.3%)	12 (38.7%)	0.111

Continuous variables that conformed to the normal distribution were expressed as mean ±SD. Continuous variables that did not conform to the normal distribution were represented by median values (25%, 75%). Categorical variables were expressed as No. (%).

Coarse P values represented statistically significant.

due to the limited data size, Delong test suggested that there was no statistical difference of AUCs among conventional, 2D and 3D models. The process and results of the Delong test are described in Supplementary Figure S2.

Calibration degree

The calibration curves of the three models were illustrated in Figure 4, which demonstrated good agreement between the predictive and actual probability. All the P value of the Hosmer-Lemeshow test were more than 0.05 in both training and testing datasets for the conventional model (P = 0.735 and 0.266, respectively), 2D model (P = 0.665 and 0.492, respectively) and 3D model (P = 0.562 and 0.448, respectively).

Clinical usefulness

DCA for the three models was performed in both training and testing datasets (Figure 5). The decision curve showed that all the three models added more benefit than using treat-all scheme (assuming all TETs are high risk) or the treat-none scheme (assuming all TETs are low risk) if the threshold probability was > 10%. When the threshold probability was betwen 25% to 60% or between 70% to 95%, using the 3D radiomics model to predict the TETs risk added more benefit than either the con-

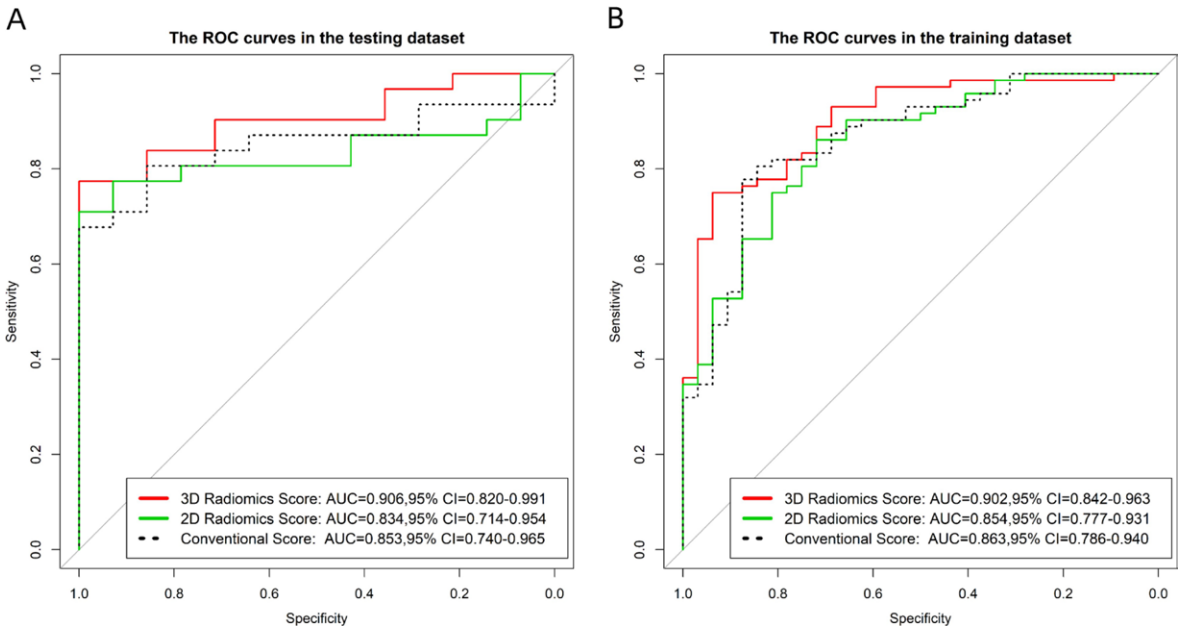

FIGURE 3. Receiver operating characteristic (ROC) curve analysis of the conventional, 2D and 3D radiomics models: **(A)** the training set; **(B)** the testing set.

ventional model or the 2D radiomics model in both training and testing datasets.

Discussion

This study evaluates three models using conventional and radiomic signatures, revealing that radiomic features from 2D and 3D imaging serve as noninvasive biomarkers for thymic epithelial tumors (TETs). These features enable preoperative risk stratification, guiding the surgical approach and resection extent. Importantly, risk stratification aids in personalized treatment planning for high-risk patients, often needing adjuvant therapy. A Phase II studies show that preoperative chemotherapy and radiotherapy enhance R0 resection rates.[16]Thus, this study highlights the significance of radiomic signatures in preoperative risk assessment and treatment planning for TETs.

In this study, three established models obtained using the conventional and radiomics signatures

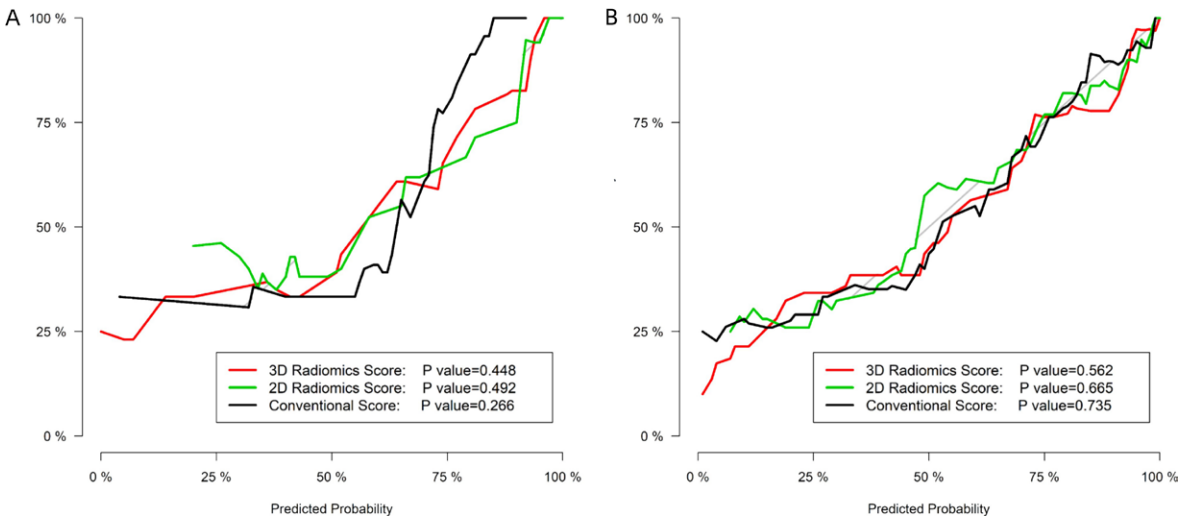

FIGURE 4. The calibration curves of the conventional, 2D and 3D radiomics models:**(A)** the training set; **(B)** the testing set.

TABLE 3. Diagnostic performance of the three models

Model	Training dataset			Testing dataset		
	Sensitivity	Specificity	AUC (95%CI)	Sensitivity	Specificity	AUC (95%CI)
Conventional models	77.8%	87.5%	0.863(0.786-0.940)	54.8%	100.0%	0.853(0.740-0.965)
2D radiomics model	86.1%	71.9%	0.854(0.777-0.931)	77.4%	85.7%	0.834(0.714-0.984)
3D radiomics model	75.0%	93.8%	0.902(0.842-0.963)	67.7%	100.0%	0.906(0.820-0.991)

AUC = area under the curve; CI = confidence interval; CT = computed tomography

were examined. The results indicated that the radiomics signatures based on conventional, 2D and 3D images could be used as noninvasive biomarkers to differentiate high-risk from low-risk TETs. Specifically, these models can provide preoperative risk stratification which informs the choice of surgical approach (minimally invasive surgery or thoracotomy) and helps define the extent of resection. By accurately predicting the risk, this model could aid in minimizing unnecessary tissue damage and reducing complications, potentially improving surgical outcomes and postoperative recovery. Since high-risk TET patients generally have poorer prognosis and often require adjuvant therapy, this stratification can guide treatment planning and improve patient outcomes by facilitating more personalized interventions.

Radiomics has shown significant potential in personalized medicine by providing non-invasive insights into tumor characteristics.[10,12] It has been applied in various diseases, such as predicting thyroid cancer nodules, differentiating the benign and malignant nature of pulmonary nodules, and supporting clinical decision-making for liver cancer patients. Radiomics studies using different imaging modalities (including ultrasound, MRI, and CT) have increasingly played a crucial role in clinical decision-making, providing new technological support for prediction, diagnosis, and prognosis.[17,18,19]

Radiomics can be used to determine the TET classification according to WHO criteria. Previous studies have applied radiomics to classify the risk levels of thymomas and predict their invasiveness[15,20,21], but the available models still need refinement and validation. Therefore, this study aimed to use radiomics based on CECT images to develop conventional and radiomics signatures, which may help the preoperative prediction of the risk of TET classified by WHO guideline.

We used a simplified classification that defines Type A, AB, and B1 thymomas as low-risk and Type B2 and B3 thymomas and TC as high-risk, which is related to patient outcome. High-risk thymic epithelial tumors reportedly have a much poorer prognosis compared with low-risk thymic epithelial tumors, the former need adjuvant therapy to improve survival. With complete resection of the tumor, the prevalence of recurrence of LTET seems low.

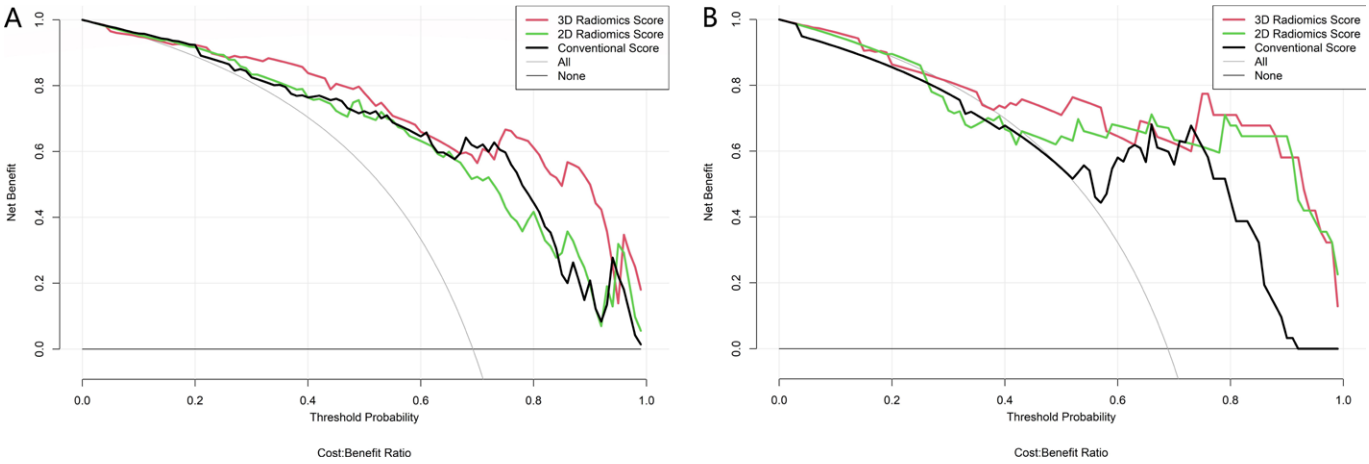

FIGURE 5. Decision curve analysis (DCA) to determine the clinical usefulness of the models by quantifying the net benefits under different threshold probabilities: **(A)** the training set; **(B)** the testing set.

Our 3D radiomics model performed better in terms of AUC, sensitivity, and specificity compared to prior models reported in the literature. For instance, Wang *et al*. reported an AUC of 0.801, with a sensitivity of 75% and specificity of 77%, while Sui *et al*. found sensitivities ranging from 71% to 74% and specificities from 65% to 74% for differentiating low-risk and high-risk TETs. The improved performance of our model may be attributed to the enhanced information captured by 3D imaging features, which provide a more comprehensive representation of tumor morphology and texture heterogeneity than 2D features. This suggests that using 3D data could offer a substantial advantage in capturing the complex structural characteristics of TETs, which is consistent with findings from previous studies on the added value of 3D features. However, it should also be noted that 3D feature extraction and analysis increase computational complexity, highlighting a potential trade-off between accuracy and practicality. In this study, the images with 5 mm thickness in CECT were used for radiomics analysis, which not only saves time but also yields satisfactory results.

Due to the small sample size, the fluctuation of individual samples affected the results greatly. The Hosemer-Lemeshow test was greater than 0.05. Although there were small fluctuations in the calibration map images of the test set, it still showed good consistency between predicted probability and true possibility without statistical deviation.

In the clinical usefulness, the 3D radiomics model was valid from 25% to 60% and from 70% to 95% for the training set, and valid from 25% to 57% and from 75% to 90% for the test set. The DCA analysis showed the 3D model to be more effective and reliable than the other two models to determine the clinical management.

Conventional features such as contour, capsule, septum and homogeneous enhancement can be used to distinguish low-risk and high-risk TETs.[7-9] Our study also compared the parameters obtained through the conventional CT features rather than software calculations, which also has some clinical significance for distinguishing high-risk from low-risk groups.

Except CT, magnetic resonance imaging (MRI) could also be used to differentiate the grading of TETs according to WHO criteria.[22,23] Nevertheless, the use and combination of multiple imaging modalities could maximize the diagnostic value, provided that all modalities are available at a given hospital, but this is not always the case, especially in developing countries like China.

This study has several limitations. First, it is a single-center, small-sample, retrospective study, which may limit the generalizability of the findings and lead to overfitting. The small sample size also means that individual sample fluctuations could have a more significant impact on the model's performance, thus affecting its robustness. To address this, we plan to expand the sample size and conduct a multi-center study for further investigation. Second, the absence of Masaoka staging information limits the model's applicability in distinguishing between different stages of thymic epithelial tumors (TETs), which is crucial for clinical decision-making. In future studies, we will incorporate this information. Third, variability in CT scan parameters and reconstruction techniques could affect the consistency and reproducibility of radiomics features, further impacting model performance. Standardizing imaging acquisition and processing methods will be essential in future studies to enhance both model robustness and clinical applicability. Additionally, AI-based automated recognition methods will be employed for more in-depth tumor analysis. Although the model demonstrates excellent performance in distinguishing risk groups, additional factors, such as tumor heterogeneity or genetic information, may further enhance predictive accuracy[24].

Conclusions

In conclusion, radiomics signatures based on conventional, 2D and 3D images could be used as non-invasive biomarkers to differentiate high-risk TETs from low-risk TETs. The 3D radiomics signature can provide complementary diagnostic information and as the most useful method to determine the clinical management.

References

1. Engels EA. Epidemiology of thymoma and associated malignancies. *J Thorac Oncol* 2010; **5(10 Suppl 4):** S260-5. doi: 10.1097/JTO.0b013e3181f1f62d

2. Travis WD, Brambilla E, Nicholson AG, Yatabe Y, Austin JHM, Beasley MB, et al. The 2015 World Health Organization Classification of Lung Tumors: impact of genetic, clinical and radiologic advances since the 2004 classification. *J Thorac Oncol* 2015; **10:** 1243-60. doi: 10.1097/JTO.0000000000000630

3. Meurgey A, Girard N, Merveilleux du Vignaux C, Maury JM, Tronc F, Thivolet-Bejui F, et al. Assessment of the ITMIG statement on the WHO histological classification and of the eighth TNM staging of thymic epithelial tumors of a series of 188 thymic epithelial tumors. *J Thorac Oncol* 2017; **12:** 1571-81. doi: 10.1016/j.jtho.2017.06.072

4. Suster S, Moran CA. Histologic classification of thymoma: the World Health Organization and beyond. *Hematol Oncol Clin North Am* 2008; **22:** 381-92. doi: 10.1016/j.hoc.2008.03.001

5. Kondo K, Yoshizawa K, Tsuyuguchi M, Kimura S, Sumitomo M, Morita J, et al. WHO histologic classification is a prognostic indicator in thymoma. *Ann Thorac Surg* 2004; **77:** 1183-8. doi: 10.1016/j.athoracsur.2003.07.042

6. Nishino M, Ashiku SK, Kocher ON, Thurer RL, Boiselle PM, Hatabu H. The thymus: a comprehensive review-erratum. *Radiographics* 2017; **37:** 1004. doi: 10.1148/rg.2017174002

7. Sadohara J, Fujimoto K, Müller NL, Kato S, Takamori S, Ohkuma K, et al. Thymic epithelial tumors: comparison of CT and MR imaging findings of low-risk thymomas, high-risk thymomas, and thymic carcinomas. *Eur J Radiol* 2006; **60:** 70-9. doi: 10.1016/j.ejrad.2006.05.003

8. Ozawa Y, Hara M, Shimohira M, Sakurai K, Nakagawa M, Shibamoto Y. Associations between computed tomography features of thymomas and their pathological classification. *Acta Radiol* 2016; **57:** 1318-25. doi: 10.1177/0284185115590288

9. Tomiyama N, Johkoh T, Mihara N, Honda O, Kozuka T, Koyama M, et al. Using the World Health Organization Classification of thymic epithelial neoplasms to describe CT findings. *AJR Am J Roentgenol* 2002; **179:** 881-6. doi: 10.2214/ajr.179.4.1790881

10. Lambin P, Leijenaar RTH, Deist TM, Peerlings J, de Jong EEC, van Timmeren J, et al. Radiomics: the bridge between medical imaging and personalized medicine. *Nat Rev Clin Oncol* 2017; **14:** 749-62. doi: 10.1038/nrclinonc.2017.141

11. Aerts HJ. The potential of radiomic-based phenotyping in precision medicine: a review. *JAMA Oncol* 2016; **2:** 1636-42. doi: 10.1001/jamaoncol.2016.2631

12. Song J, Yin Y, Wang H, Chang Z, Liu Z, Cui L. A review of original articles published in the emerging field of radiomics. *Eur J Radiol* 2020; **127:** 108991. doi: 10.1016/j.ejrad.2020.108991

13. Iannarelli A, Sacconi B, Tomei F, Anile M, Longo F, Bezzi M, et al. Analysis of CT features and quantitative texture analysis in patients with thymic tumors: correlation with grading and staging. *Radiol Med* 2018; **123:** 345-50. doi: 10.1007/s11547-017-0845-4

14. Yasaka K, Akai H, Nojima M, Shinozaki-Ushiku A, Fukayama M, Nakajima J, et al. Quantitative computed tomography texture analysis for estimating histological subtypes of thymic epithelial tumors. *Eur J Radiol* 2017; **92:** 84-92. doi: 10.1016/j.ejrad.2017.04.017

15. Wang X, Sun W, Liang H, Mao X, Lu Z. Radiomics signatures of computed tomography imaging for predicting risk categorization and clinical stage of thymomas. *Biomed Res Int* 2019; **2019:** 3616852. doi: 10.1155/2019/3616852

16. Lee GD, Kim HR, Choi SH, Kim YH, Kim DK, Park SI. Prognostic stratification of thymic epithelial tumors based on both Masaoka-Koga stage and WHO classification systems. *J Thorac Dis* 2016; **8:** 901-10. doi: 10.21037/jtd.2016.03.53

17. Zhu H, Luo H, Li Y, Zhang Y, Wu Z, Yang Y. The superior value of radiomics to sonographic assessment for ultrasound-based evaluation of extrathyroidal extension in papillary thyroid carcinoma: a retrospective study. *Radiol Oncol* 2024; **58:** 386-96. doi: 10.2478/raon-2024-0040

18. Bo Z, Song J, He Q, Chen B, Chen Z, Xie X, et al. Application of artificial intelligence radiomics in the diagnosis, treatment, and prognosis of hepatocellular carcinoma. *Comput Biol Med* 2024; **173:** 108337. doi: 10.1016/j.compbiomed.2024.108337

19. Warkentin MT, Al-Sawaihey H, Lam S, Liu G, Diergaarde B, Yuan JM, et al. Radiomics analysis to predict pulmonary nodule malignancy using machine learning approaches. *Thorax* 2024; **79:** 307-15. doi: 10.1136/thorax-2023-220226

20. Sui H, Liu L, Li X, Zuo P, Cui J, Mo Z. CT-based radiomics features analysis for predicting the risk of anterior mediastinal lesions. *J Thorac Dis* 2019; **11:** 1809-18. doi: 10.21037/jtd.2019.05.32

21. Marom EM, Milito MA, Moran CA, Liu P, Correa AM, Kim ES, et al. Computed tomography findings predicting invasiveness of thymoma. *J Thorac Oncol* 2011; **6:** 1274-81. doi: 10.1097/JTO.0b013e31821c4203

22. Abdel Razek AAK, Khairy M, Nada N. Diffusion-weighted MR imaging in thymic epithelial tumors: correlation with World Health Organization classification and clinical staging. *Radiology* 2014; **273:** 268-75. doi: 10.1148/radiol.14131643

23. Xiao G, Rong WC, Hu YC, Shi ZQ, Yang Y, Ren JL, et al. MRI radiomics analysis for predicting the pathologic classification and TNM Staging of thymic epithelial tumors: a pilot study. *AJR Am J Roentgenol* 2020; **214:** 328-40. doi: 10.2214/AJR.19.21696

24. Kostic Peric J, Cirkovic A, Srzentic Drazilov S, Samardzic N, Skodric Trifunovic V, Jovanovic D, et al. Molecular profiling of rare thymoma using next-generation sequencing: meta-analysis. *Radiol Oncol* 2023; **57:** 12-19. doi: 10.2478/raon-2023-0013

research article

Cardiac MRI for differentiating chemotherapy-induced cardiotoxicity in sarcoma and breast cancer

El-Sayed H Ibrahim[1], Lubna Chaudhary[1], Yee-Chung Cheng[1], Antonio Sosa[1], Dayeong An[2], John Charlson[1]

[1] Medical College of Wisconsin, Milwaukee, USA
[2] Northwestern University, Evanston, USA

Radiol Oncol 2025; 59(1): 79-90.

Received 12 August 2024
Accepted 21 November 2024

Correspondence to: El-Sayed H. Ibrahim, Ph.D., Medical College of Wisconsin, 8701 Watertown Plank Rd, Milwaukee, WI 53226, USA.
E-mail: sayed.phd@gmail.com

Disclosure: No potential conflicts of interest were disclosed.

Background. Over the past few decades, many studies have focused on anthracyclines effect on the heart (cardiotoxicity), but only a few have focused on sarcoma. In this study, we harness the capabilities of advanced cardiac magnetic resonance imaging (MRI) for characterizing anthracyclines-induced cardiotoxicity in sarcoma and compare the results to those from breast cancer patients.

Patients and methods. The patients receive an MRI exam at three timepoints: baseline (pre-treatment), post-treatment, and at 6-months follow-up.

Results. The results demonstrated a differential response in sarcoma, characterized by increasing left-ventricular (LV) mass and decreasing right ventricular ejection fraction (RVEF). In all patients, left ventricular ejection fraction (LVEF) remained > 50% at all timepoints. Myocardial strain was always lower than the normal threshold values and showed small changes between different timepoints. Myocardial T2 and extracellular volume (ECV) showed increasing and decreasing patterns, respectively, in sarcoma, which were the opposite patterns of those in breast cancer. While myocardium T1 showed increasing values in breast cancer, T1 in sarcoma increased post-treatment and then decreased at the 6-months follow-up. The results showed inverse correlation between dose and different strain components in sarcoma, which was not the case in breast cancer. Certain myocardial segments showed high correlation coefficients with dose, which may reflect their increased sensitivity to cardiotoxicity.

Conclusions. Cardiac MRI proved to be a valuable technique for determining anthracycline-induced changes in cardiac function and myocardial tissue composition in sarcoma and differentiating it against breast cancer. It also provides a comprehensive assessment of heart health at baseline, which is important for risk stratification.

Key words: cardiotoxicity; MRI; chemotherapy; sarcoma; breast cancer

Introduction

Despite being rare in the general population, sarcoma is the second most common cancer among children and young adults. Sarcoma tumors originate from mesenchymal cells in different body areas.[1] The number of cancer survivors has significantly increased over the past few decades due to treatment improvements.[2] Despite the development of advanced cancer therapies, anthracyclines remain a commonly used treatment for cancer, including sarcomas and breast cancer.[3] In particular, doxorubicin is considered a standard, first-line treatment of sarcoma.[4] Nevertheless, treatment with doxorubicin has the side effect of cardiotoxicity with potential development of heart failure if not prompt-

ly treated.[5] Sarcoma patients are more likely than other cancer patients to develop cardiotoxicity after receiving anthracyclines.[6] In pediatric sarcoma patients enrolled in the prospective Late Effects Surveillance System study, which included 265 patients, the cardiotoxicity incidence was 7.5%.[7] Another registry showed a 14% incidence of cardiotoxicity in 43 adult patients.[8]

Early onset cardiotoxicity is a major challenge in clinical practice due to the reliance on anthracyclines and relative lack of other systemic therapy options for treatment of advanced sarcomas.[3] Cardiotoxicity is defined by the development of heart failure symptoms or by asymptomatic decrease in baseline left ventricular ejection fraction (LVEF) ≥ 10% to a level < 50%.[1,9,10] Cardiotoxicity can cause cardiovascular complications, including ventricular dysfunction, myocardial ischemia, hypertension, arrhythmias, and heart failure.[1-14] A potential mechanism of cardiotoxicity development is myocyte free radical damage, which is emphasized by repetitive damage to myocyte mitochondria and high peak levels of plasma.[15,16] Cardiotoxicity has been well studied among patients with breast cancer[8,17]; however, there is limited data regarding cardiotoxicity and mortality rates in sarcoma patients.[18] The treatment and prognosis of sarcoma and breast cancer are different, and using results from breast cancer studies to interpret those from sarcomas may not be appropriate. Anthracyclines induced cardiotoxicity can occur after both high- and low-dose doxorubicin therapy[19] due to wide variation in individual vulnerability[20] with no clear threshold regarding safe doses of anthracyclines.[21,22] Actually, the cumulative dosage of anthracyclines used in sarcoma is higher than that in many other cancers[23] as using doxorubicin beyond the recommended cumulative dose is a promising option to improve survival in patients with advanced sarcomas.[24] Although long-term surveillance guidelines of cancer patients receiving anthracyclines are addressed in the literature, there is no clear guidelines regarding surveillance during and shortly after treatment.[25]

In clinical practice, a decrease in LVEF is the most common form of cardiotoxicity.[5,26] However, a large reduction in LVEF occurs late in the process of cancer therapy induced cardiotoxicity.[27] Therefore, it is important to stratify patients early on such that cardiac protection can be initiated as early as possible in those with increased risk of cardiotoxicity. It has been shown that MRI global longitudinal strain (GLS) is more sensitive than LVEF for detecting early signs of systolic myocardial dysfunction.[22,28] GLS may also identify patients at risk of cardiotoxicity, possibly through detection of baseline subclinical cardiac dysfunction, which may advance to heart failure.[29] Either a low absolute GLS value early during chemotherapy or a threshold relative reduction in GLS compared with baseline can be used to identify individuals at high risk of developing heart failure.[29] GLS less than 17% (in absolute value) or relative reduction in GLS by >15% from baseline has been used as a threshold for patients at risk.[27,30] Changes in other strain components, *e.g.*, global circumferential strain (GCS), have been also reported in sarcoma.[31]

It has been reported that patients with subsequent cardiotoxicity may have low myocardial T1 times and decreased LV mass; but patients do not typically develop myocardial scars or focused fibrosis from anthracyclines.[32] Nevertheless, anthracyclines can induce diffuse myocardial fibrosis later, which can be confirmed by elevated MRI T1 times.[33] However, it has been reported that myocardial MRI T2 times and serum biomarkers were not able to stratify patients and identify those at risk of developing cardiotoxicity.[32] Therefore, it is obvious that there is an ongoing myocardial remodeling process following treatment with anthracyclines. While there may be T1 reduction shortly post anthracyclines, on the long run myocardial remodeling may lead to elevated T1 times and ECV values because of diffuse interstitial fibrosis in the myocardium.[34]

We conducted a single-center, observational, prospective study to evaluate the value of cardiac MRI parameters for revealing and characterizing cardiac dysfunction associated with anthracyclines in sarcoma and breast cancer patients.

Patients and methods

All work has been conducted in accordance with the Declaration of Helsinki (1964). The study was approved by our institutional review board (IRB) and informed consent forms were collected from all subjects. Eighteen patients (5 males and 13 females; 8 sarcoma and 10 breast cancer) scheduled for doxorubicin chemotherapy were included in the study. The patients underwent a baseline (pre-treatment (18 patients)) and two follow-up (post-treatment completion (14 patients) and 6-months after treatment completion (10 patients)) visits. The treatment duration was 143 ± 65 days. Each visit included an optimized cardiac MRI exam and blood analysis. A questionnaire about risk factors and

comorbidities was collected from the patients at the first visit. The MRI exams were conducted on a 3T GE MRI scanner (GE Healthcare, Waukesha, WI, USA)) and included the following sequences: cine, tagging, modified Look-Locker (MOLLI) T1 mapping (both pre and post gadolinium (Gd) injection), T2 mapping, perfusion, and late gadolinium enhancement (LGE).

The acquired cine images included a stack of parallel short-axis slices (SAX) covering the heart from base to apex in addition to 2-chamber, 3-chamber, and 4-chamber long-axis slices. The optimized cine imaging parameters were as follows: fast imaging employing steady-state acquisition (FIESTA) acquisition, repetition time (TR) = 3.6 ms, echo time (TE) = 1.3 ms, flip angle = 55°, views per segment = 14, # averages = 1, matrix = 256 × 256, slice thickness = 8 mm, and readout bandwidth = 488 Hz/pixel. The acquired tagged images included a 3 equidistant short-axis slices (basal, mid-ventricular, and apical) in addition to 2-chamber, 3-chamber, and 4-chamber long-axis slices. Optimized tagging imaging parameters different from cine imaging were as follows: TR = 5.7 ms, TE = 3.1 ms, flip angle = 8°, views per segment = 14, readout bandwidth = 391 Hz/pixel, tag spacing = 7mm, and number of heart phases = 25.

The MOLLI images were acquired at the same 3 SAX tagged slices (basal, mid-ventricular, and apical). Optimized MOLLI imaging parameters different from cine imaging were as follows: 8 images acquired using the 5(3 s)3 acquisition pattern, TR = 2.9 ms, TE = 1.3 ms, flip angle = 35°, and readout bandwidth = 977 Hz/pixel. The T2 mapping images were acquired at the same 3 SAX tagged slices (basal, mid-ventricular, and apical). Optimized T2 mapping imaging parameters different from cine imaging were as follows: multi-echo fast spin echo sequence, TR = 895 ms, TE = 11 − 77 ms (4 echoes with 22 ms increments), echo train length (ETL) = 16, flip angle = 90°, and readout bandwidth = 651 Hz/pixel.

The perfusion images were acquired at the same 3 SAX tagged slices (basal, mid-ventricular, and apical). Optimized perfusion imaging parameters different from cine imaging were as follows: Fast gradient echo (FGRE) acquisition, TR = 2.5 ms, TE = 1.7 ms, flip angle = 20°, inversion time (TI) = 173 ms, ETL = 1, # averages = 0.75, number of multiphase images = 60, and readout bandwidth = 326 Hz/pixel. The LGE images were acquired at the same SAX and LAX cine slices. Optimized LGE imaging parameters different from cine imaging were as follows: TR = 5.1 ms, TE = 2.3 ms, flip angle = 25°, TI = 275 − 325 ms based on Look-Locker images, and readout bandwidth = 139 Hz/pixel.

Image analysis was conducted by a MRI physicist with 18 years of experience in cardiac MRI (E.I.) and independently reviewed by a cardiothoracic radiologist with 13 years of experience (A.S.). The cine images were analyzed using the cvi42 software (Circle, Calgary, Canada) function module to measure EF and myocardial mass. The T1 and T2 images were analyzed using the cvi42 software T1 and T2 mapping modules, respectively, to generate T1, T2, and ECV maps. The SinMod method (InTag, Leon, France) (35) was used to analyze the tagged images to measure myocardial global longitudinal (GLS), circumferential (GCS), and radial (GRS) strains. Finally, the cvi42 software perfusion and tissue characterization modules were used to determine the existence of ischemic perfusion defects and myocardial infarction/scars, respectively. Inter- and intra-observer variabilities of strain analysis using this technique have been previously demonstrated.[35]

The blood samples drawn at each timepoint were analyzed to measure the following biomarkers: N-terminal pro b-type natriuretic peptide (NT-proBNP), Troponin I (TnI), Troponin T (TnT), Interleukin 6 (IL-6), Tumor necrosis factor alpha (TNFα), C-reactive protein (CRP), and Galectin 3 (gal-3), as parameters associated with cardiac damage and heart failure.

Statistical analysis was conducted using Excel (Microsoft, Redmond, Washington, USA) and Python (Python Software Foundation, Wilmington, Delaware, USA) to compare measurements pre- and post-treatment or between patient subgroups and to assess correlation between different MRI parameters and dose. When examining serial longitudinal measurements, a one-way analysis of variance (ANOVA) was used. Three groups were formed depending on timepoints: baseline, post-treatment, and 6-months follow-up. The Shapiro-Wilk test and the Levene's test were performed for normality and homogeneity of variances, respectively. If either of these tests has a p-value less than or equal to 0.05, non-parametric alternatives such as the Kruskal-Wallis H-test was performed. Correlation maps between dose and different post-treatment strain components indicated a need for regional analysis at the LV base, mid-ventricle, and apex levels. Correlation coefficients greater than 0.7 were considered high, indicating high dose-response or segment-response relationships. p values < 0.05 was considered significant.

TABLE 1. Patients' demographic parameters

Parameter	All	Sarcoma	Breast
Number of patients (m/f)	5/13	4/4	1/9
Number of patients – visit A (baseline)	18	8	10
Number of patients – visit B (post treatment)	14	6	8
Number of patients – visit C (6 months post follow-up)	10	4	6
Age (years)	56 ± 13	56 ± 15	55 ± 12
Body mass index (BMI) (kg/m^2)	29 ± 6	27 ± 8	31 ± 4
White/Black race (n)	17/1	8/0	9/1
Non-Hispanic / Hispanic (n)	18/0	8/0	10/0
Patients with cardiovascular risk factors (n)	3	1	2
Patients with comorbidities (n)	7	5	2
Patients with cardiovascular disease (n)	1	1	0
Smoker patients (n)	7	3	4
Alcohol consumer patients (n)	8	3	5
Patients receiving cardiac medications (n)	4	3	1
Accumulative Dox dose (mg)	514 ± 190	564 ± 277	469±42

Dox = doxorubicin; f = female; m = male

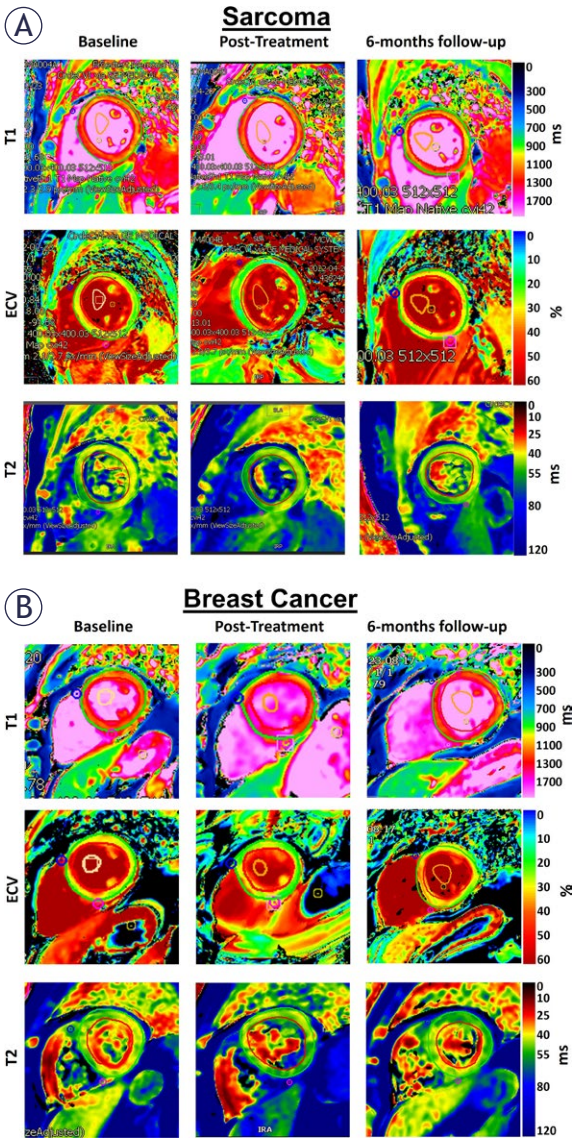

FIGURE 1. MRI tissue characterization maps in **(A)** sarcoma and **(B)** breast cancer. The figure shows myocardial T1, extracellular volume (ECV), and T2 maps. Note changes in the maps between sarcoma and breast cancer patients as well as between different study timepoints (baseline, post-treatment, 6-months follow-up).

Results

The demographic data of all patients as well as of the sarcoma and breast cancer subgroups is shown in Table 1.

Figure 1 and Figure 2 show tissue characteristics and myocardial strains, respectively, in both sarcoma and breast cancer patients at different study timepoints. The MRI measurements for all patients as well as for the sarcoma and breast cancer subgroups at the three timepoints: (A) baseline, (B) post-treatment, and (C) 6-months follow-up are shown in Table 2. One-way ANOVA showed insignificant differences in most MRI parameters between the three timepoints (baseline, post-treatment, and 6-months follow-up). However, it should be noted that all strain values at baseline (pre-treatment) were lower than normal strain threshold of 17%, which emphasizes the importance of baseline strain measurements as they reflect underlying risk factors.

Different strain measurements (GLS, GCS, and GRS) at the three study timepoints in sarcoma and breast cancer patients are shown in Figure 3. GLS and GCS are presented in absolute value (original numbers are negative) for clearer presentation along with the positive GRS. In general, in both patient subgroups, GRS was lower than GCS, which in turn was lower than GLS. In both patient subgroups, the 6-months follow-up strain were slightly higher than the post-treatment strain, especially for GCS and GRS ($p > 0.05$ for both groups).

Global measures of cardiac function (LV EF, RV EF, and LV mass) in both sarcoma and breast cancer patients at the three timepoints are shown in Figure 4. LVEF decreased at post-treatment, then

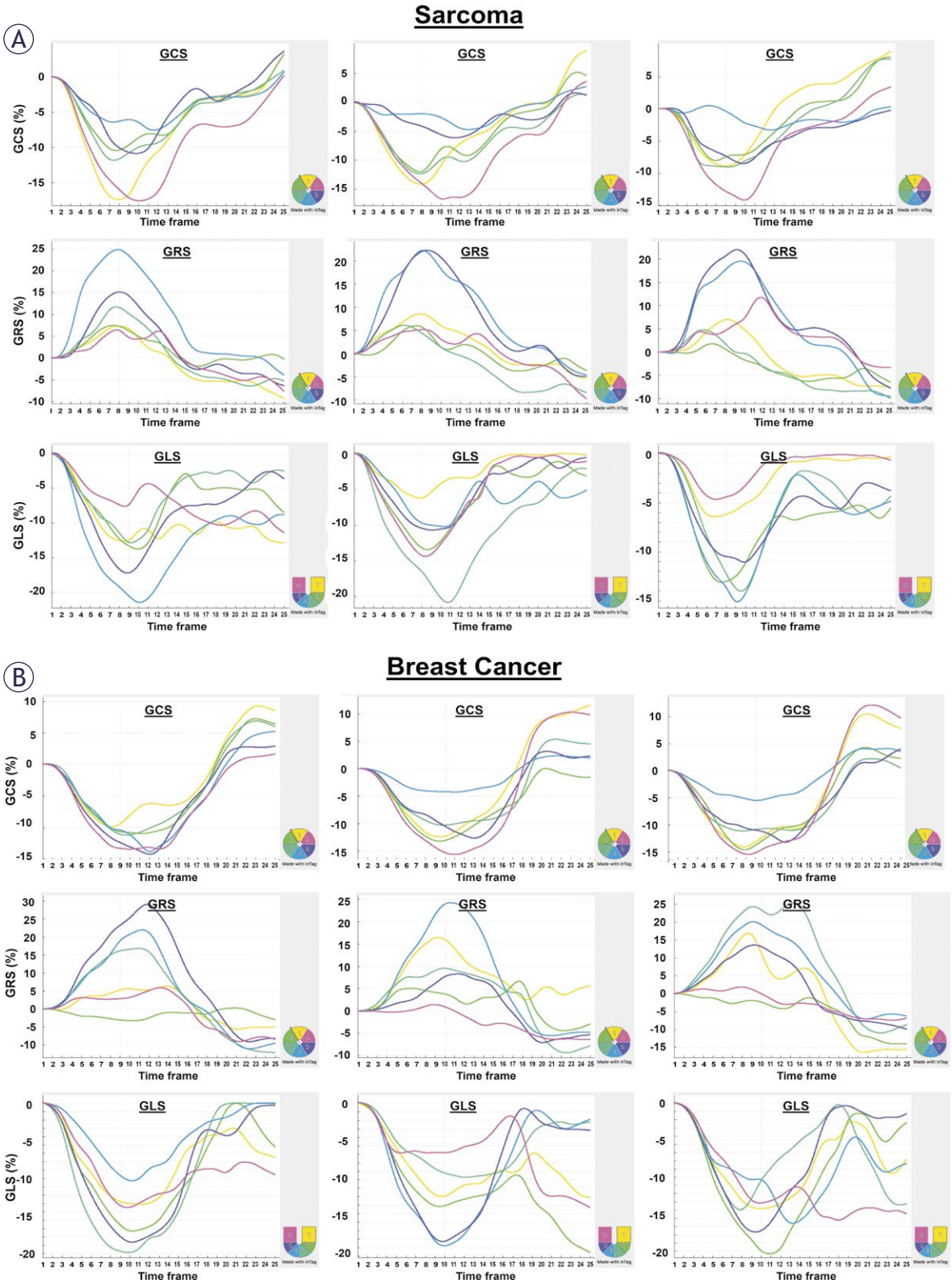

FIGURE 2. MRI strain curves in **(A)** sarcoma and **(B)** breast cancer patients. The figure shows circumferential (GCS), radial (GRS), and longitudinal (GLS) strain curves in both patient groups at different study timepoints. Myocardial strain for each case is represented by 6 segmental strain curves, color-coded based on the regional location as shown by the lower-right 6-segment illustration based on AHA standard LV model. Note changes in the strain curves between sarcoma and breast cancer patients as well as between different study timepoints (baseline, post-treatment, 6-months follow-up). Note also differences in segmental strain values within the same slice.

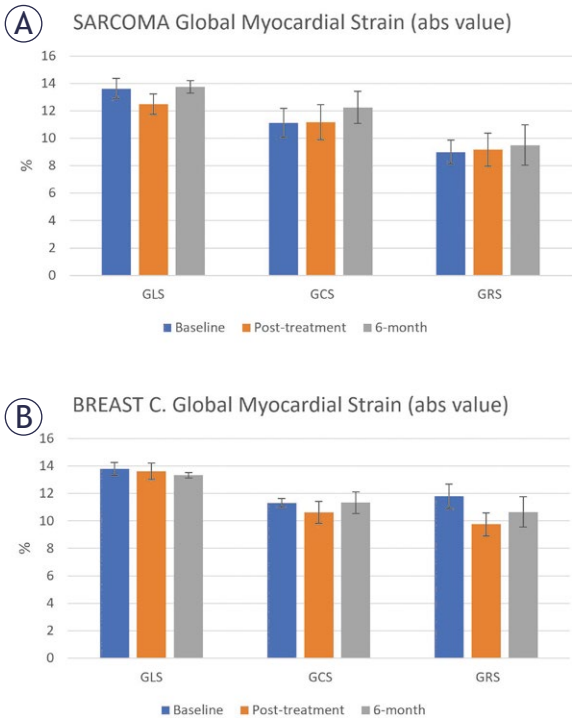

FIGURE 3. Global longitudinal (GLS), circumferential (GCS), and radial (GRS) strains at baseline, post-treatment, and 6-months follow-up in **(A)** sarcoma and **(B)** breast cancer patients. Note different patterns of change in strain between the two patient groups. In general, GRS is lower than GCS, which is lower than GLS. GCS and GLS are represented by absolute value (original values are negative) for clearer presentation along with positive GRS.

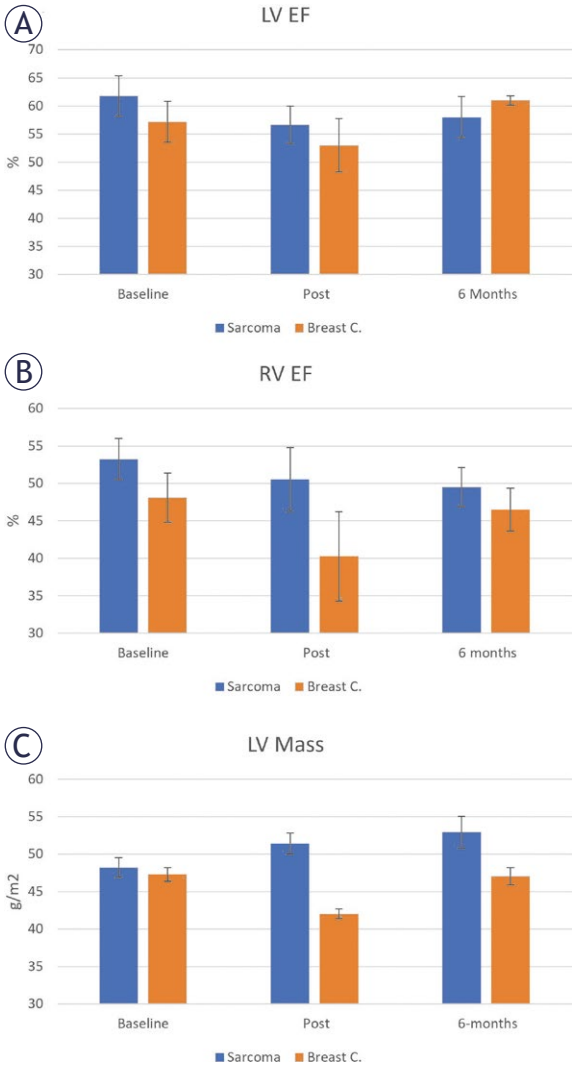

FIGURE 4. Global cardiac function parameters: **(A)** left ventricular ejection fraction (RVEF), **(B)** right ventricular ejection fraction (RVEF), and (**C**) LV mass at baseline, post-treatment, and 6-months follow-up timepoints in sarcoma and breast cancer patients. LVEF is normal in both groups at all timepoints. RV EF is lower in breast cancer compared to sarcoma. LV mass shows continuous increase with time in sarcoma.

increased back at the 6-months follow-up timepoint. LVEF was larger in the sarcoma patients, compared to the breast cancer patients, at both baseline and post-treatment timepoints. However, it was smaller at the 6-months follow-up. RV EF showed slight decrease with time in the sarcoma patients. However, in the breast cancer patients, RV EF showed large decrease at post-treatment before it increased back at the 6-months timepoint. LV mass increased with time in the sarcoma patients, while in the breast cancer patients, it decreased at post-treatment, then increased back at 6-months follow-up. Nevertheless, the changes were not statistically significant ($p > 0.05$).

Myocardium tissue characterization (T1, T2, and ECV) measurements in sarcoma and breast cancer patients are shown in Figure 5. The patterns were different between the two patient subgroups. For T1 in sarcoma patients, it slightly increased at post-treatment, then decreased at 6-months follow-up; however, T1 continuously increased with time in the breast cancer patients. For T2 in sarcoma patients, it slightly increased with time; however, it showed larger increase with time in the breast cancer patients. For ECV, it continuously decreased and increased with time in the sarcoma and breast cancer patients, respectively. Perfusion analysis revealed ischemic defects in eleven subjects (5 sarcoma and 6 breast cancer patients), mostly in the basal septal region. LGE revealed scars in five subjects (2 sarcoma and 3 breast cancer patients). There were no significant differences ($p > 0.05$) in MRI parameters between patients with perfusion defects or scars and those without them.

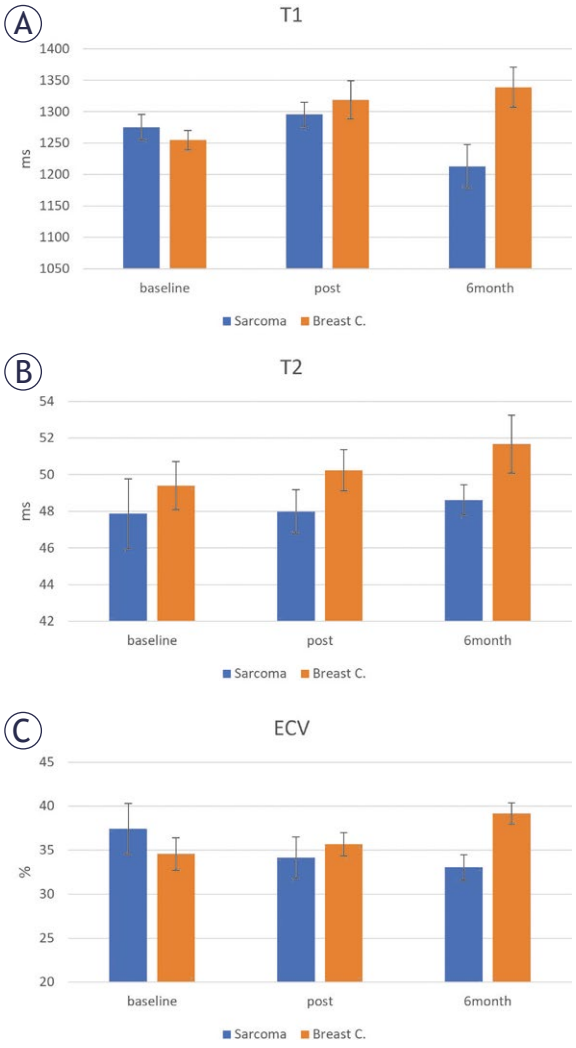

FIGURE 5. Myocardial **(A)** T1, **(B)** T2, and **(C)** extracellular volume (ECV) measurements in sarcoma and breast cancer groups at different study timepoints. All parameters show continuous increase with time in breast cancer. Sarcoma shows different patterns of change, *e.g.*, continuous decrease of ECV with time. Post-treatment and 6-months follow-up T1 values in sarcoma are lower than those in in breast cancer. T2 shows minimal increase with time in sarcoma.

TABLE 2. Cardiac MRI parameters

Parameter	All	Sarcoma	Breast	p
LVEF (%) - A	59 ± 11	62 ± 10	57 ± 12	0.398
LVEF (%) - B	55 ± 11	57 ± 8	53 ± 14	0.547
LVEF (%) - C	60 ± 5	58 ± 8	61 ± 2	0.489
LV mass (g/m²) - A	48 ± 10	48 ± 11	47 ± 9	0.849
LV mass (g/m²) - B	46 ± 8	51 ± 9	42 ± 5	0.049*
LV mass (g/m²) - C	49 ± 8	53 ± 9	47 ± 7	0.300
RVEF (%) - A	50 ± 10	53 ± 8	48 ± 11	0.256
RVEF (%) - B	45 ± 15	51 ± 11	40 ± 17	0.196
RVEF (%) - C	48 ± 6	50 ± 5	47 ± 7	0.468
GLS (%) - A	-14 ± 2	-14 ± 2	-14 ± 2	0.849
GLS (%) - B	-13 ± 2	-13 ± 2	-14 ± 2	0.272
GLS (%) - C	-14 ± 1	-14 ± 1	-13 ± 1	0.468
GCS (%) - A	-11 ± 2	-11 ± 3	-11 ± 1	0.880
GCS (%) - B	-11 ± 3	-11 ± 3	-11 ± 2	0.733
GCS (%) - C	-12 ± 2	-12 ± 2	-11 ± 2	0.546
GRS (%) - A	11 ± 3	9 ± 3	12 ± 3	0.042*
GRS (%) - B	10 ± 3	9 ± 3	10 ± 2	0.705
GRS (%) - C	10 ± 3	10 ± 3	11 ± 3	0.555
T1 (ms) - A	1264 ± 53	1275 ± 58	1255 ± 50	0.444
T1 (ms) - B	1309 ± 72	1296 ± 48	1319 ± 87	0.543
T1 (ms) - C	1289 ± 97	1213 ± 71	1339 ± 80	0.034*
T2 (ms) - A	49 ± 5	48 ± 5	49 ± 4	0.529
T2 (ms) - B	49 ± 3	48 ± 3	50 ± 3	0.204
T2 (ms) - C	50 ± 3	49 ± 2	52 ± 4	0.136
ECV (%) - A	36 ± 7	37 ± 8	35 ± 6	0.433
ECV (%) - B	35 ± 5	34 ± 6	36 ± 4	0.591
ECV (%) - C	37 ± 4	33 ± 4	39 ± 3	0.031*

A, B, and C refer to the three study timepoints (baseline, post-treatment, and 6-months follow-up), respectively.

p values are shown for all measurements. $p < 0.05$ is considered significant and marked by an asterisk (*).

ECV = extracellular volume; EF = ejection fraction; GLS, GCS, GRS = global longitudinal, circumferential, and radial strains, respectively; LV = left ventricle; RV = right ventricle

The patterns of change in the serum biomarkers are different in the two patient groups (Figure 6). In sarcoma patients, both TnT and NT-proBNP showed increase with time, TnI showed similar values at the three timepoints. CRP increased post-treatment then decreased at 6-months follow-up, while IL-6 showed the opposite pattern. Changes in Gal3 and TNFα showed small differences between the three timepoints. In breast cancer patients, both CRP and TNFα increased with time. NT-proBNP and Gal3 showed similar values at the three timepoints, while TnI, TnT, and IL-6 increased at post-treatment then decreased at 6-months follow-up. TnI and IL-6 are presented in fluorescence intensity (FI) units as the observed values were too small (out-of-range) to report. Differences in serum biomarker measurements were not statistically significant.

Correlation maps between dose and different strain components at the post-treatment timepoint are shown in Figure 7. The patterns are different for the two patient groups. In sarcoma (Figure 7), as shown in the left-most column, dose is positive-

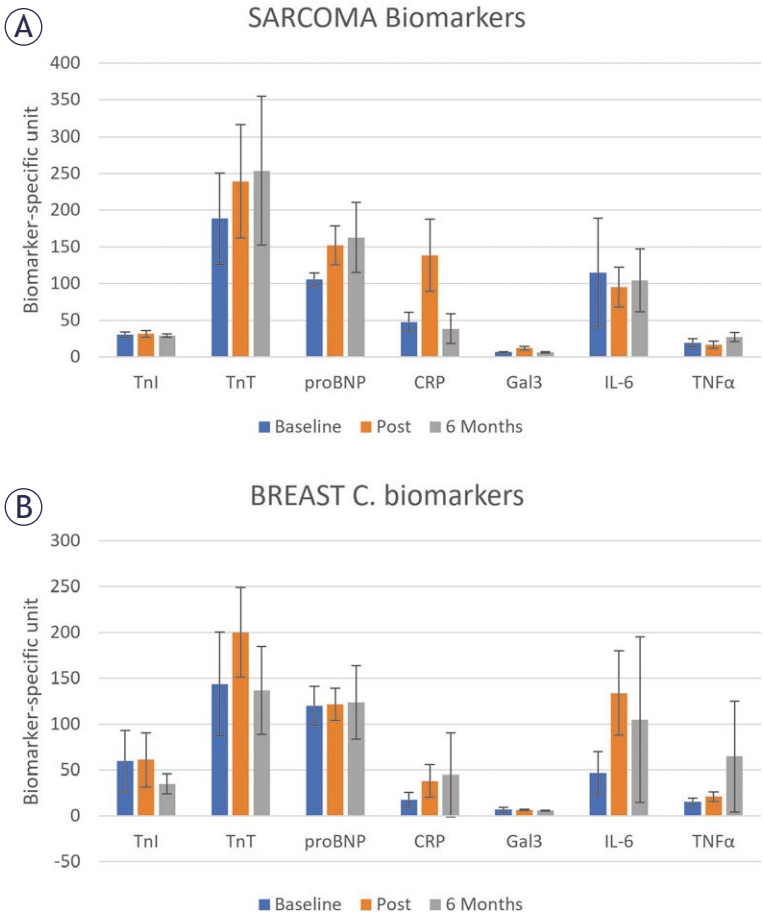

FIGURE 6. Changes in serum biomarkers at different timepoints in **(A)** sarcoma and **(B)** breast cancer.

CRP = C-reactive protein (µg/mL); Gal3 = Galectin 3 (ng/mL); IL-6 = Interleukin 6 (fluorescence intensity units); NT-proBNP = N-terminal pro b-type natriuretic peptide (pg/mL); TNFa = tumor necrosis factor alpha (pg/mL); TnI = cardiac troponin I (florescence intensity units), TnT = cardiac troponin T (pg/mL).

The figure shows different patterns of change in the biomarkers between sarcoma and breast cancer. Not all biomarkers increased post-treatment. Different parameters reflect different aspects of cardiac injury.

ly correlated with longitudinal (Ell) and circumferential (Ecc) strains, while it is negatively correlated with radial (Err) strain. This behavior is consistent for global strain as well as regional values at the base, mid-ventricular, and apical levels. The correlation coefficient values were moderate for all regions except for apical radial strain (last component in the column). These relationships demonstrate that strain gets worse (higher Ell and Ecc and lower Err) with dose, which is expected in cancer patients. However, in the breast cancer patients (Figure 7), the correlation pattern was not consistent and there existed small positive and negative correlations between dose and each of the strain components (Ell, Ecc, Err). The only (negative) high correlation existed between dose and apical radial strain, the opposite case of sarcoma patients. No correlations were statistically significant ($p > 0.05$).

At 6-months follow-up, the correlation patterns changed as shown in Figure 8. In sarcoma patients, the positive correlations between dose and Ecc was maintained, even with higher correlation coefficient compared to the post-treatment timepoint (Figure 7). Significant correlation coefficients existed between dose and both global Ecc ($p = 0.017$) and mid-ventricle Ecc (0.028), respectively. However, in the breast cancer patients, only basal Ell ($p = 0.015$) and mid-ventricular Ell ($p = 0.107$) showed high positive correlations with dose.

In the myocardial segmental level, using AHA 16-segment model (segments 1-6, 7-12, and 13-16 represent basal, mid-ventricular, and apical regions, respectively, in the longitudinal (Ell), circumferential (Ecc), and radial (Err) directions. By taking 0.7 as a threshold for correlation coefficients, the following myocardium segments showed high correlation coefficients (negative for Ell and Ecc and positive for Err) with dose in sarcoma patients at post-treatment: Ell8 ($R = 0.71$, $p = 0.114$), Ell9 ($R = 0.86$, $p = 0.028$), Ecc1 ($R = 0.78$, $p = 0.067$), Ecc7 ($R = 0.84$, $p = 0.036$), Ecc9 ($R = 0.73$, $p = 0.099$). At 6-months follow-up, the following segments had correlation coefficients above the 0.7 threshold: Ell2 ($R = 0.84$, $p = 0.036$), Ell8 ($R = 0.82$, $p = 0.46$), Ecc1 ($R = 0.74$, $p = 0.093$), Ecc4 ($R = 0.79$, $p = 0.062$), Ecc5 ($R = 0.75$, $p = 0.086$), Ecc8 ($R = 0.9$, $p = 0.015$), Ecc9 ($R = 0.75$, $p = 0.085$), Ecc11 ($R = 0.70$, $p = 0.122$), Ecc12 ($R = 0.85$, $p = 0.032$). In the breast cancer patients, only Err13 ($R = -0.89$, $p = 0.017$) and Err14 ($R = -0.74$, $p=0.093$) showed high correlation coefficients post treatment. At 6-months, the following segments showed high correlation coefficients: Ell2 ($R = 0.95$, $p = 0.004$), Ell5 ($R = 0.99$, $p <0.001$), Ell7 ($R = 0.98$, $p <0.001$), Ell9 ($R = 0.8$, $p = 0.056$), Ell11 ($R = 0.75$, $p = 0.086$), Ell14 ($R = 0.92$, $p = 0.009$), Ecc8 ($R = 0.92$, $p = 0.009$), Err2 ($R = -0.92$, $p = 0.009$), Err9 ($R = -0.8$, $p = 0.06$), Err14 ($R = -0.8$, $p = 0.06$).

Discussion

The study demonstrates important points about anthracycline-induced cardiotoxicity. The first point is that MRI strain parameters are sensitive biomarkers of cardiac dysfunction (Figure 2). While LVEF was always > 50% in both patient groups and at different study timepoints, strain parameters showed underlying subclinical dysfunction, even at baseline as all strain (absolute) values were less

(A)

SARCOMA	Dose	Ell-G	Ell-B	Ell-M	Ell-A	Ecc-G	Ecc-B	Ecc-M	Ecc-A	Err-G	Err-B	Err-M	Err-A
Dose	1.00												
Ell-G	0.54	1.00											
Ell-B	0.30	0.93	1.00										
Ell-M	0.65	0.59	0.28	1.00									
Ell-A	0.27	0.87	0.93	0.13	1.00								
Ecc-G	0.49	0.72	0.80	-0.01	0.88	1.00							
Ecc-B	0.62	0.77	0.72	0.21	0.85	0.90	1.00						
Ecc-M	0.56	0.76	0.82	0.08	0.85	0.99	0.86	1.00					
Ecc-A	0.39	0.75	0.86	-0.01	0.90	0.97	0.81	0.97	1.00				
Err-G	-0.53	-0.05	0.09	-0.46	0.27	0.05	0.18	-0.08	-0.01	1.00			
Err-B	-0.63	-0.55	-0.23	-0.97	-0.11	0.01	-0.17	-0.07	0.00	0.56	1.00		
Err-M	-0.66	-0.17	-0.03	-0.53	0.19	-0.05	0.06	-0.20	-0.08	0.95	0.57	1.00	
Err-A	-0.13	0.26	0.22	0.21	0.24	-0.07	0.22	-0.12	-0.14	0.74	-0.03	0.57	1.00

(B)

BREAST	Dose	Ell-G	Ell-B	Ell-M	Ell-A	Ecc-G	Ecc-B	Ecc-M	Ecc-A	Err-G	Err-B	Err-M	Err-A
Dose	1.00												
Ell-G	0.24	1.00											
Ell-B	0.27	0.91	1.00										
Ell-M	0.10	0.83	0.68	1.00									
Ell-A	-0.53	0.50	0.24	0.42	1.00								
Ecc-G	0.00	0.69	0.75	0.50	0.45	1.00							
Ecc-B	0.13	0.82	0.79	0.71	0.48	0.95	1.00						
Ecc-M	0.24	0.63	0.81	0.35	0.13	0.90	0.81	1.00					
Ecc-A	-0.31	0.39	0.46	0.19	0.52	0.89	0.73	0.78	1.00				
Err-G	-0.45	-0.01	-0.22	0.01	0.69	0.37	0.31	0.11	0.62	1.00			
Err-B	-0.09	-0.75	-0.85	-0.78	-0.07	-0.51	-0.59	-0.54	-0.20	0.41	1.00		
Err-M	0.13	0.36	0.24	0.39	0.40	0.65	0.67	0.52	0.60	0.68	-0.06	1.00	
Err-A	-0.77	0.09	-0.11	0.15	0.84	0.32	0.26	0.01	0.59	0.85	0.18	0.35	1.00

FIGURE 7. Correlation maps between dose and different post-treatment strain components in the **(A)** sarcoma and **(B)** breast cancer patients at the global level (G) and regional levels (base (B), mid-ventricular (M), and apical (A).

Ell, Ecc, and Err represent longitudinal, circumferential, and radial strains, respectively.

There is a clear inverse correlation between strain and dose in sarcoma, which is positive for Ell and Ecc and negative for Err, as shown in the left-most column. Such correlation pattern is not shown in the breast cancer correlation map.

than strain threshold of 17% for normal contractility. Baseline strain parameters inform about underlying risk factors, which should be taken into consideration for patient stratification and prognosis. RVEF (Table 2) in sarcoma was always higher than that in breast cancer, which may be related to the difference in tumor locations and sizes between the two patient groups.

Although previous reports pointed to decreased LV mass post treatment with anthracyclines[32], this was only demonstrated in the breast cancer patients (Table 2). The opposite pattern occurred in the sarcoma patients where myocardial mass continuously increased post-treatment and at 6-months follow-up. This may represent an undergoing LV remodeling.

The contractility pattern and changes in cardiac MRI parameters were different in sarcoma and breast cancer patients (Figure 3, Table 2). For example, while myocardial strain decreased post-treatment in breast cancer patients, this was not the case in sarcoma. This may imply different mechanisms in response to anthracyclines in breast cancer and sarcoma, especially that sarcomas can have large tumors more often than those in breast cancers, where removing a large tumor would actually result in the body being healthier after treatment.

The changes in myocardial function post-treatment were accompanied by changes in myocardial tissue characterization based on MRI relaxometry maps (Figure 5, Table 2). In breast cancer patients, all T1, T2, and ECV parameters showed continuous increase from baseline to post-treatment to 6-months follow-up, which was not the case in sarcoma. The increases in T1, T2, and ECV reflect increased diffuse fibrosis, edema, and collagen formation, respectively. These results show that breast cancer patients are more affected by changes in tissue composition compared to sarcoma patients.

Changes in serum biomarkers showed inconsistent patterns between different parameters and between the sarcoma and breast cancer patients (Figure 6). For example, only TnT (biomarkers of damage to heart muscle) and NT-proBNP (biomarker of heart failure) showed continuous increase post-treatment in sarcoma patients versus

(A)

SARCOMA	Dose	Ell-G	Ell-B	Ell-M	Ell-A	Ecc-G	Ecc-B	Ecc-M	Ecc-A	Err-G	Err-B	Err-M	Err-A
Dose	1.00												
Ell-G	0.40	1.00											
Ell-B	-0.09	0.69	1.00										
Ell-M	0.25	0.74	0.12	1.00									
Ell-A	0.51	0.17	0.44	-0.47	1.00								
Ecc-G	0.89	0.77	0.32	0.50	0.49	1.00							
Ecc-B	0.77	0.80	0.15	0.80	0.08	0.91	1.00						
Ecc-M	0.86	0.82	0.30	0.61	0.38	0.99	0.95	1.00					
Ecc-A	0.80	0.61	0.49	0.08	0.84	0.89	0.61	0.82	1.00				
Err-G	-0.13	-0.17	0.50	-0.79	0.78	-0.12	-0.51	-0.23	0.35	1.00			
Err-B	0.20	0.67	0.94	0.00	0.71	0.51	0.24	0.46	0.74	0.62	1.00		
Err-M	0.18	0.16	0.65	-0.55	0.93	0.26	-0.15	0.15	0.67	0.93	0.82	1.00	
Err-A	-0.34	-0.88	-0.33	-0.97	0.27	-0.64	-0.86	-0.73	-0.28	0.62	-0.24	0.33	1.00

(B)

BREAST	Dose	Ell-G	Ell-B	Ell-M	Ell-A	Ecc-G	Ecc-B	Ecc-M	Ecc-A	Err-G	Err-B	Err-M	Err-A
Dose	1.00												
Ell-G	-0.12	1.00											
Ell-B	0.90	0.13	1.00										
Ell-M	0.72	-0.50	0.13	1.00									
Ell-A	-0.80	0.72	-0.41	-0.77	1.00								
Ecc-G	-0.74	0.26	-0.69	-0.72	0.71	1.00							
Ecc-B	-0.81	0.49	-0.55	-0.86	0.84	0.87	1.00						
Ecc-M	-0.53	0.21	-0.39	-0.75	0.61	0.90	0.68	1.00					
Ecc-A	-0.09	0.06	-0.58	0.06	0.20	0.58	0.19	0.54	1.00				
Err-G	0.73	-0.09	0.25	0.33	-0.33	-0.06	-0.47	0.22	0.61	1.00			
Err-B	0.93	-0.52	0.29	0.76	-0.78	-0.47	-0.83	-0.26	0.33	0.82	1.00		
Err-M	0.19	0.08	0.19	-0.15	0.12	0.23	-0.12	0.59	0.49	0.80	0.43	1.00	
Err-A	0.51	0.35	0.07	0.03	0.03	0.25	-0.03	0.38	0.74	0.83	0.46	0.64	1.00

FIGURE 8. Correlation maps between dose and different 6-months follow-up strain components in the **(A)** sarcoma and **(B)** breast cancer patients at the global level (G) and regional level (base (B), mid-ventricular (M), and apical (A).

Ell, Ecc, and Err represent longitudinal, circumferential, and radial strains, respectively.

There is inverse correlation only between circumferential strain and dose in sarcoma, which is positive for Ecc. There is inverse correlation only between longitudinal base and mid-ventricular strains and dose in breast cancer, which is positive for Ell-B and Ell-M.

CRP (biomarker for inflammation) and TNFα (biomarker for heart failure) in breast cancer patients. This may reflect different mechanisms in response to anthracyclines in the two patient groups.

Post-treatment myocardial strain (Figure 7) showed good correlation with anthracycline dose in the sarcoma patients (positive correlations with GLS and GCS and negative correlation with GRS), which means deteriorated strain value is associated with higher dose. However, this pattern was not observed in breast cancer patients. At 6-months follow-up (Figure 8), only GCS in sarcoma patients showed an inverse correlation with dose, while basal and mid-ventricular GLS showed inverse correlations in the breast cancer patients. This demonstrates the importance of regional myocardial strain as early marker of cardiac dysfunction that is correlated with dose, especially in sarcoma.

On the segmental level (based on American Heart Association (AHA) 16-segment model of the LV), only few segments showed high correlation coefficients (> 0.7) with dose post-treatment. In sarcoma, these segments are septal mid-ventricular longitudinal strain, anterior circumferential strain, and basal anteroseptal radial strain. In breast cancer patients, only apical anterior and septal segmental strains had correlation coefficient values above the threshold. These results may imply different regional myocardial sensitivity to anthracyclines, a subject that is worth investigation in a separate study by itself.

A few points to be considered about this study. First, one limitation of the study is the small sample size and patients who did not complete the post-treatment or 6-months follow-up timepoints, which did not allow for statistically significant results. The small sample size also reduced the biological variability of our patient population. Although our study was underpowered to be able to detect large deteriorations in cardiac function, the clear trends in the results and differences between the two patient groups warrant a follow-up larger study to confirm these results. Secondly, we used MRI in our study, which is more powerful than CT for examining cardiac function. In our study we used standard 8-mm slice thickness as slice thickness of 8-10 mm is typically used in MRI for functional and tissue characterization

analyses of the heart in humans, which does not compromise the in-plane resolution ~ 1-2 mm. It should be noted that reduction in slice thickness is associated with reduced signal-to-noise ratio (SNR), which compromises the results accuracy. However, we use thinner slices (1-mm slice thickness) in our small-animal preclinical work on rats[36] to avoid partial volume effects in the small heart of the rat and we compensate for small SNR by acquiring multiple averages at the cost of increased scan time. Thirdly, unfortunately, histological analysis was not conducted in the patients in this study as neither biopsy nor surgery was conducted on the patients. However, we have conducted histological analysis on our recent preclinical work[37], in which we conducted hematoxylin and eosin (H&E), Masson's trichrome, and toluidine blue staining on a rat model of thoracic cancer. The histopathological results confirmed the findings by the imaging biomarkers, which was demonstrated in the samples by increased fibrosis or collagen (Masson trichrome), hemorrhage, cellular vacuolization, and/or cellular necrosis (H&E), and mast cells (toluidine) in the rat model compared to control. Finally, we used the standard American Heart Association (AHA) 16-segment model on all studied subjects and study timepoints. The model represents segmental distribution of the left ventricle myocardium at three levels (base, mid-ventricle, and apex) and different regions (anterior, inferior, septal, and lateral). This model is extensively used for standard cardiac functional analysis as reported in the literature.[38] We used the model to represent all strain components (circumferential, longitudinal, and radial) for each segment at baseline, post-treatment, and follow-up timepoints. We used correlation analysis between dose and strain parameters to examine the predictive value of different myocardial segments in response to chemotherapy. The results with high correlation ($|R| \geq 0.7$) and especially those with significant measurement ($p < 0.05$) were considered of more influence and predictivity on the dose-response effect. The results showed different segments for sarcoma vs. breast cancer at both post-treatment and 6-months follow-up timepoints.

In conclusion, cardiac MRI provides valuable information about heart function and changes in tissue composition in sarcoma receiving anthracyclines. Especially, myocardial strain is an early marker of cardiac dysfunction when EF > 50%. The generated MRI parameters may reflect a specific contractility and remodeling pattern in sarcoma that is differentiated from breast cancer.

Acknowledgement

The study was supported by the Cancer Center of the Medical College of Wisconsin, Milwaukee, USA (E.I.).

References

1. Quintana RA, Banchs J, Gupta R, Lin HY, Raj SD, Conley A, et al. Early evidence of cardiotoxicity and tumor response in patients with sarcomas after high cumulative dose Doxorubicin given as a continuous infusion. *Sarcoma* 2017; **2017:** 7495914. doi: 10.1155/2017/7495914

2. Coleman MP, Forman D, Bryant H, Butler J, Rachet B, Maringe C, et al. Cancer survival in Australia, Canada, Denmark, Norway, Sweden, and the UK, 1995-2007 (the International Cancer Benchmarking Partnership): an analysis of population-based cancer registry data. *Lancet* 2011; **377:** 127-38. doi: 10.1016/S0140-6736(10)62231-3

3. Jones RL, Wagner AJ, Kawai A, Tamura K, Shahir A, Van Tine BA, et al. Prospective evaluation of doxorubicin cardiotoxicity in patients with advanced soft-tissue sarcoma treated in the ANNOUNCE phase III randomized trial. *Clin Cancer Res* 2021; **27:** 3861-6. doi: 10.1158/1078-0432.CCR-20-4592

4. Krone RJ, Van Tine BA. More data to support a cardiac-oncologic partnership. *JACC CardioOncol* 2023; **5:** 128-30. doi: 10.1016/j.jaccao.2023.01.002

5. Swain SM, Whaley FS, Ewer MS. Congestive heart failure in patients treated with doxorubicin: a retrospective analysis of three trials. *Cancer* 2003; **97:** 2869-79. doi: 10.1002/cncr.11407

6. Mo Z, Deng Y, Bao Y, Liu J, Jiang Y. Evaluation of cardiotoxicity of anthracycline-containing chemotherapy regimens in patients with bone and soft tissue sarcomas: a study of the FDA adverse event reporting system joint single-center real-world experience. *Cancer Med* 2023; **12:** 21709-24. doi: 10.1002/cam4.6730

7. Paulides M, Kremers A, Stohr W, Bielack S, Jurgens H, Treuner J, et al. Prospective longitudinal evaluation of doxorubicin-induced cardiomyopathy in sarcoma patients: a report of the late effects surveillance system (LESS). *Pediatr Blood Cancer* 2006; **46:** 489-95. doi: 10.1002/pbc.20492

8. Shamai S, Rozenbaum Z, Merimsky O, Derakhshesh M, Moshkovits Y, Arnold J, et al. Cardio-toxicity among patients with sarcoma: a cardio-oncology registry. *BMC Cancer* 2020; **20:** 609. doi: 10.1186/s12885-020-07104-9

9. Mitani I, Jain D, Joska TM, Burtness B, Zaret BL. Doxorubicin cardiotoxicity: prevention of congestive heart failure with serial cardiac function monitoring with equilibrium radionuclide angiocardiography in the current era. *J Nucl Cardiol* 2003; **10:** 132-9. doi: 10.1067/mnc.2003.7

10. Altena R, Perik PJ, van Veldhuisen DJ, de Vries EG, Gietema JA. Cardiovascular toxicity caused by cancer treatment: strategies for early detection. *Lancet Oncol* 2009; **10:** 391-9. doi: 10.1016/S1470-2045(09)70042-7

11. Bonita R, Pradhan R. Cardiovascular toxicities of cancer chemotherapy. *Semin Oncol* 2013; **40:** 156-67. doi: 10.1053/j.seminoncol.2013.01.004

12. Khawaja MZ, Cafferkey C, Rajani R, Redwood S, Cunningham D. Cardiac complications and manifestations of chemotherapy for cancer. *Heart* 2014; **100:** 1133-40. doi: 10.1136/heartjnl-2013-303713

13. Yeh ET, Tong AT, Lenihan DJ, Yusuf SW, Swafford J, Champion C, et al. Cardiovascular complications of cancer therapy: diagnosis, pathogenesis, and management. *Circulation* 2004; **109:** 3122-31. doi: 10.1161/01.CIR.0000133187.74800.B9

14. Alvarez JA, Russell RR. Cardio-oncology: the nuclear option. *Curr Cardiol Rep* 2017; **19:** 31. doi: 10.1007/s11886-017-0844-z

15. Al-Batran SE, Meerpohl HG, von Minckwitz G, Atmaca A, Kleeberg U, Harbeck N, et al. Reduced incidence of severe palmar-plantar erythrodysesthesia and mucositis in a prospective multicenter phase II trial with pegylated liposomal doxorubicin at 40 mg/m2 every 4 weeks in previously treated patients with metastatic breast cancer. *Oncology* 2006; **70:** 141-6. doi: 10.1159/000093005

16. Alhaja M, Chen S, Chin AC, Schulte B, Legasto CS. Cardiac safety of pegylated liposomal doxorubicin after conventional doxorubicin exposure in patients with sarcoma and breast cancer. *Cureus* 2023; **15:** e44837. doi: 10.7759/cureus.44837

17. Mehta LS, Watson KE, Barac A, Beckie TM, Bittner V, Cruz-Flores S, et al. Cardiovascular disease and breast cancer: where these entities intersect: a scientific statement from the american heart association. *Circulation* 2018; **137:** e30-e66. doi: 10.1161/CIR.0000000000000556

18. Shantakumar S, Olsen M, Vo TT, Norgaard M, Pedersen L. Cardiac dysfunction among soft tissue sarcoma patients in Denmark. *Clin Epidemiol* 2016; **8:** 53-9. doi: 10.2147/CLEP.S100779

19. Ettinghausen SE, Bonow RO, Palmeri ST, Seipp CA, Steinberg SM, White DE, et al. Prospective study of cardiomyopathy induced by adjuvant doxorubicin therapy in patients with soft-tissue sarcomas. *Arch Surg* 1986; **121:** 1445-51. doi: 10.1001/archsurg.1986.01400120095016

20. Cardinale D, Iacopo F, Cipolla CM. Cardiotoxicity of anthracyclines. *Front Cardiovasc Med* 2020; **7:** 26. doi: 10.3389/fcvm.2020.00026

21. Leger K, Slone T, Lemler M, Leonard D, Cochran C, Bowman WP, et al. Subclinical cardiotoxicity in childhood cancer survivors exposed to very low dose anthracycline therapy. *Pediatr Blood Cancer* 2015; **62:** 123-7. doi: 10.1002/pbc.25206

22. Alpman MS, Jarting A, Magnusson K, Manouras A, Henter JI, Broberg AM, et al. Longitudinal strain analysis for assessment of early cardiotoxicity during anthracycline treatment in childhood sarcoma: a single center experience. *Cancer Rep (Hoboken)* 2023; **6:** e1852. doi: 10.1002/cnr2.1852

23. Heemelaar JC, Speetjens FM, Al Jaff AAM, Evenhuis RE, Polomski EAS, Mertens BJA, et al. Impact of age at diagnosis on cardiotoxicity in high-grade osteosarcoma and Ewing sarcoma patients. *JACC CardioOncol* 2023; **5:** 117-27. doi: 10.1016/j.jaccao.2022.11.016

24. Tian Z, Yang Y, Yang Y, Zhang F, Li P, Wang J, et al. High cumulative doxorubicin dose for advanced soft tissue sarcoma. *BMC Cancer* 2020; **20:** 1139. doi: 10.1186/s12885-020-07663-x

25. Ehrhardt MJ, Leerink JM, Mulder RL, Mavinkurve-Groothuis A, Kok W, Nohria A, et al. Systematic review and updated recommendations for cardiomyopathy surveillance for survivors of childhood, adolescent, and young adult cancer from the International Late Effects of Childhood Cancer Guideline Harmonization Group. *Lancet Oncol* 2023; **24:** e108-e20. doi: 10.1016/S1470-2045(23)00012-8

26. Yoon GJ, Telli ML, Kao DP, Matsuda KY, Carlson RW, Witteles RM. Left ventricular dysfunction in patients receiving cardiotoxic cancer therapies are clinicians responding optimally? *J Am Coll Cardiol* 2010; **56:** 1644-50. doi: 10.1016/j.jacc.2010.07.023

27. Plana JC, Galderisi M, Barac A, Ewer MS, Ky B, Scherrer-Crosbie M, et al. Expert consensus for multimodality imaging evaluation of adult patients during and after cancer therapy: a report from the American Society of Echocardiography and the European Association of Cardiovascular Imaging. *J Am Soc Echocardiogr* 2014; **27:** 911-39. doi: 10.1016/j.echo.2014.07.012

28. Celutkiene J, Pudil R, Lopez-Fernandez T, Grapsa J, Nihoyannopoulos P, Bergler-Klein J, et al. Role of cardiovascular imaging in cancer patients receiving cardiotoxic therapies: a position statement on behalf of the Heart Failure Association (HFA), the European Association of Cardiovascular Imaging (EACVI) and the Cardio-Oncology Council of the European Society of Cardiology (ESC). *Eur J Heart Fail* 2020; **22:** 1504-24. doi: 10.1002/ejhf.1957

29. Oikonomou EK, Kokkinidis DG, Kampaktsis PN, Amir EA, Marwick TH, Gupta D, et al. Assessment of prognostic value of left ventricular global longitudinal strain for early prediction of chemotherapy-induced cardiotoxicity: a systematic review and meta-analysis. *JAMA Cardiol* 2019; **4:** 1007-18. doi: 10.1001/jamacardio.2019.2952

30. Lyon AR, Lopez-Fernandez T, Couch LS, Asteggiano R, Aznar MC, Bergler-Klein J, et al. 2022 ESC Guidelines on cardio-oncology developed in collaboration with the European Hematology Association (EHA), the European Society for Therapeutic Radiology and Oncology (ESTRO) and the International Cardio-Oncology Society (IC-OS). *Eur Heart J* 2022; **43:** 4229-361. doi: 10.1093/eurheartj/ehac244

31. Suerken CK, D'Agostino RB, Jr., Jordan JH, Melendez GC, Vasu S, Lamar ZS, et al. Simultaneous left ventricular volume and strain changes during chemotherapy associate with 2-year postchemotherapy measures of left ventricular ejection fraction. *J Am Heart Assoc* 2020; **9:** e015400. doi: 10.1161/JAHA.119.015400

32. Muehlberg F, Funk S, Zange L, von Knobelsdorff-Brenkenhoff F, Blaszczyk E, Schulz A, et al. Native myocardial T1 time can predict development of subsequent anthracycline-induced cardiomyopathy. *ESC Heart Fail* 2018; **5:** 620-9. doi: 10.1002/ehf2.12277

33. Jordan JH, Vasu S, Morgan TM, D'Agostino RB, Jr., Melendez GC, Hamilton CA, et al. Anthracycline-associated T1 mapping characteristics are elevated independent of the presence of cardiovascular comorbidities in cancer survivors. *Circ Cardiovasc Imaging* 2016; **9**. doi: 10.1161/CIRCIMAGING.115.004325

34. Neilan TG, Coelho-Filho OR, Shah RV, Feng JH, Pena-Herrera D, Mandry D, et al. Myocardial extracellular volume by cardiac magnetic resonance imaging in patients treated with anthracycline-based chemotherapy. *Am J Cardiol* 2013; **111:** 717-22. doi: 10.1016/j.amjcard.2012.11.022

35. Ibrahim EH, Stojanovska J, Hassanein A, Duvernoy C, Croisille P, Pop-Busui R, et al. Regional cardiac function analysis from tagged MRI images. Comparison of techniques: Harmonic-Phase (HARP) versus Sinusoidal-Modeling (SinMod) analysis. *Magn Reson Imaging* 2018; **54:** 271-82. doi: 10.1016/j.mri.2018.05.008

36. Ibrahim EH, Baruah D, Budde M, Rubenstein J, Frei A, Schlaak R, et al. Optimized cardiac functional MRI of small-animal models of cancer radiation therapy. *Magn Reson Imaging* 2020; **73:** 130-7. doi: 10.1016/j.mri.2020.08.020

37. Ibrahim EH, Baruah D, Croisille P, Stojanovska J, Rubenstein JC, Frei A, et al. Cardiac magnetic resonance for early detection of radiation therapy-induced cardiotoxicity in a small animal model. *JACC CardioOncol* 2021; **3:** 113-30. doi: 10.1016/j.jaccao.2020.12.006

38. Cerqueira MD, Weissman NJ, Dilsizian V, Jacobs AK, Kaul S, Laskey WK, et al. Standardized myocardial segmentation and nomenclature for tomographic imaging of the heart. A statement for healthcare professionals from the Cardiac Imaging Committee of the Council on Clinical Cardiology of the American Heart Association. *Circulation* 2002; **105:** 539-42. doi: 10.1161/hc0402.102975

research article

Innovative strategies for minimizing hematoma risk in MRI-guided breast biopsies

Michael P Brönnimann[1,2], Matthew T McMurray[1], Johannes T Heverhagen[1], Andreas Christe[1], Corinne Wyss[1], Alan A Peters[1], Adrian T Huber[1,3], Florian Dammann[1], Verena C Obmann[1]

[1] Department of Diagnostic, Interventional and Pediatric Radiology, Inselspital, Bern University Hospital, University of Bern, Bern, Switzerland

[2] Department of Radiology, Charité – Universitätsmedizin, Berlin, Berlin, Germany

[3] Department of Nuclear Medicine and Radiology, Cantonal Hospital Lucerne, Lucerne, Switzerland

Radiol Oncol 2025; 59(1): 91-99.

Received 27 August 2024
Accepted 12 November 2024

Correspondence to: Michael P. Brönnimann, Department of Diagnostic, Interventional and Pediatric Radiology, Inselspital, Bern University Hospital, University of Bern, Rosenbühlgasse 27, 3010 Bern, Switzerland and Department of Radiology, Charité – Universitätsmedizin, Berlin, Augustenburger Platz 1, 13353 Berlin, Germany. E-mail: michael.broennimann@insel.ch / michael.broennimann@charite.de

Disclosure: No potential conflicts of interest were disclosed.

Background. The study aimed to investigate the reduction of hematoma risk during MRI-guided breast biopsies by evaluating position-dependent intervention parameters and characteristics of the target lesion.

Materials and methods. We retrospectively analyzed 252 percutaneous MRI-guided breast biopsies performed at a single center between January 2013 and December 2023. Two groups were built depending on the severity of relative hematoma formation (using a cut-off ≤ 7.62 cm^3 or > 7.62 cm^3). Potential influencing variables were assessed, such as patient demographics, interventional parameters related to anatomical landmarks, and lesion characteristics. Fisher's exact test and Mann-Whitney-U-Test were used to calculate the statistical difference between groups of categorical, dichotomous, and continuous variables. Multivariable logistic regression was used to identify the strongest association with relative hematoma formation.

Results. The univariate analysis showed that relatively larger hematoma occurred significantly more frequently when the patients were younger (P = 0.002), the relative distances from the target lesion to the nipple (P = 0.001) as well as alongside the access path (P = 0.001) were greater and when the vacuum-assisted biopsy system was used in contrast to the Spirotome® (P = 0.035). Multivariable logistic regression analysis also showed that these were independently associated with the occurrence of relatively larger hematomas. Epinephrine in the local anesthetic, lesion location classified by specific quadrant, and pathological findings did not influence the extent of the hematoma.

Conclusions. Our findings underscore the importance of strategic procedural planning to minimize hematoma occurrence and enhance patient safety during MRI-guided breast biopsy procedures.

Key words: biopsy; interventional; image-guided biopsy; magnetic resonance imaging; breast neoplasms; female; hematoma

Introduction

MRI is more sensitive than alternative imaging methods like ultrasound or mammography for women at elevated risk of breast cancer, detecting over half of lesions exclusively on MRI.[1,2] It can detect primary cancer in patients suspected of having occult breast cancer.[3-5] As per the guidelines of the American Cancer Society (ACR) and the European Society of Breast Imaging (EUSOBI), MR-guided biopsy is recommended for suspicious lesions exclusively detected by MRI (referred to as MR-only lesions).[6-8]

To minimize sampling errors and not underestimate the target lesions, percutaneous, stereotactic large core biopsies larger than 11 gauge, either with vacuum-assisted devices or with manual devices such as the Spirotome®, have prevailed over core biopsies.[9-13] Hematoma is identified as the primary complication of this procedure across different contexts, with the incidence of mammographically evident hematoma reported to be as high as 45%.[14-19] While many hematomas do not require additional intervention, the clinical significance of existing studies remains unclear.[15-20] Furthermore, the study situation is also very inconsistent in recording hematomas. Most reports attempted to record these by external observation *e.g.*[21] or indirectly *e.g.*[19] To date, no intraprocedural factors have been identified to reduce the risk of hematoma occurrence in MRI-guided breast biopsies.

A decisive aspect in developing hematomas could be the asymmetrical blood supply to the breast. Thus, 60% of the breast is supplied by perforating branches of the internal thoracic artery, which lies on the medial side.[22] Of this, at least 60% is specifically provided by the superomedial perforators.[23] Furthermore, the internal thoracic artery mainly supplies the nipple-areola complex (NAC).[24] The prone position during MRI-guided breast biopsy could aggravate this. Also, the growth and advancement of breast cancers are associated with heightened neovascularization.[25] We, therefore, hypothesize that larger hematomas are more likely to occur in the upper and outer quadrants near the NAC in malignant lesions.

The study aimed to investigate the hematoma risk during MRI-guided breast biopsies by evaluating position-dependent intervention parameters and characteristics of the target lesion.

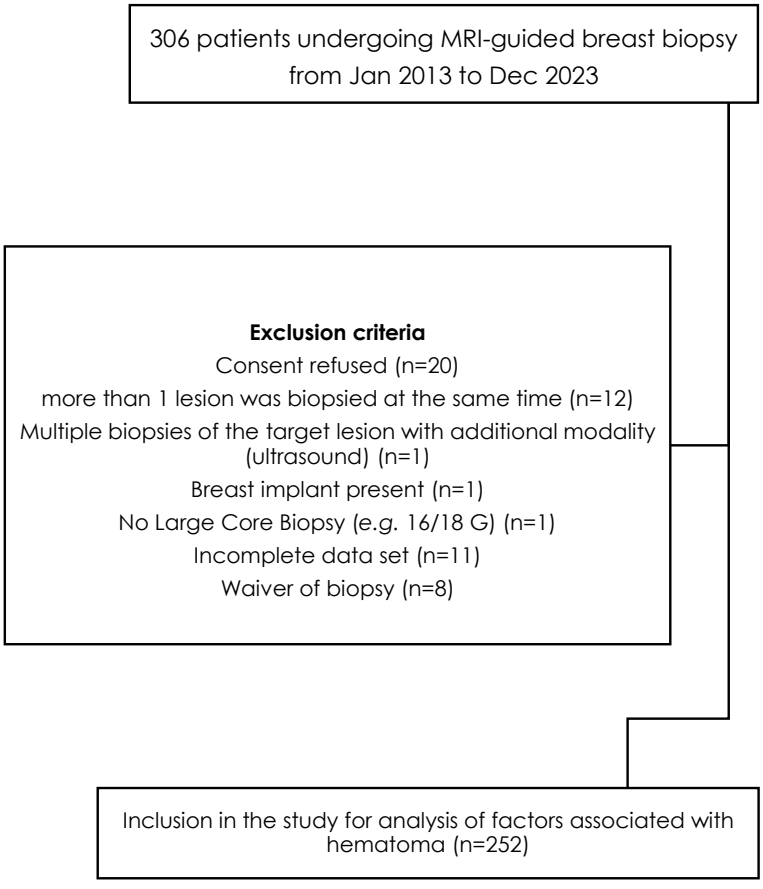

FIGURE 1. Flowchart shows the study population.

Materials and methods

The study received approval from the Ethics Committee of the Canton of Bern (BASEC Project-ID 2024-00805) and adhered to the principles outlined in the Declaration of Helsinki. The authors had complete access to the data and assumed full responsibility for its integrity. Written informed consent was obtained from all patients.

Study population

This study retrospectively analyzed 306 percutaneous MRI-guided breast biopsies conducted at our university hospital between January 2013 and December 2023 in 300 women with thus 6 women who underwent more than one biopsy.

The exclusion criteria were defined consecutively to avoid possible bias due to non-physiological local conditions (breast implant; more than one lesion was biopsied at the same time; multiple biopsies of the target lesion with additional modality) or rare intervention techniques (no large core biopsies *e.g.* 16 or 18 G and to homogenize the groups (Figure 1)).

Two groups were formed based on the severity of the relative hematoma volume. The severity was categorized dichotomously according to whether the measured relative hematoma volumes were above or below the mean value.

Baseline evaluation and biopsy technique

Before the biopsy, all patients underwent a clinical evaluation, including a thorough medical history review and standard blood tests. The procedure required an INR value below 1.5 or a Quick value above 60%, an Hb value exceeding 80 g/L,

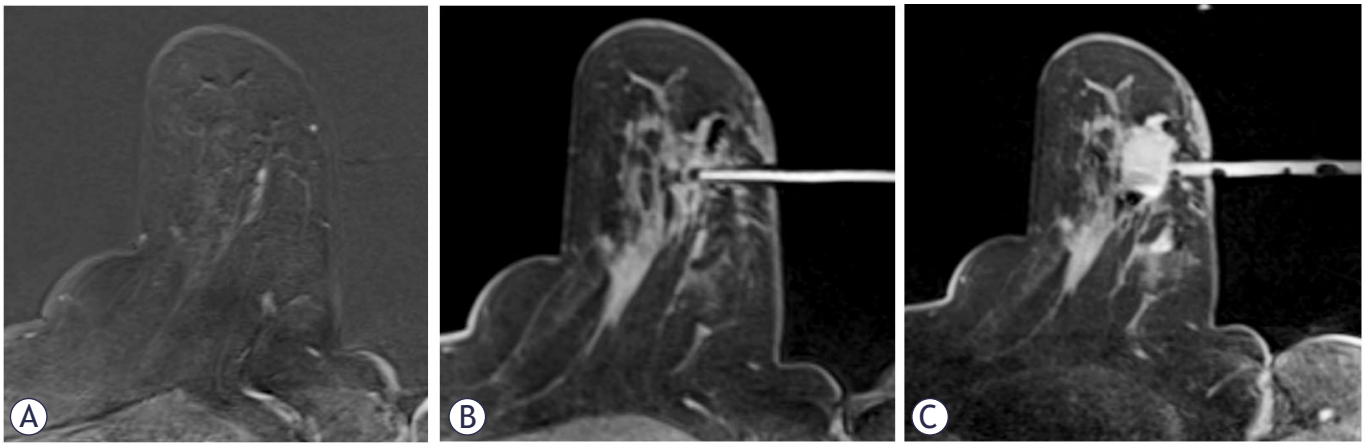

FIGURE 2. MRI-guided breast biopsy with hematoma as a sequela. **(A)** Target lesion in the lower outer quadrant. **(B)** Biopsy needle in target position. **(C)** After vacuum-assisted biopsy, a hematoma has formed. Within it, a recognizable susceptibility artifact is due to the marker.

and a platelet count of over 50 x 10^9/L. These blood values must not be older than 5 days. According to our guidelines, NSAIDs (non-steroidal anti-inflammatory drugs) and clopidogrel had to be stopped 5 days, heparin 6 hours, rivaroxaban 1 day, dabigatran and endoxaban each 3 days before intervention. Eight interventionalists, each with more than 5 years of experience, performed the biopsies. Contraindications for MRI, such as pregnancy, inability to lie prone for 60 minutes, or the administration of contrast medium containing gadolinium, were explicitly requested in advance in the questionnaire.

All biopsies were conducted utilizing a 1.5 T Siemens Magnetom Aera/SolaFit (Siemens Healthinieers, upgrade of the machine performed in 06/2022) paired with a dedicated four-channel open breast coil (Invivo Interventional Instruments, Wurzburg, Germany) and a needle positioning add-on device (Noras, Germany). Patients were positioned in the prone position on the MRI table with the affected breast compressed within the biopsy device to minimize motion during the procedure. Imaging was performed before and after administering 0.1 mmol/kg of contrast agent (Dotarem, Guerbet, France) using a T1-weighted dynamic contrast-enhanced subtraction sequence lasting 103 seconds. This imaging protocol provided coverage of the breast with nearly isotropic voxels (slice thickness 1 mm, Repetition Time (TR) of 7.62 (milliseconds) ms, Time to Echo (TE) of 4.77 ms), facilitating image reconstruction in any plane. Either the grid or pillar and post system was used. The specialized breast biopsy planning software (Siemens) was utilized to acquire lesion coordinates and guide needle positioning. The needle path was planned according to our best practices to ensure the shortest distance from the skin to the lesion while avoiding larger vessels and maintaining a safety margin from the skin. After the initial imaging, the table was retracted from the bore to facilitate disinfection and the administration of local anesthesia. Lidocaine 1% (maximum 20 ml, Streuli Pharma AG, Uznach, Switzerland), was administered to the skin, subcutaneous tissues and deep. The interventionalist could choose whether to give the one mixed with epinephrine (Lidocain-Epinephrin 2% Streuli, Streuli Pharma AG, Uznach, Switzerland). A small incision was made in the skin to facilitate the smooth entry of the device. The introducer stylet, was inserted through the needle guide to the predetermined depth. Subsequently, the stylet was withdrawn and replaced with a sterile plastic MRI-visible obturator. T1-weighted fat-saturation images were then acquired to confirm the depth and position of the introducer. Either a large volume biopsy with a manual device Spirotome® 8 gauge (G) (Bioncise, Wellen, Belgium) and max. 3 samples or a Vacuum-assisted biopsy (VAB) with an EnCore® (BD, New Jersey, USA) 7G/ 10G and max. 24 samples was done. After the marker (SenoMarkTM, BD, New Jersey, USA) was placed, a control sequence T1 and T2, again technical details were performed (Figure 2). The breast was compressed manually for 15 minutes followed by a compression bandage for the next 24 hours.

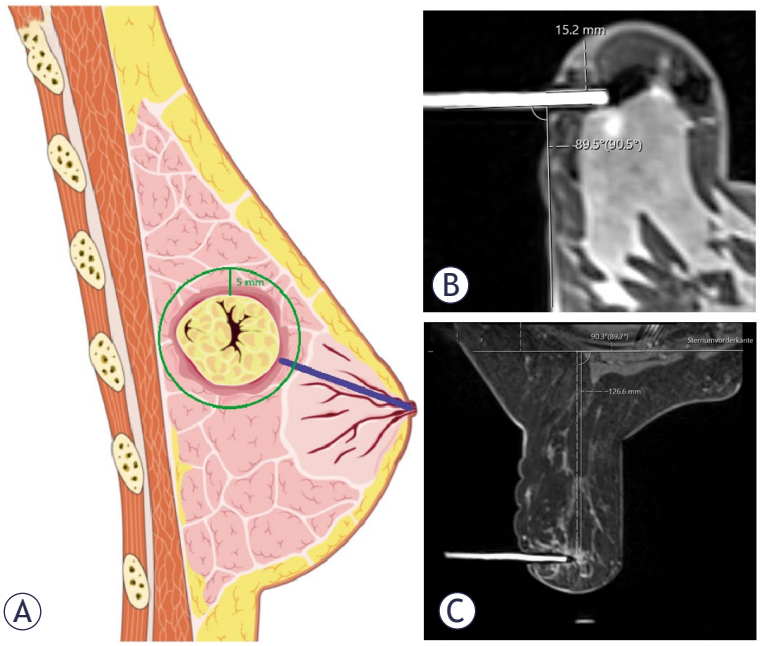

FIGURE 3. Illustration of the measurements. **(A)** In blue, the distance from the lesion to the nipple. A circle was drawn around the target lesion to capture the proportion of the surrounding mammary gland. These measurements were taken after multiplanar reconstruction (MPR) of the dynamic T1 subtraction sequence. **(B)** Access route and biopsy angle. **(C)** Perpendicular distance from the pectoralis major muscle to the lesion in T1-weighted with spectral attenuated inversion recovery (SPAIR) sequence.

Data collection

All procedures were reviewed by a board-certified interventional radiologist with eight years of experience and a radiology resident with four years of experience. Neither of them performed any of the interventions, and all were blinded to the patient`s medical history.

The perpendicular distance from the pectoralis major muscle to the lesion (in mm) was recorded with the consideration of indirectly measuring the effect of gravity. Other patient- and technique-related variables assessed on the interventional MRI images included interventional date, birth date, age of the patient (in years), procedure time (in minutes), target lesion size (in mm), biopsy side, biopsy angle, distance lesion to nipple (LN in mm), access path length measured along the needle from the skin to the lesion (in mm), lesion location according to the breast quadrants, breast and hematoma volume (cm^3). All volumes were manually obtained from the multiplanar reconstruction (MPR) of the three-dimensional (3D) T1-weighted sequence with spectral attenuated inversion recovery (SPAIR) acquisition. The manually measured hematoma volume and absolute distances were set in relation to the breast volume, as we ultimately rated this as the most meaningful in the overall context. For this purpose, we identified the mean of the relative hematoma volume of all measured volumes (7.62 cm^3) and defined this as the cut-off.

To evaluate the possible influence of surrounding mammary gland tissue on hematoma formation, a 5 mm larger circle was drawn around the target lesion to assess the amount of surrounding mammary gland tissue. The quarter rule was used for this purpose (Figure 3).

A Sectra workstation was used to review the images (IDS 7, version 24.2, 2022, Linköping, Sweden). We recorded the size of the biopsy system, type of local anesthetic and number of samples from the intervention report. The histological results from the target lesion and the patient`s history after intervention were also collected retrospectively from the electronic medical record. The following pathological reports were categorized into benign, high-risk lesions and malignancy. High-risk lesions were defined according to Heller *et al.*[26] as atypical ductal hyperplasia, lobular intraepithelial neoplasia, lobular carcinoma in situ, papilloma, atypical lobular hyperplasia, radial scar, and flat epithelial cell atypia.

Statistical analysis

We utilized IBM SPSS Statistics for Windows, version 28 (IBM, Armonk, NY), for all statistical analyses. Univariate analysis was conducted using Chi-Square and Fisher exact tests for categorical variables, and the Mann-Whitney-U-Test for continuous variables, with a significance level set at $P < 0.05$. The Kolmogorov-Smirnov test was used to test for normal distribution. Multivariable logistic regression was used to assess potential confounders and risk factors for the development of hematoma, with model goodness of fit evaluated using the Hosmer-Lemeshow test. To prevent overfitting, we adhered to the rule of ten by including five independent variables in the multiple logistic regression model, selected based on their significance or proximity to significance, while considering a minimum group size of $n \geq 25$ for categorical predictors. Therefore, we included the procedure time for the regression. The analysis was overseen by a senior statistician from the Clinical Trials Unit (CTU) of the Faculty of Medicine at the University of Bern.

Results

Study population

A total of 252 biopsies met the inclusion criteria, with a mean patient age of 51.96 ± 11.69 years (range 22–84 years). All variables in both groups were not normally distributed, as indicated by the Kolmogorov-Smirnov test (P < 0.001). There were no significant differences in pathological findings or their locations between the two groups. The majority of biopsied lesions were benign (63%, Figure 4), located in the outer quadrants of the breast (62%), and surrounded by 0–25% mammary gland tissue (42%). Slightly more than a quarter (26%) of the biopsied breasts had been previously treated (Table 1).

Hematoma formation during MRI-guided breast biopsy

On average, the MRI-guided breast biopsy lasted 41.9 minutes. In 90% of cases, the biopsy was performed as a VAB, with the majority of cases preceded by the use of local anesthetic mixed with ephedrine (68%). A hematoma occurred in 70% (178/252) of cases, with a hematoma volume of ≥14 cm^3 (diameter of 3 cm) detected in 6%, and a volume of ≥ 33.5 cm^3 (diameter of 4 cm) detected in 0.8%. The univariate analysis showed that relatively larger hematoma occurred significantly more frequently when the patients were younger (P = 0.002), the relative distances from LN (P = 0.001) as well as the access path (P = 0.001) were larger and when the VAB instead of a Spirotome system was used (P = 0.035). Both relatively smaller hematomas (11.5% *vs.* 88.5%) and relatively larger hematomas (2% *vs.* 98%) occurred significantly less with the Spirotome than the VAB. We did not observe a significantly increased frequency of relatively larger hematoma depending on epinephrine in the local anesthetic (P = 0.408), lesion location classified by specific quadrant (P = 0.399), lesion size (P = 0.425), biopsy angle (P = 0.443), the perpendicular distance from the pectoralis muscle to the lesion (P = 0.143), adjacent glandular tissue (P = 0.215) or histopathological result (benignity, P = 0,749; high-risk lesions, P = 0.581, malignancy, P = 0.825).

Association of lesion characteristics and technical parameters with the occurrence of relatively larger hematoma

Multivariable logistic regression analysis showed that lower age (OR 0.969, 95% CI 0.934 –1, P = 0.048), the use of a VAB system (OR 11.798, 95% CI 1.341–103.8, P = 0.026), the LN distance (P < 0.01) and access path length (P = 0.029) were independently associated with relatively larger hematomas (Table 2). A good model fit with an R^2 = 0.222, P < 0.001. Cohen's f2 is 0.28, corresponding to a good medium effect.[27]

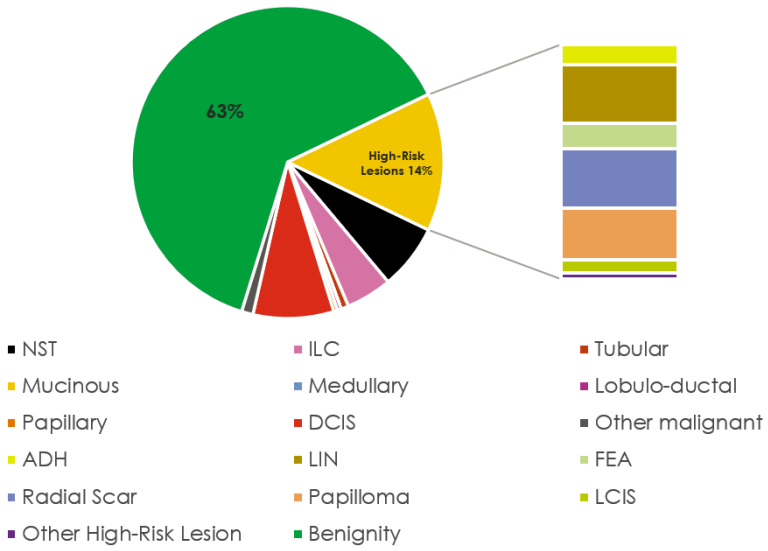

FIGURE 4. Histological findings of breast biopsies.

ADH = atypical ductal hyperplasia; DCIS; ductal carcinoma in situ; FEA = flat epithelial cell atypia; ILC = invasive lobular carcinoma; LCIS = lobular carcinoma in situ; LIN = lobular intraepithelial neoplasia; NST = non-special type

Discussion

This study aimed to assess factors influencing hematoma risk in MRI-guided breast biopsies. Through retrospective analysis of 252 cases, patients were stratified by hematoma size, and various parameters including patient demographics, anatomical features, and lesion attributes were scrutinized. Univariate analysis unveiled significant associations between larger hematoma formation and younger patient age (P = 0.002), increased LN distance (P = 0.001) and access path length (P = 0.001), and utilization of VAB instead of Spirotome® (P = 0.035). Multivariable logistic regression confirmed these associations as independent predictors of relatively larger hematomas, while factors such as epinephrine in local anesthetic, lesion location classified by specific quadrant, and pathological findings did not influence hematoma extent. Overall, hematoma incidence

TABLE 1. Univariate analysis for relatively larger hematoma with patient demographics and lesion characteristics

Survey of breast biopsies							
Parameter	**All (n=252)**		**Relatively smaller hematoma (n = 200)**		**Relatively larger hematoma (n = 52)**		***P* Value**
Age (y)	51.96	±11.69	53.09	±11.09	47.63	±12.984	0.002*
Procedure time (min)	41.83	±13.39	42.58	±13.80	38.96	±11.324	0.072
Right biopsy side	117	46%	90	45%	27	52%	0.436
Number of samples	12.08	± 4	11.81	±4.08	13.1	±3.533	0.243
Biopsy system							0.035*
VABB	228	90%	177	88.5%	51	98%	
Spirotome	24	10%	23	11.5%	1	2%	
LAE	171	68%	133	67%	38	73%	0.408
Lesion size (mm)	11.2	±6.612	11.27	±6.55	10.94	±6.89	0.425
Distance LN in RBV	0.079	± 0.05	0.07	± 0.04	0.11	±0.04	0.001*
Access path length in RBV	0.055	± 0.046	0.05	± 0.03	0.08	±0.07	0.001*
PDPectLesion in RBV	0.065	± 0.036	0.06	± 0.04	0.07	± 0.04	0.143
Biopsy angle (degree)	90.79	± 10.4	90.93	± 9.55	90.27	± 13.26	0.443
Pathological findings							0.831
Benignity	159	63%	125	63%	34	65%	
High-risk lesions	36	14%	28	14%	8	15%	
Malignancy	57	23%	47	24%	10	19%	
Pretreatment	65	26%	55	28%	10	19%	0.286
Lesion location							0.399
Upper inner q	47	19%	34	17%	13	25%	
Upper outer q	84	33%	64	32%	20	38%	
Lower inner q	24	10%	21	11%	3	6%	
Lower outer q	72	29%	61	31%	11	21%	
Areolar	25	10%	20	10%	5	10%	
Proportion of mammary gland							0.215
0–25%	105	42%	85	43%	20	38%	
25–50%	48	19%	37	19%	11	21%	
50–75%	47	19%	37	19%	10	19%	
75–100%	52	21%	41	21%	11	21%	

Unless stated otherwise, data are number of biopsies. ± standard deviations. X2 (R X 2), Fisher's exact test and Mann-Whitney-U-Test were used to calculate the statistical difference between groups of categorical, dichotomous, and continuous variables, respectively. Data are mean ± standard deviation. * Statistically significant (defined $P < 0.05$)

LAE = local anesthesia mixed with epinephrine; LN= lesion to nipple; min = minutes; mm = millimeters; PDPectLesion = perpendicular distance from the pectoralis major muscle to the lesion; Pretreatment = affected breast pretreated; RBV = in Relation to Breast Volume; VABB = vacuum-assisted breast biopsy; q = quadrant; Y = Year

was observed in 70% of cases. The results suggest that asymmetric blood supply to the breast supply and the gravitational force play a less significant role in the development of hematomas during MRI-guided breast biopsies than previously anticipated.

Our study findings align with prior research. Kettritz *et al.*[28] documented 0.87% incidence of large hematomas (≥4 cm in diameter), while our study observed a rate of 0.8% (relative to a volume of 33 cm^3). Perlet *et al.*[29] reported 1.75% occurrence of hematomas with a size of ≥3 cm. In con-

TABLE 2. Results of multivariate logistic regression analysis for relatively larger hematoma

	B	S.E.	Wald test	df	*P* value	Odds ratio	95% CI	
Variable							-	+
Age (y)	-0.031	0.160	3.927	1	0.048*	0.969	0.94	1
Biopsy system	2.468	1.11	4.947	1	0.026*	11.798	1.341	103.811
Distance LN in RBV	9.501	3.538	7.214	1	0.007*	13379	13.037	13.7 x 10^6
Access path length in RBV	7.622	3.49	4.77	1	0.029*	2043	2.186	1.9 x 10^6
Procedure time (min)	-0.025	0.015	2.759	1	0.097	0.975	0.947	1.005

The total number of cases in the cohort for the multivariate analysis was n = 252

B = Regression coefficient; CI = Confidence interval; df = Degree of freedom; LN = Lesion to nipple; min. = minutes; RBV = in relation to breast volume; S.E. = standard error; * statistically significant (defined P < 0.05); Y = years

trast, our study recorded a 6% incidence, slightly higher likely due to differing follow-up protocols. In instances of uncertainty, they conducted repeat MRI scans 24–48 hours post-biopsy. Our direct comparison between two biopsy modalities, VAB and Spirotome®, corroborates previous research. Hematoma occurrence rates were reported to be as high as 45% after VAB and 16% following large core biopsy with the Spirotome®.[14-19,30] This discrepancy is likely attributed to the increased traumatic injury associated with VAB, regardless of the sample size. Consequently, our study identified a significantly higher incidence of relatively larger hematomas associated with VAB (P = 0.035), a finding further supported as an independent predictor in multivariable logistic regression analysis.

Our investigation indicates that gravitational forces do not exert a significant influence on hematoma development in MRI-guided biopsies, as evidenced by the absence of a significant occurrence of larger hematomas despite a greater relatively perpendicular distance from the pectoralis muscle to the lesion (P = 0.143). While it is established that lesion dimensions are overestimated and exhibit a higher wash-in peak in the prone position compared to the supine position[31], McGrath *et al*.[32] observed that breast compression during MRI-guided breast biopsy may diminish perfusion and result in inadequate parenchymal enhancement. This observation is further supported by the lack of a significant difference in procedure time. Our findings suggest that future investigations could explore the influence of varying compression pressures on the risk of developing larger hematomas during breast biopsy procedures. Effective breast compression pressure should be measured and analyzed in relation to hematoma size. Adjusting compression pressure may offer a promising approach to reducing hematoma formation, meriting further investigation.

The clear difference in the extent and type of angiogenesis of breast tumors[25] is probably also reflected in our results. No significantly higher frequency of relatively larger hematomas occurred according to the different pathological findings. These potential local microvascular conditions may have little or no effect on biopsy-induced hematomas, which is supported by the lack of a significant difference in our results when epinephrine was added to the local anesthetic. Therefore, the effective benefit of the vasoconstrictive effect of local anesthetics mixed with epinephrine in MRI-guided breast biopsies should be questioned[33], as there is also a potential risk of skin necrosis.[34]

In a study by Yoen *et al*.[35], it was observed that lesion location could influence the risk of hemorrhage, with 43% of lesions experiencing hemorrhagic complications located in the lower outer quadrant (P = 0.001). However, our findings did not reveal a significant difference in hemorrhage risk among different quadrants or in the areolar region (P = 0.399).

Additionally, our conclusions find support in the research conducted by van Deventer *et al*.[24], who demonstrated considerable variability in the blood supply pattern of the breast through cadav-

eric dissections. The independent predictors identified for relatively larger hematomas, including younger age (P = 0.02), larger relative LN distances (P = 0.001), and access path length (P = 0.001), may indirectly reflect the anatomical distribution and characteristics of the perforator network relevant to our study. These perforators typically exhibit a larger diameter and closer proximity to each other in the peripheral regions of the breast near the chest wall.[24] They radiate towards the nipple and diminish in size peripherally, consistent with their nomenclature. Consequently, hypervascular zones have been delineated by Palmer and Taylor.[24,36] Notably, advancing age is associated with a significant risk factor for complications in perforator-pedicled propeller flap procedures in the lower extremities, particularly beyond 60 years or in the presence of known arteriopathy such as diabetes. Consequently, age-related impairments in perforator function may elucidate the significantly higher frequency of relatively larger hematomas observed in younger patients (P = 0.002). This phenomenon warrants further investigation, such as exploring MRI-guided biopsies and their complications in the context of recognized arteriopathy, which could yield valuable insights. Additionally, it may be worthwhile to investigate the antero-posterior approach, which is technically feasible today, and compare it to the commonly used latero-medial approach in upright tomosynthesis-guided breast biopsies *e.g.*[37] In conjunction with the hypervascular model of the breast proposed by Palmer and Taylor[37], our findings underscore potential implications regarding the risk of hemorrhage.

Our study possesses several limitations that warrant acknowledgment. Firstly, it was conducted as a retrospective analysis within a single center, resulting in a relatively limited number of cases. Secondly, the classification distinguishing between relatively smaller and larger hematomas relied on the average of our hematoma results, which may not be universally applicable and could vary in larger cohorts. Thirdly, due to the inadequate number of events in the smallest outcome categories, we were unable to incorporate all investigated variables into the multivariable logistic regression analysis. Lastly, certain variables, such as operator skill, which may influence procedural outcomes, were not evaluated in this study, presenting an area for potential investigation in future research endeavours. However, we believe that the guided approach is likely to significantly reduce the impact of operator skill on procedural outcomes, making any differences minimal or negligible.

Conclusions

Our findings underscore the importance of strategic procedural planning to minimize hematoma occurrence and enhance patient safety during MRI-guided breast biopsy procedures. Understanding these factors can lead to customized approaches to improve patient outcomes and procedural efficacy.

References

1. Berg WA, Zhang Z, Lehrer D, Jong RA, Pisano ED, Barr RG, et al. Detection of breast cancer with addition of annual screening ultrasound or a single screening MRI to mammography in women with elevated breast cancer risk. *JAMA* 2012; **307:** 1394-404. doi: 10.1001/jama.2012.388
2. Kuhl C, Weigel S, Schrading S, Arand B, Bieling H, König R, et al. Prospective multicenter cohort study to refine management recommendations for women at elevated familial risk of breast cancer: the EVA trial. *J Clin Oncol* 2010; **28:** 1450-7. doi: 10.1200/JCO.2009.23.0839
3. La Yun B, Kim SM, Jang M, Cho N, Moon WK, Kim HH. Breast magnetic resonance imaging-guided biopsy. *J Korean Soc Radiol* 2016; **74:** 351-60. doi: 10.3348/jksr.2016.74.6.351
4. Zebic-Sinkovec M, Kadivec M, Podobnik G, Skof E, Snoj M. Mammographycally occult high grade ductal carcinoma (DCIS) as second primary breast cancer, detected with MRI: a case report. *Radiol Oncol* 2010; **44:** 228-31. doi: 10.2478/v10019-010-0033-9
5. Morris EA, Schwartz LH, Dershaw DD, Van Zee K, Abramson AF, Liberman L. MR imaging of the breast in patients with occult primary breast carcinoma. *Radiology* 1997; **205:** 437-40. doi: 10.1148/radiology.205.2.9356625
6. Mann RM, Kuhl CK, Kinkel K, Boetes C. Breast MRI: Guidelines from the European Society of Breast Imaging. *Eur Radiol* 2008; **18:** 1307-18. doi: 10.1007/s00330-008-0863-7
7. Meucci R, Pistolese Chiara A, Perretta T, Vanni G, Portarena I, Manenti G, et al. MR imaging-guided vacuum assisted breast biopsy: radiological-pathological correlation and underestimation rate in pre-surgical assessment. *Eur J Radiol Open* 2020; **7:** 100244. doi: 10.1016/j.ejro.2020.100244
8. Saslow D, Boetes C, Burke W, Harms S, Leach MO, Lehman CD, et al. American Cancer Society guidelines for breast screening with MRI as an adjunct to mammography. *CA Cancer J Clin* 2007; **57:** 75-89. doi: 10.3322/canjclin.57.2.75
9. Hoorntje LE, Peeters PH, Mali WTM, Rinkes IB. Vacuum-assisted breast biopsy: a critical review. *Eur J Cancer* 2003; **39:** 1676-83. doi: 10.1016/s0959-8049(03)00421-0
10. Borstnar S, Bozovic-Spasojevic I, Cvetanovic A, Plavetic ND, Konsoulova A, Matos E, et al. Advancing HER2-low breast cancer management: enhancing diagnosis and treatment strategies. *Radiol Oncol* 2024; **58:** 258-67. doi: 10.2478/raon-2024-0030
11. Zebic-Sinkovec M, Hertl K, Kadivec M, Cavlek M, Podobnik G, Snoj M. Outcome of MRI-guided vacuum-assisted breast biopsy–initial experience at Institute of Oncology Ljubljana, Slovenia. *Radiol Oncol* 2012; **46:** 97-105. doi: 10.2478/v10019-012-0016-0
12. Brönnimann MP, Christe A, Heverhagen JT, Gebauer B, Auer TA, Schnapauff D, et al. Pneumothorax risk reduction during CT-guided lung biopsy–Effect of fluid application to the pleura before lung puncture and the gravitational effect of pleural pressure. *Eur J Radiol* 2024; 111529. doi: 10.1016/j.ejrad.2024.111529
13. Heywang-Köbrunner SH, Sinnatamby R, Lebeau A, Lebrecht A, Britton PD, Schreer I, et al. Interdisciplinary consensus on the uses and technique of MR-guided vacuum-assisted breast biopsy (VAB): results of a European consensus meeting. *Eur J Radiol* 2009; **72:** 289-94. doi: 10.1016/j.ejrad.2008.07.010
14. Ancona A, Caiffa L, Fazio V. [Digital stereotactic breast microbiopsy with the mammotome: study of 122 cases]. [Italian]. *Radiol Med* 2001; **101:** 341-7. PMID: 11438785

15. *Needles and biopsy probes*. Dershaw DD, editor. Imaging-guided interventional breast techniques. New York: Springer; 2003. p. 69-86.

16. Gebauer B, Bostanjoglo M, Moesta K, Schneider W, Schlag P, Felix R. Magnetic resonance-guided biopsy of suspicious breast lesions with a handheld vacuum biopsy device. *Acta Radiol* 2006; **47:** 907-13. doi: 10.1080/02841850600892928

17. Melotti MK, Berg WA. Core needle breast biopsy in patients undergoing anticoagulation therapy: preliminary results. *AJR Am J Roentgenol* 2000; **174:** 245-9. doi: 10.2214/ajr.174.1.1740245

18. Weikel W, Hofmann M, Steiner E, Bohrer M, Layer G. Stereotactic vacuum-assisted breast biopsy-analysis of 166 cases. *Zentralbl Gynakol* 2004; **126:** 87-92. doi: 10.1055/s-2004-818774

19. Zagouri F, Gounaris A, Liakou P, Chrysikos D, Flessas I, Bletsa G, et al. Vacuum-assisted breast biopsy: more cores, more hematomas? *In Vivo* 2011; **25:** 703-5. PMID: 21709018

20. Brönnimann MP, Tarca M, Segger L, Kulagowska J, Florian N. Fleckenstein FN, et al. Comparative Analysis of CT Fluoroscopy Modes and Gastropexy Techniques in CT-Guided Percutaneous Radiologic Gastrostomy. *Tomography* 2024; **10:** 1754-66. doi: 10.3390/tomography10110129

21. Somerville P, Seifert PJ, Destounis SV, Murphy PF, Young W. Anticoagulation and bleeding risk after core needle biopsy. *AJR Am J Roentgenol* 2008; **191:** 1194-7. doi: 10.2214/AJR.07.3537

22. Bhat SM. *SRB's surgical operations: text & atlas*. 2nd edition. New Delhi: Jaypee Brothers Medical Publishers (P) Ltd; 2017.

23. Rivard AB, Galarza-Paez L, Peterson DC. *Anatomy, thorax, breast*. Treasure Island (FL): StatPearls Publishing; 2024. PMID: 30137859

24. van Deventer PV. The blood supply to the nipple-areola complex of the human mammary gland. *Aesthetic Plast Surg* 2004; **28:** 393-8. doi: 10.1007/s00266-003-7113-9

25. Boudreau N, Myers C. Breast cancer-induced angiogenesis: multiple mechanisms and the role of the microenvironment. *Breast Cancer Res* 2003; **5:** 1-7. doi: 10.1186/bcr589

26. Heller SL, Moy L. Imaging features and management of high-risk lesions on contrast-enhanced dynamic breast MRI. *AJR Am J Roentgenol* 2012; **198:** 249-55. doi: 10.2214/AJR.11.7610

27. Cohen J. Quantitative methods in psychology: A power primer. *Psychol Bull* 1992; **112:** 155-9. doi: 10.1037//0033-2909.112.1.155

28. Kettritz U, Rotter K, Schreer I, Murauer M, Schulz-Wendtland R, Peter D, et al. Stereotactic vacuum-assisted breast biopsy in 2874 patients: a multicenter study. *Cancer* 2004; **100:** 245-51. doi: 10.1002/cncr.11887

29. Perlet C, Heinig A, Prat X, Casselman J, Baath L, Sittek H, et al. Multicenter study for the evaluation of a dedicated biopsy device for MR-guided vacuum biopsy of the breast. *Eur Radiol* 2002; **12:** 1463-70. doi: 10.1007/s00330-002-1376-4

30. Brönnimann MP, Kulagowska J, Gebauer B, Auer TA, Collettini F, Schnapauff D, et al. Fluoroscopic-guided *vs.* multislice computed tomography (CT) biopsy mode-guided percutaneous radiologic gastrostomy (prg) – comparison of interventional parameters and billing. *Diagnostics* 2024; **14:** 1662. doi: 10.3390/diagnostics14151662

31. Fausto A, Fanizzi A, Volterrani L, Mazzei FG, Calabrese C, Casella D, et al. Feasibility, image quality and clinical evaluation of contrast-enhanced breast MRI performed in a supine position compared to the standard prone position. *Cancers* 2020; **12:** 2364. doi: 10.3390/cancers12092364

32. McGrath AL, Price ER, Eby PR, Rahbar H. MRI-guided breast interventions. *J Magn Reson Imaging* 2017; **46:** 631-45. doi: 10.1002/jmri.25738

33. Flowers CI. Breast biopsy: anesthesia, bleeding prevention, representative sampling, and rad/path concordance. *Applied Radiology* 2012; **41:** 9-14.

34. Hartzell TL, Sangji NF, Hertl MC. Ischemia of postmastectomy skin after infiltration of local anesthetic with epinephrine: a case report and review of the literature. *Aesthetic Plast Surg* 2010; **34:** 782-4. doi: 10.1007/s00266-010-9528-4

35. Yoen H, Chung HA, Lee SM, Kim ES, Moon WK, Ha SM. Hemorrhagic complications following ultrasound-guided breast biopsy: A prospective patient-centered study. *Korean J Radiol* 2024; **25:** 157. doi: 10.3348/kjr.2023.0874

36. Palmer JH, Taylor GI. The vascular territories of the anterior chest wall. *Br J Plast Surg* 1986; **39:** 287-99. doi: 10.1016/0007-1226(86)90037-8

37. Vijapura CA, Wahab RA, Thakore AG, Mahoney MC. Upright tomosynthesis-guided breast biopsy: Tips, tricks, and troubleshooting. *Radiographics* 2021; **41:** 1265-82. doi: 10.1148/rg.2021210017

research article

Comparison of selective intra-arterial to standard intravenous administration in percutaneous electrochemotherapy (pECT) for liver tumors

Tim Wilke[1], Erschad Hussain[2], Hannah Spallek[3], Francesca de Terlizzi[4], Lluis M Mir[5], Peter Bischoff[6], Andreas Schäfer[6], Elke Bartmuß[6], Matteo Cadossi[4], Alessandro Zanasi[4], Michael Pinkawa[7], Attila Kovács[6]

[1] Departement of Gastroenterology, Sinzig Medical Care Center, Linz/Rhein, Germany
[2] Campus Lübeck, University Schleswig-Holstein, Lübeck, Germany
[3] Clinic for Gynaecology and Obstetrics, University Hospital Mannheim, Mannheim, Germany
[4] IGEA Clinical Biophysics, Laboratory Carpi, Modena, Italy
[5] METSY UMR 9018, Université Paris-Saclay, CNRS, Gustave Roussy, Villejuif, France
[6] Clinic for Diagnostic and Interventional Radiology and Neuroradiology, WEGE Klinik, Bonn, Germany
[7] Clinic for Radiotherapy and Radiation Oncology, WEGE Klinik, Bonn, Germany

Radiol Oncol 2025; 59(1): 100-109.

Received 23 January 2025
Accepted 4 February 2025

Correspondence to: Prof. Dr. Attila Kovács, Clinic for Diagnostic and Interventional Radiology and Neuroradiology, WEGE Klinik, Villenstr. 8, 53129 Bonn, Germany. E-mail: Attila.Kovacs@wegeklinik.com

Disclosure: No potential conflicts of interest were disclosed.

Background. Electrochemotherapy (ECT) is a local nonsurgical effective tumor treatment in the hand of the clinician for the treatment of patients with liver tumors or metastases. The study aimed to test the technical feasibility and safety of intra-arterial (i.a.) bleomycin administration compared to the established intravenous (i.v.) administration in percutaneous electrochemotherapy (pECT). Furthermore, the equivalence hypothesis was tested between the 2 modalities in terms of local short-term response and progression-free survival.

Patients and methods. Forty-four patients have been recruited and treated by pECT for hepatocellular carcinoma, cholangiocarcinoma and liver metastatic lesions from cancers of different origin: 18 were treated with standard i.v., 26 with bleomycin i.a. administration.

Results. The 2 groups were similar for anagraphic and anamnestic data, as well as for most relevant disease specific characteristics. Technical success of the treatment was obtained in 95% and 100% of patients in i.v. and i.a. groups respectively. Short-term local response was similar in the 2 groups with a slightly higher complete remission (CR) rate in the i.a. group. There were 61.9% CR, 23.8% partial remission (PR), 4.8% stable disease (SD) in the i.v. group, and 80.6%, CR 12.9% PR, 3.2% PD (p = 0.3454). One-year progression free survival was 60% (C.I. 33%–88%) in the i.v. group and 67% (C.I. 42%–91%) in the i.a. group (p = 0.5849).

Conclusions. The results of this study confirmed the safety and feasibility of super-selective i.a. bleomycin administration. Analysis of local response and progression free survival confirmed the equivalence hypothesis of the new modality compared to standard i.v. administration in the treatment of primary and secondary liver malignancies by pECT.

Key words: electrochemotherapy; percutaneous ECT; liver metastasis; liver cancer; intra-arterial administration; bleomycin

Introduction

Electrochemotherapy (ECT) is a local treatment that utilizes electric pulses application to deliver poorly permeant drugs, such as bleomycin and cisplatin, to cells by increasing permeability of the cell membrane.[1,2] Over the past 20 years, ECT proved to be effective in the treatment of cutaneous, subcutaneous, mucosal, or deep-seated tumors of various histologies and in different body sites.[3-5]

Since the results of the international, multicentre clinical study European Standard Operating Procedures for Electrochemotherapy (ESOPE) were published and were used to establish the Standard Operating Procedures for ECT on cutaneous tumors with the Cliniporator™ device (IGEA S.p.A., Carpi, Italy), a notable number of preclinical and clinical studies have been conducted on ECT by an European working-group of clinicians to confirm its safety and effectiveness on cutaneous tumors, such as malignant melanoma[6,7], breast cancer[8,9], basal cell carcinoma[10], squamous cell carcinoma[11] and others.[3,12,13] Based on these experiences, ECT application was extended and had been shown indeed to be feasible, safe, and effective for deep-seated tumors, such as liver, pancreatic and bone tumors and metastases.[14-19]

In particular, in liver malignancies, either primary or secondary, ECT can be used near collagenous structures such as vessels and bile ducts[20], it is repeatable and also suitable as a local therapy between chemotherapy cycles. Indeed, non-surgical interventional local tumor treatments are currently an additional option for the treatment of cancer patients and The European Society of Medical Oncology (ESMO) included local therapies in the current consensus guidelines on the treatment of metastatic colorectal cancer (mCRC).[21]

Local treatments for the management of liver malignant lesions can be divided into thermal (radiofrequency or microwave ablation and cryoablation) and nonthermal treatments (high precision radiotherapy, brachytherapy, irreversible electroporation and ECT).[14,19] All these treatments are ablative. Moreover, ECT is a method to vectorize the chemotherapy, being therefore highly selectively against the tumor cells whilst preserving the normal cells.

The choice of the therapy for each single case is determined by the number, size, configuration and location or environment of the target lesion. Contrary to Irreversible Electroporation (one supplementary ablative technique), ECT is also a selective approach for the vectorization of cytotoxic drugs and has gained a role in the armamentarium of local therapies available to the clinicians, enabling the treatment of i) lesions that are too large for thermal ablation, ii) non-radiosensitive tumors or iii) lesions located in the immediate vicinity of radiation- or temperature-vulnerable organs.[14] Specifically, ECT can be used in the treatment of liver lesions located centrally, close to the capsule or in proximity of the major vessels and bile ducts, which may neither be resectable nor suitable for radiofrequency or microwave ablation. The safety of ECT in the treatment of lesions located near large liver vessels was also proven in animal models.[22,23] Good tolerance, with few side effects and no relevant pain, nausea or systemic side effects were also observed.[24-26]

Conventional percutaneous ECT (pECT) in the liver is performed with intravenous (i.v.) administration of bleomycin following the Standard Operating Procedures for ECT in cutaneous and subcutaneous lesions.[27,28]

A novel procedure for the administration of bleomycin in the liver has been introduced, based on the already established liver-directed endovascular therapies, hepatic artery infusion (HAI) and transarterial chemoembolization (TACE): the selective delivery of bleomycin intra-arterially to the lesion area to be treated. The vessels supplying the lesion are accessed from the groin via a guiding catheter and a coaxially used microcatheter. The complete volume coverage of the entire lesion is ensured by contrast-enhanced Cone-Beam Computed Tomography (CBCT) scan. In this way bleomycin is directly delivered selectively into the lesion with higher concentration in loco. Since selective and superselective chemotherapy applications are already well established in interventional oncology, the aim of this work is to translate this established approach in the ECT setting. We aimed to test the technical feasibility and safety of this approach and to demonstrate the equivalence of intra-arterial (i.a.) bleomycin administration compared to the established i.v. administration.

In this study, the new method of administration is fully described and named "the intra-arterial pECT method".

Patients and methods

Patients

Forty-four patients have been recruited and treated by ECT in our centre for hepatocellular carcinoma, cholangiocarcinoma and liver metastatic lesions

from cancers of different origin: colorectal cancer, breast cancer, ovarian cancer, anal cancer, non-small cell lung cancer (NSCLC), pancreatic cancer, parotid carcinoma, neuroendocrine carcinoma, uterus carcinoma, cancer of unknown primary origin (CUP) and oesophageal carcinoma. Eighteen patients were treated with conventional intravenous administration of bleomycin (i.v. group), whilst twenty-six were treated using intra-arterial administration of the same drug (i.a. group). ECT treatments were performed between June 2018 and June 2024. The study was conducted according to the WMA Declaration of Helsinki – Ethical Principles for Medical Research Involving Human Subjects. All patients signed an informed consent form and agreed to be included in the data collection. The study was approved by the Committee for Medical Ethics of the Institution (*Ethik Kommission der Ärztekammer Nordrhein* Nr 2022314).

Imaging

Standard pretreatment evaluation of patients was performed including MRI (magnetic resonance imaging) with hepatospecific contrast agent and thorax plus abdomen CT (computed tomography), including also the pelvis, not more than 30 days before treatment. Details on MRI are reported in Spallek *et al*.[14]

Electrochemotherapy with conventional intravenous bleomycin administration

Software-based treatment planning for the correct positioning of the electrodes was performed on MRI preoperative images. The aim of the treatment planning is to obtain the electric field optimal coverage of the target lesions by including them within the needle geometry. A maximum of 6 electrodes can be activated synchronously by the pulse generator, but various spatial domains can be treated during the same session with the use of more than 6 electrodes. The needle electrodes were percutaneously inserted in and around the lesions following multimodal image guidance and stereotactic navigation, at a minimum/maximum distance of 0.5/3.0 cm one from the other. Needle electrodes have a diameter of 1.2 mm and a 16 to 24 mm length, with an active part of 3 or 4 cm long (IGEA®, Carpi, Italy). They are freely positionable and must be inserted in parallel, to ensure the correct delivery of the electric field. The direction of access of the electrodes was determined by the performing surgeon.

Once positioned, the electrodes were supplied by a suitable voltage to deliver sequential electric pulses. The goal is to ensure complete coverage of the clinical target volume with an electric field intensity above 400 V/cm and to maintain the maximum current delivered below 50A. The electric pulses were delivered by the CliniporatorTM device (IGEA®, Carpi, Italy).

When administering bleomycin intravenously, the same treatment protocol as defined by the SOP for ECT of cutaneous tumors was adopted[27,28] with regard to drug administration, dose, and electrical parameters (i.e. pulse duration and number of pulses). After having correctly positioned the electrodes, under general anesthesia, the patients were given bleomycin at a dose of 15.000 IU/m^2 body surface intravenously in bolus within 30 seconds. Eight minutes after the bleomycin administration the maximal pharmacological peak of bleomycin in the organs is expected and it is possible to start the electroporation process in liver, delivering 8 pulses of 100 μs duration between each pair of electrodes. Pulses delivery should be completed within 40 minutes.

Care was also taken to ensure that the electrical pulses were delivered only in the refractory phase of the heart by synchronizing of the Cliniporator device with the ECG (electrocardiogram) to avoid interferences with the heart rhythm.

Electrochemotherapy with intra-arterial bleomycin administration

After a local anesthesia, retrograde puncture of the right common femoral artery and insertion of a 4F sheath system were performed. The vessels supplying the tumor were probed super-selectively using a guiding microcatheter (Sidewinder 4F, Terumo®) and microcatheter (Persue 2.0 Swan Neck, Merit®) in coaxial technique. The complete volume coverage of the entire tumor was assessed in CBCT, simulating the subsequent bleomycin distribution. The microcatheter was then secured in position and the patient was transferred to the interventional CT. In the CT, the target lesion was visualized by a super-selective contrast via the microcatheter (10 cc of pure CT-contrast, followed by 10 cc saline each 1 cc/sec) and this volume data set was used for navigation. The electrodes were positioned under general anesthesia using multimodal image guidance and stereotactic navigation (CAS One, Cascination®), with the same precautions adopted for the i.v. approach. A second i.a. contrast after electrode-placement was applied to

confirm adequate coverage of the lesion, including safety margins. As soon as the electrodes were correctly positioned, 50% of the total bleomycin volume (total bleomycin dose: 15000 IU/m2 body surface) was administered intra-arterially via the microcatheter in a continuous injection. When about 50% of drug was infused, the electric pulses delivery started and during the electric pulses' delivery, the remaining 50% of the bleomycin continued to be administered intra-arterially. The injection of 100% bleomycin before electric pulses' delivery was discarded because, due to the first pass effect, there is a risk that a relevant part of the drug has passed through the tumor, making it unavailable for electroporation. After the electric pulses' delivery, a CT scan was performed to rule out therapy-associated complications. After successful electric pulses delivery, the electrodes, catheter and sheath were removed, and the puncture site was manually compressed followed by the subsequent removal of the electrodes and the application of a sterile plaster dressing. The catheter and sheath material were then removed, followed by fifteen minutes of manual compression of the puncture site until hemostasis was achieved. Then, application of a sterile plaster bandage and a pressure bandage were applied. Further standard procedures were adopted: patient monitoring, laboratory checks and post-interventional imaging according to ward protocol.

Response to treatment evaluation

Response to treatment was evaluated based on the multiparametric MRI of the liver, including multiplanar ce T1w, transversal T2w fs and transversal DWI scans at 1 to 3 months follow-up. Lesion-based treatment success was assessed using the Modified Response Evaluation Criteria in Solid Tumours (mRECIST) in terms of complete remission (CR), partial remission (PR), stable disease (SD), and progressive disease (PD). Local tumor control was defined as CR, PR or SD according to the RECIST criteria, version 1.1.[29] Objective response is obtained by the sum of CR and PR.

Statistical analysis

Continuous variables are reported as the mean and standard deviation, median and range. Categorical variables are expressed as absolute numbers and percentages. Comparisons between the two groups were performed by heteroschedastic 2 tails Student t-test for continuous variables and contingency tables with Chi square calculation for categorical variables. Progression free survival time was calculated in months as the time since ECT session date to last follow-up (in case of no progression) or to the date of progression. Progression free survival analysis was conducted by means of calculation of Kaplan Meier survival curves and logrank test for comparison between groups. A p value lower than 0.05 is considered statistically significant. Statistical analysis was performed with NCSS 9 (NCSS 9 Statistical Software [2013]).

Results

Patients were enrolled and treated in the period between June 2018 and June 2024 and were followed for a median time of 7 months (range 1–27; mean 7.8 ± 5.9 months). They were divided into two groups based on conventional intravenous or intra-arterial administration of bleomycin; 18 patients were treated with conventional i.v. and 26 with i.a. administration of chemotherapy drug.

Mean age in the two groups was similar (63 ± 11 yrs, median 64 range 41–83 in the i.v. group vs 68 ± 10 yrs, median 69 range 52–93 in the i.a. group, p = 0.2182). The two groups were similar for almost all characteristics reported in Table 1.

In total 21 lesions were treated in the i.v. group, and 31 in the i.a. group. Lesions' size was significantly larger in the i.v. group, with a mean LA (long axis) size of 5.9 ± 2.5 cm (median 4.6 cm, range 1.5–11.2), with respect to i.a. group, with a mean LA size of 4.4 ± 2.2 (median 4.0 cm, range 1.1–9.7) (p = 0.0300). Volume mean values on the other hand show only a slight not significant difference: 130 ± 137 cm^3 in the i.v. group vs 61.4 ± 81.4 cm^3 (p = 0.0501). Characteristics of the target lesions are listed in Table 2. Mean number of electrodes used in the i.v. group is 5.5 ± 1.4 (median 6, range 2–8) and in the i.a. group it is 5.0 ± 1.0 (median 5, range 3–6), values not significantly different (p = 0.1380).

Safety/toxicity

Side effects observed in both groups were only mild or moderate, such as mild pain at the treated site, C-reactive protein (CRP) elevation and leucocytosis, or haemoglobin drop. All side effects were successfully treated with appropriate medical treatments and disappeared within 10 days from occurrence. No differences were observed in the two groups with respect to onset of side effects.

TABLE 1. Descriptive characteristics of the patients in the 2 groups

PATIENTS	i.v. pECT (N = 18)		i.a. pECT (n = 26)		P value
	N	%	N	%	
Gender					0.5406
Males	8	44%	15	58%	
Females	10	56%	11	42%	
Diagnosis					
Colorectal cancer	7	39%	10	38%	0.4620
Breast cancer	4	22%	4	15%	
Hepato cellular carcinoma	2	11%	2	8%	
Cholangio cellular carcinoma	0	0%	3	12%	
Ovarian cancer	2	11%	0	0%	
Non-small cell lung cancer (NSCLC)	1	6%	2	8%	
Anal cancer	1	6%	0	0%	
Pancreatic cancer	0	0%	1	4%	
Parotis carcinoma	0	0%	1	4%	
Neuroendocrine carcinoma	0	0%	1	4%	
Uterus carcinoma	0	0%	1	4%	
Esophageal carcinoma	0	0%	1	4%	
Cancer of unknown primary origin (CUP)	1	6%	0	0%	
Liver metastases					
Synchronous	8	44%	16	62%	0.5343
Metachronous	8	44%	8	31%	
No	2	11%	2	7%	
Metastases location other than liver					
None	9	50%	17	65%	0.3613
Yes	9	50%	9	35%	
Other metastasis' location					
Lung	3	17%	3	12%	0.6025
Bone	1	6%	2	8%	
Kidney	1	6%	1	4%	
Lung + bone + brain	1	6%	0	0%	
Bone + peritoneum	1	6%	0	0%	
Pleural + bone	1	6%	0	0%	
Retroperineal	1	6%	0	0%	
Adrenal gland	0	0%	1	4%	
Lymphnode	0	0%	1	4%	
Bone + lymphnode	0	0%	1	4%	
Previous treatments					
Systemic therapy	16	89%	26	100%	0.1617
Liver surgery	4	22%	12	46%	0.1251
Local treatments	11	61%	8	31%	0.0657
Type of local treatments					
TACE	8	43%	4	15%	0.1529
TACE+RFA	1	6%	0	0%	
TACE+CP	1	6%	0	0%	
TACE/MWA/CRYOTH	0	0%	2	8%	
CRYOTH	1	6%	0	0%	
IBT	0	0%	2	8%	
Comorbidities					
Cardiac diseases	6	33%	7	27%	0.7422
Pulmonary diseases	3	17%	7	27%	0.4889
Liver diseases	9	50%	0	0%	<0.0001
Number of target lesions per patient					
1	15	83%	21	81%	1.000
2	3	17%	5	19%	

CP = chemoperfusion; CRYOTH = cryotherapy; IBT = interstitial brachytherapy; i.a. = intra-arterial; i.v. = intravenous; MWA = microwave ablation; pECT = percutaneous electrochemotherapy; RFA = radiofrequency ablation; TACE = hepatic artery chemoembolization

TABLE 2. Characteristics of target lesions in the 2 groups

LESIONS	i.v. pECT (N = 21)		i.a. pEC (N = 31)		P value
	N	%	N	%	
Type					
Hypervascular	2	9.5%	5	16.1%	0.7664
Intermediate	14	66.7%	20	64.5%	
Hypovascular	5	23.8%	6	19.4%	
Challenging location*					
Yes	19	90.5%	21	67.7%	0.0927
No	2	9.5%	10	32.3%	
Vessels or bile ducts surrounding the metastases					
Distant (> 10 mm)	4	19.0%	8	25.8%	0.5389
Close (1 mm to 10 mm)	6	28.6%	5	16.1%	
Adjacent (< 1 mm)	11	52.4%	18	58.1%	
Previous local treatments on the lesion					
Yes	7	33.3%	8	25.8%	0.7559
No	14	66.7%	23	74.2%	
Type of local treatments on the lesion					
TACE (transarterial chemoembolization)	6	28.6%	4	12.9%	0.1474
CP (chemoperfusion)	1	4.8%	0	0.0%	
IBT (interstitial brachytherapy)	0	0.0%	2	6.5%	
TACE/MWA/CRYOTH	0	0.0%	2	6.5%	
Technical success					
Yes	20	95.2%	31	100.0%	0.2199
No	1	4.8%	0	0.0%	

* Challenging location represented in liver were liver dome, vicinity of portal vein main trunk, vicinity of main bile duct

CP = chemoperfusion; CRYOTH = cryotherapy; IBT = interstitial brachytherapy; i.a. = intra-arterial; i.v. = intravenous; MWA = microwave ablation; pECT = percutaneous electrochemotherapy; TACE = hepatic artery chemoembolization

TABLE 3. Response to percutaneous electrochemotherapy (pECT) treatment in the 2 groups

RESPONSE	i.v. pECT (N = 21)		i.a. pECT (N = 31)		P value	P value
	N	%	N	%	Overall distribution	CR *vs.* non CR
CR	13	61.9%	25	80.6%	0.3454	0.1349
PR	5	23.8%	4	12.9%		
SD	1	4.8%	0	0.0%		
PD	0	0.0%	1	3.2%		
Lost to follow up	2	9.5%	1	3.2%		

CR = complete remission; i.a. = intra-arterial; i.v. = intravenous; pECT = percutaneous electrochemotherapy; PR = partial remission; SD = stable disease

Response to treatment

Response to pECT treatment was evaluated for each target lesion within the first 3 months of follow-up and the result for each single group is reported in Table 3. Despite a higher CR rate in the i.a. group, no statistically significant difference has been observed between the groups. Objective response (OR) rate was 85.7% in the i.v. group and 93.5% in the i.a. group (Figure 1).

Progression free survival is shown in Figure 2. No significant difference has been observed between groups (p = 0.5849). One-year progression free survival is 60% (C.I. 33%–88%) in the i.v. group and 67% (C.I. 42%–91%) in the i.a. group.

Discussion

This study assesses the feasibility of intra-arterial administration of bleomycin for pECT of liver tumors. Since selective and super-selective chemotherapy applications are already well established in interventional oncology, such as in TACE, HAI

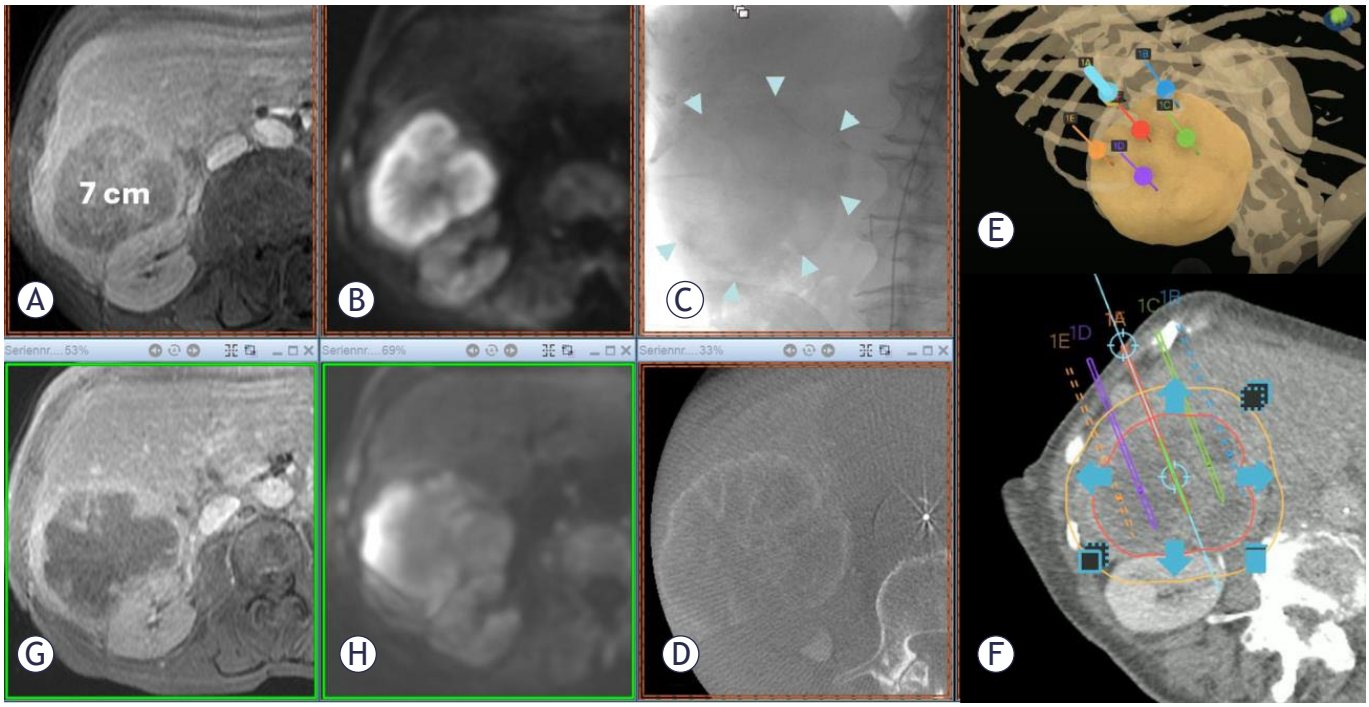

FIGURE 1. (A) Transverse contrast-enhanced T1w MR image of a pancreatic carcinoma metastasis with a maximum diameter of 7 cm in segments V/VI and VII, which no longer responds to systemic chemotherapy and is growing rapidly and progressively. **(B)** Corresponding slice to A in diffusion imaging. **(C)** Complete contrast of the metastasis in 2D angiography. **(D)** Documentation of complete contrast coverage of the metastasis in cone beam CT. **(E).** Stereotactic navigation (CAS-One® IR) of the electrodes for electroporation. **(F).** Parallel planning of the electrodes in the tumor to achieve homogeneous electroporation. **(G).** The transverse contrast-enhanced T1w MR image of the metastasis one month after the electrochemotherapy (ECT) procedure demonstrates the complete loss of perfusion in the entire metastasis. **(H)** Corresponding slice to G in diffusion imaging.

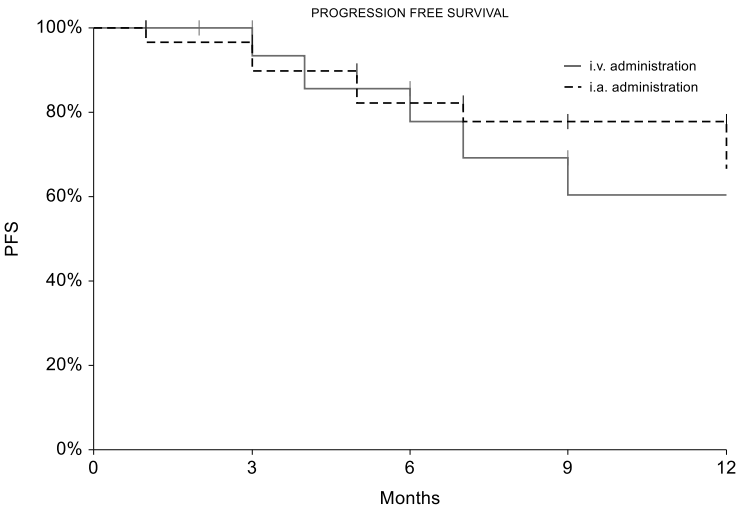

FIGURE 2. Progression free survival in the 2 groups during the 18-month follow-up period.

and IHP (isolated hepatic perfusion)[30,31], the rational was to combine this established approach with pECT. Specifically, the goal of intra-arterial therapies is to inflict lethal insult to tumors by selectively delivering anticancer treatment to its arterial supply. Regional delivery of a drug leads to its increased local concentration; this holds true for drugs demonstrating first-order kinetics (constant clearance) despite the higher dose, potentially leading to an increased response. Moreover, regional drug delivery leads to decreased systemic exposure of that drug, potentially reducing side effects and toxicity.[32] Even in pECT, the administration of the chemotherapy drug only in the tumor-bearing area to be treated, allows a higher concentration of the drug in loco, enabling a first pass effect, with less systemic bleomycin circulating in the body, i.e. decreased risk of side effects and lung toxicity, whilst off-target bleomycin already bearing low toxicity in non electroporated liver parenchyma.

The intra-arterial application of bleomycin in the liver proved to be safe and effective in the treatment of liver haemangiomas, with doses up to 45.000 IU per session[33], as well as in TACE doxorubicin resistant hepatocellular carcinomas.[34] Sporadic reports about the intra-arterial applica-

tion of bleomycin in ECT of other tumor entities can also be found in the literature.[35,36] To the best of our knowledge, this is the first study showing that the intra-arterial administration of bleomycin can be applied to pECT of liver tumors.

Intra-arterial catheter-assisted pECT also allows real-time liver tumor visualization before, during, and after placement of the probes, which may help in: improving tumor conspicuity; guiding needle advancement; verifying probe position relative to the tumor and surrounding structures; evaluation of procedure-related complications and technical success directly after the procedure, all with a significantly reduced contrast dose comparable to venous contrast and therefore reduced risk of compromising renal function.[37-39]

In this cohort study, intra-arterial administration of bleomycin is proposed as a new method of drug delivery in pECT. Here we compared this new method with the standard intravenous systemic administration of bleomycin in patients undergoing pECT for liver lesions of various histological origins. The 2 groups were similar for age, gender, histology distribution, type of metastasis (synchronous, metachronous), metastasis location, previous treatments, and comorbidities, except for surrounding liver disease. A significant difference in LA size of the lesion is observed ($p = 0.0300$), even if when calculated the entire volume of the lesion, the difference is only marginally significant ($p = 0.0501$).

The analysis of complications and side effects reveals that the conventional intravenous and the new intra-arterial methods bring the same risk of complications. Percutaneous ECT is well tolerated by the patients[14,40], no serious adverse events have been observed during procedures and during follow-up; side effects appear to be limited in number and intensity, and when occurred they were successfully treated with appropriate medical treatments and disappeared within 10 days from occurrence.

Short term results indicate a substantial equivalence between i.v. and i.a. administration modality, as non-significant differences were observed in the outcome at 1 to 3 months of follow-up. Complete response rate was 61.9%, partial response 23.8%, stable disease 4.8% and progression 9.5% in the i.v. group. Interestingly, a slightly higher CR rate was observed in the i.a. group, 80.6% with a lower PR rate, 12.9%; this non-significant difference could be ascribed to the relatively smaller target lesions treated with i.a. procedure of bleomycin administration, with a volume of 61.4 ± 81.4 cm^3 with a marginal significance in comparison with the i.v. group. In any case the objective response rate in the 2 groups is 85.7% in the i.v. group and 93.5% in the i.a. group. These data are similar to previous experiences on ECT in the liver: Edhemovic *et al*.[25] conducted a study on intraoperative ECT of colorectal liver metastases and obtained a response rate per patient of 75% (63% CR and 12% PR). In a similar study carried out on intraoperative ECT in hepatocellular carcinoma, Djokic *et al*.[41] obtained a response rate per patient of 95.8% (79.2% CR and 16.6% PR). The complete response rate at 3–6 months was 80% per patient and 88% per treated lesion, with a median size of the treated lesions of 24 mm (range 8–41 mm), slightly smaller than those treated in our study. Considering the studies on ECT of liver performed with percutaneous insertion of the electrodes, the experience of Tarantino *et al*.[42,43] on cholangiocellular carcinoma at hepatic hilum and on portal vein tumor thrombosis at hepatic hilum in patients with hepatocellular carcinoma in cirrhosis is also relevant. Even if few patients were included, they could demonstrate for the first time the feasibility and efficacy of the percutaneous procedure in the liver with intra-arterial administration of bleomycin. No important side effects and a complete response was obtained in 3 out of 5 patients and maintained for at least 18 months. Further authors reported their experiences in pECT of liver tumors[24,44] and more recently Iezzi *et al*. proved the feasibility of performing pECT under analgo-sedation, obtaining 100% OR in 5 patients with liver lesions, reporting neither major nor minor complications.[45]

In our study, the follow-up time ranges from 1 to 30 months, with a median value of 7 months, thus it is not possible to provide a very long time progression free survival evidence, nonetheless the data available show that within the first 12 months of follow-up the progression free survival is similar between the i.v. and i.a. groups ($p = 0.5849$) and this result confirms the hypothesis of equivalence in the local tumor control of i.a. procedure with respect to i.v. pECT standard procedure. This result is very important because it is complemented by several theoretical advantages of i.a. pECT, such as: targeted drug application only in the tumor-bearing area to be treated, higher concentration of bleomycin in loco using the first pass effect, less systemic drug circulating in the body and less side effects, less lung toxicity, better timing of the EP as local infusion is quicker than systemic.

By proving the equivalence of i.a. and i.v. administration, there is also the potential to reduce

the bleomycin dose in the future due to the higher on-site concentration with i.a. administration; this might be the aim of further research.

The present study has some limitations: the relatively small number of patients is mainly due to the feasibility aim of the study, and the short follow-up after treatment, even if feasibility and short-term efficacy have been clearly obtained. With a perspective of collecting more data on patients treated with i.a. pECT in the liver, it will be possible to better define the optimal indications for this new procedure with respect to conventional i.v. pECT, even if some indications can already be suggested: based on our experience, for example, for hypovascularized tumors, which seem to respond less well to i.v. ECT than hypervascularised tumors.

Conclusions

This study demonstrates the equivalence of superselective i.a. bleomycin administration compared to standard i.v. administration in the context of percutaneous electrochemotherapy for primary and secondary liver malignancies and thus opens perspectives for reducing the bleomycin dose and the associated toxicity.

References

1. Glass LF, Jaroszeski M, Gilbert R, Reintgen DS, Heller R. Intralesional bleomycin-mediated electrochemotherapy in 20 patients with basal cell carcinoma. *J Am Acad Dermatol* 1997; **37:** 596-9. doi: 10.1016/S0190-9622(97)70178-6
2. Marty M, Sersa G, Garbay JR, Gehl J, Collins CG, Snoj M, et al. Electrochemotherapy – an easy, highly effective and safe treatment of cutaneous and subcutaneous metastases: results of ESOPE (European Standard Operating Procedures of Electrochemotherapy) study. *Eur J Cancer Suppl* 2006; 4: 3-13. doi: 10.1016/j.ejcsup.2006.08.002
3. Clover AJP, de Terlizzi F, Bertino G, Curatolo P, Odili J, Campana LG, et al. Electrochemotherapy in the treatment of cutaneous malignancy: outcomes and subgroup analysis from the cumulative results from the pan-European International Network for Sharing Practice in Electrochemotherapy database for 2482 lesions in 987 patients (2008–2019). *Eur J Cancer* 2020; **138:** 30-40. doi: 10.1016/j.ejca.2020.06.020
4. Plaschke CC, Bertino G, McCaul JA, Grau JJ, de Bree R, Sersa G, et al. European Research on Electrochemotherapy in Head and Neck Cancer (EURECA) project: results from the treatment of mucosal cancers. *Eur J Cancer* 2017; **87:** 172-81. doi: 10.1016/j.ejca.2017.10.008
5. Bertino G, Sersa G, De Terlizzi F, Occhini A, Plaschke CC, Groselj A, et al. European Research on Electrochemotherapy in Head and Neck Cancer (EURECA) project: results of the treatment of skin cancer. *Eur J Cancer* 2016; **63:** 41-52. doi: 10.1016/j.ejca.2016.05.001
6. Kunte C, Letulé V, Gehl J, Dahlstroem K, Curatolo P, Rotunno R, et al. Electrochemotherapy in the treatment of metastatic malignant melanoma: a prospective cohort study by InspECT. *Br J Dermatol* 2017; **176:** 1475-85. doi: 10.1111/bjd.15340
7. Campana LG, Quaglino P, de Terlizzi F, Mascherini M, Brizio M, Spina R, et al. Health-related quality of life trajectories in melanoma patients after electrochemotherapy: real-world insights from the INSPECT register. *Acad Dermatol Venereol* 2022; 36: 2352-63. doi: 10.1111/jdv.18456
8. Matthiessen LW, Keshtgar M, Curatolo P, Kunte C, Grischke EM, Odili J, et al. Electrochemotherapy for breast cancer – results From the INSPECT database. *Clin Breast Cancer* 2018; 18: e909-17. doi: 10.1016/j.clbc.2018.03.007
9. Di Prata C, Mascherini M, Ross AM, Silvestri B, Kis E, Odili J, et al. Efficacy of electrochemotherapy in breast cancer patients of different receptor status: the INSPECT experience. *Cancers* 2023; **15:** 3116. doi: 10.3390/cancers15123116
10. Bertino G, Muir T, Odili J, Groselj A, Marconato R, Curatolo P, et al. Treatment of basal cell carcinoma with electrochemotherapy: insights from the InspECT registry (2008-2019). *Curr Oncol* 2022; **29:** 5324-37. doi: 10.3390/curroncol29080423
11. Bertino G, Groselj A, Campana LG, Kunte C, Schepler H, Gehl J, et al. Electrochemotherapy for the treatment of cutaneous squamous cell carcinoma: The INSPECT experience (2008-2020). *Front Oncol* 2022;**12:** 951662. doi: 10.3389/fonc.2022.951662
12. Campana LG, Kis E, Bottyán K, Orlando A, De Terlizzi F, Mitsala G, et al. Electrochemotherapy for advanced cutaneous angiosarcoma: a European register-based cohort study from the International Network for Sharing Practices of electrochemotherapy (InspECT). *Int J Surg* 2019; **72:** 34-42. doi: 10.1016/j.ijsu.2019.10.013
13. Sersa G, Mascherini M, Di Prata C, Odili J, de Terlizzi F, McKenzie GAG, et al. Outcomes of older adults aged 90 and over with cutaneous malignancies after electrochemotherapy with bleomycin: a matched cohort analysis from the InspECT registry. *Eur J Surg Oncol* 2021; **47:** 902-12. doi: 10.1016/j.ejso.2020.10.037
14. Spallek H, Bischoff P, Zhou W, de Terlizzi F, Jakob F, Kovàcs A. Percutaneous electrochemotherapy in primary and secondary liver malignancies – local tumor control and impact on overall survival. *Radiol Oncol* 2022; **56:** 102-10. doi: 10.2478/raon-2022-0003
15. Granata V, Fusco R, D'Alessio V, Simonetti I, Grassi F, Silvestro L, et al. Percutanous electrochemotherapy (ECT) in primary and secondary liver malignancies: a systematic review. *Diagnostics* 2023; **13:** 209. doi: 10.3390/diagnostics13020209
16. Tafuto S, von Arx C, De Divitiis C, Tracey Maura C, Palaia R, Albino V, et al. Electrochemotherapy as a new approach on pancreatic cancer and on liver metastases. *Int J Surg* 2015; **21:** S78-82. doi: 10.1016/j.ijsu.2015.04.095
17. Campanacci L, Bianchi G, Cevolani L, Errani C, Ciani G, Facchini G, et al. Operating procedures for electrochemotherapy in bone metastases: results from a multicenter prospective study on 102 patients. *Eur J Surg Oncol* 2021; **47:** 2609-17. doi: 10.1016/j.ejso.2021.05.004
18. Deschamps F, Tselikas L, Yevich S, Bonnet B, Roux C, Kobe A, et al. Electrochemotherapy in radiotherapy-resistant epidural spinal cord compression in metastatic cancer patients. *Eur J Cancer* 2023;**186:** 62-8. doi: 10.1016/j.ejca.2023.03.012
19. Kovács A, Bischoff P, Haddad H, Zhou W, Temming S, Schäfer A, et al. Long-term comparative study on the local tumour control of different ablation technologies in primary and secondary liver malignancies. *J Pers Med* 2022; **12:** 430. doi: 10.3390/jpm12030430
20. Gasljevic G, Edhemovic I, Cemazar M, Brecelj E, Gadzijev EM, Music MM, et al. Histopathological findings in colorectal liver metastases after electrochemotherapy. *PLoS One* 2017; **12:** e0180709. doi: 10.1371/journal.pone.0180709
21. Van Cutsem E, Cervantes A, Adam R, Sobrero A, Van Krieken JH, Aderka D, et al. ESMO consensus guidelines for the management of patients with metastatic colorectal cancer. *Ann Oncol* 2016; **27:** 1386-422. doi: 10.1093/annonc/mdw235
22. Brloznik M, Boc N, Sersa G, Zmuc J, Gasljevic G, Seliskar A, et al. Radiological findings of porcine liver after electrochemotherapy with bleomycin. *Radiol Oncol* 2019; **53:** 415-26. doi: 10.2478/raon-2019-0049
23. Zmuc J, Gasljevic G, Sersa G, Edhemovic I, Boc N, Seliskar A, et al. Large liver blood vessels and bile ducts are not damaged by electrochemotherapy with bleomycin in pigs. *Sci Rep* 2019; **9:** 3649. doi: 10.1038/s41598-019-40395-y

24. Cornelis FH, Korenbaum C, Ben Ammar M, Tavolaro S, Nouri-Neuville M, Lotz JP. Multimodal image-guided electrochemotherapy of unresectable liver metastasis from renal cell cancer. *Diagn Interv Imaging* 2019; **100:** 309-11. doi: 10.1016/j.diii.2019.01.001

25. Edhemovic I, Brecelj E, Cemazar M, Boc N, Trotovsek B, Djokic M, et al. Intraoperative electrochemotherapy of colorectal liver metastases: a prospective phase II study. *Eur J Surg Oncol* 2020; **46:** 1628-33. doi: 10.1016/j.ejso.2020.04.037

26. Mali B, Gorjup V, Edhemovic I, Brecelj E, Cemazar M, Sersa G, et al. Electrochemotherapy of colorectal liver metastases – an observational study of its effects on the electrocardiogram. *BioMed Eng OnLine* 2015; **14(Suppl 3):** S5. doi: 10.1186/1475-925X-14-S3-S5

27. Mir LM, Gehl J, Sersa G, Collins CG, Garbay JR, Billard V, et al. Standard operating procedures of the electrochemotherapy: instructions for the use of bleomycin or cisplatin administered either systemically or locally and electric pulses delivered by the CliniporatorTM by means of invasive or non-invasive electrodes. *Eur J Cancer Suppl* 2006; **4:** 14-25. doi: 10.1016/j.ejcsup.2006.08.003

28. Gehl J, Sersa G, Matthiessen LW, Muir T, Soden D, Occhini A, et al. Updated standard operating procedures for electrochemotherapy of cutaneous tumours and skin metastases. *Acta Oncologica* 2018; **57:** 874-82. doi: 10.1080/0284186X.2018.1454602

29. Eisenhauer EA, Therasse P, Bogaerts J, Schwartz LH, Sargent D, Ford R, et al. New response evaluation criteria in solid tumours: Revised RECIST guideline (version 1.1). *Eur J Cancer* 2009; **45:** 228-47. doi: 10.1016/j.ejca.2008.10.026

30. Dudeck O, Ricke J. Advances in regional chemotherapy of the liver. *Expert Opin Drug Deliv* 2011; **8:** 1057-69. doi: 10.1517/17425247.2011.574125

31. De Baere T, Ronot M, Chung JW, Golfieri R, Kloeckner R, Park J-W, et al. Initiative on Superselective Conventional Transarterial Chemoembolization Results (INSPIRE). *Cardiovasc Intervent Radiol* 2022; **45:** 1430-40. doi: 10.1007/s00270-022-03233-9

32. Lewandowski RJ, Geschwind JF, Liapi E, Salem R. Transcatheter intraarterial therapies: rationale and overview. *Radiology* 2011; **259:** 641-57. doi: 10.1148/radiol.11081489

33. Akhlaghpoor S, Torkian P, Golzarian J. Transarterial bleomycin-lipiodol embolization (B/LE) for symptomatic giant hepatic hemangioma. *Cardiovasc Intervent Radiol* 2018; **41:** 1674-82. doi: 10.1007/s00270-018-2010-4

34. Fu J, Wang Y, Zhang J, Yuan K, Yan J, Yuan B, et al. The safety and efficacy of transarterial chemoembolisation with bleomycin for hepatocellular carcinoma unresponsive to doxorubicin: a prospective single-centre study. *Clin Radiol* 2021; **76:** 864.e7-864.e12. doi: 10.1016/j.crad.2021.07.013

35. Shimizu T, Nikaido T, Gomyo H, Yoshimura Y, Horiuchi A, Isobe K, et al. Electrochemotherapy for digital chondrosarcoma. *J Orthop Sci* 2003; **8:** 248-51. doi: 10.1007/s007760300043

36. Domenge C, Orlowski S, Luboinski B, Baere TD, Schwaab G, Belehradek J, et al. Antitumor electrochemotherapy: new advances in the clinical protocol. *Cancer* 1996; **77:** 956-63. doi: 10.1002/(SICI)1097-0142(19960301)77:5<956::AID-CNCR23>3.0.CO;2-1

37. Van Tilborg AAJM, Scheffer HJ, Van Der Meijs BB, Van Werkum MH, Melenhorst MCAM, Van Den Tol PM, et al. Transcatheter CT hepatic arteriography-guided percutaneous ablation to treat ablation site recurrences of colorectal liver etastases: the incomplete ring sign. *J Vasc Interv Radiol* 2015; **26:** 583-7.e1. doi: 10.1016/j.jvir.2014.12.023

38. Puijk RS, Nieuwenhuizen S, Van Den Bemd BAT, Ruarus AH, Geboers B, Vroomen LGPH, et al. Transcatheter CT hepatic arteriography compared with conventional CT fluoroscopy guidance in percutaneous thermal ablation to treat colorectal liver metastases: A single-center comparative analysis of 2 historical cohorts. *J Vasc Intervent Radiol* 2020; **31:** 1772-83. doi: 10.1016/j.jvir.2020.05.011

39. Puijk RS, Dijkstra M, Van Der Lei S, Schulz HH, Vos DJW, Timmer FEF, et al. The added value of transcatheter CT hepatic angiography (CTHA) image guidance in percutaneous thermal liver ablation: an experts' opinion pictorial essay. *Cancers* 2024;**16:** 1193. doi: 10.3390/cancers16061193

40. Djokic M, Dezman R, Cemazar M, Stabuc M, Petric M, Smid LM, et al. Percutaneous image guided electrochemotherapy of hepatocellular carcinoma: technological advancement. *Radiol Oncol* 2020; **54:** 347-52. doi: 10.2478/raon-2020-0038

41. Djokic M, Cemazar M, Popovic P, Kos B, Dezman R, Bosnjak M, et al. Electrochemotherapy as treatment option for hepatocellular carcinoma, a prospective pilot study. *Eur J Surg Oncol* 2018; **44:** 651-7. doi: 10.1016/j.ejso.2018.01.090

42. Tarantino L, Busto G, Nasto A, Fristachi R, Cacace L, Talamo M, et al. Percutaneous electrochemotherapy in the treatment of portal vein tumor thrombosis at hepatic hilum in patients with hepatocellular carcinoma in cirrhosis: a feasibility study. *World J Gastroenterol* 2017; **23:** 906. doi: 10.3748/wjg.v23.i5.906

43. Tarantino L, Busto G, Nasto A, Nasto RA, Tarantino P, Fristachi R, et al. Electrochemotherapy of cholangiocellular carcinoma at hepatic hilum: a feasibility study. *Eur J Surg Oncol* 2018; **44:** 1603-9. doi: 10.1016/j.ejso.2018.06.025

44. Luerken L, Doppler M, Brunner SM, Schlitt HJ, Uller W. Stereotactic percutaneous electrochemotherapy as primary approach for unresectable large HCC at the hepatic hilum. *Cardiovasc Intervent Radiol* 2021; **44:** 1462-6. doi: 10.1007/s00270-021-02841-1

45. Iezzi R, Posa A, Caputo CT, De Leoni D, Sbaraglia F, Rossi M, et al. Safety and feasibility of analgosedation for electrochemotherapy of liver lesions. *Life* 2023; **13:** 631. doi: 10.3390/life13030631

research article

Investigation of *GSTP1* and *PTEN* gene polymorphisms and their association with susceptibility to colorectal cancer

Durr-e-Shahwar[1], Hina Zubair[1], Muhammad Kashif Raza[1,2], Zahid Khan[1], Lamjed Mansour[3], Aktar Ali[4], Muhammad Imran[1]

[1] Biochemistry Section, Institute of Chemical Sciences, University of Peshawar, Peshawar, Pakistan
[2] Department of Chemistry, Shaheed Benazir Bhutto University Sheringal Dir upper, Pakistan
[3] Department of Zoology, College of Science, King Saud University, Riyadh, Saudi Arabia
[4] Biological Screening Core, Warren Family Center for Drug Discovery, University of Notre Dame, Notre Dame, United States

Radiol Oncol 2025; 59(1): 110-120.

Received 12 July 2024
Accepted 25 October 2024

Correspondence to: Assoc. Prof. Muhammad Imran, Ph.D., Biochemistry Section, Institute of Chemical Sciences, University of Peshawar, Peshawar-25120, KP, Pakistan. E-mail: imrancl@uop.edu.pk

Disclosure: No potential conflicts of interest were disclosed.

Background. This study investigates the association of single nucleotide polymorphism in glutathione S transferase P1 (rs1695 and rs1138272) and phosphatase and TENsin homolog (rs701848 and rs2735343) with the risk of colorectal cancer (CRC).

Patients and methods. In this case-control study, 250 healthy controls and 200 CRC patients were enrolled. All subjects were divided into 3 groups: healthy control, patients, and overall (control + patients). Genotyping was performed using polymerase chain reaction-restriction fragment length polymorphism (PCR-RFLP). The demographic information, including age, gender, location, smoking status, cancer stage, and node involvement, were collected.

Results. The allele frequencies of *PTEN* rs701848 in overall subjects were 0.78 for C and 0.22 for T. Similarly, in overall individuals, allele frequencies for *PTEN* rs2735343 were 0.65 and 0.35 for G and C alleles, respectively. The CC genotype or C allele of rs701848 and CG/GG genotype of rs2735343 were observed to be a risk factor for CRC. In overall individuals, a significant ($p \leq 0.05$)) association was observed between rs701848 and rs2735343 polymorphisms CRC. Allele frequencies for *GSTP1* rs1695 were 0.68 and 0.32 for the A and G alleles, respectively. Allele frequencies for *GSTP1* rs1138272 were 0.68 and 0.32 for C and T alleles, respectively. However, a significant ($p < 0.05$) association was found in males for rs1695, while a non-significant difference was observed for the distribution of any genotypes or alleles at *GSTP1* (rs1138272).

Conclusions. Both SNPs of *PTEN* rs701848 and rs2735343 polymorphisms were significantly associated with CRC. However, in *GSTP1*, rs1695 was significantly associated with CRC risk in males, and rs1138272 showed a non-significant association with colorectal cancer risk.

Key words: colorectal cancer; GSTP1; PTEN; polymorphism; PCR-RFLP

Introduction

Colorectal cancer (CRC) is a major public health concern around the world, ranking among the top causes of cancer morbidity and mortality.[1] CRC has the third-highest incidence and second-highest mortality rate of all cancers worldwide.[2] Over 1918658 CRC cases and 900536 deaths were estimated in 2022.[3] The incidence of CRC shows considerable variation among racially or ethnically defined populations in multiracial/ethnic countries.[4] The geographical and temporal burden of this cancer provides insights into risk factor prevalence and progress in cancer control strategies.[5]

CRC causes include heterogeneous, controllable, and external factors related to lifestyle, such as diet and socioeconomic standing.[6] Chromosomal instability (CIN) or microsatellite instability (MIN) are the two main causes of the development of CRC and involve activation and inactivation of various proto-oncogenes and tumor-suppressor genes, respectively.[7] Several genes have been connected to the etiology of CRC including *GSTP1* (Glutathione S-Transferase Pi 1), *APC* (Adenomatous Polyposis Coli), and *PTEN* (Phosphatase and TENsin) *etc*.[8]

The *GSTP1* gene has six introns and seven exons and is positioned on chromosome 11q13. From aberrant crypt foci to advanced carcinomas, *GSTP1* is overexpressed in all stages of CRC.[9,10] GSTP1 dimers catalyze the conjugation of glutathione's sulfur atom to endogenous and exogenous electrophiles, such as xenobiotics, reactive oxygen species (ROS), anticancer agents, and carcinogens in the process of detoxification.[11,12] Two important genetic polymorphisms in *GSTP1* include rs1695 (Ile-105Val) resulting from an AG transition at base 1578 (c.313A>G), and rs1138272 (Ala114Val), resulting from a CT transition at base 2293 (c.341C>T).[12] These polymorphisms may predispose to CRC through deficient detoxification of carcinogens and also may have an impact on a patient's response to chemotherapy.[13]

A tumor suppressor gene called *PTEN*, which codes for a protein that has both lipid and protein phosphatase functions, is found on chromosome 10q23.3.[14] Blocking the oncogenic PI3K/Akt/mTOR pathway is the primary function of *PTEN*. Genetic alterations in *PTEN* leading to its inactivation, facilitate tumorigenesis, and are common in human cancers such as prostate cancer, breast cancer, glioblastoma, and CRC.[15] Single nucleotide polymorphisms (SNPs) in *PTEN* can decrease its activity which may lead to downstream oncogene activation and tumorigenesis.[16] The *PTEN* gene's intron and non-coding region contain SNPs like rs2735343 (located in the promoter region of the gene, C > G change) and rs701848 (found in the 3′ untranslated region (3′-UTR) of the gene T>C change), which may affect splicing, cell cycle, and protein expression.[17]

These genetic polymorphisms can affect the enzymes by either modifying enzymatic activation, their interaction with partner proteins, or their detoxification potential, which can potentially influence the susceptibility and prognosis to CRC based on ethnic disparities and inter-individual differences. The association of these polymorphisms in the candidate genes with CRC risk in the Khyber Pakhtunkhwa population has not been established yet. This study was thus designed to investigate genetic/allelic polymorphism in *GSTP1* (rs1695, rs1138272) and *PTEN* (rs701848, rs2735343), their frequency, and their association with the development of CRC.

Patients and methods

Samples collection

In this study, 250 healthy controls and 200 CRC patients of various stages from I-IV under chemotherapy or radiation therapy treatments were enrolled from Khyber Pakhtunkhwa, Pakistan. The sample size was calculated World Health Organization (WHO) formula.[18] Ethical approval for this study was obtained from the Ethical Committee Faculty of Life & Environmental Sciences, University of Peshawar, Pakistan. For the controls, healthy individuals with no sign of present or previous malignancy and no indication of CRC nor any family history of cancer were included who have no blood relation with the patients. Individuals who were unable to provide informed consent and patients who have developed CRC at the age > 60 years were excluded. Mixed ethnic backgrounds individuals and patients with comorbidities were also excluded. Blood samples (3 mL) were collected through a sterile syringe from both the patients and controls visiting the Institute of Radiation and Nuclear Medicine (IRNUM), Peshawar, Pakistan. They were stored at −20°C in sterile vacutainer tubes containing ethylenediaminetetraacetic acid (EDTA) till further analysis.

DNA extraction and genotyping

Genomic DNA was extracted using a genomic DNA extraction kit (Gene JET Genomic DNA Purification kit, Thermoscientific, USA) and quantified using a spectrophotometer (752 PC, China). A 5–10 ng DNA sample was used for the genotyping of *GSTP1* (rs1695, rs1138272) and *PTEN*(rs701848, rs2735343) polymorphisms using the polymerase chain reaction-restriction fragment length polymorphism (PCR-RFLP) technique.[19, 20] The PCR amplification was performed in a 25 mL reaction mixture, containing 100 ng genomic DNA, 0.2 mM dNTP, 0.2 mM of each primer, 2.5 U Taq DNA polymerase, and Taq buffer (Thermo Fischer Scientific USA). The primer sequences were designed using Primer 3 or Primer BLAST. The sequence of primers, PCR conditions, restriction enzymes, length of PCR, and digestion products for *GSTP1* and *PTEN*

TABLE 1. Primer sequences and amplification conditions for *GSTP1* and *PTEN* polymorphisms

Gene	Primer sequence	PCR conditions	Amplicon length (bp)	Restriction enzyme	Length of digest products (bp)	Enzyme specificity
GSTP1 (rs1695)	F:5'GGCTCTATGGGAAGGACCAGCAGG-3' R:5'GCACCTCCATCCAGAAACTGGCG3'	30 cycles of 1 min at 94°C,1 min at 66°C and 2 min at 72°C.	445	*Alw*261	330+115+270	5'GTCTC(N)1↓3' 3'CAGAG(N) 5↑5'
***GSTP1* (rs1138272)**	F:5'CAGCAGAGGCAGCGTGTGTGC-3' R:5'CCCACAATGAAGGTCTTGCCTCC-3'	30 cycles of 1 min at 94°C, 1 min at 64°C and 2 min at 72°C.	565	*AciI*	365+120+485+80	5'C↓CG↑C'3 **3'G↓GC↑G'5**
***PTEN* (rs701848)**	F:5'-GTGCTTTATTGATTTGCT-3' R:5'AGTAGTTGTACTCCGCTT-3'	5 min at 94°C, 35 cycles of 30 s at 94°C, 30 s at 55°C, 30 s at 72°C, and 10 min extension at 72°C.	199	*HaeIII*	199+81+118	5'GG↓CC3' 3'CC↑G G5'
***PTEN* (rs2735343)**	F:5'-CTCTTCCTGTTCTCCATCGTG-3' R:5'-TTCTCCAGGATTTCGTCTGC-3'	5 min at 94°C, 35 cycles of 30 s at 94°C, 30 s at 63°C, 30 s at 72°C and 10 min at 72°C.	272	*HhaI*	272+72+200	5'G↑CG↓C3' 3'C↑GC↓G'5

bp = base pair; F = forward; PCR = polymerase chain reaction; R = reverse

amplification have been described in Table 1. The PCR products were digested by respective restriction enzymes overnight at 37°C and then analyzed by electrophoresis on 2% agarose gel. The sequences of the PCR products were confirmed by Sanger sequencing. Sanger sequencing (capillary sequencing) of random samples was carried out using Applied Biosystems 3730xl DNA Analyzer (Thermo Fischer Scientific, USA). Bioedit sequence alignment editor (BioEdit version 7.7.1) was used for sequencing data analysis.

TABLE 2. Demographic information and risk factors in colorectal cancer (CRC) cases and control

Variable	Patients N = 200(%)	Control n = 250(%)	P value
***Age (Years)**			
≥ 40	132 (66.0)	151 (60.4)	0.222
< 40	68 (34.0)	99 (39.6)	
Range	10-60	11-60	-
Median	46	32	-
***Gender**			
Male	122 (61.1)	169(68)	0.273
Female	78 (39.0)	81(32)	
****Smoking status**			
Never	165 (82.3)	22 (8.8)	< 0.010
Ever	35 (17.6)	228 (91.1)	
***Site of tumor**			
Colon	102(51.00)		0.984
Rectum	98(49.00)		

*p > 0.05 patients vs control; **p ≤ 0.05 patients vs controls

Statistical analysis

The statistical package for social sciences version 20 (SPSSv.20) was used for analysis. Descriptive statistics were used to calculate proportions and percentages for each categorical variable used in univariate analysis. Adjusted odds ratios (OR) and 95% confidence interval (CI) for potential determinants of CRC were calculated by logistic regression analysis. The $p \leq 0.05$ was considered to be statistically significant. Hardy Weinberg equilibrium was tested by chi-square t-test for observed genotype frequencies.

Results

Demographic variables of the studied population

Of the 450 individuals, 200 were CRC patients; 78 (39%) were female and 122 (61%) were males. The remaining 250 were controls; 81 (32%) female and 169 (68%) males. The inter-group differences related to age, gender, and food consumption patterns were non-significant ($p > 0.05$), while smoking status was a significant factor (Table 2). The tumor location among the CRC cases was non-significant ($p > 0.05$) as 98 (49%) patients were diagnosed with rectal carcinoma and 102 (51%) had colon carcinoma.

TABLE 3. Frequency of *GSTP1* (rs1695) polymorphism and its association with colorectal cancer (CRC) risk

Models/Genotype	CRC Patients + Healthy Controls n (%)	CRC Patients n (%)	Healthy Controls n (%)	OR	P Value	95% CI	RR
Overall Subjects							
Codominant Model							
A/A	192 (43)	91 (46)	101 (40)		Referent		_
A/G	231 (51)	102 (51)	129 (52)	0.88	0.10	0.60–1.29	1.2
G/G	27 (6)	07 (4)	20 (8)	0.39	0.10	0.16–0.97	0.2
Dominant Model (A/G+G/G)	258 (57)	109 (54)	149 (60)	0.81	0.28	0.56–1.19	1.4
Recessive Model (A/A+A/G)	423	193	230	2.39	0.05*	0.99–5.79	-
Over dominant Model (A/G)	231 (51)	102 (51)	129 (52)	1.02	0.89	0.70–1.48	-
Male							
A/A	123 (42)	58 (48)	65 (38)		Referent		_
A/G	150 (52)	63 (52)	87 (51)	0.81	< 0.01*	0.50–1.31	1.3
G/G	18 (6)	01 (0.1)	17 (1)	0.07	< 0.01*	0.01–0.51	0.2
Dominant Model (A/G+G/G)	168 (58)	64 (52)	104 (52)	0.69	0.12	0.43–1.11	1.5
Female							
A/A	69 (43)	33 (42)	36 (44)		Referent		_
A/G	81 (51)	39 (50)	42 (52)	1.01	0.55	0.53–1.93	1.1
G/G	9 (6)	06 (8)	03 (4)	2.18	0.55	0.50–9.43	0.1
Dominant Model (A/G+G/G)	90 (57)	45 (58)	45 (56)	1.09	0.79	0.58–2.04	1.2
HWE (Genotype Frequencies)							
A^2	0.46	0.50	0.436	-	-	-	
2AG	0.43	0.41	0.449	-	-	-	
G^2	0.10	0.08	0.116	-	-	-	
χ^2total = 1							

*Statistically significant associations ($p \leq 0.05$), Logistic regression model adjusted by age, gender and smoking;

CI = confidence interval; CRC = colorectal cancer; OR = odd ratio; RR = relative risk

Frequency of *GSTP1* (rs1695 and rs113828) polymorphism and associated risk of CRC

The risk association of rs1695 polymorphism and CRC is shown in Table 3. Representative images of genotyping are shown in Supplementary Figure 1 and random sample sequencing analysis is in Supplementary Figure 2. Among the 450 individuals, the A allele carriers of rs1695 were more prevalent compared to the G allele carriers. Allele and genotype frequency distribution for *GSTP1* in the population are shown in Figure 1 and Figure 2 respectively. In overall individuals, allele frequencies for *GSTP1* rs1695 were 0.68 and 0.32 for the A and G alleles, respectively. The genotypes (A/G+G/G) were not associated with the risk of CRC in overall subjects (OR = 0.81, CI = 0.56 to 1.19, P = 0.28, as well as in females (OR = 1.09, CI = 0.58 to 2.04, P = 0.79,) while it was associated in males (OR = 0.81, CI = 0.50 to 1.31, P < 0.01,). The relative risk (RR) for male was 2.2 times higher than for female participants.

The risk association of *GSTP1* rs1138272 and CRC is shown in Table 4. Allele and genotype frequencies for *GSTP1* rs1138272 in the population are shown in Figure 1, 2 respectively. In overall subjects, the T allele (35%) was more prevalent than C allele (32%). In overall subjects the presence of the genotype C/T+T/T (OR = 0.75, CI = (0.47 to 1.18),

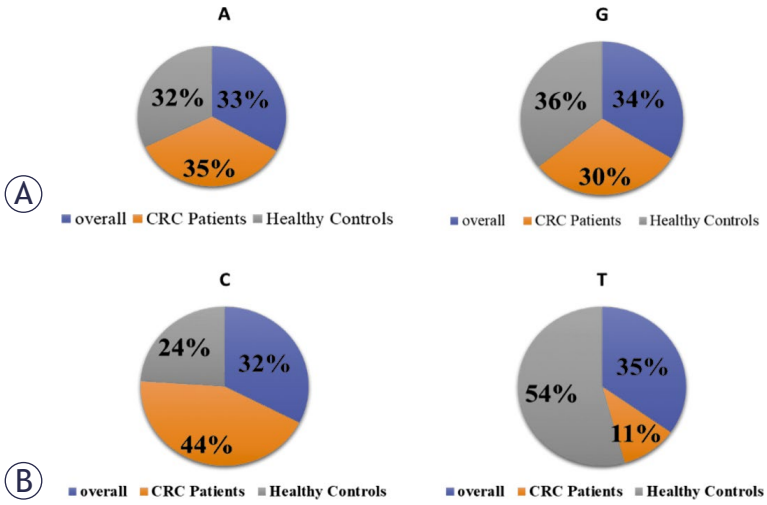

FIGURE 1. *GSTP1*Alleles frequency distribution of the rs1695 A/G **(A)** and rs1138272 C/T **(B)**.

CRC = colorectal cancer

P = 0.21) was not related to the risk of CRC and the relationship is not significant. Relative Risk for male and female is equal.

Frequency of *PTEN* (rs701848) polymorphism and associated risk of CRC

The allele frequencies of *PTEN* rs701848 in overall subjects were 0.78 for C and 0.22 for T. Representative images of genotyping are shown in Supplementary Figure 2 and random samples sequencing in Supplementary Figure 4. Among overall 450 subjects, the C allele was more prevalent compared to T allele carriers. The presence of C/C genotype was significantly associated with a higher risk of CRC in overall subjects (OR = 3.9, CI = 1.86 to 8.23, P = 0.03 in males (OR = 8.02, P = 0.001, CI = 2.29 to 28.01) as well as in females (OR = 2.05, P = 0.14, CI = 0.77 to 5.48). The RR for females was 0.8 times higher than males.

Frequency of *PTEN* (rs2735343) polymorphism and associated risk of CRC

The risk association of CG rs2735343 polymorphism and CRC is shown in Table 6. Similarly, in overall individuals, allele frequencies for *PTEN* rs2735343 were 0.65 and 0.35 for G and C alleles, respectively. In overall subjects, the G allele (C/G+G/G) was more prevalent (52%) than the C/C genotype (48%). The combined heterozygous C/G+G/G variant was observed to be 30% prevalent in healthy individuals and 80% in CRC participants. The allele frequencies and genotype count for rs2735343 are presented in Figure 3,4. The presence of genotypes (C/G, GG &C/G+G/G) was positively correlated with a higher risk of CRC in overall subjects, males and females (OR = 3.6-17.0). The RR for males is 2.8 times greater than females.

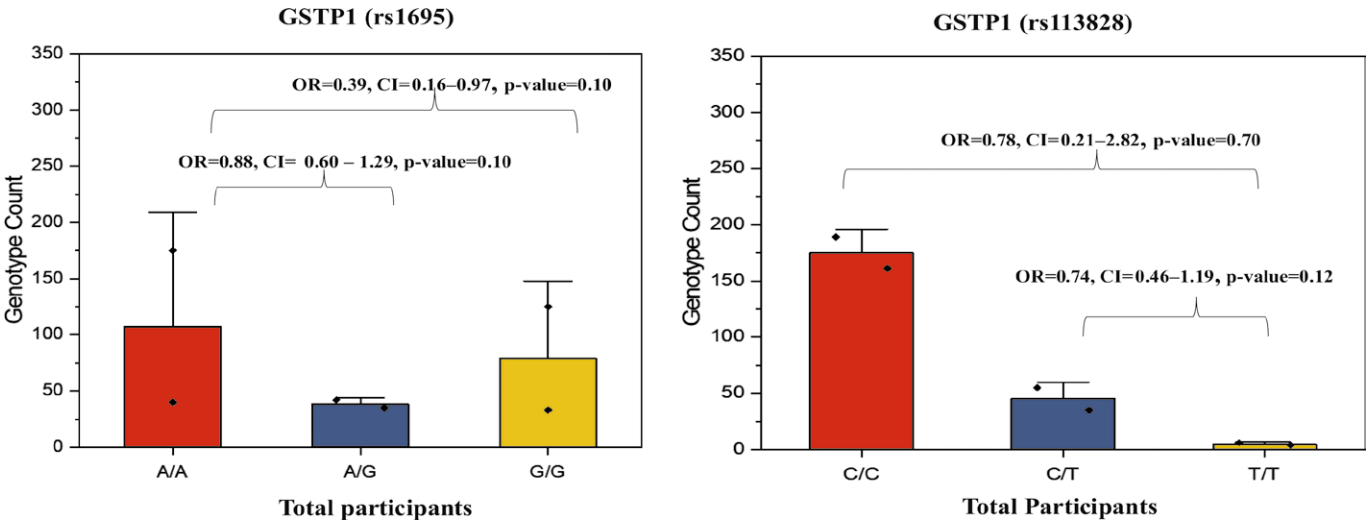

FIGURE 2. *GSTP1* genotypic count of the overall participants for rs1695 and rs1138272. The p-values and odds ratio (OR) displayed in the figure correspond to pairwise comparisons of genotypes in between the two groups. Lines typically represent trends or connections between data points and square dots mark data points or average. Genotype count means number of individuals with a specific genetic variation.

CI = confidence interval

TABLE 4. Frequency of *GSTP1*(rs1138272) polymorphism and its association with colorectal cancer (CRC) risk

Models/Genotype	CRC Patients +Healthy Controls n (%)	CRC Patients n (%)	Healthy Controls n (%)	OR	P Value	95% CI	RR
Overall Subjects							
Codominant Model							
C/C	350 (78)	161(80)	189(76)		Referent		_
C/T	90 (20)	35(18)	55(22)	0.74	0.12	0.46-1.19	0.2
T/T	10 (2)	4(2)	6 (2)	0.78	0.70	0.21-2.82	0.03
Dominant Model C/T+T/T	100 (22)	39 (19)	61 (24)	0.75	0.21	0.47-1.18	0.3
Recessive Model (C/C+C/T)	440	196	244	1.20	0.77	0.33-4.32	-
Over dominant Model (C/T)	90 (20)	35(18)	55(22)	0.75	0.23	0.46-1.20	-
Male							
C/C	229(79)	98(80)	131(78)		Referent		-
C/T	56(19)	20(17)	36(21)	0.74	0.33	0.40-1.36	0.2
T/T	6(2)	4(3)	02(1)	2.67	0.26	0.47-14.89	0.02
Dominant Model C/T+T/T	62(21)	24(20)	38(22)	0.84	0.56	0.47-1.49	0.2
Female							
C/C	121(76)	61(78)	60(74)		Referent		_
C/T	34(21)	15(19)	19(24)	0.77	0.51	0.36-1.66	0.3
T/T	4(3)	2(3)	02(2)	0.98	0.98	0.13-7.21	0.04
Dominant Model C/T+T/T	38(24)	17(22)	21(26)	0.88	0.74	0.43-1.82	0.3
HWE (Genotype Frequencies)							
C^2	0.462	0.81	0.25	-	-	-	-
2CT	0.435	0.18	0.5	-	-	-	-
T^2	0.102	0.01	0.25	-	-	-	-
χ^2total = 1							

*Statistically significant associations ($p \leq 0.05$), Logistic regression model adjusted by age, gender and smoking.

CI = confidence interval; CRC = colorectal cancer; OR = odd ratio; RR = relative risk

Association of *GSTP1* and *PTEN* polymorphism with colon and rectum cancer cases

The study analyzed CRC patients based on tumor location to assess the association of the *GSTP1* and *PTEN* polymorphism and the link between the these polymorphisms and CRC was evaluated by sub-grouping the patients into those with colon and rectum cancers (Table 7). Of the 200 CRC patients, 102 (51%) had colon cancer and 98 (49%) had rectal cancer. Heterozygous genotypes were significantly linked to increased risks of both colon and rectal cancer ($p < 0.05$) for *GSTP1*(rs1695, rs1138272) and *PTEN* (rs701848).

Discussion

CRC is a major global health issue influenced by various genetic factors. *GSTP1*, part of phase II detoxification, conjugates glutathione to detoxify and remove harmful substances, promoting detoxification.[21] Polymorphisms in these genes alter biological pathways and protein expression, contributing to tumor development.[22] *GSTP1* genotypes differ

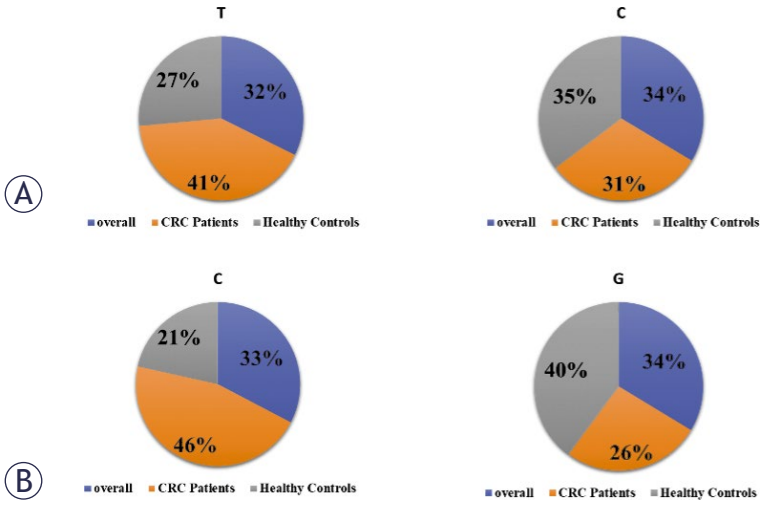

FIGURE 3. *PTEN* Alleles frequency distribution of the rs701848 T/C **(A)** and rs2735343 C/G **(B)**.

CRC = colorectal cancer

in their ability to detoxify toxic species, with enzyme activity being significantly lower in individuals with Val instead of isoleucine at position 105 (rs1695).[23] Research links *GSTP1* Ile105Val (rs1695, A>G) and *GSTP1* Ala114Val (rs1138272, C>T) mutations to various cancers, including breast, oral, and squamous cell carcinoma (SCC).[24] *GSTP1* Ile105Val (rs1695, A > G) is a missense mutation reducing enzyme activity. Santric found a significant association between *GSTP1* Ile105Val polymorphism and toxicity.[25] showed that the Kudhair *GSTP1* Ile105Val substitution increases lung cancer risk in Arab population. Watson *et al.* demonstrated that individuals with two *GSTP1* valine alleles had lower catalytic activity than those with two isoleucine alleles, with heterozygotes showing intermediate activity. Evidence on GST polymorphisms' role in CRC susceptibility is mixed.[26] *GSTP1*, highly expressed in the colon and involved in heterocyclic amine deactivation, is a candidate susceptibility gene. *GSTP1* SNPs, especially Ile105Val, are strongly associated with increased CRC risk and poorer prognosis. However, the association with rectal cancer is less robust than with colon cancer.[27]

The *GSTP1* gene variants (rs1695, rs1138272) are unlikely to significantly increase CRC risk, although a minor effect cannot be excluded, aligning with Terrazzino[27] and Osti's findings.[28] The *GSTP1* 105Val allele frequency in CRC patients was similar to previous reports in healthy Caucasians and African-Americans.[29] The frequency of both *GSTP1* polymorphisms was comparable to Australian, English, and American Caucasians (34%, 33%, and 33% Val-105; 7%, 8%, and 9% Val-114, respectively).[17] Khabaz in Saudi Arabia, and studies in Bulgaria and Kashmir populations also found no association between these genotypes and CRC risk.[30] However, Gorukmez[31] noted the *GSTP1* Ile/

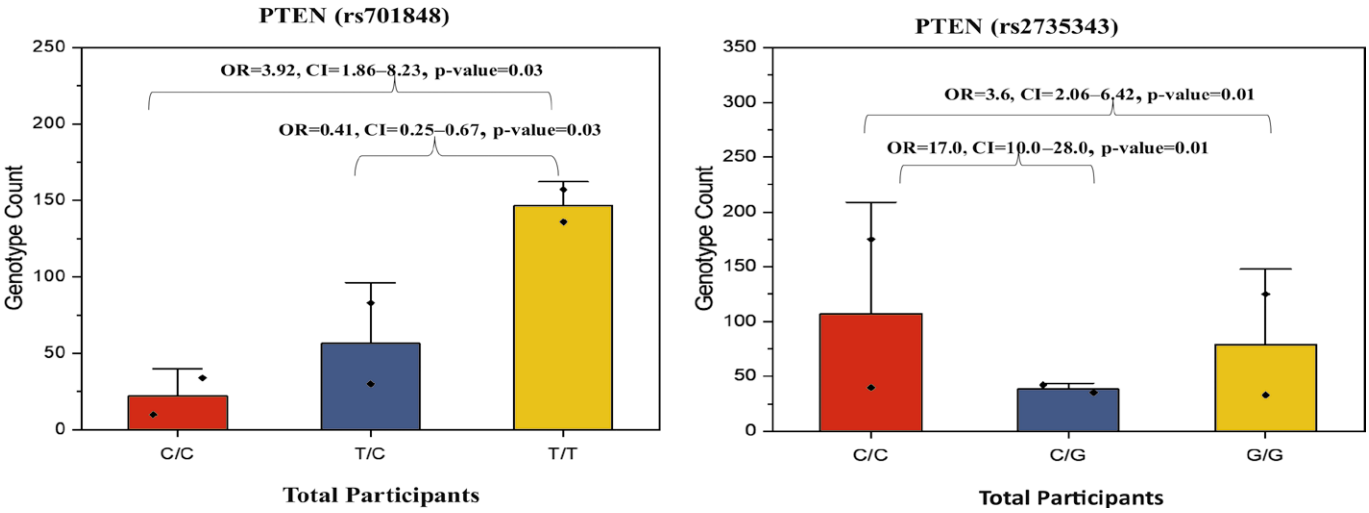

FIGURE 4. *PTEN* genotypic count of the overall participants for rs701848 and rs2735343. The p-values and odds ratio (OR) displayed in the figure correspond to pairwise comparisons of genotypes between the two groups in each of the bar graphs. Lines typically represent trends or connections between data points and square dots mark data points or average. Genotype count means number of individuals with a specific genetic variation.

CI = confidence interval

TABLE 5. Frequency of *PTEN* (rs701848) polymorphism and its association with colorectal cancer (CRC) risk

Models/Genotype	CRC Patients +Healthy Controls n (%)	CRC Patients n (%)	Healthy Controls n (%)	OR	P Value	95% CI	RR
Overall Subjects							
Codominant Model							
T/T	293 (65)	136 (68)	157 (63)		Referent		_
T/C	113 (25)	30 (15)	83 (33)	0.41	0.03*	0.25–0.67	0.5
C/C	44 (10)	34 (17)	10 (4)	3.92	0.03*	1.86– 8.23	0.06
Dominant T/C+C/C	157 (35)	64 (32)	93 (37)	0.79	0.25	0.53–1.17	0.5
Recessive Model (T/T+T/C)	406	166	240	0.20	< 0.01*	0.09–0.42	-
Over dominant Model (T/C)	113 (25)	30 (15)	83 (33)	0.35	< 0.01*	0.22–0.56	-
Male							
T/T	197 (68)	86 (70)	111 (66)		Referent		
T/C	71 (24)	17 (14)	54 (32)	0.40	0.04*	0.21–0.75	_
C/C	23 (8)	19 (16)	04 (2)	8.02	0.01*	2.29-28.01	0.04
Dominant T/C+C/C	94 (32)	36 (30)	58 (34)	0.81	0.42	0.49–1.35	0.5
Female							
T/T	96 (60)	50 (64)	46 (57)		Referent		_
T/C	42 (27)	13 (17)	29 (36)	0.41	0.02*	0.19–0.89	0.6
C/C	21 (13)	15 (19)	06 (7)	2.05	0.14	0.77-5.48	0.1
Dominant T/C+C/C	63 (40)	28 (36)	35 (43)	0.72	0.32	0.38–1.36	0.7
HWE (Genotype Frequencies)							
T^2	0.04	0.04	0.03	-	-	-	
2TC	0.34	0.32	0.29	-	-	-	
C^2	0.60	0.64	0.67	-	-	-	
χ^2total = 1							

*Statistically significant associations ($p < 0.05$), Logistic regression model adjusted by age, gender, and smoking.

CI = confidence interval; CRC = colorectal cancer; OR = odd ratio; RR = relative risk

Ile genotype was more frequent in controls than patients, while Vlaykova[32] reported a non-significant protective role for the Val allele. A mild association of CRC with heterozygous and homozygous genotypes was observed compared to the wild type of GSTP1.[30] Previous studies examining the Ile-1053Val and Ala-1143Val *GSTP1* polymorphisms in CRC reported no association, consistent with our findings.[33,34]

Phosphatase and TENsin homolog (*PTEN*) is also mutated in multiple advanced cancers and a tumor suppressor gene.[35] *PTEN* is generally cytosolic and regulates phosphatidylinositol 3,4,5-trisphosphate (PIP3) levels; a small fraction of *PTEN* is recruited to the plasma membrane. *PTEN* reduces PIP3 levels, decreasing the mTOR/AKT signaling pathway critical for cancer cell growth, survival, and progression. Many SNPs and deletion polymorphisms in *PTEN* have been reported in human cancers.[36] Both rs701848 and rs2735343 SNPs are located in the intron and non-coding region of the *PTEN* gene and increase cancer risk by probably influencing splicing, protein expression, and cell cycle. The rs701848 polymorphism influences cancer susceptibility by altering *PTEN* expression and reducing *PTEN* mRNA stability. These func-

TABLE 6. Frequency of *PTEN* (rs2735343) polymorphism and its association with colorectal cancer (CRC) risk

Models/Genotype	CRC Patients +Healthy Controls n (%)	CRC Patients n (%)	Healthy Controls n (%)	OR	P Value	95% CI	RR
Overall Subjects							
Codominant Model							
C/C	215 (48)	40 (20)	175 (70)		Referent		_
C/G	77 (17)	35 (18)	42 (17)	3.6	< 0.01*	2.06–6.42	0.2
G/G	158 (35)	125 (62)	33 (13)	17.0	< 0.01*	10.0–28.0	0.1
Dominant C/G+G/G	235 (52)	160 (80)	75 (30)	9.5	< 0.01*	6.10–14.7	0.4
Recessive Model (C/C+C/G)	292	75	217	0.09	< 0.01*	0.05–0.14	-
Over dominant Model (C/G)	77 (17)	35 (18)	42 (17)	1.09	0.71	0.67–1.79	-
Male							
C/C	139 (48)	24 (20)	115 (68)		Referent		_
C/G	47 (16)	16 (13)	31 (18)	2.47	< 0.01*	1.17–5.22	0.2
G/G	105 (36)	82 (67)	23 (14)	17.08	< 0.01*	9.02–32.3	0.2
Dominant C/G+G/G	152 (52)	98 (80)	54 (32)	8.70	< 0.01*	5.01–15.0	0.4
Female							
C/C	76 (48)	16 (21)	60 (74)		Referent		_
C/G	30 (19)	19 (24)	11 (14)	6.48	< 0.01*	2.57–16.3	0.1
G/G	53 (33)	43 (55)	10 (12)	16.12	< 0.01*	6.68–38.9	0.1
Dominant C/G+G/G	83 (52)	62(79)	21 (26)	11.07	< 0.01*	5.28–23.3	0.3
HWE (Genotype Frequencies)							
C^2	0.12	0.24	0.05	-	-	-	
2CG	0.45	0.5	0.35	-	-	-	
G^2	0.42	0.26	0.59	-	-	-	
χ^2total = 1							

*Statistically significant associations ($p < 0.05$), Logistic regression model adjusted by age, gender and smoking.

CI = confidence interval; CRC = colorectal cancer; OR = od Ratio; RR = relative risk

tional genetic polymorphisms of *PTEN* are known to participate in tumorigenesis.[30] Jang *et al* [37]. and Xu *et al*.[38] showed that the C allele of rs701848 was more susceptible than the T allele in developing esophageal squamous cell cancer (ESCC). The rs701848 is associated with an increased risk of breast cancer, renal cell cancer, CRC, and ESCC.[31] GG genotype of rs2735343 is associated with an elevated risk of ESCC while there is no association between rs2735343 (G/C) and the risk of endometrial cancer. Moreover, Asian subjects carrying the TC/CC genotype or C allele of rs701848 were associated with an increased risk of esophageal squamous cell cancer.[16] Studies have suggested a significant association between rs701848 and colon cancer risk, especially in populations with a family history of CRC. rs1903858 (G/A) and its specific association with colon, rectal, or CRC is still being researched, it has been implicated in cancer susceptibility in various populations.[39] Located in the promoter region of *PTEN*, some studies suggest rs2735343 plays a role in both colon and rectal cancers through its impact on *PTEN* expression.[40]

Our analyses demonstrated that CRC risk was associated with rs701848 in the C/C genotype and with rs2735343 in the GG and C/G genotypes and

shown that these genotypes increased the risk of CRC in the Pashtun population which supports previous findings by Jang *et al*.[37] The distribution of genotypes or alleles in cases at both genetic sites of *PTEN* was statistically different from those in controls. This study is limited by a small Pashtun sample, lack of population comparisons, and no meta-analyses. Future research should replicate these findings in larger, multi-ethnic cohorts to assess genetic links to CRC. Investigations should focus on the effects of rs701848 and rs2735343 polymorphisms on PTEN expression and function to aid in developing targeted therapies.

Conclusions

The significant association of *PTEN* rs701848 and rs2735343 polymorphisms CRC suggests their potential role as genetic risk factors in the studied population. The gender-specific association of *GSTP1* rs1695 with CRC in males warrants further investigation to elucidate the underlying mechanisms. These findings contribute to the understanding of genetic susceptibility to CRC and highlight the importance of personalized approaches in cancer prevention and treatment.

Acknowledgments

The authors would like to extend their special thanks to the volunteers who willingly participated in this study. The authors extend their appreciation to the Researchers Supporting Project number (RSP 2025R75), King Saudi University, Riyadh, Saudi Arabia for financial support.

TABLE 7. Association of *GSTP1* and *PTEN* polymorphism with colon and rectum cancer cases

Gene/rs	Genotype	Colon n = 102 (%)	Rectum n = 98 (49%)	P Value
***GSTP1* rs1695**	AA	62 (61.11)	26 (27.00)	Referent
	AG	34 (33.33)	72 (73.33)	< 0.01*
	GG	06 (5.65)	-	0.25
***GSTP1* rs1138272**	CC	91 (89)	69 (69.5)	Referent
	CT	13 (13.0)	17 (17.3)	< 0.01*
	TT	17 (17.0)	17 (17.3)	0.27
***PTEN* rs701848**	TT	72 (70.0)	64 (65.4)	Referent
	TC	13 (13.0)	17 (17.3)	< 0.01*
	CC	17 (17.0)	17 (17.3)	0.02
***PTEN* rs2735343**	CC	20 (19.6)	20 (20.4)	Referent
	CG	19 (18.6)	16 (16.3)	0.71
	GG	63(61.8)	62 (63.3)	0.96

*Statistically significant associations ($p < 0.05$)

References

1. Xi Y, Xu P. Global colorectal cancer burden in 2020 and projections to 2040. *Transl Oncol* 2021; **14:** 101174. doi: 10.1016/j.tranon.2021.101174
2. Huang P, Feng Z, Shu X, Wu A, Wang Z, Hu T, et al. A bibliometric and visual analysis of publications on artificial intelligence in colorectal cancer (2002-2022). *Front Oncol* 2023; **13:** 1077539. doi: 10.3389/fonc.2023.1077539
3. Bizuayehu HM, Dadi AF, Ahmed KY, Tegegne TK, Hassen TA, Kibret GD, et al. Burden of 30 cancers among men: Global statistics in 2022 and projections for 2050 using population-based estimates. *Cancer* 2024; **130:** 3708-23. doi: 10.1002/cncr.35458
4. Wani HA, Majid S, Bhat AA, Amin S, Farooq R, Bhat SA, et al. Impact of catechol-O-methyltransferase gene variants on methylation status of P16 and MGMT genes and their downregulation in colorectal cancer. *Eur J Cancer Prev* 2019; **28:** 68-75. doi: 10.1097/CEJ.0000000000000485
5. Morgan E, Arnold M, Gini A, Lorenzoni V, Cabasag CJ, Laversanne M, et al. Global burden of colorectal cancer in 2020 and 2040: incidence and mortality estimates from GLOBOCAN. *Gut* 2023; **72:** 338-44. doi: 10.1136/gutjnl-2022-327736
6. Hossain MS, Karuniawati H, Jairoun AA, Urbi Z, Ooi J, John A, et al. Colorectal cancer: a review of carcinogenesis, global epidemiology, current challenges, risk factors, preventive and treatment strategies. *Cancers* 2022; **14:** 1732. doi: 10.3390/cancers14071732
7. Parmar S, Easwaran H. Genetic and epigenetic dependencies in colorectal cancer development. *Gastroenterol Rep* 2022; **10:** goac035. doi: 10.1093/gastro/goac035
8. Li F, Qasim S, Li D, Dou QP. Updated review on green tea polyphenol epigallocatechin-3-gallate as a cancer epigenetic regulator. *Semin Cancer Biol* 2022; **83:** 335-52. doi: 10.1016/j.semcancer.2020.11.018
9. Franko A, Goricar K, Dodic Fikfak M, Kovac V, Dolzan V. The role of polymorphisms in glutathione-related genes in asbestos-related diseases. *Radiol Oncol* 2021; **55:** 179-86. doi: 10.2478/raon-2021-0002
10. Cui J, Li G, Yin J, Li L, Tan Y, Wei H, et al. GSTP1 and cancer: Expression, methylation, polymorphisms and signaling. *Int J Oncol* 2020; **56:** 867-78. doi: 10.3892/ijo.2020.4979
11. Gasic V, Zukic B, Stankovic B, Janic D, Dokmanovic L, Lazic J, et al. Pharmacogenomic markers of glucocorticoid response in the initial phase of remission induction therapy in childhood acute lymphoblastic leukemia. *Radiol Oncol* 2018; **52:** 296-306. doi: 10.2478/raon-2018-0034
12. Bartolini D, Torquato P, Piroddi M, Galli F. Targeting glutathione S-transferase P and its interactome with selenium compounds in cancer therapy. *Biochim Biophys Acta Gen Subj* 2019; **1863:** 130-43. doi: 10.1016/j.bbagen.2018.09.023
13. Nissar S, Sameer AS, Rasool R, Chowdri N, Rashid F. Glutathione S transferases: biochemistry, polymorphism and role in colorectal carcinogenesis. *J Carcinog Mutagen* 2017; **8:** 287. doi: 10.1007/s12253-019-00589-1
14. Wang Q, Wang J, Xiang H, Ding P, Wu T, Ji G. The biochemical and clinical implications of phosphatase and tensin homolog deleted on chromosome ten in different cancers. *Am J Cancer Res* 2021; **11:** 5833. PMID: 35018228
15. Fusco N, Sajjadi E, Venetis K, Gaudioso G, Lopez G, Corti C, et al. M. PTEN alterations and their role in cancer management: are we making headway on precision medicine? *Genes* 2020; **11:** 719. doi: 10.3390/genes11070719
16. Vodusek AL, Goricar K, Gazic B, Dolzan V, Jazbec J. Antioxidant defence-related genetic variants are not associated with higher risk of secondary thyroid cancer after treatment of malignancy in childhood or adolescence. *Radiol Oncol* 2016; **50:** 80-6. doi: 10.1515/raon-2015-0026
17. Song DD, Zhang Q, Li JH, Hao RM, Ma Y, Wang PY, et al. Single nucleotide polymorphisms rs701848 and rs2735343 in PTEN increases cancer risks in an Asian population. *Oncotarget* 2017; **8:** 96290. doi: 10.18632/oncotarget.22019
18. Lemoshow S, Hosmer Jr DW, Klar J, Lewang SK. Adecuacy of Simple size in healt studies. Chichester (England): John Wiley & Sons LTD; 1990.

19. Welfare M, Monesola Adeokun A, Bassendine MF, Daly AK. Polymorphisms in GSTP1, GSTM1, and GSTT1 and susceptibility to colorectal cancer. *Cancer Epidemiol Biomarkers Prev* 1999, **8:** 289-92. PMID: 10207630

20. Jang Y, Lu SA, Chen ZP, Ma J, Xu CQ, Zhang CZ, et al. Genetic polymorphisms of CCND1 and PTEN in progression of esophageal squamous carcinoma. *Genet Mol Res* 2013; **12:** 6685-91. doi: 10.4238/2013

21. Potęga A. Glutathione-mediated conjugation of anticancer drugs: An overview of reaction mechanisms and biological significance for drug detoxification and bioactivation. *Molecules* 2022, **27:** 5252. doi: 10.3390/molecules27165252

22. Deng N, Zhou H, Fan H, Yuan Y. Single nucleotide polymorphisms and cancer susceptibility. *Oncotarget* 2017, **8:** 110635. doi: 10.18632/oncotarget.22372

23. Deng X, Hou J, Deng Q, Zhong Z. Predictive value of clinical toxicities of chemotherapy with fluoropyrimidines and oxaliplatin in colorectal cancer by DPYD and GSTP1 gene polymorphisms. *World J Surg Oncol* 2020, **18:** 1-10. doi: 10.1186/s12957-020-02103-3

24. Farmohammadi A, Arab-Yarmohammadi V, Ramzanpour R. Association analysis of rs1695 and rs1138272 variations in GSTP1 gene and breast cancer susceptibility. *Asian Pac J Cancer Prev* 2020; **21:** 1167. doi: 10.31557/APJCP.2020.21.4.1167

25. Kudhair BK, Abdulridha FM, Hussain GM, Lafta IJ, Alabid NN. The association of combined GSTM1, GSTT1, and GSTP1 genetic polymorphisms with lung cancer risk in male Iraqi Waterpipe Tobacco (Nargila) smokers. *Cancer Epidemiol* 2024; **93:** 102689. doi: 10.1016/j.canep.2024.102689.

26. Watson MA, Stewart RK, Smith GB, Massey TE, Bell DA. Human glutathione S-transferase P1 polymorphisms: relationship to lung tissue enzyme activity and population frequency distribution. *Carcinogenesis* 1998; **19:** 275-80. doi: 10.1093/carcin/19.2.275

27. Terrazzino S, La Mattina P, Masini L, Caltavuturo T, Gambaro G, Canonico PL, et al. Common variants of eNOS and XRCC1 genes may predict acute skin toxicity in breast cancer patients receiving radiotherapy after breast conserving surgery. *Radiother Oncol* 2012; **103:** 199-205. doi: 10.1016/j.radonc.2011.12.002

28. Osti MF, Nicosia L, Agolli L, Gentile G, Falco T, Bracci S, et al. Potential role of single nucleotide polymorphisms of XRCC1, XRCC3, and RAD51 in predicting acute toxicity in rectal cancer patients treated with preoperative radiochemotherapy. *Am J Clin Oncol* 2017; **40:** 535-42. doi: 10.1097/COC.0000000000000182

29. Rodrigues-Fleming GH, Fernandes GMM, Russo A, Biselli-Chicote PM, Netinho JG, Pavarino É, et al. Molecular evaluation of glutathione S transferase family genes in patients with sporadic colorectal cancer. *World J Gastroenterol* 2018; **24:** 4462. doi: 10.3748/wjg.v24.i39.4462

30. Khabaz MN, Al-Maghrabi JA, Nedjadi T, Gar MA, Bakarman M, Gazzaz ZJ, et al. Does Val/Val genotype of GSTP1 enzyme affects susceptibility to colorectal cancer in Saudi Arabia. *Neuro Endocrinol Lett* 2016; **37:** 46-52. PMID: 26994385

31. Gorukmez O, Yakut T, Gorukmez O, Sag SO, Topak A, Sahinturk S, et al. Glutathione S-transferase T1, M1 and P1 genetic polymorphisms and susceptibility to colorectal cancer in Turkey. *Asian Pac J Cancer Prev* 2016; **17:** 3855-9. PMID: 27644629

32. Vlaykova T, Miteva L, Gulubova M, Stanilova S. Ile 105 Val GSTP1 polymorphism and susceptibility to colorectal carcinoma in Bulgarian population. *Int J Colorectal Dis* 2007; **22:** 1209-15. doi: 10.1007/s00384-007-0305-z

33. Puerta-García E, Urbano-Pérez D, Carrasco-Campos MI, Pérez-Ramírez C, Segura-Pérez A, Calleja-Hernández, et al. Effect of DPYD, MTHFR, ABCB1, XRCC1, ERCC1 and GSTP1 on chemotherapy related toxicity in colorectal carcinoma. *Surg Oncol* 2020; **35:** 388-98. doi: 10.1016/j.suronc.2020.09.016

34. Klusek J, Nasierowska-Guttmejer A, Kowalik A, Wawrzycka I, Lewitowicz P, Chrapek M, et al. GSTM1, GSTT1, and GSTP1 polymorphisms and colorectal cancer risk in Polish nonsmokers. *Oncotarget* 2018; **9:** 21224. doi: 10.18632/oncotarget.25031

35. Liu J, Pan Y, Liu Y, Wei W, Hu X, Xin W, et al. The regulation of PTEN: Novel insights into functions as cancer biomarkers and therapeutic targets. *J Cell Physiol* 2023; **238:** 1693-715. doi: 10.1002/jcp.31053

36. Papa A, Pandolfi P. The PTEN–PI3K axis in cancer. *Biomolecules* 2019; **9:** 153. doi: 10.3390/biom9040153

37. Jang HY, Kim DH, Lee HJ, Kim WD, Kim SY, Hwang JJ, et al. Schedule-dependent synergistic effects of 5-fluorouracil and selumetinib in KRAS or BRAF mutant colon cancer models. *Biochem Pharmacol* 2019; **160:** 110-20. doi: 10.1016/j.bcp.2018.12.017

38. Xu X, Chen G, Wu L, Liu L. Association of genetic polymorphisms in PTEN and additional gene–gene interaction with risk of esophageal squamous cell carcinoma in Chinese Han population. *Dis Esophagus,* 2016; **29:** 944-9. doi: 10.1111/dote.12428

39. Hassan MH, Nassar AY, Meki AMA, Nasser SA, Bakri AH, Radwan E. Pharmacogenetic study of phosphatase and tensin homolog polymorphism (rs701848) in childhood epilepsy: relation to circulating Wnt signaling. *Neurol Res* 2024; **46:** 99-110. doi: 10.1080/01616412.2023.2257465

40. Shek D, Read SA, Ahlenstiel G, Piatkov I. Pharmacogenetics of anticancer monoclonal antibodies. *Cancer Drug Resistance* 2019; **2:** 69-81. doi: 10.20517/cdr.2018.20

research article

Management of adrenocortical carcinoma in Slovenia: a real-life analysis of histopathologic markers, treatment patterns, prognostic factors, and survival

Urska Bokal[1], Jera Jeruc[2], Tomaz Kocjan[3,4], Metka Volavsek[2], Janja Jerebic[5], Matej Rakusa [3,4], Marina Mencinger[1,4]

[1] Department of Medical Oncology, Institute of Oncology Ljubljana, Ljubljana, Slovenia
[2] Institute of Pathology, Faculty of Medicine, University of Ljubljana, Ljubljana, Slovenia
[3] Department of Endocrinology, Diabetes and Metabolic Diseases, University Medical Centre Ljubljana, Ljubljana, Slovenia
[4] Faculty of Medicine, University of Ljubljana, Ljubljana, Slovenia
[5] Department of Methodology, Faculty of Organizational Sciences, University of Maribor, Kranj, Slovenia

Radiol Oncol 2025; 59(1): 121-131.

Received 5 May 2024
Accepted 5 November 2024

Correspondence to: Assist. Marina Mencinger, M.D., Ph.D., Institute of Oncology Ljubljana, Zaloška 2, SI-1000 Ljubljana, Slovenia.
E-mail: mmencinger@onko-i.si

Disclosure: No potential conflicts of interest were disclosed.

Background. Adrenocortical carcinoma (ACC) is a rare cancer that presents significant diagnostic and therapeutic challenges. We analyzed the management and estimated survival of ACC patients in Slovenia over a 17-year period.

Patients and methods. Patients registered in the National Cancer Registry and treated from 2000 to 2017 were included. The survival and prognostic factors were assessed using the Kaplan-Meier method and Cox regression, respectively.

Results. Forty-eight patients were included in our analysis. At the time of diagnosis, 6%, 42%, 25% and 27% had stage according European Network for the Study of Adrenal Tumors (ENSAT) I, II, III and IV, respectively. Adjuvant treatment with mitotane was assigned to 18 of 34 potentially eligible patients. High-risk patients treated with adjuvant mitotane showed a reduced probability of death, although the difference was not statistically significant. Relapses had numerically higher rate of R1 resection and higher Ki67. Eleven patients underwent first-line therapy with etoposide, doxorubicin, cisplatin and mitotane (EDP-M). Their median progression-free survival was 4.4 months. The median overall survival of entire cohort was 28.9 and the median disease-specific survival (DSS) was 36.2 months. The 5-year DSS rate of ENSAT I, II, III and IV were 100%, 56%, 50% and 0%, respectively. The prognostic value of ENSAT stage and Helsinki score regarding overall survival was confirmed with the multivariate analysis.

Conclusions. The 5-year DSS of our ENSAT II patients was worse than reported in contemporary cohorts. Suboptimal surgery and inconsistent adjuvant therapy with mitotane might have contributed to this outcome. Better outcomes of this rare disease might be accomplished with dedicated teams including various specialties, working towards optimal staging, diagnostic and therapeutic measures.

Key words: adrenocortical carcinoma; Helsinki score; ENSAT stage; systemic treatment; survival; prognostic factors

Introduction

Adrenocortical carcinoma (ACC) is an aggressive orphan tumour. The annual incidence is around two cases per million people.[1] The postoperative disease-free survival rate at five years is less than 50% and the 5-year survival rate for metastatic disease worldwide remains dismal.[2] About 50–60% of

patients with ACC have clinical hormone excess. In most cases, hypercortisolism (Cushing's syndrome) and/or virilisation syndrome due to androgen secretion are observed.[3]

As clinical, laboratory, and imaging features of ACC overlap with other benign and primary or secondary malignant adrenal tumours, the final diagnosis and malignant potential of an adrenal lesion depends largely on sophisticated histopathologic analysis of the surgical specimen. To facilitate and standardize the diagnosis of ACC, several multiparametric scoring systems have been developed based on combined histopathological features, such as the Weiss score and the Helsinki score.[4] The Weiss score considers nine histopathologic parameters and remains one of the most used scoring systems in clinical practice to classify conventional ACC in adults.[5] A more recently developed score, the Helsinki score, focuses on a combination of the Ki67 proliferation index, mitotic rate, and the presence of necrosis. It can be used not only for the diagnosis of conventional ACC, but also for oncocytic and myxoid variants.[6] Two staging systems have been also proposed: TNM staging, which was revised in 2017 (AJCC cancer staging[7]), and the staging system by the European Network for the Study of Adrenal Tumors (ENSAT) in 2009.[8]

According to current clinical practice guidelines, all patients with ACC and a high risk of recurrence after surgery (ENSAT stage III, R1 resection or Ki67 >10%) should receive adjuvant treatment with mitotane.[3] Recently published results of the ADIUVO trial did not support adjuvant treatment with mitotane in patients with low-intermediate risk of recurrence (ENSAT stage I-III, R0 resection and Ki67 ≤ 10%).[9] Only one phase III clinical trial (FIRM-ACT) was conducted in patients with ACC. In this trial, etoposide, doxorubicin, and cisplatin (EDP) plus mitotane resulted in higher response rates and longer progression-free survival than streptozocin plus mitotane as first-line therapy, although there was no significant difference in overall survival.[10] Recently, immune check point inhibitors and cabozantinib have been used successfully in some patients with ACC.[11,12] Other treatment options are experimental at best.[13]

Locoregional therapies are recommended for slowly progressive oligometastatic disease or when a sustained response to systemic therapy has been achieved. In addition to surgery, there are other options such as radiotherapy, radiofrequency ablation and chemoembolization.[3,14]

We performed a retrospective analysis including histopathologic assessment of primary tumours and metastases, systemic treatment patterns, and outcomes of our patients with ACC over nearly two decades (2000-2017). In addition, we identified factors influencing survival.

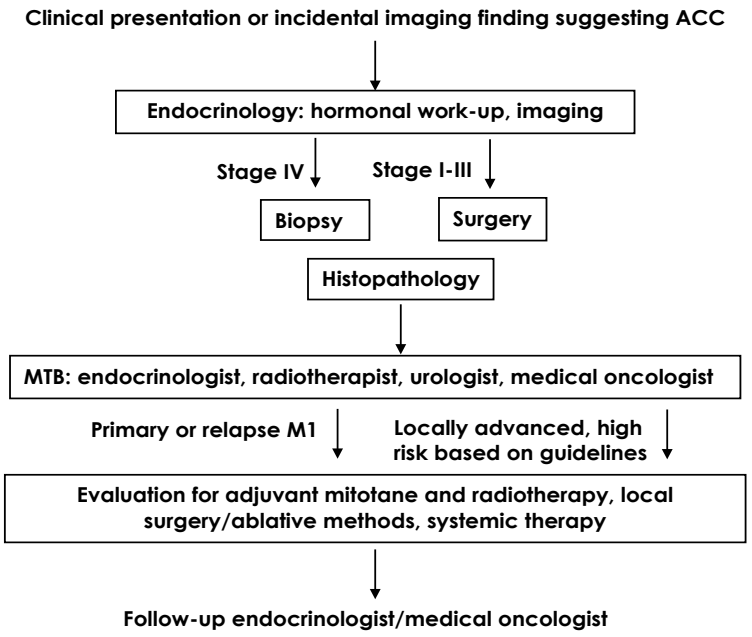

FIGURE 1. A patient flowchart describing the process of diagnostics and treatment decision-making.

ACC = adrenocortical carcinoma; MTB = multidisciplinary tumour board; M1 = metastatic disease

Patients and methods

We conducted a retrospective cross-sectional study including all adult patients who were diagnosed with ACC from year 2000 to 2017 and were treated at the University Medical Centre Ljubljana and the Institute of Oncology Ljubljana. The patient list was taken from the National Cancer Registry. The study protocol was approved by the Review Board and Committee for the Medical Ethics of the Institute of Oncology in Ljubljana (ERIDEK - 0024/2020). A flowchart detailing the diagnostics and treatment decision-making process is shown in Figure 1.

We used patients' medical records to collect their demographic and clinical parameters, data on ENSAT stage at diagnosis, tumour size (defined as the largest diameter in axial plane), biochemically confirmed hormone hypersecretion, surgical treat-

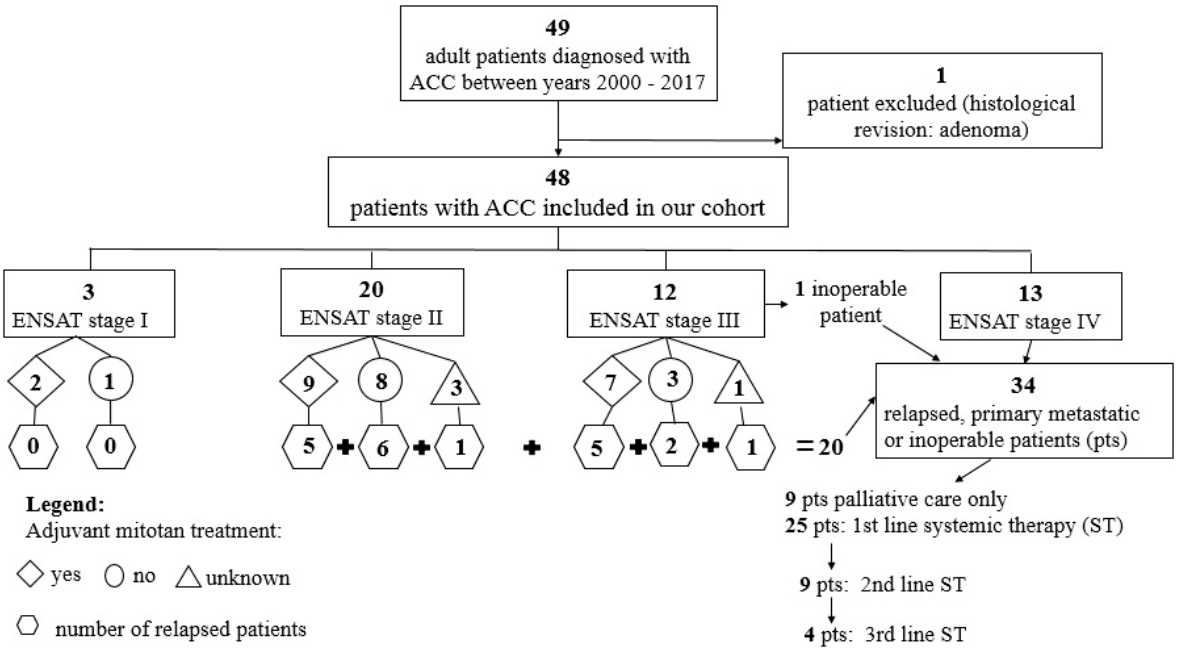

FIGURE 2. Our cohort according to European Network for the Study of Adrenal Tumors (ENSAT) stage, adjuvant mitotane treatment, relapses and different lines of systemic treatment.

ACC = adrenocortical carcinoma; ST = systemic treatment

ment of the primary tumour, status of resection margins, adjuvant radiotherapy and adjuvant mitotane treatment. We explored options for the first, the second and the third line of systemic treatment. Survival analyses and tests for prognostic factors were performed for the entire cohort. In accordance with our sample size, we chose to determine the prognostic significance of three variables: ENSAT stage (I and II versus III and IV), Helsinki score and hypercortisolism (present versus absent). The prognostic value of adjuvant mitotane treatment was analysed for the high-risk patients.[3] In addition, the prognostic value of the Ki67 index in metachronous metastasis or local recurrence (20 or more versus less than 20) was tested in univariate analysis. The cut-off value of 20 was used in analogy to the cut-off values for primary tumours.[15,16]

Two additional assessments were carried out. First, data on local treatment options for metastatic/locally recurrent disease were analysed in detail. Several survival parameters were calculated in patients who underwent surgery for local recurrence/oligometastatic disease. The median treatment-free interval (mTFI) was defined as the time from diagnosis of ACC to resection of the first metachronous metastasis. The median progression-free survival (mPFS) was defined as the time from the local therapy of the first metastasis to the systemic disease progression or death. The median overall survival of this cohort (mOS) was defined as the time from diagnosis of ACC to death.

Second, two experienced pathologists (MV and JJ) reviewed all available archival histologic tissue samples of primary tumours and metastases of the included patients. If multiple metastases or local recurrences were available, only the one that had been histologically analysed first was revised. The Weiss scoring system was used in all adrenalectomy specimens except for the two patients with the oncocytic variant of ACC in which Weiss system tends to overdiagnose malignancy and Lin-Weiss-Bisceglia criteria are applied instead.[17] The Weiss system was only used to evaluate adrenalectomy specimens, as it is not possible to perform the required assessment of venous or capsular invasion in other types of specimens (e.g. needle biopsy, metastasis, excision of recurrent disease).

The Helsinki index and the Ki67 proliferation index were determined using visual estimation method.[18] Immunohistochemistry for Ki67 antigen (clone MIB-1, Dako, 1/50, UltraView) was performed using a Benchmark XT Ventana system according to manufacturer's instructions. The correlation between the Weiss and the Helsinki score of the primary tumours was investigated. The Ki67 index and the Helsinki score of both specimens

were compared in patients in whom the tissue from both, the primary tumour and the first local recurrence or metastasis was available.

Statistical analyses

Data for continuous variables were presented as median and range and for categorical data as frequencies and percentages. The cut-off date for the survival analysis was October 15, 2020. Survival outcomes were calculated using Kaplan-Meier method with 95% confidence intervals and predictors of survival were calculated using Cox proportional hazards regression models. The p-values shown are two sided and the p-value < 0.05 was considered statistically significant. The calculations were performed using the statistic software package IBM SPSS 28.0. Correlation between Weiss and Helsinki score of primary tumours was investigated with Spearman's rank correlation coefficient test.

To further explore the prognostic power of Helsinki score receiver operating characteristic (ROC) analysis was done. Area under the ROC curve (AUC) was calculated to assess the ability of Helsinki score to differentiate between "alive" versus "death" status. The cut-off value of Helsinki score to differentiate between different prognostic groups was determined based on maximizing the Youden index in the context of the ROC curve.

Results

Patients' characteristics

Forty-nine adult patients were diagnosed with ACC at our two centres during the studied period (2000–2017). During histologic revision one patient was diagnosed with adenoma instead of ACC and was excluded from the analysis. Characteristics of all analysed patients and of the 20 patients who relapsed after radical surgery are shown in Table 1. One patient with ENSAT stage III was not treated with radical surgery as the tumour was considered inoperable.

Figure 2 shows our cohort according to ENSAT stage, adjuvant mitotane treatment, relapses and different lines of systemic treatment.

Adjuvant mitotane treatment

Thirty-four patients, who were classified as ENSAT stage I-III underwent surgical removal of the primary tumour and could have been considered eligible for adjuvant mitotane. However, 12 patients (35.3%, median age 49.5 years; 7 females), including 6 patients at high risk of recurrence after surgery (Ki67 >10%[3]); of whom three were classified as ENSAT stage II and three as stage III, were not started on this treatment. Relevant data was absent for further 4 patients (11.8%). The remaining 18 patients (52.9%, median age 63 years; 9 females,) received mitotane. Half of the treated subgroup (or 9 patients) were classified as ENSAT stage II, 38.9% (or 7) as stage III, and 11.1% (or 2) as stage I. Ki67 was > 10% in 14 of these patients (77.8%) with missing data for one patient in ENSAT stage III. Collectively, only two patients at low/intermediate risk of recurrence after surgery (R0, Ki67 ≤ 10%[3]; classified as ENSAT stage I and stage II), received mitotane.

Two patients were followed at another institution, so further data about mitotane treatment was available for 16 patients. Median time from surgery of primary tumour to start of adjuvant mitotane was 26.5 (range 6–126) days, while median duration of treatment was 17.4 (3–73) months with the median daily mitotane dose of 2750 (500 – 7000) mg. All patients were on concurrent hydrocortisone replacement therapy with median daily dose of 40 (15–45) mg. Three patients (18.7%) progressed when on mitotane after median time of 30 (10–31) months of treatment and one patient died of metastatic breast cancer in the 11th month of adjuvant mitotane treatment. All discontinuations of mitotane during adjuvant treatment were permanent. Reason for stopping were adverse effects: gastrointestinal in 2 (25.0%), hepatic in 2 (25.0%) neurocognitive in 1 (12.5%) and other in 3 (37.5%) cases. Data on mitotane plasma concentrations were not obtainable for most patients, so they were not included in the analysis. High-risk patients that received adjuvant mitotane had lower risk of death (HR 0.614, 95% CI 0.207-1.820), but the difference was not statistically significant (p = 0.379).

Adjuvant radiotherapy

Thirty-four patients classified as ENSAT stage I-III underwent surgical removal of the primary tumour. Of these 34, 16 had either R1 resection or/and ENSAT stage III disease. One of these 16 patients had both ENSAT III and R1 resection, 11 had ENSAT III and 4 had R1. Finally, only three of them received adjuvant radiotherapy (RT): one with R1 resection, one with ENSAT III and one with both criteria. All other potential candidates from this group did not receive adjuvant RT (one of them due to treatment refusal); but two other patients without criteria did.

Systemic treatment regimens for inoperable locally advanced or metastatic disease

Thirty-four out of 48 patients had inoperable locally advanced or metastatic disease, either at the time of the primary diagnosis or recurring after surgery. Nine patients were referred to palliative care only. First-line systemic treatment regimens for the remaining 25 patients are listed in Table 2.

The median age of 11 patients who were treated with standard first-line chemotherapy (EDP-mitotane) was 56 years (range 29–70). Their performance status was 0 in 6 patients (54%), 1 in 4 patients (36%) and 2 in 1 patient (9%). Median number of cycles received was 5 (range 2–7). The mPFS was 4.4 months (95% CI 1.5–7.3) and the mOS was 15.8 months (95% CI 7.7–23.8). Two patients achieved partial response (PR), 6 patients had stable disease (SD), and 3 patients had progressive disease (PD). There were no complete responses.

The patient who received treatment with dacarbazine, cyclophosphamide and vincristine were initially diagnosed with pheochromocytoma, but histologic revision from a highly specialized centre confirmed the diagnosis of ACC.

All 25 patients treated with first-line therapy progressed during the therapy or follow-up period; among them, 9 (36%) received 2nd line systemic treatment, which is listed in Table 3 together with responses achieved.

Five patients who received second line therapy with gemcitabine and capecitabine had median number of 2.5 cycles (range 2-5), median progression free survival 2.3 months (95% CI 1.5-3.1) and median overall survival 10.0 months (95% CI 1.9–18.1).

Third line therapy was prescribed to 4 patients: reintroduction of gemcitabine - capecitabine, metronomic therapy with cyclophosphamide, thalidomide plus mitotane, all of whom progressed. One patient received radionuclide therapy with ^{131}I-iodometomidate in a highly specialised centre in Würzburg, Germany, and had survived for 8 months after referral.

Survival rate of ENSAT stage I, II, III and IV

The 5-year overall survival (OS) of patients with ENSAT stage I, II, III and IV was 100%, 50%, 50% and 0%. If stages I/II and III/IV were grouped together the 5-year OS was 56.5% and 24%. The 5-year disease specific survival (DSS) was 100%, 56%, 50% and 0%, respectively. The 5-year OS of patients with ENSAT stage I-III who were diagnosed before year 2010 was 61.9% and of patients with ENSAT stage I-III who were diagnosed after the year 2010 was 42.9%; the difference was not

TABLE 1. Characteristics of all analysed patients and of the patients with European Network for the Study of Adrenal Tumors (ENSAT) I-III that relapsed after surgery with curative intent

Characteristics		All included N = 48 (%)	Relapsed N = 20 (%)
Age: median (range); years		56.6 (21–82)	54.0 (21–72)
Sex	Male	21 (44)	11 (55)
	Female	27 (56)	9 (45)
ENSAT stage at diagnosis	I	3 (6)	0
	II	20 (42)	12 (60)
	III	12 (25)	8 (40)
	IV	13 (27)	N/R
Tumour size: median (range), cm	12 (4–30)		12.5 (5–30)
	Unknown	6	2
Hormone secretion	Yes – GC*	17 (35)	5 (25)
	Yes – O	8 (17)	4 (20)
	No	20 (42)	11 (55)
	Unknown	3 (6)	/
Weiss score (median, range)	6 (4–9)		7 (5–9)
	N/D+	15	1
Ki67 score** (median, range)	20 (1–70)		24 (8–60)
	N/D°	9	1
Helsinki score** (median, range)	28 (1–78)		31 (16–68)
	N/D°	9	1
Resection margins of patients stage I –III treated with curative surgery	R0	26 (76)	17 (85)
	R1	5 (15)	3 (15)
	Rx	3 (9)	/

GC = glucocorticoids; O = other; N/D = not determined; N/R = not relevant;

* = isolated or in combination with other hormones; ** = of primary tumour;

+ due to oncocytic variant (2), unavailability of tissue samples (3): primary not operated - 1 patient; tissue not available at our institutions - 2 patients), only fine needle (6) or core needle biopsy (4) of primary tumour or metastases;

° due to unavailability of tissue samples (3) or only fine needle biopsy of primary tumour or metastases (6)

TABLE 2. First-line systemic treatment regimens for inoperable locally advanced or metastatic disease

Treatment regimen	Patients (N)
EDP-mitotane	11
mitotane (+/- local therapy)	11
etoposide + carboplatin	1
dacarbazine + cyclophosphamide + vincristine	1
tamoxifen	1

EDP = etoposide, doxorubicin and cisplatin

TABLE 3. Second line treatment regimens

Treatment	Patients (N)	Response
gemcitabine + capecitabine +/- mitotane	5	SD: 1 PD: 4
EDP-mitotane	1	PR
pembrolizumab	1	SD
dacarbazine + capecitabine + imatinib	1	PD
vinblastine + interferon alpha-2a	1	PD

EDP = etoposide, doxorubicin and cisplatin; SD = stable disease, PD = progressive disease, PR = partial response

statistically significant (p = 0.132). The mOS of patients with ENSAT stage IV who were diagnosed before and after year 2010 was 1.5 months (95% CI 0.00 – 3.89) and 8.6 months (95% CI 0.42 – 16.73), respectively. This difference was also not statistically significant (p = 0.338).

Survival analysis of the whole cohort and prognostic factors

The median follow-up of the cohort was 30.0 months; 36 (75%) patients died. The mOS was 28.9 months (95% CI 10.25-47.51). Three patients died for other reasons (not ACC). Median DSS was 36.2 months (95% CI 11.8-60.6). In univariate analysis significant impact of ENSAT stage III/IV versus I/II (HR 2.989; 95% CI 1.483-6.023; p = 0.002) and Helsinki score (HR for each additional unit of Helsinki score 1.02; 95% CI 1.003–1.042; p = 0.021) on OS was confirmed, but not of hypercortisolism (HR 1.523; 95% CI 0.772–3.006; p = 0.225). Multivariate analysis confirmed the prognostic value of the ENSAT stage (HR 2.796; CI 95% 1.258–6.212; p = 0.012) and Helsinki score (HR 1.027; 95% CI: 1.005–1.049; p = 0.015). Kaplan-Meier curves of OS according to ENSAT stage groups are shown in Figure 3.

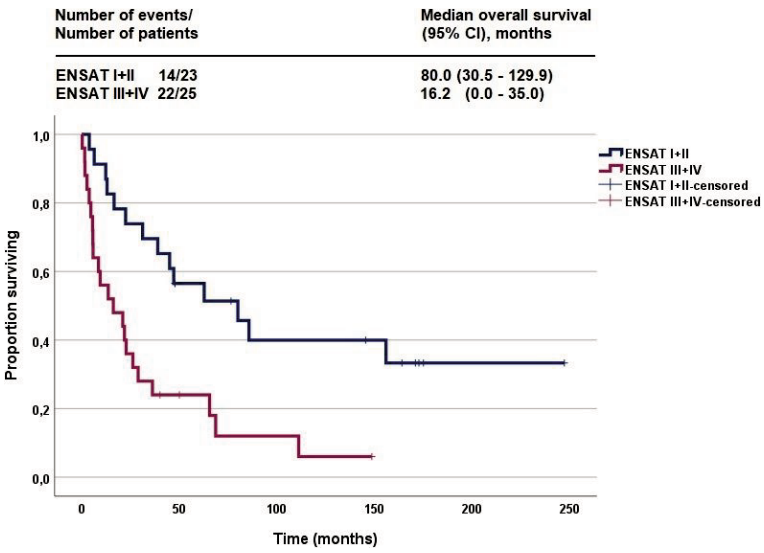

FIGURE 3. Kaplan-Meier curves of overall survival according to European Network for the Study of Adrenal Tumors (ENSAT) stage.

Fourteen of 34 patients who were operated on ACC ENSAT stage I-III remained disease free. Two patients progressed more than 5 years after surgery on primary tumour: 10 years and 9 months with local recurrence treated with surgery and RT, being alive at the time of the data cut-off; 5 years and 7 months with inoperable local recurrence, later further systemic progression and death.

To further explore the prognostic power of Helsinki score ROC analysis was performed which was statistically significant (overall model quality 0.55) with AUC 0.761 (95% CI 0.551-0.971). The cut-off value for Helsinki score determining two prognostically different groups was 19.5.

Locoregional treatment for primary metastatic or relapsing disease

Only 6 patients from our cohort were treated for local recurrence or metastatic disease with local treatment methods. As a rule, surgery was performed; which was combined with radiofrequency ablation (RFA) in only one patient. Patients who received only palliative radiotherapy were not included in this subgroup analysis. Most patients (5 out of 6 or 83%) had metachronous metastases that had occurred three months or more after surgery for the primary tumour.[19] One patient had solitary synchronous liver metastasis that was resected concomitantly with the primary tumour. In another patient, surgery was performed multiple times and combined in the third session with RFA of two liver metastases and one thoracic metastasis that had spread through the diaphragm.

Overall, local recurrences were resected in three (50%) patients, liver metastases in two (33%) patients and lung and vertebral metastases in one (16%) patient. Four patients: two with local recurrence, one with liver metastasis and one after right pneumonectomy of multiple lung metastases received RT after the local surgery. The mTFI was 32.1 months (95% CI 17.6–131.3). The mPFS was 7.29 months (95% CI 0.00-61.2) and mOS was 65.5 months (95% CI 9.4-121.55). The two patients who received RT after surgery for local recurrence both remained disease-free.

Histopathologic features

Histopathologic analysis was possible in 40 of our patients where the diagnosis was confirmed histologically by either resection or core needle biopsy of the primary tumour or metastases. In six patients, the primary tumour or metastases were only verified cytologically and in two patients adrenalectomy was performed but no tissue was available for analysis at our two institutions. Archival tissue blocks of formalin-fixed paraffin-embedded (FFPE) tissue for analysis were obtained after adrenalectomy (35: from 34 patients ENSAT stage I–III and one patient ENSAT stage IV), core needle biopsy of primary tumours (4) or metastatic deposits (2) and resection of the first local recurrences or metastases (10).

Histologic variants of ACC in our cohort were as follows: 35 had conventional ACC, two patients had oncocytic variant, two myxoid (one of them partial myxoid and partial conventional type), and one sarcomatoid variant. Survival of patients with pure myxoid (3.9 months) and sarcomatoid (6.5 months) histologic variant was less than the medium overall survival of the whole cohort (28.9 months). Both patients with oncocytic variant and the patient with partial myxoid variant (ENSAT stage I) were progression-free at the time of the data cut-off.

As far as primary tumours were concerned, Weiss score was determined in 33 patients and Ki67 proliferation index and Helsinki score in samples from 39 patients. These data are shown in Table 1. In 12 metastatic/recurrent samples, the median Ki67 index was 27.5 (range 11–60) and the median Helsinki score was 35.5 (range 19–68). There was no correlation between Weiss and Helsinki scores of primary tumours as the Spearman's correlation coefficient was - 0.092 (p = 0.612). In 11 patients, the tissue from resected primary tumours as well as from the first metastasis/local recurrence was available for investigation. Table 4 shows the comparison between their Ki67 index and Helsinki score.

Patients from 1 to 9 had local recurrence or metachronous metastasis. In the univariate analysis of this cohort those with Ki67 index of the local recurrence/metastasis of 20 or more (N = 6) had a statistically significantly shorter survival from the diagnosis of being metastatic/recurrent than the others (N = 3), HR 1.12 (95% CI 1.01 – 1.25), p = 0.033. Multivariate analysis was not performed due to small sample size.

TABLE 4. Ki67 proliferation index and Helsinki score shown for primary tumour (P) and first metastasis/local recurrence (M)

Patient	Ki67		Helsinki score	
	P	M	P	M
1	16	40	24	48
2	20	16	23	24
3	15	25	23	33
4	20	20	28	23
5	30	30	38	38
6	40	30	48	38
7	15	11	18	19
8	30	20	38	28
9	10	11	18	19
10	40	50	48	50
11	25	50	29	58

Discussion

We have confirmed the poor prognosis of patients with ACC treated in routine clinical practice. In almost half of our patients, the tumour was confined to the adrenal gland and less than one third had primary metastatic disease, which differs from the stage distribution in historic reports. In an older series of 42 patients diagnosed with ACC at Roswell Park Memorial Institute between 1929 and 1977, only 7% of patients had tumour confined to the adrenal gland, while 41% had locally advanced disease and 52% had metastatic disease.[20] Wooten *et al.* reviewed data on ACC patients described in the English literature between 1952 and 1992 and found that only 31.8% of 608 patients had tumours confined to the adrenal gland.[21] However, in contemporary reports from Portugal and Finland, stages were distributed similarly to our cohort, with 43% and 59% of tumours confined to the adrenal gland, respectively.[22,23] The observed contemporary shift in ENSAT staging is likely due to earlier ACC diagnosis, resulting from better availability of radiologic imaging, often performed for unrelated reasons (adrenal incidentalomas).[23]

In our series oncocytic and myxoid variants accounted for five percent of ACCs, while sarcomatoid variant was detected in 2.5% of all ACC included in the histopathologic analysis. The relative frequency of the variant histology is consistent with previously published data.[4] As expected, the clinical behaviour of patients with myxoid and sarcomatoid variants of ACC was

worse than in patients with the classic variant and the behaviour of oncocytic ACC was better. The patient with the partial myxoid variant who was progression-free at the time of the data cut-off, was diagnosed as ENSAT stage I, which was probably the most important factor for their good prognosis. Presumably, favourable stage distribution and access to systemic treatments impacted the median OS of our entire cohort (28.9 months), which is longer than observed historically (14 months).[20] Five-year overall survival rate of our ENSAT stage III (50%) and IV (0%) patients is comparable to published series from Portugal[22] (56%; 0%) and Finnland[23] (stage III/IV 24% for our cohort *vs*. 26%). On the other hand, five-year survival rate of our ENSAT stage II patients is inferior to both Portuguese (stage I/II 56.5% *vs*. 67%) and especially to Finnish cohort (stage I/II 96%). Worse outcome can be at least partially explained by incomplete resections[24] (four patients with ENSAT stage II had R1 resection), less than optimal surgical technique by non-expert surgeon, e.g. not performing concomitant regional lymphadenectomy (four out of five patients operated by non-urologists relapsed), and lack of adjuvant mitotane therapy (three patients with stage II should receive it due to high Ki67 but did not). In addition, some of our early ENSAT stage II patients might have been misclassified due to suboptimal staging, e.g. performing a chest X-ray instead of a CT. A higher percentage of stage I tumours in the Finnish cohort (19% versus 6% in our cohort) might have been also partially responsible for the difference. The five-year overall survival of our ENSAT I-III patients diagnosed after 2010 was not better than before 2010. Less favourable stage distribution without any ENSAT stage I patients diagnosed after year 2010 might have contributed to the lack of improvement. This indicates that during our observed period 2000 – 2017 there was no trend in detecting disease earlier; this trend was only observed in comparison to historic cohorts as discussed previously.

In the Finnish cohort, 79% of patients received adjuvant mitotane therapy, which was reported as a factor associated with better survival in this study.[23] Mitotane was prescribed to everybody after successful surgery except in cases with a very low risk for recurrence according to an expert opinion.[25] No such straight-forward reasoning was present in our cohort. Only 52.9% of the patients started therapy with mitotane, therefore, 6 patients at high risk of recurrence after surgery[3] might have been inappropriately excluded from this treatment. The main reason for this undertreatment was a lack of clinical practice guidelines on the management of ACC[3] during the observed period causing not only uncertainties in the mitotane use, but also patients' refusal of this treatment in some cases. Interestingly, similar inconsistency was also apparent in a recent Italian national cohort study where among 134 operated ACC patients selected just for surveillance 44.4% had Ki67 > 10%.[26] On the positive side, only two of our patients who were started on mitotane were at low/intermediate risk of recurrence after surgery and might have been overtreated.[9] Furthermore, most of our patients started with mitotane within the ideal 6 weeks after surgery. The drug was mostly administered for at least two years, but no longer than 5 years, as recommended.[3] Some patients did not follow this pattern and there were 9 permanent discontinuations due to adverse effects like in other cohorts.[22,23] Hydrocortisone supplementation was a uniform feature of all our patients on mitotane. However, our daily hydrocortisone replacement doses (median 40 mg, range 15–45 mg) might not have been entirely sufficient, as these patients typically require 50 mg or even up to 100 mg daily due to increased hydrocortisone clearance and increased cortisol-binding globulin.[25,27] If our high-risk patients received adjuvant mitotane, they had better survival, as it was previously shown elsewhere.[23] A lack of statistical significance could be attributed to small size of our cohort.

The most frequent combined chemotherapy used for the first line treatment was EDP-M protocol, which is the suggested treatment by the guidelines[3,14] according to the results of FIRM-ACT trial.[10] The outcomes of our patients who received the first line EDP-M treatment in real-life clinical practice were comparable to the results of that trial (mPFS 4.4 months (95% CI 1.5–7.3) versus 5.0 months (95% CI 3.5–6.9), mOS 15.8 months (95% CI 7.7-23.8) versus 14.8 months (95% CI 11.3–17.1), which probably reflects the fact that only patients with a good performance status were treated in such way (mostly WHO PS 0/1 and only 1 patient WHO PS 2). Monotherapy with mitotane was used as frequently for the first line therapy as the EDP-M protocol. Among reasons for the monotherapy with mitotane were poor performance status, comorbidities and patients' refusal of chemotherapy. No comparison between EDP-M protocol and mitotane monotherapy could be made since patients in the latter group were in worse general health.

Further lines of treatment were poorly effective, and few patients were able to receive them (36% of patients treated with the first line and 44% of

patients treated with the second line therapy). In this setting, there is no proven systemic therapy showing improved survival in a randomised controlled trial. Accordingly, the selection of second-line treatment for our patients was based on small phase 2 trials or even case reports.[28,29]

The mOS of patients who received systemic treatment for advanced disease was 13.0 months (95% CI 5.1–20.8) which is less than the mOS of 18.7 months that was observed by the Ohio State University Comprehensive Cancer Centre between years 1997 and 2016.[30] In their cohort 64% of patients received the second line treatment and they also had the possibility to participate in clinical trials. This emphasizes the importance of collaboration with international specialised centres when treating this rare disease.[31] In our cohort the mOS of patients with ENSAT stage IV diagnosed after year 2010 is higher in comparison to those who were diagnosed until year 2010 which may reflect better systemic treatment options in the recent decade, although the difference is not statistically significant. Two patients experienced relapse of the disease more than 5 years from surgery of the primary tumour, which supports the continuation of follow-up beyond 5 years as suggested by the clinical guidelines.[3]

Only six patients were treated with local therapy for relapsing/metastatic disease. Five patients had surgical resection of their solitary metastatic lesions according to the guidelines where routine use of surgery in widespread disease is not recommended.[3] The remaining patient who underwent surgery despite several synchronous metastases died after only three months reflecting the futility of the approach due to more aggressive disease. Contrary to that, the other 5 patients had a slowly progressive disease as indicated by mPFS that was 7.3 months and mTFI that was 31.1 months.

Two patients had been disease-free for more than 10 years after surgery of local recurrence, which further dictates a tight follow up with an early detection of resectable local recurrence to benefit some patients. Both patients with long lasting remission received also postoperative radiation. A large recent study in advanced ACC provided evidence that RT can be effective.[32]

Importantly, only 3 out of our 5 patients who received adjuvant RT, were appropriately selected according to current guidelines. On the other hand, 9 of 13 patients classified as ENSAT stage III and/or having R1 resection were not offered adjuvant RT after surgery for a primary tumour. According to current guidelines adjuvant RT should be considered on an individual basis (in addition to mitotane) in patients with R1 or RX resection or/and in ENSAT stage III.[3] Retrospective data showed that adjuvant RT can reduce the risk of local recurrence but does not prevent distant recurrences and, consequently, does not impact OS.[32] Randomised data on the usefulness of RT after surgical resection of primary tumour and of metastases are needed.

Only a single patient underwent RFA. Other locoregional methods such as stereotactic radiation or chemoembolization of metastases were not used. Contrary to our approach, it is currently recommended to use several local therapeutic measures on an individual basis in addition to surgery for advanced ACC.[3] Furthermore, a recent retrospective analysis of 106 patients supported the use of locoregional treatments to treat ACC recurrence.[33] It is reasonable to assume that close collaboration with an interventional radiologist could have optimised palliation in a larger proportion of our patients with metastases amenable for local treatment.

Not only the disease stage, but also margin-free (R0) resection, glucocorticoid excess and Ki67 proliferation marker were suggested as prognostic factors of survival.[14] Due to small sample size only ENSAT stage, Helsinki score and hypercortisolism were tested as prognostic factors. In multivariant analysis, both ENSAT stage and Helsinki score predicted survival. Helsinki score was validated as a prognostic marker for ACC in several other studies.[6,34,35] Unlike ENSAT stage and Ki67, Helsinki score was not found to have prognostic value in a recent series of patients with ACC from Finland.[23] Helsinki score includes two proliferation markers (Ki67 immunohistochemistry and mitotic count) and necrosis. While the prognostic value of proliferation has been validated in many studies on the Weiss parameter[15,36,37,38,39], the presence of necrosis, on the other hand, has only recently been suggested as the most powerful ominous factor and the best predictor of OS and DFS in ACC patients.[40]

No correlation between Helsinki and Weiss score was found in our cohort, which is different from the findings of another study showing strong positive correlation between these two scoring systems.[41] In addition to low number of patients included in our calculation, technical issues with respect to Ki67 immunohistochemistry on archival samples not allowing optimal evaluation could partially explain these discrepancies.

In our cohort, the cut-off value for the Helsinki score of 19.5 performed best in terms of prognostic stratification. In comparison, Pennanen *et al.*

proposed a lower cut-off value of 17 to distinguish tumours with prolonged survival from rapidly progressing tumours.[34] Duregon *et al.* used the Helsinki scores of 13 and 19 to classify patients into three prognostically distinct groups.[6] In a more recent study, the Helsinki score of 20 was identified as one of the strongest independent predictors of death, being able to distinguish tumours with prolonged survival from those with rapid progression.[35] In our cohort, there were not enough patients with low Helsinki scores to allow stratification into three groups. Several patients with a high Helsinki score had a favourable clinical course, possibly due to relatively small tumour size, complete surgical resection, and good response to treatment. Based on our and similar studies, there is probably no exact cut-off value for the Helsinki score to prognosticate disease, but rather a range between 17 and 20.

We did not find a general tendency towards a higher Ki67 index in metastases compared to primary tumours, as it was shown by study investigating the Ki67 index in primary breast cancer and corresponding metastases.[42] Nevertheless, previously published data for primary ACC tumours[15,16] and our analysis of the Ki67 index of the first local recurrence/metachronous metastasis showed that a Ki67 index < 20 might correlate with a slower progression compared to Ki67 ≥ 20. There is similarity to what was demonstrated in breast cancer, where a low Ki67 index in metastasis was associated with longer survival independently of primary tumour proliferation.[43] Beside TFI indicating aggressiveness of a disease course, analysis of Ki67 in a metastasis may be beneficial to indicate slowly progressing disease as has already been suggested in breast cancer.[43] However, more data are needed to draw any firm conclusions.

Our study has some limitations due to its retrospective methodology and incomplete information from patient charts. In addition, archived FFPE material of varying quality and age, originating from different institutions had to be re-examined. Importantly, patients treated with mitotane were not compared according to their mitotane plasma concentrations due to missing data. Small sample size allowed only few prognostic factors to be tested.

The main strength of our study is the joint effort of pathologists, endocrinologists and medical oncologists to comprehensively review the management of ACC in Slovenia over the last two decades. We tried to highlight the available good practices while also exposing the shortcomings. In particular, the importance of the appropriate histopathology diagnosis and strict adherence to the clinical guidelines if available were pointed out to improve all aspects of management from expert surgery and adjuvant mitotane treatment to locoregional therapies.

Conclusions

Research on ACC is partially hampered by the rarity of this type of cancer. Therefore, the presented real-world data might help the clinicians to improve the management of this rare and often fatal disease. A multidisciplinary approach, as highlighted here, is of paramount importance, and has already been shown to impact survival.[44]

Acknowledgments

We are indebted to Antonela Sabati Rajić, M.D. who started to systematically collect data about our patients with ACC. We also acknowledge the help of everybody else involved in the management of our patients with ACC.

References

1. Kerkhofs TM, Verhoeven RH, Van der Zwan JM, Dieleman J, Kerstens MN, Links TP, et al. Adrenocortical carcinoma: a population-based study on incidence and survival in the Netherlands since 1993. *Eur J Cancer* 2013; **49:** 2579-86. doi: 10.1016/j.ejca.2013.02.034
2. Calabrese A, Basile V, Puglisi S, Perotti P, Pia A, Saba L, et al. Adjuvant mitotane therapy is beneficial in non-metastatic adrenocortical carcinoma at high risk of recurrence. *Eur J Endocrinol* 2019; **180:** 387-96. doi: 10.1530/eje-18-0923
3. Fassnacht M, Dekkers OM, Else T, Baudin E, Berruti A, de Krijger RR, et al. European society of endocrinology clinical practice guidelines on the management of adrenocortical carcinoma in adults, in collaboration with the European network for the study of adrenal tumors. *Eur J Endocrinol* 2018; **179:** G1-G46. doi: 10.1530/EJE-18-0608
4. Gambella A, Volante M, Papotti M. Histopathologic features of adrenal cortical carcinoma. *Adv Anat Pathol* 2023; **30:** 34-46. doi:10.1097/PAP.0000000000000363
5. Weiss LM. Comparative histologic study of 43 metastasizing and nonmetastasizing adrenocortical tumors. *Am J Surg Pathol* 1984; **8:**163-9. doi: 10.1097/00000478-198403000-00001
6. Duregon E, Cappellesso R, Maffeis V, Zaggia B, Ventura L, Berruti A, et al. Validation of the prognostic role of the "Helsinki Score" in 225 cases of adrenocortical carcinoma. *Hum Pathol* 2017; **62:** 1-7. doi: 10.1016/j.humpath.2016.09.035
7. Phan AT, Grogan RH, Rohren E, Perrier ND. Adrenal cortical carcinoma. In: Amin MB, Edge S, Greene F, Byrd DR, Brookland RK, Washington MK, et al, editors. *AJCC Cancer Staging Manual.* 8th edition. New York: Springer; 2016. p. 919-26.
8. Fassnacht M, Johanssen S, Quinkler M, Bucsky P, Willenberg HS, Beuschlein F, et al. Limited prognostic value of the 2004 International Union Against Cancer staging classification for adrenocortical carcinoma: proposal for a revised TNM classification. *Cancer* 2009; **155:** 243-50. doi: 10.1002/cncr.24030

9. Terzolo M, Fassnacht M, Perotti P, Libe R, Kastelan D, Lacroix A, et al. Adjuvant mitotane versus surveillance in low-grade, localised adrenocortical carcinoma (ADIUVO): an international, multicentre, open-label, randomised, phase 3 trial and observational study. *Lancet Diabetes Endocrinol* 2023; **11:** 720-30. doi: 10.1016/S2213-8587(23)00193-6

10. Fassnacht M, Terzolo M, Allolio B, Baudin E, Haak H, Berruti A, et al. Combination chemotherapy in advanced adrenocortical carcinoma. *N Engl J Med* 2012; **366:** 2189-97. doi: 10.1056/NEJMoa1200966

11. Naing A, Meric-Bernstam F, Stephen B, Karp DD, Hajjar J, Ahnert JR, et al. Phase 2 study of pembrolizumab in patients with advanced rare cancers. *J Immunother Cancer* 2020; **8:** e000347. doi: 10.1136/jitc-2019-000347

12. Campbell MT, Balderrama-Brondani V, Jimenez C, Tamsen G, Marcal LP, Varghese J, et al. Cabozantinib monotherapy for advanced adrenocortical carcinoma: a single-arm, phase 2 trial. *Lancet Oncol* 2024; **25:** 649-57. doi: 10.1016/S1470-2045(24)00095-0

13. Altieri B, Ronchi CL, Kroiss M, Fassnacht M. Next-generation therapies for adrenocortical carcinoma. *Best Pract Res Clin Endocrinol Met* 2020; **34:** 101434. doi: 10.1016/j.beem.2020.101434

14. Fassnacht M, Assie G, Baudin E, Eisenhofer G, de la Fouchardiere C, Haar HR, et al. Adrenocortical carcinomas and malignant pheochromocytomas: ESMO-EURACAN clinical practice guidelines for diagnosis, treatment and follow-up. *Ann Oncol* 2020; **31:** 1476-90. doi: 10.1016/j.annonc.2020.08.2099

15. Beuschlein F, Weigel J, Saeger W, Kroiss M, Wild V, Daffara F, et al. Major prognostic role of Ki67 in localised adrenocortical carcinoma after complete resection. *J Clin Endocrinol Metab* 2015; **100:** 841-9. doi: 10.1210/jc.2014-3182

16. Libe R, Borget I, Ronchi CL, Zaggia B, Kroiss M, Kerkhofs T, et al. Prognostic factors in stage III-IV adrenocortical carcinomas (ACC): an European network for the study of adrenal tumor (ENSAT) study. *Ann Oncol* 2015; **26:** 2119-25. doi: 10.1093/annonc/mdv329

17. Bisceglia M, Ludovico O, Di Mattia A, Ben-Dor D, Sandbank J, Pasquinelli G, et al. Adrenocortical oncocytic tumors: report of 10 cases and review of the literature. *Int J Surg Pathol* 2004; **12**: 231-43. doi: 10.1177/106689690401200304

18. Erickson LA. Challenges in surgical pathology of adrenocortical tumours. *Histopathology* 2018; **72:** 82-96. doi: 10.1111/his.13255

19. Laubert T, Habermann JK, Hemmelmann C, Kleemann M, Oevermann E, Bouchard R, et al. Metachronous metastasis- and survival-analysis show prognostic importance of lymphadenectomy for colon carcinomas. *BMC Gastroenterol* 2012; **12**: 24. doi: 10.1186/1471-230X-12-24

20. Didolkar MS, Bescher RA, Elias EG, Moore RH. Natural history of adrenal cortical carcinoma: a clinicopathologic study of 42 patients. *Cancer* 1981; **47:** 2153-61. doi: 10.1002/1097-0142(19810501)47:9<3C2153:aid-cncr2820470908>3E3.0.co;2-6

21. Wooten MD, King DK. Adrenal cortical carcinoma. Epidemiology and treatment with mitotane and a review of the literature. *Cancer* 1993; **72:** 3145-55. doi: 10.1002/1097-0142(19931201)72:11<3145::AID-CNCR2820721105>3.0.CO;2-N

22. Souteiro P, Donato S, Costa C, Pereira CA, Simoes-Pereira J, Oliveira J, et al. Diagnosis, treatment and survival analysis of adrenocortial carcinomas: a multicentric study. *Hormones* 2020; **19:** 197-203. doi: 10.1007/s42000-019-00161-1

23. Kostiainen I, Hakaste L, Kejo P, Parviainen H, Laine T, Löyttyniemi E, et al. Adrenocortical carcinoma: presentation and outcome of a contemporary patient series. *Endocrine* 2019; **65:** 166-74. doi:10.1007/s12020-019-01918-9

24. Margonis GA, Kim Y, Prescott JD, Tran TB, Postlewait LM, Maithel SK, et al. Adrenocortical carcinoma: Impact of surgical margin status on long-term outcomes. *Ann Surg Oncol* 2016; **23:** 134-41. doi: 10.1245/s10434-015-4803-x

25. Fassnacht M, Allolio B. Clinical management of adrenocortical carcinoma. *Best Pract Res Clin Endocrinol Metabol* 2009; **23:** 273-89. doi: 10.1016/j.beem.2008.10.008

26. Puglisi S, Calabrese A, Ferrau F, Violi MA, Lagana M, Grisanti S, et al. New findings on presentation and outcome of patients with adrenocortical cancer: results from a national cohort study. *J Clin Endocrinol Metab* 2023; **108:** 2517-25. doi: 10.1210/clinem/dgad199

27. Chortis V, Taylor AE, Schneider P, Tomlinson JW, Hughes BA, O'Neil DM, et al. Mitotane therapy in adrenocortical cancer induces CYP3A4 and inhibits 5α –reductase, explaining the need for personalized glucocorticoid and androgen replacement. *J Clin Endocrinol Metab* 2013; **98:** 161-71. doi: 10.1210/jc.2012-2851

28. Henning JE, Deutschbein T, Altieri B, Steinhauer S, Kircher S, Sbiera S, et al Gemcitabine-based chemotherapy in adrenocortical carcinoma: a multicentre study of efficacy and predictive factors. *J Clni Endocrinol Metab* 2017; **102:** 4323-32. doi: 10.1210/jc.2017-01624

29. Kroiss M, Deutschbein T, Schlötelburg W, Ronchi CL, Hescot S, Körbl D, et al. Treatment of refractory adrenocortical carcinoma with thalidomide: analysis of 27 patients from the European Network for the Study of Adrenal Tumours registry. *Exp Clin Endocrinol Diabetes* 2019; **127:** 578-84. doi: 10.1055/a-0747-5571

30. Owen DH, Patel S, Wei L, Phay JE, Shirley LA, Kirschner LS, et al. Metastatic adrenocortical carcinoma: a single institutional experience. *Horm Cancer* 2019; **10:** 161-7. doi: 10.1007/s12672-019-00367-0

31. Hescot S, Debien V, Hadoux J, Drui D, Haissaguerre M, de la Fouchardiere C, et al. Outcome of adrenocortical carcinoma patients included in early phase clinical trials: Results from the French network ENDOCAN-COMETE. *Eur J Cancer* 2023; **189:** 112917. doi: 10.1016/j.ejca.2023.05.006

32. Kimpel O, Schindler P, Schmidt-Pennington L, Altieri B, Megerle F, Haak H. et al. Efficacy and safety of radiation therapy in advanced adrenocortical carcinoma. *Br J Cancer* 2023; **128:** 586-93. doi: 10.1038/s41416-022-02082-0

33. Calabrese A, Puglisi S, Borin C, Basile V, Perotti P, Pia A, et al. The management of postoperative disease recurrence in patients with adrenocortical carcinoma: a retrospective study in 106 patients. *Eur J Endocrinol* 2023; **188:** 118-24. doi: 10.1093/ejendo/lvad002

34. Pennanen M, Heiskanen I, Sane T, Remes S, Mustonen H, Haglund C, et al. Helsinki score-a novel model for prediction of metastases in adrenocortical carcinomas. *Hum Pathol* 2015; **46:** 404-10. doi: 10.1016/j.humpath.2014.11.015

35. Pato E, Srougi V, Zerbini C, Ledesma FL, Tanno F, Almeida MQ, et al. Clinical and pathological predictors of death for adrenocortical carcinoma. *J Endocr Soc* 2024; **8:** 1-6. doi: 10.1210/jendso/bvad170

36. Mete O, Gucer H, Kefeli M, Asa SL. Diagnostic and prognostic biomarkers of adrenal cortical carcinoma. *Am J Surg Pathol* 2018; **42:** 201-13. doi: 10.1097/PAS.0000000000000943

37. Giordano TJ. The argument for mitotic rate-based grading for the prognostication of adrenocortical carcinoma. *Am J Surg Pathol* 2011; **35:** 471-3. doi: 10.1097/PAS.0b013e31820bcf21

38. Martins-Filho SN, Almeida MQ, Soares I, Wakamatsu A, Alves VAF, Fragoso MCBV, et al. Clinical impact of pathological features including the Ki-67 labeling index on diagnosis and prognosis of adult and pediatric adrenocortical tumors. *Endocr Pathol* 2021; **32:** 288-300. doi: 10.1007/s12022-020-09654-x

39. Morimoto R, Satoh F, Murakami O, Suzuki T, Abe T, Tanemoto M, et al. Immunohistochemistry of a proliferation marker Ki67/MIB1 in adrenocortical carcinomas: Ki67/MIB1 labeling index is a predictor for recurrence of adrenocortical carcinoma. *Endocr J* 2008; **55:** 49-55. doi: 10.1507/endocrj.k07-079

40. Luconi M, Cantini G, van Leeuwaarde RS, Roebaar R, Fei L, Propato AP, et al. Prognostic value of microscopic tumor necrosis in adrenal cortical carcinoma. *Endocr Pathol* 2023; **34:** 224-33. doi: 10.1007/s12022-023-09760-6

41. Angelousi A, Kyriakopoulos G, Athanasouli F, Dimitriadi A, Kassi E, Aggeli C, et al. The role of immunohistochemical markers for the diagnosis and prognosis of adrenocortical neoplasms. *J Pers Med* 2021; **11:** 208. doi: 10.3390/jpm11030208

42. Kareem T, Kimler BF, Davis MK, Fan F, Tawfik O. Ki-67 expression in axillary lymph node metastases in breast cancer is prognostically significant. *Hum Pathol* 2013; **44:** 39-46. doi: 10.1016/j.humpath.2012.05.00

43. Falato C, Lorent J, Tani E, Karlsson E, Wright PK, Bergh J, et al. Ki67 measured in metastatic tissue and prognosis in patients with advanced breast cancer. *Breast Cancer Res Treat* 2014; **147:** 407-14. doi: 10.1007/s10549-014-3096-2

44. Tizianel I, Caccese M, Torresan F, Lombardi G, Evangelista L, Crimì F, et al. The overall survival and progression-free survival in patients with advanced adrenocortical cancer is increased after the multidisciplinary team evaluation. *Cancers* 2022; **14:** 3904. doi: 10.3390/cancers14163904

research article

Effectiveness of tramadol or topic lidocaine compared to epidural or opioid analgesia on postoperative analgesia in laparoscopic colorectal tumor resection

Alenka Spindler-Vesel[1,2], Matej Jenko[1,2], Ajsa Repar[3], Iztok Potocnik[2,3], Jasmina Markovic-Bozic[1,2]

[1] Clinical Department of Anaesthesiology and Intensive Care Medicine, University Medical Centre Ljubljana, Ljubljana, Slovenia

[2] Medical Faculty, University of Ljubljana, Slovenia

[3] Department of Anaesthesiology and Intensive Care, Institute of Oncology Ljubljana, Slovenia

Radiol Oncol 2025; 59(1): 132-138.

Received 18 June 2024
Accepted 24 October 2024

Correspondence to: Assist. Prof. Jasmina Markovič Božič, M.D., Ph.D., Clinical Department of Anaesthesiology and Surgical Intensive Therapy. University Medical Centre Ljubljana, Zaloška c. 7, 1525 Ljubljana, Slovenia. E-mail: jasmina.markovic1@kclj.si

Disclosure: No potential conflicts of interest were disclosed.

Background. Chronic postoperative pain is the most common postoperative complication that impairs quality of life. Postoperative pain gradually develops into neuropathic pain. Multimodal analgesia targets multiple points in the pain pathway and influences the mechanisms of pain chronification.

Patients and methods. We investigated whether a lidocaine patch at the wound site or an infusion of metamizole and tramadol can reduce opioid consumption during laparoscopic colorectal surgery and whether the results are comparable to those of epidural analgesia. Patients were randomly divided into four groups according to the type of postoperative analgesia. Group 1 consisted of 20 patients who received an infusion of piritramide. Group 2 consisted of 21 patients who received an infusion of metamizole and tramadol. Group 3 consisted of 20 patients who received patient-controlled epidural analgesia. Group 4 consisted of 22 patients who received piritramide together with a 5% lidocaine patch on the wound site. The occurrence of neuropathic pain was also investigated.

Results. Piritramide consumption was significantly lowest in group 3 on the day of surgery and on the first and second day after surgery. Group 4 required significantly less piritramide than group 1 on the day of surgery and on the first and second day after surgery. The group with metamizole and tramadol required significantly less piritramide than groups 1 and 4 on the first and second day after surgery. On the day of surgery, this group required the highest amount of piritramide.

Conclusions. Weak opioids such as tramadol in combination with non-opioids such as metamizole were as effective as epidural analgesia in terms of postoperative analgesia and opioid consumption. A lidocaine patch in combination with an infusion of piritramide have been able to reduce opioid consumption.

Key words. laparoscopic surgery; colorectal tumor; postoperative analgesia; topical analgesia; epidural analgesia; opioid analgesia

Introduction

Chronic postoperative pain is one of the most common postoperative complications that severely impair patients' quality of life. It occurs in about 10% of patients after major surgery and is a major health and economic problem. It typically starts as acute postoperative pain that is difficult

to control and gradually turns into persistent neuropathic pain. Multimodal analgesics have the potential to reduce acute postoperative pain and target multiple points in the pain pathway. For this reason, postoperative pain management should be multimodal and opioid sparing.[1] Thoracic epidural analgesia could alleviate pain after laparoscopic surgery.[2-4] Although ERAS guidelines recommend the use of less invasive techniques for pain relief[5-8], opioids are frequently used perioperatively despite their side effects.[9-11] Non-opioids and 5% lidocaine patches applied topically could effectively reduce the use of opioids and their side effects.[12,13]

Indeed, efficient perioperative pain management is important to prevent late neuropathic pain, even after laparoscopic lower abdominal surgery. The incidence is generally low compared to open surgery.[14]

In comparison to epidural or opioid analgesia, we wanted to investigate whether a lidocaine patch at the wound site or an infusion of metamizole and tramadol can reduce opioid consumption in laparoscopic colorectal surgery and whether the results are comparable to those of epidural analgesia. We also compared the incidence of postoperative neuropathic pain between the groups.

The primary outcome of this study was opioid consumption (piritramide) during the postoperative period, measured at three time points (immediately after surgery, the first postoperative day, and the second postoperative day). Secondary outcomes included pain assessment (VAS scores) and the incidence of postoperative neuropathic pain.

Patients and methods

A prospective, randomised study with four parallel groups was conducted at the University Medical Centre (UMC) Ljubljana. The study included patients from the Clinical Department of Abdominal Surgery who were categorised as high-risk ASA (American Society of Anaesthesiologists) class 2–3 surgical patients. Adult patients who had undergone laparoscopic colorectal tumor resection were included in the study. Exclusion criteria included minors, pregnant women, patients undergoing laparotomy and patients undergoing palliative procedures.

The study was approved by the Slovenian National Medical Ethics Committee (151/03/09, 220/03/09, 148/06/11) and registered with Clinical Trials under the ID number NCT04719884.

Each patient was visited by a member of the research team one day prior to surgery to obtain informed consent and clarify any questions. Patients were randomised into four groups based on the type of postoperative analgesia. They were randomly assigned to one of four treatment groups using computer-generated random numbers. Randomization was performed prior to surgery by an independent statistician (simple randomisation was used), and allocation was concealed until the intervention was applied.

Group 1 consisted of 20 patients who received an infusion of piritramide (patient-controlled analgesia, PCA). Group 2 consisted of 21 patients who received an infusion of metamizole and tramadol.

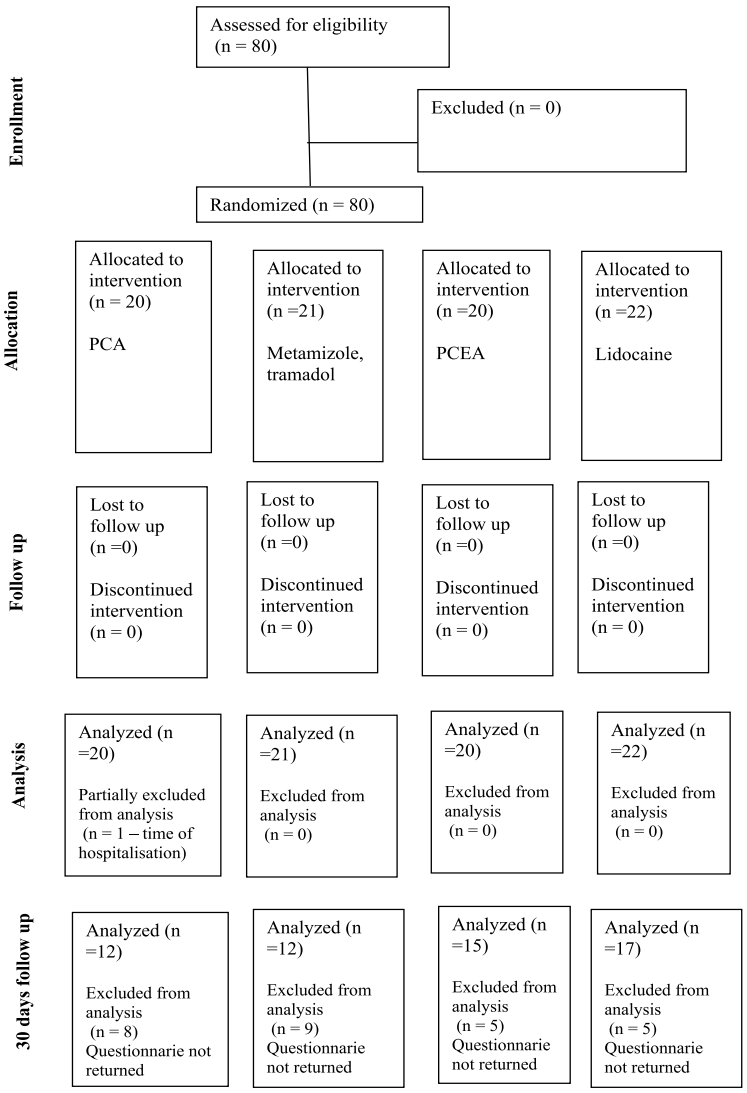

FIGURE 1. Consort chart of the study. Thet diagram shows the flow of participants through each stage of a randomized trial.

PCA = patient-controlled analgesia; PCEA = patient-controlled epidural analgesia

TABLE 1. General patients' and procedure characteristics

	Group 1 (PCA)	Group 2 (tramadol-metamizole)	Group 3 (PCEA)	Group 4 (PCA and lidocaine)	p
Age (years)	59	65	60	59	0,394
Weight (kg)	76	75	79	76	0,833
Wound length (cm)	6,55	7,17	7,45	7,90	0,286
Duration of surgery (min)	139	133	117	112	0,024
Duration of hospitalization (days)	8	9	8	10	0,380
Day of first defecation	4	4	5	4	0,571

ANOVA test was used for comparison. p value of < 0.05 is statistically significant.

PCA = patient-controlled analgesia; PCEA = patient-controlled epidural analgesia

Group 3 consisted of 20 patients who received patient-controlled epidural analgesia (PCEA). Group 4 consisted of 22 patients who received PCA together with a 5% lidocaine patch on the wound site (Figure 1).

Anaesthesia was performed by two anaesthetists, with the technique being uniform in all groups. Standard monitoring was performed. On admission, intravenous access was established, and patients were premedicated with midazolam. In group 3, a thoracic epidural catheter was inserted at the level of Th 7–8 in the left lateral position before the procedure and tested with 3 ml of 2% lidocaine.

Standard induction protocols were followed, including propofol (1–2 mg/kg) or etomidate (0.2 mg/kg), fentanyl (3–5 μg/kg) and vecuronium (0.1 mg/kg) or rocuronium (0.6 mg/kg). Anaesthesia was maintained with sevoflurane to keep the BIS value between 40 and 55. Analgesia was supplemented with fentanyl in groups 1, 2 and 4, while levobupivacaine 0.5% epidural was administered in group 2.

Muscle relaxation was monitored and vecuronium (2–4 mg) or rocuronium (10–20 mg) was administered depending on the TOF values. At the end of the procedure, the volatile agents were discontinued, and the muscle blockade was reversed with neostigmine (2.5 mg) and atropine (1 mg) or sugammadex (2 mg/kg).

Postoperative analgesia began during wound closure: in group 1 with PCA (piritramide 0.5 mg/ml; infusion 1.5 mg/h, bolus 1.5 mg, lockout 30 minutes), in group 2 with an infusion of tramadol 300 mg and metamizole 2.5 g (in 500 ml 0.9% NaCl, infusion rate 40 ml/h), in group 3 with PCEA (200 ml 0.125% levobupivacaine, 4 mg morphine, 0.075 mg clonidine; infusion 5 ml/h, bolus 5 ml, cut-off time 30 minutes) and in group 4 with PCA (piritramide 0.5 mg/ml; infusion 0.5 mg/h, bolus 1.5 mg, cut-off time 20 minutes) in combination with a 5% lidocaine patch on both sides of the wound. The plaster was removed after 12 hours and reapplied after a 12-hour break. In all groups, paracet-

TABLE 2. Comparison of piritramide consumption between the group pairs

Comparison		P value (day 0)	P value (day 1)	P value (day 2)
PCA	PCEA	0.938	< 0.001	< 0.001
PCA	tramadol-metamizole	0.083	< 0.001	< 0.001
PCA	PCA + lidocaine	0.995	0.003	0.026
PCEA	tramadol-metamizole	0.008	0.352	0.038
PCEA	PCA + lidocaine	0.862	< 0.001	< 0.001
PCA + lidocaine	tramadol-metamizole	0.030	< 0.001	< 0.001

Dwass-Steel-Critchlow-Fligner pairwise comparisons. p value of < 0.05 is statistically significant.

PCA = patient-controlled analgesia; PCEA = patient-controlled epidural analgesia

amol 1g/6–8hrs iv was administered regularly. In groups 1, 3 and 4, metamizole 2,5g/12hrs iv was also prescribed. The prescribed analgesia in all four groups was not changed during the study, as it would have made it more difficult to evaluate the difference in additional bolus consumption of piritramide. We monitored the side effects of the analgesics. Appropriate antiemetic therapy was planned, but our patients did not require it. No significant sedative effects were observed.

After the operation, the patients were transferred to the post-operative care unit (PACU) and later to the intensive care unit of the abdominal surgery department. They received additional boluses of piritramide (3 mg) if required. The duration of the operation and the length of the wound were recorded intraoperatively. In the following two postoperative days, data such as visual analogue scale (VAS) scores, piritramide consumption, length of hospital stay and readmission to hospital were recorded. VAS was evaluated every six hours and when the additional piritramide bolus was needed.

The DN4 (*Douleur Neuropathique* 4) and Pain Detect questionnaires were used to assess the occurrence of neuropathic pain 30 days after surgery.

Statistical analysis

The results were analysed with R: A language and environment for statistical computing. (R Foundation for Statistical Computing, Vienna, Austria). The ANOVA test was used to determine differences between the study groups. Pairwise comparisons were performed using the Dwass-Steel-Critchlow-Fligner test. A p-value of < 0.05 was considered statistically significant.

Power analysis

A power analysis was performed to determine the appropriate sample size. Based on previous data from patients treated at our department and clinical relevance, we assumed a minimum effect size of 0.5 (Cohen's d) for the reduction in opioid consumption between groups (based on previous data, this corresponds to 3mg of piritramide). This effect size was considered clinically significant. To detect this effect with 80% power and a significance level of 0.05, a total of 80 patients (approximately 20 per group) were required. The calculation was performed using standard formulas

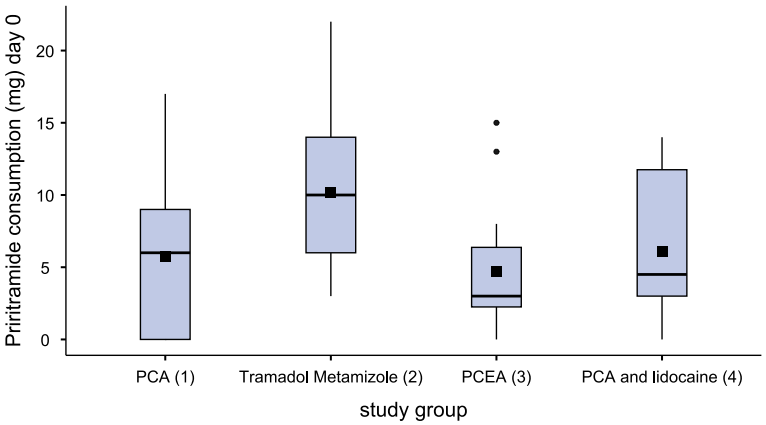

FIGURE 2. Piritramide consumption on day of surgery (day 0).

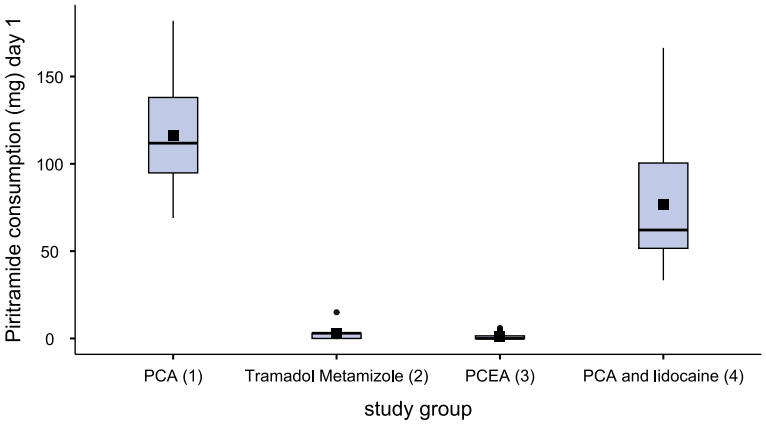

FIGURE 3. Piritramide consumption on first postoperative day (day 1).

PCA = patient-controlled analgesia; PCEA = patient-controlled epidural analgesia

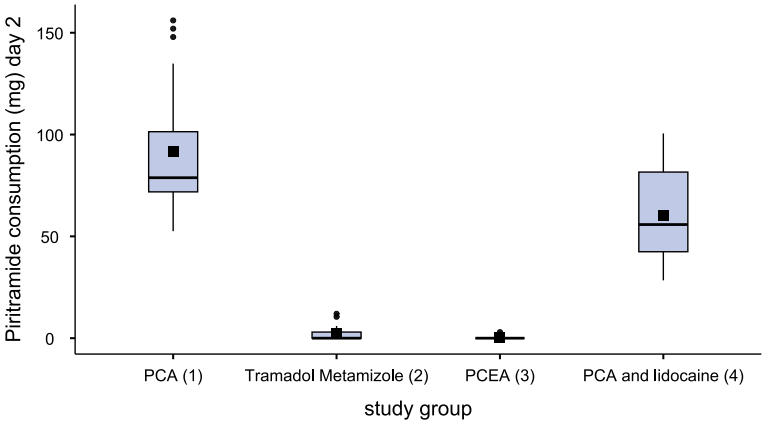

FIGURE 4. Piritramide consumption on second postoperative day (day 2).

PCA = patient-controlled analgesia; PCEA = patient-controlled epidural analgesia

TABLE 3. The scores from Pain Detect and DN4 (*Douleur Neuropathique* 4) questionnaires in the study groups

Group (No. of answers)	Pain score (mean ± SD)	DN4 (mean ± SD)
PCA (12)	0	0
Tramadol and metamizole (12)	1.2 ±2.1	0.2 ± 0.4
PCEA (15)	0.1 ± 0.5	0.1 ± 0.4
Lidocaine (17)	0.06 ± 0.2	0

ANOVA test was used for comparison. p value of < 0.05 is statistically significant.

DN4 = Douleur Neuropathique 4; PCA = patient-controlled analgesia; PCEA = patient-controlled epidural analgesia

for comparing means in four independent groups (ANOVA).

Results

We analysed the data of 20 patients in group 1, 21 patients in group 2, 20 patients in group 3 and 22 patients in group 4 (Figure 1). The general patient characteristics, length of wound and duration of surgery are shown in Table 1.

The duration of surgery was significantly shorter in the lidocaine group ($p = 0.024$). There was no statistically significant difference between the characteristics listed in Table 1 with regard to the gender or ASA status of the patients. In each group, patients were equally distributed in terms of gender.

In group 1, there were 19 colon resections and 1 rectal resection. In group 2, there were 8 rectal resections and 12 colon resections. In group 3, there were 2 rectal resections and 18 colon resections, while in group 4, there were 3 rectal resections and 19 colon resections. All surgeries were laparoscopic. Patients in our study did not undergo additional anorectal excision during rectal surgeries. The duration of rectal surgeries and the length of postoperative wounds were comparable to bowel resections; therefore, we treated all surgeries as a group of laparoscopic colorectal resections.

There was no statistically significant difference in VAS scores between the groups. The VAS scores were low (below 3).

Figures 2–4 and Table 2 show the comparison of piritramide consumption on three consecutive postoperative days.

After surgery, patients in group 3 (PCEA) required less piritramide than patients in group 2 (tramadol-metamizole) ($p < 0.08$). There were no differences in piritramide consumption between patients in groups 2 and 3 on the first day after surgery, but on the second day after surgery, patients in group 3 required less piritramide than those in group 2 ($p < 0.038$). Similarly, patients in group 4 (PCA + lidocaine) required less piritramide than patients in group 2 ($p < 0.03$) on the day of the surgery. But on the first and second day after surgery, patients in groups 2 and 3 received statistically significantly less piritramide than patients in groups 1 and 4 ($p < 0.001$). Patients in group 4 required statistically significantly less piritramide than patients in group 1 both on the first day ($p < 0.003$) and on the second day after surgery ($p < 0.026$).

There were no significant differences between groups in Pain Detect or DN4 questionnaires scores using the Anova test (Table 3).

Discussion

Postoperative pain is managed in different ways in patients undergoing elective colorectal tumor resection, affecting patient outcomes and pain scores.

The epidural catheter provides superior analgesia for colorectal surgery, whether performed laparoscopically or with laparotomy.[15] However, due to the frequent prolongation of the bowel recovery period and potential complications associated with catheter insertion, epidural analgesia is often replaced by other methods in minimally invasive procedures.[2,4,5,16] Intravenous opioid-based patient-controlled analgesia (PCA) is a common method of postoperative analgesia, but peripheral analgesics could also be used to attenuate the side effects of opioids.[7,9,11] Therefore, group 2 in our study received an infusion of the weak opioid tramadol and metamizole. We found that the consumption of piritramide was significantly reduced in this group on two consecutive days after surgery compared to group 1 (PCA) and group 4 (PCA + lidocaine). However, there was a significant requirement for additional opioids immediately after surgery. As expected, no additional analgesia was required in the epidural analgesia group.

Pain scores measured using the VAS scale were low (below 3), indicating adequate postoperative analgesia in all groups.

Several studies have shown that intravenous administration of lidocaine (for both laparoscopic and laparotomy procedures) improves postoperative analgesia in colorectal surgery, improves bowel function and shortens hospital stay.[6,17-22] Studies

have also shown potential benefits in terms of long-term cancer outcomes.[23]

Patients receiving lidocaine reported low pain scores, but piritramide consumption was relatively high due to the additional PCA infusion. It is likely that total opioid consumption would have been significantly lower if only PCA bolus infusions had been programmed.[22,24]

The use of lidocaine patches did not result in lower opioid consumption after thoracotomy and sternotomy.[25] In a study of 103 patients undergoing elective laparoscopic colorectal surgery, thoracic epidural anaesthesia, spinal diamorphine and PCA were compared. It was found that the use of patient-controlled analgesia was associated with significantly higher postoperative pain scores and higher pain intensity.[26]

Recovery of bowel function after laparoscopic colorectal surgery was similar in the epidural analgesia and intravenous lidocaine groups, although epidural analgesia provided better pain relief.[27]

In our study, topical lidocaine was applied to the wound site in group 4. Compared to the PCA group, topical lidocaine also reduced piritramide consumption but had no favourable effects on bowel function, probably due to the local effect of lidocaine rather than systemic effects. No differences were observed in the postoperative recovery of bowel function in any of our groups. This finding is consistent with observations in another study of open colon resection, in which no differences were found between the epidural, intravenous opioid or intravenous lidocaine groups in terms of recovery of bowel function, length of hospital stay and postoperative pain control.[28]

67% of participants (56/83) completed pain questionnaires and no neuropathic pain was noted 30 days after surgery, which is consistent with observations from another study of laparoscopic colorectal surgery.[29] The incidence of neuropathic pain is generally not expected in laparoscopic abdominal surgery and does not exceed 5%.[14] However, the reported incidence of chronic postoperative pain after laparoscopic colorectal surgery is 17%, similar to laparotomy.[30]

Conclusions

In laparoscopic colorectal tumor surgery, weak opioid tramadol in combination with non-opioid metamizole could be as effective as patient-controlled epidural analgesia (PCEA) in terms of postoperative analgesia and opioid consumption. A lidocaine patch in combination with an infusion of piritramide (PCA) could reduce opioid consumption.

References

1. Leslie JB, Viscusi ER, Pergolizzi JV Jr, Panchal SJ. Anesthetic routines: the anesthesiologist's role in GI recovery and postoperative ileus. *Adv Prev Med* 2010; **2011:** 976904. doi: 10.4061/2011/976904
2. Pirie K, Traer E, Finniss D, Myles PS, Riedel B. Current approaches to acute postoperative pain management after major abdominal surgery: a narrative review and future directions. *Br J Anaesth* 2022; **129:** 378-93. doi: 10.1016/j.bja.2022.05.029
3. Liu SS, Carpenter RL, Mackey DC. Effects of perioperative analgesic technique on rate of recovery after colon surgery. *Anesthesiology* 1995; **84:** 757-65. doi: 10.1097/00000542-199510000-00015
4. Novak-Jankovič V, Markovič-Božič J. Regional anaesthesia in thoracic and abdominal surgery. *Acta Clin Croat* 2019; **58(Suppl 1):** 96-100. doi: 10.20471/acc.2019.58.s1.14
5. Reidel MA, Knaebel HP, Seiler CM, Knauer C, Motsch J, Victor N, et al. Postsurgical pain outcome of vertical and transverse abdominal incision: design of a randomized controlled equivalence trial [ISRCTN60734227]. *BMC Surg* 2003; **3:** 9. doi: 10.1186/1471-2482-3-9
6. Herroeder S, Pecher S, Schonherr ME, Kaulitz G, Hahnenkamp K, Friess H, et al. Systemic lidocaine shortens length of hospital stay after colorectal surgery. *Ann Surg* 2007; **246:** 192-200. doi: 10.1097/SLA.0b013e31805dac11
7. Kietzmann D, Bouillon T, Hamm C, Schwabe K, Schenk H, Gundert-Remy U, et al. Pharmacodynamic modelling of the analgesic effects of piritramide in postoperative patients. *Acta Anaesthesiol Scand* 1997; **41:** 888-94. doi: 10.1111/j.1399-6576.1997.tb04805.x
8. Gustafsson UO, Scott MJ, Hubner M, Nygren J, Demartines N, Francis N, et al. Guidelines for perioperative care in elective colorectal surgery: Enhanced Recovery After Surgery (ERAS®) Society Recommendations: 2018. *World J Surg* 2019; **43:** 659-95. doi: 10.1007/s00268-018-4844-y
9. Salicath JH, Yeoh EC, Bennett MH. Epidural analgesia versus patient-controlled intravenous analgesia for pain following intra-abdominal surgery in adults. *Cochrane Database Syst Rev* 2018; **8:** CD010434. doi: 10.1002/14651858.CD010434.pub2
10. Lindberg M, Franklin O, Svensson J, Franklin KA. Postoperative pain after colorectal surgery. *Int J Colorectal Dis* 2020; **35:** 1265-72. doi: 10.1007/s00384-020-03580-4
11. Angst MS and Clark JD. Opioid-induced hyperalgesia: a qualitative systematic review. *Anesthesiology* 2006; **104:** 570-87. doi: 10.1007/s00384-020-03580-4
12. Smoker J, Cohen A, Rasouli MR, Schwenk ES. Transdermal lidocaine for perioperative pain: a systematic review of the literature. *Curr Pain Headache Rep* 2019; **23:** 89. doi: 10.1007/s11916-019-0830-9
13. de Queiroz VKP, da Nóbrega Marinho AM, de Barros GAM. Analgesic effects of a 5% lidocaine patch after cesarean section: a randomized placebo-controlled double-blind clinical trial. *J Clin Anesth* 2021; **73:** 110328. doi: 10.1016/j.jclinane.2021.110328
14. Shin JH and Howard FM. Abdominal wall nerve injury during laparoscopic gynecologic surgery: incidence, risk factors, and treatment outcomes. *J Minim Invasive Gynecol* 2012; **19:** 448-53. doi: 10.1016/j.jmig.2012.03.009
15. Perivoliotis K, Sarakatsianou C, Georgopoulou S, Tzovaras G, Baloyiannis I. Thoracic epidural analgesia (TEA) versus patient-controlled analgesia (PCA) in laparoscopic colectomy: a systematic review and meta-analysis. *Int J Colorectal Dis* 2019; **34:** 27-38. doi: 10.1007/s00384-018-3207-3
16. Guay J, Nishimori M, Kopp S. Epidural local anaesthetics versus opioid-based analgesic regimens for postoperative gastrointestinal paralysis, vomiting and pain after abdominal surgery. *Cochrane Database Syst Rev* 2016; **7:** CD001893. doi: 10.1002/14651858.CD001893.pub2
17. McCarthy GC, Megalla SA, Habib AS. Impact of intravenous lidocaine infusion on postoperative analgesia and recovery from surgery: a systematic review of randomized controlled trials. *Drugs* 2010; **70:** 1149-63. doi: 10.2165/10898560-000000000-00000

18. Sun Y, Li T, Wang N, Yun Y, Gan TJ. Perioperative systemic lidocaine for postoperative analgesia and recovery after abdominal surgery: a meta-analysis of randomized controlled trials. *Dis Colon Rectum* 2012; **55:** 1183-94. doi: 10.1097/DCR.0b013e318259bcd8

19. Harvey KP, Adair JD, Isho M, Robinson R. Can intravenous lidocaine decrease postsurgical ileus and shorten hospital stay in elective bowel surgery? A pilot study and literature review. *Am J Surg* 2009; **198:** 231-6. doi: 10.1016/j.amjsurg.2008.10.015

20. Kuo CP, Jao SW, Chen KM, Wong CS, Yeh CC, Sheen MJ, et al. Comparison of the effects of thoracic epidural analgesia and i.v. infusion with lidocaine on cytokine response, postoperative pain and bowel function in patients undergoing colonic surgery. *Br J Anaesth* 2006; **97:** 640-6. doi: 10.1093/bja/ael217

21. Paterson HM, Cotton S, Norrie J, Nimmo S, Foo I, Balfour A, et al. The ALLEGRO trial: a placebo controlled randomised trial of intravenous lidocaine in accelerating gastrointestinal recovery after colorectal surgery. *Trials* 2022; **23:** 84. doi: 10.1186/s13063-022-06021-5

22. Tikuišis R, Miliauskas P, Samalavičius NE, Žurauskas A, Samalavičius R, Zabulis V. Intravenous lidocaine for post-operative pain relief after hand-assisted laparoscopic colon surgery: a randomized, placebo-controlled clinical trial. *Tech Coloproctol* 2014; **18:** 373-80. doi: 10.1007/s10151-013-1065-0

23. Wall TP, Buggy DJ. Perioperative intravenous lidocaine and metastatic cancer recurrence - a narrative review. *Front Oncol* 2021; **11:** 688896. doi: 10.3389/fonc.2021.688896

24. Weibel S, Jelting Y, Pace NL, Helf A, Eberhart LH, Hahnenkamp K, et al Continuous intravenous perioperative lidocaine infusion for postoperative pain and recovery in adults. *Cochrane Database Syst Rev* 2018; **6:** CD009642. doi: 10.10 02/14651858.CD009642.pub3

25. Liu M, Wai M, Nunez J. Topical lidocaine patch for postthoracotomy and poststernotomy pain in cardiothoracic intensive care unit adult patients. *Crit Care Nurse* 2019; **39:** 51-7. doi: 10.4037/ccn2019849

26. Brown L, Gray M, Griffiths B, Jones M, Madhavan A, Naru K, et al; NoSTRA (Northern Surgical Trainees Reseach Association). A multicentre, prospective, observational cohort study of variation in practice in perioperative analgesia strategies in elective laparoscopic colorectal surgery (the LapCoGesic study). *Ann R Coll Surg Engl* 2020; **102:** 28-35. doi: 10.1308/rcsann.2019.0091

27. Wongyingsinn M, Baldini G, Charlebois P, Liberman S, Stein B, Carli F. Intravenous lidocaine versus thoracic epidural analgesia: a randomized controlled trial in patients undergoing laparoscopic colorectal surgery using an enhanced recovery program. *Reg Anesth Pain Med* 2011; **36:** 241-8. doi: 10.1097/AAP.0b013e31820d4362

28. Swenson BR, Gottschalk A, Wells LT, Rowlingson JC, Thompson PW, Barclay M, et al. Intravenous lidocaine is as effective as epidural bupivacaine in reducing ileus duration, hospital stay, and pain after open colon resection: a randomized clinical trial. *Reg Anesth Pain Med* 2010; **35:** 370-6. doi: 10.1097/AAP.0b013e3181e8d5da

29. Andjelkovic L, Novak-Jankovic V, Pozar-Lukanovic N, Bosnic Z, Spindler-Vesel A. Influence of dexmedetomidine and lidocaine on perioperative opioid consumption in laparoscopic intestine resection: a randomized controlled clinical trial. *J Int Med Res* 2018; **46:** 5143-54. doi: 10.1177/0300060518792456

30. Joris JL, Georges MJ, Medjahed K, Ledoux D, lle Damilot G, Ramquet CC, et al. Prevalence, characteristics and risk factors of chronic postsurgical pain after laparoscopic colorectal surgery. *Eur J Anaesthesiol* 2015; **32:** 712-7. doi: 10.1097/EJA.0000000000000268

research article

Interobserver and sequence variability in the delineation of pelvic organs at risk on magnetic resonance images

Wanjia Zheng[1,2], Xin Yang[1,3,4], Zesen Cheng[1,5], Jinxing Lian[1,6], Enting Li[1,7], Shaoling Mo[1,8], Yimei Liu[1], Sijuan Huang[1,3,4]

[1] State Key Laboratory of Oncology in South China, Guangdong Provincial Clinical Research Center for Cancer, Sun Yat-Sen University Cancer Center, Guangzhou, Guangdong Province, China
[2] Department of Radiation Oncology, Southern Theater Air Force Hospital of the People's Liberation Army, Guangzhou, Guangdong Province, China
[3] Guangdong Esophageal Cancer Institute, Guangzhou, Guangdong Province, China
[4] United Laboratory of Frontier Radiotherapy Technology of Sun Yat-sen University & Chinese Academy of Sciences Ion Medical Technology Co., Ltd, Guangzhou, Guangdong Province, China
[5] School of Electronic and Computer Engineering, Peking University, Shenzhen, Guangdong province, China
[6] Department of Radiation Oncology, The First Affiliated Hospital of Guangzhou University of Chinese Medicine, Guangzhou, Guangdong province, China
[7] Department of Radiology, The Eighth Affiliated Hospital of Sun Yat-sen University, Shenzhen, Guangdong province, China
[8] Department of Radiation Oncology, The First People's Hospital of Foshan, Foshan, Guangdong province, China

Radiol Oncol 2025; 59(1): 139-146.

Received 14 07 2024
Accepted 20 11 2024

Correspondence to: Sijuan Huang, Department of Radiation Oncology, Sun Yat-Sen University Cancer Center, 651 Dongfeng East Road, Yue Xiu District, Guangzhou, P. R. China. E-mail: huangsj@sysucc.org.cn

Wanjia Zheng and Xin Yang contributed equally to this work and should be considered co-first authors.

Disclosure: No potential conflicts of interest were disclosed.

Background. This study evaluates the contouring variability among observers using MR images reconstructed by different sequences and quantifies the differences of automatic segmentation models for different sequences.

Patients and methods. Eighty-three patients with pelvic tumors underwent T1-weighted image (T1WI), contrast enhanced Dixon T1-weighted (T1dixonc), and T2-weighted image (T2WI) MR imaging on a simulator. Two observers performed manual delineation of the bladder, anal canal, rectum, and femoral heads on all images. Contour differences were used to analyze the interobserver and intersequence variability. A single-sequence automatic segmentation network was established using the U-Net network, and the segmentation results were analyzed.

Results. Variability analysis among observers showed that the bladder, rectum, and left femoral head on T1WI yielded the highest dice similarity coefficient (DSC) and the lowest 95% Hausdorff distance (HD) (all three sequences). Regarding sequence variability analysis for the same observer, the difference between T1WI and T2WI was the smallest. The DSC of the bladder, rectum, and femoral heads exceeded 0.88 for T1WI–T2WI. The differences between automatic segmentations and manual delineations were minimal on T2WI. The averaged DSC of automatic and manual segmentation of all organs on T2WI exceeded 0.81, and the averaged 95% HD value was lower than 7 mm. Similarly, the sequence variability analysis of automatic segmentation indicates that the automatic segmentation differences between T2WI and T1WI are minimal.

Conclusions. T1WI and T2WI yielded better results in manual delineation and automatic segmentation, respectively. The analysis of variability among three sequences indicates that the yielded good similarity outcomes between the T1WI and T2WI cases in manual and automatic segmentation. We infer that the T1WI and T2WI (or their combination) can be used for MR-only radiation therapy.

Key words: MRI; multiple sequences; variability; automatic segmentation

Introduction

Adaptive radiotherapy (ART) is useful for detecting changes in the position, shape, size, and other characteristics of the target and organs at risk (OARs) during radiotherapy. Appropriate adjustments to the treatment plan can improve the dose consistency and protect normal tissues.[1,2]

Accurate delineation of targets and OARs is a key aspect of the ART process. Compared with computed tomography (CT), magnetic resonance imaging (MRI) has the advantage of accurate soft-tissue contrast and does not produce additional ionizing radiation doses.[3,4] Some studies[5,6] have pointed out that compared with CT, the volumes of tumor targets and OARs delineated on magnetic resonance imaging is significantly reduced such that the tumor can receive a higher dose. Simultaneously, the protection of normal tissues can be equivalent to or even better than CT.[7,8] MR-enhanced soft tissue not only improves the positioning accuracy of patients before radiotherapy but also improves the positioning of tumors and normal tissue during real-time imaging during treatment, thus making dose delivery more accurate.[9,10] Vestergaard *et al*. found that re-optimized ART for MRI-guided bladder cancer treatment has considerable sparing potential for normal tissues.[11]

For lengthy MR scans, only one sequence is used for radiotherapy. Most studies have used T2-weighted and related sequences to delineate the tumor volume, but there is no consensus on which sequence should be used to delineate OARs.[12] However, in some studies, experts recommended the use of the extended T2-weighted sequence to delineate the target and OARs.[13]

Therefore, in this study, we performed manual delineation of OARs on images reconstructed using three sequences (T1-weighted image [T1WI], contrast enhanced Dixon T1-weighted [T1dixonc], T2-weighted image [T2WI]), which are commonly used in MRI simulators, to analyze interobserver and intersequence variability. Simultaneously, we automatically segmented the images obtained using these three sequences to observe the stability of OARs in automatic segmentation.

Patients and methods

MR image acquisition

This study enrolled 83 patients diagnosed with cervical cancer and treated at the SUSYCC Cancer Center between March 2017 and December 2018. The median age of patients at the time of scanning was 54 years (22–82 years). MR images collected from 54 patients were used as the training cohort to build a single-sequence, automatic segmentation model, and images from the remaining 29 patients were used to analyze the variability of the manual segmentation outcomes of the OARs.

Patients were scanned in supine positions in a vacuum bag with their hands raised. MRI scans were conducted using a 70-cm bore Ingenia 3.0 T scanner (Philips, Netherlands), with a slice thickness of 3 mm. Three MRI sequences were selected and imported into the Monaco Planning System. The selected sequences and their respective parameters were as follows: T1WI (repetition time [TR]: 710 ms; echo time [TE]: 15 ms), T1dixonc (TR: 5.5 ms; TE: 3.7 ms), and T2WI (TR: 6088 ms; TE: 105 ms).

The basic data had been submitted to a public Research Data Deposit (RDD) platform (www.researchdata.org.cn), with an approval RDD number as RDDA2021001910.

OAR contouring

Due to the limited scanning range, this comparative study is limited to organs with complete contours within the image. According to the Radiation Therapy Oncology Group[14] and based on the delineated guidelines and clinical requirements for the female's normal pelvic tissue, bladder, rectum, anal canal, and femoral heads (left and right) were delineated on the three MRI sequences. Delineation of the rectum began at the junction of the third bone plane with the sigmoid colon and ended at the junction with the anal canal above the anorectal line. The delineation of the anal canal started at the anorectal line and ended at the anus. The bladder included all the bladder walls and their contents. Manual delineation of all organs were independently completed by two pelvic oncologists (R1 and R2) with more than five experience of career and were handed over to the same more senior pelvic oncologist for independent validation of all contours.

Automatic segmentation

There were two cohorts: a training cohort and a testing cohort. The training cohort includes 54 samples, and the testing cohort includes 29 samples. All samples encompass three sequences and are annotated with contours for both R1 and R2.

The training cohort was used for U-Net[15] networks for automatic segmentation, while the test-

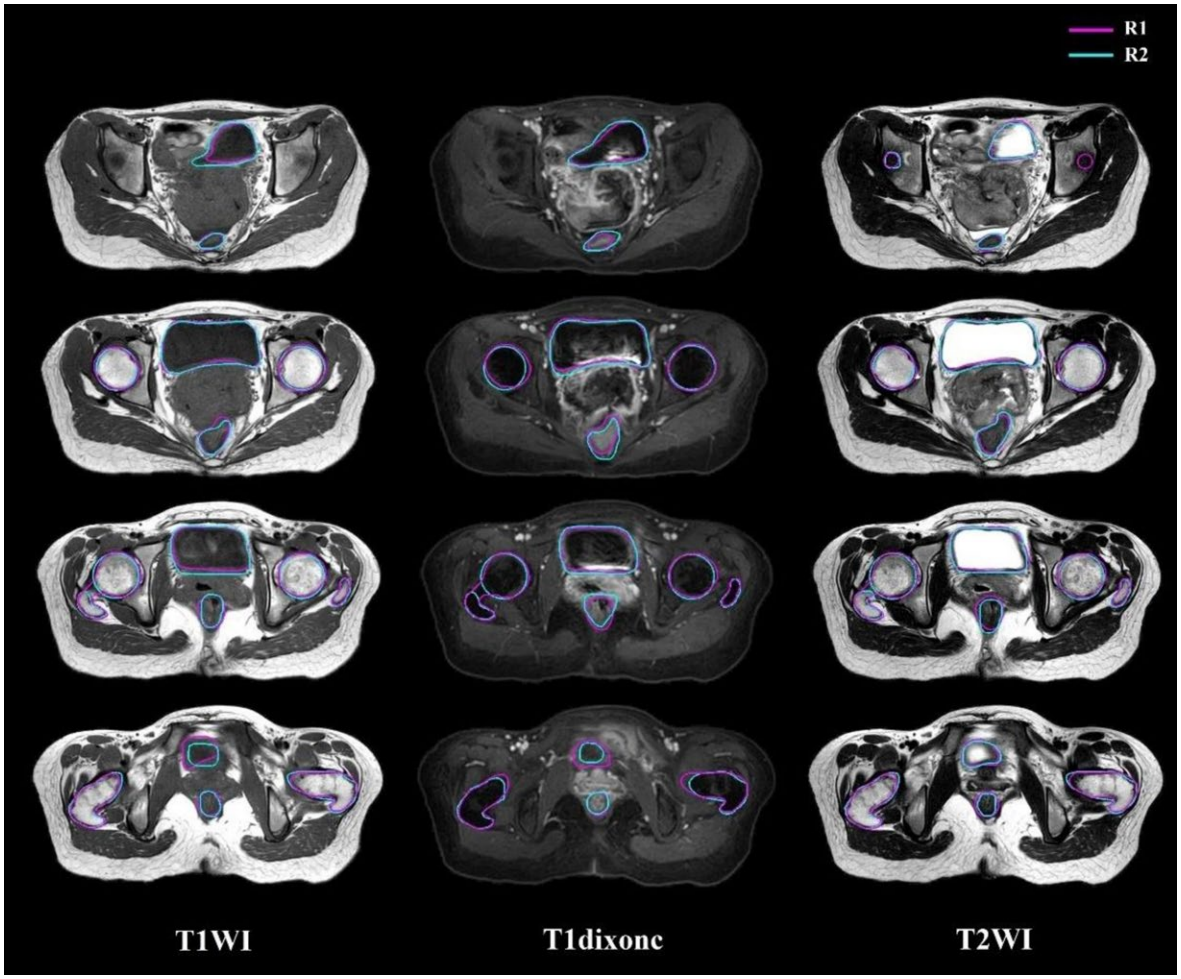

FIGURE 1. Delineation results on T1WI, T1dixonc, and T2WI performed by the two observers (magenta line: R1; blue line: R2).

ing cohort was used to evaluate the network's automatic segmentation performance.

The contour of OARs includes the bladder, rectum, anal canal, and femoral heads (left and right).

OAR evaluation

The dice similarity coefficient (DSC) and Hausdorff distance (HD) are the commonly used evaluation indicators to quantify contouring differences.[16] In this study, the DSC and 95% HD were used to assess volume- and distance-related differences, respectively.

$$D(A,B) = \frac{2|A \cap B|}{|A|+|B|} \quad [1]$$

where A and B represent two different contour volumes, and the DSC value ranges from zero to one. DSC values > 0.7 mean that the two contours coincide well[17], and a DSC value of one indicates that the two contours coincide completely.

The directed HD orientation from X to Y is the maximum distance from all the points on X to the closest point on Y.

$$\vec{d}_H(X,Y) = \max_{x \in X} \min_{y \in Y} d(x,y) \quad [2]$$

The (undirected) HD is the maximum of the two directed Hausdorff measures.

$$d_H(X,Y) = max\{\vec{d}_H(X,Y), \vec{d}_H(Y,X)\} \quad [3]$$

The 95% HD value can be used to eliminate the influence associated with the elimination of a small part of an inaccurate segmentation on the overall segmentation quality evaluation.[18] The undirected 95% HD is defined as,

$$d_{H,95\%}(X,Y) = \frac{\vec{d}_{H,95\%}(X,Y)+\vec{d}_{H,95\%}(X,Y)}{2} \quad [4]$$

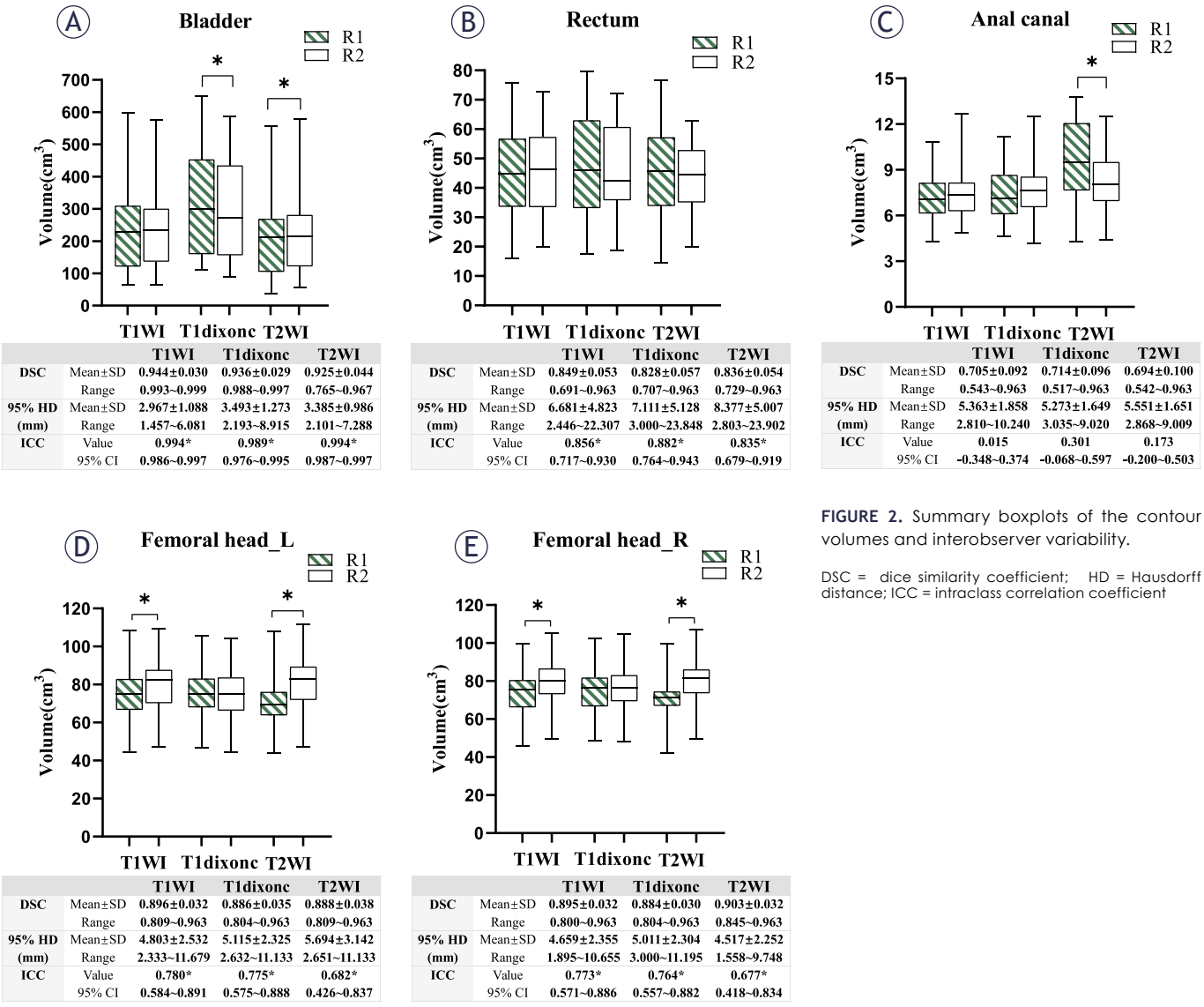

		T1WI	T1dixonc	T2WI
DSC	Mean±SD	0.944±0.030	0.936±0.029	0.925±0.044
	Range	0.993~0.999	0.988~0.997	0.765~0.967
95% HD (mm)	Mean±SD	2.967±1.088	3.493±1.273	3.385±0.986
	Range	1.457~6.081	2.193~8.915	2.101~7.288
ICC	Value	0.994*	0.989*	0.994*
	95% CI	0.986~0.997	0.976~0.995	0.987~0.997

		T1WI	T1dixonc	T2WI
DSC	Mean±SD	0.849±0.053	0.828±0.057	0.836±0.054
	Range	0.691~0.963	0.707~0.963	0.729~0.963
95% HD (mm)	Mean±SD	6.681±4.823	7.111±5.128	8.377±5.007
	Range	2.446~22.307	3.000~23.848	2.803~23.902
ICC	Value	0.856*	0.882*	0.835*
	95% CI	0.717~0.930	0.764~0.943	0.679~0.919

		T1WI	T1dixonc	T2WI
DSC	Mean±SD	0.705±0.092	0.714±0.096	0.694±0.100
	Range	0.543~0.963	0.517~0.963	0.542~0.963
95% HD (mm)	Mean±SD	5.363±1.858	5.273±1.649	5.551±1.651
	Range	2.810~10.240	3.035~9.020	2.868~9.009
ICC	Value	0.015	0.301	0.173
	95% CI	-0.348~0.374	-0.068~0.597	-0.200~0.503

		T1WI	T1dixonc	T2WI
DSC	Mean±SD	0.896±0.032	0.886±0.035	0.888±0.038
	Range	0.809~0.963	0.804~0.963	0.809~0.963
95% HD (mm)	Mean±SD	4.803±2.532	5.115±2.325	5.694±3.142
	Range	2.333~11.679	2.632~11.133	2.651~11.133
ICC	Value	0.780*	0.775*	0.682*
	95% CI	0.584~0.891	0.575~0.888	0.426~0.837

		T1WI	T1dixonc	T2WI
DSC	Mean±SD	0.895±0.032	0.884±0.030	0.903±0.032
	Range	0.800~0.963	0.804~0.963	0.845~0.963
95% HD (mm)	Mean±SD	4.659±2.355	5.011±2.304	4.517±2.252
	Range	1.895~10.655	3.000~11.195	1.558~9.748
ICC	Value	0.773*	0.764*	0.677*
	95% CI	0.571~0.886	0.557~0.882	0.418~0.834

FIGURE 2. Summary boxplots of the contour volumes and interobserver variability.

DSC = dice similarity coefficient; HD = Hausdorff distance; ICC = intraclass correlation coefficient

A lower 95% HD value indicates a smaller difference between the two contours.

All data were analyzed using SPSS (version 25.0; SPSS Inc., Chicago, Illinois, USA). The Wilcoxon rank-sum test was used to compare the results between the two observers. The intraclass correlation coefficient (ICC; two-way random method and absolute agreement for single measures) was used to measure the volume consistency between the two observers and among different sequences. A p-value of <0.05 was considered statistically significant. An ICC greater than 0.75 indicated a good correlation.[19]

Results

Interobserver variability

Figure 1 and Figure 2 shows example and results of the delineation performed by the two observers, respectively. All organs delineated by the two observers yielded the smallest average volume differences on T1WI, except for the left and right femoral heads. The volume correlation outcomes for the bladder and femoral heads showed that T1WI yielded the maximum correlation (all ICC > 0.75). The ICC of the rectum (0.882) obtained by the two observers on T1dixonc was higher than those of the other se-

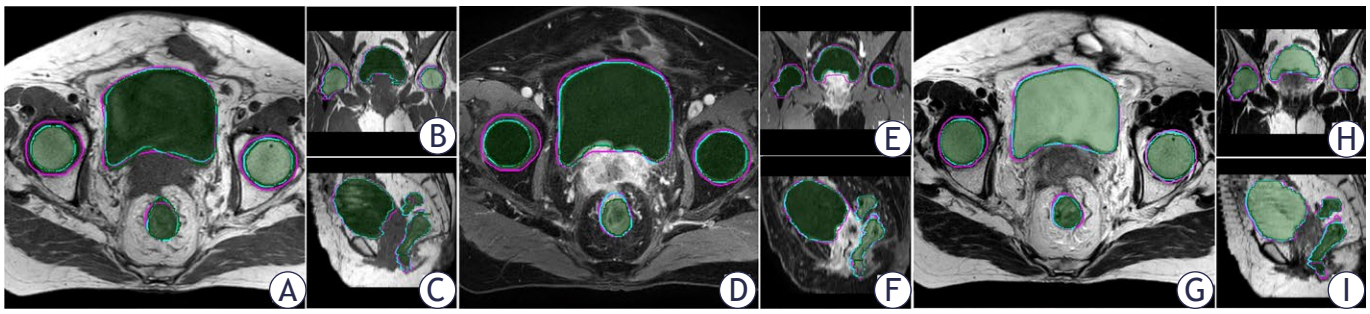

FIGURE. 3 Comparison example between automatic and manual segmentation results in the axial, coronal, and sagittal views on T1WI **(A-C)**, T1dixonc **(D-F)**, and T2WI **(G-I)**. (Magenta line: R1; blue line: R2; and automatic segmentation: shaded green)

quences. The correlation coefficient analysis of the anal canal volume showed that the two observers yielded poor correlation for the anal canal, with ICC < 0.45 on all three sequences. A detailed statistical volume comparison is presented in Supplementary Table 1. Compared with T1dixonc and T2WI, the DSC and 95% HD of the bladder, rectum, and left femoral head were improved on T1WI. The DSC (0.714) and 95% HD (5.273 mm) of the anal canal delineated by the two observers on T1dixonc were better than those on the other sequences. The highest DSC (0.903) and the lowest 95% HD (4.517 mm) of the right femoral head were observed on T2WI.

In conclusion, the contours delineated by the two observers on T1WI yielded smaller variations in the most organs.

Intersequence variability

The volume analysis results of R2 for the contour delineations (images reconstructed Supplementary Table 1. No statistically significant differences were found in the volume variation of the rectum and right femoral head between T1WI and T2WI. However, there were significant differences between the three sequences in the delineation of the bladder and left femoral head (all $p < 0.001$).

In the comparison of ICCs between the sequences Supplementary Table 2, T1WI–T2WI demonstrated an improvement in the correlation of volume compared with the respective correlations of T1WI–T1dixonc and T1dixonc–T2WI (all $p < 0.001$). Except for the anal canal (ICC, 0.614; $p < 0.001$), the ICC between T1WI and T2WI was greater than 0.9 (all $p < 0.001$). The DSC was improved, and 95% HD was reduced in the T1WI–T2WI case compared with the respective values on T1WI–T1dixonc and T2WI–T1dixonc for all OARs. The DSC on T1WI–T2WI exceeded 0.88 for the bladder, rectum, and femoral heads, and the DSC of the anal canal exceeded 0.75 (Table 1).

TABLE 1. The dice similarity coefficient (DSC) and 95% Hausdorff distance (HD) (mm) of OARs based on different MR sequences for R2 (mean ± SD)

	OARs	T1WI–T1dixonc	T1WI–T2WI	T2WI–T1dixonc
DSC	Bladder	0.877 ± 0.079	0.920 ± 0.038	0.884 ± 0.073
	Rectum	0.842 ± 0.064	0.883 ± 0.049	0.809 ± 0.050
	Anal canal	0.705 ± 0.166	0.760 ± 0.077	0.733 ± 0.125
	Femoral head _L	0.905 ± 0.062	0.952 ± 0.027	0.905 ± 0.055
	Femoral head _R	0.904 ± 0.050	0.959 ± 0.026	0.906 ± 0.049
95% HD (mm)	Bladder	6.427 ± 4.360	4.742 ± 1.574	7.092 ± 5.363
	Rectum	5.260 ± 2.934	3.408 ± 1.484	5.953 ± 3.153
	Anal canal	4.732 ± 2.398	4.076 ± 1.375	4.468 ± 2.144
	Femoral head _L	3.811 ± 1.550	2.607 ± 1.405	3.994 ± 1.596
	Femoral head _R	4.027 ± 1.275	1.181 ± 1.171	3.682 ± 1.654

L = left; OARs = organs at risk; R = right; T1dixonc = contrast enhanced Dixon T1-weighted; T1WI = T1-weighted; T2WI = T2-weighted

TABLE 2. The dice similarity coefficient (DSC) and 95% Hausdorff distance (HD) (mm) for different MR sequences of automatic segmentation (mean ± SD)

		Bladder	Rectum	Anal canal	Femoral head _L	Femoral head _R
DSC	T1WI- T1dixonc	0.789±0.096	0.686±0.111	0.691±0.121	0.865±0.083	0.876±0.037
	T1WI- T2WI	0.854±0.101	0.784±0.105	0.707±0.087	0.908±0.091	0.924±0.030
	T2WI- T1dixonc	0.756±0.130	0.860±0.912	0.709±0.134	0.891±0.032	0.892±0.037
95% HD (mm)	T1WI- T1dixonc	18.079±12.095	9.702±10.940	4.810±2.170	4.300±2.027	4.678±1.793
	T1WI- T2WI	12.459±11.094	7.978±10.469	4.826±2.361	3.362±2.441	3.188±1.413
	T2WI- T1dixonc	17.711±9.049	7.433±3.907	4.478±1.744	3.769±1.204	3.616±1.095

L = left; R = right; T1dixonc = contrast enhanced Dixon T1-weighted; T1WI = T1-weighted; T2WI = T2-weighted

The results summarized above show that when the same observer used different sequences for delineation, the similarities between T1WI and T2WI were more than those of other sequence combinations.

Automatic segmentation

Figure 3 shows example of the delineation performed by automatic and manual segmentation. The rectum volumes obtained from automatic segmentation and human observer delineation were significantly different among the three sequences (R1-Auto: all $p < 0.04$; R2-Auto: all $p < 0.03$). On T2WI, the volume correlations between automatic and manual segmentations of the bladder and right femoral head were 0.983 (T1WI = 0.933 and T1dixonc = 0.956) and 0.694 (T1WI = 0.673 and T1dixonc = 0.631), respectively Supplementary Table 3. Except for the rectum (T1WI = 0.739 and T2WI = 0.725), the best DSC outcomes of other organs on T2WI were obtained by R1 using automatic segmentation. The lowest 95% HD values of the bladder and right femoral head on T2WI were obtained by R1 using automatic segmentation, and the lowest 95% HD values of the rectum and left femoral head were found on T1dixonc. The best DSC and 95% HD outcomes of all organs were obtained by R2 and automatic segmentation on T2WI Supplementary Table 4.

We analyzed the volume of OARs, volumetric ICC, DSC, and 95% HD to observe the variability in automatic segmentation results among different sequences. There were no significant differences in the volumes of the bladder, rectum, or anal canal among the three sequences. The volumetric ICC between T1WI and T2WI exceeded 0.8 in the bladder, rectum, and right femoral head cases. However, the highest ICC between T2WI and T1dixonc was observed for the anal canal and left femoral head Supplementary Table 5. The greatest DSC and lowest 95% HD values of the bladder and femoral heads were observed in the T1WI–T2WI case compared with those obtained in the T1WI–T1dixonc and T2WI–T1dixonc cases. Compared with T1WI–T2WI and T1WI–T1dixonc, the highest DSC and lowest 95% HD of the rectum and anal canal were found between T2WI and T1dixonc (Table 2).

Discussion

Although some reports have stated that various MR sequence imaging techniques should be used to assist the positioning or delineation of the target and OARs, no study has identified the optimal sequence for pelvic tumor localization and delineation of the target and OARs. A previous report suggested that better anatomical definition can be achieved with T1-weighted images.[20] The results of this study indicated that T1WI outperformed the other two sequences in terms of volumetric ICC, DSC, and 95% HD values of the bladder, rectum, and femoral heads, this suggests that the delineated of bladder by the two observers exhibited the least interobserver variability on T1WI. This may be attributed to signal differences in the different sequences of MR images of the bladder. The bladder and urine yielded low signals on T1WI, whereas the surrounding muscles yielded high signals. Compared with T1-weighting, the bladder wall on T2WI without contrast imaging only yielded the muscular layer.[21] Because of the bright urine observed on T2WI, the filled bladder demonstrated significant contrast with the surrounding muscles, which is beneficial for delineation.[22] However, the bright urine signal obscured the signal from the

urothelium and lamina propria and resulted in an inaccurate measurement of bladder thickness and tumor dimensions on T2-weighted MR images compared with T1-weighted MR images.[21] The rectal wall had a uniformly low signal on T1WI; this yielded a significant contrast with the surrounding fat layer and is beneficial for delineating the rectum.[23] Similarly, in this study, the lowest variability between the two observers was observed for the rectum delineated on T1WI (DSC = 0.849). For the delineation of femoral heads, T1WI showed a higher signal intensity than T1dixonc. We found that the interobserver variability in the delineation of the femoral heads on T1WI were less than that on T1dixonc. In terms of variability between sequences, we compared the delineation results of different organs as assessed by a single observer and found that the results on T1WI and T2WI were the closest.

When implementing MRI–ART, the acquisition time of MR images and the optimization of radiotherapy plans are extremely time-consuming. Accurate contour delineation is the most time-consuming and essential step in radiotherapy planning. Several studies have shown that automatic segmentation saves time in real-time planning and reduces inter- and intra–observer variability.[24] Therefore, we investigated the differences among three sequences in automatic segmentation using MR images obtained from 29 patients as the test set and compared the results obtained using manual and automatic contouring.

R1 and the automatic segmentation model obtained an optimal DSC and 95% HD on T2WI. Except for the anal canal, the DSC of the bladder, rectum, and femoral heads were greater than 0.7. The DSC of the anal canal on all three sequences were greater than 0.6, with the highest DSC obtained on T2WI (0.669). R2 obtained the best DSC and 95% HD values when compared with the automatic segmentation model for all organs on T2WI. For all organs on T1WI and T2WI (excluding the anal canal), the DSCs of R2 and the automatic segmentation model were both greater than 0.75. On the three sequences, the average DSC values of the observer and the automatic segmentation model were both greater than 0.78, with the highest DSC value (equal to 0.696) observed on T2WI. Therefore, we found T2WI to be the best sequence for automatic segmentation in this study; this result is consistent with the results of another study on MRI-based automatic segmentation of the pelvis.[25]

The sequence used for the automatic segmentation of pelvic tumors in most studies is T2WI because it yields better imaging results for the target area of pelvic tumors. In this study, we compared the automatic segmentation results among the tested sequences and found that T2WI and T1WI yielded the most similar results in the automatic segmentation model (highest DSC and lowest 95% HD). This suggests that T1WI may serve as a substitute sequence for T2WI when using a single sequence for model segmentation. Our results yielded a high similarity in manual delineation and automatic segmentation models between T1WI and T2WI. This may indicate that T1WI can be used as a supplementary information input when constructing automatic segmentation models, as also shown by Chi *et al*. who used a T2-weighted image and segmented the bladder outer wall boundary using a T1-weighted image.[26]

In this study, we analyzed the differences among the three MRI sequences used in radiotherapy and provided a reference for sequence selection in an MR-only workflow. Our research exhibits certain limitations. Initially, our investigation has been confined to assessing the delineation consistency of organs at risk across various imaging modalities. However, the contouring of the target volume is equally pivotal and warrants further exploration in terms of how imaging sequences may affect its delineation. Secondly, this study involved only two observers, which may have influenced the results. In clinical settings, there is inherent variability among practitioners within the same specialty, across different specialties, and even among institutions. To mitigate these biases and enhance the generalizability of our findings, future studies will incorporate a larger cohort of observers and multi-institutional collaborations, thereby aiming to deliver more equitable and evidence-based recommendations.

Conclusions

In this study, we analyzed the variability in three MR sequences (T1WI, T2WI, and T1dixonc) based on the delineation of pelvic organs performed by human observers and automatic segmentation models. The results indicated that human observers demonstrated better results on T1WI, whereas automatic segmentation models demonstrated better results on T2WI. The difference analysis results among the sequences in manual delineation and automatic segmentation indicated good similarity between T1WI and T2WI. Therefore, T1WI, T2WI, or a combination of T1WI and T2WI can be used

for the planning of MR-only radiation therapy. To the best of our knowledge, there are few studies on interobserver variability based on pelvic MR multiple-sequence imaging.

Acknowledgments

This study was supported by Beijing Xisike Clinical Oncology Research Foundation (Y_Young2023-0156, Y-Young2024-0538), Scientific Research Cooperation Projects of UIH&SYSUCC (ZDZL-UIH-2022006) , and United Laboratory of Frontier Radiotherapy Tech-nology Fund (HT-99982024-0350).

References

1. Hardcastle N, Tomé WA, Cannon DM, Brouwer CL, Wittendorp PW, Dogan N, et al. A multi-institution evaluation of deformable image registration algorithms for automatic organ delineation in adaptive head and neck radiotherapy. *Radiat Oncol* 2012; **7:** 90. doi: 10.1186/1748-717X-7-90
2. Burridge N, Amer A, Marchant T, Sykes J, Stratford J, Henry A, et al. Online adaptive radiotherapy of the bladder: small bowel irradiated-volume reduction. *Int J Radiat Oncol Biol Phys* 2006; **66:** 892-7. doi: 10.1016/j.ijrobp.2006.07.013
3. Noel CE, Parikh PJ, Spencer CR, Green OL, Hu Y, Mutic S, et al. Comparison of onboard low-field magnetic resonance imaging versus onboard computed tomography for anatomy visualization in radiotherapy. *Acta Oncol* 2015; **54:** 1474-82. doi: 10.3109/0284186X.2015.1062541
4. Lütgendorf-Caucig C, Fotina I, Stock M, Pötter R, Goldner G, Georg D. Feasibility of CBCT-based target and normal structure delineation in prostate cancer radiotherapy: multi-observer and image multi-modality study. *Radiother Oncol* 2011; **98:** 154-61. doi: 10.1016/j.radonc.2010.11.016
5. Hunt A, Hansen VN, Oelfke U, Nill S, Hafeez S. Adaptive radiotherapy enabled by MRI guidance. *Clin Oncol (R Coll Radiol)* 2018; **30:** 711-9. doi: 10.1016/j.clon.2018.08.001
6. Ahmed M, Schmidt M, Sohaib A, Kong C, Burke K, Richardson C, et al. The value of magnetic resonance imaging in target volume delineation of base of tongue tumours – a study using flexible surface coils. *Radiother Oncol* 2010; **94:** 161-7. doi: 10.1016/j.radonc.2009.12.021
7. Sander L, Langkilde NC, Holmberg M, Carl J. MRI target delineation may reduce long-term toxicity after prostate radiotherapy. *Acta Oncol* 2014; **53:** 809-14. doi: 10.3109/0284186X.2013.865077
8. Tanaka H, Hayashi S, Ohtakara K, Hoshi H, Iida T. Usefulness of CT-MRI fusion in radiotherapy planning for localized prostate cancer. *J Radiat Res* 2011; **52:** 782-8. doi: 10.1269/jrr.11053
9. Hijab A, Tocco B, Hanson I, Meijer H, Nyborg CJ, Bertelsen AS, et al. MR-guided adaptive radiotherapy for bladder cancer. *Front Oncol* 2021; **11:** 637591. doi: 10.3389/fonc.2021.637591
10. Pathmanathan AU, van As NJ, Kerkmeijer LGW, Christodouleas J, Lawton CAF, Vesprini D, et al. Magnetic resonance imaging-guided adaptive radiation therapy: a "Game Changer" for prostate treatment? *Int J Radiat Oncol Biol Phys* 2018; **100:** 361-73. doi: 10.1016/j.ijrobp.2017.10.020
11. Vestergaard A, Hafeez S, Muren LP, Nill S, Høyer M, Hansen VN, et al. The potential of MRI-guided online adaptive re-optimisation in radiotherapy of urinary bladder cancer. *Radiother Oncol* 2016; **118:** 154-9. doi: 10.1016/j.radonc.2015.11.003
12. Kerkmeijer LGW, Maspero M, Meijer GJ, van der Voort van Zyp JRN, de Boer HCJ, van den Berg CAT. Magnetic resonance imaging only workflow for radiotherapy simulation and planning in prostate cancer. *Clin Oncol (R Coll Radiol)* 2018; **30:** 692-701. doi: 10.1016/j.clon.2018.08.009
13. Paulson ES, Crijns SP, Keller BM, Wang J, Schmidt MA, Coutts G, et al. Consensus opinion on MRI simulation for external beam radiation treatment planning. *Radiother Oncol* 2016; **121:** 187-92. doi: 10.1016/j.radonc.2016.09.018
14. Gay HA, Barthold HJ, O'Meara E, Bosch WR, El Naqa I, Al-Lozi R, et al. Pelvic normal tissue contouring guidelines for radiation therapy: a Radiation Therapy Oncology Group consensus panel atlas. *Int J Radiat Oncol Biol Phys* 2012; **83:** e353-e62. doi: 10.1016/j.ijrobp.2012.01.023
15. Ronneberger O, Fischer P, Brox T. U-Net: Convolutional Networks for Biomedical Image Segmentation. In: Navab N, Hornegger J, Wells W, Frangi A, editors. *Medical Image Computing and Computer-Assisted Intervention – MICCAI 2015*. 18th International Conference, Munich, Germany; October 5-9, 2015. Proceedings. Lecture Notes in Computer Science, vol 9351. Springer, Cham. doi: 10.1007/978-3-319-24574-4_28
16. Kieselmann JP, Kamerling CP, Burgos N, Menten MJ, Fuller CD, Nill S, et al. Geometric and dosimetric evaluations of atlas-based segmentation methods of MR images in the head and neck region. *Phys Med Biol* 2018; **63:** 145007. doi: 10.1088/1361-6560/aacb65
17. Noel CE, Zhu F, Lee AY, Yanle H, Parikh PJ. Segmentation precision of abdominal anatomy for MRI-based radiotherapy. *Med Dosim* 2014; **39:** 212-7. doi: 10.1016/j.meddos.2014.02.003
18. Pekar V, Allaire S, Qazi A, Kim JJ, Jaffray DA. Head and neck auto-segmentation challenge: segmentation of the parotid lands. In: Jang Z, Navab N, Pluim JPW, Viergever MA, editors. *Medical Image Computing and Computer-Assisted Intervention – MICCAI 2010*. 13th International Conference, Beijing, China; September 20-24, 2010. Proceedings. Lecture Notes in Computer Science, vol 6362. p. 273-80. Springer. doi: 10.1007/978-3-642-15745-5
19. Romeo V, Cavaliere C, Imbriaco M, Verde F, Petretta M, Franzese M, et al. Tumor segmentation analysis at different post-contrast time points: A possible source of variability of quantitative DCE-MRI parameters in locally advanced breast cancer. *Eur J Radiol* 2020; **126:** 108907. doi: 10.1016/j.ejrad.2020.108907
20. O'Connor LM, Dowling JA, Choi JH, Martin J, Warren-Forward H, Richardson H, et al. Validation of an MRI-only planning workflow for definitive pelvic radiotherapy. *Radiat Oncol* 2022; **17:** 55. doi: 10.1186/s13014-022-02023-4
21. Tyagi P, Moon CH, Connell M, Ganguly A, Cho KJ, Tarin T, et al. Intravesical contrast-enhanced MRI: a potential tool for bladder cancer surveillance and staging. *Curr Oncol* 2023; **30:** 4632-47. doi: 10.3390/curroncol30050350
22. Zhu QK, Du B, Yan PK, Lu HB, Zhang LP. Shape prior constrained PSO model for bladder wall MRI segmentation. *Neurocomputing* 2017; **294:** 19-28. doi: 10.1016/j.neucom.2017.12.011
23. Paley MR, Ros PR. MRI of the rectum: non-neoplastic disease. *Eur Radiol* 1998; **8:** 3-8. doi: 10.1007/s003300050328
24. Hwee J, Louie AV, Gaede S, Bauman G, D'Souza D, Sexton T, et al. Technology assessment of automated atlas based segmentation in prostate bed contouring. *Radiat Oncol* 2011; **6:** 110. doi: 10.1186/1748-717X-6-110
25. Huang S, Cheng Z, Lai L, Zheng W, He M, Li J, et al. Integrating multiple MRI sequences for pelvic organs segmentation via the attention mechanism. *Med Phys* 2021; **48:** 7930-45. doi: 10.1002/mp.15285
26. Chi JW, Brady M, Moore NR, Schnabel JA. Segmentation of the bladder wall using coupled level set methods. Proceedings of the 8th IEEE International Symposium on Biomedical Imaging: From Nano to Macro, Chicago, Illinois, USA 2011; 1653-6. doi: 10.1109/ISBI.2011.5872721

research article

Bronchial bacterial colonization and the susceptibility of isolated bacteria in patients with lung malignancy

Sabrina Petrovic[1], Bojana Beovic[2,3], Viktorija Tomic[3,4], Marko Bitenc[1], Mateja Marc Malovrh[3,4], Vladimir Dimitric[4], Dane Luznik[4], Martina Miklavcic[1], Tamara Bozic[1], Tina Gabrovec[1], Aleksander Sadikov[5], Ales Rozman[3,4]

[1] Surgery Bitenc, Medical Centre Ljubljana (MCL), Ljubljana, Slovenia
[2] Clinic for Infectious Diseases and Fever Conditions, University Medical Centre Ljubljana, Ljubljana, Slovenia
[3] Faculty of Medicine, University of Ljubljana, Ljubljana, Slovenia
[4] University Clinic of Pulmonary and Allergic Diseases Golnik, Golnik, Slovenia
[4] Faculty of Medicine, University of Ljubljana, Ljubljana, Slovenia
[5] Faculty of Computer and Information Science, University of Ljubljana, Ljubljana, Slovenia

Radiol Oncol 2025; 59(1): 147-152.

Received 15 April 2024
Accepted 19 January 2025

Correspondence to: Sabrina Petrovic, M.D., Kirurgija Bitenc d.o.o., Medical Centre Ljubljana (MCL), Vilharjev podhod 1, 1000 Ljubljana, Slovenia. E-mail: sabrina.petrovic@surgery-bitenc.com

Disclosure: No potential conflicts of interest were disclosed.

Background. Postoperative pneumonia (POP) remains a leading cause of mortality following lung surgery. Recent studies have confirmed that the respiratory tract below the vocal cords is not sterile and often harbours potentially pathogenic microorganisms (PPMs), putting patients with lung malignancies at an increased risk for pulmonary infections.

Patients and methods. The study analysed 149 patients who underwent bronchoscopy for lung lesions suspected to be lung cancer. Protected specimen brush (PSB) samples were obtained during bronchoscopy prior to any specific treatment. Bacterial identification and antimicrobial susceptibility testing were conducted on the isolated strains.

Results. Bacterial colonization was detected in 88.6% of patients, with 21.5% carrying PPMs. Notably, patients with type 2 diabetes exhibited a higher rate of PPM colonization compared to others. Antibiotic susceptibility testing showed no significant differences in efficacy between amoxicillin with clavulanic acid and first-generation cephalosporin in both colonized patients and those with PPMs. Importantly, no multidrug-resistant bacteria were identified.

Conclusions. Our findings indicate a slightly lower PPM colonization rate compared to previous studies, possibly due to the unique geographic characteristics of the study population. The absence of significant differences in bacterial susceptibility between the two tested antibiotics highlights the need for further research to refine perioperative infection management strategies.

Key words: bronchial bacterial colonization; potentially pathogenic microorganisms; antibiotic prophylaxis; lung cancer; bronchoscopy

Introduction

Postoperative pneumonia (POP) remains a significant contributor to postoperative mortality following lung surgery, with reported incidence rates ranging from 2% to 20%.[1,2] Patients with lung malignancies are particularly susceptible to pulmonary infections due to factors such as immunosuppression, impaired protective mechanisms, and localized inflammation caused by concurrent con-

ditions like bronchiectasis and chronic obstructive pulmonary disease (COPD).[2]

Recent studies have challenged the traditional belief that the respiratory tract below the vocal cords is sterile, highlighting the presence of microbial colonization.[3] However, limited research has focused on bronchial bacterial colonization (BBC) patterns in patients with lung malignancies. Existing studies report a wide range of BBC prevalence, from 10% to 83%, often involving potentially pathogenic microorganisms (PPMs) such as *Haemophilus influenzae*, *Streptococcus pneumoniae*, and *Staphylococcus aureus*.[1,2,4,5] While the clinical significance of these microorganisms within the airways remains uncertain, their presence may influence the management and prognosis of lung cancer patients.[3] Several risk factors, including age, gender, COPD, and smoking, have been associated with an increased likelihood of PPM colonization.[1,2,4] Furthermore, studies have established a link between BBC and pneumonia in these patients, though it remains unclear whether these bacteria contribute to postoperative infections after lung surgery.[1] Nevertheless, PPM colonization of the respiratory tract could elevate the risk of postoperative infections.[2]

TABLE 1. Baseline characteristics of patients

Characteristics	n	%
Patients	149	
Male	90	60.4
Median age (years)	66	
Smokers	50	33.6
Ex-smokers	71	47,7
Non-smokers	28	18,8
COPD	44	29.5
Diabetes type 2	13	8.7
Colonized patients	132	88.6
Colonized with PPMs	32	21.5
Multiple bacteria colonization	86	57.7
Adenocarcinoma	86	57.7
Squamous cell carcinoma	22	14.8
Small cell carcinoma, carcinoid or large cell carcinoma	11	7.4
Non-small cell carcinoma NOS*	17	11.4
Other, non-lung cancer malignancies (limfoma, methastases)	13	8,7

COPD = chronic obstructive pulmonary disease; NOS = not otherwise specified; PPMs = potentially pathogenic microorganisms

The effectiveness of first-generation cephalosporins as perioperative antibiotic prophylaxis, as recommended by current guidelines, is under scrutiny due to the high incidence of postoperative pneumonia and the increasing prevalence of antibiotic-resistant bacteria among isolated strains.[6-9] Addressing postoperative infections in patients with lung malignancies undergoing surgery is a critical clinical challenge, necessitating the identification of effective prophylactic strategies.

This study aims to prospectively evaluate the prevalence of PPM colonization in patients with lung malignancies, predominantly primary lung cancer, at the time of diagnosis before any specific treatment initiation. Additionally, it investigates antibiotic susceptibility among isolated bacteria to assess resistance rates and examines the potential association between PPM colonization and cancer stage.

Patients and methods

This prospective study was conducted from June 2021 to February 2023, focusing on patients presenting with lung lesions suspected to be primary lung cancer. During the initial outpatient evaluation, demographic and clinical data were collected, including age, gender, smoking history, and comorbidities. All patients were diagnosed following established guidelines for primary lung cancer diagnosis. TNM staging included chest, abdominal, and head CT scans, as well as PET-CT imaging. Flexible bronchoscopy was performed for all patients to obtain tumour tissue samples for histological diagnosis when possible. In addition, protected specimen brush (PSB) samples were collected during bronchoscopy prior to initiating any specific treatment. For cases where bronchoscopic tumour r access was not feasible, CT-guided needle biopsies were used to determine histological typing.

PSB samples were sent to the microbiology laboratory, where bacterial colonization was defined as the isolation of microorganisms at a threshold of $\geq 10^3$ CFU/mL. Antimicrobial susceptibility testing was performed on each bacterial isolate using the microbiology protocol tailored to the bacterial species.

The study received approval from the National Medical Ethics Committee of the Republic of Slovenia (no. 0120-163/2021/3), and all participants provided written informed consent.

Bronchoscopy

Bronchoscopy was performed under moderate sedation, adhering to a strict no-suction policy prior to reaching the carina. Upon entering the trachea, topical lidocaine anaesthesia was administered to the main and upper lobar bronchi. Sterile brushes (OLYMPUS disposable cytology brush BC-202D-210) were used to collect samples from the bronchi of the tumour-bearing lobe prior to diagnostic sampling to detect bacterial colonization. Each sample was preserved in 1 mL of sterile saline solution and sent to the microbiology laboratory. Peripheral tumour sampling was conducted using various bronchoscopic techniques to determine tumour histological types.

Microbiological analysis

PSB samples were promptly processed in the microbiology laboratory. Samples were vortexed, and slides were prepared before dilution and plating. Gram staining and microscopic examination assessed sample quality, bacterial morphology, and abundance. Samples were diluted to a final concentration of 10^{-3} and inoculated on various solid and liquid media, including blood agar, chocolate agar, Brucella blood agar, CHROMagar™ Orientation (CHROMagar, France), and thioglycollate broth. Plates were incubated aerobically and anaerobically at 35°C and evaluated for growth at 24, 48, and 72 hours. Liquid medium subculturing onto the same solid media plates confirmed bacterial morphotypes and colony-forming units per millilitre (CFU/mL). A threshold of $\geq 10^3$ CFU/mL was used to define positive culture results.

Bacterial identification and antimicrobial susceptibility testing were performed using the MALDI Biotyper® (Bruker Daltonics GmbH & Co, Germany) and the standardized EUCAST disc diffusion method. Bacteria were classified as PPMs (e.g., *S. pneumoniae, H. influenzae, M. catarrhalis, S. aureus, P. aeruginosa, Enterobacterales*) or non-PPMs (e.g., *Streptococcus viridans group, Neisseria spp., Corynebacterium spp.*, coagulase-negative staphylococci).[5]

Statistical analyses

Descriptive statistics were presented as median (range) for continuous variables and as frequencies and proportions for categorical variables. Comparisons of bacterial colonization rates with respect to tumour stage and comorbidities, as well

TABLE 2. Number and percentage of recovered bacteria

RECOVERED BACTERIA	No. of patients with isolated species	% of patients with isolated species
Streptococcus mitis	53	35,6%
Streptococcus salivarius	36	24,2%
Streptococcus oralis	27	18,1%
Streptococcus parasanguinis	23	15,4%
Streptococcus vestibularis	18	12,1%
Veillonella atypica	13	8,7%
Haemophilus influenzae	12	8,1%
Streptococcus pneumoniae	11	7,4%
Neisseria subflava	9	6,0%
Actinomyces odontolyticus	9	6,0%
Staphylococcus aureus	8	5,4%
Haemophilus parahaemolyticus	8	5,4%
Streptococcus gordonii	8	5,4%
Rothia mucilaginosa	7	4,7%
Escherichia coli	6	4,0%
Staphylococcus epidermidis	6	4,0%
Staphylococcus hominis	4	2,7%
Streptococcus anginosus	4	2,7%
Veillonella parvula	3	2,0%
Fusobacterium periodonticum	3	2,0%
Moraxella catarrhalis	2	1,3%
Pseudomonas aeruginosa	2	1,3%
Haemophilus parainfluenzae	2	1,3%
Corynebacterium simulans	2	1,3%
Prevotella nigrescens	2	1,3%
Streptococcus constellatus	2	1,3%
Gemella haemolysans	2	1,3%
Serratia marcescens	2	1,3%
Prevotella melaninogenica	2	1,3%
Granulicatella adiacens	2	1,3%
Streptococcus agalactiae	1	0,7%
Staphylococcus capitis	1	0,7%
Streptococcus cristatus	1	0,7%
Neisseria macacae	1	0,7%
Neisseria cinerea	1	0,7%
Neisseria flavescens	1	0,7%
Veillonella dispar	1	0,7%
Prevotella jejuni	1	0,7%
Campylobacter concisus	1	0,7%
Citrobacter koseri	1	0,7%
Prevotella pallens	1	0,7%
Enterobacter bugandensis	1	0,7%
Acinetobacter lwoffii	1	0,7%
Moraxella nonliquefaciens	1	0,7%

TABLE 3. Relationship between cancer stage and colonization with potentially pathogenic microorganisms (PPMs)

STAGE (8th TNM classification)	PPMs		Total
	no	yes	
I	50	11	61
	82.0%	18.0%	100.0%
II	25	7	32
	78.1%	21.9%	100.0%
III	16	6	22
	72.7%	27.3%	100.0%
IV	11	2	13
	84.6%	15.4%	100.0%
Total	102	26	128*
	79.7%	20.3%	100.0%

*for patients, who didn't have primary lung cancer, cTNM was not defined

TABLE 4. Relationship between colonization with potentially pathogenic microorganisms (PPMs) and chronic obstructive pulmonary disease (COPD)

COPD	PPMs		Total
	no	yes	
no	83	21	104
	79.8%	20.2%	100.0%
yes	32	12	44
	72.7%	27.3%	100.0%
Total	115	33	148*
	77.7%	22.3%	100.0%

*for 1 patient, there was no comorbidity data

TABLE 5. Relationship between colonization with potentially pathogenic microorganisms (PPMs) and diabetes type 2

DIABETES TYPE 2	PPMs		Total
	no	yes	
no	108	27	135
	80.0%	20.0%	100.0%
yes	7	6	13
	53.8%	46.2%	100.0%
Total	115	33	148*
	77.7%	22.3%	100.0%

*for 1 patient, there was no comorbidity data

as antibiotic susceptibility, were assessed using Pearson's chi-squared test or Fisher's exact test, as appropriate. A p-value < 0.05 was considered statistically significant. All p-values are two-tailed. Statistical analyses were conducted using IBM SPSS (version 21, Chicago, IL, USA).

Results

The study included 149 consecutive patients with lung malignancies, with a median age of 66 years (20–84). Baseline characteristics of the participants are summarized in Table 1. Most patients (71.8%) were diagnosed with non-small cell lung cancer, primarily adenocarcinoma (57%).

Respiratory tract colonization with at least one bacterial strain was confirmed in 132 patients (88.6%), with 86 patients (57.7%) harbouring multiple bacterial strains. Colonization with potentially pathogenic microorganisms (PPMs) was identified in 32 patients (21.5%). Antibiotic sensitivity testing for amoxicillin with clavulanic acid and first-generation cephalosporins was performed in 120 patients. Sensitivity testing for amoxicillin with clavulanic acid and first-generation cephalosporins was not conducted for 12 patients due to colonization with bacteria requiring specific antibiotic panels (*Rothia mucilaginosa, Streptococcus constellatus, Actinomyces odontolyticus, Streptococcus cristatus*, and *Fusobacterium periodonticum*), none of which were classified as PPMs.

The most frequently isolated PPMs were *Haemophilus influenzae, Streptococcus pneumoniae, Staphylococcus aureus*, and *Escherichia coli* (Table 2), while the most common non-PPMs included *Streptococcus mitis* and *Streptococcus salivarius*. Notably, 57.7% of patients exhibited colonization by multiple bacterial strains.

No statistically significant differences in PPM colonization rates were observed across different cancer stages (Table 3). Similarly, no significant association was found between COPD and colonization with potentially pathogenic bacteria (p = 0.39) (Table 4). However, type 2 diabetes emerged as an independent risk factor for colonization with potentially pathogenic bacteria (p = 0.04) (Table 5).

Antibiotic susceptibility testing revealed no significant differences in efficacy between amoxicillin with clavulanic acid and first-generation cephalosporin in both colonized patients and those colonized specifically by PPMs (Tables 6 and 7).

Discussion

In this study, we conducted a prospective investigation of BBC in patients suspected of primary lung cancer before initiating any treatment. Our methodology introduced a key distinction from previous studies by using sterile brush specimens to collect samples from the bronchi of the tumour-containing lobe. Additionally, we evaluated the antibiotic susceptibility of isolated bacteria to antibiotics commonly used for perioperative prophylaxis in thoracic surgery.

Our findings revealed a lower prevalence of colonization by PPMs (21.5%) compared to previous studies. Only two patients harboured bacteria resistant to both amoxicillin with clavulanic acid and first-generation cephalosporin. In one instance, bacteria were resistant to amoxicillin with clavulanic acid but susceptible to first-generation cephalosporin, while the reverse was observed in another case. Importantly, there were no significant differences in susceptibility between the two antibiotics, and no multidrug-resistant bacteria were identified.

In a similar study, Laroumagne *et al*. examined bronchial colonization at the time of lung cancer diagnosis. They reported a higher prevalence of PPM colonization (50%), likely due to non-sterile sampling conditions. Their findings suggested an association between bronchial colonization and lower survival rates, potentially linked to infectious complications.[4]

Ioanas *et al*. reported a PPM colonization rate of 41%, again using non-sterile sampling techniques. Their study demonstrated no resistance to conventional antibiotics, consistent with our findings. They also reported a low incidence of postoperative pulmonary infections (12%) and no pneumonia cases, likely attributable to effective prophylaxis with first-generation cephalosporin administered perioperatively and for 48 hours postoperatively. Similar complication rates were observed in colonized and non-colonized patients, although their study was limited to 41 patients.[5]

Dancewicz *et al*. also reported similar BBC rates and found no evidence of multidrug-resistant microorganisms, aligning with our results.[2] Boldt *et al*., however, reported a PPM colonization rate of 48% in patients undergoing lung surgery. They found that a single dose of sulbactam plus ampicillin was significantly more effective than first-generation cephalosporin in preventing infections, suggesting alternative regimens for prophylaxis.[10]

TABLE 6. Susceptibility among all colonized patients

Amoxicillin with clavulanic acid	First generation cephalosporin			Total
	R	S	S/R	
R	2	2	0	4
S	2	101	1	104
S/R	0	6	6	12
Total	4	109	7	120

R = resistant; S = susceptible

TABLE 7. Susceptibility among patients colonized by potentially pathogenic microorganisms (PPMs)

Amoxicillin with clavulanic acid	First generation cephalosporin			Total
	R	S	S/R	
R	1	1	0	2
S	1	20	0	21
S/R	0	5	3	8
Total	2	26	3	31

R = resistant; S = susceptible

Radu *et al*. conducted a retrospective analysis of 312 cases, highlighting the inefficacy of first-generation cephalosporin in 84% of cases, raising concerns about current prophylactic guidelines.[8] Schlusser *et al*. suggested that targeted antibiotic prophylaxis against bronchial colonizing bacteria could reduce postoperative pneumonia incidence. They observed a significant reduction when antibiotics were tailored to the identified bacteria, though their study was not randomized and warrants further validation.[6,7]

Lastly, D'Journo *et al.'s* meta-analysis established a statistical correlation between preoperative BBC and postoperative respiratory complications, emphasizing the clinical importance of preoperative colonization screening.[1]

Conclusions

This study provides valuable insights into bronchial bacterial colonization in patients with lung malignancies, predominantly primary lung cancer. The prevalence of PPM colonization and the low resistance to tested antibiotics characterize a patient population primarily from central and western Slovenia, differing from studies conducted in other geographical regions. While PPM coloniza-

tion was not associated with lung cancer stage or COPD, a significantly higher prevalence was observed in patients with type 2 diabetes.

The absence of significant differences in antibiotic susceptibility between amoxicillin with clavulanic acid and first-generation cephalosporin highlights the need for further research. Given the substantial rates of colonization and postoperative pneumonia, we recommend routine microbiological sampling during bronchoscopy for all patients suspected of primary lung cancer. This approach could enable targeted perioperative antibiotic prophylaxis in patients undergoing thoracic surgery. Future prospective studies comparing targeted *versus* standard prophylaxis are essential to establish best practices.

References

1. D'Journo XB, Rolain JM, Doddoli C, Raoult D, Thomas PA. Airways colonizations in patients undergoing lung cancer surgery. *Eur J Cardiothorac Surg* 2011; **40:** 309-21. doi: 10.1016/j.ejcts.2010.11.036
2. Dancewicz M, Szymankiewicz M, Bella M, Sviniarska J, Kowalewski J. [Bronchial bacterial colonization in patients with lung cancer]. [Polish]. *Pneumol Alergol Pol* 2009; **77:** 242-7. PMID: 9591094
3. Prat C, Lacoma A. Bacteria in the respiratory tract – how to treat? Or do not treat? *Int J Infect Dis* 2016; **51:** 113-22. doi: 10.1016/j.ijid.2016.09.005
4. Laroumagne S, Lepage B, Hermant C, Plat G, Phelippeau M, Bigay-Game L, et al. Bronchial colonization in patients with lung cancer: a prospective study. *Eur Respir J* 2013; **42:** 220-9. doi: 10.1183/09031936.00062212
5. Ioanas M, Angrill J, Baldo X, Arncibia F, Gonzalez J, Bauer T, et al. Bronchial bacterial colonization in patients with resectable lung carcinoma. *Eur Respir J* 2002; **19:** 326-32. doi: 10.1183/09031936.02.00236402
6. Schlusser O, Dermine H, Alifano M, Casetta A, Coignard S, Roche N, et al. Should we change antibiotic prophylaxis for lung surgery? Postoperative pneumonia is the critical issue. *Ann Thorac Surg* 2008; **86:** 1727-34. doi: 10.1016/j.athoracsur.2008.08.005
7. Schlusser O, Alifano M, Dermine H, Strano S, Casetta A, Sepulveda S, et al. Postoperative pneumonia after major lung resection. *Am J Respir Crit Care Med* 2006; **173:** 1161-9. doi: 10.1164/rccm.200510-1556oc
8. Radu DM, Jaureguy F, Pharm D, Seguin A, Foulon C, Destable MD, et al. Postoperative pneumonia after major pulmonary resections: an unsolved problem in thoracic surgery. *Ann Thorac Surg* 2007; **84:** 1669-74. doi: 10.1016/j.athoracsur.2007.05.059
9. Deguchi H, Tomoyasu M, Shygeeda W, Kaneko Y, Kanno H, Saito H. Influence of prophylactic antibiotic duration on postoperative pneumonia following pulmonary lobectomy for non-small cell lung cancer. *J Thorac Dis* 2019; **11:** 1155-64. doi: 10.21037/jtd.2019.04.43
10. Boldt J, Piper S, Uphus D, Fussle R, Hempelmann G. Preoperative microbiologic screening and antibiotic prophylaxis in pulmonary resection operations. *Ann Thorac Surg* 1999; **68**: 108-11. doi: 10.1016/s0003-4975(99)00400-2
11. Yamada Y, Sekine Y, Suzuki H, Iwata T, Chiyo M, Nakajima T, et al. Trends of bacterial colonisation and the risk of postoperative pneumonia in lung cancer patients with chronic obstructive pulmonary disease. *Eur J Cardiothorac Surg* 2009; **37:** 752-7. doi: 10.1016/j.ejcts.2009.05.039

Radiol Oncol 2025; 59(1): 1-22.
doi: 10.2478/raon-2025-0011

Ablacija z električnim, pulznim poljem v medicini. Nepovratna elektroporacija in elektropermeabilizacija. Teorija in uporaba

Jacobs EJ, Rubinksy B, Davalos RV

Izhodišča. Tehnike lokalne ablacije so sestavni del kirurških posegov, pri katerih je potrebno čim bolj zmanjšati poškodbe okoliškega parenhima in kritičnih struktur. Irreverzibilna elektroporacija (IRE) in visokofrekvenčna IRE (*angl. high-frequency irreversible electroporation,* H-FIRE), ki jo pogovorno imenujemo pulzna ablacija (*angl. pulsed-field ablation*, PFA), uporabljata visokoamplitudna, nizkoenergijska pulzna električna polja (*angl. pulsed electric fields*, PEF) za netermično ablacijo mehkega tkiva. PEF povzročijo celično smrt s permeabilizacijo celične membrane, kar povzroči izgubo homeostaze. Posebnost netermične narava PFA je, da omogoča selektivno celično smrt ob minimalnem vplivu na okoliške beljakovinske strukture, kar omogoča zdravljenje v bližini občutljivih anatomskih struktur, kjer sta termična ablacija ali kirurška resekcija kontraindicirani. Poleg tega PFA uporabljamo za zdravljenje, kadar po kirurški resekciji ni pričakovati tumorja v predelu kirurških robov, kar imenujemo robno poudarjanje (*angl. margin accentuatio*). V preglednem članku obravnavamo teoretične temelje PFA, podrobno opisujemo, kako PEF povzroči destabilizacijo celične membrane in selektivno ablacijo tkiva, rezultate po zdravljenju ter klinične posledice v onkologiji in kardiologiji.

Zaključki. Klinične izkušnje še vedno potekajo, vendar poročila kažejo, da PFA zmanjšuje zaplete, ki se pogosto pojavljajo pri tehnikah termične ablacije. Vse več onkoloških podatkov tudi potrjuje, da PFA stopnuje imunski odziv, ki lahko prepreči lokalne ponovitve in omili metastatsko bolezen. Kljub obetavnim rezultatom so potrebne nadaljnje raziskave izzivov, kot sta optimizacija aplikacije pulzneega električna polja in obravnavanje razlik v odzivu tkiva. Prihodnje usmeritve vključujejo izpopolnitev protokolov PFA in razširitev njene uporabe na druga terapevtska področja, kot sta benigna hiperplazija tkiva in kronični bronhitis. Focal ablation techniques are integral in the surgical intervention of diseased tissue, where it is necessary to minimize damage to the surrounding parenchyma and critical structures. IRreversible Electroporation (IRE) and High-Frequency IRE (H-FIRE), colloquially called Pulsed-Field Ablation (PFA), utilize high-amplitude, low-energy pulsed electric fields (PEFs) to nonthermally ablate soft tissue. PEFs induce cell death through permeabilization of the cellular membrane, leading to loss of homeostasis. The unique nonthermal nature of PFA allows for selective cell death while minimally affecting surrounding proteinaceous structures, permitting treatment near sensitive anatomy where thermal ablation or surgical resection is contraindicated. Further, PFA is being used to treat tissue when tumor margins are not expected after surgical resection, termed margin accentuation. Clinical experience is still progressing, but reports have demonstrated that PFA reduces complications often seen with thermal ablation techniques. Mounting oncology data also support that PFA produces a robust immune response that may prevent local recurrences and attenuate metastatic disease. Despite promising outcomes, challenges such as optimizing field delivery and addressing variations in tissue response require further investigation. Future directions include refining PFA protocols and expanding its application to other therapeutic areas like benign tissue hyperplasia and chronic bronchitis. This review explores both the theoretical foundations of PFA, detailing how PEFs induce cell membrane destabilization and selective tissue ablation, the outcomes following treatment, and its clinical implications across oncology and cardiology.

Radiol Oncol 2025; 59(1): 23-30.
doi: 10.2478/raon-2025-0010

Ponavljajoča respiratorna papilomatoza. Vloga bevacizumaba in cepljenja proti HPV. Pregled literature s predstavitvijo primerov

Sporeni S, Rifaldi F, Lanzetta I, Imarisio I, Montagna B, Serra F, Agustoni F, Pedrazzoli P, Benazzo M, Bertino G

Izhodišča. Ponavljajoča se respiratorna papilomatoza (*angl. recurrent respiratory papillomatosis* RRP) je bolezen, ki jo povzroča okužba s humanim papiloma virusom (HPV). Zdravljenja z namenom ozdravitve ni mogoče natančno opredeliti in je ohranitvena operacija pogosto najboljša možnost, da obdržimo dihalne funkcije. Doslej so monoklonska protitelesa veljala za izbiro zdravljenja z dobro učinkovitostjo in varnostnim profilom.

Metode. Opravili smo spletno iskanje člankov v angleškem jeziku po podatkovnih bazah *Medline/PubMed*, od leta 2000 do 2024. da bi našli članke, ki so vsebovali besede „*respiratorna ali laringealna papilomatoza*“ in „*HPV respiratorna okužba, zdravljenje papilomatoze, cepljenje proti papilomatozi, sistemsko zdravljenje papilomatoze*“. Nato smo ročno pregledali reference iz izvirnih člankov, da bi odkrili dodatne raziskave. Izbrali smo 34 člankov.

Rezultati. Od leta 2009 uporabljamo za zdravljenje RRP, ki se ne odziva na kirurško zdravljenje, sistemsko aplikacijo bevacizumaba. Učinkovitost monoklonskega protitelesa proti vaskularnemu endotelnemu rastnemu dejavniku (*angl. anti-vascular endothelial growth factor*, anti-VEGF) pri spremembah RRP je lahko povezana z njihovo vaskularno naravo. Glavni izziv je ponovna rast papiloma ob prenehanju zdravljenja. Možna rešitev bi lahko bila sočasna uporaba imunoterapije, s katero bi zmanjšali breme preostale bolezni in hkrati aktivirali imunski sistem proti celicam, okuženim s HPV.

Zaključki. Bevacizumab je varno zdravilo s kratkoročno lokalno zazdravitvijo HPV. Potrebne so nadaljnje prospektivne raziskave z dolgoročnim spremljanjem, da bi še bolje opredelili njegovo varnost in učinkovitost proti ponovitvi bolezni. Glede na vlogo cepiva proti HPV, tako v preventivi okužbe kot pri dopolnilnem zdravljenju, podatki kažejo potrebo po oceni njegove terapevtske učinkovitosti pri zdravljenju RRP.

Radiol Oncol 2025; 59(1): 31-42.
doi: 10.2478/raon-2025-0002

Finančno breme raka dojke. Sistematični pregled literature in prepoznavanje raziskovalnih izzivov

Ratoša I, Bavdaž M, Došenović Bonča P, Zobec Logar HB, Perhavec A, Skubic M, Vörös K, Mihor A, Zadnik V, Redek T

Izhodišča. Rak dojk je eden najbolj pogostih rakov, ki je vse bolj prisoten tudi med delovno aktivnim prebivalstvom. Ne glede na starost ima rak dojk velike neposredne in posredne stroške za bolnike, družine in družbo. Namen raziskave je bil, da s pomočjo bibliometrične analize finančnega bremena raka dojk prepozna ključne vsebine v literaturi, glavne avtorje, osrednje revije ter odprta raziskovalna področja, ki predstavljajo izzive za prihodnje raziskave.

Materiali in metode. Sistematični pregled literature je temeljil na uporabi več metod, analiza je združevala bibliometrične metode s standardnim pregledom/razpravo najpomembnejših prispevkov. Pri analizi smo uporabili programa Bibliometrics v R ter VosViewer.

Rezultati. Navajamo ključne avtorje, revije in raziskovalne vsebine v literaturi pri proučevanju finančnega bremena raka dojke. Objavljeni članki, ki opisujejo finančna bremena zaradi raka dojk, kažejo na zgostitev tako avtorjev kot revij.

Zaključki. Rezultati razkrivajo odsotnost celovitega pristopa pri preučevanju finančnega bremena ob raku dojke. Literatura se pogosto osredotoča le na enega ali nekaj izbranih vidikov finančnega bremena, obravnavajo predvsem le nekaj držav. Poseben izziv z vidika primerjalne analize predstavljajo razlike v zdravstvenih sistemih.

Radiol Oncol 2025; 59(1): 43-53.
doi: 10.2478/raon-2025-0014

Zgodnji ^{18}F-FDG-PET/CT in drugi napovedni označevalci preživetja bolnikov z metastatskim melanomom, ki so prejemali imunoterapijo

Hribernik N, Strašek K, Studen A, Zevnik K, Škalič K, Jeraj R, Reberšek M

Izhodišča. Velik delež bolnikov z metastatskim melanomom se ne odzove na zaviralce imunskih nadzornih točk, zaradi česar je potrebno razviti druge možne neinvazivne označevalce za prepoznavanje bolnikov že v obdobju zgodnjega zdravljenja, ki se na takšno imunoterapijo ne odzivajo. Namen pričujoče klinične raziskave je bil oceniti vlogo zgodnje [^{18}F]2fluoro-2-deoksi-D-glukoza PET/CT (18F-FDG-PET/CT) in drugih možnih napovednih označevalcev preživetja pri bolnikih z metastatskim melanomom, ki so prejemali zaviralce imunskih nadzornih točk, v četrtem tednu terapije (T4).

Bolniki in metode. V prospektivni neintervencijski klinični raziskavi smo bolnike z metatstatskim melanomom, ki smo jih zdravili z zaviralci imunski nadzornih točk, redno spremljali z ^{18}F-FDG PET/CT. Bolnikom smo naredili preiskavo ^{18}F-FDG PET/CT pred zdravljenjem, zgodaj v četrtem tednu (T4) in šestnajstem tednu (T16) zdravljenja in nato vsakih 16 tednov. Odgovor na zaviralce imunskih nadzornih točk v T4 smo ocenili z uporabo prilagojenih meril Evropske organizacije za raziskave in zdravljenje raka (*angl. European Organisation for Research and Treatment of Cancer*, EORTC). Bolnike z napredovanjem bolezni smo razvrstili v skupino brez klinične dobrobiti, ostale odgovore na zdravljenje pa v skupino klinične dobrobiti. Primarni cilj raziskave je bil analiza preživetja na podlagi odgovora na zdravljenje, ugotovljenega z 18F-FDG PET/CT v T4. Sekundarni cilj je bila analiza preživetja na podlagi LDH, števila metastatskih lokalizacij in imunsko pogojenih neželenih učinkov. Preživetja smo ocenili z uporabo Kaplan-Meierjeve metode in univariatne Coxove regresijske analize.

Rezultati. Skupno smo v raziskavo vključili 71 bolnikov. Srednji čas sledenja bolnikov je bil 37,1 meseca (95 % interval zaupanja [IZ] = 30,1–38,0). Trije (4 %) bolniki so imeli pred ^{18}F-FDG PET/CT v T4 le osnovni pregled zaradi hitrega napredovanja bolezni in smrti. 51 (72 %) bolnikov smo razvrstili v skupino klinične dobrobiti, 17 (24 %) pa v skupino brez klinične dobrobiti. Ugotovili smo statistično značilno razliko (p = 0,003) v srednjem celokupnem preživetju med skupino klinične dobrobiti (kjer srednje celokupno preživetje ni bilo doseženo [ND]; 95 % IZ = 17,8 meseca–ND) in skupino brez klinične dobrobiti (srednje celokupno preživetje 6,2 meseca; 95 % IZ = 4.6 meseca–ND; p = 0,003). Univariatna analiza po COX-u je pokazala razmerje obetov (RO) 0.4 (95 % IZ = 0.18–0.72; p = 0,004). Celokupno preživetje je bilo značilno daljše v skupini bolnikov z normalno serumsko vrednostjo LDH in v skupini z imunsko pogojenimi neželenimi učinki še posebej kožnimi.

Zaključki. Zgodnja preiskava z ^{18}F-FDG PET/CT v T4 lahko služi kot napovedni slikovni označevalec pri bolnikih z metastatskim melanomom, ki prejemajo imunoterapijo z zaviralci imunskih nadzornih točk. V raziskavi sta imela napovedno vrednost tudi normalna vrednost serumske LDH in pojav kožnih imunsko pogojenih neželenih učinkov.

Radiol Oncol 2025; 59(1): 54-62.
doi: 10.2478/raon-2025-0008

Razširjenost difuzne idiopatske skeletne hiperostoze in povezava s kalcifikacijami koronarnih arterij v Sloveniji

Lesjak V, Hebar T, Pirnat M

Izhodišča. Namen raziskave je bil ugotoviti prevalenco bolnikov z difuzno idiopatsko skeletno hiperostozo (DISH) v Sloveniji, oceniti povezavo med atenuacijo epikardialnega maščevja (*angl. epicardial adipose tissue*, EAT) in stopnjo kalcifikacij koronarnih arterij (*angl. coronary artery calcifications*, CAC) pri bolnikih z in brez DISH ter preučiti dejavnike, ki vplivajo na te parametre.

Bolniki in metode. V raziskavi smo obravnavali bolnike, ki so bili napoteni na koronarno CT angiografijo (CTA) zaradi kliničnega suma na koronarno arterijsko bolezen. DISH, CAC in atenuacijo EAT smo kvantificirali s preiskavo CT brez kontrastnega sredstva. Diagnoza DISH je temeljila na Resnickovih kriterijih. S CTA smo ocenili prisotnost obstruktivne koronarne arterijske bolezni. Povezavo med DISH in obsegom CAC smo ugotavljali s korelacijsko analizo in multivariatno regresijo.

Rezultati. V raziskavo smo vključili 219 bolnikov. Skupna prevalenca DISH je bila 7,8 %. Pri univariatni logistični regresiji so bili indeks telesne mase (razmerje obetov [RO] 1,133, p = 0,005), starost (RO 1,055, p = 0,032) in sladkorna bolezen (RO 3,840, p = 0,015) pomembno povezani s prisotnostjo DISH. Te povezave nismo dokazali pri multinomialni multivariatni analizi, kjer pa smo ugotovili, da so spol, starost, hipertenzija in atenuacija EAT značilno povezani z višjo stopnjo kalcifikacij koronark.

Zaključek. Ugotovljena prevalenca DISH je primerljiva s predhodnimi objavami drugih raziskav. Med razširjenostjo DISH in CACS ni bilo neodvisne povezave. Naši podatki nakazujejo na bolj kompleksno in morda nevzročno povezavo med boleznijo koronarnih arterij in DISH.

Radiol Oncol 2025; 59(1): 63-68.
doi: 10.2478/raon-2025-0006

Natančnost transtorakalnega ultrazvoka srca pri diagnostiki miksomov. Izkušnje največjega slovenskega terciarnega centra

Kačar P, Pavšič N, Bervar M, Dolenc Stražar Z, Prokšelj K

Izhodišča. Diferencialna diagnoza miksoma, najpogostejšega primarnega tumorja srca, je široka, zato je pred kirurškim zdravljenjem nujna natančna diagnostična obravnava za postavitev pravilne diagnoze. Transtorakalni ultrazvok srca (*angl. transthoracic echocardiography*, TTE) je najpogosteje prva preiskava izbora pri obravnavi bolnikov s sumom na miksom. Z raziskavo smo v želeli določiti natančnost, senzitivnost in specifičnost TTE pri diagnostiki miksoma ter določiti njihove ultrazvočne značilnosti.

Bolniki in metode. Retrospektivno smo analizirali klinične, ehokardiografske in patohistološke izvide 73 bolnikov, ki so bili napoteni v največji slovenski terciarni center zaradi suma na miksom. Kirurško smo zdravili 53 (73 %) bolnikov.

Rezultati. Na osnovi predoperativnega TTE smo bolnike razdelili v skupino z miksomom (n = 45, 85 %) in skupino z ne-miksomskim tumorjem. Od 53 perioperativnih patohistoloških vzorcev je bilo 39 (73 %) miksomov. Senzitivnost predoperativnega TTE je bila 97 % in specifičnost 50 %. Skupna natančnost je bila 85 %. Vsi ne-miksomski tumorji so imeli atipično lokacijo in 72 % miksomov je imelo tipično lokacijo v levem preddvoru ($p < 0.001$). Ne-miksomski tumorji so bili značilno manjši od miksomov (24.3 ± 13.2 mm *vs*. 37.9 ± 18.3 mm; $p = 0.017$).

Zaključki. Pričujoča raziskava je potrdila zadovoljivo natančnost TTE pri diagnostiki miksomov. Najpomembnejši ultrazvočni lastnosti za razlikovanje med miksomom in ne-miksomskim tumorjem sta lokacija in velikost tumorja. Manjši tumorji na atipični lokaciji so manj verjetno miksomi in v teh primerih je za postavitev pravilne diagnoze nemalokrat potrebna dodatna slikovna diagnostika.

Radiol Oncol 2025; 59(1): 69-78.
doi: doi: 10.2478/raon-2025-0016

Primerjava 2D in 3D radiomskih značilnosti s konvencionalnimi značilnostmi, ki so temeljila na slikah CT s povečanim kontrastom pri predoperativnem napovedovanju tveganja za tumorje timusa

Yuan YH, Zhang H, Xu WL, Dong D, Gao PH, Zhang CJ, Guo Y, Tong LL, Gong FC

Izhodišča. Namen raziskave je bil razviti in potrditi dvodimenzionalne (2D) in tridimenzionalne (3D) radiomske znake, ki so temeljili na slikah računalniške tomografije (CT) s povečanim kontrastom pri predoperativnem napovedovanju tveganja za epitelne tumorje v timusu, pa tudi primerjati napovedno učinkovitost takšnega radiološke metode s slikami konvencionalne preiskave CT.

Bolniki in metode. V raziskavo smo retrospektivno vključili 149 bolnikov z epitelnim tumorjem timusa od januarja 2016 do decembra 2018. Razdelili smo jih v skupino z visokim tveganjem (B2/B3/TCs, n = 103) in skupino z nizkim tveganjem (A/AB/B1, n = 46). Vse bolnike smo naključno razporedili v učni (n = 104) in testni (n = 45) niz. Zbrali smo 14 konvencionalnih značilnosti slik CT in 396 radioloških značilnosti, pridobljenih iz 2D oziroma 3D slik CT s povečanim kontrastom. Z multivariatno logistično regresijsko analizo smo vzpostavili tri modele: konvencionalni model, 2D radiomski in 3D radiomski model. Različno učinkovitost modelov smo prikazali s krivuljami sprejemlivk operativnih karakteristik (ROC).

Rezultati. Pri konvencionalnem modelu sta bili vrednosti območij pod krivuljo (AUC) v učnem in testnem nizu 0,863 in 0,853, občutljivost 78 % in 55 %, specifičnost pa 88 % in 100 %. Pri 2D-modelu sta bili vrednosti AUC 0,854 in 0,834, občutljivost 86 % in 77 %, specifičnost pa 72 % in 86 % v učnih in testnih nizih. Model 3D je pokazal AUC 0,902 in 0,906, občutljivost 75 % in 68 % ter specifičnost 94 % in 100 % v učnih in testnih nizih.

Zaključki. Radiomske značilnosti, ki temeljijo na 3D-slikah, lahko razlikujejo med epitelnimi tumorji timusa z visokim in nizkim tveganjem ter zagotavljajo dopolnilne diagnostične informacije.

Radiol Oncol 2025; 59(1): 79-90.
doi: 10.2478/raon-2025-0012

Z MR srca ugotavljamo različno kardiotoksičnost, ki jo povzroča kemoterapija pri sarkomu in raku dojke

Ibrahim ESH, Chaudhary L, Cheng YC, Sosa A, An D, Charlson J

Izhodišča. V zadnjih nekaj desetletjih so se številne raziskave osredotočile na vpliv antraciklinov na srce (kardiotoksičnost) pri raku dojke, le nekaj pa na sarkom. V pričujoči raziskavi uporabljamo zmogljivosti naprednega slikanja z magnetno resonanco (MR) srca za opredelitev kardiotoksičnosti, ki jo povzročajo antraciklini pri sarkomu in rezultate primerjamo z rezultati pri bolnicah z rakom dojke.

Bolniki in metode. Bolniki so opravili preiskavo z magnetno resonanco v treh časovnih točkah: v izhodišču (pred zdravljenjem), po zdravljenju in po šestih mesecih.

Rezultati. Izsledki preiskav so pokazali različen odziv srca na zdravljenje pri sarkomu, za katerega je bilo značilno povečanje mase levega prekata (*angl. left ventricle*, LV) in zmanjšanje iztisnega deleža desnega prekata (*ang. right ventricular ejection fraction*, RVEF). Pri vseh bolnikih je iztisni delež levega prekata (*ang. left ventricular ejection fraction*, LVEF) ostal > 50 % v vseh časovnih točkah. Deformacija miokarda je bila vedno nižja od običajnih mejnih vrednosti in je med različnimi časovnimi točkami kazala majhne spremembe. T2 miokarda in zunajcelični volumen (ECV) sta se pri sarkomu povečevala oziroma zmanjševala, kar je bilo nasprotno od vzorcev pri raku dojke. Medtem ko je T1 miokarda pri raku dojke pokazal naraščajoče vrednosti, se je T1 pri sarkomu po zdravljenju povečal in se nato zmanjšal ob 6-mesečnem spremljanju. Rezultati so pokazali obratno korelacijo med odmerkom in različnimi komponentami deformacije pri sarkomu, kar pa ni veljalo za raka dojke. Nekateri segmenti srčne mišice so pokazali visoke koeficiente korelacije z odmerkom, kar lahko odseva njihovo večjo občutljivost na kardiotoksičnost.

Zaključki. MR srca se je izkazala za dragoceno tehniko za ugotavljanje antraciklinskih sprememb srčne funkcije in sestave miokardnega tkiva pri sarkomu in kaže različno kardiotoksičnost, kot se pojavlja pri raku dojke po zdravljenju z antraciklini. Prav tako omogoča celovito oceno zdravja srca pred zdravljenjem, kar je pomembno za opredelitev tveganja.

Radiol Oncol 2025; 59(1): 91-99.
doi: 10.2478/raon-2025-0004

Inovativne strategije za zmanjšanje tveganja hematoma pri biopsijah dojk, vodenih z magnetno resonanco

Brönnimann MP, McMurray MT, Heverhagen JT, Christe A, Wyss C, Peters AA, Huber AT, Dammann F, Obmann VC

Izhodišča. Namen raziskave je bil proučiti možnost zmanjšanja tveganja hematoma med biopsijami dojk, vodenimi z magnetno resonanco (MR). Ocenjevali smo parametre posega, ki so bili odvisni od položaja ter ovrednotili značilnosti biopsirane lezije.

Bolniki in metode. Retrospektivno smo analizirali 252 perkutanih biopsij dojk, ki smo jih izvedli s pomočjo MR, opravljenih v terciarnem centru med januarjem 2013 in decembrom 2023. Glede na resnost nastanka relativnega hematoma (z uporabo mejne vrednosti ≤ 7,62 cm^3 ali > 7,62 cm^3) smo oblikovali dve skupini. Ocenili smo potencialne vplive spremenljivk, kot so bili bolničini demografski podatki, intervencijski parametri, povezani z anatomskimi podatki in značilnosti lezije. Za izračun statistične razlike med skupinami kategoričnih, dihotomnih in zveznih spremenljivk smo uporabili Fisherjev natančni test in Mann-Whitneyev U test. Za opredelitev najmočnejše povezave z relativnim nastankom hematoma smo uporabili multivariatno logistično regresijo.

Rezultati. Univariatna analiza je pokazala, da so se relativno večji hematomi pojavili bistveno pogosteje pri mlajših bolnicah (P = 0,002), kadar so bile primerljive razdalje od biopsirane lezije do bradavice (P = 0,001) in dostopnost poti (P = 0,001) večji ter kadar smo uporabili sistem za vakuumsko biopsijo v primerjavi s sistemom Spirotome® (P = 0,035). Tudi multivariatna logistična regresijska analiza je pokazala, da so bili ti dejavniki neodvisno povezani s pojavom relativno večjih hematomov. Epinefrin v lokalnem anestetiku, lokacija lezije, razvrščene po posameznih kvadrantih, in patohistološke ugotovitve niso vplivali na obseg hematoma.

Zaključki. Ugotovitve raziskave poudarjajo pomen strateškega načrtovanja postopka za zmanjšanje pojava hematoma in za povečanje varnosti bolnikov med postopki biopsije dojk z MR.

Radiol Oncol 2025; 59(1): 100-109.
doi: 10.2478/raon-2025-0017

Primerjava selektivne intraarterijske in standardne intravenske aplikacije pri perkutani elektrokemoterapiji (pECT) jetrnih tumorjev

Wilke T, Hussain E, Spallek H, de Terlizzi F, Mir LM, Bischoff P, Schäfer A, Bartmuß E, Cadossi M, Zanasi A, Pinkawa M, Kovács A

Izhodišča. Elektrokemoterapija (ECT) je lokalno nekirurško učinkovito zdravljenje tumorjev, ki jo izvajamo tudi pri obravnavi bolnikov z jetrnimi tumorji ali metastazami. Namen raziskave je bil preveriti tehnično izvedljivost in varnost intraarterijske aplikacije bleomicina v primerjavi z uveljavljeno intravensko aplikacijo pri perkutani elektrokemoterapiji (pECT). Želeli smo tudi primerjati učinkovitost obeh načinov zdravljenja glede na lokalni odgovor na zdravljenje in preživetje brez napredovanja bolezni.

Bolniki in metode. V raziskavo smo vključili 44 bolnikov, ki smo jih zdravili s pECT zaradi hepatocelularnega karcinoma, holangiokarcinoma in jetrnih metastaz raka različnih izvorov. 18 bolnikom smo aplicirali bleomicin na standardni način intravenozno, 26 bolnikom pa intraarterijsko.

Rezultati. Obe skupini sta si bili podobni po splošnih anagrafskih in po anamnestičnih podatkih ter po bolezenskih značilnostih. Zdravljenje smo lahko tehnično izvedli pri 95 % bolnikov z intravensko aplikacijo in pri 100 % bolnikov z intararterijsko. Kratkoročni lokalni odgovor na zdravljenje je bil v obeh skupinah bolnikov podoben, z nekoliko višjo stopnjo popolnega odgovora v skupini z intararterijsko aplikacijo. V skupini z intravensko aplikacijo bleomicina je bilo 61,9 % popolnih odgovorov; 23,8 % delnih in 4,8 % stagnacije bolezni, v skupini z intraarterijsko aplikacijo pa je bila lokalna kontrola bolezni glede na odgovor na zdravljenje 80,6 %; 12,9 % in 3,2 % (p = 0,3454). Enoletno preživetje brez napredovanja bolezni je bilo pri intravenski aplikaciji 60 % (I.Z. 33 % – 88 %), pri intararterijski pa 67 % (I.Z. 42 % – 91 %) (p = 0,5849).

Zaključki. Rezultati raziskave potrjujejo varnost in izvedljivost superselektivne intraarterijske aplikacije bleomicina. Lokalni odgovor na zdravljenje in preživetja brez napredovanja bolezni sta v raziskavi pokazala primerljivo učinkovitost intraarterijskega načina dovajanja bleomicina v primerjavi s standardnim intravenoznim pri zdravljenju primarnih in sekundarnih jetrnih malignomov s pECT.

Radiol Oncol 2025; 59(1): 110-120.
doi: 10.2478/raon-2025-0001

Raziskava polimorfizmov genov GSTP1 in PTEN ter njihove povezave z dovzetnostjo za kolorektalni rak

Shahwar D-e, Zubair H, Kashif Raza M, Khan Z, Mansour L, Ali A, Imran M

Izhodišča. Preučevali smo povezavo enonukleotidnega polimorfizma (*ang. Single-Nucleotide Polymorphism*) v glutation S transferazi P1 (rs1695 in rs1138272) ter fosfatazi in homologu TENsin (rs701848 in rs2735343) s tveganjem za kolorektalni rak.

Bolniki in metode. V raziskavo primerov in kontrol smo vključili 200 bolnikov s kolorektalnim rakom in 250 zdravih subjektov za kontrolo. Vsi preiskovanci so bili razdeljeni v 3 skupine: bolniki, zdravi subjekti za kontrolo ter skupna skupina (bolniki in kontrolni subjekti). Genotipizacijo smo naredili z verižno reakcijo s polimerazo in polimorfizmom dolžine restrikcijskih fragmentov. Zbrali smo demografske podatke, vključno s starostjo, spolom, mestom bolezni, kadilskim statusom, stadijem raka in prizadetostjo bezgavk.

Rezultati. Pogostost alelov PTEN rs701848 pri vseh osebah je bila 0,78 za C in 0,22 za T. Podobno je bila pri vseh osebah pogostost alelov PTEN rs2735343 0,65 in 0,35 za alela G in C. Ugotovili smo, da sta bila genotip CC ali alel C rs701848 in genotip CG/GG rs2735343 dejavnika tveganja za kolorektalni rak. Pri vseh posameznikih smo opazili pomembno ($p \leq 0,05$) povezavo med polimorfizmoma rs701848 in rs2735343 ter kolorektalnim rakom. Pogostosti alelov za rs1695 GSTP1 sta bili 0,68 oziroma 0,32 za alela A in G. Pogostosti alelov za GSTP1 rs113828 sta bili 0,68 oziroma 0,32 za alela C in T. Vendar smo za rs1695 ugotovili pomembno ($p < 0,05$) povezavo pri moških, medtem ko smo videli za porazdelitev vseh genotipov ali alelov pri GSTP1 (rs113828) nepomembno razliko.

Zaključki. Oba enonukleotidna polimorfizma PTEN rs701848 in rs2735343 sta bila pomembno povezana s kolorektalnim rakom. Pri GSTP1 pa je bil rs1695 pomembno povezan s tveganjem za rak debelega črevesa in danke pri moških, med tem ko je rs113828 pokazal nepomembno povezavo s tveganjem za kolorektalni rak.

Radiol Oncol 2025; 59(1): 121-131.
doi: 10.2478/raon-2025-0013

Obravnava karcinoma skorje nadledvične žleze v Sloveniji. Klinična analiza histopatoloških kazalcev, vzorcev zdravljenja, napovednih kazalcev in preživetja

Bokal U, Jeruc J, Kocjan T, Volavšek M, Jerebic J, Rakuša M, Mencinger M

Izhodišča. Karcinom skorje nadledvične žleze (*angl. adrenocortical carcinoma*, ACC) je redek rak, ki predstavlja izziv pri diagnosticiranju in zdravljenju. Preučili smo zdravljenje in preživetje bolnikov z ACC v Sloveniji v obdobju 17-ih let.

Bolniki in metode. V raziskavo smo vključili bolnike, ki so bili vpisani v Register raka RS in smo jih zdravili od leta 2000 do 2017. Preživetje in napovedne dejavnike smo ocenili s Kaplan-Meierjevo metodo in Coxovo regresijo.

Rezultati. Vključenih je bilo 48 bolnikov. Ob postavitvi diagnoze je 6 %, 42 %, 25 % oziroma 27 % bolnikov imelo stadij bolezni glede na klasifikacijo Evropske zveze za raziskavo nadledvičnih tumorjev (*angl. European Network for the Study of Adrenal Tumors*, ENSAT) I, II, III oziroma IV. 18 od 34 potencialno primernih bolnikov smo dopolnilno zdravili z mitotanom, Bolniki z visoko rizičnimi karcinomi, ki so bili dopolnilno zdravljeni z mitotanom, so imeli nižje tveganje za smrt, čeprav razlika ni bila statistično značilna. Bolniki s ponovitvijo bolezni so imeli višji Ki67 in številčno bolj pogoste R1 resekcije. Enajst bolnikov je prejelo prvi red zdravljenja z etopozidom, doksorubicinom, cisplatinom in mitotanom (*angl.* EDP-M). Njihovo srednje preživetje brez napredovanja bolezni je bilo 4,4 meseca. Srednje celokupno preživetje celotne kohorte je bilo 28,9 in srednje specifično preživetje 36,2 meseca. Odstotek bolnikov s petletnim specifičnim preživetjem glede na stadij ENSAT I, II, III in IV je bil 100 %, 56 %, 50 % in 0 %. Stadij ENSAT in ocena po Helsinkih sta se izkazala kot napovedna dejavnika za preživetje v multivariantni analizi.

Zaključki. Petletno specifično preživetje naših bolnikov s karcinomom skorje nadledvične žleze in stadijem ENSAT II je bilo manjše v primerjavi z nekaterimi drugimi sodobnimi kohortami. K temu sta lahko prispevala neoptimalno kirurško zdravljenje in nedoslednost pri izvedbi dopolnilnega zdravljenja z mitotanom. Preživetje bolnikov s to redko boleznijo bi lahko izboljšali tudi z optimiziranjem diagnostičnih in zamejitvenih postopkov ter večjim poudarkom na multidisciplinarnosti pri načrtovanju zdravljenja.

Radiol Oncol 2025; 59(1): 132-138.
doi: 10.2478/raon-2025-0003

Učinkovitost tramadola ali topičnega lidokaina v primerjavi z epiduralno ali opioidno analgezijo na pooperativno analgezijo pri laparoskopski resekciji tumorjev debelega črevesa in danke

Spindler-Vesel A, Jenko M, Repar A, Potočnik I, Markovič-Božič J

Izhodišča. Kronična pooperativna bolečina poslabša kakovost življenja. Postopoma se razvije v nevropatsko bolečino. Kombinirana analgezija vpliva na mehanizme nastanka kronične bolečine.

Bolniki in metode. Raziskovali smo, ali lahko lidokainski obliž na mestu rane ali infuzija metamizola in tramadola zmanjšata porabo opioidov med laparoskopsko kolorektalno operacijo in ali so rezultati primerljivi z učinkovitostjo epiduralne analgezije. Bolnike smo naključno razdelili v štiri skupine. V prvo skupino smo vključili 20 bolnikov, ki so prejemali infuzijo piritramida, v drugo skupino pa 21 bolnikov, ki so prejemali infuzijo metamizola in tramadola. V tretji skupini je bilo 20 pacientov deležnih epiduralne analgezije, v četrti je 22 pacientov prejelo piritramid in 5 % lidokainski obliž na mestu rane. Raziskovali smo tudi pojavnost nevropatske bolečine.

Rezultati. Poraba piritramida je bila značilno najmanjša v tretji skupini na dan operacije ter prvi in drugi dan po operaciji. Četrta skupina je potrebovala bistveno manj piritramida kot prva na dan operacije ter prvi in drugi dan po operaciji. Skupina z metamizolom in tramadolom je prvi in drugi dan po operaciji potrebovala bistveno manj piritramida kot skupina 1 in 4 prvi in drugi dan po posegu. Na dan operacije je ta skupina potrebovala največjo količino piritramida.

Zaključki. Za pooperativno analgezijo po laparoskopski resekciji kolorektalih tumorjev je bil tramadol v kombinaciji z metamizolom enako učinkovit kot epiduralna analgezija ali infuzija piritramida. Lidokainski obliž v kombinaciji z infuzijo piritramida je zmanjšal porabo opioidov.

Radiol Oncol 2025; 59(1): 139-146.
doi: 10.2478/raon-2025-0006

Različnost med opazovalci in zaporedij pri razmejitvi ogroženih medeničnih organov na slikah z magnetno resonanco

Zheng W, Yang X, Cheng Z, Lian J, Li E, Mo S, Liu Y, Huang S

Izhodišča. Raziskava ocenjuje različnost (variabilnost) oblikovanja kontur med opazovalci z uporabo slik magnetne resonance (MR), rekonstruiranih z različnimi zaporedji in kvantificira razlike med modeli samodejne segmentacije za različna zaporedja.

Bolniki in metode. 83 bolnikov s tumorji medenice je na simulatorju opravilo magnetnoresonančna slikanja: T1 obteženo (*angl. T1-weighted image*, T1WI), kontrastno ojačano T1 Dixon obteženo (*angl. contrast enhanced Dixon T1-weighted*, T1dixonc) in T2 obteženo (*angl. T2-weighted image,* T2WI). Dva opazovalca sta na vseh posnetkih ročno razmejila mehur, analni kanal, danko in glave stegnenice. Za analizo različnosti med opazovalci in med zaporedji slikanja smo upoštevali razlike v konturah. S pomočjo omrežja *U-Net* smo vzpostavili mrežo za samodejno segmentacijo posamezne sekvence (*angl. single-sequence segmentation*), rezultate segmentacije pa smo analizirali.

Rezultati. Analiza različnosti med opazovalci je pokazala, da so mehur, danka in glava levega stegnenice pri T1WI pokazali najvišji koeficient podobnosti (*angl. dice similarity coefficient,* DSC) in najnižjo 95% Hausdorffovo razdaljo (*angl. Hausdorff distance*, HD), kar je bilo vidno pri vseh treh sekvencah. Pri analizi različnosti zaporedij za istega opazovalca je bila razlika med T1WI in T2WI najmanjša. DSC mehurja, danke in stegneničnih glavic je pri sekvencah T1WI-T2WI presegel 0,88. Razlike med samodejnimi segmentacijami in ročnimi razmejitvami (delineacijami) so bile pri T2WI minimalne. Povprečje DSC samodejne in ročne segmentacije vseh organov na T2WI je preseglo 0,81, povprečna 95-odstotna vrednost HD pa je bila nižja od 7 mm. Podobno analiza različnosti zaporedja samodejne segmentacije je pokazala, da so bili razlike v samodejni segmentaciji med T2WI in T1WI minimalne.

Zaključki. S T1WI in T2WI smo dosegli boljše rezultate pri ročni razmejitvi oziroma pri samodejni segmentaciji. Prav tako je analiza različnost med tremi zaporedji pokazala, da smo dobili dobre rezultate podobnosti med primeroma T1WI in T2WI pri ročni in samodejni segmentaciji. Sklepamo, da se lahko sekvence T1WI in T2WI (ali njuna kombinacija) uporabljajo za radioterapijo samo z MR.

Radiol Oncol 2025; 59(1): 147-152.
doi: 10.2478/raon-2025-0018

Bronhialna bakterijska kolonizacija in občutljivost izoliranih bakterij pri bolnikih z rakom na pljučih

Petrović S, Beović B, Tomič V, Bitenc M, Marc Malovrh M, Dimitrić V, Lužnik D, Miklavčič M, Božič T, Gabrovec T, Sadikov A, Rozman A

Izhodišča. Pooperativna pljučnica ostaja pomemben vzrok smrtnosti po operaciji pljuč. Nedavne raziskave so potrdile, da dihalne poti pod glasilkami niso sterilne in pogosto vključujejo potencialno patogene mikroorganizme, zato se bolniki s pljučnimi malignimi boleznimi izpostavljeni povečanemu tveganju za pljučne okužbe.

Bolniki in metode. V raziskavo smo vključili 149 bolnikov, pri katerih smo naredili bronhoskopijo zaradi za rak sumljivih sprememb na pljučih. Pri vsakem bolniku smo pred specifičnim zdravljenjem ob bronhoskopiji odvzeli vzorce z zaščitenim sterilnim katetrom. Vzorce smo poslali v mikrobiološki laboratorij, kjer smo identificirali izolirane bakterije in testirali njihovo občutljivost na protimikrobna zdravila.

Rezultati. Bakterijsko kolonizacijo smo odkrili pri 88,6 % bolnikov, med njimi jih je 21,5 % imelo potencialno patogene mikroorganizme. Bolniki s sladkorno boleznijo tipa 2 so pokazali višjo stopnjo kolonizacije s potencialno patogenimi mikroorganizmi v primerjavi z drugimi bolniki v raziskavi. Testiranje občutljivosti ni pokazalo pomembne razlike med amoksicilinom s klavulansko kislino in cefalosporini prve generacije tako pri koloniziranih bolnikih kot pri tistih, ki so bili kolonizirani s potencialno patogenimi mikroorganizmi. Nismo pa našli bakterij, ki bi bile odporne na več zdravil.

Zaključki. Rezultati v pričujoči raziskavi so pokazali nekoliko nižjo stopnjo kolonizacije s potencialno patogenimi mikroorganizmi v primerjavi z dosedanjimi raziskavami. Vzrok je verjetno edinstvena geografska značilnost obravnavane populacije. Odsotnost statistično pomembnih razlik v občutljivosti bakterij med obema testiranima antibiotikoma poudarja potrebo po nadaljnjih raziskavah za izboljšanje strategij perioperativnega obvladovanja okužb.

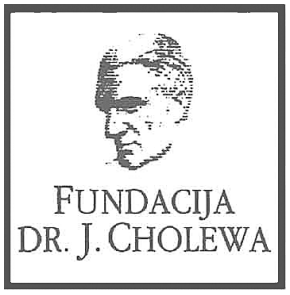

Fundacija ''Docent dr. J. Cholewa''
je neprofitno, neinstitucionalno in nestrankarsko
združenje posameznikov, ustanov in organizacij, ki želijo
materialno spodbujati in poglabljati raziskovalno
dejavnost v onkologiji.

Dunajska 106
1000 Ljubljana
IBAN: SI56 0203 3001 7879 431

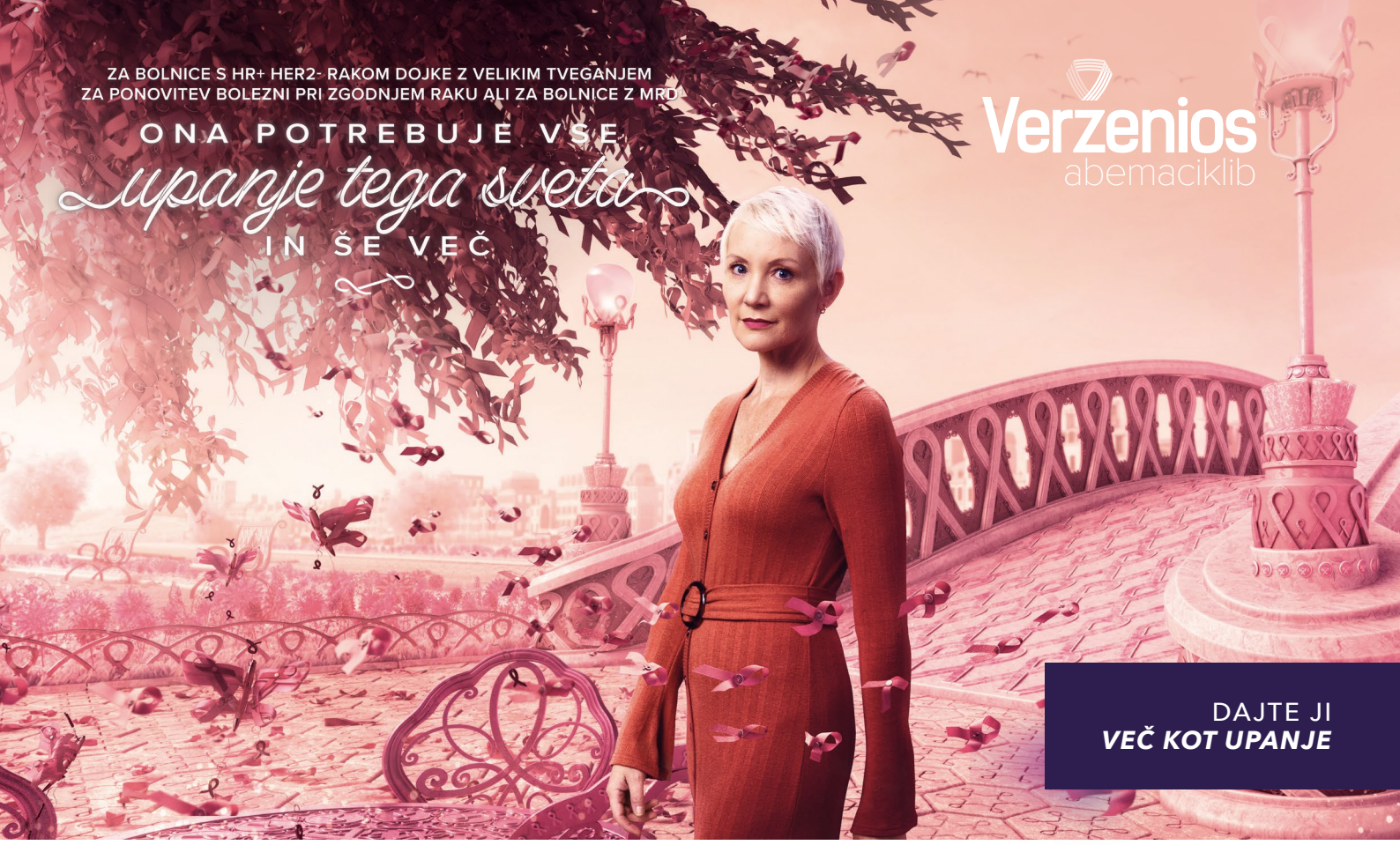

SKRAJŠAN POVZETEK GLAVNIH ZNAČILNOSTI ZDRAVILA

IME ZDRAVILA: Verzenios 50 mg/100 mg/150 mg filmsko obložene tablete **KAKOVOSTNA IN KOLIČINSKA SESTAVA:** Ena filmsko obložena tableta vsebuje 50 mg/100 mg/150 mg abemacikliba. Ena filmsko obložena tableta vsebuje 14 mg/28 mg/42 mg laktoze (v obliki monohidrata). **Terapevtske indikacije**: Zgodnji rak dojk: Zdravilo Verzenios je v kombinaciji z endokrinim zdravljenjem indicirano za adjuvantno zdravljenje odraslih bolnikov z na hormonske receptorje (HR) pozitivnim, na receptorje humanega epidermalnega rastnega faktorja 2 (HER2) negativnim zgodnjim rakom dojk s pozitivnimi bezgavkami, pri katerih obstaja veliko tveganje za ponovitev. Pri ženskah v pred- ali perimenopavzi je treba endokrino zdravljenje z zaviralcem aromataze kombinirati z agonistom gonadoliberina LHRH – luteinizing hormone-releasing hormone). Napredovali ali metastatski rak dojk: Zdravilo Verzenios je indicirano za zdravljenje žensk z lokalno napredovalim ali metastatskim, na hormonske receptorje (HR) pozitivnim in na receptorje humanega epidermalnega rastnega faktorja 2 (HER2) negativnim rakom dojk v kombinaciji z zaviralcem aromataze ali s fulvestrantom kot začetnim endokrinim zdravljenjem ali pri ženskah, ki so prejele predhodno endokrino zdravljenje. Pri ženskah v pred- ali perimenopavzi je treba endokrino zdravljenje kombinirati z agonistom LHRH. **Odmerjanje in način uporabe**: Zdravljenje z zdravilom Verzenios mora uvesti in nadzorovati zdravnik, ki ima izkušnje z uporabo zdravil za zdravljenje rakavih bolezni. Priporočeni odmerek abemacikliba je 150 mg dvakrat na dan, kadar se uporablja v kombinaciji z endokrinim zdravljenjem. *Zgodnji rak dojk:* Zdravilo Verzenios je treba jemati neprekinjeno dve leti, ali do ponovitve bolezni ali pojava nesprejemljive toksičnosti. *Napredovali ali metastatski rak dojk:* Zdravilo Verzenios je treba jemati, dokler ima bolnica od zdravljenja klinično korist ali do pojava nesprejemljive toksičnosti. Če bolnica bruha ali izpusti odmerek zdravila Verzenios, ji je treba naročiti, da naj naslednji odmerek vzame ob predvidenem času; dodatnega odmerka ne sme vzeti. Obvladovanje nekaterih neželenih učinkov lahko zahteva prekinitev in/ali zmanjšanje odmerka. Zdravljenje z abemaciklibom prekinite v primeru povišanja vrednosti AST in/ali ALT >3 x ZMN SKUPAJ s celokupnim bilirubinom > 2,0 x ZMN v odsotnosti holestaze ter pri bolnicah z intersticijsko pljučno boleznijo (ILD)/pnevmonitis stopnje 3 ali 4. Sočasni uporabi močnih zaviralcev CYP3A4 se je treba izogibati. Če se uporabi močnih zaviralcev CYP3A4 ni mogoče izogniti, je treba odmerek abemaciklibа znižati na 100 mg dvakrat na dan. Pri bolnicah, pri katerih je bil odmerek znižan na 100 mg abemaciklibа dvakrat na dan in pri katerih se sočasnemu dajanju močnega zaviralca CYP3A4 ni mogoče izogniti, je treba odmerek abemaciklibа dodatno znižati na 50 mg dvakrat na dan. Pri bolnicah, pri katerih je bil odmerek znižan na 50 mg abemaciklibа dvakrat na dan in pri katerih se sočasnemu dajanju močnega zaviralca CYP3A4 ni mogoče izogniti, je mogoče z odmerkom abemaciklibа nadaljevati ob natančnem spremljanju znakov toksičnosti. Alternativno je mogoče odmerek abemaciklibа znižati na 50 mg enkrat na dan ali prekiniti dajanje abemaciklibа. Če je uporaba zaviralca CYP3A4 prekinjena, je treba odmerek abemaciklibа povečati na odmerek, kakršen je bil pred uvedbo zaviralca CYP3A4 (po 3-5 razpolovnih časih zaviralca CYP3A4). Prilagajanje odmerka glede na starost in pri bolnicah z blago ali zmerno ledvično okvaro ter z blago (Child Pugh A) ali zmerno (Child Pugh B) jetrno okvaro ni potrebno. Pri dajanju abemaciklibа bolnicam s hudo ledvično okvaro sta potrebna previdnost in skrbno spremljanje glede znakov toksičnosti. Način uporabe: Zdravilo Verzenios je namenjeno za peroralno uporabo. Odmerek se lahko vzame s hrano ali brez nje. Zdravila se ne sme jemati z grenivko ali grenivkinim sokom. Bolnice naj odmerke vzamejo vsak dan ob približno istem času. Tableto je treba pogoltniti celo (bolnice tablet pred zaužitjem ne smejo gristi, drobiti ali deliti). **Kontraindikacije**: Preobčutljivost na učinkovino ali katero koli pomožno snov. **Posebna opozorila in previdnostni ukrepi**: Pri bolnicah, ki so prejemale abemaciklib, so poročali o nevtropeniji, o večji pogostnosti okužb kot pri bolnicah, zdravljenih s placebom in endokrinim zdravljenjem, o povečanih vrednostih ALT in AST. Pri bolnicah, pri katerih se pojavi nevtropenija stopnje 3 ali 4, je priporočljivo prilagoditi odmerek. Do primerov nevtropenične sepse s smrtnim izidom je prišlo pri < 1 % bolnic z metastatskim rakom dojk. Bolnicam je treba naročiti, naj o vsaki epizodi povišane telesne temperature poročajo zdravstvenemu delavcu. Bolnice je treba spremljati za znake in simptome globoke venske tromboze (VTE) in pljučne embolije ter jih zdraviti, kot je medicinsko utemeljeno. Glede na stopnjo VTE bo morda treba spremeniti odmerek abemaciklibа. Pri bolnikih, pri katerih se pojavi resni arterijski trombembolični dogodek (ATE), je treba oceniti koristi in tveganja nadaljnjega zdravljenja z abemaciklibom. Glede na povečanje vrednosti ALT ali AST je mogoče potrebna prilagoditev odmerka. Driska je najpogostejši neželeni učinek. Bolnice je treba ob prvem znaku tekočega blata začeti zdraviti z antidiaroiki, kot je loperamid, povečati vnos peroralnih tekočin in obvestiti zdravnika. Sočasni uporabi induktorjev CYP3A4 se je treba izogibati zaradi tveganja za zmanjšano učinkovitost abemaciklibа. Bolnice z redkimi dednimi motnjami, kot so intoleranca za galaktozo, popolno pomanjkanje laktaze ali malapsorpcija glukoze/galaktoze, tega zdravila ne smejo jemati. Bolnice je treba spremljati glede pljučnih simptomov, ki kažejo na ILD/pnevmonitis, in jih ustrezno zdraviti. Glede na stopnjo ILD/pnevmonitisa je morda potrebno prilagajanje odmerka abemaciklibа. **Medsebojno delovanje z drugimi zdravili in druge oblike interakcij**: Abemaciklib se primarno presnavlja s CYP3A4. Sočasna uporaba abemaciklibа in zaviralcev CYP3A4 lahko poveča plazemsko koncentracijo abemaciklibа. Uporabi močnih zaviralcev CYP3A4 sočasno z abemaciklibom se je treba izogibati. Če je močne zaviralce CYP3A4 treba dajati sočasno, je treba odmerek abemaciklibа zmanjšati, nato pa bolnico skrbno spremljati glede toksičnosti. Pri bolnicah, zdravljenih z zmernimi ali šibkimi zaviralci CYP3A4, ni potrebno prilagajanje odmerka, vendar jih je treba skrbno spremljati za znake toksičnosti. Sočasni uporabi močnih induktorjev CYP3A4 (vključno, vendar ne omejeno na: karbamazepin, fenitoin, rifampicin in šentjanževko) se je treba izogibati zaradi tveganja za zmanjšano učinkovitost abemaciklibа. Abemaciklib in njegovi glavni aktivni presnovki zavirajo prenašalce v ledvicah, in sicer kationski organski prenašalec 2 (OCT2) ter prenašalca MATE1. *In vivo* lahko pride do medsebojnega delovanja abemaciklibа in klinično pomembnih substratov teh prenašalcev, kot je dofelitid ali kreatinin. Trenutno ni znano, ali lahko abemaciklib zmanjša učinkovitost sistemskih hormonskih kontraceptivov, zato se ženskam, ki uporabljajo sistemske hormonske kontraceptive, svetuje, da hkrati uporabljajo tudi mehansko metodo. **Neželeni učinki**: Najpogostejši neželeni učinki so driska, okužbe, nevtropenija, levkopenija, anemija, utrujenost, navzea, bruhanje in zmanjšanje apetita. *Zelo pogosti:* okužbe, nevtropenija, levkopenija, anemija, trombocitopenija, limfopenija, zmanjšanje apetita, glavobol, disgevzija, omotica, driska, bruhanje, navzea, stomatitis, alopecija, pruritus, izpuščaj, pireksija, utrujenost, povečana vrednost alanin-aminotransferaze, povečana vrednost aspartat-aminotransferaze *Pogosti:* povečano solzenje, venska trombembolija, ILD/pnevmonitis, dispepsija, spremembe na nohtih, suha koža, mišična šibkost *Občasni:* febrilna nevtropenija, fotopsija **Rok uporabnosti**: 3 leta **Posebna navodila za shranjevanje** Za shranjevanje zdravila niso potrebna posebna navodila. **Imetnik dovoljenja za promet z zdravilom**: Eli Lilly Nederland B.V., Papendorpseweg 83, 3528BJ, Utrecht, Nizozemska. Datum prve odobritve dovoljenja za promet: 27. september 2018. Datum zadnjega podaljšanja: 23. junij 2023. **Datum zadnje revizije besedila**: 4. 7. 2024 **Režim izdaje:** Rp/Spec - Predpisovanje in izdaja zdravila je le na recept zdravnika specialista ustreznega področja medicine ali od njega pooblaščenega zdravnika.

Reference: 1. Povzetek glavnih značilnosti zdravila Verzenios, zadnja odobrena verzija.

Pomembno: Predpisovanje in izdaja zdravila je le na recept zdravnika specialista ustreznega področja medicine ali od njega pooblaščenega zdravnika. Pred predpisovanjem zdravila Verzenios si preberite zadnji veljavni Povzetek glavnih značilnosti zdravil. Podrobne informacije o zdravilu so objavljene na spletni strani Evropske agencije za zdravila http://www.ema.europa.eu

Eli Lilly farmacevtska družba, d.o.o., Dunajska cesta 167, 1000 Ljubljana, telefon 01 / 580 00 10, faks 01 / 569 17 05

PP-AL-SI-0306, 24.9.2024. Samo za strokovno javnost.

PR/BSI/BEN/2024/008

TANTUM VERDE®

benzidaminijev klorid

Za lajšanje bolečine in oteklin v ustni in žrelu, ki so posledica radiomukozitisa

Bistvene informacije iz Povzetka glavnih značilnosti zdravila

Tantum Verde 1,5 mg/ml oralno pršilo, raztopina
Tantum Verde 3 mg/ml oralno pršilo, raztopina

Sestava: 1,5 mg/ml: 1 ml raztopine vsebuje 1,5 mg benzidaminijevega klorida, kar ustreza 1,34 mg benzidamina. V enem razpršku je 0,17 ml raztopine. En razpršek vsebuje 0,255 mg benzidaminijevega klorida, kar ustreza 0,2278 mg benzidamina. **Sestava 3 mg/ml:** 1 ml raztopine vsebuje 3 mg benzidaminijevega klorida, kar ustreza 2,68 mg benzidamina. V enem razpršku je 0,17 ml raztopine. En razpršek vsebuje 0,51 mg benzidaminijevega klorida, kar ustreza 0,4556 mg benzidamina. **Terapevtske indikacije:** Samozdravljenje: Lajšanje bolečine in oteklin pri vnetju v ustni votlini in žrelu, ki so lahko posledica okužb in stanj po operaciji. Po nasvetu in navodilu zdravnika: Lajšanje bolečine in oteklin v ustni votlini in žrelu, ki so posledica radiomukozitisa. **Odmerjanje in način uporabe:** Uporaba: 2- do 6-krat na dan (vsake 1,5 do 3 ure). Odmerjanje 1,5 mg/ml: Odrasli: 4 do 8 razprškov 2- do 6-krat na dan. Pediatrična populacija: Mladostniki, stari od 12 do 18 let: 4-8 razprškov 2- do 6-krat na dan. Otroci od 6 do 12 let: 4 razprški 2- do 6-krat na dan. Otroci, mlajši od 6 let: 1 razpršek na 4 kg telesne mase; do največ 4 razprške 2- do 6-krat na dan. Odmerjanje 3 mg/ml: Odrasli: 2 do 4 razprški 2- do 6-krat na dan. Pediatrična populacija: Mladostniki, stari od 12 do 18 let: 2 do 4 razprški 2- do 6-krat na dan. Otroci od 6 do 12 let: 2 razprška 2- do 6-krat na dan. Otroci, mlajši od 6 let: 1 razpršek na 8 kg telesne mase; do največ 2 razprška 2- do 6-krat na dan. Starejši bolniki, bolniki z jetrno okvaro in bolniki z ledvično okvaro: niso potrebni posebni previdnostni ukrepi. Trajanje zdravljenja ne sme biti daljše od 7 dni. Način uporabe: Za orofaringealno uporabo. Zdravilo se razprši v usta in žrelo. **Kontraindikacije:** Preobčutljivost na učinkovino ali katero koli pomožno snov. **Posebna opozorila in previdnostni ukrepi:** Pri nekaterih bolnikih lahko resne bolezni povzročijo ustne/žrelne ulceracije. Če se simptomi v treh dneh ne izboljšajo, se mora bolnik posvetovati z zdravnikom ali zobozdravnikom, kot je primerno. Uporaba benzidamina ni priporočljiva za bolnike s preobčutljivostjo na salicilno kislino ali druga nesteroidna protivnetna zdravila. Pri bolnikih, ki imajo ali so imeli bronhialno astmo, lahko pride do bronhospazma. Pri takih bolnikih je potrebna previdnost. To zdravilo vsebuje 13,6 mg alkohola (etanola) v enem razpršku (0,17 ml), kar ustreza manj kot 0,34 ml piva oziroma 0,14 ml vina. Majhna količina alkohola v zdravilu ne bo imela nobenih opaznih učinkov. To zdravilo vsebuje metilparahidroksibenzoat (E218). Lahko povzroči alergijske reakcije (lahko zapoznele). To zdravilo vsebuje manj kot 1 mmol (23 mg) natrija v enem razpršku (0,17 ml), kar v bistvu pomeni 'brez natrija'. Zdravilo vsebuje aromo poprove mete z benzilalkoholom, cinamilalkoholom, citralom, citronelolom, geraniolom, izoevgenolom, linalolom, evgenolom in D-limonen, ki lahko povzročijo alergijske reakcije. Zdravilo z jakostjo 3 mg/ml vsebuje makrogolglicerol hidroksistearat 40. Lahko povzroči želodčne težave in drisko. **Medsebojno delovanje z drugimi zdravili in druge oblike interakcij:** Študij medsebojnega delovanja niso izvedli. **Nosečnost in dojenje:** O uporabi benzidamina pri nosečnicah in doječih ženskah ni zadostnih podatkov. Uporaba zdravila med nosečnostjo in dojenjem ni priporočljiva. **Vpliv na sposobnost vožnje in upravljanja strojev:** Zdravilo v priporočenem odmerku nima vpliva na sposobnost vožnje in upravljanja strojev. **Neželeni učinki:** Neznana pogostnost (ni mogoče oceniti iz razpoložljivih podatkov): anafilaktične reakcije, preobčutljivostne reakcije, odrevenelost, laringospazem, suha usta, navzea in bruhanje, oralna hipestezija, angioedem, fotosenzitivnost, pekoč občutek v ustih. Neposredno po uporabi se lahko pojavi občutek odrevenelosti v ustih in v žrelu. Ta učinek se pojavi zaradi načina delovanja zdravila in po kratkem času izgine. **Način in režim izdaje zdravila:** BRp-Izdaja zdravila je brez recepta v lekarnah in specializiranih prodajalnah. **Imetnik dovoljenja za promet:** Aziende Chimiche Riunite Angelini Francesco – A.C.R.A.F. S.p.A., Viale Amelia 70, 00181 Rim, Italija **Datum zadnje revizije besedila:** 05. 04. 2022

Pred svetovanjem ali izdajo preberite celoten Povzetek glavnih značilnosti zdravila.

Samo za strokovno javnost.

Datum priprave informacije: julij 2024

Odgovoren za trženje: Bonifar d.o.o.

ANGELINI

NADGRAJUJEMO ZDRAVLJENJE
PLJUČNEGA RAKA

ADAURA

Resektabilni EGFRm NSCLC (stadiji IB-IIIA), katerega EGFR ima Del19 ali L858R

51% manjša verjetnost

za smrt v primerjavi
s placebom v celokupni populaciji

ROg=0,62 ROg = 0,49 (95% IZ: 034, 0,70; p<0,001)[2]

FLAURA

Lokalno napredovali ali metastatski NSCLC, katerega EGFR ima aktivirajoče mutacije

38,6 vs **31,8**

mediano OS
v primerjavi z gefitinib/erlotinib

ROg: 0,80 (95,05% IZ: 0,641, 0,997; p<0,001)[3]

TAGRISSO®
osimertinib

LAURA

Lokalno napredovali neresektabilni EGFRm NSCLC

39,1 vs **5,6** mesecev

mediano PFS
v primerjavi s placebom

ROg=0,16 (95% IZ: 0,10, 0,24); p<0.001)[5]
Ocenjeno s slepim, neodvisnim centralnim pregledom (BICR)

FLAURA 2

Lokalno napredovali ali metastatski NSCLC, katerega EGFR ima aktivirajoče mutacije

29,9 vs **19,4** mesecev

mediano PFS zdravilo Tagrisso v kombinaciji s kemoterapijo v primerjavi z monoterapijo

ROg=0,62 (95% IZ; 0,48, 0,80)[4]
Ocenjeno s slepim, neodvisnim centralnim pregledom (BICR)

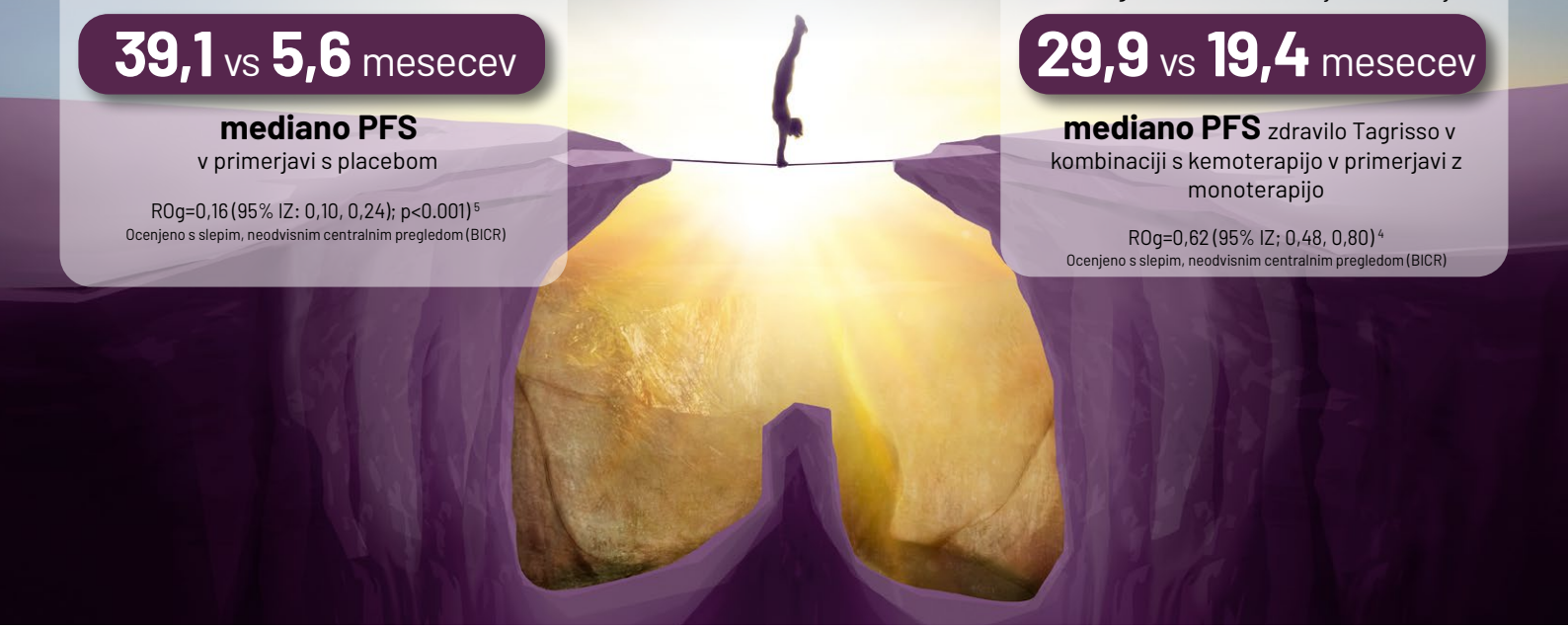

SKRAJŠAN POVZETEK GLAVNIH ZNAČILNOSTI ZDRAVILA

TAGRISSO 40 mg filmsko obložene tablete / TAGRISSO 80 mg filmsko obložene tablete

SESTAVA: Ena filmsko obložena tableta vsebuje 40 ali 80 mg osimertiniba. **INDIKACIJE:** Zdravilo Tagrisso je kot monoterapija indicirano za: adjuvantno zdravljenje po popolni resekciji tumorja pri odraslih bolnikih z nedrobnoceličnim rakom pljuč v stadiju IB-IIIA (NSCLC - non-small cell lung cancer), pri katerem ima tumorski receptor za epidermalni rastni faktor (EGFR - epidermal growth factor receptor) delecije eksona 19 ali substitucije eksona 21 (L858R). • prvo linijo zdravljenja odraslih bolnikov z lokalno napredovalim ali metastatskim nedrobnoceličnim rakom pljuč (NSCLC - "non-small-cell lung cancer"), katerega receptor za epidermalni rastni faktor (EGFR - "epidermal growth factor receptor") ima aktivirajoče mutacije. • zdravljenje odraslih bolnikov z lokalno napredovalim ali metastatskim NSCLC, pozitivnim za mutacijo T790M EGFR. • zdravljenje odraslih bolnikov z lokalno napredovalim, neoperabilnim NSCLC, katerih tumorji imajo delecije eksona 19 ali substitucijske mutacije eksona 21 (L858R) EGFR in jim bolezen med kemoradioterapijo na podlagi platine ali po njej ni napredovala. Zdravilo Tagrisso je indicirano v kombinaciji s: pemetreksedom in kemoterapijo na podlagi platine za prvo linijo zdravljenja odraslih bolnikov z napredovalim NSCLC, ki imajo tumorje z delecijo eksona 19 EGFR ali substitucijsko mutacijo eksona 21 (L858R) EGFR. **ODMERJANJE IN NAČIN UPORABE:** Zdravljenje z zdravilom Tagrisso mora uvesti zdravnik, ki ima izkušnje z zdravili za zdravljenje raka. Pri odločanju o uporabi zdravila Tagrisso je treba določiti stanje mutacije EGFR (v vzorcih tumorja pri adjuvantnem zdravljenju ali za zdravljenje lokalno napredovalih, neoperabilnih tumorjev in v vzorcih tumorja ali plazme pri lokalno napredovalem ali metastatskem raku) z uporabo validirane testne metode. Odmerjanje: Priporočeni odmerek je 80 mg osimertiniba enkrat na dan. Bolniki na adjuvantnem zdravljenju morajo zdravili jemati do ponovitve bolezni ali nesprejemljivih toksičnih učinkov. Zdravljenja, daljšega od 3 let, niso preučili. Bolniki z lokalno napredovalim ali metastatskim rakom pljuč morajo zdravilo jemati do napredovanja bolezni ali nesprejemljivih toksičnih učinkov. Če bolnik izpusti odmerek zdravila Tagrisso, ga mora vzeti, razen če je do naslednjega odmerka že manj kot 12 ur. Zdravilo Tagrisso je mogoče vzeti s hrano ali brez nje, vsak dan ob istem času. Med uporabo s pemetreksedom in kemoterapijo na podlagi platine je priporočeni odmerek zdravila Tagrisso 80 mg osimertiniba enkrat na dan. Prilagoditve odmerka: Glede na varnost in prenašanje pri posameznem bolniku je lahko potrebna prekinitev odmerjanja in/ali zmanjšanje odmerka. V primeru potrebe po zmanjšanju odmerka je treba odmerek zmanjšati na 40 mg enkrat na dan. Smernice za zmanjšanje odmerka v primeru neželenih učinkov/toksičnosti so navedene v preglednici v Povzetku glavnih značilnosti zdravila. To zdravilo je namenjeno za peroralno uporabo. Tableto je treba zaužiti celo z vodo in se je ne sme drobiti, lomiti ali gristi. Odmerek pemetrekseda, cisplatina ali karboplatina je treba prilagoditi v skladu z navodili v ustreznih povzetkih glavnih značilnosti zdravil. Cisplatin in/ali karboplatin je treba uporabljati do 4 cikle. **KONTRAINDIKACIJE:** Preobčutljivost na učinkovino ali katerokoli pomožno snov. Šentjanževke se ne sme uporabljati skupaj z zdravilom Tagrisso. **OPOZORILA IN PREVIDNOSTNI UKREPI:** Pri odločanju o uporabi zdravila TAGRISSO pri bolnikih z lokalno napredovalim, neoperabilnim NSCLC, ki jim bolezen ni napredovala med kemoradioterapijo na podlagi platine ali po njej, za adjuvantno zdravljenje bolnikov z NSCLC po popolni resekciji tumorja ali če je zdravilo TAGRISSO uporabljeno v kombinaciji s pemetreksedom in kemoterapijo na podlagi platine za prvo linijo zdravljenj je pomembno določiti prisotnost mutacije EGFR (delecije eksona 19 (Ex19del) ali substitucije eksona 21 (L858R)). V kliničnem laboratoriju je treba opraviti validirano preiskavo tumorske DNK iz vzorca tkiva, pridobljenega z biopsijo ali kirurškim posegom. Pri odločanju o uporabi zdravila Tagrisso za zdravljenje lokalno napredovalega ali metastatskega NSCLC je pomembno določiti stanje mutacije T790M EGFR. Opraviti je treba validirano preskavo tumorske DNK, dobljene iz vzorca tkiva, ali tumorske DNK v obtoku (ctDNA – circulating tumor DNA), dobljene iz vzorca plazme. Določitev prisotne mutacije EGFR (aktivacijske mutacije EGFR pri prvi linij zdravljenja ali mutacije T790M po napredovanju bolezni med zdravljenjem ali po zdravljenju z zaviralcem tirozin kinaze receptorja za epidermalni rastni faktor) v vzorcu tkiva ali plazme pomeni, da je bolnik primeren za zdravljenje z zdravilom TAGRISSO. A če je uporabljena preiskava za ctDNA iz plazme in je izvid negativen, je priporočljivo opraviti še preiskavo tkivnega vzorca, če je le mogoče. Pri preiskavah vzorcev plazme namreč obstaja možnost lažno negativnih rezultatov. Uporabiti se sme le robustne, zanesljive in občutljive preiskave z dokazano uporabnostjo za določanje stanja mutacije EGFR v tumorski DNK (iz vzorca tkiva ali plazme). O intersticijski bolezni pljuč (IBP) ali neželenih učinkih, podobnih IBP, so poročali pri 4,3 % od 1956 bolnikov, ki so v študijah ADAURA, FLAURA, FLAURA2, AURA in LAURA prejemali zdravilo Tagrisso. Poročali so o 8 dogodkih s smrtnim izidom. Pri adjuvantnem zdravljenju niso poročali o smrtnih primerih. Pojavnost IBP je bila pri bolnikih japonske etnične pripadnosti 10,4 %, pri bolnikih azijske etnične pripadnosti 2,8 % in pri neazijskih bolnikih 3,2 %. Vse bolnike z akutnim nastankom in/ali nepojasnjenim poslabšanjem pljučnih simptomov (dispneja, kašelj, zvišana telesna temperatura) je treba skrbno pregledati, da bi izključili IBP. V času preiskovanja teh simptomov je treba zdravljenje s tem zdravilom prekiniti. Če je diagnosticirana IBP, je treba ukiniti zdravljenje z zdravilom Tagrisso in uvesti ustrezno zdravljenje, kot je potrebno. Ponovna uvedba zdravila Tagrisso pride v poštev le po skrbnem pretehtanju koristi in tveganj pri posameznem bolniku. Radiacijski pnevmonitis: V študiji LAURA so po definitivni kemoradioterapiji na podlagi platine o radiacijskem pnevmonitisu poročali pri 48 % od 143 bolnikov, ki so prejemali zdravilo TAGRISSO in pri 38 % od 73 bolnikov, ki so prejemali placebo.V skupini z zdravilom TAGRISSO so imeli učinke 3. stopnje trije bolniki (2,1 %), v nobeni skupini pa niso poročali o učinkih 4. ali 5. stopnje. Mediani čas od prvega odmerka do pojava radiacijskega pnevmonitisa je bil v skupini z zdravilom TAGRISSO 1,7 meseca in v skupini s placebom 1,8 meseca. Mediani čas od zadnjega odmerka radioterapije do pojava radiacijskega pnevmonitisa je bil v skupini z zdravilom TAGRISSO 2,5 meseca in v skupini s placebom 2,6 meseca. Hudi kožni neželeni učinki (SCARs - Severe Cutaneous Adverse Reactions): V povezavi z zdravljenjem z zdravilom TAGRISSO so poročali o primerih Stevens-Johnsonovega sindroma (SJS), s kategorijo pogostnosti redko in o primerih toksične epidermalne nekrolize (TEN) s kategorijo pogostnosti neznano. Pred uvedbo zdravljenja je treba bolnike seznaniti z znaki in simptomi SJS in TEN. Če se pojavijo znaki ali simptomi, ki nakazujejo SJS ali TEN, je treba zdravljenje z zdravilom TAGRISSO prekiniti. Če se diagnosticira SJS ali TEN se mora zdravljenje z zdravilom TAGRISSO nemudoma ukiniti. Podaljšanje intervala QTc: Bolnikom, zdravljenim z zdravilom Tagrisso, se pojavi podaljšanje intervala QTc. Takšno podaljšanje lahko poveča tveganje za ventrikularne tahiaritmije (npr. torsade de pointes) ali nenadno smrt. V študijah ADAURA, LAURA, FLAURA, FLAURA2 ali AURA nso poročali o motnjah srčnega ritma, povezanih s QTc. Uporabi zdravila Tagrisso se je treba pri bolnikih s prirojenim sindromom dolgega intervala QT izogniti, če je le mogoče. O rednih kontrolah elektrokardiograma (EKG) in elektrolitov je treba razmisliti pri bolnikih s kongestivnim srčnim popuščanjem, elektrolitskimi motnjami in prejemnikih zdravil, za katera je znano, da podaljšajo interval QTc. Prekinite uporabo pri bolnikih, ki se jim interval QTc podaljša preko 500 msec na vsaj 2 ločenih posnetkih EKG, in ga ne uporabljajte, dokler ni interval QTc manj kot 481 msec oziroma do njegove vrnitve na izhodiščno vrednost, če je izhodiščni interval QTc 481 msec ali več. Potem začnite zdravilo Tagrisso znova uporabljati v manjšem odmerku. Trajno ukinite zdravljenje z zdravilom Tagrisso, če se bolniku pojavi podaljšanje intervala QTc v kombinaciji s čimer koli od naslednjega: torsade de pointes, polimorfna ventrikularna tahikardija, znaki/simptomi resne motnje srčnega ritma. Spremembe v krčljivosti srca: V kliničnih preskušanjih se je zmanjšanje iztisnega deleža levega prekata (LVEF "left ventricular ejection fraction") za ≥ 10 odstotnih točk ali na manj kot 50 % pojavilo pri 4,2 % (65/1557) bolnikov, zdravljenih z monoterapijo z zdravilom TAGRISSO, ki so imeli LVEF izmerjen izhodiščno in vsaj še enkrat med obdobjem spremljanja. Pri bolnikih s srčnimi dejavniki tveganja in bolnikih s stanji, ki prizadenejo LVEF, je treba razmisliti o nadziranju delovanja srca, vključno z ocenjevanjem LVEF izhodiščno in med zdravljenjem. Pri bolnikih, ki se jim med zdravljenjem pojavijo pomembni srčni znaki ali simptomi, je treba razmisliti o nadziranju delovanja srca, vključno z ocenjevanjem LVEF. V s placebom nadzorovanem preskušanju adjuvantnega zdravljenja (ADAURA) se je zmanjšanje LVEF za ≥ 10 odstotnih točk ali na manj kot 50 % pojavilo pri 1,5 % (5/335) bolnikov, zdravljenih z zdravilom TAGRISSO, in 1,5 % (5/331) bolnikov, zdravljenih s placebom. V študiji LAURA se je med bolniki, ki so imeli izhodiščno in poizhodiščno oceno LVEF, po kemoradioterapiji na podlagi platine pojavilo zmanjšanje LVEF za 10 odstotnih točk ali več ter za manj kot 50 % po kemoradioterapiji na podlagi platine pojavilo pri 3,0 % (4/135) prejemnikov zdravila TAGRISSO in pri nobenem prejemniku placeba. V študiji FLAURA2 se je LVEF zmanjšal za 10 odstotnih točk ali več oziroma je upadel na manj kot 50 % pri 8,0 % (21/262) bolnikov, ki so prejemali zdravilo TAGRISSO v kombinaciji s pemetreksedom in kemoterapijo na podlagi platine ter so imeli LVEF izmerjen izhodiščno in vsaj še enkrat med obdobjem spremljanja. Keratitis: O keratitisu so poročali pri 0,6 % bolnikov, zdravljenih z zdravilom Tagrisso v študijah ADAURA, FLAURA, FLAURA2, LAURA in AURA. Bolnike z znaki in simptomi, ki nakazujejo keratitis (na primer vnetje očesa, solzenje, občutljivost na svetlobo, zamegljen vid, bolečine v očesu in/ali pordelost očesa), je treba nemudoma napotiti k specialistu oftalmologu. Aplastična anemija: V povezavi z zdravljenjem z zdravilom Tagrisso so poročali o redkih primerih aplastične anemije, vključno s smrtnimi primeri. Pred uvedbo zdravljenja je treba bolnike seznaniti z znaki in simptomi aplastične anemije, ki vključujejo, a niso omejeni le na dolgotrajno zvišano telesno temperaturo, podplutbe, krvavitve, bledico, okužbe in utrujenost. Če se pojavijo znaki in simptomi, ki kažejo na aplastično anemijo, je treba razmisliti o natančnem nadziranju bolnika ter o prekinitvi ali prenehanju zdravljenja z zdravilom Tagrisso. Pri bolnikih s potrjeno aplastično anemijo je treba zdravljenje z zdravilom Tagrisso ukiniti. Starost in telesna masa: Pri bolnikih starih nad 65 let ali bolnikih z telesno maso pod 50 kg je lahko prisotno povečano tveganje za pojav neželenih učinkov 3. ali višje stopnje. Pri teh bolnikih je priporočeno skrbno spremljanje. **NEDSEBOJNO DELOVANJE Z DRUGIMI ZDRAVILI:** Močni induktorji CYP3A lahko zmanjšajo izpostavljenost osimertinibu. Osimertinib lahko poveča izpostavljenost substratom BCRP in P-glikoproteina (P-gp). Študije in vitro so pokazale, da poteka presnova I. faze osimertiniba pretežno s CYP3A4 in CYP3A5. Podatki iz klinične farmakokinetične študije so pokazali, da ni verjetno, da bi zaviralci CYP3A4 vplivali na izpostavljenost osimertinibu. Dodatnih katalizacijskih encimov niso odkrili. Podatki klinične farmakokinetične študije o sočasni uporabi z rifampicinom kažejo, da se je sočasni uporabi močnih induktorjev CYP3A (npr. fenitoina, rifampicina, karbamazepina) in zdravila Tagrisso priporočljivo izogniti. Izpostavljenost osimertinibu lahko zmanjšajo tudi zmerni induktorji CYP3A4 (npr. bosentan, efavirenz, etravirin, modafinil), zato jih je treba uporabljati previdno oziroma se jim je treba izogniti, če je mogoče. Klinični podatki, ki bi omogočali priporočilo za prilagoditev odmerka zdravila Tagrisso, ni na voljo. Sočasna uporaba šentjanževke je kontraindicirana. Glede na podatke klinične farmakokinetične študije je pri sočasni uporabi zdravila Tagrisso in rosuvastatina ter ostalih zdravil, katerih odstranjevanje je odvisno od BCRP in imajo ozek terapevtski indeks, treba bolnike skrbno spremljati glede znakov spremenjenega prenašanja zaradi večje izpostavljenosti sočasnemu zdravilu med prejemanjem zdravila Tagrisso. Tveganja za manjšo izpostavljenost hormonskim kontraceptivom ni mogoče izključiti. Bolnike, ki sočasno jemljejo zdravila, katerih odstranjevanje je odvisno od P-gp in imajo ozek terapevtski indeks (npr. digoksin, dabigatran, in aliskiren), je treba skrbno spremljati glede znakov spremenjenega prenašanja zaradi večje izpostavljenosti sočasnemu zdravilu v času prejemanja zdravila Tagrisso. **NEŽELENI UČINKI:** Podatki iz petih randomiziranih študij III. faze (ADAURA – adjuvantno zdravljenje, FLAURA in FLAURA2 (skupina z monoterapijo) – prva linija LAURA (po kemoradioterapiji na podlagi platine) in AURA3 - le druga linija) in iz dveh študij z eno samo skupino (AURAex in AURA2 - druga linija ali več) in eni študiji I. faze (AURA1 – prva linija ali več) povzemajo izpostavljenost zdravilu Tagrisso pri 1956 bolnikih z nedrobnoceličnim rakom pljuč in pozitivno mutacijo EGFR. Večina neželenih učinkov je bila glede na resnost 1. ali 2. stopnje. Najpogostejši neželeni učinki zdravila so bili driska (46 %), izpuščaj (45 %), paronihija (33 %), suha koža (31 %) in stomatitis (23 %). V vseh študijah skupaj je bilo neželenih učinkov 3. stopnje 11 % in 4. stopnje 0,2 %. Med bolniki, ki so prejemali zdravilo Tagrisso 80 mg enkrat na dan, so zaradi neželenih učinkov odmerek zmanjšali 3,4 % bolnikom. Ukinitev uporabe zdravila zaradi neželenih učinkov je bilo 5,5 %. Varnost zdravila TAGRISSO v kombinaciji s pemetreksedom in kemoterapijo na podlagi platine temelji na podatkih 276 bolnikov z NSCLC in pozitivno mutacijo EGFR in se sklada z varnostjo monoterapije z zdravilom TAGRISSO in znanimi varnostnimi značilnostmi pemetrekseda in kemoterapije na podlagi platine. Najpogosteje poročani neželeni učinki med uporabo zdravila TAGRISSO v kombinaciji s pemetreksedom in kemoterapijo na osnovi platine, so bili izpuščaj (48 %), driska (43 %), zmanjšan apetit (31 %), stomatitis (31 %), paronihija (27 %) in suha koža (24 %). Zelo pogosti neželeni učinki: zmanjšan apetit, driska, stomatitis, izpuščaj, suha koža, paronihija, srbenje ter zmanjšano število levkocitov, limfocitov, trombocitov in nevtrofilcev. Pogosti neželeni učinki: epistaksa, intersticijska bolezen pljuč, alopecija, urtikarija, sindrom palmarno-plantarne eritrodizestezije, zvišanje ravni kreatinina v krvi, zvišanje ravni kreatin fosfokinaze v krvi, zmanjšan iztisni delež levega prekata. **VRSTA IN VSEBINA OVOJNINE:** Al/Al perforirani pretisni omoti za enkratni odmerek. Škatle z 28 x 1 tableto (4 pretisni omoti). **NAČIN IZDAJANJA ZDRAVILA:** samo na recept **DATUM REVIZIJE BESEDILA:** 19.12.2024. (SI-3575) **IMETNIK DOVOLJENJA ZA PROMET:** AstraZeneca AB, S-151 85, Södertalje. Švedska

Pred predpisovanjem, prosimo, preberite celoten povzetek glavnih značilnosti zdravila. Dodatne informacije so na voljo pri družbi AstraZeneca UK Limited, Podružnica v Sloveniji, Verovškova 55, Ljubljana, telefon +386 1 51 35 600.

NSCLC... nedrobnocelični rak pljuč, ROg...razmerje ogroženosti, IZ...interval zaupanja, OS...celokupno preživetje, PFS...preživetje brez napredovanja bolezni

1.Povzetek glavnih značilnosti zdravila Tagrisso. 2. Tsuboi M, Wu YL, Grohe C, et al. Osimertinib as adjuvant therapy in patients with resected EGFRm stage IB-IIIA NSCLC: updated results from ADAURA. Presented at: ESMO Congress 2022; September 9-13, 2022; Paris, France. 3.Vansteenkiste J, Planchard D, et al; FLAURA Investigators. Overall survival with osimertinib in untreated, EGFR-mutated advanced NSCLC. N Engl J Med. 2020;382(1):41-50. 4. FLAURA-2 5. LAURA, 4, Ramalingam SS, Vansteenkiste J, Planchard D, et al; FLAURA Investigators. Overall survival with osimertinib in untreated, EGFR-mutated advanced NSCLC. N Engl J Med. 2020;382(1):41-50. 5. Planchard D et al. Osimertinib with or without Chemotherapy in EGFR-Mutated Advanced NSCLC. N Engl J Med. 2023 Nov 23;389(21):1935-1948.

Samo za strkovno javnost. Informacija pripravljena januarja 2025.

SI-4748

AstraZeneca

DOVOLI SI VERJETI

Lynparza®
olaparib
tablete 100 mg
tablete 150 mg

*Prvi in edini zaviralec PARP odobren za 5 različnih lokalizacij tumorjev[1-5] **

RAK JAJČNIKOV

Prvi zaviralec PARP odobren za vzdrževalno zdravljenje napredovalega raka jajčnikov v monoterapiji (v 1L pri bolnicah z mutacijo *gena BRCA1/2* in 2L) ali kombinaciji z bevacizumabom (pri bolnicah s HRD).[1-3, 5]

RAK TREBUŠNE SLINAVKE

Edini zaviralec PARP odobren za vzdrževalno zdravljenje bolnikov z zarodno mutacijo gena *BRCA1/2*, ki imajo razsejani adenokarcinom trebušne slinavke in jim bolezen ni napredovala po najmanj 16 tednih prvega reda zdravljenja s kemoterapijo na osnovi platine.[1-4]

RAK DOJK

Prvi zaviralec PARP odobren za zdravljenje, pri bolnikih z zarodno mutacijo gena *BRCA1/2*, ki imajo HER2-negativni zgodnji, lokalno napredovali ali razsejan rak dojk.[1-2, 4]

RAK PROSTATE

Edini zaviralec PARP odobren za zdravljenje bolnikov z razsejanim KORP v monoterapiji za bolnike z mutacijami gena *BRCA1/2*, ki jim je bolezen napredovala po zdravljenju z novim hormonskim zdravilom, in v kombinaciji z abirateronom ne glede na status mutacij.[1-4]

RAK ENDOMETRIJA

Prvi in edini zaviralec PARP odobren za vzdrževalno zdravljenje odraslih bolnic s primarno napredovalim ali ponovljenim rakom endometrija v kombinaciji z durvalumabom za bolnice, ki nimajo okvare popravljanja neujemanja pri podvojevanju DNA (pMMR), bolezen pa jim ni napredovala med zdravljenjem prve linije z durvalumabom v kombinaciji s karboplatinom in paklitakselom.[1-4, *]

SKRAJŠAN POVZETEK GLAVNIH ZNAČILNOSTI ZDRAVILA

LYNPARZA 100 mg filmsko obložene tablete / LYNPARZA 150 mg filmsko obložene tablete

SESTAVA: Ena filmsko obložena tableta vsebuje 100 mg olapariba ali 150 mg olapariba.

INDIKACIJE: Rak jajčnikov: 1) *zdravilo Lynparza je indicirano kot monoterapija za*:
• vzdrževalno zdravljenje odraslih bolnic z napredovalim (stadij III in IV po FIGO) epitelijskim rakom visokega gradusa jajčnikov, jajcevodov ali primarnim peritonealnim rakom z mutacijo gena *BRCA1/2* (germinalno in/ali somatsko), ki so v odzivu (popolnem ali delnem) po zaključeni prvi liniji kemoterapije na osnovi platine.
• vzdrževalno zdravljenje odraslih bolnic, pri katerih je prišlo do ponovitve epitelijskega raka visokega gradusa jajčnikov, jajcevodov ali primarnega peritonealnega raka, občutljivega na platino, ki so v popolnem ali delnem odzivu na kemoterapijo na osnovi platine.
2) *zdravilo Lynparza je v kombinaciji z bevacizumabom indicirano za:*
• vzdrževalno zdravljenje odraslih bolnic z napredovalim (stadij III in IV po FIGO) epitelijskim rakom visokega gradusa jajčnikov, jajcevodov ali primarnim peritonealnim rakom, ki so v popolnem ali delnem odzivu po zaključeni prvi liniji kemoterapije na osnovi platine v kombinaciji z bevacizumabom, pri katerih je rak povezan s pozitivnim stanjem pomanjkanja homologne rekombinacije (HRD – homologous recombination deficiency), opredeljenim z mutacijo gena *BRCA1/2* in/ali genomsko nestabilnostjo.
Rak dojk: *zdravilo Lynparza je indicirano kot:*
• monoterapija ali v kombinaciji z endokrinim zdravljenjem za adjuvantno zdravljenje odraslih bolnikov z germinalnimi mutacijami gena *BRCA1/2*, ki imajo HER2-negativnega zgodnjega raka dojk z velikim tveganjem in so bili predhodno zdravljeni z neoadjuvantno ali adjuvantno kemoterapijo.
• monoterapija za zdravljenje odraslih bolnikov z germinalno mutacijo gena *BRCA1/2*, ki imajo HER2-negativnega lokalno napredovalega ali metastatskega raka dojk. Bolniki morajo biti predhodno zdravljeni z antraciklinom in taksanom v okviru (neo)adjuvantnega zdravljenja ali zdravljenja metastatske bolezni, razen če za ti zdravljenji niso primerni. Pri bolnikih, ki imajo raka dojk s pozitivnimi hormonskimi receptorji (HR), je morala bolezen prav tako napredovati med predhodnim hormonskim zdravljenjem ali po njem, ali morajo bolniki veljati za neprimerne za hormonsko zdravljenje.
Adenokarcinom trebušne slinavke: zdravilo Lynparza je kot monoterapija indicirano za vzdrževalno zdravljenje odraslih bolnikov z germinalno mutacijo gena BRCA1/2, ki imajo metastatski adenokarcinom trebušne slinavke in njihova bolezen ni napredovala po najmanj 16 tednih zdravljenja s platino v shemi prve linije kemoterapije.
Rak prostate: *zdravilo Lynparza je indicirano:*
• kot monoterapija za zdravljenje odraslih bolnikov z metastatskim, na kastracijo odpornim rakom prostate (mKORP) in mutacijami gena *BRCA1/2* (germinalnimi in/ali somatskimi), pri katerih je bolezen napredovala po predhodni terapiji, ki je vsebovala novo hormonsko zdravilo.
• v kombinaciji z abirateronom in prednizonom ali prednizolonom za zdravljenje odraslih bolnikov z mKORP, pri katerih kemoterapija ni klinično indicirana.
Rak endometrija: Zdravilo Lynparza je v kombinaciji z durvalumabom indicirano za vzdrževalno zdravljenje odraslih bolnic s primarno napredovalim ali ponovljenim rakom endometrija, ki nimajo okvare popravljanja neujemanja pri podvojevanju DNA (pMMR), bolezen pa jim ni napredovala med zdravljenjem prve linije z durvalumabom v kombinaciji s karboplatinom in paklitakselom.

ODMERJANJE IN NAČIN UPORABE: Priporočeni odmerek zdravila Lynparza pri monoterapiji ali v kombinaciji z drugimi zdravili je 300 mg (dve 150 mg tableti) dvakrat na dan; to ustreza celotnemu dnevnemu odmerku 600 mg. 100 mg tablete so na voljo za zmanjšanje odmerka. Bolnice s ponovitvijo raka jajčnikov morajo začeti zdravljenje z zdravilom Lynparza najpozneje v 8 tednih po zadnjem odmerku sheme zdravljenja na osnovi platine. Če je zdravilo Lynparza uporabljeno v kombinaciji z bevacizumabom za prvo linijo vzdrževalnega zdravljenja po dokončanju prve linije zdravljenja na osnovi platine in z bevacizumabom, je odmerek bevacizumaba 15 mg/kg enkrat na 3 tedne. Glejte celotne informacije o zdravilu za bevacizumab. Za priporočeno odmerjanje partnerskega zdravila/partnerskih zdravil (zaviralec aromataze/antiestrogen in/ali LHRH) v kombinaciji endokrinega zdravljenja glejte celotne informacije o zadevnem zdravilu. Če je zdravilo Lynparza uporabljeno v kombinaciji z abirateronom za zdravljenje bolnikov z mKORP, je odmerek abiraterona 1000 mg peroralno enkrat na dan. Abirateron je treba dajati s 5 mg prednizona ali prednizolona peroralno dvakrat na dan. Glejte celotne informacije o zdravilu za abirateron. Če je zdravilo Lynparza uporabljeno v kombinaciji z durvalumabom za vzdrževalno zdravljenje odraslih bolnic s primarno napredovalim ali ponovljenim rakom endometrija brez okvare MMR (pMMR), ki jim bolezen ni napredovala med zdravljenjem prve linije z durvalumabom v kombinaciji s karboplatinom in paklitakselom, je odmerek durvalumaba 1500 mg na 4 tedne. Glejte celotne informacije o zdravilu za durvalumab. Prvo linijo vzdrževalnega zdravljenja napredovalega raka jajčnikov z mutacijo gena BRCA in prvo linijo vzdrževalnega zdravljenja HRD-pozitivnega napredovalega raka jajčnikov v kombinaciji z bevacizumabom je priporočljivo nadaljevati do radiološkega napredovanja bolezni ali nesprejemljive toksičnosti ali do največ 2 leti, če po 2 letih ni radioloških znakov bolezni. V primeru znakov bolezni po 2 letih, se lahko zdravljenje nadaljuje, če bi le to po mnenju zdravnika bilo koristno za bolnico. Glejte informacije o zdravilu bevacizumab za priporočeno celotno trajanje zdravljenja največ 15 mesecev, vključno z obdobji v kombinaciji s kemoterapijo in kot vzdrževalno zdravljenje. Pri adjuvantnem zdravljenju zgodnjega raka dojk je prporočljivo, da bolniki prejemajo zdravljenje do 1 leto ali do ponovitve bolezni ali do nesprejemljive toksičnosti, kar od tega se zgodi najprej. Zdravljenje ponovitve raka jajčnikov, raka dojk, adenokarcinoma trebušne slinavke,raka prostate in napredovalega ali ponovljenega raka endometrija je priporočljivo nadaljevati do napredovanja osnovne bolezni ali nesprejemljive toksičnosti. Učinkovitost in varnost ponovnega vzdrževalnega zdravljenja z zdravilom Lynparza po prvi ali poznejši ponovitvi bolezni pri bolnicah z rakom jajčnikov nista bili dokazani. Podatkov o učinkovitosti in varnosti ponovnega zdravljenja pri bolnicah z rakom dojk ni. Pri raku prostate je treba pri bolnikih, ki niso bili kirurško kastrirani, nadaljevati z medicinsko kastracijo z analogom luteinizirajočega hormona sproščajočega hormona. Če je zdravilo Lynparza uporabljeno v kombinaciji z abirateronom in prednizonom ali prednizolonom, je zdravljenje priporočljivo nadaljevati do napredovanja osnovne bolezni ali do nesprejemljivih toksičnih učinkov. Pri vseh bolnikih je treba med zdravljenjem še naprej uporabljati analoge GnRH (gonadotropin sproščajočega hormona) ali pa morajo bolniki pred tem opraviti obojestransko orhidektomijo. Glejte informacije o zdravilu za abirateron. Podatkov o učinkovitosti ali varnosti ponovnega zdravljenja z zdravilom Lynparza pri bolnikih z rakom prostate ni. Če je zdravilo uporabljeno v prvi liniji vzdrževalnega zdravljenja napredovalega ali ponovljenegaraka endometrija, ki nima okvare MMR (pMMR), v kombinaciji z durvalumabom je zdravljenje je priporočljivo nadaljevati do napredovanja osnovne bolezni ali do nesprejemljivih toksičnih učinkov. Glejte informacije o zdravilu za durvalumab. V primeru potrebe po zmanjšanju odmerka zaradi neželenih učinkov je priporočeno zmanjšanje odmerka na 250 mg dvakrat na dan (to ustreza celotnemu dnevnemu odmerku 500 mg). Če je potrebno še dodatno zmanjšanje odmerka, je priporočljivo zmanjšanje odmerka na 200 mg dvakrat na dan (to ustreza celotnemu dnevnemu odmerku 400 mg). Zdravljenje z zdravilom Lynparza mora uvesti in nadzorovati zdravnik, ki ima izkušnje z uporabo zdravil proti raku. Mutacijsko stanje *BRCA* in/ali genomsko nestabilnost morajo imeti bolniki potrjeno z validiranim testom. Pred uporabo zdravila Lynparza v kombinaciji z abirateronom in prednizonom ali prednizolonom za zdravljenje bolnikov z mKORP genomsko testiranje ni potrebno. Pri zdravljenju v prvi liniji vzdrževalnega zdravljenja napredovalega ali ponovljenega raka endometrija, ki nima okvare MMR (pMMR), v kombinaciji z durvalumabom je pred uvedbo zdravljenja treba z validiranim testom potrditi, da ima bolnica stanje tumorja brez okvare MMR (pMMR). Genetsko svetovanje bolnikom z mutacijami *BRCA* je treba opraviti v skladu z lokalnimi predpisi. Zdravilo Lynparza se lahko pri bolnikih z blago okvaro ledvic (očistek kreatinina 51 do 80 ml/min) uporablja brez prilagoditve odmerka. Pri bolnikih z zmerno okvaro ledvic (očistek kreatinina 31 do 50 ml/min) je priporočen odmerek 200 mg dvakrat na dan. Uporaba zdravila se pri bolnikih s hudo okvaro ali končno odpovedjo ledvic (očistek kreatinina ≤ 30 ml/min) ne priporoča, ker varnost in farmakokinetika pri tej skupini bolnikov nista bili raziskani. Zdravilo Lynparza se lahko daje bolnikom z blago ali zmerno okvaro jeter (klasifikacija Child-Pugh A ali B) brez prilagoditve odmerka. Uporabe zdravila Lynparza se ne priporoča pri bolnikih s hudo okvaro jeter (klasifikacija Child-Pugh C), ker varnost in farmakokinetika pri tej skupini bolnikov nista bili raziskani. Zdravilo Lynparza je za peroralno uporabo. Tablete zdravila Lynparza je treba pogoltniti cele in se jih ne sme gristi, drobiti, raztapljati ali lomiti. Lahko se jih jemlje ne glede na obroke. **KONTRAINDIKACIJE:** Preobčutljivost na učinkovino ali katero koli pomožno snov. Dojenje med zdravljenjem in en mesec po zadnjem odmerku. **POSEBNA OPOZORILA IN PREVIDNOSTNI UKREPI:** *Hematološki toksični učinki:* Pri bolnikih, zdravljenih z zdravilom Lynparza, so bili opisani hematološki toksični učinki, vključno s klinično diagnozo in/ali laboratorijskimi izsledki, na splošno blage ali zmerne (stopnja 1 ali 2 po CTCAE) anemije, nevtropenije, trombocitopenije in limfopenije. Če je bilo zdravilo Lynparza uporabljeno v kombinaciji z durvalumabom, so poročali o čisti aplaziji rdečih krvnih celic (PRCA) in/ali o avtoimunski hemolitični anemiji (AIHA). Bolniki ne smejo začeti zdravljenja z zdravilom Lynparza, dokler ne okrevajo po hematoloških toksičnih učinkih predhodnega zdravljenja proti raku. Preiskava celotne krvne slike je priporočljiva na začetku zdravljenja, potem vsak mesec prvih 12 mesecev zdravljenja in pozneje redno. Če se pri bolniku pojavijo hudi hematološki toksični učinki ali je odvisen od transfuzij krvi, je treba zdravljenje z zdravilom Lynparza prekiniti in uvesti ustrezno hematološko testiranje. Če krvne vrednosti ostanejo klinično nenormalne še 4 tedne po prekinitvi uporabe zdravila Lynparza, je priporočljivo opraviti preiskavo kostnega mozga in/ali krvno citogenetsko analizo. Če je PRCA ali AIHA potrjena, je treba zdravljenje z zdravilom Lynparza in durvalumabom prenehati. *Mielodisplastični sindrom/akutna mieloična levkemija (MDS/AML):* Celokupna pojavnost MDS/AML je bila pri bolnikih, ki so v kliničnih preizkušanjih prejemali monoterapijo z zdravilom Lynparza, vključno v obdobju dolgoročnega spremljanja preživetja, < 1,5 %, z večjo pojavnostjo pri bolnicah z *BRCA*m, pri katerih je prišlo do ponovitve na platino občutljiva raka jajčnikov, ki so predhodno prejele vsaj dve liniji kemoterapije s platino in so jih spremljali 5 let. Večina teh primerov je bila s smrtnim izidom. Če obstaja sum na MDS/AML, je potrebno bolnico napotiti na nadaljnje preiskave k hematologu, vključno z analizo kostnega mozga in odvzemom krvi za citogenetiko. Če se po preiskavi dolgotrajne hematološke toksičnosti potrdi MDS/AML, je treba uporabo zdravila Lynparza prekiniti in bolnico ustrezno zdraviti. *Venski tromboembolični dogodki:* Med zdravljenjem z zdravilom Lynparza so poročali o venskih tromboemboličnih dogodkih, predvsem o pljučni emboliji, vendar ti dogodki niso imeli kakšnega dosledenega kliničnega vzorca. V primerjavi z drugimi odobrenimi indikacijami so opažali večjo pojavnost pri bolnikih z metastatskim, na kastracijo odpornim rakom prostate, ki so prejemali tudi androgeno deprivacijsko zdravljenje. Bolnike spremljajte glede kliničnih znakov in simptomov venske tromboze in pljučne embolije, ter jih zdravite kot je medicinsko ustrezno. Bolniki z anamnezo VTE imajo morda večje tveganje za njeno ponovitev in jih je treba ustrezno spremljati. *Pnevmonitis:* V kliničnih študijah je bil pnevmonitis, vključno s smrtnim izidom, opisan pri < 1,0 % bolnikov, ki so prejemali zdravilo Lynparza, spremljali pa so jih številni predispozicijski dejavniki. Če se pri bolniku pojavijo novi ali poslabšajo obstoječi dihalni simptomi, npr. dispneja, kašelj in zvišana telesna temperatura, ali je ugotovljen nenormalen radiološki izvid prsnih organov, je treba zdravljenje z zdravilom Lynparza prekiniti in takoj opraviti preiskave. Če je pnevmonitis potrjen, je treba zdravljenje z zdravilom Lynparza prekiniti in bolnika ustrezno zdraviti. *Hepatotoksičnost:* Če se pojavijo klinični simptomi ali znaki, ki kažejo na razvoj hepatotoksičnosti, je treba takoj izvesti klinično oceno bolnika in preiskave delovanja jeter. V primeru suma na z zdravilom povzročeno okvaro jeter (DILI - drug-induced liver injury) je treba zdravljenje prekiniti. V primeru hude DILI je treba razmisliti o ukinitvi zdravljenja, kot je klinično primerno. **MEDSEBOJNO DELOVANJE Z DRUGIMI ZDRAVILI IN DRUGE OBLIKE INTERAKCIJ:** Zdravilo Lynparza se uporablja kot monoterapija in ni primerno za uporabo v kombinaciji z mielosupresivnimi zdravili proti raku, vključno z zdravili, ki poškodujejo DNA. Sočasna uporaba olapariba s cepivi ali imunosupresivnimi zdravili ni raziskana. Za presnovni očistek olapariba so pretežno odgovorni izoencimi CYP3A4/5. Sočasna uporaba zdravila Lynparza z znanimi močnimi ali zmernimi zaviralci tega izoencima ni priporočljiva. Če je treba sočasno uporabiti močne ali zmerne zaviralce CYP3A, je treba odmerek zdravila Lynparza zmanjšati. Prav tako med zdravljenjem z zdravilom Lynparza ni priporočljivo pitje grenivkinega soka. Prav tako olapariba ni priporočljivo uporabljati z znanimi močnimi ali zmernimi do močnimi induktorji tega izoencima, ker obstaja možnost, da se učinkovitost zdravila Lynparza bistveno zmanjša. Olaparib *in vitro* zavira CYP3A4 ter *in vivo* predvidoma blago zavira CYP3A. Zato je potrebna previdnost pri sočasni uporabi olapariba z občutljivimi substrati CYP3A4 ali substrati, ki imajo ozko terapevtsko okno. Bolnike, ki sočasno z olaparibom prejemajo substrate CYP3A z ozkim terapevtskim oknom, je priporočljivo ustrezno klinično spremljati. *In vitro* so ugotovili indukcijo CYP1A2, 2B6 in 3A4, prav tako ni mogoče izključiti možnosti, da olaparib inducira CYP2C9, CYP2C19 in P-gp, zato lahko olaparib po sočasni uporabi zmanjša izpostavljenost substratom teh presnovnih encimov in prenašalne beljakovine. Učinkovitost nekaterih hormonskih kontraceptivov se lahko zmanjša, če so uporabljeni sočasno z olaparibom. *In vitro* olaparib zavira efluksni prenašaleca P-gp, zato je potrebno bolnike, ki sočasno prejemajo substrate P-gp, ustrezno klinično spremljati. *In vitro* olaparib zavira BCRP, OATP1B1, OCT1, OCT2, OAT3, MATE1 in MATE2K. Ni mogoče izključiti možnosti, da olaparib poveča izpostavljenost BCRP, OATP1B1, OCT1, OCT2, OAT3, MATE1 in MATE2K. Še zlasti je previdnost potrebna, če se olaparib uporablja v kombinaciji s katerim koli statinom. Izvedli so klinično študijo za oceno kombinacije olapariba z anastrozolom, letrozolom in tamoksifenom, vendar klinično pomembnih medsebojnih delovanj niso opazili. **NEŽELENI UČINKI:** Zdravilo Lynparza je bilo povezano z neželenimi učinki, ki so bili na splošno blage ali zmerne resnosti (stopnja po CTCAE 1 ali 2) in na splošno niso zahtevali prekinitve zdravljenja. Če je zdravilo Lynparza uporabljeno v kombinaciji z bevacizumabom pri raku jajčnikov, v kombinaciji z abirateronom in prednizonom ali prednizolonom pri raku prostate, ali v kombinaciji z durvalumabom po zdravljenju z durvalumabom v kombinaciji s kemoterapijo na osnovi platine za raka endometrija, se varnostni profil na splošno sklada z varnostnim profilom vsakega posameznega zdravila. Varnostni profil temelji na kumulativnih podatkih 4499 bolnikov s solidnimi tumorji, ki so bili v kliničnih preskušanjih zdravljeni z monoterapijo z zdravilom Lynparza v priporočenem odmerku. *Zelo pogosti neželeni učinki:* anemija, nevtropenija, levkopenija, zmanjšanje apetita, omotica, glavobol, spremenjen okus, kašelj, dispneja, bruhanje, driska, navzea, dispepsija in utrujenost (vključno z astenijo). *Pogosti neželeni učinki:* limfopenija, trombocitopenija, zvišanje transaminaz, stomatitis, bolečine v zgornjem delu trebuha, izpuščaj, zvišanje kreatinina v krvi in venska trombembolija. Pri bolnicah, ki so prejemale zdravilo Lynparza v kombinaciji z durvalumabom po zdravljenju z durvalumabom v kombinaciji s kemoterapijo na osnovi platine, so se v večjo pogostnostjo pojavili neželeni učinki: trombocitopenija in izpuščaj (zelo pogosti) ter preobčutljivost (pogosti). Ugotovili so tudi dodatni neželeni učinek čiste aplazije rdečih krvnih celic. **PLODNOST, NOSEČNOST IN DOJENJE:** Ženske v rodni dobi ne smejo biti noseče na začetku zdravljenja z zdravilom Lynparza in ne smejo zanositi med zdravljenjem in še 6 mesecev po prejetju zadnjega odmerka. Pri vseh ženskah v rodni dobi je potrebno pred zdravljenjem opraviti test nosečnosti in ga redno izvajati med celotnim zdravljenjem. Priporočljivi sta dve visoko učinkoviti in komplementarni obliki kontracepcije. Zaradi možnega medsebojnega delovanja olapariba s hormonsko kontracepcijo je treba razmisliti o dodatni nehormonski kontracepciji. Pri ženskah s hormonsko odvisnim rakom je treba razmisliti o dveh nehormonskih načinih kontracepcije. Zdravilo Lynparza je kontraindicirano med obdobjem dojenja in še en mesec po prejetju zadnjega odmerka. Moški bolniki morajo med zdravljenjem in še 3 mesece po prejetju zadnjega odmerka zdravila Lynparza med spolnimi odnosi z nosečo žensko ali žensko v rodni dobi uporabljati kondom. Tudi partnerke moških bolnikov morajo uporabljati visoko učinkovito kontracepcijo, če so v rodni dobi. Moški bolniki med zdravljenjem z zdravilom Lynparza in še 3 mesece po zadnjem odmerku tega zdravila ne smejo darovati sperme. **REŽIM PREDPISOVANJA IN IZDAJE ZDRAVILA:** Rp/Spec. **DATUM ZADNJE REVIZIJE BESEDILA:** 12.8.2024 (SI-4324) **IMETNIK DOVOLJENJA ZA PROMET**: AstraZeneca AB, SE-151 85 Södertälje, Švedska. Dodatne informacije so na voljo pri podjetju AstraZeneca UK Limited, Podružnica v Sloveniji, Verovškova 55, 1000 Ljubljana, telefon: 01/51 35 600. **Pred predpisovanjem, prosimo, preberite celoten povzetek glavnih značilnosti zdravila.**

PARP – poli (ADP-riboza) polimeraza, **1L** – v prvem redu zdravljenja, **2L** – v drugem redu zdravljenja,
HRD – pomanjkanje homologne rekombinacije, **KORP** – na kastracijo odporen rak prostate
*Zdravili Lynparza in durvalumab za zdravljenje raka endometrija še nista razvrščeni na listo zdravil ZZZS

Literatura: 1. Povzetek glavnih značilnosti zdravila Lynparza, 12.8.2024, **2.** https://www.ema.europa.eu/en/medicines/human/EPAR/rubraca, dostopano 1.9.2024, **3.** https://www.ema.europa.eu/en/medicines/human/EPAR/zejula, dostopano 1.9.2024, **4.** https://www.ema.europa.eu/en/medicines/human/EPAR/talzenna, dostopano 1.9.2024, **5.** https://www.ema.europa.eu/en/news/lynparza-recommended-approval-ovarian-cancer, dostopano 1.9.2024

AstraZeneca

AstraZeneca UK Limited, Podružnica v Sloveniji,
Verovškova 55, 1000 Ljubljana, tel: 01/51 35 600

Samo za strokovno javnost. Datum priprave gradiva: september 2024 SI-4341

5 NA NOVO razvrščenih indikacij:[1]

KEYTRUDA®
(pembrolizumab, MSD)

NEDROBNOCELIČNI PLJUČNI RAK:

> samostojno adjuvantno zdravljenje odraslih z visokim tveganjem za ponovitev bolezni po popolni kirurški odstranitvi in kemoterapiji na osnovi platine[2]

> neoadjuvantno zdravljenje v kombinaciji s kemoterapijo, ki vključuje platino in v nadaljevanju samostojno adjuvantno zdravljenje odraslih z operabilnim NDPR z visokim tveganjem za ponovitev bolezni[2]

ADENOKARCINOM ŽELODCA ali GASTROEZOFAGEALNEGA PREHODA:

> lokalno napredovali neoperabilni ali metastatski HER2-pozitiven rak: 1L zdravljenja v kombinaciji s trastuzumabom, fluoropirimidinom in kemoterapijo, ki vključuje platino, pri odraslih s tumorsko izraženostjo PD-L1 s CPS ≥ 1[2]

> lokalno napredovali neoperabilni ali metastatski HER2-negativen rak: 1L zdravljenja v kombinaciji s fluoropirimidinom in kemoterapijo, ki vključuje platino, pri odraslih s tumorsko izraženostjo PD-L1 s CPS ≥ 1[2]

RAK MATERNIČNEGA VRATU:

> v kombinaciji s kemoterapijo, z bevacizumabom ali brez njega, za zdravljenje persistentnega, ponovljenega ali metastatskega RMV, pri odraslih bolnicah s tumorsko izraženostjo PD-L1 s CPS ≥ 1[2]

Skenirajte QR kodo in izvedite več o osredotočenosti družbe MSD na zdravljenje raka.

Okrajšave: 1L - prva linija; CPS - kombinirana pozitivna ocena ; NDPR – nedrobnocelični pljučni rak; PD-L1 - ligand programirane celične smrti 1; RMV – rak materničnega vratu

Referenci: 1. ZZZS. E-gradiva. Spremembe seznama B. Dostopano 16.12.2024 na https://www.zzzs.si/?id=126&detail=F641B38F0189A2BFC1257B2D0047239C 2. Povzetek glavnih značilnosti zdravila KEYTRUDA

SKRAJŠAN POVZETEK GLAVNIH ZNAČILNOSTI ZDRAVILA • Pred predpisovanjem, prosimo, preberite celoten Povzetek glavnih značilnosti zdravila! • Ime zdravila: KEYTRUDA 25 mg/ml koncentrat za raztopino za infundiranje vsebuje pembrolizumab. • **Terapevtske indikacije:** Zdravilo KEYTRUDA je kot samostojno zdravljenje indicirano za zdravljenje: odraslih in mladostnikov, starih 12 let ali več, z napredovalim (neoperabilnim ali metastatskim) melanomom; za adjuvantno zdravljenje odraslih in mladostnikov, starih 12 let ali več, z melanomom v stadiju IIB, IIC ali III, in sicer po popolni kirurški odstranitvi; za adjuvantno zdravljenje odraslih z nedrobnoceličnim pljučnim rakom, ki imajo visoko tveganje za ponovitev bolezni po popolni kirurški odstranitvi in kemoterapiji na osnovi platine; metastatskega nedrobnoceličnega pljučnega raka (NSCLC) v prvi liniji zdravljenja pri odraslih, ki imajo tumorje z ≥ 50 % izraženostjo PD-L1 (TPS) in brez pozitivnih tumorskih mutacij EGFR ali ALK; lokalno napredovalega ali metastatskega NSCLC pri odraslih, ki imajo tumorje z ≥ 1 % izraženostjo PD-L1 (TPS) in so bili predhodno zdravljeni z vsaj eno shemo kemoterapije, bolniki s pozitivnimi tumorskimi mutacijami EGFR ali ALK so pred prejemom zdravila KEYTRUDA morali prejeti tudi tarčno zdravljenje; odraslih in pediatričnih bolnikov, starih 3 leta ali več, s ponovljenim ali neodzivnim klasičnim Hodgkinovim limfomom (cHL), pri katerih avtologna presaditev matičnih celic (ASCT) ni bila uspešna, ali po najmanj dveh predhodnih zdravljenjih kadar ASCT ne pride v poštev kot možnost zdravljenja; lokalno napredovalega ali metastatskega urotelijskega raka pri odraslih, predhodno zdravljenih s kemoterapijo, ki je vključevala platino; lokalno napredovalega ali metastatskega urotelijskega raka pri odraslih, ki niso primerni za zdravljenje s kemoterapijo, ki vsebuje cisplatin in imajo tumorje z izraženostjo PD-L1 ≥ 10, ocenjeno s kombinirano pozitivno oceno (CPS); ponovljenega ali metastatskega ploščatoceličnega raka glave in vratu (HNSCC) pri odraslih, ki imajo tumorje z ≥ 50 % izraženostjo PD-L1 (TPS), in pri katerih je bolezen napredovala med zdravljenjem ali po zdravljenju s kemoterapijo, ki je vključevala platino; za adjuvantno zdravljenje odraslih z rakom ledvičnih celic s povišanim tveganjem za ponovitev bolezni po nefrektomiji, ali po nefrektomiji in kirurški odstranitvi metastatskih lezij, za zdravljenje odraslih z MSI-H (microsatellite instability-high) ali dMMR (mismatch repair deficient) kolorektalnim rakom v naslednjih terapevtskih okoliščinah: prva linija zdravljenja metastatskega kolorektalnega raka; zdravljenje neoperabilnega ali metastatskega kolorektalnega raka po predhodnem kombiniranem zdravljenju, ki je temeljilo na fluoropirimidinu; in za zdravljenje MSI-H ali dMMR tumorjev pri odraslih z: napredovalim ali ponovljenim rakom endometrija, pri katerih je bolezen napredovala med ali po predhodnem zdravljenju, ki je vključevalo platino, v katerih koli terapevtskih okoliščinah, in ki niso kandidati za kurativno operacijo ali obsevanje; neoperabilnim ali metastatskim rakom želodca, tankega črevesa ali biliarnega trakta, pri katerih je bolezen napredovala med ali po vsaj enem predhodnem zdravljenju. Zdravilo KEYTRUDA je kot samostojno zdravljenje ali v kombinaciji s kemoterapijo s platino in 5-fluorouracilom (5-FU) indicirano za prvo linijo zdravljenja metastatskega ali neoperabilnega ponovljenega ploščatoceličnega raka glave in vratu pri odraslih, ki imajo tumorje z izraženostjo PD-L1 s CPS ≥ 1. Zdravilo KEYTRUDA je v kombinaciji s kemoterapijo, ki vključuje platino, indicirano za neoadjuvantno zdravljenje, in v nadaljevanju kot samostojno zdravljenje za adjuvantno zdravljenje odraslih z operabilnim nedrobnoceličnim pljučnim rakom, ki imajo visoko tveganje za ponovitev bolezni; v kombinaciji s pemetreksedom in kemoterapijo na osnovi platine je indicirano za prvo linijo zdravljenja metastatskega neploščatoceličnega NSCLC pri odraslih, pri katerih tumorji nimajo pozitivnih mutacij EGFR ali ALK; v kombinaciji s karboplatinom in bodisi paklitakselom bodisi nab-paklitakselom je indicirano za prvo linijo zdravljenja metastatskega ploščatoceličnega NSCLC pri odraslih; v kombinaciji z enfortumab vedotinom je indicirano za prvo linijo zdravljenja neoperabilnega ali metastatskega urotelijskega raka pri odraslih; v kombinaciji z aksitinibom ali v kombinaciji z lenvatinibom je indicirano za prvo linijo zdravljenja napredovalega raka ledvičnih celic (RCC) pri odraslih; v kombinaciji s kemoterapijo s platino in fluoropirimidinom je indicirano za prvo linijo zdravljenja lokalno napredovalega neoperabilnega ali metastatskega raka požiralnika pri odraslih, ki imajo tumorje z izraženostjo PD-L1 s CPS ≥ 10; v kombinaciji s kemoterapijo za neoadjuvantno zdravljenje, in v nadaljevanju kot samostojno adjuvantno zdravljenje po kirurškem posegu, je indicirano za zdravljenje odraslih z lokalno napredovalim trojno negativnim rakom dojk ali trojno negativnim rakom dojk v zgodnjem stadiju z visokim tveganjem za ponovitev bolezni; v kombinaciji s kemoterapijo je indicirano za zdravljenje lokalno ponovljenega neoperabilnega ali metastatskega trojno negativnega raka dojk pri odraslih, ki imajo tumorje z izraženostjo PD-L1 s CPS ≥ 10 in predhodno niso prejeli kemoterapije za metastatsko bolezen; v kombinaciji s karboplatinom in paklitakselom je indicirano za prvo linijo zdravljenja primarno napredovalega ali ponovljenega raka endometrija (EC) pri odraslih, ki so kandidati za sistemsko zdravljenje; v kombinaciji z lenvatinibom je indicirano za zdravljenje napredovalega ali ponovljenega raka endometrija pri odraslih z napredovalo boleznijo med ali po predhodnem zdravljenju s kemoterapijo, ki je vključevala platino, v katerih koli terapevtskih okoliščinah, in ki niso kandidati za kurativno operacijo ali obsevanje; v kombinaciji s kemoradioterapijo (zdravljenje z zunanjim obsevanjem, ki mu sledi brahiterapija) je indicirano za zdravljenje lokalno napredovalega raka materničnega vratu v stadiju III - IVA po FIGO 2014 pri odraslih, ki niso prejeli predhodne definitivne terapije; v kombinaciji s kemoterapijo, z bevacizumabom ali brez njega, je indicirano za zdravljenje persistentnega, ponovljenega ali metastatskega raka materničnega vratu pri odraslih bolnicah, ki imajo tumorje z izraženostjo PD-L1 s CPS ≥ 1; v kombinaciji s trastuzumabom, fluoropirimidinom in kemoterapijo, ki vključuje platino, je indicirano za prvo linijo zdravljenja lokalno napredovalega neoperabilnega ali metastatskega HER2-pozitivnega adenokarcinoma želodca ali gastroezofagealnega prehoda pri odraslih, ki imajo tumorje z izraženostjo PD-L1 s CPS ≥ 1; v kombinaciji s fluoropirimidinom in kemoterapijo, ki vključuje platino, je indicirano za prvo linijo zdravljenja lokalno napredovalega neoperabilnega ali metastatskega HER2-negativnega adenokarcinoma želodca ali gastroezofagealnega prehoda pri odraslih, ki imajo tumorje z izraženostjo PD-L1 s CPS ≥ 1; v kombinaciji z gemcitabinom in cisplatinom je indicirano za prvo linijo zdravljenja lokalno napredovalega neoperabilnega ali metastatskega raka biliarnega trakta pri odraslih. • **Odmerjanje in način uporabe:** Testiranje PD-L1: Če je navedeno v indikaciji, je treba izbiro bolnika za zdravljenje z zdravilom KEYTRUDA na podlagi izraženosti PD-L1 tumorja potrditi z validirano preiskavo. Testiranje MSI/MMR: Če je navedeno v indikaciji, je treba izbiro bolnika za zdravljenje z zdravilom KEYTRUDA na podlagi MSI-H/dMMR statusa tumorja potrditi z validirano preiskavo. Odmerjanje: Priporočeni odmerek zdravila KEYTRUDA pri odraslih je bodisi 200 mg na 3 tedne ali 400 mg na 6 tednov, apliciran z intravensko infuzijo v 30 minutah. Priporočeni odmerek zdravila KEYTRUDA za samostojno zdravljenje pri pediatričnih bolnikih s cHL, starih 3 leta ali več, ali bolnikih z melanomom, starih 12 let ali več, je 2 mg/kg telesne mase (do največ 200 mg) na 3 tedne, apliciran z intravensko infuzijo v 30 minutah. Za uporabo v kombinaciji glejte povzetke glavnih značilnosti zdravil sočasno uporabljenih zdravil. Če se zdravilo KEYTRUDA uporablja kot del kombiniranega zdravljenja skupaj z intravensko kemoterapijo, je treba zdravilo KEYTRUDA aplicirati prvo. Če se zdravilo KEYTRUDA uporablja kot del kombiniranega zdravljenja skupaj z enfortumab vedotinom, je treba zdravilo KEYTRUDA aplicirati po enfortumab vedotinu, kadar sta uporabljena na isti dan. Bolnike je treba zdraviti do napredovanja bolezni ali nesprejemljivih toksičnih učinkov (in do maksimalnega trajanja zdravljenja, če je le to določeno za indikacijo). Pri adjuvantnem zdravljenju melanoma, NSCLC ali RCC je treba zdravilo uporabljati do ponovitve bolezni, pojava nesprejemljivih toksičnih učinkov oziroma mora zdravljenje trajati do enega leta. Za neoadjuvantno in adjuvantno zdravljenje operabilnega NSCLC morajo bolniki neoadjuvantno prejeti zdravilo KEYTRUDA v kombinaciji s kemoterapijo, in sicer 4 odmerke po 200 mg na 3 tedne ali 2 odmerka po 400 mg na 6 tednov ali do napredovanja bolezni, ki izključuje definitivni kirurški poseg, ali do pojava nesprejemljivih toksičnih učinkov, čemur sledi adjuvantno zdravljenje z zdravilom KEYTRUDA kot samostojnim zdravljenjem, in sicer 13 odmerkov po 200 mg na 3 tedne ali 7 odmerkov po 400 mg na 6 tednov ali do ponovitve bolezni ali do pojava nesprejemljivih toksičnih učinkov. Bolniki, pri katerih pride do napredovanja bolezni, ki izključuje definitivni kirurški poseg, ali do nesprejemljivih toksičnih učinkov, povezanih z zdravilom KEYTRUDA kot neoadjuvantnim zdravljenjem v kombinaciji s kemoterapijo, ne smejo prejeti zdravila KEYTRUDA kot samostojnega zdravljenja za adjuvantno zdravljenje. Za neoadjuvantno in adjuvantno zdravljenje TNBC morajo bolniki neoadjuvantno prejeti zdravilo KEYTRUDA v kombinaciji s kemoterapijo, in sicer 8 odmerkov po 200 mg na 3 tedne ali 4 odmerke po 400 mg na 6 tednov, ali do napredovanja bolezni, ki izključuje definitivni kirurški poseg, ali do pojava nesprejemljivih toksičnih učinkov, čemur sledi adjuvantno zdravljenje z zdravilom KEYTRUDA kot samostojnim zdravljenjem, in sicer 9 odmerkov po 200 mg na 3 tedne ali 5 odmerkov po 400 mg na 6 tednov ali do ponovitve bolezni ali pojava nesprejemljivih toksičnih učinkov. Bolniki, pri katerih pride do napredovanja bolezni, ki izključuje definitivni kirurški poseg, ali do nesprejemljivih toksičnih učinkov povezanih z zdravilom KEYTRUDA kot neoadjuvantnim zdravljenjem v kombinaciji s kemoterapijo, ne smejo prejeti zdravila KEYTRUDA kot samostojnega zdravljenja za adjuvantno zdravljenje. Za lokalno napredovalega raka materničnega vratu morajo bolnice prejeti zdravilo KEYTRUDA sočasno s kemoradioterapijo, čemur sledi samostojno zdravljenje z zdravilom KEYTRUDA. Zdravilo KEYTRUDA se lahko daje v odmerku 200 mg na 3 tedne ali 400 mg na 6 tednov do napredovanja bolezni, pojava nesprejemljivih toksičnih učinkov ali do 24 mesecev. Če je aksitinib uporabljen v kombinaciji s pembrolizumabom, se lahko razmisli o povečanju odmerka aksitiniba nad začetnih 5 mg v presledkih šest tednov ali več. V primeru uporabe v kombinaciji z lenvatinibom je treba zdravljenje z enim ali obema zdraviloma prekiniti, kot je primerno. Uporabo lenvatiniba je treba zadržati, odmerek zmanjšati ali prenehati z uporabo, v skladu z navodili v povzetku glavnih značilnosti zdravila za lenvatinib, in sicer za kombinacijo s pembrolizumabom. Pri bolnikih starih ≥ 65 let, bolnikih z blago do zmerno okvaro ledvic, bolnikih z blago ali zmerno okvaro jeter prilagoditev odmerka ni potrebna. Odložitev odmerka ali ukinitev zdravljenja: Zmanjšanje odmerka zdravila KEYTRUDA ni priporočljivo. Za obvladovanje neželenih učinkov je treba uporabo zdravila KEYTRUDA zadržati ali ukiniti, prosimo, glejte celoten Povzetek glavnih značilnosti zdravila. • **Kontraindikacije:** Preobčutljivost na učinkovino ali katero koli pomožno snov. • **Povzetek posebnih opozoril, previdnostnih ukrepov, interakcij in neželenih učinkov:** Imunsko pogojeni neželeni učinki (pnevmonitis, kolitis, hepatitis, nefritis, endokrinopatije, neželeni učinki na kožo in drugi): Pri bolnikih, ki so prejemali pembrolizumab, so se pojavili imunsko pogojeni neželeni učinki, vključno s hudimi in smrtnimi primeri. Večina imunsko pogojenih neželenih učinkov, ki so se pojavili med zdravljenjem s pembrolizumabom, je bila reverzibilnih in so jih obvladali s prekinitvami uporabe pembrolizumaba, uporabo kortikosteroidov in/ali podporno oskrbo. Pojavijo se lahko tudi po zadnjem odmerku pembrolizumaba in hkrati prizadanejo več organskih sistemov. V primeru suma na imunsko pogojene neželene učinke je treba poskrbeti za ustrezno oceno za potrditev etiologije oziroma izključitev drugih vzrokov. Glede na izrazitost neželenega učinka je treba zadržati uporabo pembrolizumaba in uporabiti kortikosteroide – za natančna navodila, prosimo, glejte Povzetek glavnih značilnosti zdravila Keytruda. Zdravljenje s pembrolizumabom lahko poveča tveganje za zavrnitev pri prejemnikih presadkov čvrstih organov. Pri bolnikih, ki so prejemali pembrolizumab, so poročali o hudih z infuzijo povezanih reakcijah, vključno s preobčutljivostjo in anafilaksijo. Pembrolizumab se iz obtoka odstrani s katabolizmom, zato presnovnih medsebojnih delovanj zdravil ni pričakovati. Uporabi sistemskih kortikosteroidov ali imunosupresivov pred uvedbo pembrolizumaba se je treba izogibati, ker lahko vplivajo na farmakodinamično aktivnost in učinkovitost pembrolizumaba. Vendar pa je kortikosteroide ali druge imunosupresive mogoče uporabiti za zdravljenje imunsko pogojenih neželenih učinkov. Kortikosteroide je mogoče uporabiti tudi kot premedikacijo, če je pembrolizumab uporabljen v kombinaciji s kemoterapijo, kot antiemetično profilakso in/ali za ublažitev neželenih učinkov, povezanih s kemoterapijo. Ženske v rodni dobi morajo med zdravljenjem s pembrolizumabom in vsaj še 4 mesece po zadnjem odmerku pembrolizumaba uporabljati učinkovito kontracepcijo, med nosečnostjo in dojenjem se ga ne sme uporabljati. Varnost pembrolizumaba pri samostojnem zdravljenju so v kliničnih študijah ocenili pri 7631 bolnikih, ki so imeli različne vrste raka, s štirimi odmerki (2 mg/kg telesne mase na 3 tedne, 200 mg na 3 tedne in 10 mg/kg telesne mase na 2 ali 3 tedne). V tej populaciji bolnikov je mediani čas opazovanja znašal 8,5 meseca (v razponu od 1 dneva do 39 mesecev), najpogostejši neželeni učinki zdravljenja s pembrolizumabom pa so bili utrujenost (31 %), diareja (22 %) in navzea (20 %). Večina poročanih neželenih učinkov pri samostojnem zdravljenju je bila po izrazitosti 1. ali 2. stopnje. Najresnejši neželeni učinki so bili imunsko pogojeni neželeni učinki in hude z infuzijo povezane reakcije. Pojavnost imunsko pogojenih neželenih učinkov pri uporabi pembrolizumaba samega za adjuvantno zdravljenje je znašala 37 % za vse stopnje in 9 % od 3. do 5. stopnje, pri metastatski bolezni pa 25 % za vse stopnje in 6 % od 3. do 5. stopnje. Pri adjuvantnem zdravljenju niso zaznali nobenih novih imunsko pogojenih neželenih učinkov. Varnost pembrolizumaba pri kombiniranem zdravljenju s kemoterapijo ali kemoradioterapijo (CRT) so ocenili pri 6093 bolnikih z različnimi vrstami raka, ki so v kliničnih študijah prejemali pembrolizumab v odmerkih 200 mg, 2 mg/kg telesne mase ali 10 mg/kg telesne mase na vsake 3 tedne. V tej populaciji bolnikov so bili najpogostejši neželeni učinki naslednji: anemija (53 %), navzea (52 %), diareja (36 %), utrujenost (35 %), zaprtost (32 %), bruhanje (28 %), zmanjšano število nevtrofilcev (28 %) in zmanjšanje apetita (27 %). Pojavnost neželenih učinkov 3. do 5. stopnje je pri bolnikih z NSCLC pri kombiniranem zdravljenju s pembrolizumabom znašala 69 % in pri zdravljenju samo s kemoterapijo 61 %, pri bolnikih s HNSCC pri kombiniranem zdravljenju s pembrolizumabom 85 % in pri zdravljenju s kemoterapijo v kombinaciji s cetuksimabom 84 %, pri bolnikih z rakom požiralnika pri kombiniranem zdravljenju s pembrolizumabom 86 % in pri zdravljenju samo s kemoterapijo 83 %, pri bolnikih s TNBC pri kombiniranem zdravljenju s pembrolizumabom 80 % in pri zdravljenju samo s kemoterapijo 77 %, pri bolnicah z rakom materničnega vratu pri kombiniranem zdravljenju s pembrolizumabom (kemoterapija z ali brez bevacizumaba ali v kombinaciji s CRT) 77 % in pri zdravljenju s kemoterapijo z ali brez bevacizumaba ali samostojno s CRT 71 %, pri bolnikih z rakom želodca pri kombiniranem zdravljenju s pembrolizumabom (kemoterapija z ali brez trastuzumaba) 74 % in pri kemoterapiji v kombinaciji z ali brez trastuzumaba 68 %, pri bolnikih z rakom biliarnega trakta pri kombiniranem zdravljenju s pembrolizumabom 85 % in pri samostojni kemoterapiji 84 %, in pri bolnicah z EC pri kombiniranem zdravljenju s pembrolizumabom 59 % in pri samostojni kemoterapiji 46 %. Varnost pembrolizumaba v kombinaciji z aksitinibom ali lenvatinibom pri napredovalem RCC in v kombinaciji z lenvatinibom pri napredovalem EC so ocenili pri skupno 1456 bolnikih z napredovalim RCC ali napredovalim EC, ki so v kliničnih študijah prejemali 200 mg pembrolizumaba na 3 tedne skupaj s 5 mg aksitiniba dvakrat na dan ali z 20 mg lenvatiniba enkrat na dan, kot je bilo ustrezno. V teh populacijah bolnikov so bili najpogostejši neželeni učinki diareja (58 %), hipertenzija (54 %), hipotiroidizem (46 %), utrujenost (41 %), zmanjšan apetit (40 %), navzea (40 %), artralgija (30 %), bruhanje (28 %), zmanjšanje telesne mase (28 %), disfonija (28 %), bolečine v trebuhu (28 %), proteinurija (27 %), sindrom palmarno-plantarne eritrodizestezije (26 %), izpuščaj (26 %), stomatitis (25 %), zaprtost (25 %), mišično-skeletna bolečina (23 %), glavobol (23 %) in kašelj (21 %). Neželenih učinkov od 3. do 5. stopnje je bilo pri bolnikih z RCC med uporabo pembrolizumaba v kombinaciji z aksitinibom ali lenvatinibom 80 % in med uporabo sunitiniba samega 71 %. Pri bolnicah z EC je bilo neželenih učinkov od 3. do 5. stopnje med uporabo pembrolizumaba v kombinaciji z lenvatinibom 89 % in med uporabo kemoterapije same 73 %. Varnost pembrolizumaba v kombinaciji z enfortumab vedotinom so ocenili pri 564 bolnikih z neoperabilnim ali metastatskim urotelijskim rakom, ki so prejemali 200 mg pembrolizumaba 1. dan in 1,25 mg/kg enfortumab vedotina 1. in 8. dan vsakega 21-dnevnega ciklusa. Na splošno so opazili, da je bila pojavnost neželenih učinkov za pembrolizumab v kombinaciji z enfortumab vedotinom višja kot pri samostojnem zdravljenju s pembrolizumabom, kar odraža prispevek enfortumab vedotina in daljšega trajanja kombiniranega zdravljenja. Neželeni učinki so bili na splošno podobni neželenim učinkom, ki so jih opazili pri bolnikih, ki so prejemali pembrolizumab ali enfortumab vedotin kot samostojno zdravljenje. Pojavnost makulopapuloznega izpuščaja vseh stopenj je bila 36 % (10 % od 3. do 4. stopnje), kar je višje, kot je bilo opaženo pri samostojnem zdravljenju s pembrolizumabom. Na splošno so bile pogostnosti neželenih učinkov višje pri bolnikih, starih ≥ 65 let, v primerjavi z bolniki, starimi < 65 let, predvsem za resne neželene učinke (56,3 % pri bolnikih, starih ≥ 65 let, in 35,3 % pri bolnikih, starih < 65 let) in učinke ≥ 3. stopnje (80,3 % pri bolnikih, starih ≥ 65 let, in 64,2 % pri bolnikih, starih < 65 let), podobno kot opažanja pri primerjalni kemoterapiji. Za celoten seznam neželenih učinkov, prosimo, glejte celoten Povzetek glavnih značilnosti zdravila. Za dodatne informacije o varnosti v primeru uporabe pembrolizumaba v kombinaciji glejte povzetke glavnih značilnosti zdravila za posamezne komponente kombiniranega zdravljenja. • **Način in režim izdaje zdravila:** H – Predpisovanje in izdaja zdravila je le na recept, zdravilo se uporablja samo v bolnišnicah. • **Imetnik dovoljenja za promet z zdravilom:** Merck Sharp & Dohme B.V. , Waarderweg 39, 2031 BN Haarlem, Nizozemska.

Merck Sharp & Dohme inovativna zdravila d.o.o.
Ameriška ulica 2, 1000 Ljubljana, Slovenija; Telefon: 01/ 520 42 01, faks: 01/ 520 43 50
Veeva code: SI-KEY-00735; Pripravljeno v Sloveniji, 01/2025. Vse pravice pridržane.

Samo za strokovno javnost

H - Predpisovanje in izdaja zdravila je le na recept, zdravilo pa se uporablja samo v bolnišnicah. Pred predpisovanjem, prosimo, preberite celoten Povzetek glavnih značilnosti zdravila Keytruda, ki je na voljo pri naših strokovnih sodelavcih ali na lokalnem sedežu družbe.

▼PHESGO®

PERTUZUMAB-TRASTUZUMAB

Roche

85 % bolnikov daje prednost zdravilu PHESGO v primerjavi z intravenskima oblikama pertuzumaba in trastuzumaba[1]

Moj čas. Moja izbira.[2]

Ime zdravila: Phesgo 600 mg/600 mg in 1200 mg/600 mg raztopina za injiciranje
Kakovostna in količinska sestava: Ena viala z 10 ml raztopine vsebuje 600 mg pertuzumaba in 600 mg trastuzumaba. En ml raztopine vsebuje 60 mg pertuzumaba in 60 mg trastuzumaba (Phesgo 600 mg/600 mg). Ena viala s 15 ml raztopine vsebuje 1200 mg pertuzumaba in 600 mg trastuzumaba. En ml raztopine vsebuje 80 mg pertuzumaba in 40 mg trastuzumaba (Phesgo 1200 mg/600 mg). **Terapevtske indikacije:** Zgodnji rak dojk: Zdravilo Phesgo je v kombinaciji s kemoterapijo indicirano za neoadjuvantno zdravljenje odraslih bolnikov s HER2-pozitivnim, lokalno napredovalim, vnetnim ali zgodnjim rakom dojk z visokim tveganjem za ponovitev in adjuvantno zdravljenje odraslih bolnikov s HER2-pozitivnim zgodnjim rakom dojk z visokim tveganjem za ponovitev. Razsejani rak dojk: Zdravilo Phesgo je v kombinaciji z docetakselom indicirano za zdravljenje odraslih bolnikov s HER2-pozitivnim, razsejanim ali lokalno ponovljenim neoperabilnim rakom dojk, ki pred tem še niso prejeli anti-HER2 terapije ali kemoterapije za razsejano bolezen. **Odmerjanje in način uporabe:** Zdravilo Phesgo je lahko uvedeno le pod nadzorom zdravnika, ki ima izkušnje z uporabo zdravil proti raku. Zdravilo Phesgo mora dajati zdravstveni delavec, ki je usposobljen za obvladovanje anafilaksije, in v okolju, kjer je takoj na voljo celotna oprema za oživljanje. Bolniki, ki trenutno prejemajo pertuzumab in trastuzumab intravensko, lahko preidejo na zdravilo Phesgo. Odmerjanje: Bolniki, zdravljeni z zdravilom Phesgo, morajo imeti HER2-pozitivni tumor, imunohistokemijsko opredeljen kot 3+ in/ali razmerje pri ISH ≥ 2,0. Bolniki, ki prejemajo taksan, morajo zdravilo Phesgo dobiti pred taksanom. Kadar se zdravilo Phesgo uporablja sočasno z docetakselom, je priporočeni začetni odmerek docetaksela 75 mg/m², nato pa se ga poveča na 100 mg/m² glede na izbrano shemo in prenašanje začetnega odmerka. Druga možnost je odmerek docetaksela 100 mg/m² po 3-tedenskem razporedu že od začetka, ponovno glede na izbrano shemo. Če se uporablja shemo, ki temelji na karboplatinu, je priporočeni odmerek docetaksela ves čas 75 mg/m². Kadar se zdravilo Phesgo uporablja sočasno s paklitakselom v adjuvantnem zdravljenju, je priporočeni odmerek paklitaksela 80 mg/m² enkrat na teden v 12-tedenskih ciklih. Bolniki, ki prejemajo shemo na osnovi antraciklina, morajo zdravilo Phesgo dobiti po koncu celotne sheme na osnovi antraciklina. *Razsejani rak dojk:* Zdravilo Phesgo je treba uporabljati v kombinaciji z docetakselom. Zdravljenje z zdravilom Phesgo se lahko nadaljuje do napredovanja bolezni ali pojava neobvladljivih toksičnih učinkov, tudi če se zdravljenje z docetakselom ukine. *Zgodnji rak dojk:* Pri neoadjuvantnem zdravljenju, ki predstavlja del celostnega zdravljenja zgodnjega raka dojk, je treba zdravilo Phesgo dajati 3 do 6 ciklov v kombinaciji. V okviru adjuvantnega zdravljenja je treba zdravilo Phesgo uporabljati v skupnem trajanju eno leto, ki predstavlja del celostnega zdravljenja zgodnjega raka dojk in ne glede na čas operacije. Zdravljenje mora vključevati standardno kemoterapijo na osnovi antraciklina in/ali taksana. Zdravilo Phesgo naj se začne uporabljati 1. dan prvega cikla, ki vsebuje taksan, in ga je treba uporabljati še naprej, tudi če se kemoterapija ukine. *Zamujeni ali izpuščeni odmerki:* ***Če je čas med dvema zaporednima injiciranjema:*** krajši od 6 tednov: vzdrževalni odmerek zdravila Phesgo 600 mg/600 mg je treba dati čimprej. Nato nadaljujte s 3-tedenskim režimom. 6 tednov ali več: ponovno je treba dati polnilni odmerek zdravila Phesgo 1200 mg/600 mg, sledi pa mu vzdrževalni odmerek zdravila Phesgo 600 mg/600 mg na vsake 3 tedne. *Prilagoditev odmerka:* Za zdravilo Phesgo ni priporočljivo zmanjševanje odmerka. Po presoji zdravnika bo morda potrebna prekinitev zdravljenja z zdravilom Phesgo. *Prehod z intravenskega pertuzumaba in trastuzumaba na zdravilo Phesgo:* Bolnikom, ki so zadnji odmerek intravenskega pertuzumaba in trastuzumaba prejeli pred manj kot 6 tedni, je treba dati vzdrževalni odmerek zdravila Phesgo 600 mg pertuzumaba/600 mg trastuzumaba in ta odmerek uporabljati tudi za nadaljnje aplikacije na vsake 3 tedne. Bolnikom, ki so zadnji odmerek intravenskega pertuzumaba in trastuzumaba prejeli pred 6 tedni ali več, je treba dati polnilni odmerek zdravila Phesgo 1200 mg pertuzumaba/600 mg trastuzumaba, ki mu sledi vzdrževalni odmerek 600 mg pertuzumaba/600 mg trastuzumaba na vsake 3 tedne. Način dajanja: Zdravilo Phesgo moramo dajati le kot subkutano injekcijo. Zdravilo Phesgo ni namenjeno intravenskemu dajanju. Mesto injiciranja je treba izmenjevati le med levim in desnim stegnom. Polnilni odmerek je treba dati v 8 minutah, vzdrževalni odmerek pa v 5 minutah. Zaradi z injiciranjem povezanih reakcij je priporočljiv čas opazovanja 30 minut po danem polnilnem odmerku in 15 minut po zaključku vzdrževalnega odmerka zdravila Phesgo. **Kontraindikacije:** Preobčutljivost na učinkovino ali katero koli pomožno snov. **Posebna opozorila in previdnostni ukrepi:** Disfunkcija levega prekata (vključno s kongestivnim srčnim popuščanjem): Med uporabo zdravil, ki zavirajo aktivnost HER2, so poročali o zmanjšanju LVEF. Večino primerov simptomatskega srčnega popuščanja v okviru adjuvantnega zdravljenja so zabeležili pri bolnikih, zdravljenih s kemoterapijo na osnovi antraciklina. Bolniki, predhodno zdravljeni z antraciklini ali obsevanjem v predelu prsnega koša, imajo lahko večje tveganje za zmanjšanje LVEF glede na študije z intravenskim pertuzumabom v kombinaciji s trastuzumabom in kemoterapijo. Pred uvedbo zdravila Phesgo je treba oceniti vrednost LVEF in jo nato med zdravljenjem tudi redno spremljati ter zagotoviti, da LVEF ostaja znotraj normalnih vrednosti. Če se LVEF poslabša in se ob naslednjem merjenju ne izboljša ali se še dodatno poslabša, je treba resno razmisliti o prenehanju zdravljenja z zdravilom Phesgo, razen če koristi za posameznega bolnika odtehtajo tveganja. Pred uporabo zdravila Phesgo skupaj z antraciklinom je treba skrbno razmisliti o kardiološkem tveganju in ga pretehtati glede na zdravstvene potrebe posameznega bolnika. Z upoštevajnjem farmakološkega delovanja zdravil, usmerjenih proti HER2, in antraciklinov je med sočasno uporabo zdravila Phesgo in antraciklinov mogoče pričakovati večje tveganje za kardiotoksičnost kot med zaporedno uporabo. Z injiciranjem povezane reakcije/z infundiranjem povezane reakcije: Uporabo zdravila Phesgo so spremljale z injiciranjem povezane reakcije. Opredeljene so bile kot katera koli sistemska reakcija s simptomi, kot so zvišana telesna temperatura, mrzlica, glavobol, najverjetneje zaradi sproščanja citokinov, ki se je pojavilo v 24 urah po dajanju zdravila Phesgo. Priporoča se skrbno opazovanje bolnika med dajanjem polnilnega odmerka in še 30 minut po njem ter med dajanjem vzdrževalnega odmerka zdravila Phesgo in še 15 minut po njem. Če se pojavi pomembna z injiciranjem povezana reakcija, injiciranje upočasnimo ali prekinemo ter nudimo ustrezno zdravljenje. Oceniti je treba stanje bolnika in ga skrbno spremljati, dokler znaki in simptomi popolnoma ne izzvenijo. Pri bolnikih s hudo reakcijo je treba razmisliti o dokončni prekinitvi zdravljenja. Klinična ocena mora temeljiti na tem, kako huda je bila prejšnja reakcija, in na odzivu na zdravljenje neželenega učinka. Preobčutljivostne reakcije/anafilaksija: Bolnike je treba skrbno opazovati glede preobčutljivostnih reakcij. Pri pertuzumabu v kombinaciji s trastuzumabom in kemoterapijo so opazili hude reakcije preobčutljivosti, vključno z anafilaksijo in dogodki s smrtnim izidom. Zdravilo Phesgo je treba dokončno ukiniti v primeru preobčutljivostne reakcije 4. stopnje po merilih NCI-CTCAE, bronhospazma ali akutnega respiratornega distresnega sindroma. Febrilna nevtropenija: Pri bolnikih, ki se zdravijo z zdravilom Phesgo v kombinaciji s taksanom, obstaja večje tveganje za nastanek febrilne nevtropenije. Pri bolnikih, ki se zdravijo z intravenskim pertuzumabom v kombinaciji s trastuzumabom in docetakselom, obstaja večje tveganje za nastanek febrilne nevtropenije v primerjavi z bolniki, ki se zdravijo s placebom, trastuzumabom in docetakselom, še posebej med prvimi 3 cikli zdravljenja. Driska: Zdravilo Phesgo lahko izzove hudo drisko. Driska je najpogostejša med sočasnim prejemanjem terapije s taksanom. Starejši bolniki (≥ 65 let) imajo večje tveganje za drisko v primerjavi z mlajšimi bolniki (< 65 let). Zlasti pri starejših bolnikih in v primeru hude ali dolgotrajne driske je treba razmisliti o zgodnjem zdravljenju z loperamidom in nadomeščanju tekočin ter elektrolitov. Razmisliti je treba o prekinitvi zdravljenja z zdravilom Phesgo, če ne dosežemo izboljšanja bolnikovega stanja. Pljučni dogodki: Pri uporabi trastuzumaba so v obdobju po prihodu zdravila na trg poročali o hudih pljučnih dogodkih. Ti dogodki so bili občasno smrtni. Poleg tega so poročali o primerih intersticijske pljučne bolezni, vključno s pljučnimi infiltrati, sindromom akutne respiratorne stiske, pljučnico, pnevmonitisom, plevralnim izlivom, dihalno stisko, akutnim pljučnim edemom in respiratorno insuficienco. Dejavniki tveganja, povezani z intersticijsko pljučno boleznijo, vključujejo predhodno ali sočasno zdravljenje z drugimi antineoplastičnimi terapijami, za katere je znano, da so z njo povezane, kot so taksani, gemcitabin, vinorelbin in radioterapija. Ti dogodki se lahko pojavijo kot del z infuzijo povezane reakcije ali imajo zapoznel nastop. Bolniki z dispnejo v mirovanju zaradi zapletov napredovale maligne bolezni in sočasnih bolezni imajo lahko večje tveganje za pljučne dogodke. Zato teh bolnikov ne smemo zdraviti z zdravilom Phesgo. Pri pnevmonitisu je potrebna previdnost, zlasti pri bolnikih, ki se sočasno zdravijo s taksani. **Medsebojno delovanje z drugimi zdravili in druge oblike interakcij:** Formalnih študij medsebojnega delovanja niso izvedli. **Neželeni učinki**: Najpogostejši neželeni učinki zdravila (≥ 30%), o katerih so poročali pri bolnikih, zdravljenih z zdravilom Phesgo ali intravenskim pertuzumabom v kombinaciji s trastuzumabom in kemoterapijo, so bili alopecija, driska, navzea, anemija, astenija in artralgija. Najpogostejši resni neželeni dogodki (≥ 1 %), o katerih so poročali pri bolnikih, zdravljenih z zdravilom Phesgo ali intravenskim pertuzumabom v kombinaciji s trastuzumabom, so bili febrilna nevtropenija, srčno popuščanje, zvišana telesna temperatura, nevtropenija, nevtropenična sepsa, zmanjšanje števila nevtrofilcev in pljučnica. Poročanje o domnevnih neželenih učinkih: Poročanje o domnevnih neželenih učinkih zdravila po izdaji dovoljenja za promet je pomembno. Omogoča namreč stalno spremljanje razmerja med koristmi in tveganji zdravila. Od zdravstvenih delavcev se zahteva, da poročajo o katerem koli domnevnem neželenem učinku zdravila na: Javna agencija Republike Slovenije za zdravila in medicinske pripomočke, Sektor za farmakovigilanco, Nacionalni center za farmakovigilanco, Slovenčeva ulica 22, SI-1000 Ljubljana, Tel: +386 (0)8 2000 500, Faks: +386 (0)8 2000 510, e-pošta: h-farmakovigilanca@jazmp.si, spletna stran: www.jazmp.si. Za zagotavljanje sledljivosti zdravila je pomembno, da pri izpolnjevanju obrazca o domnevnih neželenih učinkih zdravila navedete število serije biološkega zdravila. **Režim izdaje zdravila:** H. **Imetnik dovoljenja za promet:** Roche Registration GmbH, Emil-Barell-Strasse 1, 79639 Grenzach-Wyhlen, Nemčija
Za podrobnejše informacije glejte celoten Povzetek glavnih značilnosti zdravila. **Verzija: 1.0/24**

▼Za to zdravilo se izvaja dodatno spremljanje varnosti. Tako bodo hitreje na voljo nove informacije o njegovi varnosti. Zdravstvene delavce naprošamo, da poročajo o katerem koli domnevnem neželenem učinku zdravila. Kako poročati o neželenih učinkih, si poglejte v povzetku glavnih značilnosti zdravila pod poglavjem "Poročanje o domnevnih neželenih učinkih"

Če bolnica med zdravljenjem z zdravilom Phesgo ali v 7 mesecih po prejemu zadnjega odmerka zdravila Phesgo zanosi, vas prosimo, da nosečnost takoj poročate podjetju Roche farmacevtska družba d.o.o. (na e-naslov: slovenia.drugsafety@roche.com ali po telefonu na številko 01 3602 606). Prosili vas bomo za dodatne informacije med izpostavljenostjo zdravilu Phesgo v času nosečnosti in v prvem letu otrokovega življenja. S tem bomo v družbi Roche bolje razumeli varnost zdravila Phesgo in zagotovili ustrezne informacije zdravstvenim oblastem, zdravstvenim delavcem in bolnikom.

Za dodatne informacije glejte Povzetek glavnih značilnosti zdravila Phesgo.

Referenci: 1. O´Shaughnessy J, Sousa S, Cruz J, et al., Preference for the fixed-dose combination of pertuzumab and trastuzumab for subcutaneous injection in patients with HER2-positive early breast cancer (PHranceSCa): A randomised, open-label phase II study, European Journal of Cancer 2021; 152: 223 – 232. **2.** Povzetek glavnih značilnosti zdravila Phesgo https://ec.europa.eu/health/documents/community-register/2020/20201221150167/anx_150167_sl.pdf (dostopano septembra 2024).

DODATNE INFORMACIJE SO NA VOLJO PRI:
Roche farmacevtska družba d.o.o., Stegne 13G, Ljubljana

Datum priprave informacije: oktober 2024
M-SI-00001285 (v1.0)

SKRAJŠAN POVZETEK GLAVNIH ZNAČILNOSTI ZDRAVILA Onivyde pegylated liposomal 4,3 mg/ml
SESTAVA*: Onivyde pegylated liposomal 4,3 mg/ml koncentrat za disperzijo za infundiranje: ena viala z 10 ml koncentrata vsebuje 43 mg brezvodnega irinotekana (v obliki irinotekanijeve soli saharoznega oktasulfata v pegilirani liposomski formulaciji). **TERAPEVTSKE INDIKACIJE*:** Zdravilo Onivyde pegylated liposomal je v kombinaciji z oksaliplatinom, 5-fluorouracilom (5-FU) in levkovorinom (LV) indicirano za prvo izbiro zdravljenja metastatskega adenokarcinoma trebušne slinavke pri odraslih bolniki in v kombinaciji s 5-FU in LV za zdravljenje metastatskega adenokarcinoma trebušne slinavke pri odraslih bolnikih, pri katerih je bolezen po zdravljenju na osnovi gemcitabina napredovala. **ODMERJANJE IN NAČIN UPORABE*:** Onivyde pegylated liposomal smejo bolnikom predpisati in dajati samo zdravstveni delavci, ki imajo izkušnje pri uporabi zdravil za zdravljenje raka. Zdravilo Onivyde pegylated liposomal ni enakovredno drugim neliposomskim formulacijam irinotekana, zato jih ne smemo zamenjevati. Zdravilo Onivyde pegylated liposomal se ne daje kot samostojno zdravilo. Z zdravljenjem je treba nadaljevati, dokler bolezen ne napreduje ali bolnik zdravljenja z zdravilom ne prenaša več. Priporočeni odmerek zdravila Onivyde pegylated liposomal v kombinaciji z oksaliplatinom, LV in 5-FU je 50 mg/m^2 v obliki 90-minutne intravenske infuzije, ki ji sledi 120-minutna intravenska infuzija oksaliplatina v odmerku 60 mg/m^2, nato 30-minutna intravenska infuzija LV v odmerku 400 mg/m^2 in zatem 46-urna intravenska infuzija 5-FU v odmerku 2400 mg/m^2, vsaka 2 tedna. Priporočeni začetni odmerek zdravila Onivyde pegylated liposomal pri bolnikih z znano homozigotnostjo za alel UGT1A1*28 je nespremenjen. Priporočeni odmerek in režim odmerjanja zdravila Onivyde pegylated liposomal v kombinaciji s 5-FU in LV je 70 mg/m^2 intravensko 90 minut, čemur sledi LV 400 mg/m^2 intravensko 30 minut in nato 5 FU 2400 mg/m^2 intravensko 46 ur, vsaka 2 tedna. Pri bolnikih z znano homozigotnostjo za alel UGT1A1*28 je treba razmisliti o manjšem začetnem odmerku zdravila Onivyde pegylated liposomal 50 mg/m^2. Če zdravilo bolniki dobro prenašajo, lahko v naslednjih ciklih razmislimo o odmerku zdravila Onivyde pegylated liposomal 70 mg/m^2. Prilagajanje odmerka se priporoča za obvladovanje toksičnosti, povezane z zdravilom Onivyde pegylated liposomal. **KONTRAINDIKACIJE*:** Anamneza hude preobčutljivosti na irinotekan ali katero koli pomožno snov. Dojenje. **OPOZORILA*:** *Mielosupresija/nevtropenija:* Med zdravljenjem z zdravilom Onivyde pegylated liposomal se priporoča nadziranje celotne krvne slike. Bolniki se morajo zavedati tveganja za nevtropenijo in pomena povišane telesne temperature. Febrilno nevtropenijo je treba nujno zdraviti v bolnišnici s širokospektralnimi intravenskimi antibiotiki. Pri bolnikih, ki doživijo hude hematološke neželene učinke, se priporoča zmanjšanje odmerka ali prekinitev zdravljenja. Bolnikov s hudo odpovedjo kostnega mozga ne smemo zdraviti z zdravilom Onivyde pegylated liposomal. Anamneza predhodnega obsevanja trebuha poveča tveganje za hudo nevtropenijo in febrilno nevtropenijo po zdravljenju z zdravilom Onivyde pegylated liposomal. Pri bolnikih, ki hkrati prejemajo zdravilo Onivyde pegylated liposomal in so obsevani, je potrebna previdnost. Bolniki s pomanjkljivo glukuronidacijo bilirubina, kot so bolniki z Gilbertovim sindromom, imajo med zdravljenjem z zdravilom Onivyde pegylated liposomal lahko večje tveganje za mielosupresijo. *Imunosupresivni učinki in cepiva:* Dajanje živih ali atenuiranih cepiv bolnikom z oslabljenim imunskim sistemom lahko povzroči resne ali smrtne okužbe. *Interakcije z močnimi induktorji encima CYP3A4, močnimi zaviralci encima CYP3A4 in močnimi zaviralci encima UGT1A1:* Zdravila Onivyde pegylated liposomal ne smemo dajati skupaj z močnimi induktorji encima CYP3A4, močnimi zaviralci encima CYP3A4 ali z močnimi zaviralci encima UGT1A1, razen če ni drugih terapevtskih možnosti. Zdravljenje z močnimi zaviralci encima CYP3A4 moramo prekiniti vsaj 1 teden pred začetkom zdravljenja z zdravilom Onivyde pegylated liposomal. *Driska:* Zdravilo Onivyde pegylated liposomal lahko povzroči hudo in smrtno nevarno drisko. Zdravila Onivyde pegylated liposomal se ne sme dajati bolnikom s črevesno obstrukcijo in kronično vnetno črevesno boleznijo.Pri bolnikih, ki doživijo zgodnji pojav driske (v ≤ 24 urah po začetku zdravljenja z zdravilom Onivyde pegylated liposomal) ali holinergične simptome, je treba razmisliti o terapevtskem in profilaktičnem zdravljenju z atropinom, razen če je kontraindicirano. Bolnike je treba opozoriti na tveganje za zapoznelo drisko (> 24 ur), ki je izčrpavajoča in v redkih primerih tudi življenjsko nevarna. Loperamid je treba uvesti ob prvem pojavu neoblikovanega ali mehkega blata ali takoj, ko odvajanje blata postane pogostejše kot običajno. Loperamid je treba dajati, dokler bolnik ni brez driske vsaj 12 ur. Da bi se izognili hudi driski, opustite vse izdelke, ki vsebujejo laktozo, ohranjajte hidracijo in uživajte dieto z nizko vsebnostjo maščob. Če driska traja tudi, ko bolnik prejema loperamid več kot 24 ur, je treba razmisliti o dodatni peroralni antibiotični podpori. Loperamida zaradi tveganja za paralitični ileus ne smemo uporabljati več kot 48 ur zaporedoma. Nov cikel zdravljenja se ne sme pričeti, dokler se driska ne umiri do ≤ 1. stopnje (2–3 odvajanja/dan več kot pred zdravljenjem). *Holinergične reakcije:* Zgodnjo drisko lahko spremljajo rinitis, povečano slinjenje, zardevanje, diaforeza, bradikardija, mioza in hiperperistaltika. Pri bolnikih s holinergičnimi simptomi moramo uporabiti atropin. *Preobčutljivostne reakcije, vključno z akutnimi infuzijskimi reakcijami:* V primeru hudih preobčutljivostnih reakcij je treba zdravljenje z zdravilom Onivyde pegylated liposomal prekiniti. *Predhodna Whipplova operacija:* Večje tveganje za resne okužbe. Bolnike je treba spremljati glede znakov okužbe. *Žilne bolezni:* Zdravilo Onivyde pegylated liposomal je bilo povezano s trombemboličnimi dogodki, kot so pljučna embolija, venska tromboza in arterijska trombembolija. Treba je pridobiti podrobno zdravstveno anamnezo, da bi prepoznali bolnike z več dejavniki tveganja poleg osnovne neoplazme. Bolnike je treba obvestiti o znakih in simptomih trombembolije in jim svetovati, da se v primeru katerega od teh znakov ali simptomov takoj obrnejo na svojega zdravnika ali medicinsko sestro. *Pljučna toksičnost:* Pri bolnikih, ki so prejemali neliposomski irinotekan, so se pojavili dogodki, podobni intersticijski pljučni bolezni (IPB), ki so vodili do smrtnih primerov. Pri bolnikih z dejavniki tveganja (obstoječo pljučno boleznijo, uporabo pnevmotoksičnih zdravil, kolonije stimulirajočimi dejavniki ali predhodnim zdravljenjem z obsevanjem) je treba pred zdravljenjem z zdravilom Onivyde pegylated liposomal in po njem skrbno nadzirati respiratorne simptome. Dokler ni opravljena diagnostična ocena, je treba ob pojavu nove ali napredovale dispneje, kašlja in povišane telesne temperature zdravljenje z zdravilom Onivyde pegylated liposomal začasno prekiniti. Pri bolnikih s potrjeno diagnozo IPB moramo zdravljenje z zdravilom Onivyde pegylated liposomal dokončno prekiniti. *Jetrna okvara:* Bolniki s hiperbilirubinemijo so imeli povišane koncentracije skupnega SN-38, zato je tveganje za nevtropenijo povečano. Pri bolnikih z vrednostjo skupnega bilirubina 1,0–2,0 mg/dl je treba redno nadzirati celotno krvno sliko. Previdnost je potrebna pri bolnikih z jetrno okvaro (bilirubin > 2-kratna zgornja meja normalnih vrednosti [ULN]; aminotransferaze > 5-kratna ULN). Previdnost je potrebna, če zdravilo Onivyde pegylated liposomal dajemo v kombinaciji z drugimi hepatotoksičnimi zdravili. *Bolniki s premajhno telesno maso (indeks telesne mase < 18,5 kg/m²):* Potrebna je previdnost. *Pomožne snovi:* To zdravilo vsebuje 33,1 mg natrija na vialo, kar je enako 1,65 % največjega dnevnega vnosa natrija za odrasle osebe, ki ga priporoča SZO in znaša 2 g. En mililiter zdravila Onivyde pegylated liposomal vsebuje 0,144 mmol (3,31 mg) natrija. **INTERAKCIJE*:** *Previdnostni ukrepi:* Sočasno dajanje z induktorji encima CYP3A4 (npr. antikonvulzivi, rifampicin, rifabutin in šentjanževka) lahko zmanjša sistemsko izpostavljenost zdravilu Onivyde pegylated liposomal. Sočasno dajanje z zaviralci encima CYP3A4 (npr. grenivkinim sokom, klaritromicinom, indinavirjem, itrakonazolom, lopinavirjem, nefazodonom, nelfinavirjem, ritonavirjem, sakvinavirjem, telaprevirjem, vorikonazolom) ali encima UGT1A1 (npr. atazanavirja, gemfibrozila, indinavirja, regorafeniba) lahko poveča sistemsko izpostavljenost zdravilu Onivyde pegylated liposomal. Sočasna uporaba z zdravili z delovanjem na novotvorbe (flucitozinom) lahko poslabša neželene učinke zdravila Onivyde pegylated liposomal. **PLODNOST*:** Pred začetkom zdravljenja z zdravilom Onivyde pegylated liposomal premislite o svetovanju bolnikom glede shranjevanja spolnih celic. **NOSEČNOST*:** Uporaba ni priporočljiva. **DOJENJE*:** Zdravilo je kontraindicirano. **KONTRACEPCIJA*:** Ženske v rodni dobi morajo med zdravljenjem in še 7 mesecev po zdravljenju z zdravilom Onivyde pegylated liposomal uporabljati učinkovito kontracepcijo. Moški morajo med zdravljenjem z zdravilom Onivyde pegylated liposomal in 4 mesece po zdravljenju uporabljati kondome. **VPLIV NA SPOSOBNOST VOŽNJE IN UPRAVLJANJA STROJEV*:** Bolniki morajo biti med zdravljenjem pri vožnji in upravljanju strojev previdni. **NEŽELENI UČINKI*:** Zdravilo Onivyde pegylated liposomal v kombinaciji z oksaliplatinom, 5-fluorouracilom in levkovorinom: *Zelo pogosti:* anemija, nevtropenija, trombocitopenija, hipokaliemija, zmanjšan apetit, periferna nevropatija, disgevzija, parestezija, driska, navzea, bruhanje, bolečine/nelagodje v trebuhu, stomatitis, alopecija, astenija, vnetje sluznic, zmanjšana telesna masa. *Pogosti:* sepsa, infekcija urinarnega trakta, okužba s kandido, nazofaringitis, febrilna nevtropenija, levkopenija, limfopenija, dehidracija, hiponatriemija, hipofosfatemija, hipomagneziemija, hipoalbuminemija, hipokalciemija, tremor, nevrotoksičnost, disestezija, holinergični sindrom, glavobol, omotica, zamegljen vid, tahikardija, hipotenzija, trombembolični dogodki, pljučna embolija, kolcanje, dispneja, epistaksa, kolitis, enterokolitis, zaprtje, suha usta, napenjanje, napihnjenost trebuha, dispepsija, gastroezofagealna refluksna bolezen, hemoroidi, disfagija, hiperbilirubinemija, suha koža, sindrom palmarno-plantarne eritrodizestezije, izpuščaj, hiperpigmentacija kože, mišična šibkost, mialgija, mišični krči, akutna poškodba ledvic, pireksija, edem, mrzlica, zvišana raven transaminaz (ALT in AST), zvišana raven alkalne fosfataze v krvi, zvišana raven gama-glutamil transferaze, zvišana raven kreatinina v krvi, z infuzijo povezana reakcija. *Občasni:* divertikulitis, pljučnica, analni absces, febrilna okužba, gastroenteritis, okužba sluznice, oralna glivična okužba, okužba s Clostridium difficile, konjuktivitis, furunkel, herpes simpleks, laringitis, parodontitis, pustulozni izpuščaj, sinusitis, okužba zob, vulvovaginalna glivična okužba, peritumoralni edem, pancitopenija, hemolitična anemija, elektrolitsko neravnovesje, hiperkalciemija, celična smrt, hipokloremija, protin, hiperglikemija, hiperkaliemija, pomanjkanje železa, podhranjenost, nespečnost, zmedenost, depresija, nevroza, napadi, možganska krvavitev, možganska ishemija, ishemična možganska kap, anozmija, agevzija, motnje ravnotežja, hipersomnija, hipestezija, motnje v duševnem razvoju, letargija, motnje spomina, presinkopa, sinkopa, prehodni ishemični napad, draženje oči, zmanjšana ostrina vida, vrtoglavica, angina pektoris, akutni miokardni infarkt, palpitacije, hipertenzija, periferna hladnost, hematom, flebitis, orofaringealna bolečina, kašelj, hiperoksija, vnetje nosu, atelektaza, disfonija, pnevmonitis, gastrointestinalna toksičnost, obstrukcija dvanajstnika, analna inkontinenca, afta, oralna disestezija, bolečina v ustni votlini, motnje jezika, analna razpoka, angularni heilitis, dishezija, oralna parestezija, zobni karies, eruktacija, želodčne motnje, gastritis, motnje dlesni, boleče dlesni, hematohezija, hiperestezija zob, paralitični ileus, otekanje ustnic, razjede v ustih, spazem požiralnika, parodontalna bolezen, rektalna krvavitev, holangitis, toksični hepatitis, holestaza, hepatična citoliza, pruritus, hiperhidroza, bulozni dermatitis, generalizirani eksfolativni dermatitis, eritem, toksičnost za nohte, papule, petehije, luskavica, občutljiva koža, luščenje kože, kožna lezija, teleangiektazija, urtikarija, artralgija, bolečine v hrbtu, bolečine v kosteh, bolečine v okončinah, poliartritis, okvara ledvic, odpoved ledvic, disurija, proteinurija, vulvovaginalna suhost, slabo počutje, splošno poslabšanje telesnega zdravja, vnetje, sindrom večorganske disfunkcije, gripi podobna bolezen, nesrčna bolečina v prsnem košu, aksilarna bolečina, bolečina v prsnem košu, hipotermija, bolečina, otekel obraz, temperaturna intoleranca, kseroza, zvišano mednarodno umerjeno razmerje, znižana raven celokupnih beljakovin, zmanjšan ledvični očistek kreatinina, podaljšan QT interval na elektrokardiogramu, povečano število monocitov, zvišana raven troponina I. Zdravilo Onivyde pegylated liposomal v kombinaciji s 5-fluorouracilom in levkovorinom: *Zelo pogosti:* nevtropenija, levkopenija, anemija, trombocitopenija, hipokaliemija, hipomagneziemija, dehidracija, zmanjšan apetit, omotica, driska, bruhanje, navzea, bolečine v trebuhu, stomatitis, alopecija, pireksija, periferni edem, vnetje sluznic, utrujenost, astenija, zmanjšana telesna masa. *Pogosti:* septični šok, sepsa, pljučnica, febrilna nevtropenija, gastroenteritis, oralna kandidoza, limfopenija, hipoglikemija, hiponatriemija, hipofosfatemija, nespečnost, holinergični sindrom, dizgevzija, hipotenzija, pljučna embolija, trombembolični dogodki, dispneja, disfonija, kolitis, hemoroidi, hipoalbuminemija, pruritus, akutna ledvična odpoved, z infuzijo povezana reakcija, edem, zvišana raven bilirubina, zvišana raven transaminaz (ALT in AST), zvišano mednarodno umerjeno razmerje. *Občasni:* biliarna sepsa, preobčutljivost, hipoksija, ezofagitis, proktitis, urtikarija, izpuščaj, obarvanje nohtov. *Neznana pogostnost:* anafilaktična/anafilaktoidna reakcija, angioedem, eritem. **PREVELIKO ODMERJANJE*:** Za preveliko odmerjanje zdravila ni znanega antidota. Treba je uvesti maksimalno podporno nego, s katero preprečimo dehidracijo zaradi driske in zdravimo zaplete zaradi okužb. **FARMAKODINAMIČNE LASTNOSTI*:** Irinotekan (zaviralec topoizomeraze I), inkapsuliran v vezikel z lipidnim dvoslojem oziroma liposom. Irinotekan je derivat kamptotecina. Kamptotecini delujejo kot specifični zaviralci encima DNA-topoizomeraza I. Irinotekan in njegov aktivni presnovek SN-38 se reverzibilno vežeta na kompleks topoizomeraze I in DNA ter sprožita poškodbe v enoverižni DNA, kar zaustavi replikacijske vilice pri podvajanju DNA in povzroča citotoksičnost. Irinotekan se presnavlja s karboksilesterazo do SN-38. SN-38 je približno 1.000-krat močnejši kot irinotekan kot zaviralec topoizomeraze I, očiščene iz tumorskih celičnih linij človeka in glodavcev. **PAKIRANJE*:** Pakiranje vsebuje eno vialo z 10 ml koncentrata. **NAČIN PREDPISOVANJA IN IZDAJE ZDRAVILA: H - Predpisovanje in izdaja zdravila je le na recept, zdravilo pa se uporablja samo v bolnišnicah. DATUM ZADNJE REVIZIJE BESEDILA: 04. 2024. Imetnik dovoljenja za promet:** Les Laboratoires Servier, 50, rue Carnot, 92284 Suresnes cedex, Francija. ***Pred predpisovanjem preberite celoten povzetek glavnih značilnosti zdravila. Celoten povzetek glavnih značilnosti zdravila in podrobnejše informacije so na voljo pri: Servier Pharma d. o. o., Podmilščakova ulica 24, 1000 Ljubljana, www.servier.si.**

Zdravilo je na slovenskem trgu na voljo v tuji ovojnini. Za uporabnika so informacije v slovenskem jeziku dostopne na uradni spletni strani www.cbz.si. Navodila za uporabo v slovenskem jeziku so na voljo tudi na https://servier-pro.si/.

Kratice in literatura:
NALIRIFOX: liposomski irinotekan v kombinaciji z oksaliplatinom, 5-fluorouracilom in levkovorinom; mPaCa: metastatski rak trebušne slinavke; mOS: mediana celokupnega preživetja; mPFS: mediana preživetja brez napredovanja bolezni; ORR: skupna stopnja odziva.

1. Povzetek glavnih značilnosti zdravila ONIVYDE pegylated liposomal, april 2024.
2. Melisi D et al. Annals of Oncology. 2023;34:S896-S897.

SERVIER moved by you

ONI AD1 C1 2024-25. Samo za strokovno javnost. Datum priprave informacije: avgust 2024.

Instructions for authors

The editorial policy

Radiology and Oncology is a multidisciplinary journal devoted to the publishing original and high-quality scientific papers and review articles, pertinent to oncologic imaging, interventional radiology, nuclear medicine, radiotherapy, clinical and experimental oncology, radiobiology, medical physics, and radiation protection. Papers on more general aspects of interest to the radiologists and oncologists are also published (no case reports).

The Editorial Board requires that the paper has not been published or submitted for publication elsewhere; the authors are responsible for all statements in their papers. Accepted cannot be published elsewhere without the written permission of the editors.

Submission of the manuscript

The manuscript written in English should be submitted to the journal via online submission system Editorial Manager available for this journal at: www.radioloncol.com.

In case of problems, please contact Sašo Trupej at saso.trupej@computing.si or the Editor of this journal at gsersa@onko-i.si

All articles are subjected to the editorial review and when the articles are appropriated they are reviewed by independent referees. In the cover letter, which must accompany the article, the authors are requested to suggest 3-4 researchers, competent to review their manuscript. However, please note that this will be treated only as a suggestion; the final selection of reviewers is exclusively the Editor's decision. The authors' names are revealed to the referees, but not vice versa.

Manuscripts which do not comply with the technical requirements stated herein will be returned to the authors for the correction before peer-review. The editorial board reserves the right to ask authors to make appropriate changes of the contents as well as grammatical and stylistic corrections when necessary. Page charges will be charged for manuscripts exceeding the recommended length, as well as additional editorial work and requests for printed reprints.

Articles are published printed and on-line as the open access:

(https://content.sciendo.com/raon).

All articles are subject to 1500 EUR + VAT publication fee. Exceptionally, waiver of payment may be negotiated with editorial office, at the time of article submission.

Manuscripts submitted under multiple authorship are reviewed on the assumption that all listed authors concur in the submission and are responsible for its content; they must have agreed to its publication and have given the corresponding author the authority to act on their behalf in all matters pertaining to publication. The corresponding author is responsible for informing the co-authors of the manuscript status throughout the submission, review, and production process.

Preparation of manuscripts

Radiology and Oncology will consider manuscripts prepared according to the Uniform Requirements for Manuscripts Submitted to Biomedical Journals by International Committee of Medical Journal Editors (www.icmje.org). The manuscript should be written in grammatically and stylistically correct language. Abbreviations should be avoided. If their use is necessary, they should be explained at the first time mentioned. The technical data should conform to the SI system. The manuscript, excluding the references, tables, figures and figure legends, must not exceed 5000 words, and the number of figures and tables is limited to 8. Organize the text so that it includes: Introduction, Materials and methods, Results and Discussion. Exceptionally, the results and discussion can be combined in a single section. Start each section on a new page, and number each page consecutively with Arabic numerals. For ease of review, manuscripts should be submitted as a single column, double-spaced text. The template for preparation of the manuscript is available in the editorial manager.

The Title page should include a concise and informative title, followed by the full name(s) of the author(s); the institutional affiliation of each author; the name and address of the corresponding author (including telephone, fax and E-mail), and an abbreviated title (not exceeding 60 characters). This should be followed by the abstract page, summarizing in less than 250 words the reasons for the study, experimental approach, the major findings (with specific data if possible), and the principal conclusions, and providing 3-6 key words for indexing purposes. Structured abstracts are required. Slovene authors are requested to provide title and the abstract in Slovene language in a separate file. The text of the research article should then proceed as follows:

Introduction should summarize the rationale for the study or observation, citing only the essential references and stating the aim of the study.

Materials and methods should provide enough information to enable experiments to be repeated. New methods should be described in details.

Results should be presented clearly and concisely without repeating the data in the figures and tables. Emphasis should be on clear and precise presentation of results and their significance in relation to the aim of the investigation.

Discussion should explain the results rather than simply repeating them and interpret their significance and draw conclusions. It should discuss the results of the study in the light of previously published work.

Charts, Illustrations, Images and Tables

Charts, Illustrations, Images and Tables must be numbered and referred to in the text, with the appropriate location indicated. Charts, Illustrations and Images, provided electronically, should be of appropriate quality for good reproduction. Illustrations and charts must be vector image, created in CMYK color space, preferred font "Century Gothic", and saved as .AI, .EPS or .PDF format. Color charts, illustrations and Images are encouraged, and are published without additional charge. Image size must be 2.000 pixels on the longer side and saved as .JPG (maximum quality) format. In Images, mask the identities of the patients. Tables should be typed double-spaced, with a descriptive title and, if appropriate, units of numerical measurements included in the column heading. The files with the figures and tables can be uploaded as separate files.

References

References must be numbered in the order in which they appear in the text and their corresponding numbers quoted in the text. Authors are responsible for the accuracy of their references. References to the Abstracts and Letters to the Editor must be identified as such. Citation of papers in preparation or submitted for publication, unpublished observations, and personal communications should not be included in the reference list. If essential, such material may be incorporated in the appropriate place in the text. References follow the style of Index Medicus, DOI number (if exists) should be included.

All authors should be listed when their number does not exceed six; when there are seven or more authors, the first six listed are followed by "et al.". The following are some examples of references from articles, books and book chapters:

Dent RAG, Cole P. In vitro maturation of monocytes in squamous carcinoma of the lung. *Br J Cancer* 1981; **43:** 486-95. doi: 10.1038/bjc.1981.71

Chapman S, Nakielny R. *A guide to radiological procedures*. London: Bailliere Tindall; 1986.

Evans R, Alexander P. Mechanisms of extracellular killing of nucleated mammalian cells by macrophages. In: Nelson DS, editor. *Immunobiology of macrophage.* New York: Academic Press; 1976. p. 45-74.

Authorization for the use of human subjects or experimental animals

When reporting experiments on human subjects, authors should state whether the procedures followed the Helsinki Declaration. Patients have the right to privacy; therefore, the identifying information (patient's names, hospital unit numbers) should not be published unless it is essential. In such cases the patient's informed consent for publication is needed, and should appear as an appropriate statement in the article. Institutional approval and Clinical Trial registration number is required. Retrospective clinical studies must be approved by the accredited Institutional Review Board/Committee for Medical Ethics or other equivalent body. These statements should appear in the Materials and methods section.

The research using animal subjects should be conducted according to the EU Directive 2010/63/EU and following the Guidelines for the welfare and use of animals in cancer research (Br J Cancer 2010; 102: 1555 – 77). Authors must state the committee approving the experiments, and must confirm that all experiments were performed in accordance with relevant regulations.

These statements should appear in the Materials and methods section (or for contributions without this section, within the main text or in the captions of relevant figures or tables).

Transfer of copyright agreement

For the publication of accepted articles, authors are required to send the License to Publish to the publisher on the address of the editorial office. A properly completed License to Publish, signed by the Corresponding Author on behalf of all the authors, must be provided for each submitted manuscript.

Conflict of interest

When the manuscript is submitted for publication, the authors are expected to disclose any relationship that might pose real, apparent or potential conflict of interest with respect to the results reported in that manuscript. Potential conflicts of interest include not only financial relationships but also other, non-financial relationships. In the Acknowledgement section the source of funding support should be mentioned. The Editors will make effort to ensure that conflicts of interest will not compromise the evaluation process of the submitted manuscripts; potential editors and reviewers will exempt themselves from review process when such conflict of interest exists. The statement of disclosure must be in the Cover letter accompanying the manuscript or submitted on the form available on www.icmje.org/coi_disclosure.pdf

The use and explanation of AI and AI-assisted technologies in scientific writing

When authors use artificial intelligence (AI) and AI-assisted technologies in the writing process, they should consider that:

- These technologies should only be used to improve readability and language and to assist in the investigation of data. They should not replace researchers' primary tasks of explaining, the interpretation of data and drawing valid scientific conclusions.
- Apply the technology under human supervision and control, and carefully review and edit the result, because AI can produce authoritative-sounding results that may be incorrect, incomplete, or biased.
- Do not list AI or AI-assisted technologies as authors or co-authors, and do not cite AI as an author. Authorship carries with it responsibilities and tasks that only humans can perform.
- Disclose in your manuscript the use of AI and AI-enabled technologies in the writing process by following the instructions below. An appropriate statement should appear in the published paper. Please note that authors are ultimately responsible and accountable for the content of the paper.

Disclosure notes

Authors must disclose the use of AI and AI-assisted technologies in the writing process by adding a statement at the end of their manuscript in the main manuscript file before the bibliography, at the time of manuscript submission. The statement should be included in a new section titled 'Statement on the Use of AI and AI-Assisted Technologies in the Writing Process'.

Statement: during the preparation of this paper, the author(s) used [NAME TOOL / SERVICE] to create [REASON]. After using this tool/service, the author(s) have reviewed and edited the content as required and take full responsibility for the content of the publication.

This statement does not apply to the use of basic tools to check grammar, spelling, references, etc. If there is nothing to disclose, it is not necessary to add a statement.

Page proofs

Page proofs will be sent by E-mail to the corresponding author. It is their responsibility to check the proofs carefully and return a list of essential corrections to the editorial office within three days of receipt. Only grammatical corrections are acceptable at that time.

Open access

Papers are published electronically as open access on https://content.sciendo.com/raon, also papers accepted for publication as E-ahead of print.

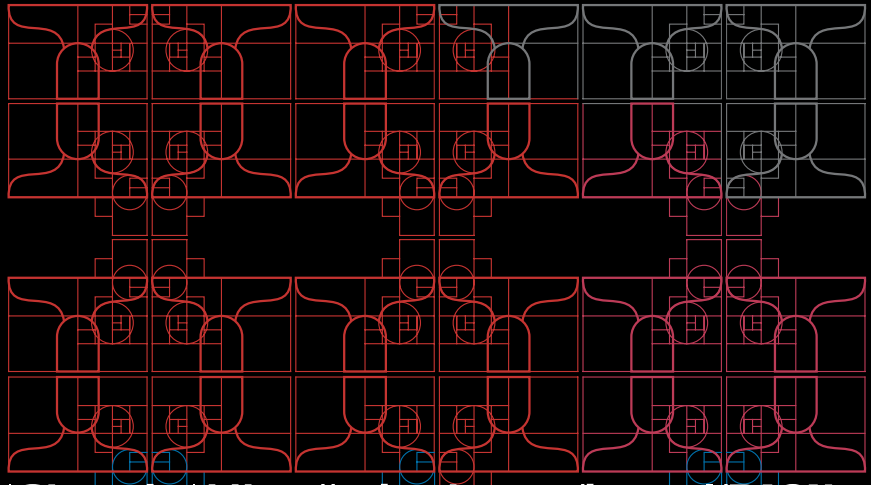

Radiology and Oncology | Ljubljana | Slovenia | https://sciendo.com/journal/RAON

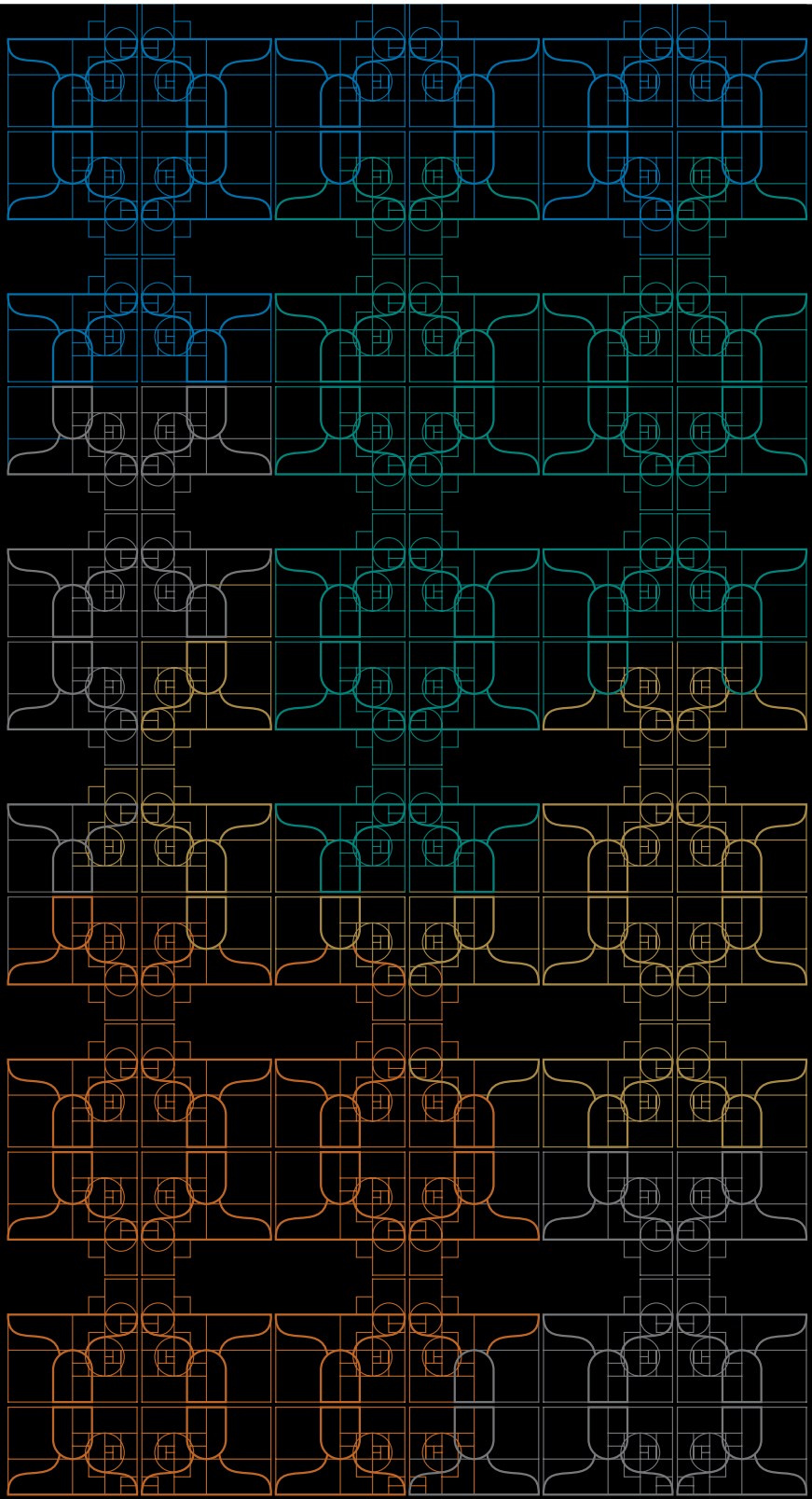

ISSN 1318 - 2099